JRC Scientific and Technical Reports

GLOBAL MONITORING FOR SECURITY AND STABILITY (GMOSS)

INTEGRATED SCIENTIFIC AND TECHNOLOGICAL RESEARCH SUPPORTING SECURITY ASPECTS OF THE EUROPEAN UNION

Edited by

Gunter Zeug & Martino Pesaresi

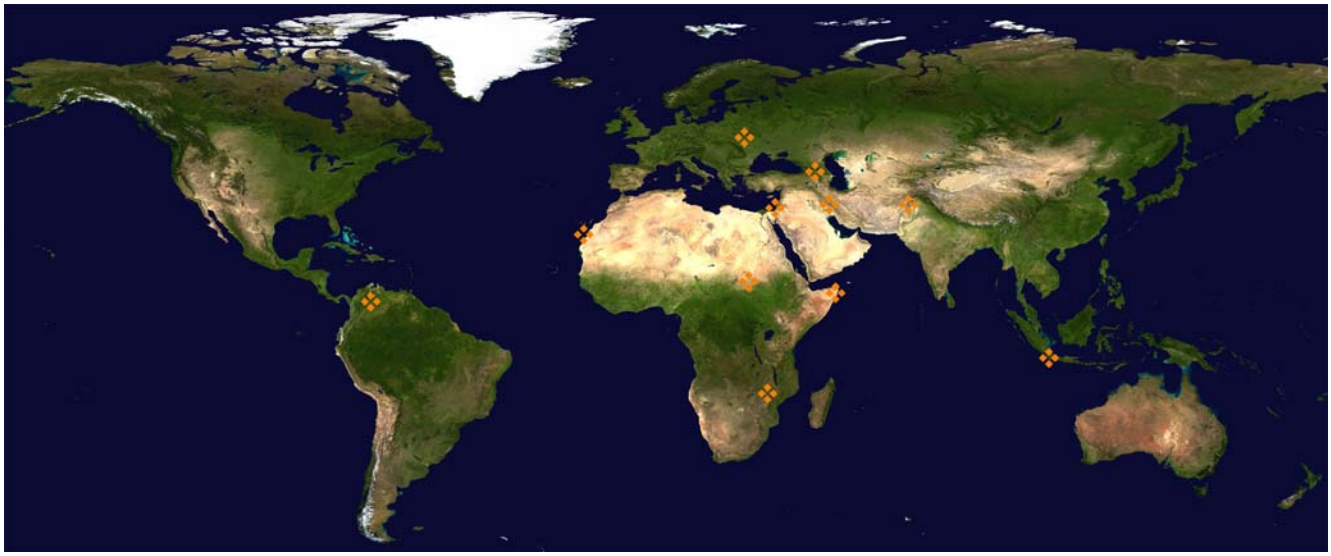

EUR 23033 EN - 2007

JRC EUROPEAN COMMISSION

ipsc Institute for the Protection and Security of the Citizen

ISFEREA

GMOSS Global Monitoring for Security and Stability

The Institute for the Protection and Security of the Citizen provides researchbased, systems-oriented support to EU policies so as to protect the citizen against economic and technological risk. The Institute maintains and develops its expertise and networks in information, communication, space and engineering technologies in support of its mission. The strong crossfertilisation between its nuclear and non-nuclear activities strengthens the expertise it can bring to the benefit of customers in both domains.

European Commission
Joint Research Centre
Institute for the Protection and Security of the Citizen

Contact information
Address:
European Commission – Joint Research Centre
Institute for the Protection and Security of the Citizen – Support to External Security
TP 267, Via E. Fermi, 2749
I-21027 Ispra (VA), Italy

E-mail: gunter.zeug@jrc.it
Tel.: +39-0332-786550
Fax: +39-0332-785154

http://ses.jrc.it
http://ipsc.jrc.ec.europa.eu
http://www.jrc.ec.europa.eu

JRC 41424

EUR 23033 EN
ISBN 978-92-79-07584-1
ISSN 1018-5593

DOI: 10.2788/53480

Luxembourg: Office for Official Publications of the European Communities

Printed in Italy

The cover photo is based on a Terra/MODIS Image Mosaic of the Earth - Copyright by NASA. The image can be downloaded from the Visible Earth website (http://visibleearth.nasa.gov).

GLOBAL MONITORING FOR SECURITY AND STABILITY (GMOSS)

INTEGRATED SCIENTIFIC AND TECHNOLOGICAL RESEARCH SUPPORTING SECURITY ASPECTS OF THE EUROPEAN UNION

Edited by

GUNTER ZEUG & MARTINO PESARESI

Acknowledgements

We wish to express our sincere thanks to all the contributors to this report for making this endeavour possible. The work presented here was conducted by partners of the GMOSS Network of Excellence in the Aeronautics and Space priority of the Sixth Framework Programme funded by the European Commission's Directorate General Enterprise & Industry. The authors and editors are grateful for the support through this programme. It is our hope that this publication will provide stimulation to researchers and decision makers from the wide thematic field of *security* to perform and support more in-depth work and analysis to face today's challenges of a changing world.

Contents

Global Monitoring for Security and Stability – A Network of Excellence promoting Europe's civil security research capacity

Gunter Zeug* & Martino Pesaresi

European Commission, Joint Research Centre, Institute for the Protection and Security of the Citizen (IPSC), Support to External Security Unit, Ispra 21027 (VA), Italy

* gunter.zeug@jrc.it

Introduction

With the fall of the Berlin Wall and the end of the East-West confrontation the traditional security concept of protecting state borders, territory and citizens needs radical revision. After a decade of apparent security and freedom of threats in the nineties of the 20iest century the world situation changed in recent years: international terrorism, state failure, proliferation of weapons of mass destruction, and organized crime emerged as new challenges for global security. Besides, coping with climate change, natural hazards, and environmental degradation, poverty, under-development, and diseases are facts that also affect human security and which no single state can master alone. The complexity of these facts, their action and interaction still show a lot of gaps in our knowledge. Obviously these gaps can only be filled with collective research under common responsibility and following common strategies.

New technologies play a crucial role in changing the scenario of collective threats and security strategies; new technology makes the scenario more and more complex and is an accelerator of change. Since early 90s, civilian satellite remote sensing technologies have reached the sophistication necessary for having an impact on security issues. Spatial, radiometric, and time resolution of the data obtained by new satellite platforms and sensors have increased dramatically the capacity to impact on our security and safety by monitoring more and more detailed information in a multi-scale and synoptic way.

Synoptic, multi-scale, objective, independent and almost censure-free, consistent, automatically collected, are positive characteristics of the data source provided by satellite platforms.

Last-generation very-high spatial resolution data are challenging the available technology for accessing and interpreting these imageries and forcing to new paradigms. New image data storing, access, visualization and internet streaming paradigms have been successfully developed in these recent years, and the world-wide success of systems like Google Earth or Microsoft Virtual Earth demonstrate the technological possibility to multi-scale multiple and distributed access to a shared world-wide central database of very high resolution images.

Technology is proposing now solutions mature enough for the visual access to world-wide detailed imageries but the same level of reliability is not available yet for automatic image understanding and image information mining tasks. Actually the operational image interpretation of last-generation satellite data is done largely by visual inspection and reporting: this methodology is sustainable only for limited areas and limited number of targets to be detected in the image data, but became rapidly unfeasible and/or inconsistent if applied to large areas with the need to have rapid and reliable assessments.

The increase of detail available in the new-generation satellite data brings to a dramatic increase of data complexity, including massive volume of data to be managed, increase of statistical variability of the signal detected and increase of geometrical complexity of the image as the presence of parallax and panoramic distortion. All these factors are contributing to the increasing of the computational complexity and to the instability of the inferential models used for automatic image understanding. Paradoxically (and contrary to the expectations of the remote sensing scientific community), the increase of the detail on the available satellite images seems to decrease our capacity to interpret those using automatic inferential systems.

Beside these scientific and technical challenges related to the nature of the new data source to be managed, some others are related to the nature of the applications explored in the contributions presented in this volume: we can list below some constraints and challenges related to the use of remotely-sensed data in security applications:

i) The need of *multi-temporal* analysis as in pre-post event assessment, trends, anomalies detection;

ii) The need of *rapid assessment* on sometime large areas (hours, days);

iii) The need to *integrate heterogeneous geo-information sources* often of unknown quality;

iv) The fact that often basic *information is missing* because the areas under analysis are inaccessible for security reasons (e.g. regarding data geo-coding, interpretation keys, validation);

v) The fact that the output of the assessment is often highly controversial, as in the case of presence of conflict or politically or economically sensitive topics, so the need to show a shared and *convincing* inferential model;

vi) The possible presence of disinformation originated by political or economic interests and consequently the necessity to handle the *credibility* of the sources used in the assessments;

vii) The possible existence of *camouflage* in the observed scene, consequently the necessity to handle a possible intelligent strategy of the observed entity.

All these issues are characteristics of the use of satellite data in security applications and they are challenging the traditional methodologies for image data processing, automatic image data understanding and output validation developed by the scientific remote sensing community. In particular the first four listed characteristics force to design robust systems able to handle more consistently semantic and spatial information uncertainly while the last three characteristics force the scientist to exit from the classical natural science paradigm (largely dominant in the remote sensing scientific community) postulating complete dichotomy between the observer and the observed "external" reality eventually directly accessible as "truth".

All these technical, scientific and epistemological challenges are only partly addressed in the contributions presented in this volume: anyhow we have to consider these contributions as a first consistent and important step forward the definition of the sense and the limits of a new technology in a radically new context of use.GMOSS

The four year project Global Monitoring for Security and Stability (GMOSS) was established to strengthen and integrate Europe's civil security research capacities putting a special focus on satellite earth observation as tool for global monitoring. It was organized as Network of Excellence (NoE) in the Aeronautics and Space priority of the Sixth Framework Programme funded by the European Commission's Directorate General Enterprise & Industry.

NoEs were designed to enhance scientific and technological excellence on a particular research topic to provide European leadership by gathering the available but mostly fragmented expertise.

Scientifically GMOSS aimed at identifying and analysing user needs and providing related information, tools and methods to support crisis management and conflict prevention. By linking socio-economic and political sciences with remote sensing and geoinformation technologies the thematic view of each research area should be exceeded and the value of the results for potential end-users like the European Commission, EU agencies, UN institutions, and national authorities be expanded.

Integration could simply be understood as the bringing together of several parties working in the same project. Figure 1 shows this impressively: 22 contractors together with another 11 associated partners formed an effective working partnership. But GMOSS was going beyond a basic union of researchers working on the subject named security. In GMOSS integration meant networking and linking of different fields of research to form an integrated whole. This can also be read out of Figure 1: the partner organisations' names and acronyms illustrate and confirm the manifold thematic background of the GMOSS partners ranging from defence to conflict analysis and peacebuilding as well as from information technology to remote sensing and geoinformation carried out by partners with institutional, industrial and research background.

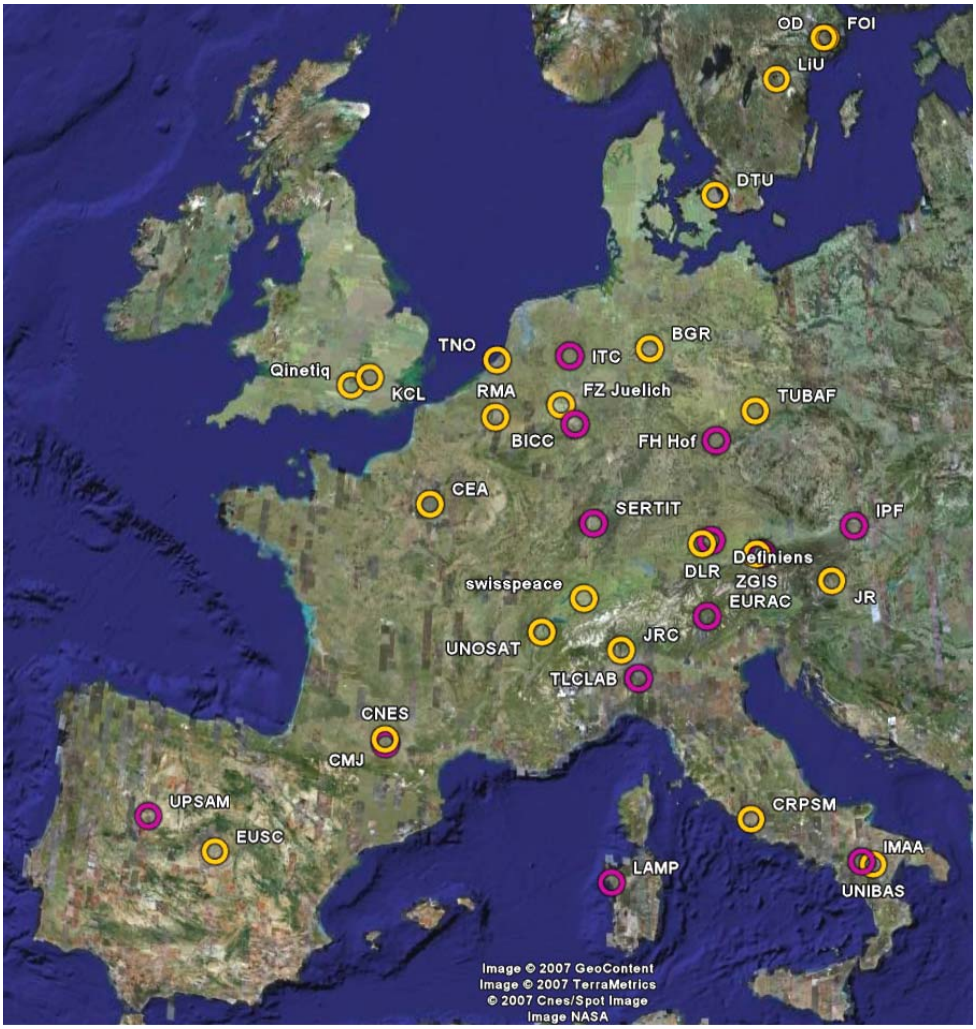

Fig.1: The GMOSS Partnership: in orange contractors of GMOSS, in pink: associated partners of GMOSS (map based on Google Earth)

This variety is also represented in the work-package structure of GMOSS. It consists of three main groups of activities: *integration – research – training* which again were subdivided into several work-packages.

Integration

As mentioned above integration meant the creation of close networks between the partners and the common development of solutions. All activities in this group were established to promote and supervise the overall integration of the GMOSS network. The common work on agreed testcases, and the investigation and development of tools and methods were coordinated in these work-packages just as the sharing of information and knowledge in frequent workshops, seminars and meetings. Staff exchanges were another method allowing common work and establishing a common knowledgebase among the scientists. Harmonised working in crisis response and the provision of high quality products need agreed working standards which were developed by another working group. Shared infrastructure might speed up and facilitate the processes.

Research

The research activities within the network encompassed three main groups:

I. *Generic tools:*

After identifying application needs, the development, evaluation and comparison of tools and environments were conducted based on case studies. These included feature recognition, change detection and visualisation techniques.

II. *Applications:*

Several security related applications were selected for evaluating remote sensing for its potential use. Examples are the effective monitoring of international treaties protecting against proliferation of weapons of mass destruction, the provision of early warning to avoid or reduce risk of natural hazards, better estimates of static and dynamic population numbers on different scales, monitoring critical infrastructure and borders, and finally rapidly assessing of damages.

III. *Security concepts:*

Based on current EU security strategies and other relevant documents a first work-package aimed at analysing which threats and risks can be monitored and managed with the support of remote sensing. The work-package on crisis response investigated strategies and patterns of responding to crisis events relevant for European citizens and organisations for getting a more harmonized and common understanding of crisis scenarios and response patterns. The work of the scenario analysis WP aimed at the analysis of issues and priorities of the European security policy towards the identification and ranking of major threats to security and stability. The results were used for the definition of scenarios to be assessed by the researchers and the identification of early warning indicators and ‘keys’ (footprints), which can be monitored and evaluated.

Training

The spreading of excellence (also beyond the boundaries of the NoE’s partnership) was another aim of NoEs. GMOSS outcomes were continuously disseminated to experts in- and

outside of the European research area and end users like the European Commission. GMOSS provided also information for security aspects of the European Union's Global Monitoring for Environment and Security initiative (GMES). The network members themselves were offered technical training courses, summer schools, seminars and workshops with the aim of facilitating integration and transfer knowledge.

This report

This report is a collection of success stories about achievements and activities of the GMOSS network members during the past years. State of the art scientific and technological research supporting security aspects of the European Union are presented. The report structure reflects GMOSS' work breakdown structure illustrated above. It consists of four parts. Part I addresses *Concepts and Integration.* A first chapter is dealing with the analysis of European security policies and strategies providing a summary of the strategic challenges facing the EU and its response. A second article analyses and evaluates the current geographic priorities of the EU security policy. The role and feasibility of earth observation (EO) technologies in order to meet the needs of safety and security is discussed in a third paper.

The GMOSS network defined test-cases to provide a real-life context within which to place the technical applications that have been developed. One article explains reasons for selecting the different test cases and gives general background information on the selected regions as well as about the activities that were conducted within the network.

Further articles describe concepts for risk assessment of armed conflicts and conflict mapping methods. Besides technical concepts for retrieval of security related information from the internet and an overview about the GRID approach developed by UNOSAT is given. The chapter ends with a contribution about the GMOSS Gender Action program summarizing the general problem of weak participation of women in scientific research careers and in management positions. In addition it reflects results from a gender workshop about the perspective of women in conflict, post conflict reconstruction and peace building.

Part II of this book presents various *Application* activities conducted by the network partners. The contributions range from GIS analysis in the field of infrastructure monitoring of pipelines to an investigation of probable causes for increased cases of cancer after the first Gulf War in 1991. Robust satellite techniques for early warnings in security applications are presented as well as groundwater vulnerability studies in the Near East. Regional studies from Zimbabwe are concerned with population density estimations and post conflict assessments and reconstruction monitoring in Harare. The assessment of the state of built-up features after their destruction as well as the process of their rehabilitation is investigated and described in another contribution. A border permeability study defines several factors that describe the permeability of land borders and uses them to model the accessibility and permeability of borders on continental and local scale. Flooding is a common natural hazard causing often damage to humans, infrastructure and land. An article tries to focus on the impact of floods and economic and environmental damage in risk areas along two lakes in Sweden showing the potential of GIS for decision makers.

The automatic transformation of imaged scenarios into policy-relevant information is another subject described in a paper. Therein the use of pseudo-realistic visualizations for providing a 'true' depiction of e.g. a certain crisis area is described. This is compared to analytical 3D views for displaying analytical items, and to communicate scientific results.

A further chapter investigates the use of geoinformation technologies for local emergency management. The main questions addressed are how municipalities can implement GIS effectively and how risk analysis can be implemented using these tools.

Part III focuses on the research and development of image processing methods and *Tools*. These range from the determination of moving targets velocity and direction using one single optical VHR satellite imagery to the use of differential SAR interferometry for the measurement of surface displacement caused by underground nuclear explosions.

The four following papers describe the use of Robust Satellite techniques for monitoring (natural) hazards like floods, volcanoes and earthquakes.

Another chapter presents the concepts of Multi-Stationary orbits and the analysis of the variability of the images spatial resolution and illumination conditions based on change detection methods and texture analysis for detecting small changes in a satellite scene. This is followed by an article about the use of mathematical morphology for detecting versatile objects, belonging to very different contexts, like dwelling units in refugee camps, roads of complex shapes and different background, main structures in nuclear plants.

The modelling of buildings in urban areas from high resolution stereo satellite images for population estimation and change detection is illustrated in another chapter. The modelling of buildings is also addressed by another contribution about the localization of industrial areas in the context of risk assessment. The approach is based on the detection of long linear segments on an image whose intensity is related to the vegetation index. Part III finishes with a chapter about the progress in the field of change detection, including the introduction of an iterative re-weighting scheme into the MAD algorithm, the use of regularization to avoid numerical instabilities with high-dimensional data, the application of MAD to automatic radiometric normalization of image time series and the unsupervised clustering of changes in the MAD feature space.

The report closes with Part IV. The author looks back on four years of integrated work and depicts challenges and achievements. He ends with an outlook about a possible way forward for integrated European security research.

Concepts & Integration

European Security Strategy and Earth Observation

Anthony Cragg*

King's College London, Centre for Defence Studies, Strand Bridge House, 138-142 Strand, London WC2R 1HH

* anthonycragg@yahoo.co.uk

1. Overview

This paper draws on the European Security Strategy and other major EU policy documents in this field to provide a summary account for the general reader of the strategic challenges facing the EU and its response. It then considers the role which earth observation (EO) technologies can play in the European Union's strategy for responding to these contingencies with particular reference to the wide range of potential customers for EO product within EU structures and the contribution which it can make to crisis management.

2. A new security landscape

There has been a radical change in European security priorities since the establishment of governments in Central and Eastern Europe in 1989, committed to democratic principles and to membership of NATO and the EU. With the dissolution of the Warsaw Pact in 1991 and the gradual emergence of the EU as a significant player in international security, the focus of European security has moved from the confrontation of massed forces on the inner German border and in the North Atlantic to a commitment to a broadly-based concept of international security – ranging from diplomatic and humanitarian intervention to military action - within and beyond Europe and efforts to counter international terrorism and the proliferation of weapons of mass destruction (WMD).

New philosophies and strategies have been developed which reflect this fundamental shift in European and wider international security priorities. These include, in particular, the UN's Agenda for Peace (1992 and 1995); NATO's Strategic Concept (1999); and the European Security Strategy (2003). All acknowledge new threats and risks and see crisis management and peacekeeping in their widest interpretation as key security instruments.

A wide choice of instruments is at the disposal of the EU in its approach to international security , ranging from political and diplomatic initiatives through measures such as trade, aid and humanitarian relief to the possibility of military intervention within the framework of the Petersberg Tasks set out in Article 17 of the Treaty on the European Union. These tasks are an integral part of the Common Foreign and Security Policy (CFSP) and the European Security and Defence Policy (ESDP) and range from humanitarian and rescue operations to crisis management including peacemaking. Joint disarmament operations, support for third countries in combating terrorism and security sector reform are also seen as potential roles.

3. Major threats and risks

The principal security challenges faced today by the EU were set out in the European Security Strategy (ESS) approved by Heads of State and Government in December 2003. These are:

- Terrorism;
- Proliferation of WMD;
- Regional Conflicts;

- State Failure;
- Organised Crime.

The ESS also recognises that poverty, disease and economic failure can lead to the breakdown of societies and that competition for natural resources is likely to lead to instability, with energy dependence a special concern for Europe. Climate change and the denial of human rights have also risen high on the agenda of EU concerns with a security dimension.

4. Strategic objectives and policy implications

Against this background, the ESS identifies three main strategic objectives:

- To tackle these key threats by means of a mix of military, political, economic and other instruments, including humanitarian intervention and law enforcement. The EU is particularly well equipped to respond to crises in a multi-faceted way;
- To build security in the EU's neighbourhood by promoting a ring of well governed states to the east of the Union and on the borders of the Mediterranean. The stability of the Balkans region and a resolution of the Arab/Israeli conflict are strategic priorities for Europe;
- To support the development of an effective system of international security based on a strong United Nations and other international bodies, a flourishing transatlantic relationship and commitment to upholding and developing international law.
- To achieve these objectives, the ESS sets out a broad policy framework which envisages that the EU should:
- Become more active in pursuing strategic objectives by developing a culture which fosters early, rapid and, where necessary, robust intervention, including a willingness to act preventatively;
- Enhance its military and diplomatic capability, including by means of common threat assessments, the pooling of sharing of military assets and a greater capacity to bring the necessary civilian resources to bear in crisis and post-crisis situations;
- Improve coordination and coherence among EU policy instruments, including the military and civilian capabilities of member states, diplomatic efforts, development, trade and environmental policies, and assistance programmes;
- Foster multilateral cooperation in international organisations and seeking strategic partnerships with nations and regional groupings which share the EU's goals and values.

5. The information requirement

An up to the minute, clear and all-embracing information picture is an essential requirement to enable the EU to conduct the full spectrum of its security policy from situation monitoring to crisis management. Earth observation from microwave, infra-red and optical means of acquisition, is an essential contributor to this picture and complements other information ranging from open source data to classified material such as confidential political reporting and secret intelligence.

Information support to EU policy makers in the conduct of CFSP/ESDP and of security-oriented business managed by the European Commission will need to be fast, precise and flexible. Significant requirements include :

- A broadly based approach. This is needed in order to manage today's security issues as compared with the military 'bean counting' of the Cold War. A consolidated analysis of a wide range of factors – whether humanitarian or military – is required, drawing on information provided from many sources, including earth observation.
- ESS also makes it clear that the EU must be ready to act before a crisis occurs by pre-emptive engagement to prevent a situation from deteriorating. This will require flexibility in responding to demands for information by policy makers. Practical experience demonstrates that a stream of information in near real time is required by policy makers exercising strategic political control over an operation.
- Peacekeeping operations demand precisely focused information to help define and support the minimum force required to secure an operational objective. The successful handling of a humanitarian crisis also demands similarly precise and focussed information to support the delivery of aid as rapidly and effectively as possible.

Given the complex institutional framework of EU security policy, the range of customers for satellite imagery is considerable. It ranges in the policy –making field from bodies such as the European Council, the Policy and Security Committee and the Military Committee to the Situation Centre and the EU Military Staff. European agencies such as the European Maritime Security Agency (EMSA), the European Disease Prevention and Control Agency (ECDC), (EMSA) and FRONTEX, the body charged with fostering operational cooperation in the field of border control are also potential customers, as are Commission services dealing with external relations, humanitarian aid, transport and energy security, public health, civil protection and many others.

More recently, in mid-2007, the multifaceted nature of the EU's commitment to international security encouraged the creation of a new Civilian Planning and Conduct Capability (CPCC) designed to exercise strategic command and control over civilian ESDP operations and to contribute to a joint civil-military planning capability with the aim of ensuring close cooperation from the planning phase onwards. As it develops, the CPCC too could become a significant customer for satellite imagery.

6. Targets for Earth Observation

It is possible to identify from the ESS and other key EU policy statements – notably the Declaration on Combating Terrorism and the Strategy against the Proliferation of WMD – a range of priority targets. These include:

- Regional Problems: EU Neighbourhood, including the Wider Middle East and the Western Balkans; the Great Lakes; Kashmir, the Korean Peninsula.
- State Failure: Somalia
- Terrorism: Security of transport systems; protection of key points; essential services (e.g. water, energy, communications); consequence management. Many of these requirements will, of course, be national responsibilities but it is possible to envisage a coordinated international response under some circumstances.
- WMD Proliferation: Treaty verification; monitoring of export controls; interdiction of illegal procurement; security of procurement-sensitive items (e.g. spent nuclear fuels); illegal trafficking; cooperative threat reduction; monitoring regional instability and state proliferators.
- Organised Crime: Heroin trafficking from Afghanistan via Balkans criminal networks; trafficking of women; illegal migration; maritime piracy; illegal weapons trading.

- Humanitarian Relief: The extent and impact of natural disasters and humanitarian crises.

7. Earth Observation and Crisis Management

Much practical experience of the gathering, processing and dissemination of information in a crisis management situation is available from recent operations. Against this background, the following broad approach to the principal demands for earth observation support can be envisaged, which is equally relevant to EO applications in other sectors in which the EU is active, including border security, civil protection, critical infrastructure protection and maritime security:

- Pre-crisis: broadly-based routine observation in the context of the ESS, counter-terrorism and counter-proliferation policies to support the Situation Centre and other bodies as required. Other useful areas for pre-crisis or conflict prevention include the monitoring of resources in developing countries which are potential focal points for crises (including, for example, diamonds, timber and water) as well as applications for humanitarian purposes such as the monitoring of crops for food security.
- Developing crisis: flexibility to facilitate rapid focus on emerging problem and crisis management planning. This might include on the one hand assessing the impact of natural disasters or of indicators of potential crises, such as movements of troops and refugees and on the other supporting the preparation of humanitarian or military operations.
- Crisis situation: contribution to political management of crisis including humanitarian interventions and any military or police involvement in crisis management, especially by EU battle groups and the EU Rapid Reaction Force. Both will require high quality information in near real time.
- Post-crisis: contribution to management of post-crisis phase will require flexibility, accuracy and precision. This will include supporting damage assessment and tracking post-crisis humanitarian aid, recovery and reconstruction programmes, the monitoring of military disengagement, including disarmament and demobilisation and possibly specific observation tasks linked to the implementation of peace building agreements, such as the monitoring large-scale movements of displaced persons and refugees, borders or other disputed areas, critical infrastructure etc.

8. European Security Today

The EU's practical experience of major military operations has been limited to the short-term operations: Artemis (DRC -2003); Concordia (FYROM - 2003); EUFOR Congo (2006) and the longer-lasting and potentially more demanding Operation Althea, which saw the takeover of responsibility from NATO in Bosnia-Herzegovina towards the end of 2004. It has broader experience, however, of the use of 'soft power', including in particular, police and other law-enforcement operations, often underpinned by medium and longer term assistance, including institution building, aimed at further contributing to stability and security. Indeed, of the 16 operations which it has mounted to date, 12 have been of this nature, ranging from border monitoring in Indonesia to extensive engagement in Africa and the Middle East.

Ongoing operations in mid-2007 include military and police operations in Bosnia and Herzegovina, a range of police and border monitoring missions and support for police and security sector reform.

Work is also actively in train for a comprehensive engagement in Kosovo under which the EU would be charged with overseeing the implementation of a status settlement. This will be a broadly-based mission designed to help the Kosovo authorities in their task of ensuring security, stability and the rule of law.

9. Earth Observation in practice

Examples of the contribution of high resolution satellite imagery to the information pool on which decision makers could draw in the management of recent crises, whether humanitarian or man-made, include:

- A very short notice initial damage and needs assessment of Beirut and Southern Lebanon in the wake of the major inter-communal disturbances of summer 2006. This and other information was integrated into a database for use by the Lebanese authorities and the donor community.
- The provision of very high resolution data and technical support to the Indonesian and Sri Lankan authorities following the South Asian tsunami in December 2004. This facilitated the speedy production of accurate maps for damage assessment purposes and future planning
- Support for the Pakistani authorities following the earthquake of October 2005 through the collection and analysis of high resolution imagery
- Participation in an EU initiative to identify and map illegal diamond mining as a contribution to the Kimberley Process – a joint governmental and mining industry initiative to stem the flow of 'conflict diamonds' used to finance rebel movements in Africa.
- Monitoring poppy cultivation in Afghanistan as a contribution to efforts to develop alternative livelihoods for farmers.

10. GMOSS and the way ahaead

The GMOSS research programme concentrates on a range of applications of potential value to the conduct of EU security policy. This includes treaty monitoring, early warning, damage assessment, and population, infrastructure and border monitoring. In order to support this programme and as part of the overall objective of developing advice and operational guidelines on EU priority security issues for the GMOSS research community, a range of examples have been identified in which earth observation might be able to contribute to managing the major threats and risks faced by the EU. These include the following:

Regional conflicts or potential conflict (including failed states). Earth observation is likely to be able to contribute significantly to the monitoring and managing of such situations. This includes border monitoring, change detection, monitoring of longer term infrastructure developments in military facilities or important infrastructure of civilian nature and the provisions of early warning of troop movements, particularly in border areas. This may also include the identification of ecological changes and/or disputes about natural resources (for example water, oil and other minerals etc) that can lead or contribute to regional instability.

Counter-terrorism. Earth observation might be able to assist in the identification of training camps in states supporting terrorism or the movement of personnel and weapons and perhaps contribute to the monitoring of key points for security purposes.

WMD proliferation. Nuclear facilities appear to be suitable for monitoring. Chemical capabilities are likely to be more problematic both to identify and monitor and biological the

most difficult. Earth observation also has the potential to help in sustaining the basic policy building blocks of counter-proliferation policy, notably: multilateral agreements; the promotion of a stable international environment; close cooperation with key partners; and political action against state proliferators.

Organised crime. There is potential for using earth observation to detect poppy, coca or other illicit crops and the illegal exploitation of natural resources such as logging or mining. On the maritime front, the space-based detection of vessels might be used in order to support action against maritime piracy and organised trafficking of persons, arms or other illicit items.

Humanitarian Relief. Earth observation could be used for the identification of useable infrastructure such as ports, roads, railways and airstrips; checking possible locations for establishing relief facilities such as refugee camps and temporary hospitals; and obtaining information on the extent and impact of natural disasters.

References

Council of the European Union (2003): A Secure Europe in a Better World, European Security Strategy, Adopted by the Heads of State and Government at the European Council in December 2003, Brussels.

Council of the European Union (2005): ESDP Newsletter, Issue 1, Brussels, December 2005.

Council of the European Union (2006): ESDP Newsletter, Issue 2, Brussels, June 2006.

Council of the European Union (2007): ESDP Newsletter, Issue 3, Brussels, January 2007

Council of the European Union (2007): ESDP Newsletter, Issue 4, Brussels, July 2007

North Atlantic Treaty Organization (NATO) (1999): NATO Strategic Concept, NAC-S(99)64, Washington, April 1999;

NATO, Summit Communiqués: Madrid: M-1(97)81, 24 April 1997, Washington: NAC-S(99)81, 24 April 1997; Prague: Presse Release 2002(127), 21 November 2002;

United Nations (UN) (1992): UN Agenda for Peace, New-York, June 1992

Western European Union (WEU) (1992): Petersberg Declaration, Meeting of WEU Council of Ministers, Bonn, 19 June 1992.

USEFUL URLs

EU Common Foreign Security Policy (CFSP) and Defence Policies (ESDP):

http://www.iss-eu.org/

http://www.consilium.europa.eu/cms3_fo/showPage.asp?id=248&lang=EN&mode=g

http://www.consilium.europa.eu/cms3_applications/applications/newsRoom/loadBook.asp?BID=80&LANG=1&cmsid=978

http://www.weu.int/documents/920619peten.pdf

EU External Relations (General and CFSP):

http://ec.europa.eu/comm/external_relations/index.htm

http://ec.europa.eu/comm/external_relations/cfsp/intro/index.htm

Global Monitoring for Environment and Security/GMES:

http://www.gmes.info/index.php?id=home

NATO (on-line library):

http://www.nato.int/docu/home.htm

OSCE (politio-military dimension):

http://www.osce.org/activities/18803.html

UN (peace&security issues):

http://www.un.org/peace/

WEU (historical archives):

http://www.weu.int

European Security Policy: Proposal for Country Prioritisation

Dirk Buda*

European Commission, Joint Research Centre, Institute for the Protection and Security of the Citizen (IPSC), Support to External Security Unit, Ispra 21027 (VA), Italy

* dirk.buda@ec.europa.eu

Abstract

The identification of security challenges primarily derives from a global analysis. This evaluation of the current geographic priorities of EU security policy takes into account the EU's programmatic orientations, as set out in particular in the European Security Strategy (ESS, the EU's main instrument and tool to address global security and current application to third countries).

The reasons for EU concern or action differ from one country to another, and are influenced by the EU's capacity to effectively address security challenges in collaboration with international partners. The EU's capacity to act varies depending political will, existence of necessary instruments and on the country (or region) concerned.

The approach to country prioritisation and ranking with respect to EU Security Policy is based on EU programmatic orientations and relevant EU actions. It has been developed on the basis of information generally drawn from publicly available EU sources.

The resulting overall scores, rankings and classification according to the proposed model generally confirm geographical priorities of EU security/external policy as set out in the European Security Strategy or associated documents.

Introduction

The rationale of this proposal for Country Prioritisation is that advice and operational guidelines on EU priority security issues in support of the management of scientific, technical or other activities (training, development of games etc) within GMOSS should include an evaluation of the current geographic priorities of EU security policy. The reasons for EU concern or action with respect to an individual country clearly differ from one to another, including for example, the absence of government authority, concerns over weapons of mass destruction (WMD), state support to terrorism or significant presence of listed terrorist entities or organisations in a third country and, last but not least, the risk of regional instability.

From a European perspective, the situation is at the same affected by the EU's capacity to effectively address these threats or security challenges (mostly in consensus and strong cooperation with the international community, UN, NATO etc). In turn, this capacity is defined by both (1) the EU's political will (and interests) and (2) the existence of necessary instruments and means to address these threats or security challenges. In both respects, the EU's capacity varies indeed a lot depending on the country (or region) concerned.

Parameters and criteria chosen

The proposed approach for country prioritisation and ranking with respect to EU Security Policy is based on **two main categories**:

(1) EU programmatic orientations and

(2) relevant EU actions.

It has been developed on the basis of information generally drawn from publicly available EU sources. The matrix used (See Annex) containing a number of parameters and relevant criteria can be summarized as follows:

The EU's main programmatic orientations for EU Security Policy with respect to external relations

1) General threats and security challenges

1) Terrorism

2) WMD

3) Regional stability

2) General policy orientations

   a) Preventive engagement

   b) Effective multilateralism

   c) Transatlantic partnership

   d) Other strategic partnerships

Use of existing EU instruments and tools for action in the area of EU Security Policy/external relations

3) CFSP/ESDP

   a) ESDP/EU security missions (military, police)

   b) CFSP/Joint Actions

   c) Presence of EU Special Representatives

   d) CFSP/Common Positions

4) Other external action relevant to security

   a) Common Strategies

   b) Restrictive measures in place against third countries

   c) EU Official Development Assistance (EC and EU Member States).

The assessment of the programmatic orientations under in part 1 is based on the ESS and other important public policy documents established as follow-up to the ESS (such as: WMD Action Plan, EU Strategy for the Wider Middle East etc) and relevant European Council Conclusions and General Affairs and External Relations Council Conclusions. While the main threats and security challenges are clearly identified in part I of the ESS, the parameters used to classify countries according to its general policy orientations may need some explanation.

The proposed matrix follows mainly the strategic objectives as set out in part II of the ESS (addressing the threats through conflict prevention/early action, building security in the Neighbourhood and support to UN/multilateralism). In addition, some elements of part III of the ESS (policy implications for Europe) have been taken into account, namely the transatlantic partnership and other strategic partnerships. Indeed, the EU does define itself as an actor on the international scene willing to address global (or regional) security challenges

not only in accordance with international law, it wants key institutions and regimes of the international system (above all the UN) to be strengthened. At the same time, the EU is more than aware that it must act together with partners in the international arena in order to become effective.

The existence of an UN peacebuilding or peacekeeping mission can therefore be considered as an important parameter for policy orientation and in practice this is often confirmed by relevant UN-EU co-operation or even an EU action or mission in place in the country concerned. The same applies for OSCE missions in the Balkans, the Caucasus and Central Asia (EU Member States already on board by definition) that exemplify already transatlantic partnership and at the same time strategic partnership with Russia.

The assessment of EU action under 2 is based on relevant Council conclusions and also draws from other more specific EU sources and listings (Situation as of December 2005). This part comprises all EU external action relevant to security. Apart from CFSP/ESDP ('second pillar') there are parameters for relevant 'first pillar' (Community) action (restrictive measures, aid) as well as 'cross-pillar' action (Common Strategies).

Strictly speaking, two of the instruments mentioned under 2, i.e. the Common Positions within CFSP and the EU Common Strategies, are also mainly of programmatic nature. However, they are very often directly linked to EU policies and action, for example sanctions (negative measure) or concrete EC programmes in support of the country concerned (positive measure). Therefore, it is proposed to class these instruments with the EU action part.

The EU's Official Development Assistance (ODA) is included on the grounds that aid is generally encouraging stability and underpinning other action in the area of external security. Thereby, it does not only contribute to stability and security, but also becomes an important factor in efforts to encourage security. In addition, it can be assumed that the EU has also an interest to "secure" its own resources spent elsewhere.

Scores, rankings and classifications

The proposed approach is above all guided by the objective of achieving an overall balance between programmatic parameters (7 in total) and EU action related parameters (7 in total). Apart from this, it also aims at maintaining a reasonable proportion within these two main categories, between:

- Threats/security challenges (3 parameters) and General policy orientations (4 parameters) in the programmatic part; and
- CFSP/ESDP (4 parameters) and other external action (3 parameters) in the EU action part.

When fulfilling (or falling into the range of) an individual parameter (programmatic or related to concrete EU action) a point is being attributed for each country. For the scores, a cumulative approach (without specific weighting factor) has been chosen for all parameters (except for the EU ODA, see below).

In practice, this means that countries that fall within the programmatic focus of the ESS and are subject of concrete EU action get cumulative high scores. This score is of course even higher when this country is identified with threats/security challenges, fits with the general policy orientations (all programmatic) and many EU instruments over the whole spectrum are being used.

For the EU ODA, a more complex composite score has been developed in order to include all relevant EU aid (including from Member States). This score combines two individual indicators:

a) EC commitments in 2003 (rated in accordance with four classes established on €/ per habitants of the country concerned), and

b) EU (Community and EU Member States) disbursements over the period during 1999-2002 (rated in accordance with four classes established on EU share of global assistance in favor of the country concerned).

Based on the overall scores (and the resulting ranking), the countries have been classified into four basic categories of importance as follows:

I. VERY HIGH priority (RED: ranking 1-5),

II. HIGH priority (ORANGE: ranking 6-10);

III. MEDIUM priority (YELLOW: ranking 11-15).

IV. LOW priority (GREEN: ranking 16-21)

For illustrative purposes, such classification from LOW to VERY HIGH priority has also been carried out for the following sub-scores:

a) Programmatic orientations;

b) EU action (except ODA);

c) EU ODA.

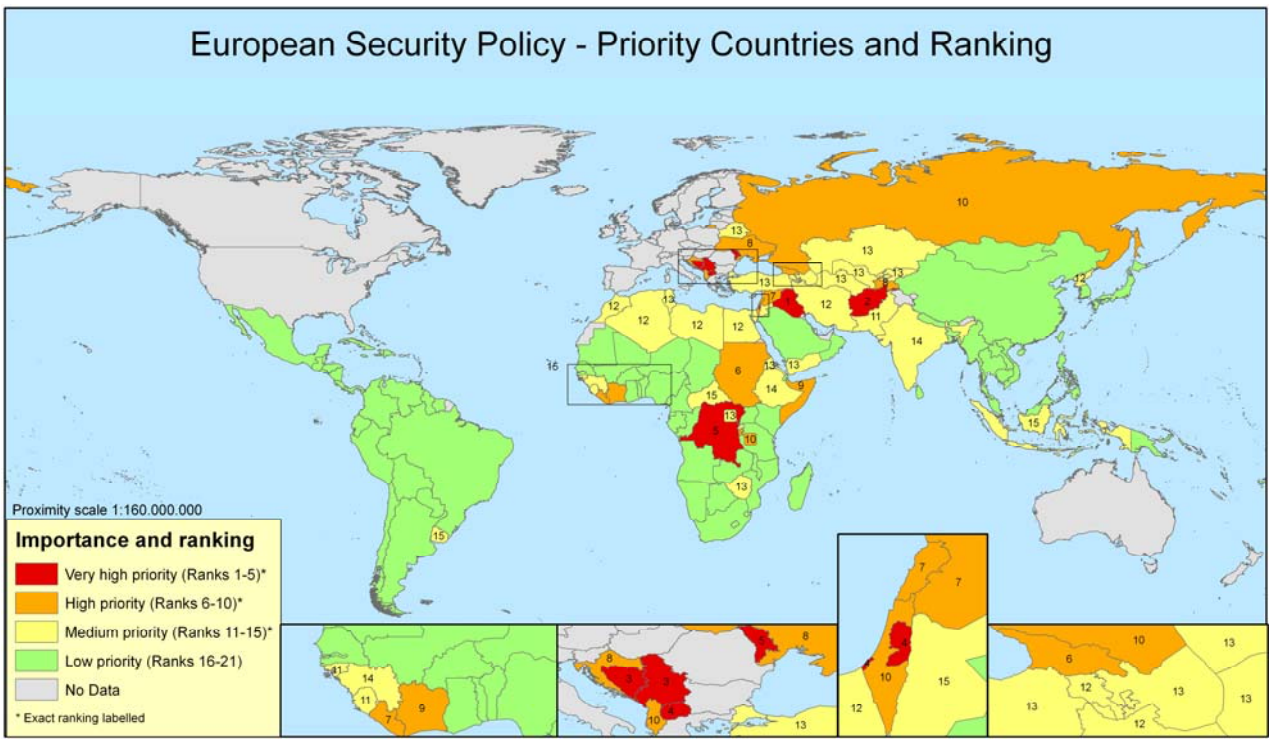

Fig. 1: European Security Policy – Priority Countries and Ranking

A few remarks on the results

The resulting overall scores, rankings and classification according to the proposed model generally confirm geographical priorities of EU security/external policy as set out in the European Security Strategy or main policy documents. The resulting picture may be defined as the (current) areas of particular EU interest:

- The Western Balkans and the European Neighbourhood (almost all countries are classified VERY HIGH to MEDIUM), with extension to several countries of the Wider Middle East and adjacent Asian countries (incl. Afghanistan, Pakistan and several countries of Central Asia),
- Great Lakes Region and some other selected developing countries in Africa and Asia.

It is no surprise that countries of conflict (or post-conflict) such as Iraq, Afghanistan, Serbia and Montenegro/Kosovo or Bosnia and Herzegovina are ranked VERY HIGH or HIGH. This is underpinned by a high level of EU assistance granted precisely to these countries (post-conflict reconstruction).

From a geographical point of view, unsurprisingly Latin America has overall LOW priority for the EU even if development aid reaches sometimes high levels. The priorities of EU security policy in Africa and Asia seem to be selective, most likely dominated by regional instability concerns, resulting in more or less numerous EU action in place.

What is striking is the complementarity between the EU and multilateral actors (UN, OSCE etc). In practice, the EU is almost always present or supporting countries when multilateral action (based on UN Security Council resolutions) is in place. Generally, this concern CFSP and/or ESDP instruments, but very often even the whole range of EU instruments (including aid) is being used.

Development aid visibly supports security policy, but is of course not only directed to post-conflict (or conflict prevention) situations. Countries of serious concern (WMD, terrorism etc) or being subject of restrictive measure get relatively little aid for obvious reasons, while the countries in Africa, the Caribbean and the Pacific (so-called ACP countries) still get relatively important aid. The latter fact does not really affect overall scores and classifications with few exceptions (e.g. Cap Verde).

Earth observation use determination

Albert Nieuwenhuijs* & Bert van den Broek

TNO Defence, Security, Safety, Oude Waalsdorperweg 63, P.O. Box 96864, 2509 JG, The Hague, The Netherlands

* albert.nieuwenhuijs@tno.nl

Introduction

Goal of this paper

This paper will deliver a quick assessment method for the feasibility of earth observation in order to meet the needs in the context of safety and security of companies and institutions interested in the adoption of earth observation services. This method will be based on a classification that will describe possible earth observation information services in such a way that it has meaning and is understandable for both the (potential) customer and the supplier of earth observation information services.

Use of the classification

The reason for having a classification of earth observation information services (hereafter to be briefly called services), is to facilitate a systematic analysis of uses for earth observation. The classification of services contributing to security and stability has several uses. Uses that are foreseen are:

- By categorizing all possible uses for earth observation, the classification contributes to a common language about information within (and possibly outside) the GMOSS community;
- By providing a complete list of all possible contributions of earth observation to security and stability, the classification can be used as a check-list to determine if all possible aspects of a scenario have been covered;
- The classifications of services can be used as a intermediate layer of communication between the user which formulates his requirements for a certain task and the provider, which formulates his possibilities.
- By separating user requirements and provider possibilities, the classification makes a quick determination possible of which needs of the user can be provided for by earth observation and which can't.

Delineation

The classification developed in this paper focuses solely on objects on land or water that can be monitored from space. Objects in the air are left out of consideration in this document.

The classification of services

The classification aims to provide a common base of communication between user and providers of the types of information that are required on the one hand and can be provided at the other. Provision of a certain type of information by earth observation is called an earth

observation information service, or more briefly a service. As such, the classification should define the possible services in terms that can be clearly and univocally interpreted by both parties. This is why the services are defined in non-technical terms. The terms, on the other hand have been defined on such a detail level that a translation to technical requirements is possible. For example, although all possible uses of the frequency spectrum are foreseen, these are not part of the classification as customers can in general not decide on such a technical aspect of their need.

The classification is constructed as a branched structure. It starts with very general aspects of the information service and develops to more specific aspects. In the classification, combinations of features that are impossible (such as moving buildings) are left out. Every line in the structure thus represents exactly one possible service. A graphical representation of (a part of) the classification tree is given in Figure 1.

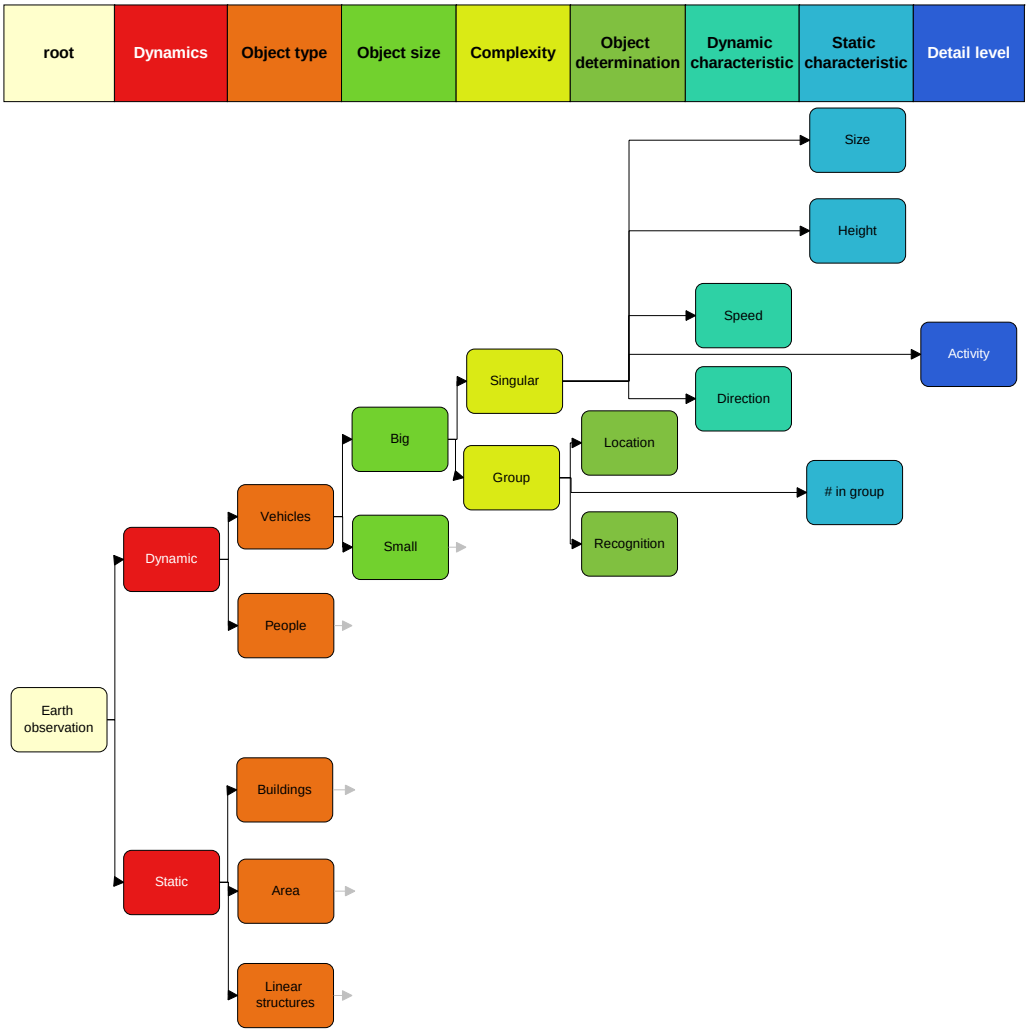

Fig. 1: Illustration of the branched nature of the service classification

In the following paragraph, we will first describe the aspects in which the information is divided, after which each aspect is described in more detail in its own paragraph.

Defined aspects:

The classification uses eight aspects to describe the service. These aspects are divided into four aspects describing the object and four aspects describing the type of information. The four aspect that describe the object are:

- Dynamics;
- Object type;
- Object size;
- Complexity;

The type of information is described in the following four aspects:

- Object determination;
- Dynamic characteristic;
- Static characteristic;
- Detail level;

Each aspect and the options within these aspects (so-called 'strata') are described below.

Dynamics

Defines whether the service concerns observation of static (stationary) or dynamic (moving) objects.

Object type

Defines which type of object is to be observed. Objects are categorized in:

- Vehicles: moving constructions, such as cars, trucks, boats and ships;
- People: moving biological objects, i.e. humans or animals;
- Buildings: stationary constructions with similar length and width (not linear structures), such as bridges, towers, factories, docks, launch pads, landing strips, hangars, etc.;
- Area: ground or water surface;
- Linear structures: stationary structures with a length many times (>100) its with. i.e. (rail)roads, dikes, pipelines, cables, transport infrastructures;

Object size

Differentiates between different sizes of objects. The defined strata depend on the type of object:

- • Vehicles:
    - o 'big' are vehicles bigger than 20 m2 ground surface.
    - o 'small' are all vehicles smaller than or equal to 20m2 ground surface.
- • People: are not differentiated in sizes.
- • Constructions:
    - o 'big' are constructions bigger than 500m2 ground surface.
    - o 'small' are constructions smaller than or equal to 500m2 ground surface.
- • Area:
    - o 'big' are areas bigger than 10km2 ground surface.

  - 'small' are areas smaller than or equal to 10km2 ground surface, but bigger than 100m2 ground surface.
  - 'point' are areas smaller than or equal to 100m2 ground surface.
- • Linear structures:
  - 'big' are structures wider than 5m,
  - 'small' are structures with a width smaller than or equal to 5m.

Complexity

Defines whether observation is to concern either a singular object, or a group of objects.

Object determination

Determines whether an object with certain properties needs to be found (location) or the identity of an known object need to be determined (recognition). An example of 'location' is to look for all buildings within a certain area, an example of 'recognition' would be to identify a certain (known) building as a chemical factory.

Dynamic characteristic

Differentiates between different types of movement information; respectively speed and direction.

Static characteristic

Differentiates between different characteristics to be observed in objects. Defined strata are:

- Count number of objects in group
- Measure size (ground surface) of group
- Measure object height
- Measure object size (ground surface)

Detail level

Determines which aspects of the status of an object is to be determined. Defined strata are:

- Activity (object is in use)
- Construction (object is being built or adapted)
- Damage (object is out of function)
- Cultivation (area is being used for growing plants)

Interpretation

Every line in the tree represents exactly one service. It is very likely that in practice, a request from a customer requires more than one of the services, in combination or as alternatives. In this case, all underlying services should be considered.

Description of the method

The process of matching user needs with the feasibilities of a earth observation provider takes a total of five steps. The first step, numbered ‘step 0’ is common to all analyses and only has to be performed once. Steps 1 to 4 are steps that will have to be repeated in each analysis.

The steps are defined as follows:

step 0. Determine which services are feasible

A team of specialist will determine the measure of feasibility of services under certain generic circumstances. This assessment need not cover every eventuality, as the tool will only be use as a quick scan to eliminate the needs that are without doubt NOT suited to be met by earth observation.

step 1. Determine possible ‘customers’

A possible way to do this is to take a generic list of threats, both natural and man-made (such as the one define in the EU project ‘VITA’) and from that identify parties that are concerned with the threat.

step 2. Determine their needs

Either by an interview or some other quizzing instrument, the needs of these parties that have not yet been fulfilled are surveyed.

step 3. Translation of these needs in required and optional services and their boundary conditions

Using the list of EO services, the combination of required and optional services are composed that will (partially) fulfil the need of the customer. Additional requirements of the services can be specified in the notes, such as: ‘required to work both by night and in daytime’, ‘only usable if scanned more than once per hour’, etc. Also, required combinations are specified in the notes. For example: service A,B and C only useful in combination with service D.

The context of a need of a customer is to be translated as much as possible into the defined services, for example a chemical factory with electricity supply and nearby river will be translated into a service of identifying a large building and locating linear structures.

The need of the customer does not always have to be to gain absolute proof by EO; it can also be enough to augment the already existing base of evidence.

step 4. Compare the results of step 0. and step 3. to assess the feasibility of the customer need.

With the feasibility list and the customer need list, the needs that cannot be met by EO can by crossed off. The remainder of the needs need more investigation to see if Earth observation will deliver a reasonable added value. The defined additional requirements can offer a valuable start for the investigation.

The relationship between the various terms used is illustrated in Figure 2.

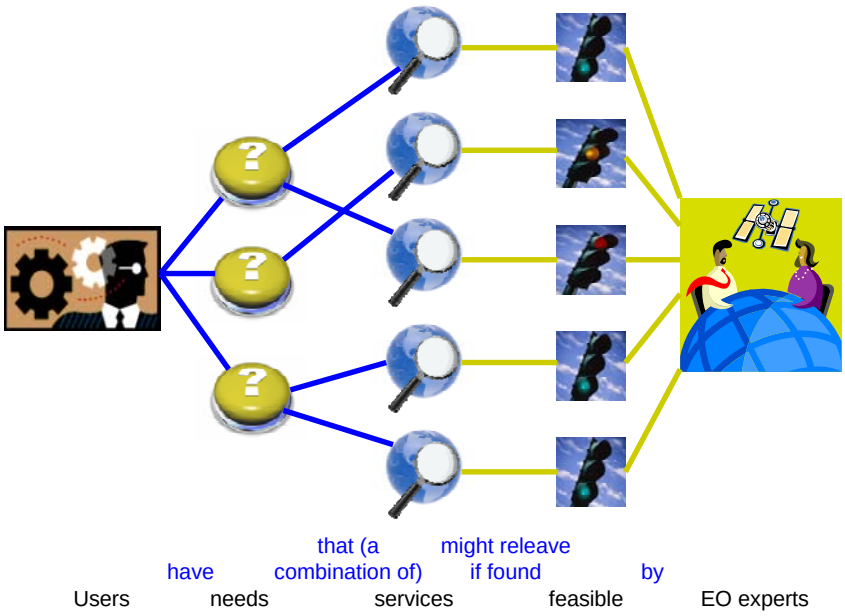

Fig. 2: relationship between users, services and EO experts

Result of the method is an assessment of the feasibility to use earth observation to meet the needs of the concerning user. In general, earth observation will not be the only possibility to meet the needs of the user. Therefore, after completion of the method, the user has to decide the which of his options he will pursue. In case the user decides to contemplate using earth observation, the option should be examined in more detail: because the feasibility assessment done by the team of EO experts is a generic one, the specific requirements of the user should be closer considered.

Application of the method

Introduction

In order to illustrate the application of the method, a fictive case will be used that will be as close to reality as possible. The case has been chosen to closely align with the Iraq Pipeline test case that was developed within GMOSS. Its fictiveness lies mainly in the fact that no actual problem holder could be found. The replies of this problem holder have been simulated as realistically as possible by members of the project that are professionally aware of the needs and problems of the oil sector.

In this chapter the results of every step are presented in its entirety to illustrate the method. The information of step 2 and 3 is therefore repeated in the following steps. Normally, One would only present the information gathered in step 1 and 4 which would contain the information of all steps.

The application of the method is not only meant as illustration for the reader, it was also used for validation of the method for the writers.

Case description

The case is situated in the IRAQ region. The region is highly dependent on oil production, but the instability in the country provides for regular attacks on the oil infrastructure.

The infrastructure owners – The Iraqi government together with several big oil companies – have formed a investigatory commission to investigate what can be done to reduce the risk on

the oil infrastructure with respect to these attacks. One of the angles this commission will consider, is protection by earth observation. In order to determine what earth observation can offer them, they decide to use the use the method presented in this paper.

Step 0: Determine which services are feasible

This step was performed by specialists of TNO. The results can be found in appendix A.

Step 1: determine possible customers

In this case, the investigatory commission will function as the customer.

Step 2: Determine the needs

The needs of the commission were divided into the following categories:

1) Prevention
2) Crisis management
3) Recovery and reconstruction

A brainstorm session was held on each of these categories what could reduce the risk. In this session, little attention was paid to the attainability of the goal by earth observation; this was left for later stages of the method.

Ways of reducing risk that were generated in the brainstorm were:

Prevention

a) Monitoring of public unrest;
b) Find preparatory activities for actions (for example training camps);
c) Public announcement of monitoring, thereby increasing the perceived danger to potential attackers;
d) Monitoring of oil loss through tapping and corruption;
e) Description of perpetrators for the benefit of tracing and neutralizing;
f) Early investigation of attack scene (look for tracks before others can disturb them).

Crisis management

a) Early alerting of incident
b) Time of attack
c) Location information
    i) Accessibility of stricken area by road, air or water. Condition of access roads and bridges, possible landing areas for helicopters, etc.
    ii) availability of resources (like water, sand, people, etc.)
    iii) presence of people, animals and infrastructures that might be threatened.
d) Afflicted area
    i) Dimensions
    ii) Gravity

Recovery/reconstruction

a) Monitoring progress

b) Monitoring for trespassers in area

Step 3: Translation of needs in services

In this step, we express the needs for reaching these goals in terms of earth observation services. In the description we will always specify:

- the conditions under which these services are useful to the cause, for example the frequency required, what features can be provided to be able to locate or recognize an object, what features need to be observed, etcetera;
- the combination of services that is required or helpful to the cause, i.e. specify exactly what you need (also combinations) and what you want, but is optional. For example, specify that if you want to find trucks at a building site, that you need to specify that both services (Buildings – big/small – construction and Vehicles – big – singular – recognition) have to be met at the same time.

Prevention

a) Monitoring of public unrest

People – group - location: see if there are gatherings at places or times that are circumspect.

People – group – recognition / extent of group / # in group: see the shape of the group to see if there is a common centre (for example a speaker), see if the group is concentrated and if the group is big. Religious meetings with a single speaker near (or in) religious objects and a size between 10 and 100 persons have been known to function as recruiting sessions for activists. All aspects have to be met in order to identify a possible hearth of public unrest.

b) Find preparatory activities for actions (for example training camps);

Buildings – small – group – location / recognition / activity: find training camps for activists. They can be recognized by the fact that they are located in remote areas. Campsites or constructed in a relatively short timespan (from 1 day for a small camp to 1 month for an extensive camp). Campsites are accessible by car. Sometimes traces of the use of explosives can be found. Camp buildings are usually hidden or camouflaged. A camp can have a lifespan of 1 month to several years. There will be cooking at the campsite, either in open fire or in a camp kitchen. The camp site will be in the vicinity of water or tanks will be present with regular supply by truck. Location of secluded camp-sites is helpful, but recognition of the specific properties of a training camp would have much more added value.

Area – big – activity: look for explosions that are used to train attacks.

Linear structure – activity: Look for unscheduled activity next to pipelines, for example for reconnoitring for a place to attack.

c) Public announcement of monitoring, thereby increasing the perceived danger to potential attackers;

This does not require any earth observation services; the announcement would be equally effective with or without observation.

d) Monitoring of oil loss through tapping and corruption;

Linear structure – activity: look for illegal tapping of oil at taps meant for inspection and maintenance. This is done with trucks driving to the tapping point and filling up.

Vehicles – singular – recognition: look for oil tankers arriving in the port which do not appear on the official records.

e) Description of perpetrators for the benefit of tracing and neutralizing;

People – recognition – singular: description of the number and appearance of the perpetrators. Characteristics like sex, colour and type of clothing, colour and type of car, used materials, etcetera.

f) Early investigation of attack scene (look for tracks and traces before others can disturb them).

Area – small/point – damage/activity: look for tracks of vehicles and people and changes in the direct surrounding of the incident.

2) Crisis management

a) Early alerting of incident

i. **Linear structures – damage:** look for fires on the pipelines.

ii. **Linear structures – damage:** look for oil spills around the pipelines.

b) Time of attack

Linear structures – damage: record the time the incident took place.

c) Location information

(i) Accessibility of stricken area by road, air or water. Condition of access roads and bridges, possible landing areas for helicopters, etc.

Linear structures – damage: look for the condition of the access roads toward the stricken area.

Area – big – height/cultivation: look for the accessibility of the terrain for service vehicles (treeless patches for helicopter landing and firm, smooth terrain for trucks). Both services are needed at the same time to effectively be used in crisis management.

(ii) Availability of resources (like water, sand, people, etc.)

Area – big – cultivation: give a up-to-date map of the vicinity of the stricken area. Water levels, overgrowth – to indicate where water and sand for extinguishing or dykes can be found – and indications of local townships and other aggregations of people who might be helpful in managing the incident.

(iii)Presence of people, animals and infrastructures that might be threatened.

d) Buildings – big / small – group – location: locate buildings or groups of buildings that might be threatened by the incident. Any of the specified services is helpful in itself.

Area – big – cultivation/height: Generate a detailed geographical report of the immediate surroundings of the incident, in order to predict the way the incident will develop (for instance, farmland, forests, local depressions, hills or waterways or even local wind direction that could shape the development of a fire or an oil spill). Both services are needed at the same time to effectively be used in crisis management.

e) Afflicted area

(i) Dimensions

Area – small – damage: provide quick and accurate information about the stricken area and, if possible about the rate of proliferation.

(ii) Gravity

Area – small – damage: provide quick and accurate information about the damage done within the stricken area.

3) Recovery/reconstruction

a) Monitoring progress

Area – small – damage/activity/cultivation: monitor remaining damage and return of cultivation, for instance to monitor the health of the returning vegetation. Any of the specified services is helpful in itself.

b) Monitoring for trespassers in area

People – singular - location: monitor for trespassing of people into the recovery site, for example for sabotage.

Step 4: Compare needs with feasibility

In this step, we evaluated the feasibility of the required earth observation services for the task. This was sometimes done iteratively; when a service was identified not to be feasible, a review was done if the task could be performed by a set of different or relaxed earth services which might be better feasible.

Prevention

a) Monitoring of public unrest

People – group - location: see if there are gatherings at places or times that are circumspect	Only feasible if both location and time are knows on beforehand due to limitations on revisit time and a required high resolution. Limited feasibility
People – group – recognition / extent of group / # in group: see the shape of the group to see if there is a common centre (for example a speaker), see if the group is concentrated and if the group is big. Religious meetings with a single speaker near (or in) religious objects and a size between 10 and 100 persons have been known to function as recruiting sessions for activists.	Only feasible if both location and time are knows on beforehand due to limitations on revisit time and a required high resolution. If this is true, the shape of the group is recognizable. Feasible (but only when observed)

b) Find preparatory activities for actions (for example training camps);

Buildings – small – group – location / recognition / activity: find training camps for activists. They can be recognized by the fact that they are located in remote areas. Campsites or constructed in a relatively short time span (from 1 day for a small camp to 1 month for an extensive camp). Campsites are accessible by car. Sometimes traces of the use of explosives can be found. Camp buildings are usually hidden or camouflaged. A camp can have a lifespan of 1 month to several years. There will be cooking at the campsite, either in open fire or in a camp kitchen. The camp site will be in the vicinity of water or tanks will be present with regular supply by truck.	If observable from the sky, detection of new training camps might be feasible by change detection. Not all camps shall be detectable however. Limited feasibility.
Area – big – activity: look for explosions that are used to train attacks.	Depend heavily on the visibility of the explosions. Only big explosions often leave visible craters, by using change detection using high resolution data. Limited feasibility.
Linear structure – activity: Look for unscheduled activity next to pipelines, for example for reconnoitring for a place to attack.	Revisit times will be too long, so that monitoring of the actual activity is unlikely. Might be feasible if tracks of illegal activity can be seen. This requires special measures on the ground to ensure visibility of the tracks, or special algorithms not yet developed. Not yet feasible

c) Public announcement of monitoring, thereby increasing the perceived danger to potential attackers;

This does not require any earth observation services; the announcement would be equally effective with or without observation.

d) Monitoring of oil loss through tapping and corruption;

Linear structure – activity: look for illegal tapping of oil at taps meant for inspection and maintenance. This is done with trucks driving to the tapping point and filling up.	Revisit times will be too long, so that monitoring of the actual activity is unlikely. Might be feasible if tracks of illegal activity can be seen. This requires special measures on the ground to ensure visibility of the tracks, or special algorithms not yet developed. Not yet feasible

Vehicles – singular – recognition: look for oil tankers arriving in the port which do not appear on the official records.	Recognition of oil-tanker type ships is feasible. Is feasible, but comparison with official records is not trivial.

e) Description of perpetrators for the benefit of tracing and neutralizing;

People – recognition – singular: description of the number and appearance of the perpetrators. Characteristics like sex, colour and type of clothing, colour and type of car, used materials, etcetera.	Requires resolution higher than can be obtained from space. Also long revisit times are a problem here. Not feasible.

f) Early investigation of attack scene (look for tracks and traces before others can disturb them).

Area – small/point – damage/activity: look for tracks of vehicles and people and changes in the direct surrounding of the incident.	Tracks may be observed. Required effort is limited, but yielded information is limited too. Limited feasibility

Crisis management

a) Early alerting of incident

Linear structures – damage: look for fires on the pipelines.	Feasible by detection of high temperature, even at low resolution. Revisit time should therefore be high however. Feasible.
Linear structures – damage: look for oil spills around the pipelines.	Feasible by detection of oil spills, but only at medium or high resolution. Long revisit times may hinder the observation. Limited feasibility.

b) Time of attack

Linear structures – damage: record the time the incident took place.	If the consequence of incident is a big fire feasible with a time resolution of about 15 minutes. If medium resolution (oil spills) time resolution of about a day. Limited feasibility.

c) Location information

i) Accessibility of stricken area by road, air or water. Condition of access roads and bridges, possible landing areas for helicopters, etc.

Linear structures – damage: look for the condition of the access roads toward the stricken area.	In medium resolution, a revisit time of once a day is possible. Data will be up-to-date until the last day. Feasible.
Area – big – height/cultivation: look for the actual accessibility of the terrain for service vehicles. (treeless patches for helicopter landing and firm, smooth terrain for trucks)	Is feasible with medium resolution multispectral data. Feasible.

ii) Availability of resources (like water, sand, people, etc.)

Area – big – cultivation: give a up-to-date map of the vicinity of the stricken area. Water levels, overgrowth – to indicate where water and sand for extinguishing or dykes can be found – and indications of local townships and other aggregations of people who might be helpful in managing the incident.	Is feasible with medium resolution multispectral data. Feasible with high and medium resolution data. Revisit times are less important here. Feasible.

iii) presence of people, animals and infrastructures that might be threatened.

Buildings – big / small – group – location: locate buildings or groups of buildings that might be threatened by the incident.	Is feasible with medium resolution multispectral data. Feasible with high and medium resolution data. Revisit times are less important here. Feasible.
Area – big – cultivation/height: Generate a detailed geographical report of the immediate surroundings of the incident, in order to predict the way the incident will develop (for instance, farmland, forests, local depressions, hills or waterways or even local wind direction that could shape the development of a fire or an oil spill).	Is feasible with medium resolution multispectral data. Feasible with high and medium resolution data. Revisit times are less important here. Feasible.

d) Afflicted area

i) Dimensions

Area – small – damage: provide	Rate of proliferation or other

quick and accurate information about the stricken area and, if possible about the rate of proliferation.	changes can only be detected between passes. At medium resolution revisit times will be in the order of one day. Feasible.

ii) Gravity

Area – small – damage: provide quick and accurate information about the damage done within the stricken area.	Analysis of the current state as well as change detection with the situation before the incident can deliver relevant information. However, not all damage is easily recognisable by earth observation. Limited feasibility.

Recovery/reconstruction

a) Monitoring progress

Area – small – damage/activity/cultivation: monitor remaining damage and return of cultivation, for instance to monitor the health of the returning vegetation.	Feasible with high and medium resolution multispectral data. Revisit times are less important here. Feasible.

b) Monitoring for trespassers in area

People – singular - location: monitor for trespassing of people into the recovery site, for example for sabotage.	Requires resolution higher than can be obtained from space. Also long revisit times are a problem here. Not feasible.

Summary of results from the analysis

The most interesting applications of earth observation for this case are:

- Early alerting of incidents, related to fires;
- Provision of actual location information, including presence of people, animals and infrastructures in the vicinity;
- Monitoring the progress of recovery.

Depending on the seriousness of the limitations of the services for the application, possible services that could prove useful are in the fields of:

- Monitoring of public unrest;
- Finding prepatory activities for actions;

- Recognition of illegal oil tankers;
- Early investigation of the attack scene and an early estimation of the damage done;
- Early alerting of oil-spill related incidents;

Conclusions on the use of the method

The analysis as illustrated above shows that the methodological approach described in this paper can be used to quickly and systematically identify areas where earth observation can or can't be of interest for safety and security. The method delivers a list of earth observation services that might be feasible and can directly contribute to the needs of the organisation at hand.

The method contributes in two ways:

- It provides a systematic way by which the potential value of earth observation services can be of use, minimising the risk of oversight.
- It provides a quick elimination of potential uses that are theoretically not feasible.

After performing the method, further investigations are needed to determine if the services that are theoretically feasible are also economically and practically advisable.

A Feasibility matrix

A.1 General feasibility properties

In the feasibility matrix below, some restrictions are common to all earth observation services. These concern:

- Revisit time vs. resolution
- Resolution vs. orbit?
- Advantages and disadvantages of optical and radar observation
- Context as feature of objects

Each of these restrictions will be discussed in the paragraphs below.

A.1.1 Revisit time vs. resolution

Spatial resolution and short revisit times (temporal resolution) are in practice complementary and depend on the number of satellites and the resolution in meters. The restriction is mainly due to physical and technical restrictions such as the time needed to scan a swath (width of the scanned path) and the forward speed of the satellite.

The higher the speed, the shorter the revisit time, but also the bigger the distance between adjacent swaths.

In practice, revisit times vary with the resolution as follows:

- Very low resolution (>500m): stationary satellites, not revisit time, rescan time up to once every 15 minutes
- Low resolution (50m – 500m): daily revisit
- Medium resolution (5 – 50 m): daily to weekly revisit
- High resolution (<5 m): weekly revisit

A.1.2 Orbit vs. resolution

The height of the orbit determines the required speed of the satellite in order to keep the orbit and thereby the speed with respect to the ground, which is an important factor in the revisit time. In practice this orbit cannot be much lower than 500 km, as the friction below this height will destabilize lower orbits. As the resolution of a picture is directly dependent on the distance between the object and the sensor , this poses a limit to the resolution of the pictures attainable. For optical pictures this limit is about 1 meter and for radar this is limited to a resolution of about 2 meters.

Another popular orbit is the geo- stationary orbit at an altitude of 35786 km. At this altitude, the satellite rotates around the earth exactly once a day and the position of the satellite with respect to the ground is therefore stationary. At this altitude, the optical resolution is about 1 kilometer.

A.1.3 Advantages and disadvantages of optical and radar observation

Optical observation

- Clouds can obscure the view, thereby frustrating observation

- Atmospheric circumstances (like fog and haziness) can affect the picture, creating differences in otherwise identical observations, which can hamper automatic change detection.
- Optical observation uses more oblique viewing angles. Observation of the same spot from different angels can hamper automatic change detection.
- Optical observation uses ambient (sun)light, which introduces shadows. This can be both an advantage (for example in estimating the height of an object by the length of its shadow) and a disadvantage (shadows can complicate the picture and hamper automatic change detection).
- Optical observation delivers more easily recognizable and thereby more easily interpretable pictures than radar observation.
- The better resolution of optical observation makes height extraction by stereography more feasible.
- Multi-spectral observation, giving information on the property of objects (such as the infra-red spectrum which is a good indication of plantlife), is better feasible optically than by radar.
- Radar observation:
- Radar pictures are more ‘abstract’ and thus more difficult to extract specific objects from.
- Radar offers the possibility to measure Doppler shift, that can be used to measure the speed of objects directly
- Radar interferometry offers the possibility of measuring the height of objects directly (without stereoscopy)

A.1.4 Context as a feature of objects

In the feasibility matrix, context is sometimes mentioned as an enabling factor or condition. Context describes the relation of an object with its surroundings, in order to facilitate the interpretation of that object. To illustrate what is meant by this, some examples are given below:

- A round, high structure can be interpreted differently depending on the surroundings. Such a structure in a built-up area, connected to a cross-shaped building could be interpreted as a church tower. A similar structure in the rural areas with cattle could be interpreted as a food silo.

Church with tower

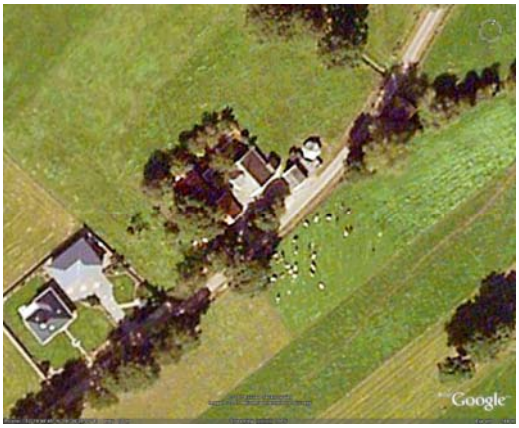

Farm with silo

- The function of an industrial building is usually very hard to interpret. However, an industrial building close to water connected to many electricity wires could be interpreted as a electricity plant.

A2 Specific feasibility properties

In the matrix, numbers between accolades, such as {1}, refer to illustrations in appendix 2.

#	Dynamics	Object type	Object size	Complexity	Determination level	Dynamic characteristic	Static characteristic	Detail	Feasibility
1	Moving	Vehicles	Big	Group	Location				Optical: feasible in high resolution on water or land indifferent of speed.
2	Moving	Vehicles	Big	Group	Recognition				Groups recognizable only by features of the group (for example formation) or context (for example vehicles accompanying a group of refugees)
3	Moving	Vehicles	Big	Group		Direction			On land on a road direction can in high or medium resolution be determined by the side of the road the vehicles are driving. Depending on the underground, sometimes tracks can be seen. Sometimes in high resolution the direction the vehicle is facing is visible. On sea the wake of vehicle can be used to determine direction both optical and by radar. {6}
4	Moving	Vehicles	Big	Group		Speed			Optical speed determination on land can only be done be measuring distance traveled in two

#	Dynamics	Object type	Object size	Complexity	Determination level	Dynamic characteristic	Static characteristic	Detail	Feasibility
									consecutive snapshots. Radar doppler shift can be used to determine the speed (MTI). Radar on water: feasible by detection of shift in wake. {13}
5	Moving	Vehicles	Big	Group			# in group		Is feasible by counting the objects.
6	Moving	Vehicles	Big	Group			extent of group		Is feasible by measuring the group.
7	Moving	Vehicles	Big	Group			Size of object		Is feasible to measure the objects individually. Optical precision up to 1 meter, radar up to 2 meters. {9}
8	Moving	Vehicles	Big	Group				Damage	Not recognizable in general.
10	Moving	Vehicles	Big	Group				Activity	Only feasible by contexts or features.
11	Moving	Vehicles	Big	Singular	Location				Optical: feasible in high resolution on water or land indifferent of speed. Radar on land is feasible with MTI Radar on water: feasible by detection of shift in wake. {13}
12	Moving	Vehicles	Big	Singular	Recognition				Sometime feasible via context or features. For example: red cross on back, truck travelling off-road.
13	Moving	Vehicles	Big	Singular		Direction			On land on a road direction can in high or medium resolution be determined by the side of the road the vehicles are driving. {7} Depending on the underground, sometimes tracks can be seen. Sometimes in high resolution the direction the vehicle is facing is visible. On sea the wake of vehicle can be used to determine direction both optical and by radar. {6}
14	Moving	Vehicles	Big	Singular		Speed			Optical speed determination on land can only be done be measuring distance travelled in two consecutive snapshots.

#	Dynamics	Object type	Object size	Complexity	Determination level	Dynamic characteristic	Static characteristic	Detail	Feasibility
									Radar Doppler shift can be used to determine the speed (MTI). Radar on water: feasible by detection of shift in wake. {13}
15	Moving	Vehicles	Big	Singular			Size of object		Is feasible to measure the objects individually. Optical precision up to 1 meter, radar up to 2 meters. {9}
16	Moving	Vehicles	Big	Singular			Height of object		Optical sometimes possible via shadow, but dependent on circumstances. Optical en radar via stereoscopy (for objects higher than 5 m). {8}
17	Moving	Vehicles	Big	Singular				Damage	Not recognizable in general.
19	Moving	Vehicles	Big	Singular				Activity	Only feasible by contexts or features. For example, activity of a fishing boat can sometimes be determined by the presence of nets behind the boat.
20	Moving	Vehicles	Small	Group	Location				Object size should be at least twice the resolution. Optical, objects up to one meter can be detected, by radar, objects up to two meters can be detected. If a group is concentrated enough, a group of very small objects is sometimes visible. {10}
21	Moving	Vehicles	Small	Group	Recognition				Groups recognizable only by features of the group (for example formation) or context (for example vehicles accompanying a group of refugees)
22	Moving	Vehicles	Small	Group		Direction			On land on a road direction can in high or medium resolution be determined by the side of the road the vehicles are driving. {7} Depending on the underground, sometimes tracks can be seen. On sea sometimes the wake of the vehicles can be used to determine direction both optical and by

#	Dynamics	Object type	Object size	Complexity	Determination level	Dynamic characteristic	Static characteristic	Detail	Feasibility
									radar. {6} In all cases, detection is not easy and depends on circumstances and object features.
23	Moving	Vehicles	Small	Group		Speed			Optical speed determination on land can only be done be measuring distance travelled in two consecutive snapshots. Radar Doppler shift can be used to determine the speed (MTI). In all cases, detection is not easy and depends on circumstances and object features.
24	Moving	Vehicles	Small	Group			# in group		Is sometimes feasible by counting the objects in the group. Otherwise an estimation can sometimes be made from the combination of the extent of the group and its density. {14}
25	Moving	Vehicles	Small	Group			extent of group		Feasible for the visible vehicles.
26	Moving	Vehicles	Small	Group			Size of object		Not feasible
27	Moving	Vehicles	Small	Group				Damage	Not feasible
29	Moving	Vehicles	Small	Group				Activity	Not feasible
30	Moving	Vehicles	Small	Singular	Location				Object size should be at least twice the resolution. Optical, objects up to one meter can be detected, by radar, objects up to two meters can be detected.
31	Moving	Vehicles	Small	Singular	Recognition				Is difficult because of limited number of pixels Recognition only by context or special features.
32	Moving	Vehicles	Small	Singular		Direction			Due to small wake, direction of vehicles on water is hard to determine. Determination of direction of vehicles on land is very hard, but sometimes possible by determining the side of the road they are following {7} or (in

#	Dynamics	Object type	Object size	Complexity	Determination level	Dynamic characteristic	Static characteristic	Detail	Feasibility
									exceptional cases) by identifying tracks.
33	Moving	Vehicles	Small	Singular		Speed			Optical speed determination on land can only be done be measuring distance travelled in two consecutive snapshots.
34	Moving	Vehicles	Small	Singular			Size of object		Feasible, but with optical accuracy of up to one meter and radar accuracy up to two meters.
35	Moving	Vehicles	Small	Singular			Height of object		Not feasible
36	Moving	Vehicles	Small	Singular				Damage	Not feasible
39	Moving	People		Group	Location				If a group is concentrated enough, a group of very small objects is sometimes (under very favourable circumstances) visible. (for example a market) {10}
40	Moving	People		Group	Recognition				Groups recognizable only by features of the group (for example formation) or context. {14}
41	Moving	People		Group		Direction			Optical determination of direction can only be done be measuring distance travelled in two consecutive snapshots.
42	Moving	People		Group		Speed			Optical speed determination can only be done be measuring distance travelled in two consecutive snapshots.
43	Moving	People		Group			# in group		An estimation can sometimes be made from the combination of the extent of the group and its density. {14}
44	Moving	People		Group			extent of group		Feasible, as far as the group is clearly determinable. {14}
45	Moving	People		Group				Damage	Not feasible
46	Moving	People		Group				Activity	Only via context (for example the results of the activity)
47	Moving	People		Singular	Location				Not possible

#	Dynamics	Object type	Object size	Complexity	Determination level	Dynamic characteristic	Static characteristic	Detail	Feasibility
48	Moving	People		Singular	Recognition				Not possible
49	Moving	People		Singular		Direction			Not possible
50	Moving	People		Singular		Speed			Not possible
51	Moving	People		Singular				Damage	Not possible
52	Moving	People		Singular				Activity	Only via context (for example the results of the activity)
67	Static	Buildings	Big	Group	Location				Feasible both optical and by radar in high or medium resolution
68	Static	Buildings	Big	Group	Recognition				Feasible by specific features (for example silo's) or context (for example supply by trucks) in high or medium resolution
69	Static	Buildings	Big	Group			# in group		Feasible by counting in high or medium resolution
70	Static	Buildings	Big	Group			extent of group		Feasible by measurement in high or medium resolution
71	Static	Buildings	Big	Group			Size of object		Feasible in high or medium resolution
72	Static	Buildings	Big	Group				Damage	Feasible in high optical resolution, depending on sort and location of damage. With radar difficult, due to difficult interpretation of radar image. In specific cases, radar can be very useful. {12}
73	Static	Buildings	Big	Group				Construction	Feasible in high or medium optical resolution. Radar more difficult due to interpretation of radar image. In all cases, context needs to be present (for example building trucks supplying building materials) {5}
74	Static	Buildings	Big	Group				Activity	Feasible in high resolution via context (for example use of parking space, supply of goods, smoke from chimney). {4}
75	Static	Buildings	Big	Singular	Location				Feasible both in high and medium resolution

#	Dynamics	Object type	Object size	Complexity	Determination level	Dynamic characteristic	Static characteristic	Detail	Feasibility
76	Static	Buildings	Big	Singular	Recognition				Feasible based on specific features both in medium and high resolution
77	Static	Buildings	Big	Singular			Size of object		Feasible in high and medium resolution
78	Static	Buildings	Big	Singular			Height of object		Feasible with stereoscopy in high resolution
79	Static	Buildings	Big	Singular				Damage	Depending on sort and location of the damage feasible in high resolution. Example of bad recognizable damage is a vertically collapsed building after an earthquake.
80	Static	Buildings	Big	Singular				Construction	Feasible in high optical resolution. Radar more difficult due to interpretation of radar image. In all cases, context needs to be present (for example building trucks supplying building materials) {5}
81	Static	Buildings	Big	Singular				Activity	Feasible in high resolution via context (for example use of parking space, supply of goods, smoke from chimney). {4}
82	Static	Buildings	Small	Group	Location				Feasible in high resolution
83	Static	Buildings	Small	Group	Recognition				Feasible by specific features (for example layout) or context (for example location within a residential area) in high or medium resolution. Recognition in radar pictures is sometimes difficult. {11}
84	Static	Buildings	Small	Group			# in group		Feasible by counting in high resolution
85	Static	Buildings	Small	Group			extent of group		Feasible by measuring in high or medium resolution
86	Static	Buildings	Small	Group			Size of object		Feasible in high resolution
87	Static	Buildings	Small	Group				Damage	Seldom feasible. Depends on extent and location of the damage.
88	Static	Buildings	Small	Group				Construction	Feasible in high optical resolution. Radar more difficult due to interpretation of radar image.

#	Dynamics	Object type	Object size	Complexity	Determination level	Dynamic characteristic	Static characteristic	Detail	Feasibility
									In all cases, context needs to be present (for example building trucks supplying building materials) {5}
89	Static	Buildings	Small	Group				Activity	Sometimes feasible in high resolution via context (for example use of parking space, supply of goods, smoke from chimney). {4}
90	Static	Buildings	Small	Singular	Location				Feasible in high resolution. Recognition in radar pictures is sometimes difficult. {11}
91	Static	Buildings	Small	Singular	Recognition				Sometimes feasible based on features and context.
92	Static	Buildings	Small	Singular			Size of object		Feasible in high resolution
93	Static	Buildings	Small	Singular			Height of object		Feasible in optimal conditions in high resolution , accuracy up to 2 meters
94	Static	Buildings	Small	Singular				Damage	Seldom feasible
95	Static	Buildings	Small	Singular				Construction	Sometimes feasible on basis of context.
96	Static	Buildings	Small	Singular				Activity	Sometimes feasible on basis of context.
97	Static	Area	Big		Location				Feasible in low, medium or high resolution.
98	Static	Area	Big		Recognition				Usually feasible based on spectrum analysis in medium or high resolution or texture in high resolution {3}
99	Static	Area	Big				Size of object		Feasible in low, medium or high resolution
100	Static	Area	Big				Height of object		Changes in height can be done by stereography in medium or high resolution or (with radar only) by inteferometry. A global elevation model is obtained through the SRTM mission.
101	Static	Area	Big					Damage	Feasible by comparing two snapshots, or sometimes by inference of features.
102	Static	Area	Big					Construction	Feasible in medium or high resolution by

#	Dynamics	Object type	Object size	Complexity	Determination level	Dynamic characteristic	Static characteristic	Detail	Feasibility
									inference of features.
103	Static	Area	Big					Activity	Often feasible by specific features.
104	Static	Area	Big					Cultivation	By multi-spectral or polarimetric measurements often feasible. {3}
105	Static	Area	Small		Location				Feasible in medium or high resolution.
106	Static	Area	Small		Recognition				Usually feasible based on spectrum analysis in medium or high resolution or texture in high resolution. {3}
107	Static	Area	Small				Size of object		Feasible in medium or high resolution.
108	Static	Area	Small				Height of object		Changes in height can be done by stereography in medium or high resolution or (with radar only) by inteferometry. A global elevation model is obtained through the SRTM mission.
109	Static	Area	Small					Damage	Feasible by comparing two snapshots, or sometimes by inference of features.
110	Static	Area	Small					Construction	Sometimes feasible in medium or high resolution by inference of features. For small area more difficult.
111	Static	Area	Small					Activity	Often feasible by specific features.
112	Static	Area	Small					Cultivation	By multi-spectral or polarimetric measurements often feasible. {3}
113	Static	Area	Point		Location				Feasible in medium or high resolution. {2}
114	Static	Area	Point		Recognition				Usually feasible based on spectrum analysis in medium or high resolution or texture in high resolution. {2}
115	Static	Area	Point				Size of object		Feasible at high resolution. Accuracy will be limited due to relative small dimensions of object. {2}
116	Static	Area	Point				Height of object		Changes in height can be done by stereography in medium or high resolution or (with

#	Dynamics	Object type	Object size	Complexity	Determination level	Dynamic characteristic	Static characteristic	Detail	Feasibility
									radar only) by inteferometry. Height of all locations is recorded via SRTM project.
117	Static	Area	Point					Damage	Only when damage is extensive enough and visible. {15}
118	Static	Area	Point					Construction	Sometimes feasible in high resolution by inference of features.
119	Static	Area	Point					Activity	Sometimes feasible in high resolution by inference of features.
120	Static	Area	Point					Cultivation	Only general conclusions like difference between covering or pavement.
121	Static	Linear structure			Location				Feasible at high resolution.
122	Static	Linear structure			Recognition				Sometimes feasible based on features and context.
123	Static	Linear structure					Size of object		Feasible at high resolution. Accuracy will be limited due to relative small width of object.
124	Static	Linear structure						Damage	Feasible if dimensions of damage big enough, otherwise possibly by effects of damage if of sizable proportions. {15}
125	Static	Linear structure						Construction	Detection of construction of roads and pipelines is often feasible due to the greater dimensions of the work in comparison to the linear structure. {1}
126	Static	Linear structure						Activity	Often feasible in high resolution by features or context.

GMOSS Test Cases

Klaus Granica[1], Stefan Lang[2], Peter Zeil[2], Bert van den Broek[3], Irmgard Niemeyer[4], Bhavini Rama[5*]

[1] *Joanneum Research, Graz, Austria*

[2] *Z_GIS - Centre for Geoinformatics, Salzburg, Austria*

[3] *The Netherlands Organisation for Applied Scientific Research (TNO),The Hague, Netherlands*

[4] *Freiberg University of Mining and Technology, Germany*

[5] *King's College London, UK*

* bhavini.rama@kcl.ac.uk

1. Introduction

The purpose of the test cases that were carried out within the framework of the GMOSS project was to provide a real-life context within which to place the technical applications that have been developed. Furthermore, the test cases assisted in coordinating the studies carried out by the GMOSS partners. The selected test case countries were: Kashmir, Zimbabwe, Iraq, and Iran.

Kashmir was selected as a test bed for the installation, completion and exercising of the GMOSS expertise in the field of remote sensing and crisis management. After the strong earthquake that occurred in Pakistan on 8th October 2005, the partners decided to work on this application case. Zimbabwe was chosen in order to demonstrate the importance of a crisis-alert system with a focus on monitoring humanitarian crisis situations and providing evidence for human rights violations. In addition to overall damage assessment, remote sensing capabilities can – and should be – used to monitor progress made on reconstruction efforts and the effectiveness of humanitarian support. The test case on Iraq was chosen in order to demonstrate the use of remote sensing for the monitoring and analysis of pipeline attacks (thus affecting the country's economy) and the unstable situation in Baghdad. Finally, the test case on the Iran investigated whether satellite imagery analysis could give indications on the civil or military purposes of the Iranian nuclear programme. Different pre-processing, change detection, classification and visualisation techniques were applied to radar, multispectral, hyperspectral satellite imagery in order to monitor the development of some relevant sites: Arak, Bushehr, Esfahan, Natanz and Saghand.

The aim of this paper is to provide a description of the image analysis techniques developed and utilised in order to secure data for each of the countries. The paper is divided on a country-by-country basis. Remote sensing techniques can be applied to a number of scenarios in a complementary and synergistic manner. Of course, it must be noted that imagery only reveals what has changed, but cannot account for the reasons behind what caused these changes. Therefore, evidence drawn from image information in security-related issues should not be treated in an isolated manner but coupled with local expertise and knowledge in order to provide accurate awareness of the overall situation in a particular region and/or country.

2. Kashmir

Kashmir is a highly interesting region for a number of security-related reasons; this is not only from the point of view of natural disasters but also in regards to other topics such as terrorism, nuclear proliferation, treaty monitoring and border monitoring. The hazard of earthquakes has a long history along the rim of the Himalayas and is directly related to the tectonic movement of the Indian subcontinent. For the geologists it is a well-known region and it is evident that earthquakes will accompany the inhabitants of this region in the future.

The Charter on Disaster Management was automatically triggered in response to the occurrence of the 8th October 2005 earthquake. As a result of this activation, DLR, ITUK, JRC, Map Action, SERTIT, and UNOSAT immediately initiated their production of 'value-adding' satellite image maps of the identified damaged region (see Figure 1). A series of different satellites from medium to very high resolution data were used, including: Ikonos, QuickBird, SPOT 4, SPOT 5, Radarsat, Landsat TM, ASTER, and SRTM.

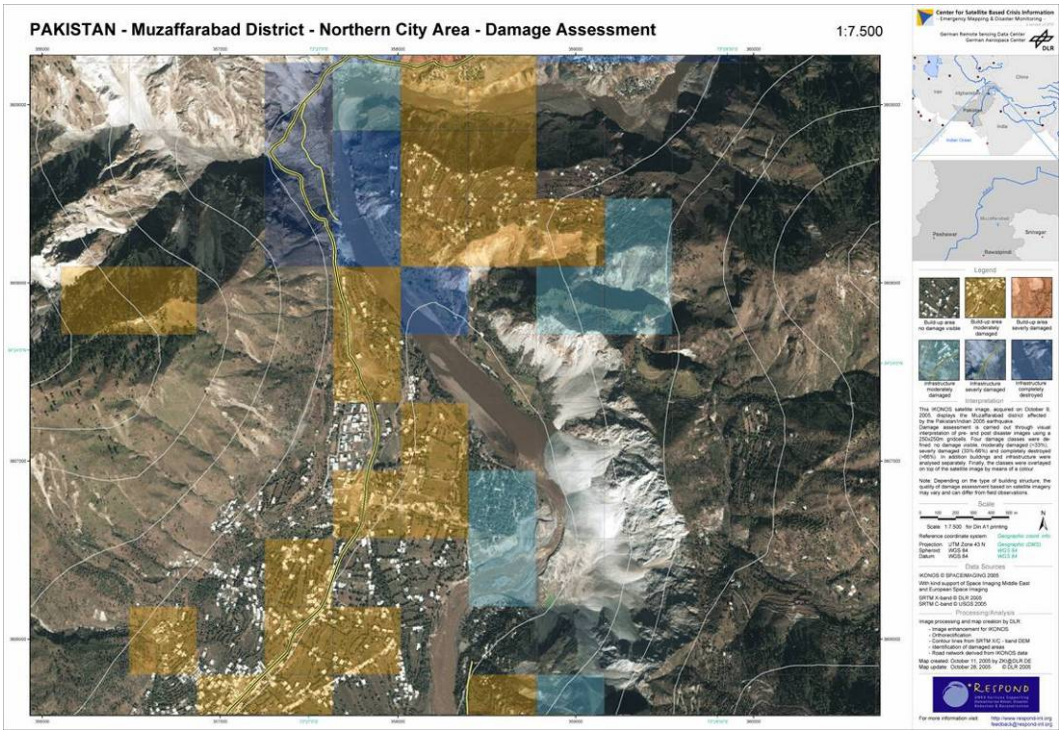

Fig. 1: Example of a damage map from the Muzaffarabad district.

The first overview map was delivered to the international humanitarian aid community on 9th October 2005. On 11th October the DLR provided the first very high-resolution (VHR) (1m) satellite maps of the destroyed areas. The users of these products included: UN OCHA, UNDAC, IFRC, the Pakistani authorities, national and international relief agencies and the UN donor conference.

- In the aftermath of the rescue phase the GMOSS partners were able to provide more information on the following topics:
- Installation of a **WebServer**
- **Landcover classification** using spaceborne imagery

- Generation of **High Resolution DSMs** from spaceborne imagery
- **Automatic detection of changes** on medium spatial resolution satellite images
- **Identification of damaged zones** in urban areas from nighttime imagery
- **Assessment of damaged areas** (infrastructure, houses, etc.)
- **Finding of new areas** for relocation of the affected population
- **3D** approach for modelling & change detection
- **Monitoring border** region

Although it was possible to deliver the products via e-mail or on public websites, some actors were not able to download the products due to the lack of an Internet connection, and some were not even aware of the existence of the service. Furthermore, as a result of the political sensitivity linked to the disaster region, publishing of the products via public web pages was delayed for several days. Despite this, the feedback was very positive regarding the level of quality and the thematic content of all products. The fast availability of the overview maps was very useful for planning and highly appreciated as the users stressed the importance of timely delivery of post-disaster information.

2.1 Methodologies

As the Kashmir region is located in a highly mountainous region characterised by steep terrain, it was necessary to perform accurate pre-processing of the satellite images in order to generate detailed Digital Elevation Models (DEM) and perform accurate geo-coding and geo-referencing. Due to the large expanse of area to be covered, a two-fold strategy was developed using a combination of medium-sized (Figure 2) and very high resolution (VHR) DEMs (Figure 3). The VHR DEMs had a smaller coverage (i.e. 250km^2), compared to the larger but less detailed coverage of 3600km^2, therefore these were used for more detailed analysis of selected hotspots in urban areas, during the damage interpretation. Joanneum has developed a new method using three SPOT images for deriving DEMs with higher accuracy.

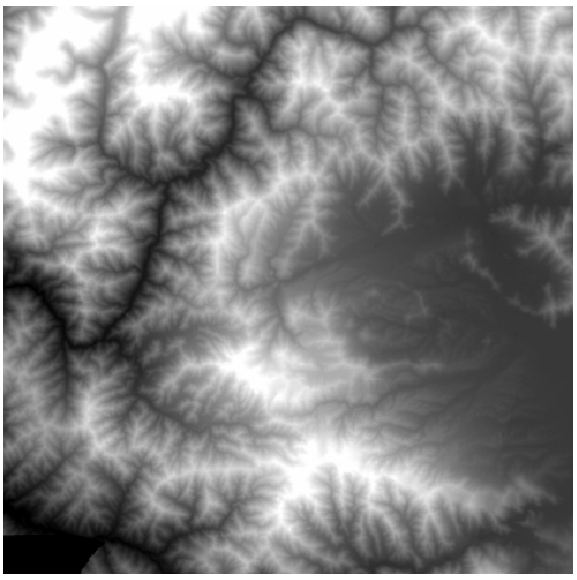

Fig. 2: Overview of the DEM from SPOT5 imagery having 5 m resolution and 60 km x 60 km coverage.

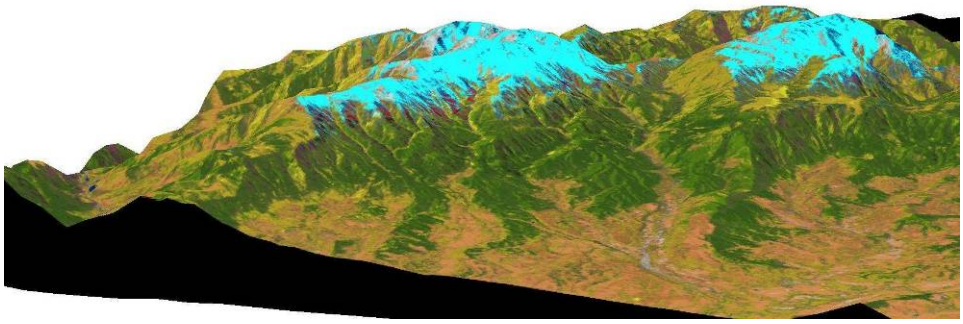

Fig. 3: DEM from IKONOS imagery having 1 m resolution.

After an earthquake, one of the most urgent information needs is to know the distribution of the population within the affected region. The 8th October 2005 earthquake resulted in a high death toll, massive destruction of electricity and infrastructure in the regions surrounding Muzzafarabad, Manshera and Abottabad; and a significant number of internally displaced persons (IDPs). In order to survive, the IDPs would have had to light fires (to keep warm) as well as look for nutrition. Therefore, in this context the use of a specific type of satellite imagery, namely OLS – DMSP, night-time images were used to derive indicators on the location of the survivors. The *European Union Satellite Centre (EUSC)* proved that these types of images demonstrate the appearance of new lights from bonfires and the disappearance of regular lights, as a result of destroyed electricity in urban areas.

For the proper use of this type of data it was a prerequisite to perform an exact matching and registration. The DMSP satellite delivers wide orbit strips which do not match from one to other. Therefore, the image mosaics of more than one rectified OLS images and the quality of rectification is different between the two time epochs, but also within the images of one epoch. Based on these findings a correction has been applied on the OLS-DMSP (by Joanneum) improving the rectification quality and consequently some false signals could be removed.

It is relatively simple to extract, by visual interpretation, changes that have occurred in an affected area when using expensive high spatial resolution images (like QuickBird, IKONOS, SPOT, etc). Therefore, an important approach that was developed within the network is the automatic detection of changes on medium spatial resolution satellite images. This new automated method, will estimate changes by exploiting lower cost and coarse spatial resolution satellite images like, for example, the ASTER sensor images (15 m resolution).

Disastrous events such as earthquakes, wars, tsunamis (etc) cause change in the order and regularity of the affected areas. Therefore, it is possible to detect such changes using a technique called textural analysis (developed by CRPSM). This technique was applied to two ASTER images (15m resolution) of Muzaffarabad, before and after the earthquake (Figure 4 and 5).

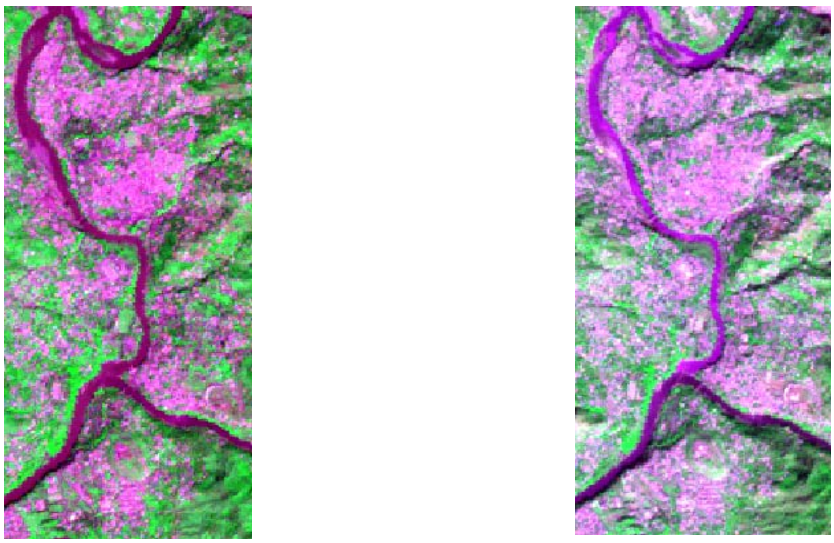

Fig. 4: Muzaffarabad City before (left, 09/09/05) and after (right, 10/18/05) earthquake.

It is highly likely that the same sections of each image (before and after) with higher differences possibly correspond to areas strongly affected by the earthquake. Since an area wider than the zone corresponding to the city has been considered, we introduce a parameter, called *Urbanization Index*, which can be used to emphasize changes that have occurred in the urban areas, thus avoiding other types of changes such as the changes in vegetation due to season (images have more than 1 month's temporal difference).

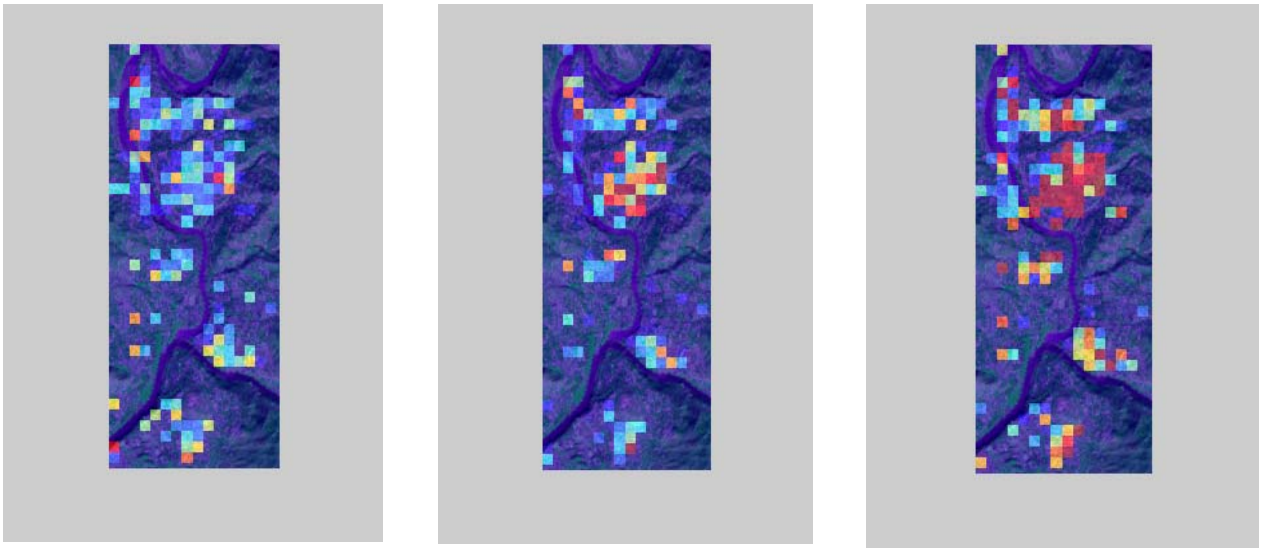

Fig. 5: Results of the Texture Analysis applied to the images and superimposed on the original image.

SPOT5 panchromatic imagery provided an excellent means of identifying relevant indicators for feature recognition within the border regions. Roads, settlements, buildings, power stations, and other infrastructure features can easily be recognized (see Figure 6). The destruction after the earthquake can also be observed easily in the post-disaster image.

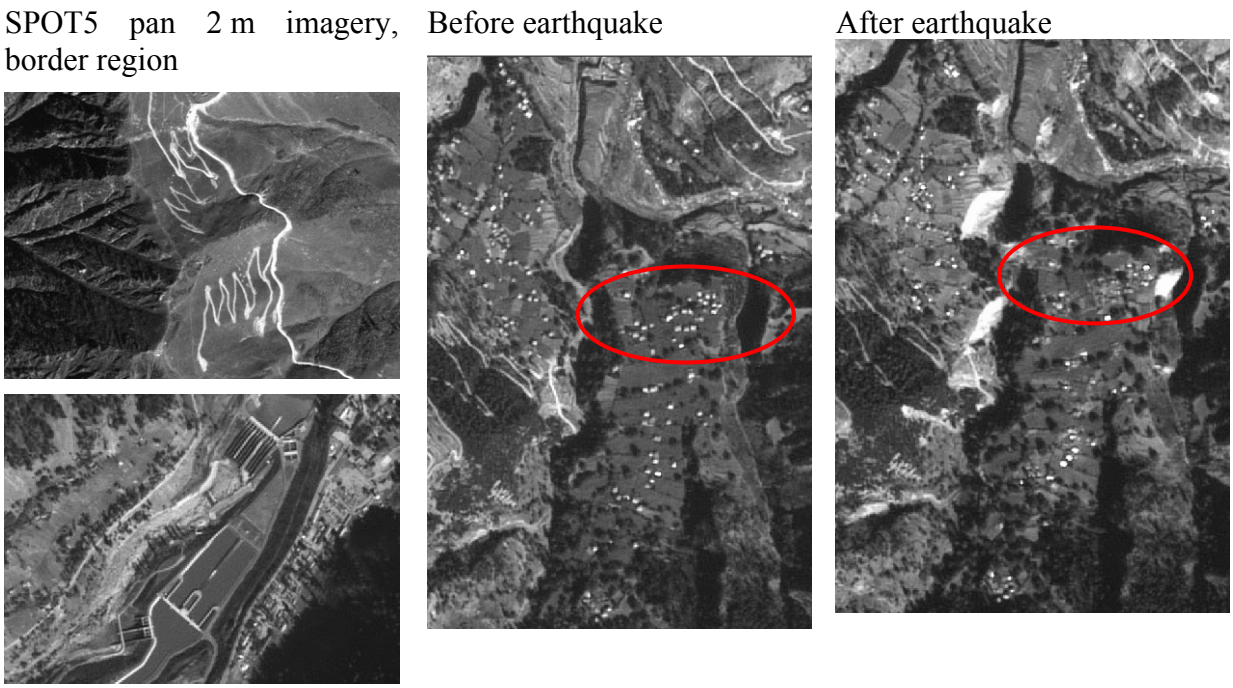

Fig. 6: Examples from SPOT5 Pan imagery showing roads network and power station (left), houses before (middle) and destroyed houses and landslides after the Earthquake (right).

2.2 Conclusions

After a disaster, it is important that the relief units and disaster management teams have comprehensive and accurate information delivered to them as quickly as possible. In order to satisfy these requirements the development of automized or semi-automized tools were seen as a priority focus for the GMOSS partners. Within the lifetime of the Network the processing chain proved, that it is possible to derive decisive information from remote sensing images. The use of DEMs in a mountainous terrain is mandatory for getting precise data, and it was shown that using new methods it is possible to obtain high quality DEMs from space borne imagery (Figure 7).

Finally, it is important to note that in order to carry out an accurate assessment, it is necessary to define which features or indicators need to be derived and to what extent. This definition influences the decision of which type of space borne data will ultimately be used. Data availability is not always given, thus the methods have to be flexible and comprehensive in order to obtain the appropriate information on the affected area.

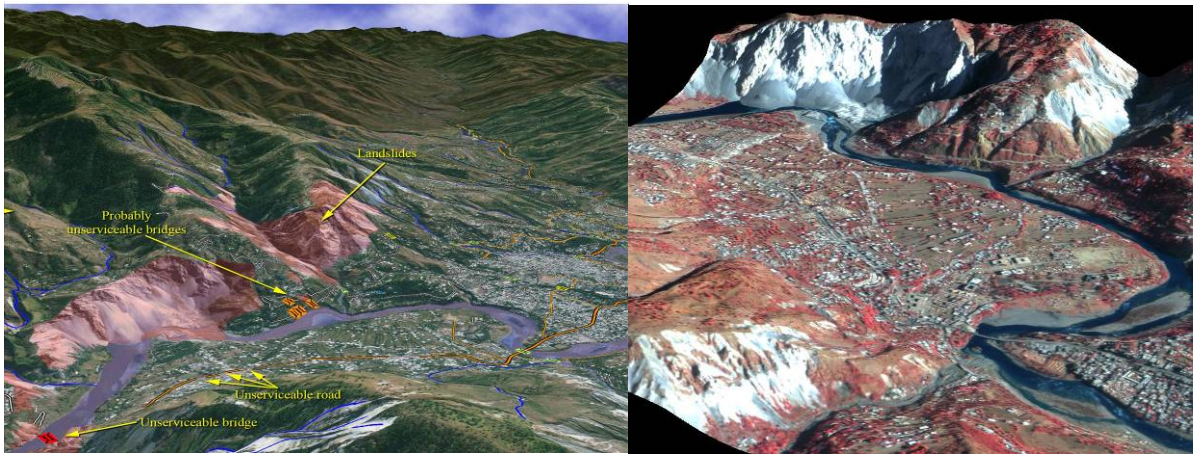

Fig. 7: 3D views from space borne imagery in Muzzafarabad after the Earthquake.

3 Zimbabwe

Geographically, Zimbabwe is a landlocked country. Surrounded by the countries of Mozambique, South Africa, Botswana and Zambia it is enclosed to the North by the Zambezi River, to the South by the Limpopo river and to the East by the Eastern Highlands.

Zimbabwe's major industries were agriculture, mining, manufacturing and tourism, at least before destabilization. The deterioration of the overall situation in Zimbabwe, as indicated by the large numbers of emigrants and an increasing number of internally displaced persons (IDPs), which are reflected by the collapse of investments, the souring inflation, and the economic decline in general, is of increasing international concern. However, the ongoing political instability in Zimbabwe is a slow-onset protracting crisis, in which a critical peak or 'outbreak' can hardly be identified. Whereas the severity of the ongoing crisis is widely acknowledged (Zimbabwe ranks as number 6 in the 'Failed state Index'), response from external actors or aid and relief organizations is hardly triggered. A crisis-alert system for monitoring humanitarian crisis situations and providing evidence for human rights violations relies on EO-based information as a ubiquitous, direct and unfiltered source of information. In order to observe and assess crisis situations, EO data – together with eyewitness accounts, reports or other means of communication – may support the international community in collecting evidence for the implications of the fast-track land transformation process or the effects of 'cleaning' operations carried out by the government.

3.1 Land use / land cover change

By means of medium-resolution satellite imagery, indicators were investigated for monitoring the stability of livelihoods in rural areas and land-use changes with respect to agricultural activity, water availability, patterns of subsistence farming (Figure 8). Besides altering natural conditions with changing precipitation patterns in the rainy season that lead to regional droughts, the following reasons account for the ongoing changes in land use and land cover patterns: (1) political conditions embracing the failures in land use policy and the fast-track land reform; (2) socio-economical conditions including the lack of money and expertise to properly use irrigation systems, an increasing pressure on land, the segregation of rural population and the prevalence of HIV/AIDS.

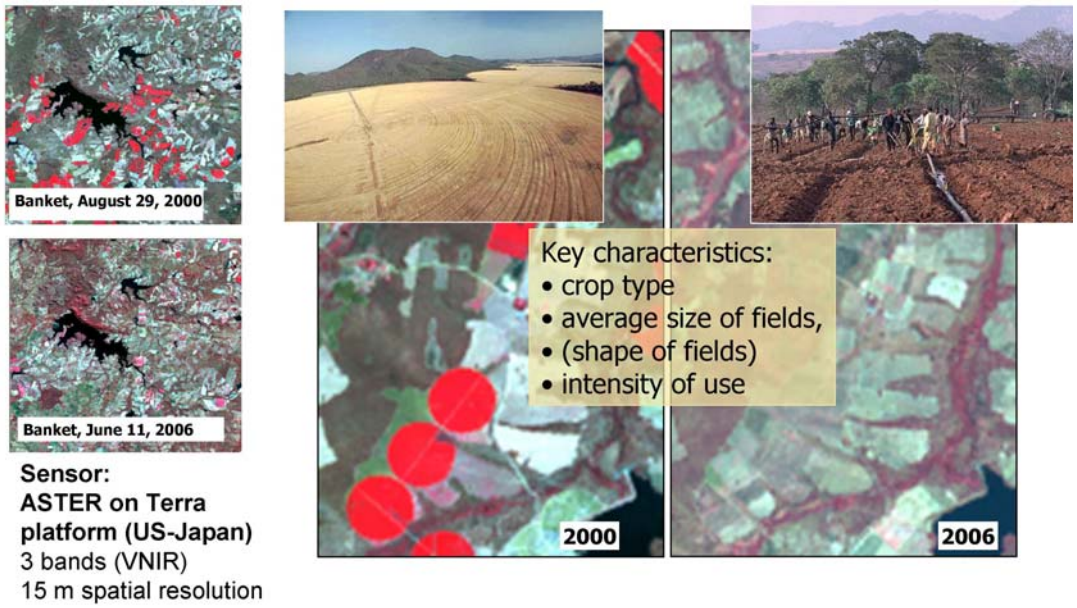

Fig. 8: Formerly pivot-irrigated agricultural fields lay fallow as shown on two ASTER scenes from 2000 and 2006 from Banket, a town located about 95 km north-west of Harare in the province of. Mashonaland West. This example shows Zimbabwe's change in land use from intensive agricultural use (cotton, maize, tobacco, sugar, wheat) to smaller homesteads and subsistence farming, as triggered by the fast-track land reform program.

Land has been a source of conflict in Zimbabwe since colonial times. The redistribution of land by means of resettlement has been carried out since the 1990's on a willing-seller/willing-buyer basis. The political dimension of the land issue figured in the foreground when, in 2000, the government came under pressure from former combatants ('freedom fighters') which requested delivery on promises made at independence. A fast-track version was initiated which was characterised by chaos, violence and land invasions. The uncertainties created badly hit the commercial farming sector, jeopardised investors' confidence and subsequently caused the loss of 400000 jobs in the farming and tourist industry.

3.2 Disaggregating population figures in rural areas

Land cover information has also been used together with other spatial information to disaggregate census-based population figures, which – when being reported on enumeration units – are too coarse for detailed studies of population dynamics, especially in rural areas. Disaggregating population figures was done in an area in the centre of the country including the capital Harare accounting for approximately 25% of the overall Zimbabwean population (Figure 9). The resulting map shows the estimated population densities in a resolution appropriate for activities at district level (Schneiderbauer and Ehrlich, 2005).

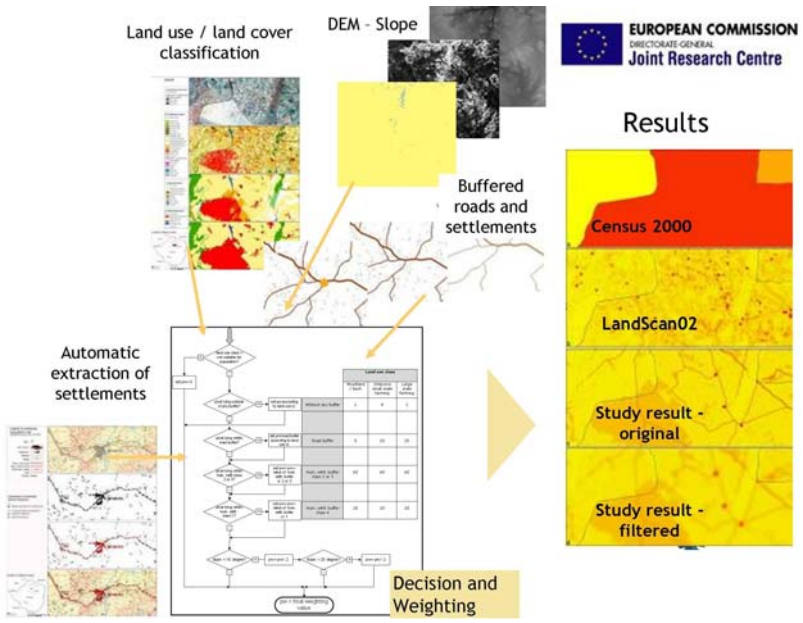

Fig. 9: Disaggregating population figures utilizing auxiliary geo-information, modelled according to terrain, proximity to roads, etc. (see text for further explanation).

3.3 Assessment of damage / deconstruction and reconstruction

The availability of very high spatial resolution (VHSR) remote sensing data offers the opportunity to produce accurate assessments of the spatial extent of damages and estimates about numbers of affected people. The combined use of VHSR imagery with other information layers requires rigorous preprocessing procedures to be applied to the data. For the area of the city of Harare three Quickbird (QB) scenes (25.08.2004, 22.06.2005 and 02.08.2005) were geometrically processed (Figure 10).

Fig. 10: Methods applied for data pre-processing of high resolution optical satellite imagery (here: QuickBird).

From situation awareness to policy-relevant products – a general workflow for providing conditioned information for security scenarios has been outlined by Lang et al., 2006. It foresees transformation of complex imaged scenarios into policy-relevant information, being itself embraced by the decision support chain. Starting from situation analysis and needs assessment it provides targeted information, conditioned for decision support. Within GMOSS we have developed and tested integrated GIS/RS methods for (1) indicating changes and quantifying them and (2) extracting and analyzing damaged structures during operation Murambatsvina (see Figure 11). A similar approach is used to monitor progress/failure of the agreement (announced by the Government in June 2005) to resettle the internally displaced in suburban areas.

Fig. 11: Comparison of two time slices (2004 and 2005) of QuickBird imagery showing demolitions in the townships of Mbare (left) and Glen Norah (right) during operation Murambatsvina (see text for more information).

Operation *Murambatsvina*, also known as *Operation Restore Order*, was a countrywide operation, carried out by the Zimbabwean Government, of forced mass evictions, the demolition of homes and informal trading stores (Schöpfer et al., 2007). The United Nations (UN) has estimated that in six weeks between May and July 2005, 700,000 people across Zimbabwe lost their homes and their livelihoods as a consequence of Operation *Murambatsvina*. In some areas entire settlements were razed to the ground. While the demolitions took place right across the country, the majority of the destruction occurred in high-density urban areas in Harare, Chitungwiza, Bulawayo, Mutare, Kariba and Victoria Falls. Zimbabwe stands not alone for forced demolitions of homes in informal settlements and acting on informal sector operators as such actions are also occurring in other parts of Africa and elsewhere in the world.

Different methods and algorithms for change indication have been applied (based on both optical and SAR data). The following illustration (Figure 12) shows respective results. These approaches of change indication approach saves time as the classification procedure can be reproduced by any user to check the images for damaged areas prior to intensive change detection analysis. Only in a second step, may focus on the indicated affected areas, which are otherwise hardly to be found. Within a focused area, the number of structures or affected houses or the density of buildings can be further analyzed. The usability and reusability of rule sets enhance the efficiency of image analysis and contribute to efficient and constant monitoring.

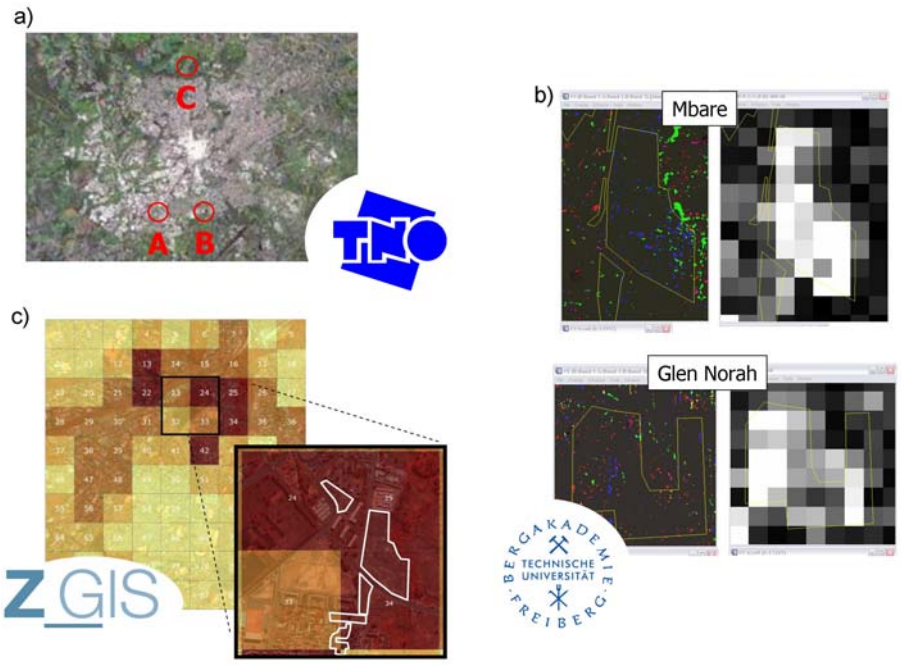

Fig. 12: Different methods for change indication with respect to damages and/or reconstruction. a) multitemporal color-composit based on ASAR data (2005 and 2006); b) MAD change detection algorithm applied to VHSR optical satellite data (2004 and 2005); c) change indication based on object-based image analysis on VHSR optical satellite data (2004 and 2005) (aggregated to 500 * 500 m cells)

Via the visual detection of shacks in Mbare and Glen Norah (see Figure 13), it was possible to differentiate between small huts (covering a minimum area of 4m²) and larger, more stable houses with mostly a walled fundament. By visual interpretation we were able to identify 99 units. Therefore, when considering an average number of 8 to 10 people per unit, 116 extracted buildings would account for about 1000 to 1200 people.

Fig. 13: Visual detection and automated extraction of dwelling units in Mbare and Glen Norah.

When *Murambatsvina* was still going on, the Zimbabwean Government officially launched a reconstruction effort, called Operation *Garikayi* (Reconstruction / Resettlement). This new operation involves financing for the construction of houses, factory shells and market stalls (Sunday Mail, 26 June 2005), see Figure 14. While the Government will provide stands (plots), those rendered homeless will build their new homes supported by loans. Evidence on the ground however suggests that the operation was hastily put together, did not meet the immediate needs of the people affected, and progress against the planed objectives was slow (Schöpfer et al., 2007).

Fig. 14: Operation Garikayi taking place in the area of Hatcliffe (2006 and 2007).

For online visualisation of geo-data a WebGIS client based on the open source software UMN MapServer has been applied (see Figure 15). UMN MapServer is compiled according to the following principles: (a) the user requests data from the server; (b) The web server handles the request; (c) if geo-data are requested, the request will be forwarded to the MapServer; (d) the MapServer accesses the geo-data base including raster and vector data and processes them according to the request; (e) a raster image is sent back via the Web sever and presented at client side. Requests for maps like web map service (WMS) and web feature service (WFS) are conform to OGC (Open Geospatial Consortium) specifications. The following figure shows a WebGIS client as been established by Ioanneum Research for the GMOSS test case Zimbabwe. The client is based on HTML and Javascript and thus can be used with standard Internet browsers. It offers an intuitive graphical user interface allowing the presentation of maps and additional data as well as basic GIS functionalities like distance measuring and buffering. (JR)

Fig. 15: Web-GIS client for the test case Zimbabwe.

Visualization of results is a key prerequisite to the usability of the extracted information in a decision support context. Depending on the objectives we differentiate between two different types of visualization products, see Figure 16: (1) Pseudo-realistic visualization aims at providing a 'true' depiction of e.g. a certain crisis area, complemented by figures, graphs and numbers describing the situation more quantitatively. This may be used to directly support relief actions or other fine-scale operations. (2) 3D analytical views that display analytical items, and communicate scientific results, put in a familiar context. We use virtual globes as tools for seamless combination of 3D enabled and geo-referenced data. Freely available virtual globes with HSR contextual data enable disseminating analytical information derived EO data to a broad audience. Analytical 3D views provide conditioned information layers on different spatial aggregation levels (administrative or grid based units) using extrusion as a means for displaying the relevant variable (Tiede & Lang, 2007).

Fig. 16: Visualisation of information on globe viewers. Left: normal, terrain-based 3D visualisation, right: analytical 3D view.

4. Iraq

Oil dominates the economy, providing around 95% of foreign exchange earnings. Post-war looting, insurgent attacks, and sabotage have all undermined efforts to rebuild the economy. In particular, attacks on key economic facilities, such as oil pipelines and infrastructure have prevented Iraq from maximising exports.

Iraq's oil production currently stands at some 2.3 million bbl/day. Due to attacks on oil infrastructure and the workforce, it has been difficult to increase production to pre-war levels of about 2,5 million bbl/day. Domestic oil consumption is at an approximate rate of 351,000 bbl/day, while oil exports are at a rate of 1.42 million bbl/day. Reserves are estimated to stand at around 112.5 billion bbl.

Some 97% of the population are of Muslim faith, of which, approximately 60% are Shia and 40% are Sunni. Christian and other religions constitute the remaining 3%. The greater part of the population – some 75-80% - are of Arab ethnicity, while 15-20% are Kurdish and the remaining 5%, either Turkoman, Assyrian or other ethnic groups. The distribution of the various groups is shown in Figure 17.

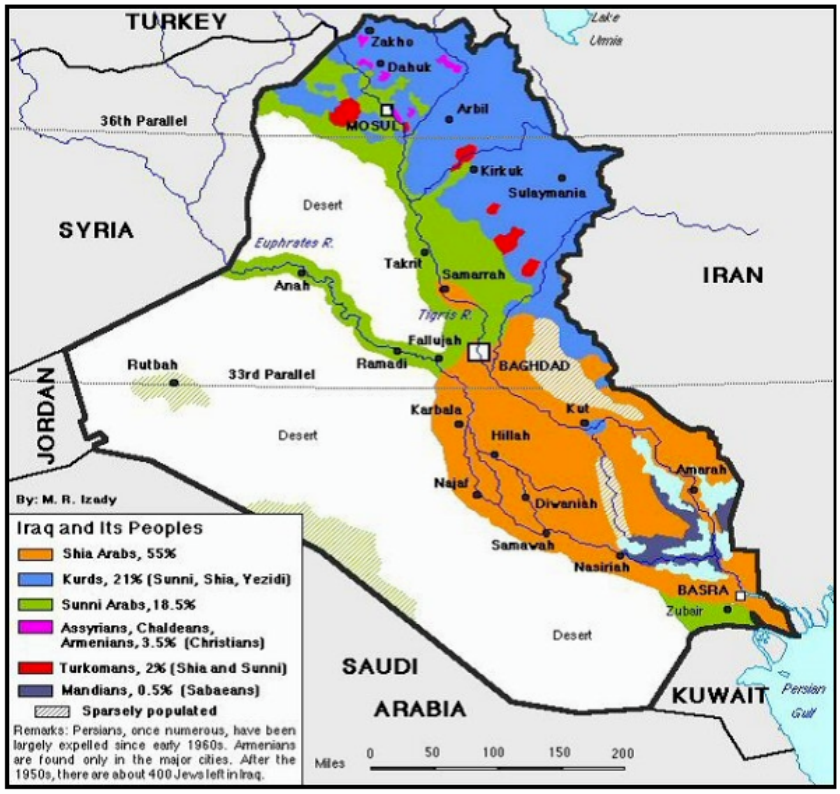

Fig. 17: Ethnic distribution in Iraq

The unity of the central government is weak, however, especially in its central provinces with a Sunni majority. The Kurds have established a separate government in the north. Kurds want to establish an own state including Kirkuk. This is of importance because control of Kirkuk also means access to huge oil reserves enabling the Kurds to have a basis for a independent economy in their region.

In this situation numerous attacks on the oil infrastructure have taken place, especially on pipelines between Kirkuk and Bayji where a crucial oil refinery is located in Sunni area. The continuing aspiration of the Kurds for independence possibly leads to a regional conflict with Turkey. Even within the Shia south, there is widespread unrest. Sectarian cleansing in mixed

areas is common. Many commentators argue that the country is beginning to fragment or that civil war is either imminent or already happening.

4.1 Methodologies

Monitoring and analysis of pipeline attacks

For observing attacks from space, satellites with a high temporal resolution are needed. The spatial resolution is rather low. An instrument such as SEVIRI (Spinning Enhanced Visible and InfraRed Imager), onboard the second generation weather satellite for Europe (MSG system) produces images with a resolution of 1-3 km and produces images every 15 minutes. The high monitoring frequency makes this instrument interesting for purposes such as hot spot detection (at 3.9 micrometer) and to determine the actual time of the fire event with an accuracy of 15 minutes. An example is given for Iraq on 2 March 2005 in Figure 18.

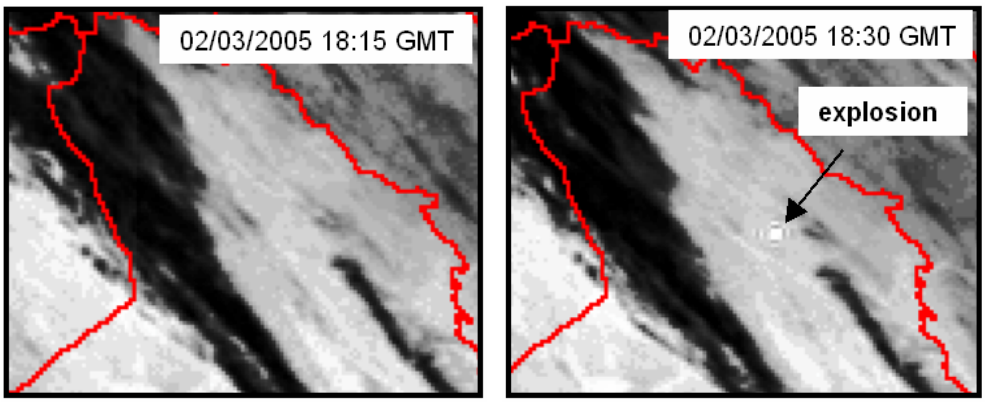

Fig. 18: Seviri image of Iraq showing a hot spot on the second

A so-called Robust Satellite Technique (RST) can be used to automatically extract hot spots due to man-induced hazards from the Seviri data (Filizolla et al., 2004). The SEVIRI data give a precise identification of the event (within 15 minutes), and can be combined with data at higher spatial resolution obtained from MODIS for a more accurate spatial location of the events. MODIS (MODerate resolution Imaging Spectroradiometer) is the main sensor on board of the Terra and Aqua satellites, which are part of the Earth Observing System (EOS) of NASA. The combined use of both satellites (EOS AM Terra and EOS PM Aqua) gives a daily monitoring frequency.

These observations are then compared with online reports of pipeline attacks that have occurred. These reports are collected and listed online by the Institute of Analysis of Global Security (IAGS). The online reports often do not provide precise information in regards to the area affected by the explosion and the time of the event; therefore, satellite data proves to be immensely useful in regards to providing this missing information. The content of the reports and the information from the satellites can be analyzed using a program called Paranoid (Program for Analysis Retrieval And Navigation On Intelligence Data), which was developed at TNO and is utilised for quick processing of structured and unstructured information for the provision of intelligence. Using this software, information relating to the various oil companies, means of the attack, and persons mentioned in the online reports are analyzed and combined with information about the time and location of the attack in order to search for possible motives and responsible terrorists.

In order to analyse geospatial trends in the reported and detected attacks a GIS product of Iraq was designed in ArcGis. This product contains the pipelines and other oil and gas infrastructure (pumping stations, refineries, substations, gas tankers, etc) as well as the locations of attacks. The EUSC team undertook the task of creating the vector maps of a complete pipeline network of Iraq. Complementary and context data were also used in this study and included open sources such as population, land-use, infrastructure (e.g. road densitites) and ethnic data. These data were integrated with the Landscan data-set of Iraq to calculate geostatistics for the different ethnic groups in Iraq.

Subsequently, a vulnerability analysis was carried out on the main oil pipeline sections within Iraq, using the integrated data and a selection of criteria for attacks on a pipeline. The criteria used are listed here in descending order of importance:

1. Closeness to populated areas and public transportation infrastructure for larger impact and easier escape of the perpetrators
2. Location near infrastructure to produce more damage.
3. Impact on the national and international economy.
4. Unguarded pipelines, unfenced sections, lack of buffered areas and areas without surveillance.
5. Pipeline above the ground.
6. Pipeline accessibility (isolated areas in Iraqi desert or in difficult mountainous terrain).

Four levels of vulnerability have been defined and the results are shown in Figure 19. Comparison of the levels of vulnerability with the numbers of attack derived from the IAGS list have been confirmed and localized by the satellite observations.

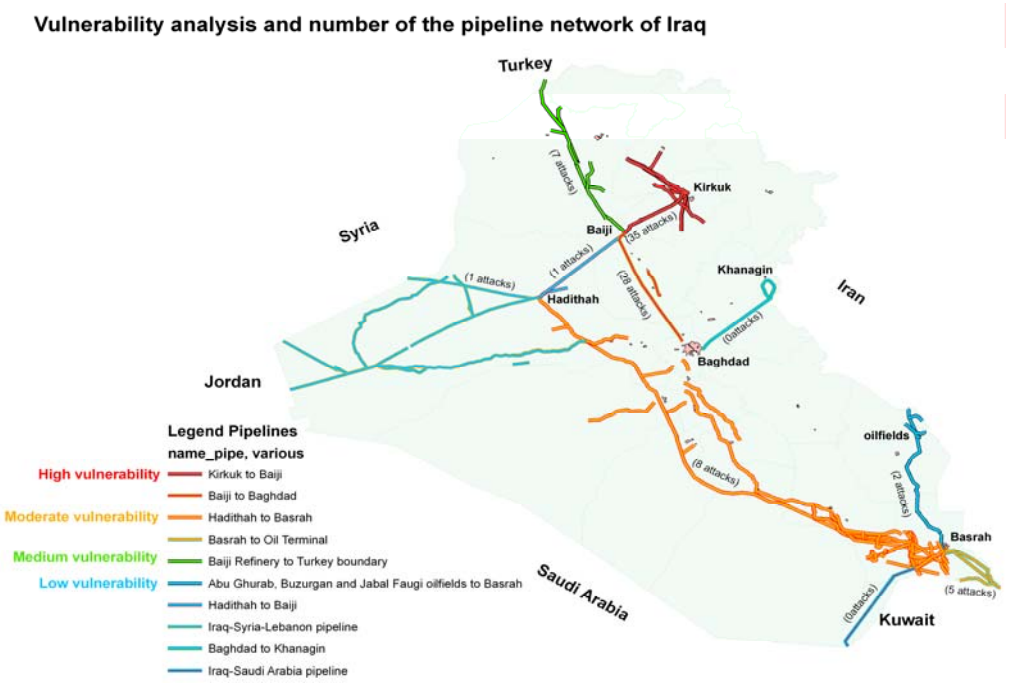

Fig. 19: Overview of pipeline vulnerability

Comparing these results with the population density data shows that:

1) High vulnerability sections of the pipeline network coincide with moderate to high population.
2) Medium vulnerability sections also coincide with significant levels of population density.
3) Low vulnerability sections coincide with low population density. This occurs in areas such as the western Iraqi desert.

Most probably, the direct relationship between concentration of attacks and a significant population density is due to the hiding possibilities that the perpetrators can find in areas of high population where public transportation is available (the saboteurs would be easily located and identified if attacks took place in isolated areas).

Comparing the vulnerability results with ethic population data shows that:

1) High vulnerability sections are located mostly within the Sunny Arab areas with some parts in areas of Shia Turkomen near Kirkuk.
2) Moderate vulnerability sections are mostly under the influence of the Shia Arab in a large area that extends from the centre to the southeastern parts of the country. However, there are moderate vulnerability sections in areas of Sunni Arab in the central and in the southeastern parts of Iraq, near the border with Kuwait).
3) Medium vulnerability section occupying the northern part of the country extends across areas dominated by Fayli Kurd, Shia turkomen, Sunni Arab and Sunni Kurd.
4) Low vulnerability sections in populated areas have the following distribution of ethnic groups, the section from Khanegin to Baghdad extends along areas of Sunni Kurd, Sunni Arab and Sunni Turkomen, the section from the oilfields in the proximity of Kuwait crosses an area sparsely populated by the Shia Arab, and the section from Hadithah to the Syrian border traverses the Iraqi desert sparsely populated by the Sunni arab.

The analysis above indicates that most of the pipeline attacks have taken place in areas of Sunni Arab and Shia Arab. Clearly these groups have a predominant role in the attacks.

Instability and situational awareness in Baghdad

Baghdad is the capital of Iraq. With a metropolitan area estimated at a population of 7,000,000, it is the largest city in Iraq. By the beginning of summer 2007, the on-going sectarian violence has divided the city of Baghdad into distinct and hostile zones consisting of a larger Shia city, nearly all of the city east of the Tigris, and a smaller Sunni city, west of the Tigris. The destruction of the Sarafiya bridge across the Tigris in spring 2007 is illustrative for this situation. This study addressed the question how well high-resolution satellite images are able to provide information on the actual situation in urban areas such as Baghdad. The study comprises the use of radar and optical imagery for monitoring infrastructural change and damage assessment and the generation of an urban digital surface model from satellite stereo data.

Radar satellites are important for geospatial intelligence about urban areas and urban situational awareness, since these satellites can collect data at day and night and independently of weather conditions ensuring that the information can be obtained at regular intervals and in time. A drawback of SAR imagery is the poor ability to recognise the detected changes in the scene. The changes therefore need to be characterised using complementary data and context information. For this purpose the urban digital surface model derived from Ikonos stereo imagery that contains building heights was used.

Five images over Baghdad were analysed from 17 January 2003, 30 March 30 2003, 23 April 2003, 17 July 2005, and 2 April 2007 which were collected with Radarsat in the same orbit, so that for all images the same imaging geometry is applicable. These so-called fine beam images have a resolution of 10 meter. In Figure 20 we show the Baghdad area of 25 by 25 km which has been analysed. The image shows three dates in the RGB colours channels. This method is an easy way for visual inspection in order to find changes since for no change the image is grey, while a change shows up in colour. Of course when more than three dates have to be analysed this visualisation method is inadequate. In Figure 20 various colours related to changes are visible. For example blue implies that (23 April 2003) enhanced scattering occurred just after the war, while yellow indicates the presence of enhanced scattering in 2005, which remained in 2007. Red indicates recent changes indicated by enhanced radar scattering. Changes have been extracted from these data using change detection techniques, which include accurate co-registration, speckle filtering techniques and multi-temporal feature extraction. (Ghauharali et al. 2006, Dekker 1998, van den Broek et al., 2007).

Fig. 20: Multi-temporal Radarsat image of the Baghdad area from 23 April 2003 (blue), 17 July 2005 (yellow) and 2 April 2007 (red).

At Joanneum Research the in-house developed software package RSG has been used to process the Ikonos stereo imagery for retrieving height information and to produce a urban surface model. Four main steps are needed for the processing of the data which are summarised here: 1) geometric modelling of the stereo data, 2) coarse registration of the stereo data using a coarse DEM (e.g. the C-band DEM of the SRTM mission), 3) automatic matching of stereo images and 4) generation of the surface model. Especially the automatic matching can give problems for high-resolution data over urban area due to occlusions and repetitive patterns. A more detailed description of the processing can be found in Raggam et al. (2004).

In Figure 21 we show areas of change for the so-called Green Zone, the heavenly guarded government area in Baghdad and the digital surface model.

This area shows significant changes between 2003 and 2005 using Radarsat. In Figure 21 three spots with the main changes are numbered and overlaid on the Ikonos image. The digital surface model is also shown in Figure 21 and has a somewhat noisy appearance due to problems in the matching of the stereo image pair. Typical height for the river (dark area) is about 30 meters above sea level. There are also some higher areas in the river, which are due to matching problems. The average ground level is 34-35 meters above sea level, and the highest buildings such as the presidential palace have heights up to 60 meters above sea level. i.e. a building height of 25 meters. Using the digital surface model, average heights for the spots have been calculated, which are 36.7, 37.0 and 38.5 meters for spot 1,2 and 3, respectively. We can use these heights as an indicator for the appearance of new buildings when the height above ground level is more than 2 meters. This is true for spot 2 and 3. When we inspect the corresponding Ikonos images for the three spots we find that spot 1 is a parking area and spots 2 and 3 are areas where barracks have been deployed after the war in 2003. These barracks are probably in use for military accommodation. The presence of the barracks enhances the scattering in the Radarsat image of 2005. The enhanced scattering for spot 1 indicates that the parking area is used after the war and not or less before the war.

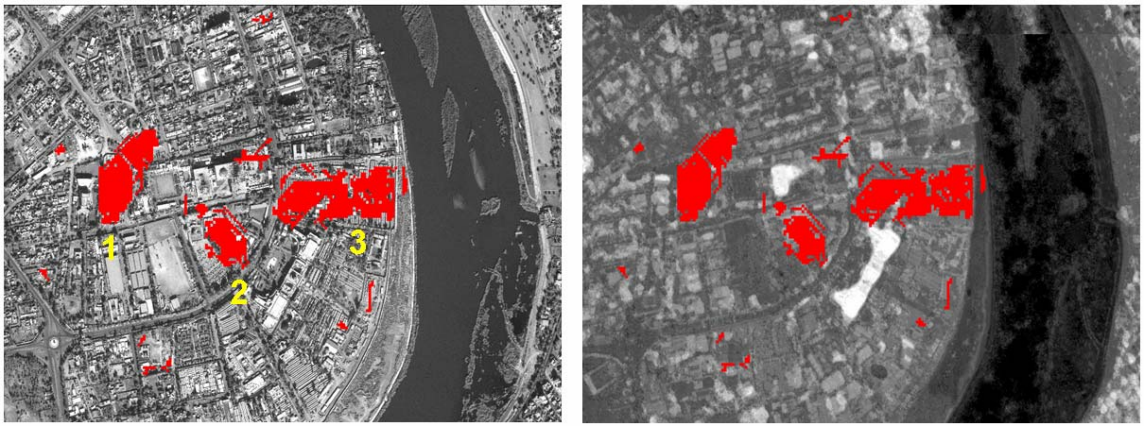

Fig. 21: (Left) Ikonos image of 9 December 2005, with changes from Radarsat in a red overlay for area 1 (Green Zone). (Right) DSM of the same area.

Other changes found with the radar data could be associated with the destruction of buildings (due to the war in 2003), population change (appearance of dwellings) and economical activity (disuse and reuse of storage places, market places and assembly places for trucks). A more detailed description of the changes and the methods can be found in van den Broek and Dekker (2007).

4.2 Conclusions

At the moment (2007) it is not clear how the situation in Iraq will develop further. The various possibilities vary between quietly resolving of the conflict and escalation towards a regional conflict with global consequences. Most probable for the near future is continuing instability, resembling a Lebanon scenario or a civil war leading to partition of the country.

Earth observation data provides information for the geospatial context of the conflict/crisis, which is basic information for policy makers and which is required for all kinds of actions and decision scenarios. Earth observation provides quick overview of large areas (e.g. Seviri, Modis) and can provide detailed information (of remote areas) after an event through current high-resolution imagery (e.g. Ikonos, Quickbird, Radarsat, TerraSAR). Problem here is the availability of up-to-date high-resolution data due to limited revisit times, access, and distribution possibilities, which clearly has to be improved.

5. Iran

Is the Iran developing nuclear weapons? The test case on the Iran investigated whether satellite imagery analysis could give answers to this question.

International Atomic Energy Agency (IAEA) inspections since 2003 have revealed two decades' worth of undeclared nuclear activities in Iran, including uranium enrichment and plutonium separation efforts.

Iran says its nuclear ambitions are peaceful. It is a signatory of the Non-Proliferation Treaty (NPT); its nuclear programme began in the Shah's era, including a plan to build 20 nuclear power reactors. Iran also signed the important additional protocol of the NPT safeguards agreements, however, this was not ratified by the Iranian parliament. Two power reactors in Bushehr, on the coast of the Persian Gulf, were started but remained unfinished when they were bombed and damaged by the Iraqis during the Iran-Iraq war. Following the revolution in 1979, all nuclear activity was suspended, though subsequently work was resumed on a somewhat more modest scale. Current plans extend to the construction of 15 power reactors and two research reactors. The first nuclear power station is building with Russian help[1]

Given Iran's insufficient uranium reserves, Iran cannot achieve its goal of nuclear energy independence. Moreover, indigenous fuel cycle costs are substantially greater than importing nuclear fuel at market prices.[2] The country has an abundance of energy resources, with reserves of natural gas (second only to those of Russia) and substantial oil reserves (third in world behind Saudi Arabia and Iraq). However, Iran's uranium reserves could give Iran a significant number of nuclear weapons. It has been assessed by at least one source that the Natanz facility might produce uranium for 5 bombs/yr and Arak facility might produce plutonium for 3 bombs/yr[3]. Iran's facilities are scaled exactly like another state's facilities that were designed to produce fissile material for nuclear weapons.[4]

The UN Security Council has repeatedly legally required Iran to suspend its enrichment and reprocessing activities. But Iran has ignored the Security Council resolutions, refused to consider the idea of suspending its enrichment activities and made substantial progress in putting in place many hundreds of uranium enrichment centrifuges and learning how to operate them, bringing closer the possible future day when Iran might be able to produce highly enriched uranium. Efforts to restart negotiations with Iran on the nuclear issue have failed so far, as the United States and its European partners have insisted that that they will not negotiate until Iran suspends its enrichment activity and Iran has refused to suspend that activity again. (Bunn 2007)

5.1. Investigations

The aim was to monitor the development of some relevant sites in the Iran: Arak, Bushehr, Esfahan, Natanz and Saghand (see Figure 22). In particular it was investigated

- what significant features of nuclear facilities / activities / processes are identifiable from space?

[1] http://www.globalsecurity.org/wmd/world/iran/nuke.htm

[2] US Department of State: Iran's Nuclear Fuels Cycle Facilities: :A Pattern of peaceful Intent? Briefing slides presented by the US to foreign diplomats in Vienna, September 2005

[3] http://www.globalsecurity.org/wmd/world/iran/nuke.htm

[4] US Department of State: Iran's Nuclear Fuels Cycle Facilities: :A Pattern of peaceful Intent? Briefing slides presented by the US to foreign diplomats in Vienna, September 2005

- how these signature could be utilised for image analysis (visual interpretation / semantic modelling)

Different pre-processing, change detection, classification and visualisation techniques were applied to multispectral, radar, and hyperspectral satellite imagery, such as QuickBird, ASTER, Radarsat and HYPERION, see Figures 23 to 26.

Fig. 22: Overview on some Iranian nuclear facilities: Arak, Bushehr, Esfahan, Natanz, Saghand © Forschungszentrum Jülich

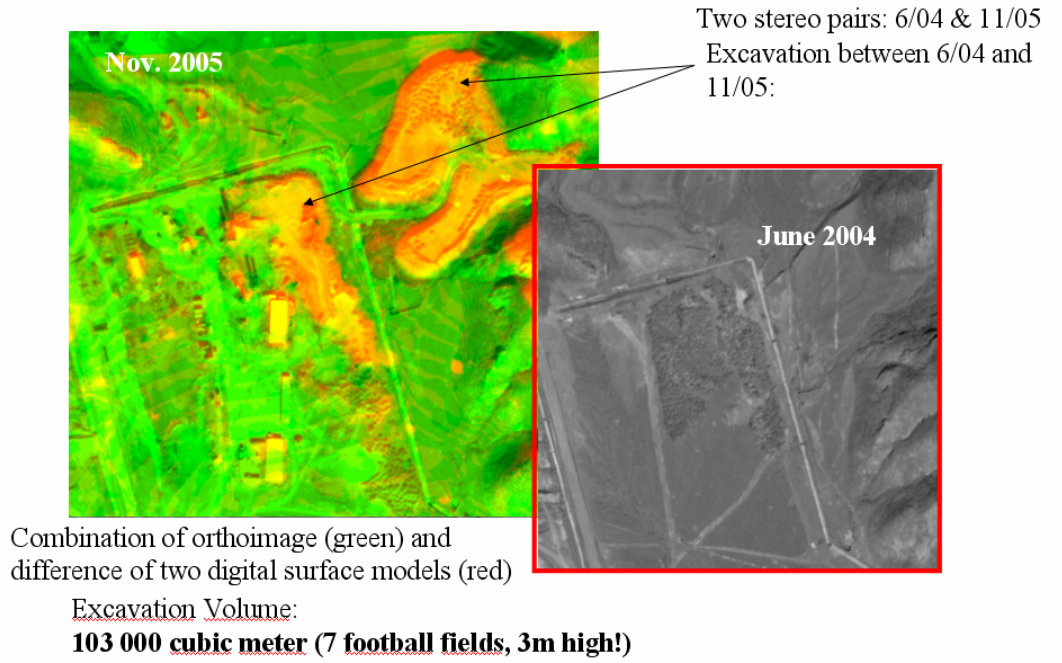

Fig. 23: Subsurface constructions, underground activities at Esfahan. 3D change detection using stereo pairs of June 2004 and November 2005 © DLR

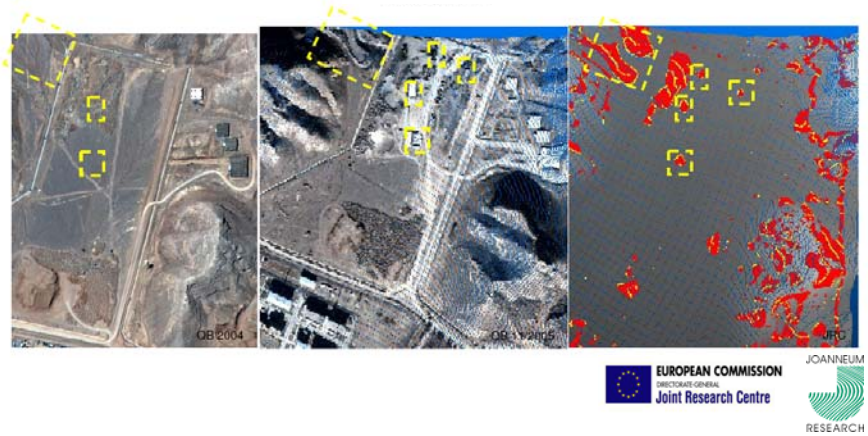

Fig. 24: 3D Change detection (right) using QuickBird stereo pairs of June/July 2004 (left) and November 2005 (middle), Esfahan (Hollands et al. 2007)

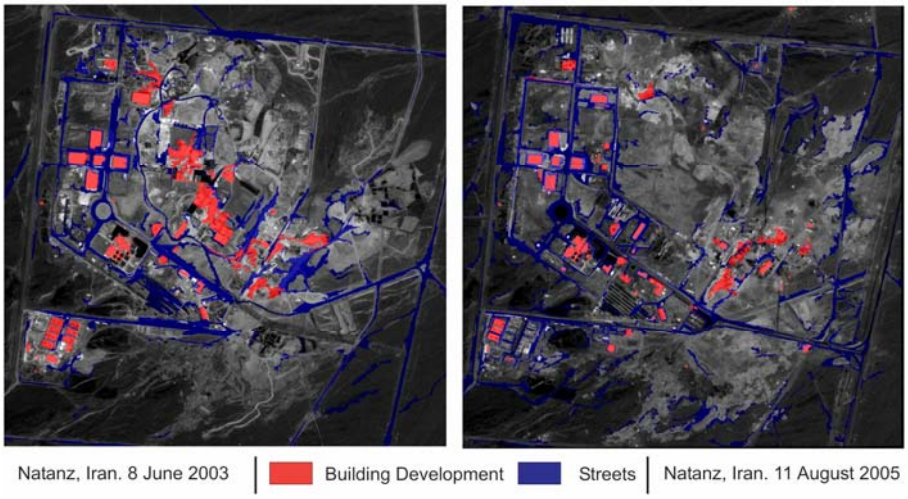

Fig. 25: Automated object-based classification for Natanz, June 2003 and August 2005 (Nussbaum & Niemeyer 2007)

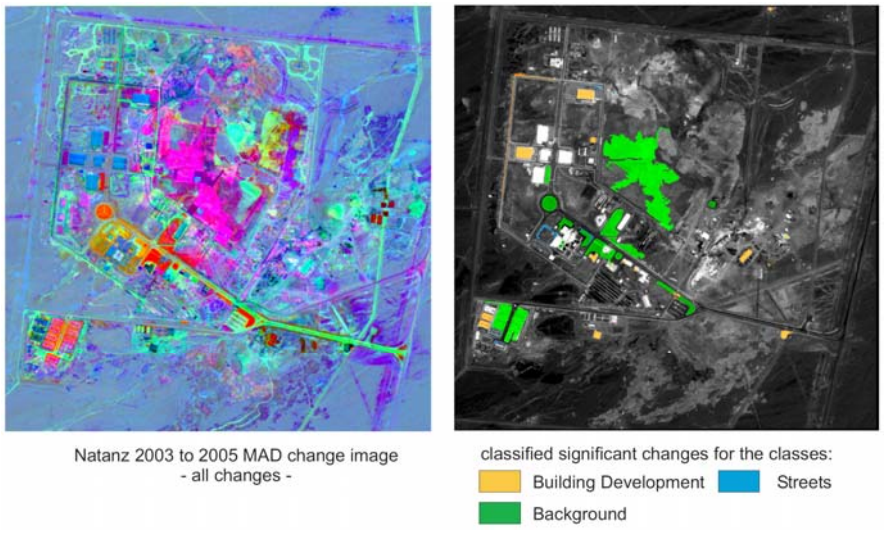

Fig. 26: Detection (left) and classification (right) of changes at Natanz between June June 2003 and August 2005 (Nussbaum & Niemeyer 2007)

5.2 Conclusions:

Remote sensing data ranging from the visible to the microwave region of the electromagnetic spectrum could provide nuclear safeguards-relevant information. Digital image processing are essential for wide-area monitoring and detailed detection of small-scale infrastructure. However, the sensor characteristics still restrict the application of satellite imagery analysis for verifying the Treaty compliance.

6. References

Bunn, M., 2007, Securing the bomb. Nuclear Threat Initiative, Washington D. C. www.nti.org/securingthebomb.

Dekker, R.J., 1998, Speckle filtering in satellite SAR change detection imagery, *International Journal of Remote Sensing, Vol. 19, No. 6*, pp. 1133-1146.

Filizzola, C., Pergola, N., Pietrapertosa, C., and Tramutoli, V., 2004, Robust satellite techniques for seismically active areas monitoring: a sensitivity analysis on September 7th 1999 Athens's earthquake, *Seismo Electromagnetics and Related Phenomena*. *Physics and Chemistry of the Earth*, vol. 29, pp 517-527, 2004

Ghauharali, R.I., Dekker, R.J., van den Broek, A.C., van Maarseveen, R.A., 2006, Automated detection and categorisation of changes in satellite imagery, *NIVR report 53501VB*, August 2006.

Hollands, T., Boström, G., Gonçalves, J.G.M., Gutjahr, K., Niemeyer, I. & V. Sequeira (2007): 3D Scene Change Detection from Satellite Imagery. In: Proc. 29th Symposium on Safeguards and Nuclear Material Management, Aix-en-Provence, 22–24 May 2007

Lang, S., D. Tiede, F. Hofer, 2006 Modeling ephemeral settlements using VHSR image data and 3D visualisation – the example of Goz Amer refugee camp in Chad. In: PFG - Photogrammetrie, Fernerkundung, Geoinformatik, Special Issue: Urban Remote Sensing, 4/2006, 327 – 338.

Niemeyer, I. & S. Nussbaum (2006): Change detection - the Potential for Nuclear Safeguards. In: Avenhaus, R., Kyriakopoulos, N., Richard, M. & G. Stein (ed.) (2006): *Verifying Treaty Compliance. Limiting Weapons of Mass Destruction and Monitoring Kyoto Protocol Provisions.* Springer, Berlin: 335-348

Nussbaum, S. & I. Niemeyer (2007): Automated extraction of change information from multispectral satellite imagery. *ESARDA Bulletin* 36, 20007, 19-25

Raggam, H., Franke, M., Gutjahr, K, 2004, Surface Model Extraction from High Resolution Stereo Data over Alpine Terrain, *24th Earsel Symposium "New Strategies for European Remote Sensing*, Dubrovnik, May 25 – 27, 2004.

Schneiderbauer, S. and D. Ehrlich, (2005). Population density estimations for disaster management. Case study rural Zimbabwe. In: van Oosterom, P., Zlatanova, S., Fendel, E.M. (Eds.): Geo-information for Disaster Management. Proc. of the 1st International Symposium on Geo-information for Disaster Management, Delft, The Netherlands, March 21-23, 2005. Springer, 901-922.

Schöpfer, E., D. Tiede, S. Lang and P. Zeil 2007. Damage assessment in townships using VHSR data - The effect of Operation Murambatsvina / Restore Order in Harare, Zimbabwe. Urban Remote Sensing Joint Event. Paris 2007, CD-ROM.

Van den Broek, A.C. and Dekker R.J, 2007, Geospatial intelligence about urban areas using SAR, *Proceedings SPIE Remote Sensing Europe*, Florence, 17-20 September 2007

Van den Broek, A.C., Dekker R.J, Gutjahr, K., Raggam, H., 2007, Use of high resolution optical and radar imagery for intelligence and situational awareness in urban areas*, proceedings Urban Remote Sensing Joint Event*, Paris 11-13 April 2007.

Armed conflict risk assessment - towards an operational approach.

Clementine Burnley, Dirk Buda, and François Kayitakire*

European Commission, Joint Research Centre, Institute for the Protection and Security of the Citizen (IPSC), Support to External Security Unit, Ispra 21027 (VA), Italy

* francois.kayitakire@jrc.it

Introduction

In the field of conflict studies, automated data processing for relevant information extraction is essential to process the huge amounts of data being collected on countries and political groups. Communication facilities and broad use of digital documents also provide the potential for automated quantitative information analysis to support political decision makers to make timely evaluations of the risk of severe crises. Such tools are more and more required in the framework of early warning systems. This study aims to provide a scientifically sound approach to build a statistical model to assess quantitatively the risk of intra-state armed conflict on the global level. A particular attention is paid to the operationalization of the approach in early situation assessment.

Quantitative methods applied to conflict risk assessment can be classified into two categories according to the type of independent variables used to predict or estimate the risk: (i) methods that use structural indicators as independent variables to explain/predict the conflict events; (ii) methods that use past conflict events to estimate the current risk. The last category try to detect changes in the trends of a given measure of (in)stability. Risk assessment seeks to assess the probability of future instability on the basis of estimable relationships between structural risk factors, while early warning seeks to flag emerging crises as early as possible on the basis of monitoring recognisable patterns.

In fact, Jenkins and Bond (2001), citing Davies and Gurr (1998), point out that risk assessment focuses on the structural conditions leading to political tensions while early warning identifies the dynamic factors leading to political crises. Schrodt and Gerner (1997) propose a distinction based on the type of source data variables. Yiu and Mabey (2005) categorize the two concepts as knowable (risk assessment) and complex (early warning) processes. This paper concentrates on the risk assessment. It is worth noting that the concept of risk should include also estimation of the conflict impact. This is not dealt with in the present study. For the sake of brevity the term risk is however used in place of the probability of occurrence of an armed conflict.

Conflict studies aiming to find a causal relation between structural indicators and the risk of armed conflict have recently gained great interest in political science research. These studies aim usually to find the relation between the risk of armed conflict and a given set of indicators like economic indicators (GDP, GDP growth, exports and imports), demographic and societal indicators (total population, population density, life expectancy, infant mortality, school enrollment, social fractionalization, etc.), political indicators (regime type and duration, involvement in international organizations, peace duration, political rights, neighboring countries in war, etc.) and environmental factors (spatial dispersion of the population, mountainous terrain, forest cover, cropland area, irrigated land, etc.). From this list we can already see that some variables are not actually explanatory variables, but just correlates of

risk of war (e.g. infant mortality, life expectancy). We must, therefore, be careful in interpreting the regression results.

Once the regression model is estimated, it might be used to predict the probability of conflict outbreak and used operationally for warning about the risk of war in any country. However, most of these studies limit their investigations on the effect of the independent variables in the model (causal explanation), and they do not discuss the prediction, or forecast, issue. Although this shortcoming was pointed out by Beck et al. (2000) most later studies do not consider the issue (see e.g. Collier and Hoeffler, 2004, 2002; Elbadawi and Sambanis, 2002; Fearon, 2005). Regression models are evaluated solely on the basis of their quality of fit. This paper goes further by discussing predicted probabilities for several countries and comparing the prediction with the index of political instability that is established by the World Bank (Kaufmann et al., 2006).

Method

Most empirical conflict studies aim to predict the probability of conflict onset based on a set of risk factors. In that case, the dependent variable is commonly coded 0 for all country-years records with no war, 1 for the year a war started, and missing for periods of ongoing war (Hegre and Sambanis, 2006; Collier and Hoeffler, 2004; Beck et al., 2000; Goldstone et al., 2005; Bennett and Stam, 2000), whereas some authors code these periods as 0 (Fearon and Laitin, 2003). Other studies consider modelling the incidence of armed conflict and the dependent variable is coded 1 for all periods of ongoing war (Reynal-Querol, 2002; Elbadawi and Sambanis, 2002; Hauge and Ellingsen, 1998; Urdal, 2005). The first approach is theoretically the most appropriate for modelling the probability of conflict onset, that is the risk of a new "country-conflict" occurrence. However, in practice, it turns out to be inefficient.

Firstly, the start and end dates of a conflict are not always obvious. They depend on the criteria used in building the conflict dataset. For instance, the PRIO dataset records a conflict when and only while it reaches the threshold of 25 battle-related deaths a year or 1000 deaths in total (Gleditsch et al., 2002).

Secondly, removing periods of ongoing war reduces the sample, and especially the number of cases. This is critical because the number of cases is already small. For instance, we have 843 cases in total between 1971 and 2004 whereas there were only about 70 new cases, compared to about 7600 total countryyears records. Some scholars argued that the different approaches gave similar results at least when studying the effect of particular factors (Urdal, 2005; Hegre and Sambanis, 2006), but did not provide details of their evidence. In this study, we preferred the third design and coded as ones all ongoing war periods.

As independent variables, we selected 21 structural indicators: the GDP per capita (gdpc), GDP growth (gdpg), merchandise exports (expm), exports of goods and services as a percent of GDP (expgdp), merchandise imports (impm), imports of goods and services as a percent of GDP (impgdp), fuel exports (expf), foreign investment (inve), official development assistance par capita (odac), official development assistance as percentage of Gross National Income (odag), total external debt (debt), total population (popu), population density (pdens), population growth (pgro), secondary school enrollment (secs), religious fractionalisation index (ref), religious polarisation index (rep), ethno-linguistic fractionalisation index (elf), ethno-linguistic polarisation index (elp), democracy level (democ) and accessibility index (geog).

These factors are the most studied and have been shown to be related more or less to the risk of armed conflict. The availability of data was also taken into account for the variable selection. The literature review on which is based this selection and a discussion on data sources are detailed in Burnley and Kayitakire (2007).

We checked the distribution of all the variables and were eventually transformed for normalisation and variance stabilisation. They were then standardised to mean 0 and variance 1. Some variables had missing observations simply because they had not been reported. For example, if exports data are missing for a country and for some years, we can reasonably assume that this country did actually export, but did not report the statistics. We used a Markov Chain Monte Carlo (MCMC) method (Schafer and Olsen, 1998) that assumes multivariate normality to impute all missing values. Missing values for any variable are predicted taking into account the correlation between all variables used in the imputation model. Multiple imputation preserves therefore the relation between variables, and accounts for uncertainty in the model by creating different complete datasets. We created 5 versions of imputed data sets, and combined the results of their analysis. In other cases, data are missing because the combination variable-country-year is not relevant. For example, the countries of the former soviet republics that became independent in the 1990's lack information on most economical indicators before 1990. Such entries are kept empty.

Risk related to structural factors

Let Y_{it} be a random variable that records the event "an armed conflict occurs in country *i*, in year *t*", so that

$Y_{it} = 1$ if the event is realised (armed conflict), and

$Y_{it} = 0$ otherwise (peace).

We are interested in $\pi_{it}=P(Y_{it}=1)$ the probability that an armed conflict occurs in country *i* in year *t*. As we do a panel analysis, we can draw the subscript t. We need to estimate π on the basis of some explanatory variables (or covariates) $x = (x_1, ..., x_r)$. These explanatory variables are typically the structural indicators as income measures, regime type, social fractionalisation index, etc.

We suppose that the dependence of π on *x* occurs through the linear combination:

$$f(\pi) = \sum_{j=1}^{r} x_j \beta_j$$

The logit function is the most appropriate to model this dependence as it bears several interesting properties (McCullagh and Nelder, 1995; p. 109). Thus, the regression model can be written as follows:

$$\log(\frac{\pi}{1-\pi}) = \beta_0 + \beta_1 x_1 + \beta_2 x_2 + ... + \beta_r x_r + \varepsilon$$

where β_j are the unknown model parameters and ε is the error term.

Risk related to previous conflicts

Countries that experience an armed conflict are more prone to another conflict in the future. This effect is usually taken into account by including a variable that reflects the history of conflicts (Mousseau et al., 2003; Gleditsch and Ward, 2005; Urdal, 2005). In this paper, we propose to separate the effect of past conflicts from the effect of other independent variables. The risk related to past conflicts is hereafter modelled in an innovative way inspired by the

capture-recapture methods that are used in Ecology studies (Jolly, 1982; Seber, 1982). Interested reader can find the details of the approach in Burnley and Kayitakire (2007).

Results

As a first step, we provide a brief description of the variables distribution. From table 1 it can be noted that some variables could not be used in the model at all because the missing data proportion is too high. We excluded variables that lack data for more than 20% of the observations in the conflict cases. These variables are *expf, gdppc* and *secs*. Location statistics of most factors are in the line of the expected trends, even if the differences in mean values are often small in comparison with their standard deviation, excepted for the indicators of religious fractionalisation and polarisation whose mean values are lower in conflict than in non-conflict cases.

Table 1: Summary statistics of the explanatory variables

	Conflict	Nomiss	Miss(%)	Mean	Median	Std
gdpc	1	745	11	2148	787	4011
	0	4497	32	5789	1910	8126
gdpg	1	738	12	0.0	1.6	7.6
	0	4583	31	1.8	2.0	6.0
expm	1	828	1	10284	1472	24131
	0	4997	25	19984	1049	66593
impm	1	826	2	10993	2154	25600
	0	4988	25	20505	1383	75248
expf	1	498	41	16.6	2.6	32.8
	0	3278	51	17.4	3.1	29.0
expgdp	1	725	14	23.6	20.4	15.2
	0	4329	35	37.2	31.9	23.6
impgdp	1	725	14	29.1	25.4	16.1
	0	4327	35	44.1	37.6	24.9
inve	1	808	4	724	33	3539
	0	4707	29	1858	23	11215
odag	1	738	12	5.9	2.4	9.1
	0	4272	36	7.3	2.3	12.8
odac	1	815	3	29.9	13.4	53.9
	0	4761	28	69.8	18.8	195.6
debt	1	717	15	16767	4083	31275
	0	3787	43	7535	909	22477
popu	1	839	0	59279	18380	156551
	0	6542	1	18751	3234	85944
gdppc	1	667	21	3246	1872	3920
	0	3801	43	6976	4083	7692

secs	1	39	95	40.3	48.0	28.6
	0	560	92	64.7	72.0	25.8
REF	1	839	0	0.40	0.43	0.23
	0	5537	16	0.44	0.47	0.23
REP	1	839	0	0.57	0.64	0.26
	0	5537	16	0.62	0.71	0.26
ELF	1	835	0	0.50	0.51	0.23
	0	5322	20	0.42	0.42	0.25
ELP	1	835	0	0.59	0.64	0.20
	0	5322	20	0.54	0.60	0.25
democ	1	839	0	0.03	0.00	6.32
	0	6626	0	0.20	0.00	6.08
geog	1	838	0	34.96	22.94	36.01
	0	4678	29	31.35	18.29	39.79
Note: The total number of observations was 7465, among which 839 (11%) conflict cases (ones in the second column).						

Note: The total number of observations was 7465, among which 839 (11%) conflict cases (ones in the second column).

Regression analysis

We consider several specifications of the model and data processing in order to select the method that offers the best trade-off between quality of fit and completeness in the possibility of prediction. We start with the naive model, including all the explanatory variables and using the original dataset before imputation of missing values. The observations with at least one missing variable were excluded from the analysis. The results of this first analysis are reported in table 2. They show that the likelihood of armed conflict is significantly associated with the GDP growth rate, the ODA per capita, the ODA per unit of GDP, the level of foreign investment, the size of the population, the level of democracy and with the different indices of social fractionalisation/ polarisation, excepted for the ethno-linguistic polarisation index. The overall model fitting statistics denote an acceptable model. The coefficient of determination R^2, adjusted according to Nagelkerke (1991), of 0.28 is an acceptable value in social sciences. The Hosmer-Lemeshow statistics (Hosmer and Lemeshow, 2000) is sufficiently small (not statistically significant) denoting an overall good fit.

Table 2: Parameter estimates of the full model using the original dataset, and its goodness-of-fit statistics (Model 1)

Parameter	DF	Estimate	Standard error	Wald χ^2	*p*-value
Intercept	1	-6.6480	1.8170	13.3872	0.0003
lgdpc	1	-0.1797	0.1242	2.0957	0.1477
gdpg	1	-0.0505	0.0093	29.6620	<.0001
lexpm	1	-0.0646	0.1389	0.2165	0.6417
lexpgdp	1	-0.3451	0.2400	2.0677	0.1504

limpm	1	-0.2978	0.1633	3.3250	0.0682
limpgdp	1	0.2983	0.2911	1.0500	0.3055
lodag	1	-0.4351	0.1501	8.4027	0.0037
lodac	1	0.3248	0.1140	8.1162	0.0044
ldebt	1	-0.0065	0.0331	0.0391	0.8432
inve	1	-0.00003	0.000014	4.7356	0.0295
lpopu	1	0.9650	0.1429	45.5839	<.0001
lref	1	-1.3843	0.2411	32.9514	<.0001
lrep	1	1.2756	0.2648	23.2026	<.0001
lelf	1	0.3071	0.1510	4.1367	0.0420
lelp	1	-0.0985	0.1942	0.2571	0.6121
democ	1	0.0282	0.0086	10.7950	0.0010
lgeog	1	-0.0312	0.0539	0.3360	0.5621
Observations (1/0)				623/3003	
Log likelihood				-1330	
Wald χ^2				447.06	
Adjusted R^2				0.28	
Hosmer-Lemeshow χ^2				6.16	

However, when we examine the coefficient estimates of the different regressors, we can note some "inconsistencies" with our initial hypotheses. The sign of the coefficient of *lodag* (ratio ODA/GDP) is negative (less assistance is associated with higher risk of armed conflict) whereas the sign for *lodac* is positive (more assistance is associated with higher risk of armed conflict). We expected similar signs for both variables. The religious fractionalisation index has also an "unexpected" negative coefficient whereas the associated polarisation index coefficient is in the expected direction. Montalvo and Reynal-Querol (2005) observed the same pattern and interpreted this as meaning that, conditional on a given degree of polarization, more religious diversity decreases the probability of a civil war. Indeed, a high number of different groups increases the coordination problems and, therefore, given a level of polarization, the probability of civil wars may be smaller.

Another "inconsistency" with our initial hypotheses is that the coefficients of most of the economic indicators (income, exportation and importation volumes, debt service) are not statistically significant at 5% level. Some have either "unexpected" signs. Thus, *lgdpc, lexpm* and *limpm* are not significant but have the expected sign, whereas *ldebt* is not significant and has an "unexpected" sign. This is perhaps due to multicollinearity problems.

We found also that the observations of several countries in recent years (namely in 2004, the last reporting year) were discarded because of missing data. We could speculate on the availability of data in the future, but this is a factor that we can not control. We tested the model with a dataset augmented by imputation of missing data.

The imputation model was mainly based on the expected correlation between economic indicators. However, we excluded the variable *inve* from the analysis because it was not used in the imputation model.

We should underline that the results of a model similar to the one presented in table 2 don't almost change if *inve* is put aside. This may indicate that the test of significance of its effect

may not be valid probably because its distribution was highly skewed. The results of the imputed dataset are summarised in table 3. Statistics of goodness-of-fit are less good than in Model 1. The coefficient of determination is lower (0.22) and the Hosmer-Lemeshow statistics is higher, even statistically significant at 5% level. Factors with significant effect are almost the same: GDP growth rate, official development assistance, population size, religious fractionalisation, ethno-linguistic fractionalisation, and democracy level. Only the religious polarisation factor *lrep* is not significant in Model 2 whereas it was in Model 1, and vice-versa for *lexpgdp* (share of exportation of merchandise in the GDP). The "inconsistencies" we noted in Model 1 are also present in Model 2. Coefficient estimates have the same sign, and they are quite similar for both model as it can be seen on figure 1. The largest changes are noted for the intercept, *gdpg, lexpm, lodac, lpopu, lref* and *lrep*. The number of imputations has no effect on the model estimates. If the calculation load is an issue (large dataset for example), single imputation will be preferred to multiple imputation. A more detailed sensitivity analysis should allow documenting the variability of the model parameters and the exact effect of missing data imputation.

Table 3: Parameter estimates of the full model using the imputed dataset, and its goodness-of-fit statistics (Model 2)

Parameter	DF	Estimate	Standard error	Wald χ^2	*p*-value
Intercept	1	-2.7931	0.0877	1013.6268	<.0001
lgdpc	1	-0.2099	0.1202	3.0492	0.0808
gdpg	1	-0.2392	0.0437	29.9952	<.0001
lexpm	1	-0.1759	0.2743	0.4111	0.5214
lexpgdp	1	-0.3364	0.1240	7.3596	0.0067
limpm	1	-0.4914	0.2637	3.4718	0.0624
limpgdp	1	0.2224	0.1225	3.2944	0.0695
lodag	1	-0.7090	0.1377	26.5158	<.0001
lodac	1	0.7959	0.1446	30.2963	<.0001
ldebt	1	-0.00104	0.0822	0.0002	0.9899
lpopu	1	1.9908	0.1640	147.4034	<.0001
lref	1	-0.4548	0.1846	6.0673	0.0138
lrep	1	0.2555	0.1810	1.9909	0.1582
lelf	1	0.3387	0.1179	8.2602	0.0041
lelp	1	-0.0514	0.1177	0.1910	0.6621
democ	1	0.0335	0.00687	23.7944	<.0001
lgeog	1	-0.0937	0.0511	3.3560	0.0670
Observations (1/0)				832/4141	
Log likelihood				-1896	
Wald χ^2				513.35	
Adjusted R^2				0.22	
Hosmer-Lemeshow χ^2				18.97*	

From a statistical point of view, Model 1 should be preferred to Model 2. However, the model based on imputed dataset can provide estimates of conflict probability for more countries than

the one based on the original dataset. If we consider the estimates of 2004, Model 2 provides predictions for 157 out of 226 countries/territories whereas Model 1 provides predictions for only 103 out of 226 countries/territories. This is a significant operational advantage.

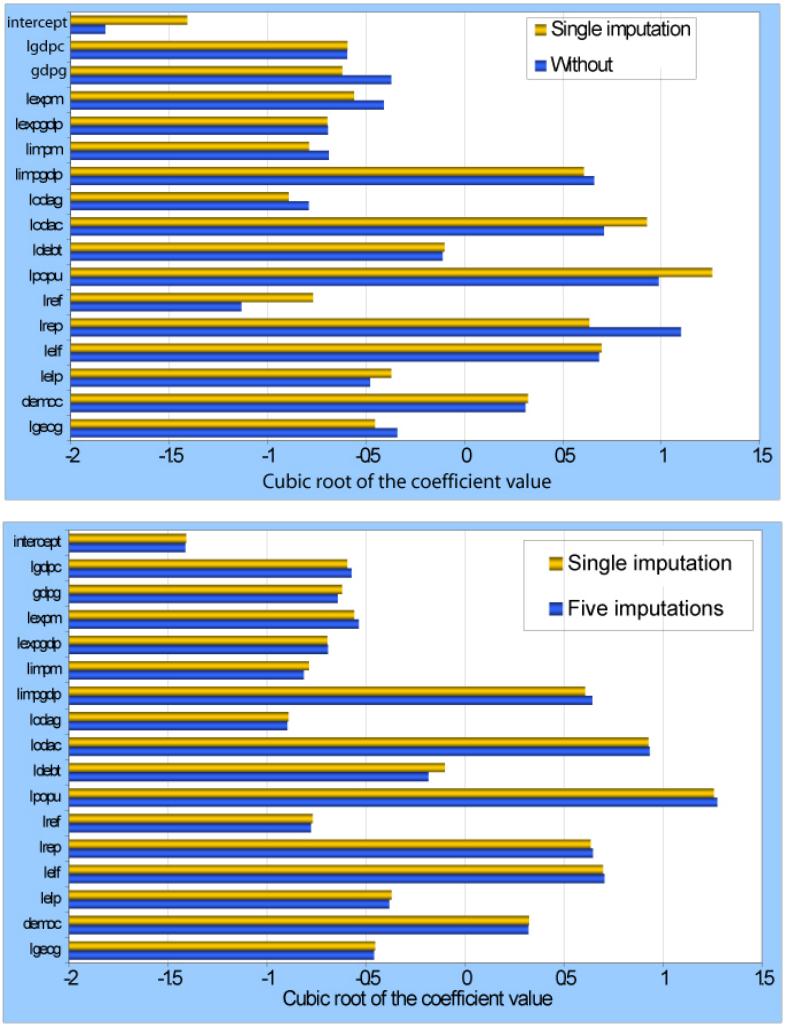

Fig. 1: Comparison of coefficient estimates of model without imputations and model with single imputation (top), and the effect of the number of imputations (bottom).

Alternative specifications of the model

We noted that some factors had unexpected coefficient values in the full models that are detailed in the previous section. Alternative specifications of the model, aiming to reduce multicollinearity effect, were tested.

Firstly, we avoid using simultaneously variables that are expected to measure the same driving force. For example, when the variable *lexpm* that measures the exportation volume is entered into the model, then *limpm* is put aside, and vice-versa, because they are supposed to proxy the trade openness of the country. We found that (results not shown here) the alternative specifications lead to quite similar results with regards to overall fitting quality of the model. The suspected multicollinearity effect was evidenced for some factors even if it did not seem to affect substantially the overall results.

Secondly, we tested a forward stepwise procedure that selects variables on the basis of their explanatory power. Starting with the full model with 16 variables (Model 2), the selection procedure resulted in a 10-variable model, with a Wald χ^2 of 505.1, an adjusted R^2 of 0.22 and

H-L χ^2 of 13.03 (not significant at 5% level). The fact that the model assessment statistics are close to, even better than, those of the full model indicates that some factors are redundant or do not add much more in the explanation of the response variability. The variables that are retained in the final model are *lgdpc, gdpg, lexpm, lexpgdp, lodag, lodac, lpopu, lref, lelf* and *democ*. Variables that were firstly seen as candidates for removal from the model on the basis of their correlation to other variables remain in the model.

It is worth noting however that the correlation coefficients of these variables with the remaining factors are below 0.90. This is in line with the observation made in the previous paragraph and tends to confirm that the multicollinearity effect may be a problem for correlations stronger than the 0.90 threshold.

As a third approach, we replaced in the regression model the original variables by their principal components. The principal components regression has been indeed used by several authors to deal with multicollinearity among explanatory variables (Massy, 1965; Aguilera et al., 2006;Wold et al., 1984; Heij et al., 2007). In usual principal components analysis, fewer components than the number of original variables are selected based on the amount of variance they convey. For regression analysis, the components are selected according to their explanatory power in the model by using the stepwise selection method described in the previous section. The selection of components to use in the regression model lead to 9 out of 16 principal components. It is worth noting that the components retained in the model (Model 3) are not necessary ordered according to their eigenvalues. For instance, in the final model we have the first, second and seventh components, but not the others in between (3rd to 6th). Not surprisingly, the overall statistics of model quality were similar to those of the reduced model obtained from the stepwise variable selection procedure: a Wald χ^2 of 507.3, an adjusted R^2 of 0.22 and H-L χ^2 of 8.6 (not significant at 5% level). The nine components that we retained account for 63% of the total variance in the explanatory variables. The principal component approach and the stepwise variable selection method can be equally applied. The latter method has however the advantage that it is readily interpretable whereas the principal components do not have necessary a clear interpretation in terms of initial variables. On the other hand, the principal components method could be advantageous in the case of strong multicollinearity.

Risk predictions based on structural indicators

We report hereafter results obtained mainly with the method that combines the principal components regression and the stepwise variable selection (Model 3). Estimated probabilities for two periods (2000 and 2004) are mapped on figures 2 and 3. With these periods, we can assess the consistency of our model through time for the recent past. Similarly, we present estimated probability time series for some countries.

To help reading these maps, we list in table 4 the top 20 countries with high estimated probability for armed conflict occurrence. There are 17 countries that are in the top 20 for 2000 and 2004. This shows that the model is consistent over time. These maps show a number of things that merit to be discussed further. Countries like China, India, Brazil and Turkey are reported to have high risk of armed conflict whereas they are usually seen as stable. In fact, all these countries, as well as Indonesia and Nigeria, have large populations and relatively low GDP per capita and have experienced at least one armed conflict –according to the definition we adopted in this study– in the recent past. For instance Turkey has been on war for several years against the PKK (Kurdistan Worker's Party) rebellion; several "small" conflicts have been active up to now in India; Indonesia and Nigeria also have their domestic rebellions still active. The estimated high risk for China and Brazil is obviously due to their large populations because they did not experience any internal armed conflict since 1971, whereas the high risk for Tanzania is obviously due to its very poor economic performance.

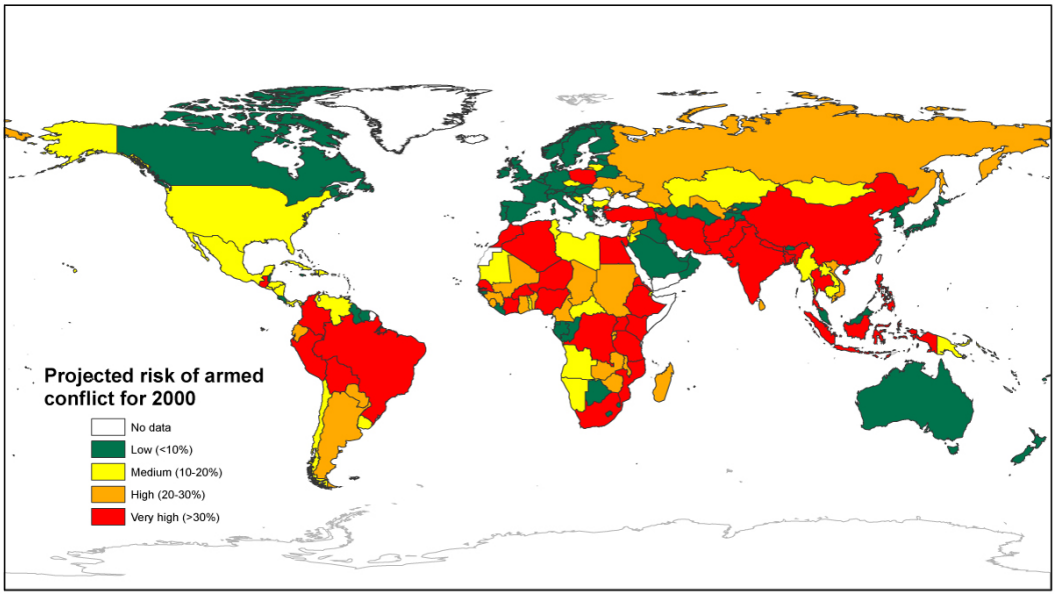

Fig. 2: Risk of armed conflict in 2000 estimated with Model 3 (see text for details on the model).

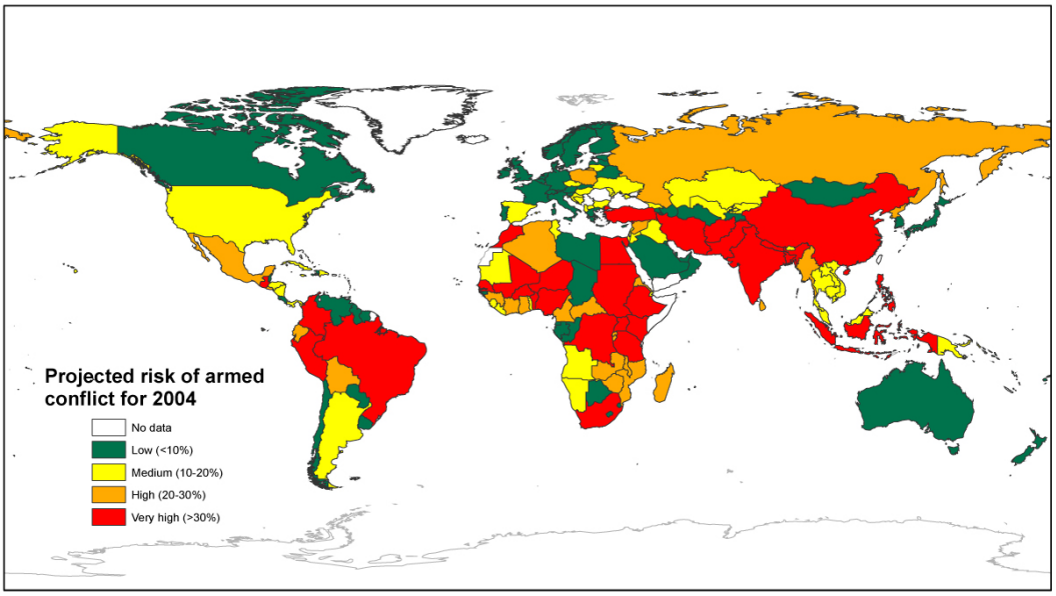

Fig. 3: Risk of armed conflict in 2004 estimated with Model 3 (see text for details on the model).

Table 4: Top 20 countries ranked according to the projected probability of internal armed conflict in 2000 and 2004.

2000		2004	
Country	Probability	Country	Probability
India	0.79	India	0.71
Afghanistan	0.58	Pakistan	0.52
Indonesia	0.54	Morocco	0.49
Congo, Dem. Rep.	0.53	Indonesia	0.45
Pakistan	0.52	Colombia	0.45
Turkey	0.47	Nigeria	0.43
Ethiopia	0.47	Niger	0.43
Morocco	0.46	Kenya	0.43
Brazil	0.44	Bangladesh	0.41
China	0.43	Congo, Dem. Rep.	0.40
Tanzania	0.41	Peru	0.40
Bangladesh	0.41	Nepal	0.39
Egypt	0.41	Brazil	0.38
Nigeria	0.40	Turkey	0.37
Colombia	0.40	Mali	0.37
Nepal	0.39	Burkina Faso	0.36
Kenya	0.38	Guatemala	0.36
Niger	0.37	Tanzania	0.36
Thailand	0.37	Egypt	0.36
Peru	0.37	Ethiopia	0.34

Risk related to previous conflicts

The probability that an armed conflict occurs in a country was estimated on the basis of the history of armed conflicts from 1971 to 2004. As it can be seen on figure 4, this probability was almost constant during the cold war period (until 1991), diminished slightly around 1995 and raised again in early 2000s'. This means that on the global level, the probability to observe an armed conflict has been almost constant with a mean value of 0.73 and a mode of 0.78 (most likely value). Another interesting thing to observe on this figure is that the end of the cold war period is marked by a pick in the number of countries at war (s_i) and in the potential number of countries prone to armed conflict (S_i) whereas the probability p_i of risk related to previous conflict is at the minimum. This means that this period marked a change in the pattern of armed conflicts. If we examine the different components of the number of countries at war each year (figure 5), we can observe that the end of the cold war period is marked by more new armed conflicts than other periods, whereas the number of resolved conflicts in the same period is relatively low. Moreover, in the next years, we observe less new conflicts and more resolved conflicts. It is important to understand that we put in the category of resolved conflicts the countries that were at war during the year under consideration and that have not yet returned to war at the end of the studied period, i.e. 2004. The probability p_i takes into

account this and does not necessary follow the trend of s_i, the number of countries at war. A number of countries that resolved their conflicts between 1990 and 1995, did not actually return to conflict afterward.

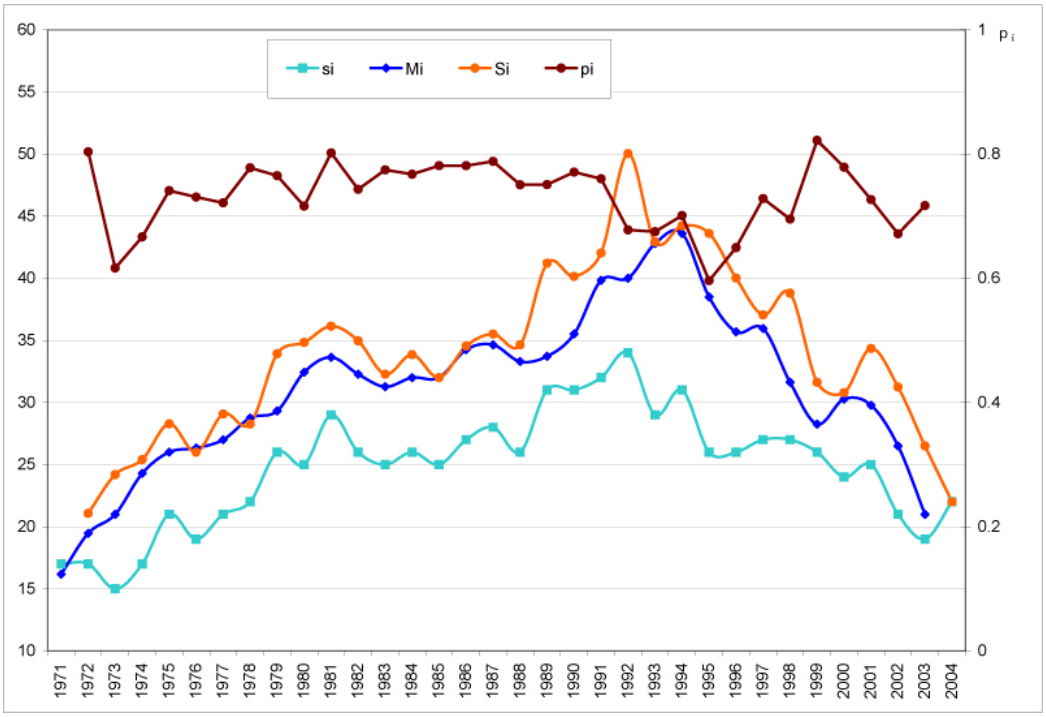

Fig. 4: Evolution of the probability of armed conflict based on the history of conflicts (pi), the frequency of armed conflicts (si), estimate of the number of countries prone to armed conflicts (Si), and estimate of the number of countries that are prone to two or more episodes of armed conflict (Mi).

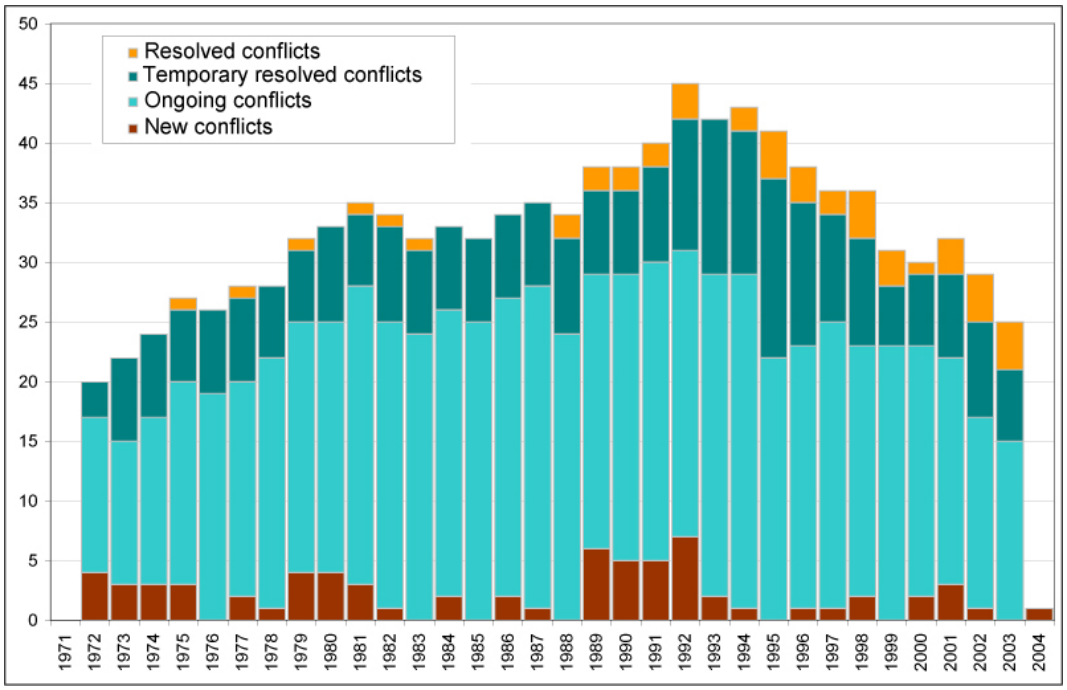

Fig. 5: Evolution of the total number of countries involved in or are prone to an armed conflict each year with a breakdown into different categories (new, resolved, temporary resolved and ongoing conflicts). Note that some categories can not be calculated for the first and last years (1971 and 2004, respectively). For instance, it is not possible to calculate the number of new conflicts in the first year of the period under consideration, and the number of resolved conflicts for the last year.

The risk α_{kj} related to previous conflict is calculated as follows. Let's consider i the first year the country j has experienced a conflict ($Y_{ij} = 1$), and $k>i$ so that $Y_{kj} = 0$. Then,

(3) $$\alpha_{ij} = \prod_{l=i}^{l=k} p_l$$

For each country and for each year, we estimated α_{ij} the probability of conflict due to the conflict history by applying formula 3. The values of p_i at the first and last years (1971 and 2004) could not be directly estimated. They were replaced by the mode value. We finally took the average value between the probability estimated with Model 3 (structural factors) and that related to the history of conflicts. This can be regarded as the overall risk of armed conflict given the socio-economic situation of the country in the recent past.

Figure 6 shows the map of risk of armed conflict in 2004 as estimated in this study. Countries are classified into four categories with breakpoints defined as follows: low risk (< 10%), medium risk (10 − 20%), high risk (20 − 30%) and very high risk (> 30%). In the context of armed conflicts, we are talking about rare events (the cases represent 7% of the observations), and probabilities greater than 20% can already be regarded as high (King and Zeng, 2001).

The estimates for some countries must be interpreted with caution as their socioeconomic data were actually sparse. This is especially the case for Iraq and Afghanistan. The model can be updated easily as new data become available.

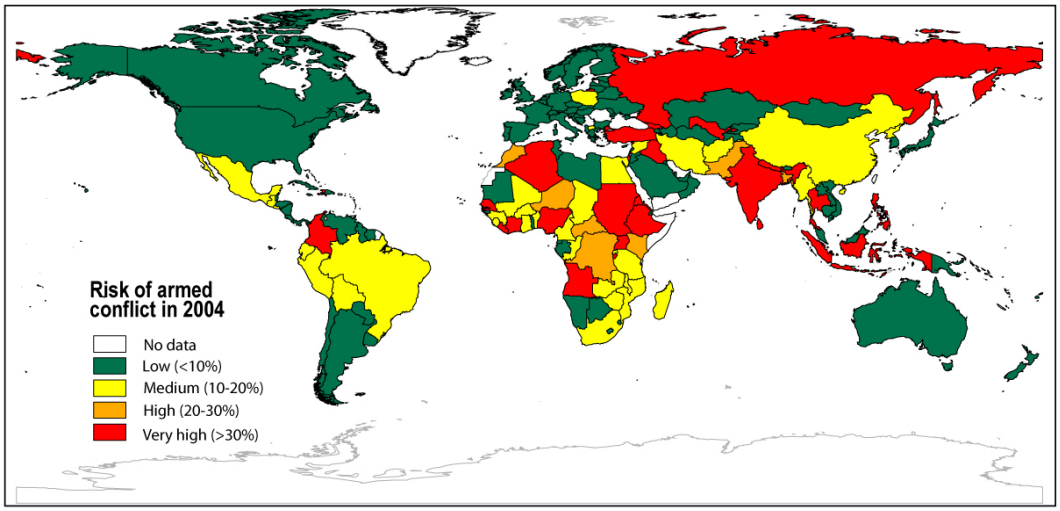

Fig. 6: Risk of armed conflict in 2004 as estimated with Model 3 (see text for details on the model) and adjusted for the effect of previous conflicts.

On the basis of these results, we can note that the ten countries with highest risk are in the order India, Indonesia, Colombia, Nigeria, Nepal, Turkey, Ethiopia, Uganda, Sudan and Philippines. All these countries have indeed strong central governments that have been challenged for a long time by different kind of rebellions. They will perhaps never explode into total war and collapse, but they remain in somehow fragile. We think however that the model overestimate the risk for India and Turkey. Their estimates are systematically high for the last 20 years, even 30 years for India. In the same time they showed a remarkable economic development. These countries succeeded in keeping at low level the influence of their rebellions and concentrating to economic development rather than trying to resolve all conflict cases before moving ahead for economic activities. If they maintain the current economic growth, the rebellion activities could be significantly lowered by the fact that the central government will have more capacity for security forces and incentives for rebellion supporters to take part and benefit the country's economic prosperity. Low intensity conflicts

can maintain without really destabilising the country. Such situations have been observed in Spain (Basque country), France (Corsica), Northern Ireland, etc.

Conclusion

At the beginning of this paper we hypothesized that a number of widely used structural indicators might be strongly correlated with the risk of armed conflict in a country. Our study findings were that despite widespread discussion in academic papers, the most commonly used indicators (GDP growth rate, official development assistance, level of foreign investment, population size, level of democracy, social fractionalisation/ polarisation) did not unequivocally emerge after regression analysis as causal factors, in part due to multicollinearity effects. Future work can address the reasons for these inconsistences with the initial hypothesis. Nevertheless, the method outlined may be used operationally for estimation of conflict probability and for prediction of conflict for countries for which structural data exists. Estimated probability times series show, that our model is consistent over time. Recognising the dependence of such predictions on data availability and quality, we have also described a procedure for imputation of missing data, which produced adequate results.

References

A. Aguilera, M. Escabias, and M. Valderrama. Using principal components for estimating logistic regression with high-dimensional multicollinear data. Computational Statistics and Data Analysis, 50(8):1905–1924, 2006.

N. Beck, G. King, and L. Zeng. Improving quantitative studies of international conflict: A conjecture. American Political Science Review, 94(1):21–35, March 2000.

D. S. Bennett and A. C. Stam. Research design and estimator choices in the analysis of interstate dyads. Journal of conflict resolution, 44(5):653–685, October 2000.

C. Burnley and D. B. F. Kayitakire. Conflict risk assessment based on structural indicators. Report, European Commission - Joint Research Centre, 2007.

P. Collier and A. Hoeffler. On the incidence of civil war in Africa. Journal of conflict resolution, 46(1):13–28, August 2002.

P. Collier and A. Hoeffler. Greed and grievance in civil war. Oxford Economic Papers, 56(4):563–596, October 2004.

J. Davies and T. R. Gurr. Preventive Measures: Building Risk Assessment and Crisis Early Warning Systems. Rowman & Littlefield, 1998.

I. Elbadawi and N. Sambanis. How Much War Will We See? Explaining the Prevalence of Civil War. Journal of Conflict Resolution, 46(3):307–334, 2002.

J. D. Fearon. Primary Commodity Exports and Civil War. Journal of Conflict Resolution, 49(4):483–507, 2005.

J. D. Fearon and D. D. Laitin. Ethnicity, insurgency, and civil war. American Political Science Review, 97(1):75–90, February 2003.

K. Gleditsch and M. Ward. Visualization in International Relations. In A. Mintz and B. Russett, editors, New Directions for International Relations: Confronting the Method of Analysis Problem, pages 65–91. Lexington Books, Lanham, MD, 2005.

N. P. Gleditsch, P. Wallensteen, M. Eriksson, M. Sollenberg, and H. Strand. Armed Conflict 1946-2001: A New Dataset. Journal of Peace Research, 39(5):615–637, 2002.

J. A. Goldstone, R. H. Bates, T. R. Gurr, M. G. Marshall, J. Ulfelder, and M. Woodward. A global forecasting model of political instability. In Annual meeting of the American Political Science Association, Washington, D.C., September 2005.

W. Hauge and T. Ellingsen. Beyond Environmental Scarcity: Causal Pathways to Conflict. Journal of Peace Research, 35 (3):299–317, 1998.

H. Hegre and N. Sambanis. Sensitivity analysis of empirical results on civil war onset. Journal of Conflict Resolution, 50 (4):508–535, 2006.

C. Heij, P. J. Groenen, and D. van Dijk. Forecast comparison of principal component regression and principal covariate regression. Computational Statistics & Data Analysis, 51(7):3612–3625, April 2007.

D. Hosmer and S. Lemeshow. Applied Logistic Regression. John Wiley & Sons, New York, 2000.

J. C. Jenkins and D. Bond. Conflict-carrying capacity, political crisis, and reconstruction. a framework for the early warning of political system vulnerability. Journal of conflict resolution, 45(1):3–31, February 2001.

G. Jolly. Mark-recapture models with parameters constant in time. Biometrics, 38(2):301–321, 1982.

D. Kaufmann, A. Kraay, and M. Mastruzzi. Governance Matters V: Governance Indicators for 1996–2005. Technical report, The World Bank, New York, 2006.

G. King and L. Zeng. Explaining rare events in international relations. International Organization, 55(3):693–715, 2001.

W. Massy. Principal Components Regression in Exploratory Statistical Research. Journal of the American Statistical Association, 60(309):234–256, 1965.

J. G. Montalvo and M. Reynal-Querol. Ethnic polarization, potential conflict, and civil wars. The American Economic Review, 95(3):796–816, June 2005.

M. Mousseau, H. Hegre, and J. R. O'neal. How the Wealth of Nations Conditions the Liberal Peace. European Journal of International Relations, 9(2):277–314, 2003.

N. Nagelkerke. A note on a general definition of the coefficient of determination. Biometrika, 78(3):691–692, 1991.

M. Reynal-Querol. Ethnicity, Political Systems, and Civil Wars. Journal of Conflict Resolution, 46(1):29–54, 2002.

J. Schafer and M. Olsen. Multiple Imputation for Multivariate Missing-Data Problems: A Data Analyst's Perspective. Multivariate Behavioral Research, 33(4):545–571, 1998.

P. Schrodt and D. Gerner. Cluster-Based Early Warning Indicators for Political Change in the Contemporary Levant. American Political Science Association, 94(4):803-817, 2000.

G. Seber. The estimate of animal abundance and other related parameters. Griffin, London, 1982.

H. Urdal. People vs. Malthus: Population Pressure, Environmental Degradation, and Armed Conflict Revisited. Journal of Peace Research, 42(4):417–434, 2005.

S. Wold, A. Ruhe, H. Wold, and W. Dunn III. The Collinearity Problem in Linear Regression. The Partial Least Squares (PLS) Approach to Generalized Inverses. SIAM Journal on Scientific and Statistical Computing, 5:735, 1984.

C. Yiu and N. Mabey. Countries at risk of instability: practical risk assessment, early warning and knowledge management. Background paper. Prime Minister's Strategy Unit, United Kingdom, February 2005.

Conflict Mapping in Kosovo

Christof Roos & Dirk Buda*

European Commission, Joint Research Centre, Institute for the Protection and Security of the Citizen (IPSC), Support to External Security Unit, Ispra 21027 (VA), Italy

* dirk.buda@ec.europa.eu

Objectives

- Integrate information on conflict events in Kosovo during 2005/2006 and ongoing Community assistance into an interactive map;
- Evaluate potential impact of conflict events on Community assistance.

Results

In the context of the ongoing negotiations on the final status of Kosovo, a project of mapping conflict in Kosovo was carried out. in co-operation with FAST/Swisspeace (period: 2005 and 2006). Given that data/information on conflict from UNMIK or KFOR was not available and that obtained from OSCE not suitable (not sufficiently pre-structured and geolocated), information on conflict events in Kosovo was purchased from FAST/Swisspeace (period: 2005 and 2006). This data was further processed by the JRC (geolocation, conflict category, actor, target/background etc), integrated into a database and mapped. A website was established providing access to this data:

http://global-atlas.jrc.it/kosovo/main.htm

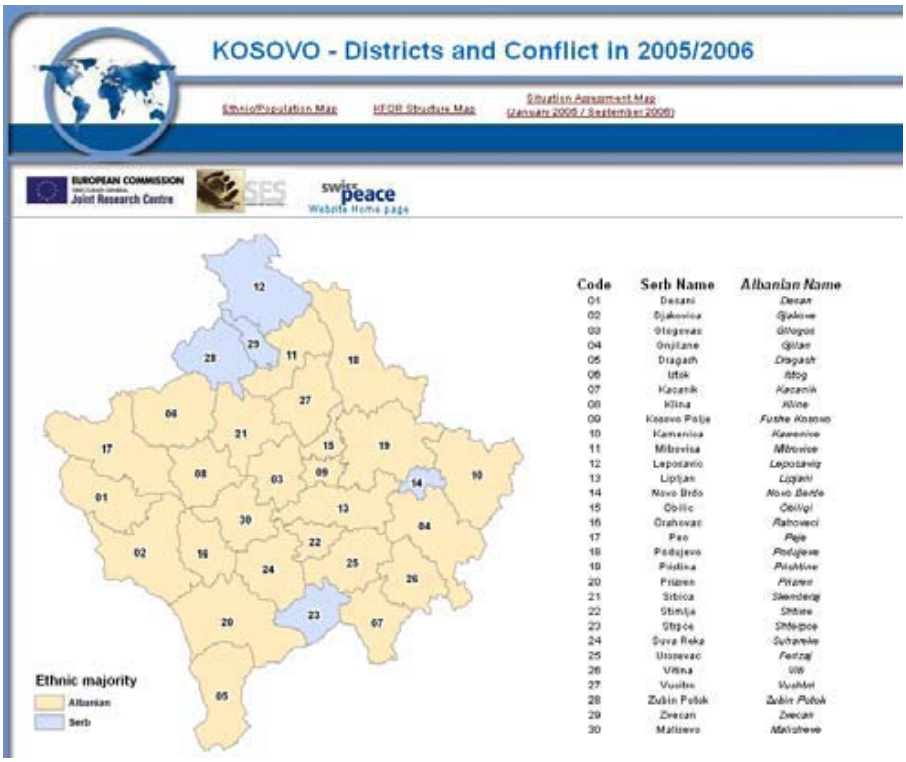

Fig. 1: Kosovo Conflict Maps

When clicking on a given district, the geolocated data both for events of violent conflict (use of force) and selected other conflict events (sanctions, demonstrations etc), classified in accordance with the Swisspeace Event Coding System, are provided in a chronological order:

Mitrovica/Mitrovice

Total events reported: **36**
Violent events: **16**
Other events: **20**

***Origin: FAST/SWISSPEACE** **KPS**:Kosovo Police Service **KFOR**:Kosovo Force led by NATO **UNMIK**:United Nations Mission in Kosovo

Date	Event Type*	Event Category*	Target/Background	Description*
28 Sep 2006	Call for action	Propose	Serb	Mitrovica. 28.09.2006 US Assistant Secretary of State Daniel Fried during a meeting with political leaders of the Kosova Serb community called on the Serb community to join the Kosovar institutions. They discussed about the current situation in Kosova and the future status process. Fried is quoted saying that there will be no partition of Kosova, but a decentralisation so that people can control their lives.
28 Sep 2006	Criticize or denounce	Accuse	Albanian	Mitrovica. 28.09.2006 UNMIK regional administrator in Mitrovica Gerard Galluci accused Albanians of the latest incidents in Mitrovica. He said that a 16-year-old Albanian was arrested right after the attack against 'Dolce Vita' bar for throwing a bomb, and the last incident on the bridge was also provoked by Albanians, and for that there is evidence.

Fig. 2: Events at District level

The database was updated in 2006 on a quarterly basis (now dataset integrated until 31.12.2006). It also contains several static maps on the level of violent and non violent events by municipality and maps on KFOR as well as the ethnic composition in Kosovo.

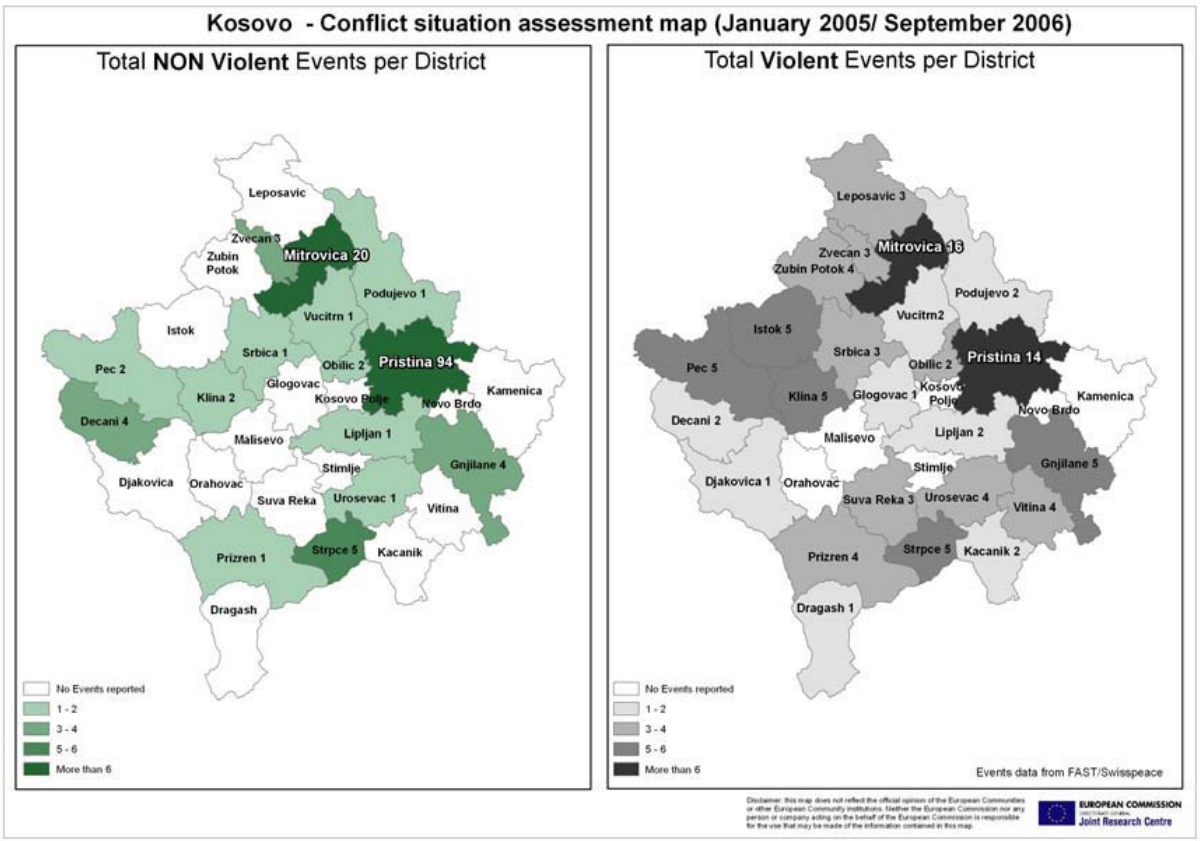

Fig. 3: Kosovo Conflict Assessment Map

Overall, 2006 (as 2005) was marked by a rather low level of conflict, in particular regarding the number of violent events (use of force). Therefore and because it proved difficult to obtain relevant data on Community assistance local/regional projects), no assessment was made of potential impact of local conflict on Community assistance.

Computer Science Challenges for Retrieving Security Related Information from the Internet

Richard Göbel[1]*, Antonio de la Cruz[2]

[1] *Hochschule Hof, 95028 Hof, Germany*

[2] *European Satellite Center – EUSC, 28850 Torrejon de Ardoz, Madrid Spain E-28850*

* richard.goebel@fh-hof.de

Abstract

The Internet becomes increasingly important as a source of information for disaster prevention and disaster management. Starting point for the acquisition of information from the Internet are usually search engines. Current search engines, however, fell short to provide sufficient support in this context. A key issue is the missing support for spatial search criteria. Without spatial search criteria it is difficult or even impossible to define sufficiently precise conditions for retrieving documents referring to a certain location.

This paper proposes a concept for a spatial search engine in this application concept and discusses the challenges for implementing such a concept. In particular the document focuses on so called index structure facilitating efficient searches using both textual and spatial criteria. The paper introduces a new hybrid index structure overcoming the weaknesses of existing indexing methods.

Introduction

Disaster prevention and disaster management both require complete pictures of usually complex situations for decision makers. The required information typically comes from a wide range of data sources. As an example this information may come from aid workers, local authorities, local sensors and remote sensing. The Internet is increasingly used as well because it supports fast access to recent information on the context of an evolving crisis. Of specific interest are news paper articles providing for example information on events (e.g. increasing number of criminal or terroristic activities), economical and environmental key data as well as information on the current social and political environment.

The starting point for an Internet search is often a search engine like Google. Although these search engines already provide an impressive level of support it is still difficult to define sufficiently specific search conditions to reduce the number of irrelevant documents in a search result. The key issue here is the limitation of search engines to so called full text searching. A full text search defines a set of terms (word or phrases) where some of these terms need to be contained and other are not allowed being present in a document. Unfortunately this approach fails short to support basic search conditions like time and space which are essential for security related applications. This means that a search condition like "return all documents containing the phrase 'terror attack' and the word 'pipeline' referring to locations in 'Iraq' in the 'year 2006'" cannot be formulated due to the reference to locations in Iraq and the time frame 'year 2006'.

The support for time in search engines is not difficult and already supported in several specialized news search engines. The support of spatial search conditions is however not yet available on an operational basis. The two key problems are the derivation of positions for a document from its content (geo-coding) and the fast access to a large number using search conditions combining space and time (efficient searching).

A reliable geo-coding would require a full semantic analysis of a text which is probably very difficult according to the state of the art of language processing. Nevertheless already more simple solutions will help which assign documents also to few wrong locations in addition to the real location. This approach would return some wrong documents in addition to every valid search result which is probably acceptable for a search engine.

Supporting efficient search in a large number of documents is however a key issue for spatial search engines since quick response times are a key requirement in this application context. In fact very little is known about efficient searching for combined textual and spatial search criteria. Therefore one focus of our research is on hybrid index structure facilitating efficient searching.

This paper summarises the current state of the art in geo-coding and indexing related to this application context. The paper also includes experiences from first experiments with algorithms for geo-coding and index structures which were performed via a first prototype. From the experiences gained with index structure this paper proposes a new index structure which will most likely reduce search times significantly for combined textual and spatial searching.

The next chapter introduce a concept for a spatial search engine. The following two chapters discuss the geo-coding and the index challenge for spatial search engines. The last chapter provides some application examples clarifying the potential application context of this technology.

Search Engine Concept

Today the Internet is the starting point for the search of information in nearly every domain. Search engines like Google provide good access to this wealth of information by supporting full text searches. A full text search facilitates the finding of all documents containing one or more given terms (words or phrases). Modern search engines support also additional criteria as for example the combination of terms via Boolean operators, automatic extension of search conditions with similar terms or the restriction of searches to certain sites.

A search engine typically includes at least the following components:

- A Crawler navigates the Internet by starting at a given set of URI's and retrieving all documents reachable directly or indirectly from these initial URI's. The Crawler may be further divided into a Finder following URI's, a Document Builder aggregating documents from these URI's and a URI Database providing the initial URI's and further parameters. The Crawler may also provide an administration interface for setting all needed parameters.
- The Data Archive holds all information about documents needed to support searches. For this purpose an Analyser extracts terms and phrases together with auxiliary information (e.g. document metadata) and stores this information in a Metadata Database. If needed also the found documents could be stored in a Document Archive. A Search Engine provides the search functionality on top of the Metadata Database and Document Database
- A User Interface (typically a web interface) provides access to the Search Engine for end users.

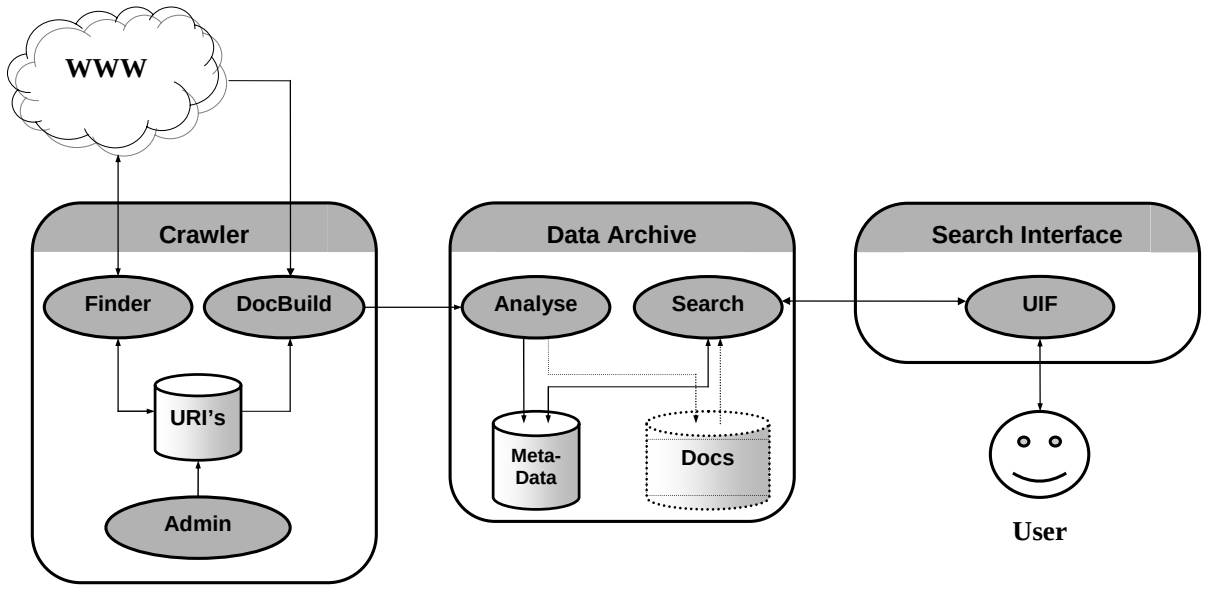

Fig. 1: Components of a typical search engine

The support of spatial search criteria requires several extensions for this concept:

- The Analyser needs to be extended to derive geographical positions for a document if the document refers to positions. This process is often called geo-coding or geo-referencing.
- The Metadata Database needs to manage geographical positions in addition to words and phrases. The efficient support of combined search criteria is not obvious in this context (e.g. find all documents containing the term "Nuclear Thread" referring to "Iran").
- The User Interface needs to support the specification of locations in addition to the provision of terms and phrases.

The key challenges for the implementation of a spatial search engine are the geo-coding of documents and the efficient support of combined spatial and textual search criteria. The implementation of an appropriate user interface is, however, straight forward.

The geo-coding would be simple if documents provide already their geographical position for example via geotags (see for example [9]). Although an increasing number of web pages use this concept, most documents from the Internet do not yet provide their positions. Even in the foreseeable future a large number of documents will not provide this information. Therefore different approaches are investigated for deriving the position automatically from a text (see for example [1], [11] and [12]). A fully correct approach in this context is currently out of scope according to the current state of the art of natural language processing. Nevertheless a sufficiently reliable method would be sufficient for a search engine since human users need to analyse the found documents anyhow to identify relevant documents. But even this goal is not easy to achieve for a general purpose search engine.

The other key topic is the efficient support of combined spatial and textual search criteria. Efficient access to data in databases is usually supported by so called index structures. These index structures support the navigation to search results without the need to check every single entry separately. So far very little is known about specific index structures for this purpose. A very early result is given in [20]. This approach is discussed together with a new concept for an improved index structure in chapter 5.

A general spatial search engine is still difficult to implement. A search engine for a limited domain seems to be, however, more feasible. In the case of the security domain the search engine would focus probably on a limited number of web sites providing just news articles.

Usually news articles define their positions by place names (typically via a city or larger town). In this case the geo-coding procedure could focus on the identification of relevant place names in a document. The place names would be mapped to geographical point positions using a so called Gazetteer. Even though this approach still generates some challenges (see chapter 4) the geo-coding is significantly easier than in the general case.

The limitation of the search engine to selected sites reduces the efficiency challenge for combined spatial and textual searches. Also the limitation to point positions for documents eases the development of an appropriate index structure.

Geo-coding of Documents

The Analyser needs to extract words and phrases from the document. In our case it needs to derive also a spatial reference given by geographical coordinates. For this purpose the Analyser identifies place names using a gazetteer.

A simple Analyser could generate a position for every found place name and link it to the document. Already this approach would facilitate the search for regions which are not directly mentioned in the document. As an example a search for "Iraq" would also return all documents containing the word "Baghdad".

Using this simple analysis would result in many mismatches as well:

- Certain terms would be misinterpreted as place names because they have the same spelling as entries from the gazetteer. As an example the term "BUSH" could be considered as the name of a person, a plant or a place name ("place name twins").
- Most place names are not unique ("ambiguous place names"). As an example "Paris" could be the name of the capital of France or a town in Texas.
- A document may contain different place names. In this case it is not clear to which location the document refers ("multiple place names"). As an example the sentence:

  "In contrary to previous attacks in and around Baghdad the target of the current attack in Basra was not a military infrastructure"

  contains the place names "Baghdad" and "Basra". From the sentence it becomes however clear that the article would probably refer to Basra and not to Baghdad.
- In some cases a document contains relative positions ("relative positions"):

  "The target of this terror attack was a pipeline 60 km south of Baghdad"

All these issues have been investigated in depth by [12]. A complete resolution of the mentioned problems would be possible by analysing the semantic of a document. A fully reliable text understanding method is however not yet available and currently beyond the capabilities of science and technology. Therefore methods need to be selected and/or developed which remove some of these invalid references without removing too many correct references.

In general methods for removing invalid references could make use of the following additional information:

- Source of a document: In some cases a source of the document limits the set of place names which can be expected. As an example articles from a regional newspaper will primarily contain place names from the related region. This means that the analyser may use only place names of this region from the Gazetteer (probably together with some general place names).
- Context of a place name: The context of a candidate place name inside a document consists of words before and after this place name. This context could be used to distinguish valid place names from "place name twins". As an example place names will be often used together with "location terms" (e.g. "in", "around", "close", etc.). In English the analyser may also take advantage from the fact that place names start with a capital letter.
- Information about place names: Most Gazetteers provide further information about the role of a place name (e.g. capital, major city, minor city). This information could be used to rank place names and to keep only the highest ranked locations. This is in particular important for a single ambiguous place names referring to different locations.

All information together would need to be used to remove unlikely location candidates avoiding too many mismatches. The use of this information by the Analyser will however be configurable to balance the number of false accepts relative to false rejects.

A first implementation for the prototype included the following ideas:

- Geographical positions start with a capital letter in English
- No stop words like "and", "this", "for", etc. are accepted as place names even if they occur in a Gazetteer (language specific).
- A frequent place name in a document wins over an infrequent place names
- Larger and more important locations win over smaller and less important place name (e.g. the capital of France is assumed instead of a town in Texas if Paris is found in a document).

Further rules were implemented after first experiments with the prototype of a search engine:

- Short words (less than 3 characters) are ignored as place names even if they occur in the Gazetteer
- Words following a full stop are not accepted as a place name
- Words completely in upper case are not accepted as place names
- Acronyms followed by bracketed acronym explanations are ignored for geo-coding process. Example: "DoD (Department of Defense)"

The implemented methods already provide reasonable result in some but not all situations. Further work is currently performed to reduce the number of mismatches and to widen the scope of the methods to more documents.

Index Structure

A key challenge for the spatial search engine is the management of a very large metadata database containing the terms, phrases and geographical positions of all analysed documents. The metadata database needs to facilitate fast searching via the user client. Key for fast searching is a so called "index structure". Index structures support quick navigation to search results avoiding the checking of every individual entry. A typical index structure is the B-Tree

(see [3]) which is available in every Object/Relational Database Management System. Text Databases use an "Inverted Index" which is more appropriate in this context. An inverted index manages a set of terms where every term points to all documents containing it. This approach might be combined with other index methods (e.g.: [15], [16]) to improve efficiency (e.g. for substring searches).

Spatial searches are usually supported by the so called R-Tree (see [7]). Although R-Trees are probably the best index method for spatial searches at present, it is difficult to ensure fast response for very large databases in every case (see for example [18]). For some special cases however this tree could be optimised to meet efficiency requirements (see for example: [6]).

The spatial search engine needs to support search conditions combining textual and spatial search criteria. This means that also specific search indexes need to be available for this purpose. In general three different options are possible:

1. Independent indexes are built for the spatial criteria and the full text search. Separate searches are executed for every criterion. The intersection of all intermediate result sets will provide the final result set. The approach for generating the intersection would probably use a marking algorithm or bit lists. Note that this approach is slow if very large intermediate result sets need to be handled.
2. The index structures for spatial and full text search are connected with each other. One approach is a single R-Tree containing all locations and every location is the starting point for an inverted index organising documents related to this location (option 2.1). The other approach is an inverted index where every term is a starting point for an R-Tree organising the geographical positions of documents with this term (option 2.2).
3. A search could be supported by a single index managing both positions and terms in a single tree.

The existing prototype uses an index structure starting with an R-Tree containing all geographical locations. Every geographical location in this tree points to an inverted index managing all documents for this location (option 2.1). This option and the other option 2.2 were also described in [20]. The paper [20] compares these two structures by applying them to some test data. These first tests seem to indicate that searches can be processed faster for option 2.2. This paper, however, does not provide any worst case analysis for time and space. In particular the space requirements are not considered at all.

A formal worst case analysis requires the precise definition of a complexity measure. In this particular case it makes sense to relate the search effort with the number of nodes which need to be visited in the index structure. In addition the number of results for a search needs to be considered as well since a large result set will also justify the navigation to a larger number of nodes. Therefore it probably makes sense to define the complexity measure as follows:

- If a search returns at least one result then the measure is the number of visited nodes divided by the number of search results.
- If a search returns no search results, then the measure is the number of visited nodes.

With this measure the processing of a search is inefficient if a large number of nodes are visited while the search returns only few or even no results. The worst case would be if all nodes of the index structures need to be searched even though the search does not return results.

Unfortunately the worst case cannot be avoided for option 2.1. This worst case may occur for a large geographical region where most or even all nodes of the R-Tree need to be searched. If

we further assume a word which does not occur in any document then all nodes of the R-Tree and all connected inverted indexes need to be searched without returning any search results.

On the other hand the space requirements for option 2.1 are moderate. The space requirements for an R-Tree are usually acceptable. If we assume that every document refers only to a small number of p positions then a document will be considered by not more than p inverted indexes connected to the R–Tree. This moderate amount of redundancy is probably acceptable.

Option 2.2 is clearly more efficient. With this approach the search word is used in the initial inverted index to identify a specialised R-Tree containing all positions of documents containing this particular word. Then the search continues only in this R-Tree. Here the search complexity depends on the search efficiency for R-Tree. The method from [6] could for example ensure a search time growing logarithmic with the number of positions in the R-Tree in some cases.

Unfortunately the space requirements of option 2.2 are prohibitive for a general application of this index structure. Many words will occur in a large number of documents resulting in very similar R-Tree for these words. This means that this index structure will have a high degree of redundancy and the space requirements grow significant faster than linear with the number of documents managed by the index structure.

According to this analysis option 2.1 is probably the only feasible solution so far. This option ensures reasonable access times for small geographical regions. Nevertheless an improved solution is needed for the general case combining efficient search times with moderate space requirements.

To overcome the weaknesses of both options this paper proposes a new index structure combing textual and spatial criteria in one node. Here a node will define:

- lower and upper bounds for the longitude of a circumscribing rectangle
- lower and upper bounds for the latitude of a circumscribing rectangle
- bitlist indicating words contained in all documents for a subtree starting with this node

An index structure using these nodes could be generated as follows:

1. Derive document descriptions for all documents. These descriptions contain references to the original document, one or more geographical positions defined by their longitudes and latitudes and the contained words (e.g. organised via a Patricia Tree [16]). The index structures will point to these document descriptions and not to the original documents.
2. Generate an inverted index for all documents with terms pointing to document descriptions. The index will be generated in main memory using an appropriate search structure for term (e.g. a Patricia Tree).
3. Shift all documents pointing to less than r documents (e.g. r = 100) to an index for “rare terms”. Searches containing rare terms will only use this index structure. All other search conditions (further terms and geographical region) are directly checked against document descriptions.
4. Generate a bitlist for the remaining index. The first bit indicates the presence of the first word from the inverted index, the second refers to the second word, etc.
5. Generate a single R-Tree for all locations. The positions in all leaf nodes point to the corresponding document descriptions. All nodes of the R-Tree already contain empty bitlists (with zeros at all positions).

6. Add an appropriate bitlist for every document description indicating which words are present in this description with the exception of rare terms.
7. Compute the bitlist for every leaf node of the R-Tree by joining the bitlists of the referenced document descriptions (using logical OR).
8. Compute the bitlist of every inner node of the R-Tree by joining the bitlists of all subnodes which were already processed using logical OR).

This index structure would reduce redundancy significantly but still facilitate efficient searching. A problem is the large node size due to the contained bit list. If we consider bitlists for 100,000 words then the bitlist would have a size of more than 12 Kbytes. The size of the bitlist can, however, be reduced if we allow a certain degree of redundancy. For this purpose the inverted index would be split into parts which contain not more than a predefined limit of l words after step 3. Each part is characterised by a lower bound and an upper bound containing all strings of the corresponding inverted index according to the lexicographical ordering on strings. The next steps are performed for all split indexes. This means that a separate R-Tree needs to be generated for every tree.

The formal analysis of this new index structure is a bit more complex than for the previous one. Again we need to analyse the number of nodes which need to be visited here. For this purpose we consider nodes of every level (same depth counting from root node) from an index structure separately. In addition we split the set of nodes which need to be visited into two sets:

- Nodes N+ contributing at least one item to the search result
- Nodes N- contributing no item to the set of search results

As a first observation we can state the size of the result R is an upper bound for the N+ nodes because every of these nodes contributes at least as single item to the result set:

$$|R| > |N+|$$

This also means that N+ grows not faster than linearly with the size of a result set and not at all with the number of items in a database.

Now the key question is whether an upper bound can be found for the number of N- nodes. If this set is limited by a constant c not dependent on the total number of nodes (growing proportional with the number of entries) then the number of visited nodes grows only linear with the size of the result set and not at all with the number of entries. If we assume log(|E|) levels (E set of entries) for a search tree then the search effort is limited by log(|E|)*(|R|+c).

Our index structure is basically a two dimensional R-Tree containing additional bitlists. All nodes of such a two dimensional R-Tree can be considered as rectangles in two dimensional space, where the sorted value spaces of the involved columns represent the two dimensions. A rectangle defines lower and upper bounds for both dimensions. A rectangle of a parent node includes all rectangles of its child nodes and the leaf nodes contain entries as points. Note that for an R-Tree all rectangles are minimal (minimal bounding rectangle). A search condition is also a rectangle (search rectangle). A search starts at the root node and continues recursively at all child nodes which overlap the search rectangle. On the leaf level all points are checked for the search condition.

With this structure some of the theoretical results for R-Trees are also applicable in this case. Of particular interest are the results from [6]. This paper introduces constraints for which the search time grows not faster than logarithmic with the number of entries. For this purpose the paper makes the following assumptions:

- Two distinct nodes from a single level of the R-Tree do not strongly overlap. This means that edges or corners may meet but there is no common inner point for two nodes.
- The form for the bounding boxes of all nodes needs to be optimised according to the forms of the expected search region. This means that the ratio of nodes needs to deviate at maximum by a chosen factor k from the ratio of envisaged search conditions.

With these preconditions the paper divides the number of nodes overlapping with a search range into three different categories:

- The set EGDE contains all nodes for which an edge is fully included in the search region. In the two dimensional case an edge contains always a point position (otherwise a tighter rectangle would be possible for the node). This means that the search region contains at least one point (entry) and this node is member of the set N+.
- The set CORNER contains all nodes overlapping at least one corner of the search region. If these nodes do not strongly overlap, every corner is not overlapped by more than 4 nodes. This means that the set CORNER contains not more than 4 □ 4 = 16 nodes.
- All other nodes overlapping the search region belong to the set CROSS. These nodes have a shorter edge in one dimension and a larger edge in the other dimension than the search region. The overlap has the form of a cross (see figure 2).

The number of nodes in the set CROSS depends on the on the deviation factor k defining the maximum allowed differences between the form of nodes and search regions. The paper proofs that this set does not contain more than 6k+12.

The two sets CORNER and CROSS form together the set N- which contains not more than 6k+28 nodes. As a consequence the total number of nodes which need to be visited is limited by log(|E|)*(6k+28+|R|)

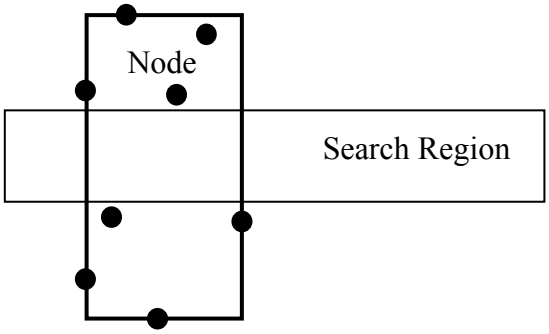

Fig. 2: Cross Overlap

A tree packing method generating optimised R-Tree structures according to these requirements is also provided in [6]. It should be noted that this packing method does not always guarantee the required form for all nodes. But for nearly all sample data sets the method could ensure the required form for all nodes apart from very few exceptions.

The processing of the spatial part of a search condition would follow exactly these rules. In a similar way a pure textual search only continues the search at nodes where the bit for the search term is set. This means that we can expect at least a single document below this node containing the search term. This also means that the set N- is empty in this case.

Unfortunately this situation is not given for a combined search. If we just consider leaf nodes then the spatial search region may overlap a large number of leaf nodes which spatial extend is not fully contained in this search region. This means that some locations from these leaf nodes

are not contained in the search region. In the worst case these specific locations could point to the only documents containing the search term.

The described worst case condition is a very unlucky situation which is unlikely to happen if a larger number of leaf nodes need to be searched. If we assume that terms and locations are not strongly correlated then there is fair chance that a least some locations from searched leaf nodes point to documents with the specified word.

For an average case analysis we need to consider the number b of locations in a leaf node. If we have to search p nodes contributing at least one location to the search region then we can expect at least p/b documents containing the word in average. This means that we need to search at maximum b leaf nodes for finding a single document. As a consequence an upper bound for the average case is log(|E|)*(6k+28+|R|)*b.

Note that this result is not yet satisfactory. We have mixed the upper bound from a worst case analysis (clearly also an upper bound in an average) with a bound from an average case analysis. This approach results in an upper bound which is probably not sufficiently tight for an average case analysis. It would be also interesting to analyse the upper bound for the worst case which grows probably faster than logarithmic for the general case. It should be also investigated under which additional constraints a logarithmic behaviour can be ensured.

The investigation of the proposed index structure is still in a very early stage. Nevertheless first analysis shows promising results. At present an experimental implementation is on its way to perform first tests with data from the search engine prototype.

Application Context and Interfaces

The technology of a spatial search engine will enhance the access to data from the Internet in many different application contexts for disaster prevention and disaster management. Some examples are:

- Collection of background information about specific events in given regions. These events could be natural disaster, technical accidents, terror attacks or conflicts. As an example a query may address articles on terror attacks to pipelines in Iraq.
- Continuous Monitoring of a given region by visualizing events in a map triggered by articles with predefined keywords. This approach might be for example useful for the monitoring of border conflicts in critical areas.
- Harvesting of information from the Internet about activities in a crisis region which are not directly related to the disaster but may influence aid operations. In the case of an earthquake it may be useful to know about festivals or other organized events to assess the number of affected person and to focus help activities in the right region.
- Monitoring of activities around critical infrastructure. Here the system may collect articles in the area around this infrastructure containing specific keywords. As an example the system may collect articles on unusual events like unauthorized persons entering a secure area or vehicles parking in prohibited areas. A significant increase of these types of events could then trigger an alarm.

In general applications of the spatial search engine technology could divided in two different areas:

- A conventional search engine provides a passive interface waiting for user triggered searches. This means that the search engine will only deliver results after a user has

initiated a search. It is important to understand that the crawler will automatically harvest the Internet even in this context.

- The system could actively provide information to users if the analyzer encounters documents which meet a certain condition. In this case the data is automatically transferred to users for example by an email or the insertion of events in a map.

The initial prototype supported only the first option of a passive interface. Meanwhile another interface has been developed to support the automatic transfer of search results to other systems. This interface provides search results in an internal XML format. This XML format is the basis for the generation of other formats like KML (Google Earth), GML (Geographical Markup Language) or SVG (Scalable Vector Graphics). The transformation to these other formats is defined by providing an appropriate configuration file using XSLT (Extensible Stylesheet Language Transformations). With this approach transformations also in other formats can be easily achieved. So far the visualization of search results in Google Earth could be fully demonstrated.

References

1. E. Amitay, N. Har'El, R. Sivan, A. Soffer: "Web-a-Where: Geotagging Web Content", Proceedings SIGIR'04, ACM Press, pages 273 – 280, Sheffield, UK, 2005

2. Bär: „Implementierung, Optimierung und Vergleich ausgewählter Tree-Packing-Verfahren für den R-Baum im Rahmen einer räumlichen Datenbank", Diplomarbeit, Fachhochschule Hof, 2005

3. R. Bayer, C. McCreight: „Organization and Maintenance of Large Ordered Indexes", Acta Informatica 1(3), pages 173 - 189, 1972

4. R. Göbel: Effiziente Verwaltung geographischer Daten mit räumlichen Datenbanksystemen – Möglichkeiten und Grenzen, Tagungsband AGIT 2005, Salzburg, Wichmann Verlag, 2005

5. R. Göbel, A. Almer, T. Blaschke, G. Lemoine, A. Wimmer: „Towards an Integrated Concept for Geographical Information Systems in Disaster Management", Proceedings First International Symposium on Disaster Management, Delft, Springer 2005

6. R. Göbel: "Towards Logarithmic Search Time Complexity for Two-Dimensional R-Trees", Proceedings of Second International Conference on Systems, Computing Sciences and Software Engineering 2006, Springer, to appear in 2007

7. A. Guttman: „R-Trees: A Dynamic Index Structure for Spatial Searching" Proc. ACM SIGMOD Conference, Boston, pages 47 - 57, 1984

8. P. Hall, G. Dowling: „Approximate string matching" Computing Surveys, 12(4):381-402, 1980

9. Jan Torben Heuer, Sören Dupke: "Towards a Spatial Search Engine Using Geotags", Proceedings GI-Days 2007 - Young Researchers Forum, Florian Probst and Carsten Keßler (Eds.), IfGIprints 30. ISBN: 978-3-936616-48-4, 2007

10. ISO 2788: „Documentation – Guidelines for the establishment and development of monolingual thesauri", International Organization for Standardization", 1986

11. C. B. Jones, A. I, Abdelmoty, D. Finch, G. Fu, S. Vaid: "The SPIRIT Spatial Search Engine: Architecture, Ontologies and Spatial Indexing", Proceedings Third International Conference on Geographic Information Sciences, pages 125 – 139, Adelphi, MD, USA, 2004

12. M. Kimler: „Geo-Coding: Recognition of geographical references in unstructured text and their visualisation", Diplomarbeit, Fachhochschule Hof, 2004

13. C. Kohlschütter: „The Fuzzy Gazetteer - A world wide place name searching engine supporting imprecise queries", Internal Project Report, Fachhochschule Hof, 2002

14. K.V.R. Kanth, A.K. Singh: „Optimal Dynamic Range Searching in Non-replicating Index Structures", Proc. International Conference on Database Theory, LNCS 1540, pages 257-276, 1999

15. E. McCreight: „A space-economical suffix tree construction algorithm" J. ACM, 23(1): 262 - 272, 1976

16. D. R. Morrison: „PATRICIA - Practical Algorithm To Retrieve Information Coded in Alphanumeric", J. ACM 15(4): 514-534, 1968

17. S. Neupert: „Entwurf und Realisierung einer räumlichen Datenbank auf der Basis optimierter R-Bäume", Diplomarbeit, Fachhochschule Hof, 2005

18. K.V. Ravi Kanth, A. Singh: "Optimal Dynamic Range Searching in Non-Replicating Index Structures" Proc. International Conference on Database Theory, pages 257 - 276, Springer Verlag Berlin Heidelberg, 1999

19. S. Rill: „SARA Semi Automatic Research Archiv - Entwicklung eines Konzepts zur ortsbezogenen Archivierung von Nachrichten und Fakten - Demonstration dieses Konzepts in Form eines Prototyps", Diplomarbeit, Fachhochschule Hof, 2005

20. Y. Zhou, X. Xie, C. Wang, Y. Gong, W.Y. Ma: „Hybrid Index Structures for Location-based Web Search", Proceedings of the 14th ACM international conference on information and knowledge management, Bremen 2005

UNOSAT Grid – an overview

Ana Silva and Einar Bjorgo*

Operational Satellite Applications Programme (UNOSAT), United Nations Institute for Training and Research (UNITAR), Palais des Nations, CH - 1211 Geneva 10, Switzerland

* einar.bjorgo@**unosat**.org

The UNOSAT Grid project was created mainly to simplify the access of humanitarian relief workers to Earth Observation (EO) information with no background knowledge of EO data, but it will also be able to offer an infrastructure and service to advanced users of EO data. The need for satellite imagery support to the humanitarian community has been well documented for several years (Bjorgo, 2002). With the assistance of GMOSS, UNOSAT-Grid will be able to provide GRID technology solutions to developing countries (Moran and Mendez Lorenzo, 2005, Sandoval, 2006), UN field staff and their implanting partners.

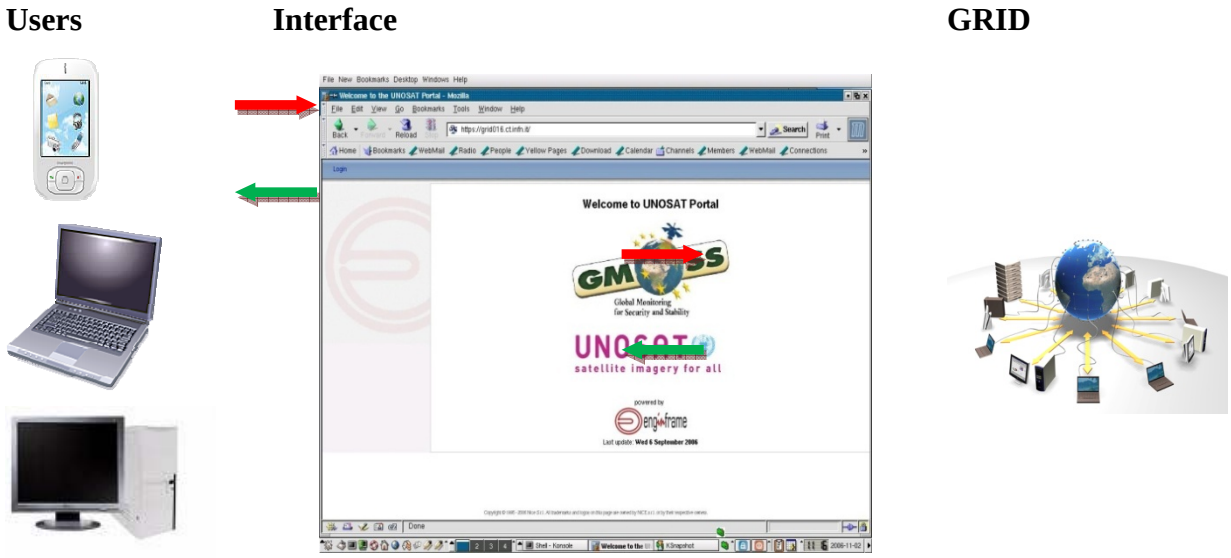

Fig. 1: UNOSAT Grid structure

With the creation of the necessary infrastructure to run UNOSAT jobs on the Grid as well as the software to upload and process the satellite imagery, with the mobile phone access in pilot phase (Mendez Lorenso, 2006); UNOSAT-Grid is aiming for the creation of a user-interface that allows the users to perform image processing and produce their own maps, through the UNOSAT portal.

The software chosen to be implemented in the Grid environment as part of the UNOSAT project is a known GIS Free Open Software: Geographic Resources Analysis Support System (GRASS). This software is a hybrid and modular structured Geographic Information System (GIS) with raster oriented and vector oriented functions. Tests on GRASS GIS were already conducted by UNOSAT in a single PC and also in the Grid environment. The results obtained show that GRASS GIS is an adequate alternative to Proprietary Software and can also be used in a GRID environment.

The functionality trough UNOSAT web would provide users a complete WebGIS for imagery analysis and maps production of data stored on a central database, as well data requested by UNOSAT in emergency situations. This functionality will also allow developing nations to have access to GIS tools without worrying about software licensing costs, computing power and storage capacity.

The humanitarian field workers with access to mobiles phones or internet will be able to request satellite imagery over their current location to UNOSAT mobile phone Grid interface or the normal web interface. This data would be received in a short time after the request is done. The same humanitarian field workers can also edit and create new maps of the field with more detailed assessment.

References

Bjorgo, Einar, 2002. Space Aid – Current and Potential Uses of Satellite Imagery in UN Humanitarian Organization. United States Institute for Peace (USIP) Virtual Diplomacy Series No. 12.
Link: http://www.usip.org/virtualdiplomacy/publications/reports/12.html

Mendez Lorenzo, Patricia, 2006. Project Gridification: The UNOSAT Experience. Enabling Grids for E-sciencE (EGEE) User Forum, CERN
Link: http://www.unosat.org/Grid/Lorenzo_gridification_unosat.pdf

Moran, Sean and Patricia Mendez Lorenzo, 2005. Using the Grid for Satellite Imagery with UNOSAT. Internal UNOSAT-CERN report
Link: http://www.unosat.org/Grid/Moran_Lorenzo_grid_unosat.pdf

Sandoval, Walter Daniel Lagrava, 2006. Access to satellite image metadata on the Grid. Master of Science thesis, University of Geneva
Link: http://www.unosat.org/Grid/Sandoval_thesis.pdf

GMOSS Gender Action Plan

Vinciane Lacroix[1*], Nathalie Stephenne[2], Clementine Burnley[2], and Irmgard Niemeyer[3]

[1] *Signal and Image Center, Royal Military Academy, Belgium*

[2] *European Commission, Joint Research Centre, Institute for the Protection and Security of the Citizen (IPSC), Support to External Security Unit, Ispra 21027 (VA), Italy*

[3] *Freiberg University of Mining and Technology, Germany*

* Vinciane.Lacroix@elec.rma.ac.be

Abstract

The European Commission considers that without gender equality in science and without a better use of the human resources available, scientific excellence will never be truly achieved within the European research area. This is why it has developed a gender equality policy in particular to promote the participation of women scientists in EU Framework Programme activities and to ensure that the gender dimension is properly addressed in EU-funded research content.

In this context, the GMOSS network of excellence (NoE) set up a Gender Action Programme including two major actions. In order to address the gender dimension in security, the NoE organized a workshop looking at the perspective of women in conflict, post conflict reconstruction and peace building. The workshop involved the participation of keynote speakers and panel experts drawn from political geography, from national and international network of women with both research and field expertise in peace building.

On the other hand, the NoE indirectly addresses the problem of a weak participation of women in scientific research careers and in management positions, in an artistic exhibition. It is indeed often argued that women do not engage themselves in such careers because they believe their private life would suffer from such a choice. While it is difficult to be sure of the reasons for lack of career progression, according to the figures available women do engage (30%) but are not promoted (14%). In this respect, the artistic exhibition featuring some male and female GMOSS researchers, questioning them about the sharing of their private and professional life, stresses that having a rich private life can be compliant with excellence at work, for both women and men.

This paper summarizes the GMOSS Gender Action Plan (GAP), starting from its early experience, with a focus on the gender dimension in security research workshop, and then presenting the exhibition concept before providing an overall conclusion on the lesson learned on its GAP.

1. Introduction

In order to support the goals of research excellence and economic competitiveness the European Commission (EC) has set a 40% target for representation for women at all levels of implementing and managing research programs in the EU[5]. In EU science or engineering jobs, figures for female participation were 31% (2004), in R&D 15.9% (2003), and 14% in the most senior academic staff positions (Annex 1). In the specific field of security research largely driven by the military and defense community, female participation figures are even lower[6].

Women and Science, 2005, *Excellence and Innovation – gender equality in Science*, EUR 21784, Science and Society, European Commission, DG Research-DirC Unit C4

[6] Tickner, J. Ann, (1992) *Gender In International Relations*, Columbia University Press.

Mahoney-Norris, Kathleen. and Hampton, Mary**.** "Women Faculty at Civilian and Military Institutions of Higher Education: More Alike than Different?" *Paper presented at the 47th annual meeting of the*

The call for gender equality is a central objective of gender mainstreaming in EC-funded European research[7]. A second objective of EC gender mainstreaming is to analyse and address any gender dimension in research content "to ensure that research funded by the Union meets the needs of its female as well as its male citizens"[8]. A third objective is to support research which gives an understanding on the gender question itself: "knowledge… of gender and gender relationships and of the impact of these concepts on European society[9]. Together, the three objectives are to promote research by women, research addressing men and women's needs and research about men and women in European research.

The Global Monitoring of Security and Stability (GMOSS) network of excellence (NoE) has been asked to work towards the EC's 3 objectives through a monitoring of gender mainstreaming actions. After one year of GMOSS activity, the Gender Action Plan (GAP) was still vague and no programme had been clearly defined. Thus, to fulfill its contractual obligation[10], the NoE has been asked to set up a female task force with the task of proposing a GAP. The compendium of good practices[11] compiled by the EC in order to provide guidance on how to design a Gender Action Plan for Integrated Project (IP) or Network of excellence (NoE), was discussed at this first "Gender Action Meeting" that took place in October 2005 at DLR premises, under the JRC lead. These early discussions are summarized in section 2.

At about the end of the funded period of the NoE, looking back to these initial ideas, GMOSS has at least completed two important actions besides the work on reporting gender participation statistics in its reports and in "Sesam", the European Commission online reporting tool for Research and Technological projects[12].

The first action addressed the relevance of gender in security research by means of an international workshop held in Belgirate in March 2006, as summarized in section 3. The aim of the workshop was to analyse the gender dimensions either in the security concepts or in the application tools developed and used within GMOSS NoE. We tried to build a consensus definition of the gender dimension in security research, to improve awareness inside the GMOSS network using a set of definitions produced by the BRIDGE project (Annex 2).

The second action questions the work/private life balance, often seen as one of the brakes for women in choosing management or research at a high level as a career, by means of an artistic exhibition in December 2007 whose concept is summarized in section 4.

Besides these two actions, two researchers participated to the European Workshop on Gender Mainstreaming[13] which aim was to bring together some of the actors of various European networks of excellence to discuss and exchange gender-linked activities and to debate on the topic "How to manage professional and private life".

International Studies Association, Town & Country Resort and Convention Center, San Diego, California, USA , on March 22-25 .
ETAN Report *Science policies in the European Union – Promoting excellence through mainstreaming gender equality* - Osborn *et. al.* (2000)

[8] Ibid. p. 11

[9] Ibid, p. 11

European Commision funded projects like GMOSS NOE are explicitly required as a contractual condition, to define and implement gender action plans, a fact not widely known among participating institutions.
Gender Action Plans A compendium of good practices European Commission Research directorate-General Directorate C- Science and Society Women and Science

[12] http://webgate.ec.europa.eu/**sesam**/

[13] http://www.l2mp.fr/CMA-VIUgmWorkshop/

The last section concludes the paper at two levels: the first one addressing the specific gender security problem in the context of GMOSS, and the second one, more general, discussing the lessons learned from building up such a GAP.

2. Early Gender Actions

The NoE has been introduced as a new tool for the 6th Framework Programme. It is specific in the sense that its programme is updated every year and that it aims at the integration of the partners rather than on the creation of products.

The EC demand on GAP has been initially seen by the overall network as an additional administrative burden. Indeed, the NoE funding only concerns integration, all other activity is seen as additional work, if not already part of the researcher everyday task. Therefore it relies on the researchers themselves and their respective Institutions to work on such a matter.

Another reason for the slow starting activity of the GMOSS GAP is that there was a tendency to consider gender perspectives in research as a field proper for women, thus suggesting that women scientists should take over the task, while they do not necessarily hold the appropriate expertise. Moreover, initially, most of the network male researchers saw in the gender issue only the problem of low participation of women in scientific careers and in management positions, which they still see as a fatality, thus ignoring the gender perspective in security. Several male researchers showed even some hostility towards the setting up of such a GAP, and would consider that if it is mandatory, it should fully be conducted by women, showing reluctance to embed the GAP inside the outreach activity under the responsibility of a man.

On the other hand, female researchers do not want to be promoted only because they are women. Some may be afraid of being considered as feminists or even as aggressive if they are part of a feminine team dealing with gender issues. Others have the feeling that fighting for their position in their own environment is already enough, so that they do not want to start a new battle, even if shared with other women.

The first gender meeting has thus been set on these rather unstable bases, as it most probably happened in many IP or NoE. The main reason being that quite often ‘gender’ connotes ‘female’ and this point of view tends to divide rather than to integrate.

This meeting, taking place at DLR premises in October 2005 was intended to discuss

- general gender action aspects,
- the situation of women in science and science institutions,
- the gender dimension of security issues.

With regard to the first two points, a questionnaire was answered by the participants: (i) What means gender action for you? (ii) How is it handled at your institute? (iii) What are your personal experiences? It turned out, that gender equality is formally installed at most of the present institutions, however, the actual equality of women in the professional life in some case still suffers from the contradictoriness of work and family, misogyny and the exclusion from the “old boys network”.

The gender dimension of security issues was discussed for impacts of armed conflicts on women and women’s role in peace-building[14]. Women and men experience conflict differently as refugees, internally displaced persons, combatants, heads of household and community

[14] Women, War, Peace: The Independent Experts’ Assessment on the Impact of Armed Conflict on Women and Women’s Role in Peace-Building (Progress of the World’s Women 2002, Vol. 1). Download at http://www.unifem.org/resources/books_reports.php

leaders, as activists and peace-builders[15]. Gender issues to be discussed in this regard are the following[16]:

- Violence against women: The magnitude of violence suffered by women before, during and after conflict is overwhelming.
- Displacement: The gender dimensions of displacement are overwhelmingly neglected.
- Health: Sometimes even basic health care is lacking for women in conflict situations.
- HIV/AIDS: Wherever a woman lives with conflict and upheaval, the threat of HIV/AIDS and its effects are multiplied.
- Organizing for peace: Women organize for peace in their communities and at the national and regional level, but they are rarely a part of the official peace process.
- Peace operations: A gender perspective must inform all aspects of mission planning and operation, beginning with the very concept of the operation.
- Justice and accountability: The impunity that prevails for widespread crimes against women in war must be redressed.
- Media and communications: The media supplies information for good or ill; it presents images of women that resound throughout communities in complex ways, especially during conflict and post-conflict periods, when tensions are high.
- Reconstruction: In the aftermath of conflict, when nations begin to rebuild, they must recognize and provide for women's specific needs.
- Prevention: Information from and about women in conflict situations has not informed preventive actions.

As many of these aspects do not only apply to armed conflicts but to crisis situations in general, a gender perspective is indispensable for security research.

3. Main Gender Action: A workshop to address the gender dimension in security

To address the gender dimension in security research the Belgirate workshop in March 2006 considered the distinction between women and men in the concepts, data and tools used to understand security. One challenge of the GMOSS network resides in the concept of demand and supply driven work flow between socio-political analysis and earth observation technology (Fig. 1). Within integrated discussion groups the socio-political partners analyse the European security policy demands and threat scenarios to improve the information provided to the decision makers. On the other side of the flow, the existing technologies of earth observation are improved efficiently to address the decision makers' needs. In this concept of demand and supply driven work flow, the workshop aimed to bring together two communities of scientists: technological scientists using earth observation (EO) data, and socio-political scientists specialising in gender studies. These socio-political scientists were expected to define the gender dimensions of common security concepts that should be applied by technological scientists.

[15] Ibid. p. 1
[16] Ibid. p. 6f

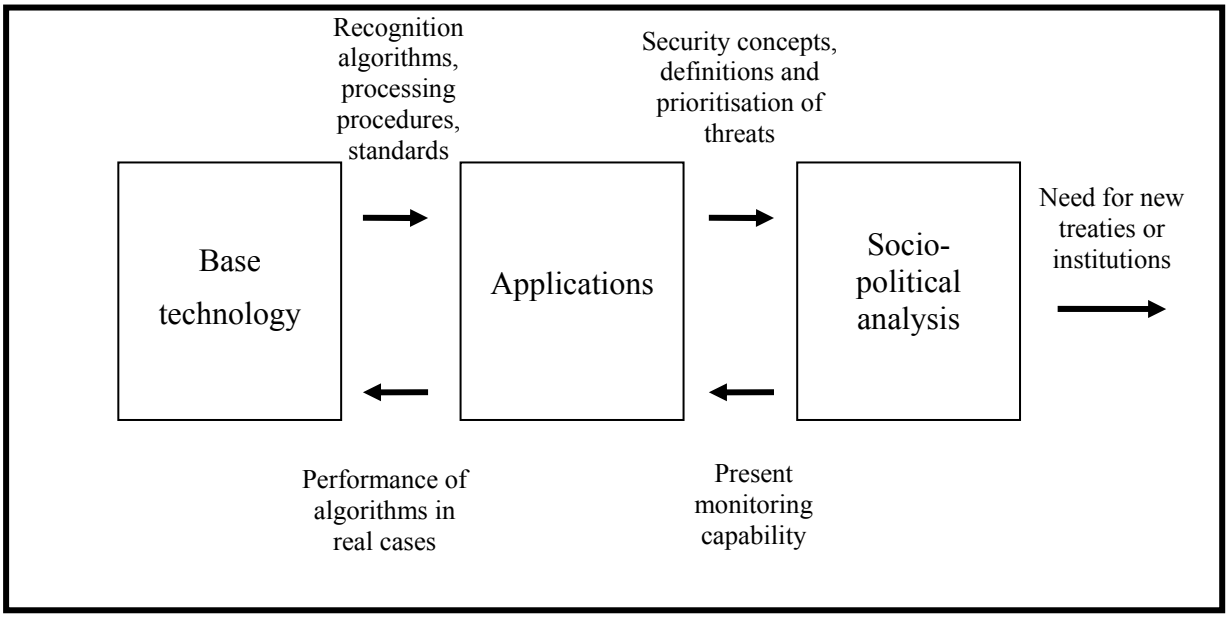

Fig. 1: Workflow between technological and socio-political work packages within GMOSS

Four questions have been asked at the workshop: (i) what can be a general definition of security, including gender security; (ii) what is the gender dimension in security (i.e gender roles in governance and decision making, gender participation in peace building, gender actions in natural disaster response); (iii) how do we measure the gender dimension in security and, (iv) what is the geospatial translation of these measures, for example in a vulnerability analysis.

3.1 Security concepts

Two main schools of thought in international relations, realism, later followed by neorealism, and critical security studies are distinguished (Buzan 1998).

Realist definition : State security

In realist security concepts the main threat to states was interstate conflict. The interests of states were presumed to be the interests of the individuals and communities they contained (Morgenthau 1948, Lyn-Jones and Miller 1995). However post-structuralist and other theorists (including neorealists) have challenged the realist view of violent conflict as natural and inevitable, seeing interdependence and international collaboration as both needed and possible (Buzan 1991, Sample 2000, Vasquez 2000, Raymond 2000).

Changes in definition : Human security

The human security definition relies on concepts of universal, indivisible, interdependent human rights, recognised and protected by international law enforced by states and international institutions. According to UNDP, human security translates into freedom from fear, wars and pervasive threats to people's right, safety and lives (UNDP 1994). This definition is finding acceptance the international community and also within the security policymaking community.

The human security approach can be distinguished by its focus on addressing structural causes of security threats like conflict by building institutional, civil and state capacity and by

fostering equitable economic development. While states remain the primary international actors, civil society and non state-institutional actors are establishing a stronger role. In this view state security capabilities are seen to have increased through improvements in the scientific knowledge base, in technology, and in political coordination. Ecosystem protection agreements like the Kyoto protocol are an example of collaborative responses to global threats.

Security definitions in GMOSS

Both EU security policy and GMOSS work encompass the full scope of the human security definition. The scientific challenge is to provide evidence-based theories, models and qualitative and quantitative data on causes, linkages and effective responses to security threats, however defined. The GMOSS NoE focuses on civil security. The definition used at the beginning of the project is quite broad: "Security is one of the basic needs of mankind, both individually and collectively. It is the single most important prerequisite for economic growth, investments and job creation and a powerful driving force for human ingenuity. It is an area of social concern where there is a unanimous expectation of citizens for government responsibility."[17]

Gender and security

Within the realist security concept, since the object at risk is the state and the interests of individuals are collapsed into those of the state, gender issues are ostensibly irrelevant. The difference in interests and situations, of women and men is broadly assumed to be insignificant. The human security concept, with individuals as its focus, identifies civilians, particularly women and children as extremely vulnerable to all types of security threats and thus eligible for special protective measures. Gender discrimination and gender equity are well recognised dimensions of human security. This approach is still deemed insufficient by some feminist theorists who nevertheless advance a normative and multi-level view of security which, by emphasizing the group position of women, only partially overlaps the human security definition.

The socio-political experts in Gender studies at this workshop agreed on the use of the human security definition as a definition of security as it takes into account individual rights, where gender can be specifically identified to play a part in determining different levels and types of security. In their view only this definition can be used in a gender mainstreaming process in security research and policy design (workshop presentations, Jacobson, Breines, Teigeler 2006).

The GMOSS workshop focused on Gender and Conflict, presenting conflict as a case study of the gender dimension in security. The gender perspective on conflict describes a specific, gendered experience of conflict, which is different for women and men due to their different social roles. It also argues that women and men have different roles in conflict, and that, just as women are excluded from political participation they are also not sufficiently represented in peace building and reconstruction processes.

[17] GMOSS Technical Annex1-Part 1, p. 2.

3.2 Human security and human equality – gender studies approach

Gender roles in conflict and post-conflict situations

The gender studies approach uses the gender perspective to reveal significant differences in the actual situations of men and women both during peacetime and during conflict mainly related to gender role and cultural distinctions.

In the social construction of gender roles, stereotypically "feminine" qualities such as nurturing, emotion, intuition are negatively opposed to "masculine" qualities such as strength, rationality, and logic. Despite this construction of femininity, women are not naturally peaceful or nurturing, especially during conflicts, where a general culture of violence prevails. The gender construction simply reflects the usual female responsibility for the care, welfare and survival of the family, which, according to some theorists gives them an important role in conflict and also in reconstruction (Reimann 2004). It is not at all established as fact that women are more peaceful than men, indeed women also indirectly support and incite violence although they perpetrate violence to a much lesser degree than men (ICRC 2001; Turshen 1998).

The view of gender roles as active, on-going social constructions which vary across cultures means that gender roles can be challenged within gender studies using contradicting examples and proposing alternative constructions (Teigeler 2006). For instance, changes in roles are said to be progressively arising, especially in developed countries, where men are taking on primary care of children in families and are participating in groups against violence toward women. But these changes, if they are ongoing, still need a lot of reinforcement in our society (workshop presentation, Teigeler 2006).

By destroying the existing socio-political structure, conflicts or natural disaster can provides new roles to both genders. This gender studies approach proposes a spatial multi-scale approach to analysing power relations (Wastl-Walter and Staeheli 2004) that is a particularly interesting dimension to address through a geospatial modeling approach. People's vulnerability to environmental stresses, natural disasters or conflicts, is affected by differential access to resources (food, healthcare, information, markets) and role in society. The effects of war [and possibly natural disasters] on women (and men) are influenced by the position of the woman [or man] in that conflict (Lindsey 2001). This gender vulnerability at the time of the disaster/conflict has an unarguable spatial component that could be integrated and studied by new geographical technologies.

Participation in decision making

For many liberal and some socialist feminists, comprehensive security would include an equity dimension, meaning full participation of women and men in political processes, policy decision making and economic activities[18]. Rather than creating a feminist dominated "matriarchy" this approach would support sharing of the male and female outlook. Human dignity is seen to be based on the same access for all to decision making processes and participation in the community's life (workshop presentation, Giles 2006). In the positive sense, gender equity in decision making and participation brings a plurality of perspectives to the decision process and this guarantees more qualitative (and fit for purpose) decisions. Empowerment and security for women are seen as indivisible, with the elimination of inequality for women requiring access to societal power and resources.

[18] Tickner, (1992) op. cit.

3.3 Gender researchers and geospatial technicians: unfeasible partnership?

Four questions guided the development of the GMOSS workshop; so far, only the first two have been addressed. The last two questions:'(iii) how do we measure the gender dimension in security' and '(iv) what is the geospatial translation of these measures', were not effectively responded to at the workshop. Moreover, they were the reason for a lively discussion between the speakers and the audience. Definitively, they proved that a relevant gap exists between the different communities -gender studies researchers and geospatial technicians[19]- dealing with security. We use the names 'geospatial researchers', 'geospatial scientists' and 'technology technicians' to refer to experts working in the area of producing geospatial models for interpreting security issues, which are the main profile of scientists working in the GMOSS Network and attending the workshop we analyse in this paper. The response to the questions revealed the two communities to approach the security topic in radically different and apparently irreconcilable ways.

The global datasets relevant to security are national level, and so do not provide coverage of the majority of conflicts, which now take place inside states, or of natural disasters which are highly localised. The specific challenge in introducing a gender perspective within geospatial tools is, to develop precisely geolocated and gender disaggregated data on impact of conflicts/disasters; baseline economic data, baseline development data, and coping strategies. For instance, in an analysis of a violent conflict including a gender insight, a starting point could be (i) to examine differential gender impacts, using disaggregated data for instance on conflict/disaster mortality and displacement; (ii) to better understand the link between political participation, socio-economic status and coping strategies at different social scales (iii) to communicate insights to response actors. However, valid information especially on conflict cannot be collected exclusively via quantitative methods. Qualitative methods are required to understand the reality of conflict processes – the incentives of actors, the rules and institutions informing the strategies of actors and possible causal links with political, social and economic framework conditions. This is best done by combining information on contextual factors influencing conflict processes with in-depth case studies.

The dialogue between speakers and audience concluded that land use changes could indicate a gender pattern in specific geographical contexts. For instance, extensive monoculture is led by men, while subsistence and small-field agriculture carried out mainly by women, could be observed in some African contexts. Interestingly, the epistemological gap between the two communities emerged again after this initial consensus: a participant in the audience was willing, to map land use characteristics for large territories and determine gender patterns. That proposal little to the gender researchers: they maintained, that local socio-cultural and economic variability is a main characteristic of gender relations, large-scale analysis and foresight may be condemned to failure.

More critically, research support of both communities is necessary to explore and determine which geospatial variables may give indications about gender inequities in security. For instance, as commented in the gender studies approach, gender equity in decision-making

19 Speakers invited at the gender and security meeting of the GMOSS workshop were gender studies researchers and NGOs officials working on gender and security projects. It could be pointed out, following the logic of our argument, that there are also fundamental differences between the purposes and ways of work of these two groups. However, in accordance with the interests of the GMOSS workshop, during the meeting specific controversies emerged between speakers, working on gender issues, and the audience, mainly consisting of geospatial researchers. Our interest is to reflect on this phenomenon, and this is the reason why we omit the difference between gender researchers and practitioners in the present article. For facilitating the fluidity of the text we include under the name 'gender researchers' or 'gender scientists' the position of both, gender studies researchers and NGO practitioners participating in the meeting.

bodies has been pointed as an indicator of more social stability and security for women. Another example is the new coping capacities and decision-making roles sometimes provided to women by the conflict context. Such patterns could be tested through statistical analysis, e.g. could we find a correlation between gender equity at different decision making scales and regional or country security stability? Or the other way around, could we find links between differential gender impacts of conflicts and power imbalances between men and women?

Through the gender approach, we identified vulnerabilities specifically attributable to gender in the different roles, levels of decision, stage of conflict and spatial scales. Technological models and tools have to integrate these gender dimensions. However, more resources should be invested from both communities.

As a theoretical example, a gendered vulnerability assessment model using geo-spatial tool and earth observation images would require: (i) to take into account the gender dimension in the spatial components of the vulnerability analysis by using disaggregated data (women heads of household as a first step). (ii) to better understand the link between gendered land uses and visible changes in land cover on satellite images, (iii) to study the appropriate scale or resolution of the gender dimensions (family, household, community, state and international), (iv) to interact with decision makers in the understanding of the components.

3.4 Conclusion: Integration of socio-political concepts in EO applications and technologies

The workshop considered ways to introduce a gender perspective in the concepts, data and tools used in earth observation, which could theoretically fit within the current GMOSS work flow between the socio-political and the technological workpackages, to benefit European decision makers (Figure 2).

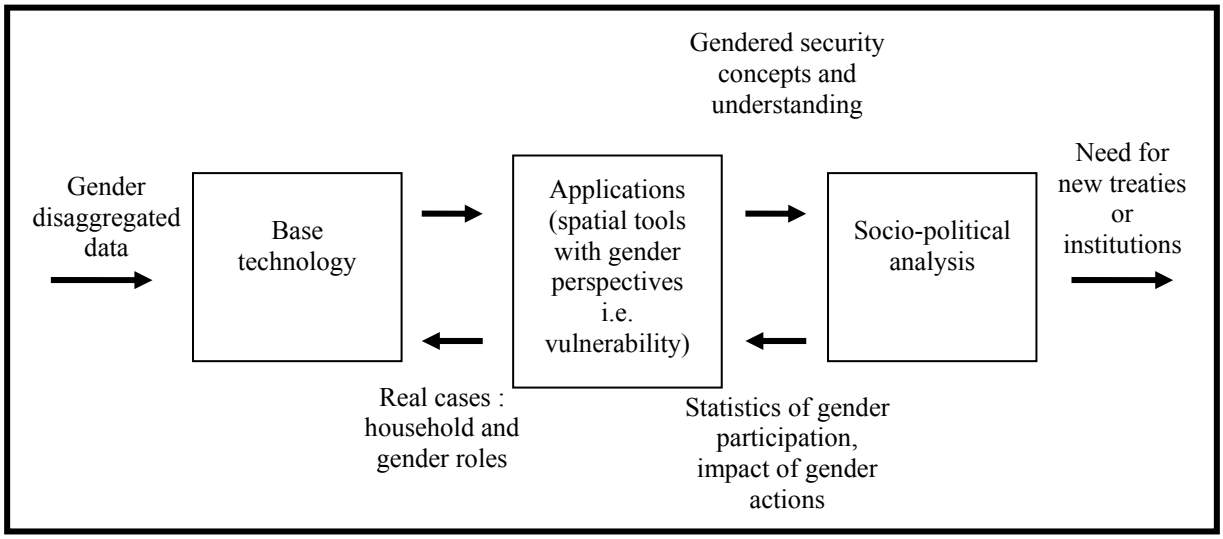

Figure 2: Hypothetical workflow including gender dimension between technological and socio-political work packages within GMOSS

We started the workshop overview by presenting theoretical contributions of gender studies to security definitions, and by pointing out their specific approach to the analysis of social and political dimensions of security. We demonstrated gender is not only a significant variable for obtaining disaggregated data, but that gender inequities in social roles and decision-making, and female-directed violence, or gender-based impacts of natural disasters, are fundamental aspects of security problems themselves.

We have pointed to differences in goals, epistemological foundations and methodological practices which create a significant gap between the two communities. However, our analysis has aimed at providing exploratory paths for promoting mutual understanding between the two research areas, with the global aim of providing a more complete and complex (holistic), qualitative, efficient and democratic account of security problems.

4. Outreach Gender Action: An Artistic Exhibition

The aim of the artistic exhibition shown first in Brussels, December 2007, is to show that a rich private life is compliant with excellence at work, both for men and women. As a career in sciences, especially in research, is often seen as highly demanding and offering little room for a family or for a very active private life, we have looked for some counter examples inside the network. It resulted in a selection of "portraits" of a few researchers, men and women. A photographic portrait, some artworks, and the answers to a questionnaire illustrate each character. Most of the portraits have been taken during some GMOSS event. As it was not possible to follow each of these researchers in their private life, it was asked them to provide a few pictures showing them at work, during field missions, in their leisure time, or with their family and friends. These pictures served as a basis for the artworks: printed on A4 paper, they have been manually processed: some parts could be covered with acrylic painting, others left as such; some sketches or collages illustrating hobbies, relatives or suggesting specific activities could have been added. Part of such a painted photograph is shown in Figure 3.

Fig. 3: Part of a painted photograph illustrating one member of GMOSS after Tai-Chi.

The same image was used several times, in order to generate a series like a game, illustrating the various aspects of the researcher, as perceived by the artist, photographer and painter, herself being member of the NoE.

The questionnaire is made of four general questions, plus a question related to the researcher biography :

1. *What is your understanding of security?* This question was meant to provide a unifying framework for all the characters, while gathering them around GMOSS main issue: security.
2. *How does your professional experiences help you to address security issues?* The purpose of this question was to provide to the young generation, to their parents, and to adults in charge of advising for some career, a flavor of the various possible backgrounds useful for dealing with security issues.
3. *How does your professional life benefit from your private life?* This third question aims at underlying the positive aspects of a rich private on the professional performances.
4. *What should be changed to have a better balance of your private and professional life?* Answering this question enables each researcher to highlights the actual problems and to suggest solutions for today's society.
5. *Provide a small bibliography as answer to this question: who am I*?

All these questions tend to show that the benefit of a rich private life is not only to be seen at an individual level, but also at the society level, including the employers themselves who should not think that people working 10 hours per day are necessarily more efficient than some others working 8 hours but having a satisfying rich private life.

In its initial version, the artistic exhibition was seen as a gallery of pictures showing only women portraits. However, only a few women were willing to participate. It should be noted that the project aroused more interest inside the network when it had been enlarged in order to encompass men portraits, and the subject discussed was the balance between the private and professional life.

5. Conclusions

5.1 Conclusion on the GMOSS GAP

Building a GAP in GMOSS has been a difficult task, because, presented as such, it rather divided the researchers than it integrated them. Indeed, this obligation has been taken as a separate task, while, if integrated already in the different thematic work packages when applicable, it could have been more easily accepted. The workshop itself had been announced as a separate event, while it took place just after the annual GMOSS integration meeting, in the very same place.

The tendency is to consider gender perspectives in research a field proper of "women". This may explain why, when institutions decide to introduce gender topics into their daily practices, gender specialists are not hired, but, instead, women scientists in the current working groups are assigned the job of dealing with gender issues, although in many cases they may not hold the proper expertise[20]. The simple and mistaken argument behind this decision is that because of being women, they are 'natural' specialists in gender studies. Nevertheless, although it is not always the rule that women scientists want to deal with gender issues, we could find many women highly motivated and determined to introduce gender topics in their research field, which constitutes an important research potential for gender studies. This may indicate many women intuit or experience gender imbalances and biases in the fundaments and practice of their own scientific disciplines, work environments and research areas. Gender studies imply a

20 The GMOSS 18 month Review Report, reads: "Starting from the assumption that the female researchers of GMOSS should be in charge of the expertise to develop an appropriate concept, a female task force on gender actions was proposed…" P 20, Section 2.1.2 Gender Action Plan
http://gmoss.jrc.it/Documents/Members/Documents/Documents/GMOSS_18month_review_report_V2.pdf

response to the concerns of women. However, this female potentiality should not mean that men cannot deal with gender topics (they could bring many interesting insights to the gender field as well as open fundamental reflections into their own research area and experience), nor that women scientists should not receive the training, time and financial support that the project of introducing a gender perspective into an existing research environment requires.

The GAP obligation of the 6th forced the NoE to think about gender in security research. This reflection provided some basis for future research in gender in security. Seeing these interesting outcomes, the release of this obligation in the 7th is regrettable.

Annex I:

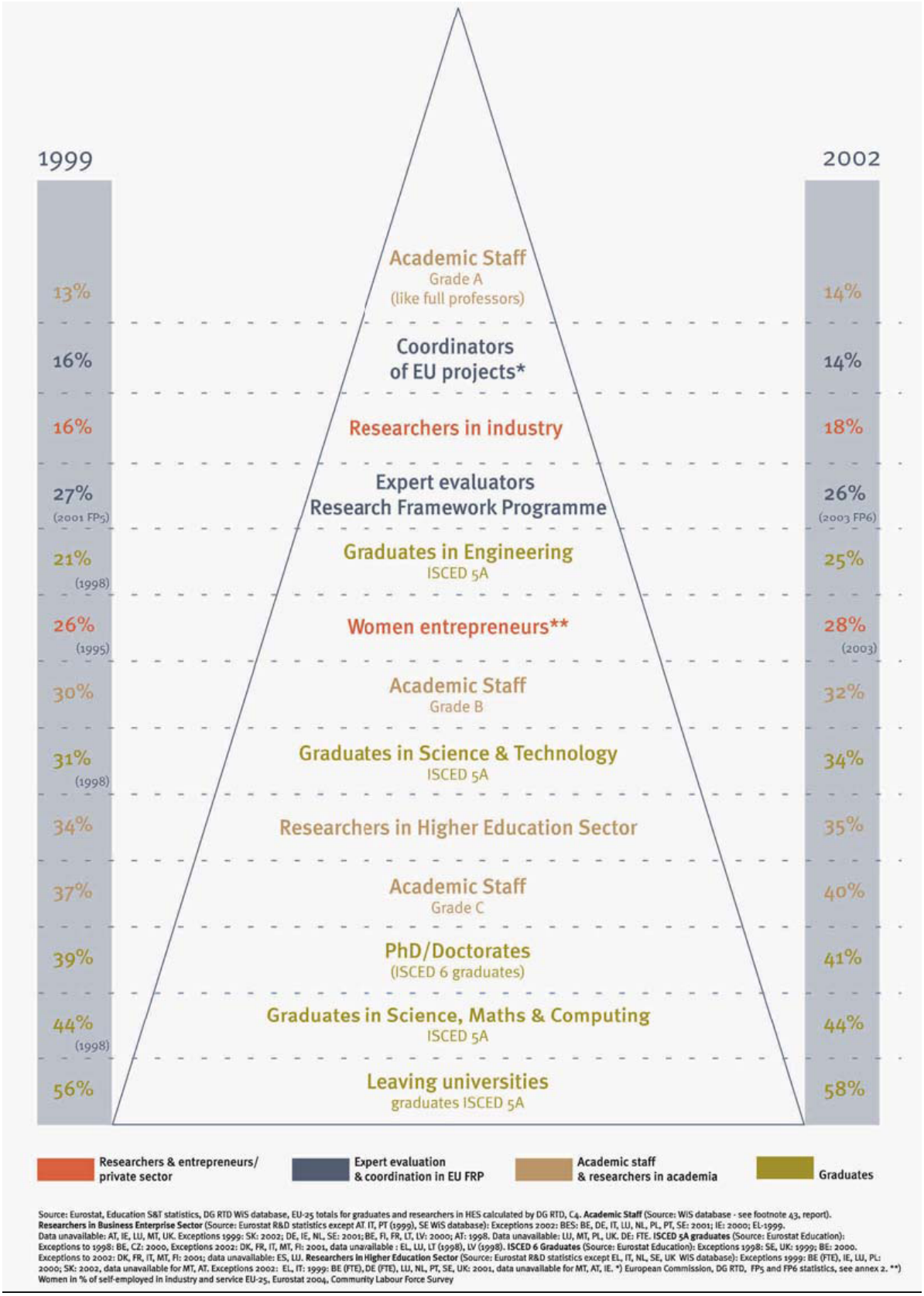

Women and Science, 2005, *Excellence and Innovation – gender equality in Science*, EUR 21784, Science and Society, European Commission, DG Research-DirC Unit C4

Annex 2: Definitions

Culture	The distinctive patterns of ideas, beliefs, and norms which characterise the way of life and relations of a society or group within a society
Gender Analysis	The systematic gathering and examination of information on gender differences and social relations in order to identify, understand and redress inequities based on gender
Gender Discrimination	The systematic, unfavourable treatment of individuals on the basis of their gender, which denies them rights, opportunities or resources
Gender Division of Labour	The socially determined ideas and practices which define what roles and activities are deemed appropriate for women and men
Gender Equality and Equity	Gender equality denotes women having the same opportunities in life as men, including the ability to participate in the public sphere
	Gender equity denotes the equivalence in life outcomes for women and men, recognising their different needs and interests, and requiring a redistribution of power and resources
Gender Mainstreaming	An organisational strategy to bring a gender perspective to all aspects of an institution's policy and activities, through building gender capacity and accountability
Gender Needs	Shared and prioritised needs identified by women that arise from their common experiences as a gender
Gender Planning	The technical and political processes and procedures necessary to implement gender-sensitive policy
Gender Relations	Hierarchical relations of power between women and men that tend to disadvantage women
Gender Training	A facilitated process of developing awareness and capacity on gender issues, to bring about personal or organisational change for gender equality
Gender Violence	Any act or threat by men or male-dominated institutions, that inflicts physical, sexual, or psychological harm on a woman or girl because of their gender
Intra-household Resource Distribution	The dynamics of how different resources that are generated within or which come into the household, are accessed and controlled by its members
National Machineries for Women	Agencies with a mandate for the advancement of women established within and by governments for integrating gender concerns in development policy and planning
Patriarchy	Systemic societal structures that institutionalise male physical, social and economic power over women
Sex and Gender	Sex refers to the biological characteristics that categorise someone as either female or male; whereas gender refers to the socially determined ideas and practices of what it is to be female or male
Social Justice	Fairness and equity as a right for all in the outcomes of development, through processes of social transformation
WID/GAD	The WID (or Women in Development) approach calls for greater attention to women in development policy and practice, and emphasises the need to integrate them into the development process
	In contrast, the GAD (or Gender and Development) approach focuses on the socially constructed basis of differences between men and women and emphasises the need to challenge existing gender roles and relations
Women's Empowerment	A 'bottom-up' process of transforming gender power relations, through individuals or groups developing awareness of women's subordination and building their capacity to challenge it
Women's Human Rights	The recognition that women's rights are human rights and that women experience injustices solely because of their gender

Hazel Reeves and Sally Baden, 2000, Bridge Report 55

Applications

Geospatial Trends of Pipeline Sabotages and Vulnerability Analysis of the Pipeline Network of Iraq to Terrorist Activities: A GIS Development

Antonio de la Cruz*, Marcin Mielewczyk, Daniele Cerra, and Gracia Joyanes

European Union Satellite Centre – EUSC, E-28850 Torrejon de Ardoz, Madrid, Spain

* a.delacruz@eusc.europa.eu

Note: Published also in ESRI -GISDIC "GIS for Defence and Intelligence Communities", Volume 4.

Abstract

As part of the GMOSS (Global Monitoring for Stability and Security) project funded by the European Commission, a GIS has been developed to assess the geospatial distribution of pipeline sabotages and analyse the vulnerability of the Iraqi pipeline network to terrorist activities. This task has been undertaken due to the large impact of these activities at national and international level. The database of sabotages has been generated from searches on the Internet but a recurrent problem has been the lack of georeferencing data of the sabotages. The shape files of MODIS hotspots provided by NASA Web Fire Mapper / MODIS Rapid Response have been used to solve this problem and to confirm and extend the database. This is an interesting security application of algorithms originally designed for environmental applications such as forest fires.

The vectorization of the pipeline network and related oil and gas infrastructures have been obtained at the best possible scale from available maps and imagery (TPC, JOG, Russian maps, Landsat 7 mosaic of Iraq etc.)

The GIS results suggest several vulnerability factors such as (in decreasing vulnerability order): 1. Closeness to populated areas; 2. Nearby infrastructures; 3. Impact on the national and international economy; 4. Unguarded pipelines; 5. Pipelines above ground; and 6. Pipeline accessibility. These factors have been weighted and vulnerability levels have been generated as follows:

High vulnerability. Includes the pipeline sections from Kirkuk to Baiji (35 sabotages); and the section from Baiji to Baghdad (sabotages)

Moderate vulnerability. This level affects the pipeline sections of Hadithah to the city of Basrah (8 sabotages); and city of Basrah to the Basrah oil terminal (5 sabotages).

Medium vulnerability. This level includes the section from Baiji refinery to the Turkish border (7 sabotages)

Low vulnerability. The sections included are the pipeline connecting the oil fields of Abu Ghurab, Buzurgam, and Jabal Faugi with the city of Basrah (2 sabotages); the pipeline section between Baiji and Hadithah (1 sabotage); the Iraq-Syria-Lebanon pipeline (1 sabotage); the Iraq-Saudi Arabia pipeline (0 sabotages); and the Baghdad and Khanagin pipeline (0 sabotages).

As a general trend, pipeline sabotages are more common in eastern Iraq near highly populated areas with dense infrastructures and are less common in the isolated areas of the western Iraqi desert.

1. Introduction

The large number of sabotages on the pipeline network and related oil and gas infrastructure of Iraq, is a clear indication that terrorist groups have selected these objectives as the most relevant targets to undermine the Iraqi economy, prevent reconstruction in the country and destabilize peace efforts. The incidence of these sabotages in related installations such as oil-export terminals (e.g. Basrah) is having a major impact on the reduction of international oil supplies and therefore has an influence on the global economy (Fig. 1). Furthermore, the

sabotages in Iraq have accentuated this strategy by terrorist groups in other large oil-producing countries.

The GMOSS team at the EUSC has developed a full GIS product that contains a database of sabotages to oil and gas pipelines and related installations in Iraq (IAGS, Pipeline Watch and other internet sources), dating from June 2003 when the sabotages started, until very recent (more than 300 entries). The mapping of the pipeline network and related oil and gas infrastructure has been digitized from the best available maps such as TPC, JOG, Russian military maps and Landsat mosaic of Iraq kindly provided by EUSC.

The objectives of this work are to develop a methodology to georeference security events such as pipeline sabotages and also to to derive conclusions from the geospatial trends of these pipeline sabotages as well as to undertake vulnerability analysis of the pipeline network and related infrastructure.

Additional GIS layers have been developed to generate relevant vulnerability factors such as population areas that could be related to terrorist groups, vulnerability of the nearby population to the oil and gas fires and related pollution following the pipeline sabotages, etc. These and other research issues are in progress with GMOSS partners that will be using the present GIS as seed data for security research activities (see additional details in section 2).

Note: For the purpose of this research, we have only considered the sabotages that can be georeferenced with the coordinates and dates of MODIS hotspots. The actual number of sabotages that have taken place in the Iraqi pipelines is actually much larger.

Current research on the response of MODIS hotspots to the real conditions of Iraq will allow a better estimation of false alarms and to georeference a more realistic number of sabotages.

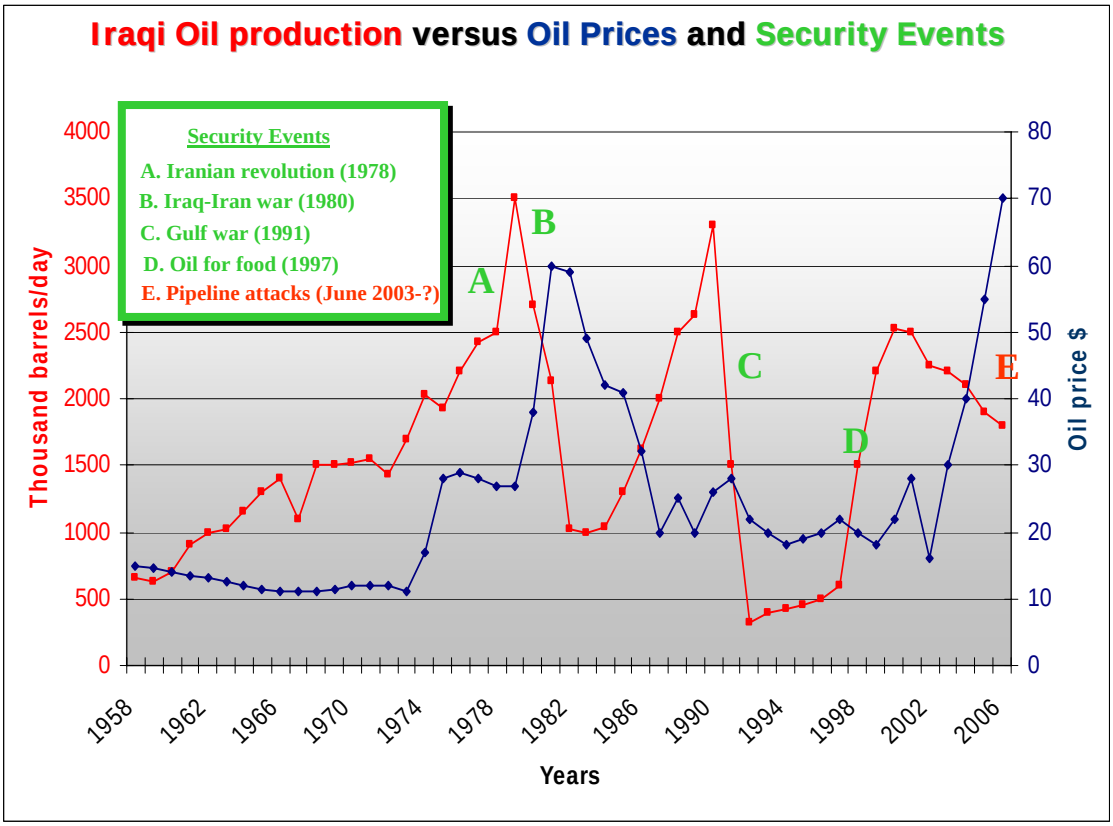

Fig. 1: Impact of pipeline sabotages on Iraqi Oil production and Oil Prices (E)

2. GIS Description: Database of Sabotages and Vectorization of the Pipeline Network and Related Oil and Gas Infrastructures

2.1 Database of Pipeline Sabotages

The database of the GIS has been developed from different open sources and searches on the Internet such as the website of the Institute for the Analysis of Global Security (IAGS) that has extensive records of sabotages on the pipelines in Iraq. Unfortunately, many of these records lack georeferencing data to locate the sabotages along the pipelines (or these data are not very precise), as this was not the purpose of IAGS. Therefore, additional searches were undertaken to obtain this information and to extend the number of entries of the database. Relevant findings were also obtained by searching digital news of the sabotages by CNN, BBC, NBC, etc. This searching, however, has been time-consuming. Therefore, and in view of the importance of compiling databases for security applications, realized during this period, a new research activity has been started with Hof University to develop crawler and data mining techniques that will allow the design of a search engine able to compile databases by automatic or semi-automatic means.

It should also be considered that information of all the sabotages is not published (e.g. those taking place in distant and isolated areas), thus, the importance of detecting them by automatic means such as hotspots. However, further research is needed to fine tune MODIS algorithms for a more realistic response to a larger number of sabotages.

2.1.1. The Use of Modis Hotspots to Compile the Database

The burning and explosions of oil and gas caused by the sabotages can last several days and they produce high temperatures that are recorded as hotspots by suitable algorithms using the IR bands from sensors such as MODIS (Terra and Aqua), SEVIRI (MSG) and AATSR (Envisat). Therefore, the database has been partially completed with the shape files of MODIS hotspots containing dates, coordinates, temperature, etc. related to the sabotages (Fig. 2). This is a new security application of sensors originally designed for environmental applications such as forest fires.

The shape files of MODIS hotspots from June 2003 until recently (83,000 files) were kindly provided by NASA Web Fire Mapper / MODIS Rapid Response to confirm and to extend the database. A very large number of hotspots responded to the gas flares of Iraqi refineries and gas wells (a redundant way to detect these infrastructures). Therefore, all these hotspots were eliminated as well as many other hotspots unrelated to the pipeline network. However, MODIS hotspots could only confirm 35-40% of the sabotages. Nevertheless, the high temperatures anomalies can be observed in the MODIS IR bands. We think, therefore, that the MODIS detection algorithms have to be fine-tuned by considering the specific conditions of Iraq such as the hot-surface temperatures of the western Iraqi desert. In this way, the resulting hotspots could confirm a much higher number of pipeline sabotages. Research is also in progress with other GMOSS partners such as University of Basilicata to use the hotspots of SEVIRI (MSG) and AATSR (Envisat) to confirm and extend the results of the database. Preliminary results are encouraging.

The use of hotspots to generate databases for security applications has the following benefits:

- The shape files of the hotspots have records of dates, coordinates, temperatures and level of confidence on their registration by the algorithm.

- They can provide useful data for the acquisition of suitable H.R. imagery (date and location)
- They can provide unbiased data when information from a crisis area has been censored.

The database of sabotages to the pipeline network and related oil and gas installations has been compiled in MS Access and is composed of text (Internet searches) and images (MODIS, SEVIRI and AATSR (Envisat) hotspots.

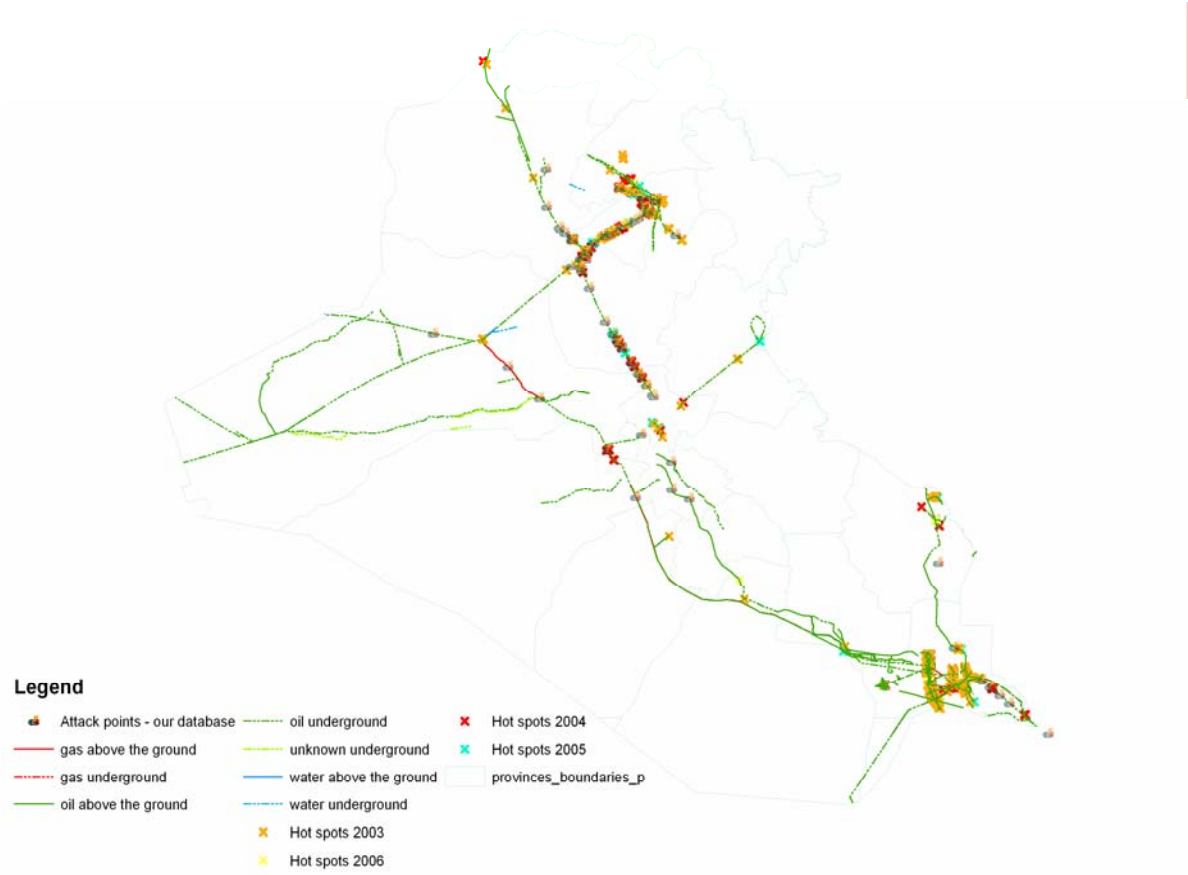

Fig. 2: Distribution of pipeline sabotages correlated with MODIS hotspots during 2003, 2004, 2005 and 2006 provided by NASA Web Fire Mapper / MODIS Rapid Response.

2.2 Vectorization of the Pipeline Network and Related Oil and Gas Infrastructures

In order to display graphically the events of the database, a relative large-scale map of the pipeline network and related infrastructure was needed. As this product was not available it was decided to produce our own product (Fig. 4). The mapping of the pipeline network has been vectorized from the best available maps at different scales, dates and levels of detail on oil and gas infrastructures such as JOG (Joint Operations Graphic), TPC (Tactical Pilot Charts), DCW (Digital Chart of the World), Russian military maps and the Landsat 7 (true color band combination) mosaic of Iraq. The final EUSC product is superior in scale and level of detail to other existing products such as VMAP 0 and VMAP 1 due to the fact that all the sources above have been used in the EUSC product as opposed to VMAP1 that uses only the JOG maps. Furthermore, the distribution of VMAP 1 is restricted.

The related oil and gas infrastructures that have been mapped are also substantial. These include oil and gas fields, refineries, pumping stations, power stations, oil/gas export terminals, etc. (Fig. 5)

High resolution imagery available at EUSC (Spot 5, Ikonos, Quickbird) has been used in the areas that coincided with the pipeline network and oil and gas infrastructures. In addition, the resulting product has been compared and improved with the seamless mosaic of Google Earth of Iraq formed by Quickbird imagery. These comparisons have improved the mapping quality of the pipeline network and the related oil and gas infrastructures.

As a result of the different sources that have been used, the number of attributes of layers in the EUSC product is also considerably larger. Attributed tables have been generated for the pipeline network, for the database of the sabotages and for the related infrastructures. The attributes for the pipeline include the differentiation of pipelines for oil and gas, the number (oil/gas) tracks running in parallel, the pipeline sections below and above ground, etc. (Fig. 3).

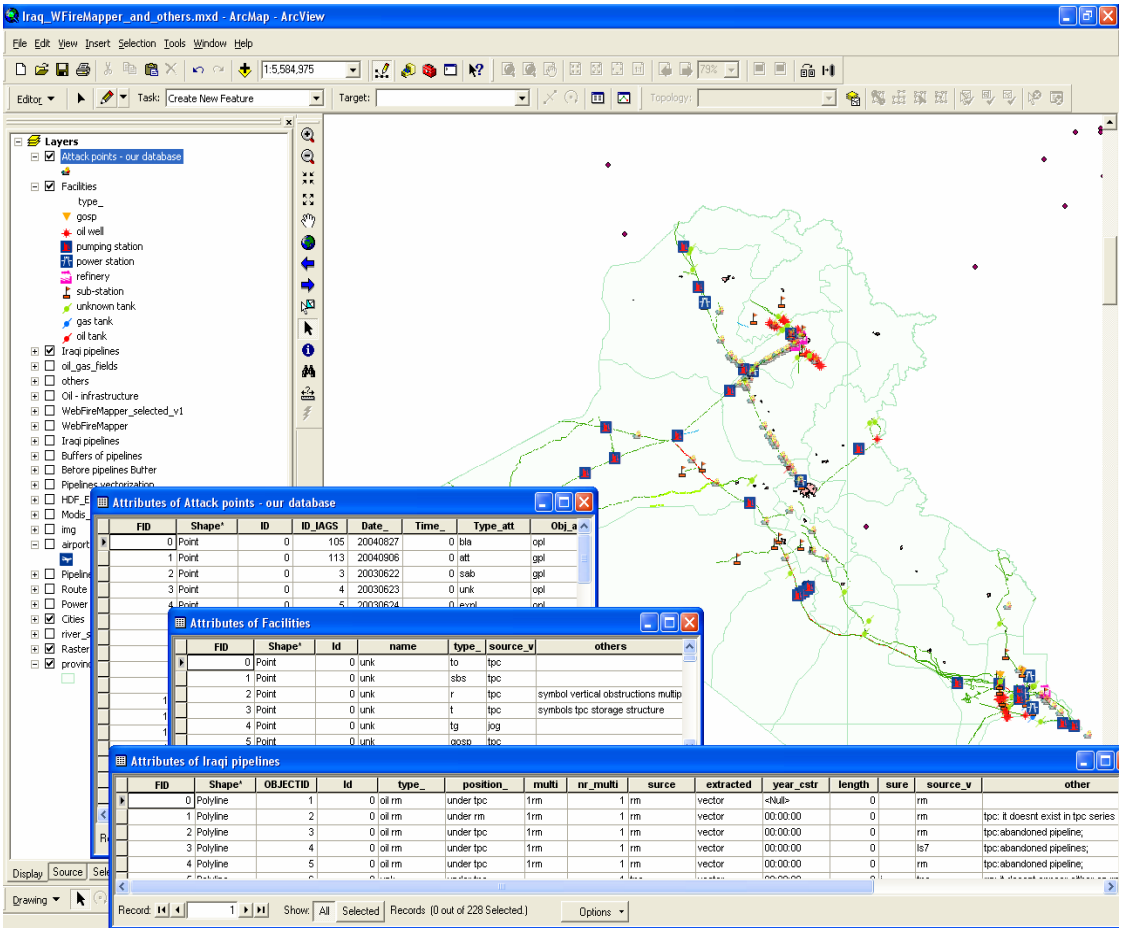

Fig. 3: GIS overview with attribute tables for the database, pipeline network and related infrastructures

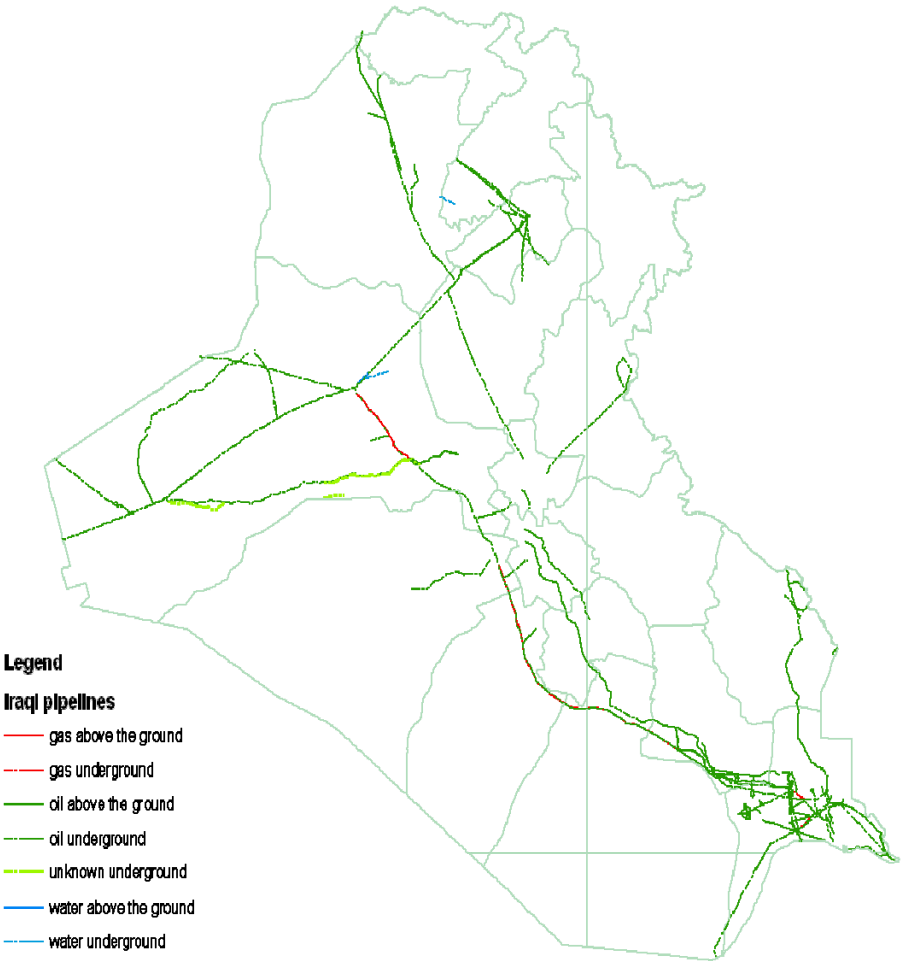

Fig. 4: Vectorization of the pipeline network of Iraq

3. GIS Results: The Geospatial Distribution and Types of Sabotages in the Pipeline Network of Iraq

Pending the fine-tuning of the MODIS algorithms to confirm the geolocation of additional sabotages, the results below are only preliminary. Final results will be provided in the next delivered report.

The database of pipeline sabotages (preliminary at this stage) together with the mapping of the pipeline network and related oil and gas infrastructures (from imagery and maps) have allowed the geospatial display of these sabotages in order to derive relevant security information as follows (Fig. 6):

- The oil pipeline section between Kirkuk and the Baiji Refinery has received most of the sabotages (35). This underground pipeline section is part of the Iraq-Turkey pipeline. These sabotages have taken place during 2003 (4 sabotages), 2004 (24 sabotages), 2005 (6 sabotages) and 2006 (1 sabotage) and they were carried out by explosions (20 sabotages – 57% of all the sabotages in this section), undefined sabotages (14 sabotages – 40%), automatic weapons (1 sabotage).

- The oil pipeline that follows in number of sabotages (28) is the underground section between Baiji and Baghdad. The sabotages took place during 2003 (9 sabotages), 2004 (15 sabotages), 2005 (4 sabotages) and were made by explosions (21 sabotages – 75%), undefined (7 sabotages – 25%).
- Following in number of sabotages (8) is the Iraq Strategic Pipeline (both gas and oil) in the above-ground section between Hadithah and the City of Basrah. The sabotages took place during 2003 (2 sabotages), 2004 (4 sabotages), 2005 (1 sabotage), 2006 (1 sabotage) and were produced by explosions (3 sabotages – 37%), undefined (5 sabotages – 63%).
- Next in number of sabotages is the Iraq-Turkey pipeline (oil) in the underground section between Baiji refinery and the Turkish border (7). These sabotages took place during 2003 (4 sabotages), 2004 (3 sabotages) and were carried out by explosions (5 sabotages – 71%), undefined (1 sabotage) and automatic weapons (1 sabotage).
- The pipelines with fewer sabotages are (in decreasing order):
    - The oil pipeline section between the city of Basrah and the Basrah Oil terminal. This pipeline underground section had 5 sabotages in 2004 (3 explosions, 2 undefined).
    - The oil pipeline section connecting the oil fields of Abu Ghurab, Buzurgam, and Jabal Faugi with the city of Basrah displays 2 sabotages in 2004 (1 explosion, 1 undefined). This oil pipeline has sections above the surface and underground. The sabotages took place in the sections above the surface.
    - The oil pipeline section between Baiji and Hadithah had 1 sabotage in 2004 (1 explosion). This pipeline runs underground.
    - The Iraq-Syria-Lebanon pipeline (oil) suffered 1 sabotage in 2003 (undefined). This pipeline goes underground.
    - The Basrah Oil terminal suffered 1 suicide bomb sabotage on April 2004 in spite of the deployment of Coalition Forces
    - The pipeline of Iraq-Saudi Arabia and the pipeline from Baghdad to Khanagin did not suffer any sabotages.

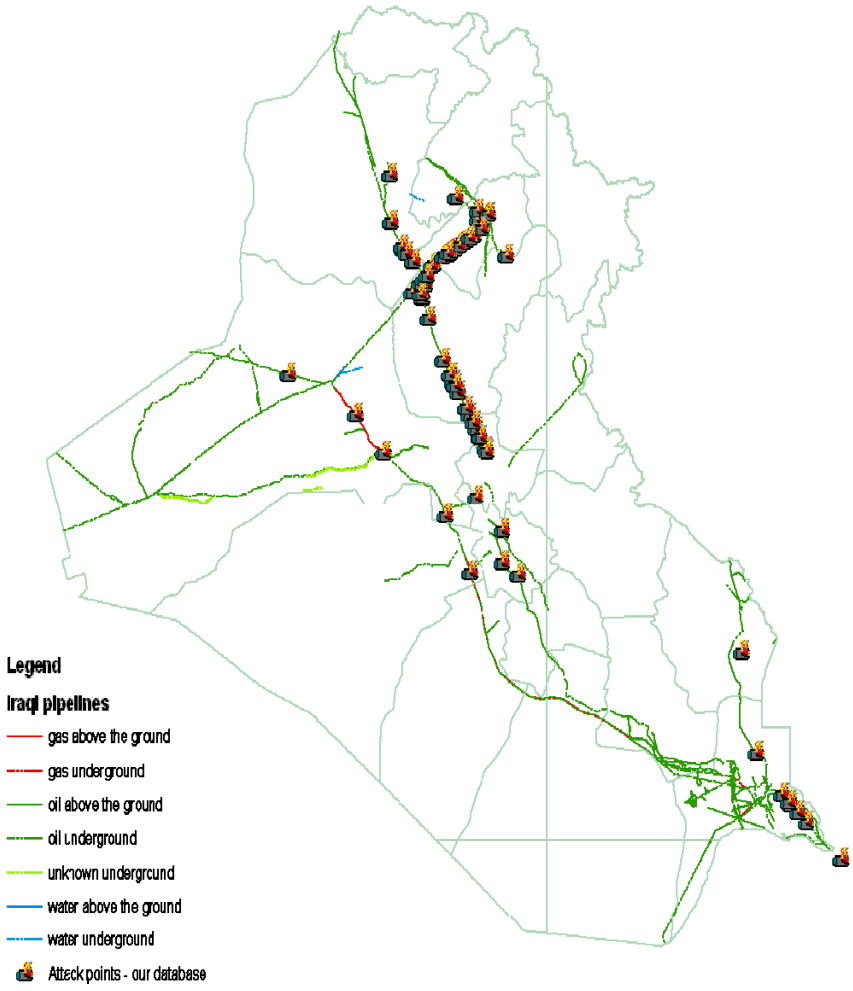

Fig. 6: Distribution of the georeferenced sabotages by pipeline

4. Vulnerability Analysis

Several vulnerability factors have been selected by querng the GIS (database and layers) as having the most important input in the vulnerability of the pipeline network. These factors have been ranked and weighted accordingly (in decreasing order) as follows:

1. Closeness to populated areas and public transportation infrastructure for larger impact and easier escape of the perpetrators (Fig. 8). Weight 20.
2. Location of nearby infrastructures (for additional damages). Weight 15.
3. Impact in the national and international economy. Weight 13.
4. Unguarded pipelines, unfenced sections, lack of buffered areas and areas without surveillance. Weight 10.
5. Pipeline above the ground. Weight 6.
6. Pipeline accessibility (isolated areas in the Western Iraqi desert or in difficult mountainous terrain have received less sabotages). Weight 3.

Considering the factors above, four vulnerability levels have been established as follows (Fig. 7):

I. High vulnerability. This level includes factors 1, 2, 3, 4 and 5 above. Its weight range is 67-48. This vulnerability level includes the pipeline sections of:

   a) Kirkuk to Baiji. The presence of military police at the end of 2004 patrolling the pipeline, has reduced the vulnerability level of this pipeline since then.

   b) Baiji to Baghdad.

II. Moderate vulnerability. This level includes factors 2, 3, 4 and 5 above. Its weight ranges between 47-33. This level includes the pipelines sections of:

   a) Hadithah to the City of Basrah.

   b) City of Basrah to the Basrah Oil terminal

III. Medium vulnerability. This level includes factors 3, 4 above and a weight range of 32-20. This level includes the pipeline section of:

   a) Baiji refinery to the Turkish border

IV. Low vulnerability. This level includes factors 4, and 6 and has a weight range of 19-0. The pipeline sections included are:

   a) Pipeline connecting the oil fields of Abu Ghurab, Buzurgam, and Jabal Faugi with the city of Basrah

   b) Pipeline section between Baiji and Hadithah

   c) The Iraq-Syria-Lebanon pipeline

   d) The Iraq-Saudi Arabia pipeline

   e) The Baghdad and Khanagin pipeline

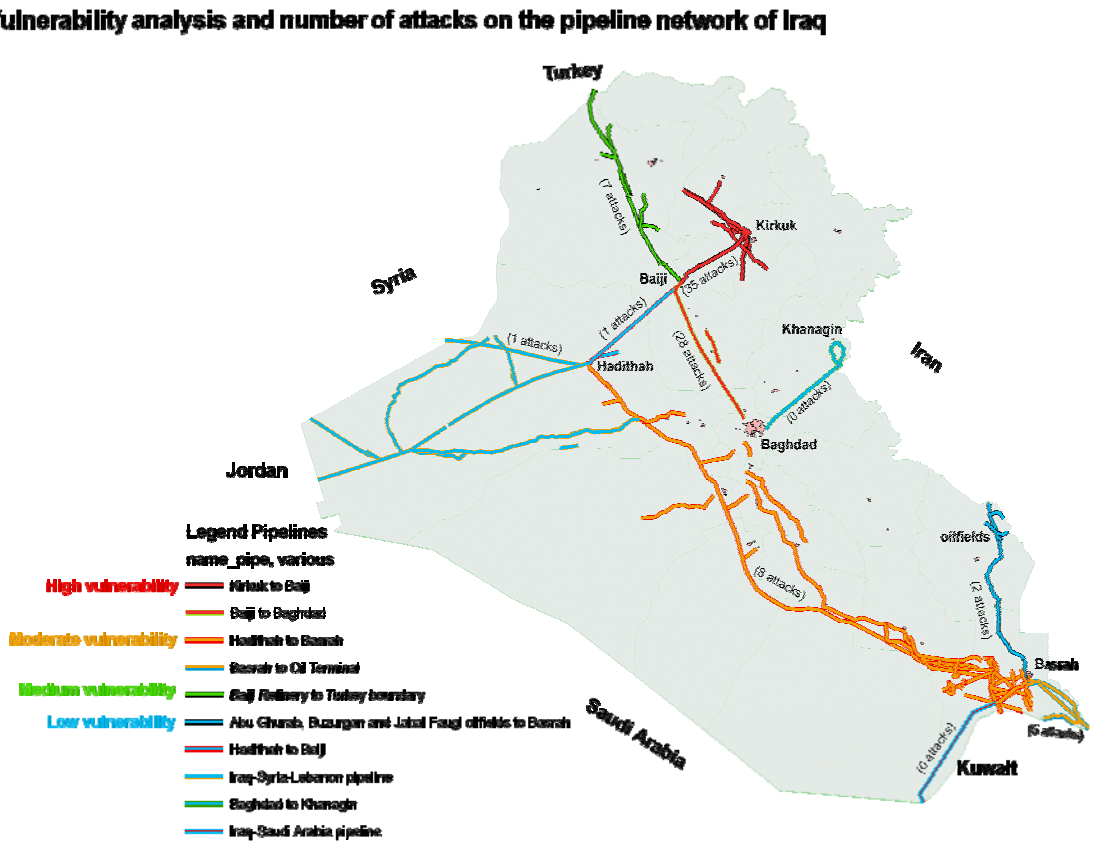

Fig. 7: Vulnerability analysis of the pipeline network of Iraq

5. Conclusions and Future Work

The database of pipeline sabotages together with the mapping of the pipeline network and related oil and gas infrastructures (from imagery and maps) have allowed the geospatial display of the sabotages and to derive the following levels of vulnerability:

Level I. High vulnerability (pipeline sections of Kirkuk to Baiji refinery -35 sabotages- and Baiji to Baghdad -28 sabotages-).

Level II. Moderate vulnerability (pipeline sections of Hadithah to the city of Basrah – 8 sabotages- and City of Basrah to the Basrah Oil Terminal - 5 sabotages -).

Level III. Medium vulnerability (pipeline section of Baiji refinery to the Turkish border – 7 sabotages)

Level IV. Low vulnerability. This level includes the following sections:

a) Pipeline connecting the oil fields of Abu Ghurab, Buzurgam, and Jabal Faugi with the City of Basrah (2 sabotages).

b) Pipeline section between Baiji and Hadithah (1 sabotage).

c) The Iraq-Syria-Lebanon Pipeline (1 sabotage)

d) The Iraq-Saudi Arabia Pipeline (0 sabotages)

e) The Baghdad and Khanagin Pipeline (0 sabotages).

Future work includes the refinement of the MODIS algorithm with the specific conditions in Iraq to confirm and extend the database of sabotages as well as to develop timely alarms for pipeline sabotages that would reduce the lost of oil and gas in the sabotages and to continue the work on the security research subjects outlined in section 2 of this report (Relevancy to the Security Research activities of the GMOSS project).

6. Acknowledgments

The shapefiles of MODIS hotspots over Iraq from March 2003 to June 2006 of NASA Web Fire Mapper / MODIS Rapid Response, were kindly provided by D. Davies, Geography Dept. of Maryland University.

The opportunity to participate in the GMOSS project (Global Monitoring for Stability and Security) contract SNE3-CT-2003-503699 of the 6th FP of the European Commission, is gratefully acknowledged.

7. References

Institute for the Analysis of Global Security (IAGS) 2006: Sabotages on Iraqi pipelines, oil installations and oil personnel. Iraq Pipeline Watch.

GIS and Remote Sensing Based Study on Probable Causes of Increase in Cancer Incidences in Iraq after Gulf War 1991

Hassan Muhammad[a*], Iman Aloan[b], and Åke Sivertun[a]

[a] *Dept. of Compuer. & Information Science, Linköping University, Sweden*

[b] *Phd Orthopedic Oncology, Linköping Hospital, Sweden*

* hasmu331@student.liu.se

Abstract

Accuse of using banned toxic weapons in Iraq during Gulf War 1991 started new debates. The increase in cancer cases was the main focus of these issues. The gap in literature motivated this study to find out the correlation between use of Depleted Uranium (DU) weapons and its assumed effects on human health. The different probable causes of increase in cancer cases, in Iraq after Gulf War 1991, have been discussed in this study. Three potential causes; DU, brick kilns smoke near Basra and Kuwait oil fire smoke have been selected. The major emphasis in this study is to study the correlation between cancers and the use of Depleted Uranium. Different statistical data sets have been used and analyzed in the form of maps and graphs using Geographical Information Systems (GIS) and Remote Sensing methodologies. It is, however, hard to proof - after this GIS based study - that the fired Depleted Uranium is the sole cause of increase in cancer incidences in Iraq. Some trends and risk factors at least can be observed where increase in cancer cases in different Governorates in Iraq, where DU was used, is clearly visible after Gulf War 1991. After analyzing satellite images of different dates, the second part of this study concludes that Kuwait oil wells smoke is probably not responsible for increase in cancer incidences in Iraq. A small debate has been initiated regarding smoke from brick kilns near Basra as the source for malignancy. No study has been found in this regard which can provide evidences that brick kiln smoke is the cause of increase in cancer incidences in southern Iraq.

It's not easy to carry out a full fledge GIS and Remote Sensing based study to identify DU as cause of increase in cancer cases. The main limitation in this regard is shortage of required data. Therefore a new GIS based methodology has been devised which can be used to study relationship between exposure to DU and increase in cancer cases in Iraq. This new methodology is also dependent on specific data sets. Hence this methodology also recommends the collection of specific data sets required for this study.

At the end, an extended study, has been suggested to fill up the gaps found in literature investigating the harmfulness of DU.

1. Introduction

The Gulf War 1991 has significance in many ways. One of the significant issues is the use of some banned toxic weapons. After the Gulf War 1991, different issues have been raised by different societal, journalist and research groups but one issue was quite common in all these and that was the suspected effects of DU on environment and human health. The reason to raise this issue was the notable increase in cancer incidences in Iraq. Lung cancer, leukaemia and birth defects are the most common malignancies which enormously increased after 1991 Gulf war. Depleted Uranium (DU) is a hard and dense metal, which was used in bomb shells and ammunition basically in the battle against Iraqi tanks by US army and allied forces. It is still a controversial debate whether DU is the cause of increase the number of cancer incidences or not. This statement can be proved after analyzing statistical cancer data. These data sets then can be analyzed and presented on the maps to get the pattern of development of

this malignancy so that the organizations responsible to make health policies could focus on certain areas.

Cancer is a kind of malignancy that if it could be found in early stages is relatively easy to cure. There are some other techniques to find the cancer malignancy in individuals but at higher level e.g. health ministry or officials related to health field usually need to know a situation in a proper time so that they can take measures accordingly. For this reason, some early warning systems can be made to find out the alarming situations. In this scenario GIS and RS Technologies can help, with other technologies, to find out any geographical correlations, cluster detection or trends in increase of cancer incidences in specific regions. These kinds of information systems can help making proper policies and to take measures before it gets too late.

2. GIS in Epidemiology

There are several terms in geography like location, space, distance, longitude, latitude, etc. which are now getting used in epidemiological studies. With the advancement of computer technologies, geographical issues have been able to take under deeper consideration. In the early days of computer and geo-technologies, only the graphical maps had been displayed on the screens (Hjalmars. 1998). Later on the analytical functions have been developed significantlly. Geographical Information System is not only helpful in most technological and scientific fields including epidemiology. It is for example easier to connect the spatial phenomena with population patterns and environmental parameters. Health and disease mapping and analysis is then one of the possible applications made available here (Krieger et al, 2003).

GIS is a system for capturing, storing, retrieval, analyzing and displaying spatially referenced data (Hjalmars 1998). These systems give the possibility to attach attribute data to specific geographic entities. These attached attribute data then can be used together with the mapped objects for these advanced analyses.

The correlation between health and its related causes have been studied in the past. The British physician John Snow, studied in 1854 pattern of outbreak of cholera and identified the relation between the disease and infected water. It was definitely not a computer operated study, but at least was a first step towards these kinds of analyses. Different researches in health issues were basically dependent on medical and biological data bases but etiologies are related to geographical conditions (Schærström, 1996). After 1960, things were getting computerized and different scientific fields were trying to make use of their analytical processes with computers. The same happened with the field of geography. Some certain disciplines in geography had been using computers to produce at least graphic maps. The use of GIS in health related issues was not common in late 80's, but even then some studies had been published related to epidemiology, GIS and cancer (Hjarmars, 1998 Gatrell et al, 1998, Swedish Oncological Centres 1995, Geoffrey 1998, Löfman et al. 1996, Rytköne & Robert, 1998, Kulldroff Brody et al, 2004, and othera have shown tha GIS can be used in epidemiological studies with success.

Geographical studies have important role in the public health in many ways. Several factors affect our health where we work and live. Some important geographical analyses have been discussed in the study by Wilkinson et al, 1998. The stated important analyses are:

- "Examination of disease rates and other health statistics by geographical area to assess the health of the population.

- Examination of variation in health and use of health services as comparative approach to needs assessment and resource allocation.
- Examination of time trends in disease at a local level.
- Analysis of the spatial distribution of health care facilities and referral patterns to aid decisions about optimal location of health services.
- Studies of variation in health treatments and outcome for planning the development of health services.
- Studies of health and health promotion interventions at community level.
- Disease surveillance, for example of communicable diseases, congenital malformations.
- Analytical epidemiological studies of factors affecting the occurrence, progression or outcome of disease.
- Investigations of putative environmental hazards including industrial source of pollution.
- Investigations of disease clusters or clustering.

Selection of geographically ordered population samples for surveys".

In this study is made an attempt to verify or falsify the different theories regarding the causal reasons behind the increase in cancer rates in Iraq after the 1991 war.

3. Depleted Uranium, its Different forms and its effects of human body

3.1 Uranium and Depleted Uranium

Uranium is a heavy metal found in nature. It can be found in all soils, rocks, rivers, lakes, oceans, plants and animals in various chemical forms (Bordujenko, 2002). It can also be found in food and drinking water (WHO, 2001).

Approximately 90 μg (micrograms) uranium exists in human body (WHO, 2001). Approximately 66% of total uranium is found in skeleton, 16% in liver, 8% in the kidneys and 10% in other tissues (Bleise 2003). In our daily life normally we consume 1–2 μg uranium in our food and 1.5 μg in water. The food, especially cereals, vegetables and table salt, are the major sources of uranium we found in human body. (Bleise 2003).

Naturally Uranium occurs in oxidized form because it easily oxidizes in air (Bleise 2003). It's a heavy metal with silvery white color (Bleise 2003). It's slightly paramagnetic, slightly softer than steel and pyrophoric (Bleise 2003) (ie, it has a tendency to spontaneously ignite in air when in the form of fine particles) (Bordujenko 2002). In finely divided state it reacts with cold water. Uranium in nature is a combination of three radioactive isotopes. Their mass numbers are ^{238}U (99.27% by mass), ^{235}U (0.72%) and ^{234}U (0.0054%). All uranium isotopes are radioactive (Bleise 2003). Its specific gravity is 5.0 or greater and has very high density (18.95 g/cm^3, 1.7 times higher than lead's density of 11.35 g/cm^3). The melting point of metallic uranium is 1132 °C and its boiling point is 4131 °C (Bordujenko 2002).

According to the WHO (2001) report, during the enrichment process of uranium the content of ^{235}U is enriched from 0.72% to 3%. The remaining uranium contains almost ^{238}U 99.8%, ^{235}U 0.2% and ^{234}U 0.0006% by mass. This remaining Uranium is called Depleted Uranium (DU). DU has about 60% of radioactivity of uranium for the same mass (Mitchel et al. 2004). DU can be called a weakly radioactive heavy metal due to its 40% less radioactivity than Uranium.

Most of the ^{235}U and ^{234}U having removed from uranium to make enriched uranium for weapons or nuclear fuels, but still its chemical and biological properties still remain the same that natural uranium has (Fetter 1999). According to ATSDR estimates, four tons of uranium can be found in one square mile of soil with one foot depth (comparable to 1.4 t/km²) (Bordujenko 2002).

All natural uranium isotopes emit alpha particles. These are positive charged ions. These have relatively large size and charge, so these particles rapidly loose their kinetic energy and have little penetration power (Bleise 2003). These particles can not penetrate even into human skin so these are not harmful for human health. In the decaying process of uranium isotopes, beta and gamma radiation is emitted. Beta and gamma particles have ability to penetrate into human body, but gamma particles have the highest possibility to penetrate into the human body thus can cause hazard both internally and externally (Bordujenko 2002, Fetter 1999).

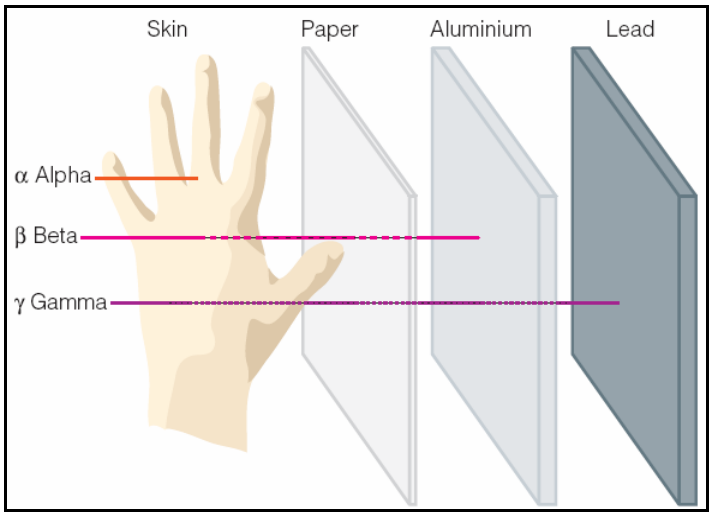

Fig 3.1: Relative penetration of alpha, beta and gamma emissions (Source: Bordujenko 2002)

3.2 Applications of DU:

3.2.1 Civilian applications:

DU has been used as a fluorescent content in dental crowns. It also has been used as X-ray radiation shielding. In commercial aircrafts DU has been used as counter weight, in fork lifters as balancer, in yellow enamel powder for jewelry and badges industry, in the keels of sailing yatches, in satellite blasts, in coloring glass and ceramics, in photographic films, in petroleum exploration (drilling equipment) and also has been used as a catalyst in production of synthetic ammonia (Bordujenko 2002, Bleise 2003, Betti 2003).

In 1992, October the 4th, a cargo plane was crashed with a public residential building in Amsterdam. DU was used as counter balance in that plane. After cleaning the crash site, 150 out of 282 kg of DU was missing out of total amount. Few years after crash, a number of people started reporting health complaints. The substances after the crash were called a possible reason of these health complaints. Six years after crash, a study was carried out to verify if exposure to DU was the reason for health complaints. After using different techniques it was found that its "highly improbable that exposure to DU would result in the health complaints reported" (Haag Uijt de et al. 2000).

3.2.2 Military Applications:

Military applications of DU are almost similar in view of different authours. These authours are Bleise 2003, Bordujenko 2002, Giannardi et al. 2003, Snihs & Åkerblom (2000) In the beginning, DU and Tungsten were under consideration for penetrators and tank amours. Both metals are high density materials. At the end, DU was selected because of its availability, pyrophoricity and price. DU penetrators are hardened during processing by reducing its carbon contents and by alloying with titanium. DU penetrator ignites on high temperature by impact and it melts quickly because of relatively low melting point of uranium. Normally 10-35% and at maximum 70% of DU penetrators become aerosol on impact and contaminate environment. The size of dust particle is normally less than 5 μm and has black color. These particles can be airborne for longer periods. The target hit by DU can be recognized by the black dust cover on it. This dust can be spread by the wind. In controlled tests, it has been experienced that DU dust can be deposited within the distance of 100 m and can be wind transported up to 40 km. DU hit on soft targets do not produce significant DU dust and can penetrate up to 50 cm in the soil. Besides wind the DU dust can be spread with water. Besides all attacking uses, DU also been used as protective shields in tanks.

Depleted Uranium has been used in Iraq, Kuwait, Bosnia and Kosovo in wars. Gulf war is the only war where DU ammunition was fired on large scale. Air force fired approximately 259 ton, army fired approximately 50 tons and marine aviation fired almost 11 tons of DU in Gulf War. Almost 3 tons of DU ammunition was fired during NATO air strike in Bosnia around Sarajevo and almost 10 tons of DU ammunition was fired in Kosovo.

3.3 Exposure to DU:

Exposures may be of two types, external or internal.

3.3.1 External Exposure:

As it's already been stated that alpha particles can not penetrate even into the human skin that's why only beta and gamma components can be considered for external exposure. External exposures can be occurred when somebody passes through the DU dust or when DU fragments are picked up. No visible health effects are expected from external radiation caused by DU left in the field (Bleise 2003).

Fetter, S. (1999) discussed in his research article about the DU exposure in case of individual persons and in case of whole population. He argues with different assumptions regarding individual exposure and finally concludes that it´s dose rate is considerably less to be hazardous. However, direct contact with DU fragments may result in exposure of a higher dose to the skin and become hazardous. Similarly in the case of population exposure he tried to defend his hypotheses on the basis of assumed statistics and in this way conclude that population exposure to DU is also not fatal.

3.3.2 Internal Exposure:

There are three path ways for internal exposure i.e. ingestion, inhalation and contaminated wounds.

Ingestion is not considered the major exposure pathway (WHO 2001). But through soil and by hand contamination it may be considered as a major source. Children may for example be a possible target group for such hand contamination. Contaminated animals can also be a pathway to humans through consumption of their meat and through the milk etc. As the

contaminated areas are small, the food contamination may be considering negligible (Bleise 2003).

Water intake is, however, considered as one of the major pathways to ingest uranium.

According to Bleise et. el. (2003), on the basis of current information, 2-5% amount of DU is absorbed into the blood from intestines and rest of 95-98% is eliminated rapidly. Approximately 90% of the absorbed amount in the blood is rapidly cleared through urine within the first week of intake. The remaining will get distributed in different tissues and body organs. Kidneys are the most effected organs and about 10% deposits can be found here. The amount of uranium deposited in bones remains their, for much longer duration than kidney. About 1% uranium can be seen in bones even after 5 and 25 years.

Inhalation is considered a major pathway for exposure. If the target is harder, then the DU aerosol generation will be higher and softer targets generates limited DU aerosols (Bleise 2003). Particle size also differs from bigger fragments to finest particles. According to estimations, about 60%-69% of aerosols are respirable (Bordujenko 2002). In view of Bleise (2003), inhaled Particles below 10 μm AED (aerodynamic equivalent diameter) can reach deeper pulmonary regions (bronchioles and alveoli) and deposit for considerable time. We can classify the uranium containing particles into two classes, soluble and insoluble, however solubility also depends on the size of particle. If the chemical is soluble then it may take few days to absorb in blood and insoluble may take few months to years. Soluble forms of uranium are associated with toxic chemical effects and insoluble forms are more related to radiation effects. Some amount of soluble and insoluble uranium ultimately goes to the kidneys and the acute longer exposure may impair the kidney function leads to irreversible damage. The persons present at the time of impact may expose considerably. Fires can also be another source of DU particles generation. Fire can produce uranium oxide from a contaminated object which is chemically less harmful than the radiotoxicity.

Wound contamination may occur in combat or later by accidentally bruising the skin on contaminated objects. Small scars can be cleaned effectively and may not have considerable exposure. However, embedded contaminated fragments not removable by surgical mean result in chronic internal exposure (Bleise 2003).

The royal society (2002) working group on the health hazards of DU munitions have produced two research articles considering increased radiation risk from exposure to DU in battlefield and the risks from chemical toxicity and long term environmental effects of DU. Some other aspects are also included raised by public in different meetings. According to these articles there are no or very few chances of hazardous health effects in both short term and long term exposure. There are some studies show short term health effects of DU on human health but were not lead to cancer or other fatal diseases, but, long term effects of DU exposure are not clear yet. Some environmental aspects are also considered in these articles but not showing any long term or fatal effects on human health. Some recommendations for further research are given at the end of the discussion mentioning the areas of required information in future.

Dr. Doug Rokke has a PhD in health physics and is a Vietnam and Gulf War Vet. He was originally trained as a forensic scientist. When the Gulf War started, he was assigned to prepare soldiers to respond to nuclear, biological, and chemical warfare, and sent to the Gulf. He headed the US Army's DU Project after the Gulf War, and advocates a ban on the manufacture and use of DU munitions. He has been attending different conferences regarding uranium weapons and its effects on human health. He has presented a paper on the uses of DU and hazards related, to the British House of Commons, London in December 1999. He mentioned the uses of DU and its effects on human health in different situations. He also

mentioned some areas other than Gulf War, where DU has been fired. These areas are in different parts of the world and even in USA. The residents of these areas have been reporting health complaints. The symptoms of these diseases are very similar to the symptoms of veterans of different battles. Concerning officials are ignoring these situations and not ready to provide proper treatment to the effected population. He also experienced the adverse health effects during Gulf War. He discussed some outcomes of research articles where no significant hazardous health effects were mentioned, but he stressed on the need to conduct screening of DU affected patients right after exposure to DU than after 8 years. He also discussed significant negative health effects. He also mentioned the fact that the governments of US and UK have significant proves of negative health effects but they don't want to publish this material in media.

In a commentary by R. F. Mould (2001) published in British Journal of Radiology, most of the exposure ways to DU and their effects on human health have been discussed. Different groups of affected people have been discusses like uranium miners, Japanese atomic bomb survivors, workers in uranium associated industries, and lung cancer & leukaemia in Gulf War veterans. Thereafter, Iraqi cancer statistics have also been discussed. In uranium minors, several lung cancer cases had been reported but radon exposure was called for the reason of lung cancer. Workers exposed to uranium in uranium associated industries, it was concluded that "there is limited evidence of no association between exposure to uranium and lung cancer at cumulative internal dose levels lower than 200 mSv. However, there is insufficient evidence to determine whether an association does or does not exist between exposure to uranium and lung cancer at higher levels of cumulative exposure." In the case of Gulf War veterans, author states that reported lung cancer and leukaemia cases are not the results of well designed epidemiological surveys and "no significantly higher than expected incidence of these two neoplasms has yet been proven". He referred to another study based on surveillance of gulf war veterans where 60 veterans were included and 15 out of which had DU fragments in their soft tissues and none of them had lung cancer or leukaemia. Another place, author mentioned the published statistics of patients registered in Mosul hospitals. There is a significant increase in cancer cases before and after Gulf war but this data cannot be equated to 100,000 population. He also stated that there may be several other reasons for increase in absolute numbers, so these figures cannot be correlated with exposure to DU. Author tries to prove no relation between DU and said cancer cases by presenting two more cases, possible influence of chemical carcinogens and DU in Balkans. He says that cancer incidences may be due to exposure to chemical carcinogens generated due to smoke in burning Kuwait oil fields and this smoke was carried by the winds over Iraq. He also mentioned that these cancer cases may be generated by chemical warfare between Iraq and Iran where sulphur mustard were used. The long term effects of these chemicals on human health can damage the immune system, birth defects and elevated incidences of leukaemia and lymphoma. In Balkan case, he states that during Kosovo conflict, fuel storages, oil refineries and fertilizer plants were severely damaged, so environmental contamination should be considered while assessing causes of health effects.

- If DU is not hazardous for health then why this issue is still widely being discussed?
- There may be a possibility that cancer incidences may be the reasons of affected environment due to war where most of the chemical and toxic (DU) weapons have been used. Means indirect effects of DU on health.

There is no controversy on the properties and uses of depleted uranium in civil or in military uses. However there are some big gaps present in the literature about health effects of depleted uranium on human body. Most of the researchers explains in their literature (especially US researchers) that DU is totally safe for the human health and some small disorders may happen for time being, short after the exposure to DU. It includes the amount of uranium in urine.

Most of the researchers in their articles tried to present their views on the basis of assumed situations and then to put those situations into mathematical and statistical equations and proved at the end that DU is not hazardous. On the other hand some researchers (Dr. Jawad Al-Ali, Basra Hospital, Iraq) who got the real time primary data from the field or from the exposed population and then found some results which show DU a major cause of different cancers. So there is a big gap between the research on assumptions and research on real time data. No article has been found which states the real situations during the war. So this information is needed that what happened really in the war situation and why the results are different of those researchers who worked on assumptions and who worked on really exposed people in the war situation.

4. Methodology

There are two types of research models have been developed in this research. One is the model on which this research is based. Second is the proposed model. GIS can play a very important role to find out the reasons for increase in cancer incidences. A specifically collected primary data is needed to clearly verify the causes of cancer increase in Iraq. Unfortunately, data required for a detailed research is not available right now. Therefore a detailed and advanced GIS research model has been devised which can be helpful to verify if DU is the reason for cancer increase in Iraq or not. The advanced research plan is devised in different parts. These parts are shown in the following pages.

4.1 Adopted Research Model:

The first research model has three parts. As the topic of this research is to study the probable causes of increase in cancer incidences in Iraq, therefore three possible causes have been studied to find out most appropriate reason for increase in cancer incidences. First part illustrates about the DU as a cause. Iraqi cancer incidence data has been collected from different sources e.g. Iraqi cancer registry and from published and presented articles in international conferences, sources of each datasets are given under relevant tables and its representations. Temporal analysis is the basic analysis for this research. Data has been collected keeping in mind to show the increase pattern in cancer incidences before and after Gulf War 1991. Two types of data sets have been devised i.e. total cancer data for year 1989 and 1994 by province and cancer data by site.

Sorting of data is the next step. Initial data was in paper printing form. The required data has been sorted from these pages. Iraq cancer registry has presented data in different ICD classification in different years. Translation of data sets was an important part to get the actual figures by including actual disease categories.

Tabulation process comes after translation. Data has been stored in table forms using Microsoft Excel software. Different categories and mathematical functions have been applied to get the final required data.

At this step, population data set has been included too to convert data from total cancer incidences to 100,000 population. After getting data by 100,000 population, percentage increase, relative risk and odd ratios have been calculated. Percentage increase and relative risk calculations were available by Iraqi Governorate. These resultant tables then have been converted into the GIS supported format that is DBF.

Thematic layers have been used for temporal mapping showing Iraqi Governorates. The name of each Governorate has been included in the attribute table to join with external cancer incidence tables in DBF format. The common fields “Governorate”, both in attribute tables of

thematic layer and in external tables, have been edited keeping in mind that entries in both types of tables should be identical.

External data tables then have been joined with thematic layer one by one according to the requirement. This joined data then has been carefully classified to show the temporal change in cancer incidence pattern in Iraqi Governorates. These maps then have been presented in the form of layouts.

Second part of the first research model is to verify, if the Kuwait oil well smoke is the cause of increase in cancer incidences in Iraq or not. Satellite images of different time periods have been used for temporal analysis. These images have been acquired by different sources e.g. NOAA, Kuwait Data Archive (KuDA) and from different published and presented articles in international conferences.

Geo-rectification of these satellite images was the first step to start a temporal analysis. Background literature study to understand the phenomenon and interpretation of images has been done in the meanwhile. These Geo-rectified images then have been interpreted visually. The results of these images then have been presented in the form of layouts along with their interpretation in the text form.

Third part of first research model is to verify, if the brick kilns northwards to Basra region is the cause of increase in cancer incidences especially in Basra Governorate or not.

Location of these brick kilns and wind direction information was required for this analysis. Location of brick kilns and along with the interpretation of wind direction has been done to find out the reason. This was the only information available for this analysis. Therefore interpretation has been given.

4.2 Proposed Research model:

The second research model has two major parts. One is statistical data collection and analysis, and second is GIS analysis part. In statistical part, there are further four sub categories have been devised. First one is “total number of incidences by province”. In this part the model, only total number of cancer incidences in whole Iraq has been included by province. Second category “cancer incidences by site for each province” deals with the cancer incidences in Iraq by type, for all Governorates. Third category is similar to first two categories but this not only deals with cancer incidences by site but also by age. The results of these first three categories can also be presented by charts and maps using GIS tools. These three categories make an epidemiological study complete in this scenario.

Fourth category deals with another analysis called odd ratio calculation. There are two groups required to carry on this study. One is Experimental group and other is Control group. This analysis is used to find out the significance and relationship between cause and incidences. It’s important to collect data according to the requirements. Data required for this analysis is not yet available due to the current situation in Iraq. Therefore the confidence level of this analysis depends on the quality of data used.

The second part of advanced research methodology represents a specific GIS analysis study. This study cannot be carried out for whole Iraq due to its nature. It is proposed to carry out this study on one Governorate in Iraq. The most suitable Governorate to start this study is Basra because this area had received maximum DU quantity than others and because of its higher rate of increase in cancer per 100,000 population. This study requires intensive data sets. These specific data sets are not available right now in Iraq’s current situation. This type of data has to be collected yet.

The primary data layers required for this study are, point location of the areas received DU, Residence location of cancer patients and the location of the point where a patient had exposure to DU.

The situation in study area makes it difficult to Geo-code patients' location on the basis of their residential addresses. A whole new database development is required for this purpose. A GPS study is proposed to record all the locations for three basic layers, required for this study.

Attribute data collection for each recorded point is an important part in this study too. This data can store the cancer type and its further attributes. This collected data then will be helpful to find out the morphology of cancer in the area and its epidemiology.

Anisotropy analysis has a key importance in this study. Wind direction and speed analysis will help to make a layer showing the areas having influence of DU radiation. This anisotropic layer then will be overlaid with rest of the two layers, residence location of cancer patients and location of the point where a patient exposed to DU.

Anisotropic analysis, relative risk analysis and odd ratio calculations will provide a final result if DU is the cause for increase in cancer incidences or not.

4.3 Some Important Concepts:

4.3.1 International Disease Classification (ICD):

ICD, International Classification of Disease is a national standard to record the cause of the death under a specific class. Data for Iraqi cancer incidences was available in ICD-9 and ICD-10. World Health Organization took over the responsibility for ICD creation in 1948. After 1948, there comes a 7th revision in ICD called ICD-7 and so on. ICD-10, the 10th revision or the latest classification, has been used by WHO member states since 1994. It was important to translate this data before using it into further manipulation.

4.3.2 Anisotropy:

"Anisotropy is the property of being directionally dependent. Something which is anisotropic, may appear different, or have different characteristics in different directions" (Wickipedia Encyclopedia). It's important in the proposed methodology because the wind speed and wind direction in Iraq has played its role to spread DU all around the deployed place. It requires wind direction and speed data for a required specific time period. Analysis on location of DU deployment layer and wind speed & direction data returns a surface which shows influence of DU in the surrounding area and its magnitude.

4.3.3 Relative Risk:

The relative risk of two groups is simply the ratio of risk between them. It tells us how much risk is increase or decreased from an initial level. If the risk ratio is 0.5, it reduces the chance of having an event to half. If the risk ratio is 3, it increases the chance of having an event by threefold.

4.3.4 Odd Ratio:

"The odds ratio is one of a range of statistics used to assess the risk of a particular outcome (or disease) if a certain factor (or exposure) is present. The odds ratio is a relative measure of risk, telling us how much more likely it is that someone who is exposed to the factor under study

will develop the outcome as compared to someone who is not exposed" (Westergren et al. 2001).

5. Results:

Different data sources have been used to draw some results with selected methodology. Though Iraqi cancer data is not readily available, so the only data which has been gathered from different sources has been presented in graphic and map forms. Some tabular data and their corresponding graphs have been shown in this chapter and then some important maps have also been shown.

5.1 Iraqi Cancer Data Results:

First of all, situation in whole Iraq is been discussed and then emphasis is given on selected areas. These areas have been selected on the basis of availability of data.

In Table 5.1 and its corresponding graph (figure 5.1) shows the continuous increase in each cancer type especially Leukemia, Lung cancer, Lymphoma, Brain/Nerve cancer and Breast cancer. Increase in breast cancer is significantly high almost double.

Tab. 5.1: Incidence/100,000 population of selected cancer types by site by year. Source: Iraq cancer registry 1988, 1991, 1994, 1997 and Iraqi cancer board / cancer registry center for the data of year 2000

Cancer by Site	1986-1988	1989-1991	1992-1994	1995-1997	1998-2000
Nerve,	3.90	4.36	3.91	6.67	5.72
Brain	2.04	2.07	2.17	2.37	2.83
Kidney	1.58	1.85	1.51	1.65	2.11
Bone	5.81	6.07	7.01	7.2	8.95
Leukemia	9.95	10.11	9.09	12.51	12.85
Lung	12.07	12.59	11.71	15.16	13.1
Breast	12.15	12.93	12.71	19.44	21.98
Prostate	1.91	2.14	2.02	2.39	2.8
Bladder	10.28	10.71	11.31	10.15	10.11
Thyroid	2.18	2.63	2.06	2.3	2.91
Multiple Myeloma	0.86	0.97	1.05	1.28	0.91

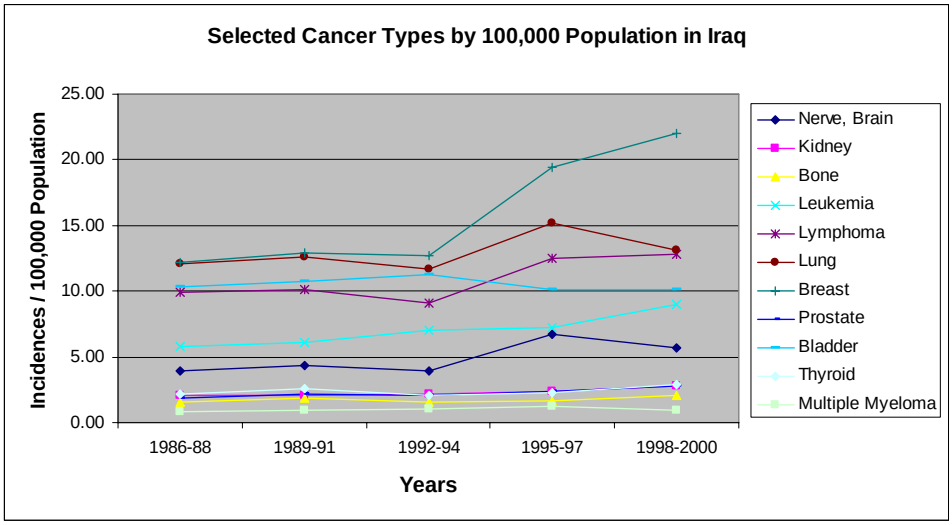

Fig 5.1: Graph showing increase in cancer types by site by 100,000 population

Tab. 5.2: Statistics showing total number of cancer cases and incidences by 100,000 population before and after Gulf war 1991. Source: Jubury, 1998.

	Total Incidences		Incidence / 100,000 Population		
Governorate	**1989**	**1994**	**1989**	**1994**	**% increase**
Baghdad	4183	6427	84.00	149.12	77.53
Ninevah	1500	1629	94.94	89.02	-6.24
Basra	180	461	19.35	37.18	92.08
Taamim	86	114	13.23	17.81	34.63
Misan	37	218	7.12	37.59	428.24
Anbar	51	95	5.80	9.69	67.27
Salahudin	90	94	11.69	10.93	-6.49
Thi-Qar	72	489	7.06	41.79	492.09
Muthanna	27	59	7.94	14.75	85.74
Wasit	44	69	7.33	10.30	40.43
Diyala	69	134	6.70	11.55	72.44
Babil	73	166	6.13	11.94	94.68
Najaf	70	126	11.11	16.58	49.21
Kerbala	28	45	5.49	6.62	20.54
Qadisia	0	86	0.00	13.23	0.00

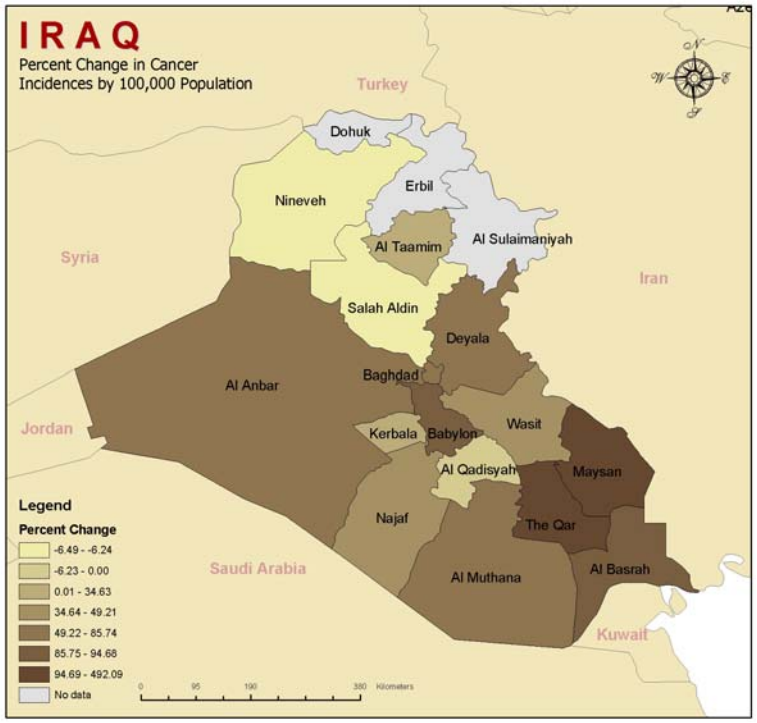

Fig. 5.2: Map showing Percent Change in Cancer Incidences by 100,000 Population from 1989 to 1994

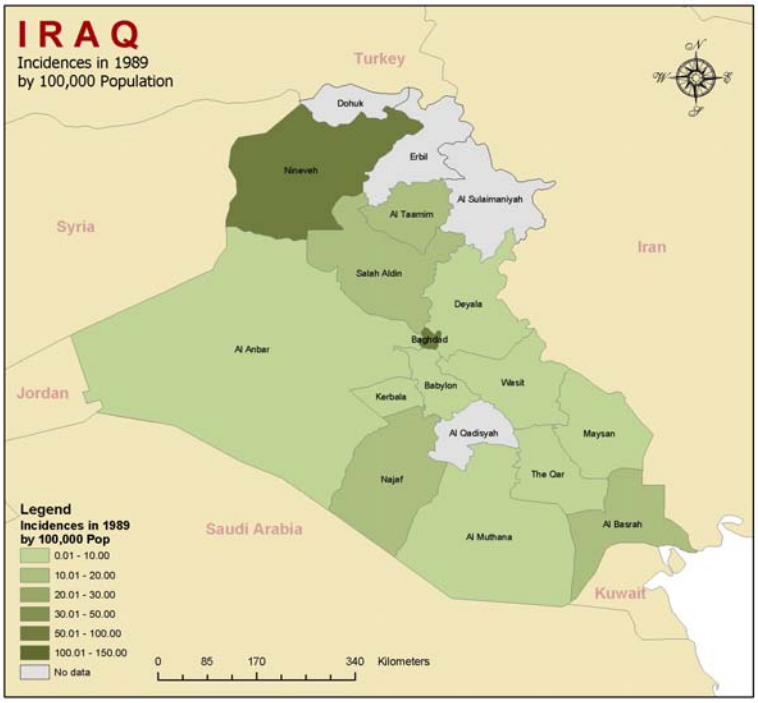

Fig. 5.3: Map showing Cancer Incidences in 1989 by 100,000 Population

A clear change is visible in both maps shown in figure 5.3 and 5.4. These figures represent a temporal analysis. In 1989, Basrah and surrounding Governorates were not having much cancer incidences per 100,000 population but after the Gulf war, Basrah, Meysan and The-Qar Governorates have observed an enormous increase as shown according to data of year 1994 in figure 5.4. Basrah in 1989 had 19.35 incidences per 100,000 population but in 1994 it showed up almost double increase in incidences per 100,000 population. The Maysan and The-Qar Governorates have shown almost 5 times increase in incidences. Most of the other

Governorates have entered into the next level classes where increase was almost double. These changes are quite obvious in figures 5.3 and 5.4.

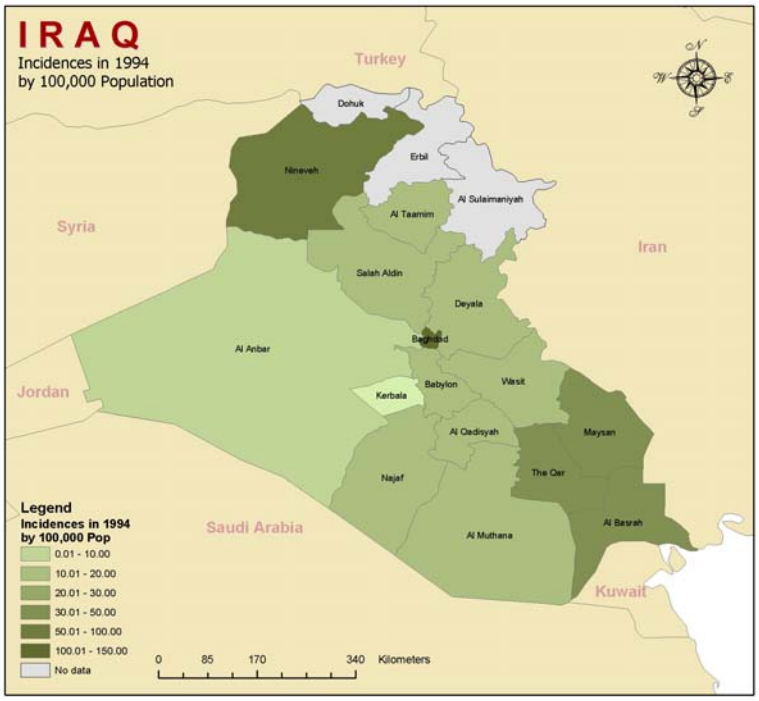

Fig. 5.4: Map showing Cancer Incidences in 1994 by 100,000 Population

It has been discussed already that data availability for Iraqi cancer incidences is very inconsistent due to this reason a continuous data was not available.

Table 5.3: Military personals involved in battle and exposed to explosions

Cancer by site	1991	1992	1993	1994	1995	1996	1997
Lymphomas	10	16	70	85	80	106	82
Leukemias	10	28	45	53	65	70	40
Lung CA	4	6	39	40	41	40	40
Brain CA	1	2	20	30	35	40	34
Bone CA	2	3	5	10	10	12	15

Table 5.4: Military personals involved in battle but not exposed to explosions

Cancer by site	1991	1992	1993	1994	1995	1996	1997
Lymphomas	-	2	8	11	9	8	6
Leukemias	1	4	7	11	7	12	6
Lung	2	6	7	15	11	23	14
Brain	-	-	-	2	4	7	10
Bone	-	-	2	12	7	3	3

Some different data sets are available from Iraqi Cancer Registry and other published material presented in different conferences. Iraqi Cancer Registry provides information of cancers by sites but it doesn't provide information with geographical contexts. That's why it's a difficult rather near to impossible task to conduct a full fledge GIS based study on available data. It is recommended that data collection should be the first stage for any related GIS bases study in Iraq for cancer incidences. It should have made possible to get a smooth data for GIS analysis. This study even provides some significant trends on the basis of available data.

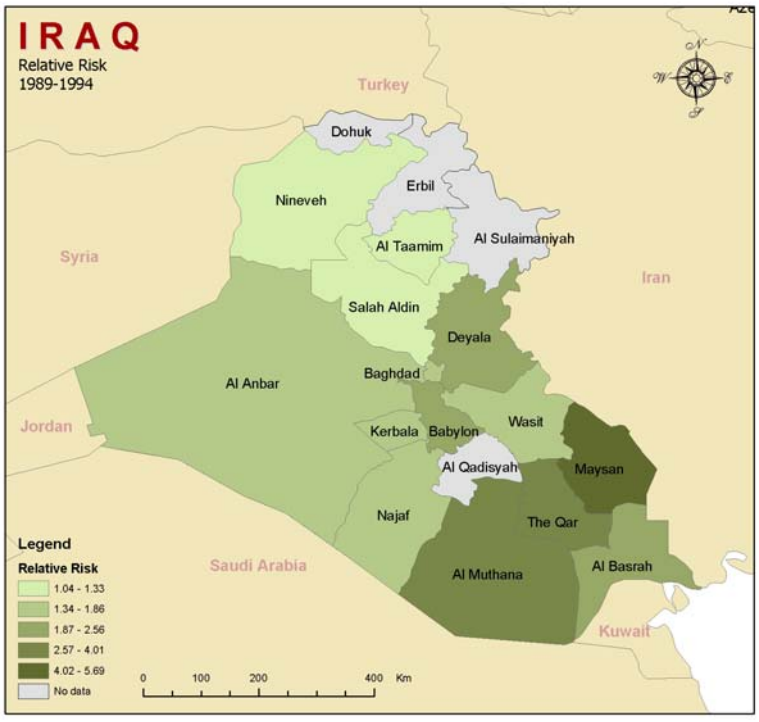

Fig. 5.5: Map showing Relative Risk 1989-1994

5.2 Basra:

Basra is the region which had received maximum amount of Depleted Uranium. The percentage increase in cancer cases has also been maximum in Basra and surrounding The-Qar and Muthana Governorates. A study has been carried out on the data of the military personals who were involved and the personals who were not involve. The results according to the data represent high rate of increase in cancer incidences the personals who were exposed to DU and lower rate of increase in personals who were involved in the battle but were not exposed to the DU explosions. The detailed discussion is as follows:

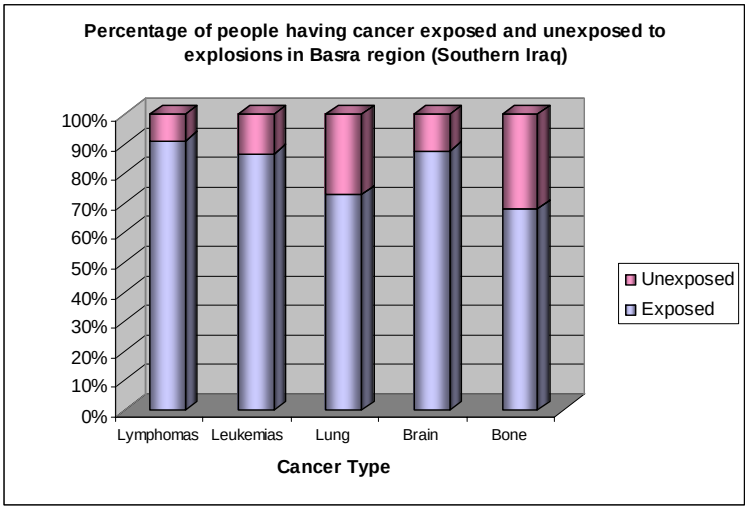

Fig. 5.6: Graph showing Percentage of military personals having cancer exposed and unexposed to explosions in Basra

Tables 5.3 and 5.4 show the number of cancer incidences of military personals that were exposed and unexposed to the explosions, while, Figure 5.6 shows the percentage of military personals having cancers and who were involved in battle and were exposed or unexposed to the explosions. The personals that were unexposed to the explosions showed up with less cancer cases but on the other hand the personal that were exposed to the explosions showed up with huge number of cancer cases in the battle around Basra.

Figure 5.7 shows the increase in cancer cases per 100,000 populatoin in Basra Region where a significant increase is visible between year 1988 and 1998.

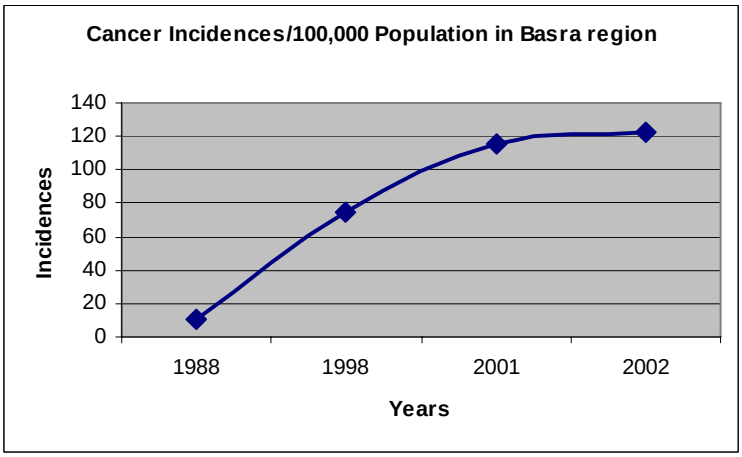

Fig. 5.7: Graph showing Cancer incidences in Basra Region

5.3 Baghdad:

Baghdad, the capital of Iraq, also presents the increase in cancer incidences per 100,000 population, detail of which is as follows:

Table 5.5: Cancer Incidences by site per 100,000 population in Baghdad. Source: Iraqi cancer registeries

Cancer by Site	1986-88	1989-91	1992-94
Nerve, Brain	4.32	10.56	12.27
Kidney	2.68	5.58	7.09
Bone	2.01	4.74	5.32
Leukemia	9.58	18.05	23.18
Lymphoma	11.17	24.79	31.59
Lung	17.86	35.53	42.95
Breast	20.29	41.49	52.09
Prostate	2.68	4.93	7.95
Bladder	12.45	24.84	34.23
Thyroid	2.58	6.09	6.82
Multiple Myeloma	1.72	3.26	4.68

The situation in Baghdad governorate is the same as Basra. The increase in cancer cases per 100,000 population is quite visible. Breast, Lung, Leukemia and Lymphoma showed up almost double to triple increase in cancer incidences by 100,000 population.

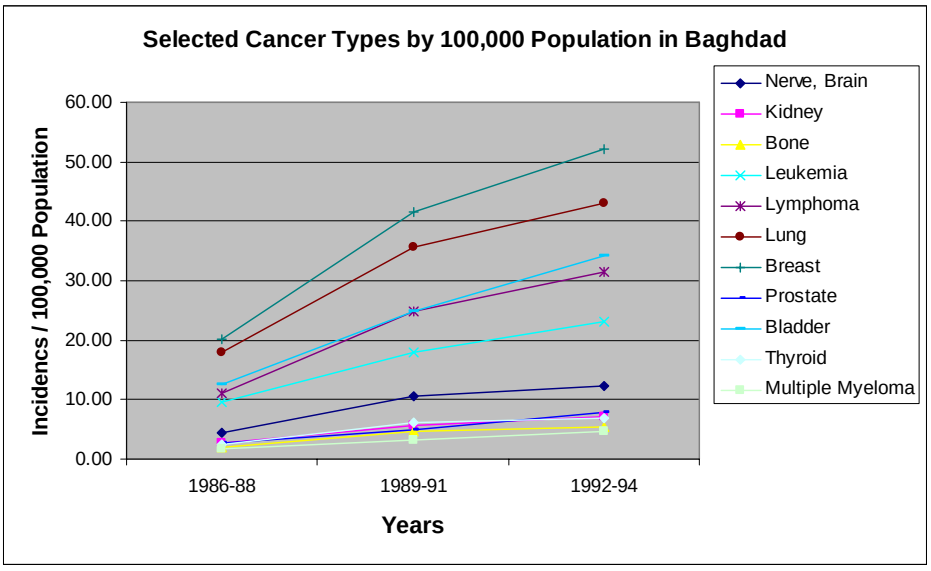

Fig. 5.8: Graph showing Selected Cancer types by 100,000 population in Baghdad

5.4 Mousal:

Situation in Mousal city is also not different than other regions. This is the bigger city in Ninevah Governorate. Ninevah Governorate has been showing already a higher rate of cancer incidences per 100,000 population before Gulf War but the rate of cancer incidences just got even higher after the Gulf War. Lung, Breast, Leukemia and Lymphoma have shown a great increase in cancer incidences as shown in Table 5.6 and corresponding graph in Figure 5.9.

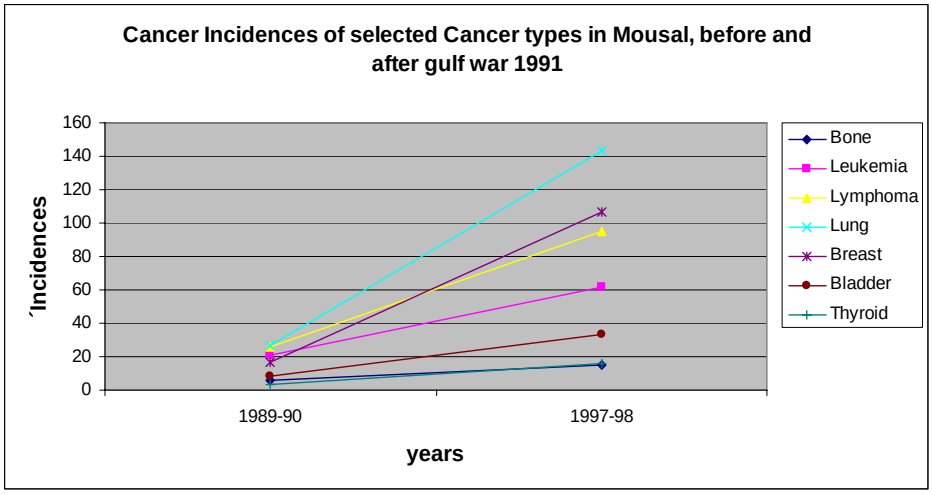

Fig. 5.9: Graph showing Increase in Cancer Incidences in Mousal before and after Gulf War

6. Brick Kiln Smoke Study:

Brick kilns near Basra have also been accused as probable cause of increase in cancer incidences in southern Iraq. The relevant data and literature is not available, rather study of this causal factor is still to be carried out. This causal factor still has to be explored fully. There are some questions which should be answered correctly in this regard, e.g. what is the trend of wind direction in Iraq? What is the location of brick kilns in Iraq? What has been using in brick kilns in the name of fuel? The information and data required for this study is; wind direction information in the form or maps and textual interpretation, the fuel used in these brick kilns and their precise location.

Some assumptions have been made by author regarding this issue. Wind direction is the first scenario in this case. The location of brick kilns (figure 6) is at the northward direction of Basra. The detailed wind direction and speed record is not available but this information can be assessed by the satellite images showing Kuwait oil fire smoke (this issue has been discussed in detail in part 7). The wind direction, which has been observed by satellite images, is mostly towards southeast direction. This means the smoke of these kilns goes directly towards the direction of wind and obviously there is Basra region at southeastern direction.

Secondly, the nature of fuel is the major factor which should be analyzed properly. We consider the study of Kuwait oil fire smoke in this context. The smoke from burning oil has not been proven as a cause of long term serious health effects, e.g. cancer, in Kuwait scenario. Eye and upper respiratory tract irritation, shortness of breath, cough, rashes, and fatigue were the complaints from the exposed population and officials (see part 7). Therefore if crude oil has been using in these brick kilns then the smoke of brick kiln should not be called the cause of increase in cancer cases. The situation can be different if the fuel, which has been using in these kilns, is different than crude oil.

The map displayed in figure 5.10 shows industrial contamination sites while the location of brick kilns is highlighter with a circle. Arrows shown in the map describe the direction of wind.

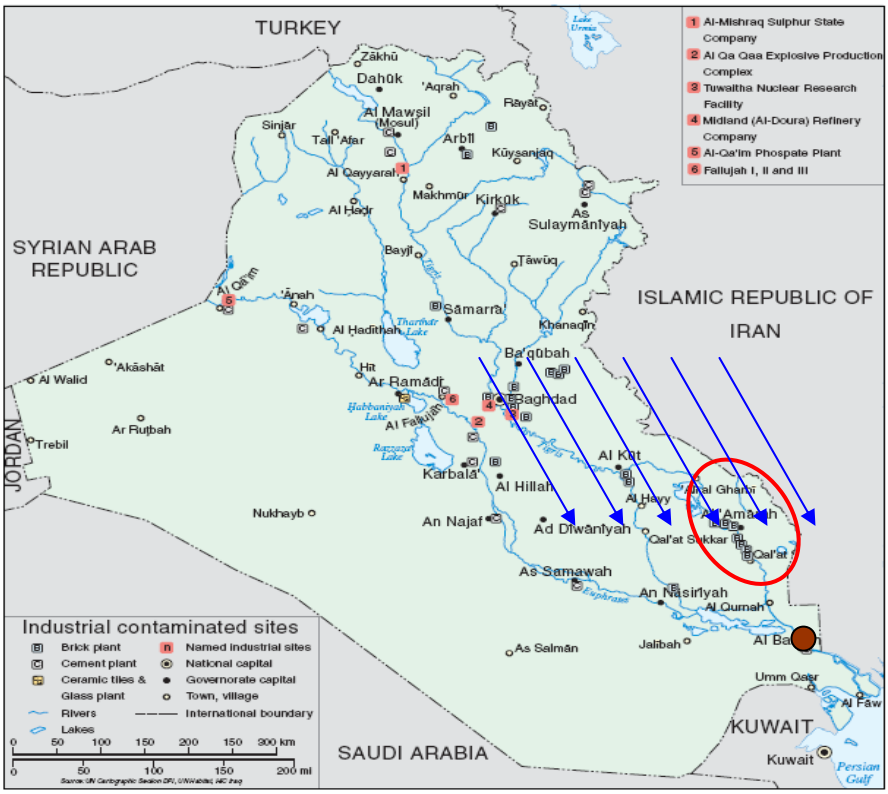

Fig. 6: Map showing Industrial contaminated sites while showing Brick Kilns at north of Basra. Source: UN Cartographic section DPI, UN Habitat, HIC Iraq "Environment in Iraq: UNEP Progress Report" October 2003.

7. Fire at Kuwait Oil Wells:

In the beginning of year 1991, Iraqi troops withdrew from Kuwait and set fire to more than 600 oil wells and pools of spilled oil in Kuwait. This fire burned for more than eight months from third week of February 1991 to November 6, 1991. This was a threat to the environment and human life. This was rather a beginning of a new war between allied forces and Iraqi forces. During this war DU weapons have been used in Iraq. After four years of this war an increase in cancer incidences in Iraq has been observed. DU has been called as a major cause for increase in cancer incidences but some of the journalist and social circles mentioned that smoke from Kuwait oil wells may also be one of the causes increase in cancer incidences in Iraq and especially in Basra, southern Iraq.

There have been several studies on Kuwait oil wells fire and its effects on environment and human health. These studies show some heath issues caused by this thick smoke in Kuwait and surrounding areas. Before going towards GIS study on this topic it is worth to include some extracts of different relevant publications.

7.1. Background Study:

The OTA Background paper (1994) assesses the Kuwait oil fire health risks. One of the findings of this multi dimensional study was "using state-of-the-art risk assessment methods, the risks to health from exposure to the smoke and the background air contaminants in the Persian Gulf are likely to be extremely small. If aspects of the Persian Gulf experience are causing illness, they are likely to be other than oil fire smoke, according to DoD's risk assessment".

In another research by Petruccelli et al (1999) on US troops, after their return, a sample of 1599 soldiers was taken who have been on mission for three months in Kuwait. They have been inquired about the symptoms before, during and after the mission. The symptoms were eye and upper respiratory tract irritation, shortness of breath, cough, rashes, and fatigue. The decreasing trend of these symptoms has been observed in soldiers after leaving the Kuwait. Thus concluded the oil fire smoke is one of the factors for these symptoms.

In a research to find the relationship between asthma and bronchitis in Gulf War veterans and Kuwait oil fires by Jeffrey et al (2002), states that there is no relation proved. The sample of 1560 Gulf War veterans was taken after five year of Gulf War. This study proves that exposure to oil fire smoke doesn't cause respiratory symptoms among Gulf War veterans. The 94% of veterans were well exposed to oil fire smoke and 21% of which were remained there for more than 100 days.

In another study by Kelsall et al (2004), 1456 Australian Gulf War veterans were examined. This study doesn't support any long term effects of oil fire or dust storm exposure.

Dr. John Andrew, Administrator for Science for the Agency for Toxic Substances and Disease Registry within the Public Health Service, with his other two colleagues has been appointed for the assessment and planning for public health needs in Kuwait. He presented a Congressional Testimony "Potential Adverse Health Effects of Service in the Persian Gulf War" before the subcommittee on Hospitals and Health Care Committee on Veterans' affairs. He has been involved in several research studies on the health effects of Kuwait oil fire smoke. In this testimony he resumes all the studies and stated all the facts about health effects of oil fire smoke. According to him, Sulfur dioxide and Nitrogen dioxide, two major pollutants, never reached to harmful levels. Carbon monoxide levels rarely exceed the US alert levels and the reason told was the possible increase in vehicular traffic. Levels of particulate matters also exceed US alert levels but this situation has been observed in Kuwait so often before oil well fire due to sand and dust storms. Furthermore, army personals, fire fighters and Kuwaiti citizens exposed to the smoke, have been examined. After using several models and analysis of real time data sets it's summarized that "Based on the exposure information that has been assembled, we do not believe that there will be a detectable increase in lung cancer in Gulf War Veterans as a result of the oil well fires".

According to mentioned studies none of these pointed out cancer as emerging or prevailing threat due to oil fire smoke. Now let's have a look at some studies about the direction and speed of the wind during these months.

Regarding direction of the smoke, a study has been carried out by Limaye et al (1992). This smoke was visible from weather satellites in polar and geosynchronous orbits. Meteosat visible and infrared satellite observations indicate the smoke direction that it often traveled southeastward along the western coast of Persian Gulf and then turned towards west and then southwards to the Arabian coast. Some dust storms, formed in Syria and Iraq changed its direction towards southwest Kuwait and sometime towards northwest Saudi Arabia.

In another study, Kuwait Data Archive (KuDA) had been developed. It was an initiative taken by National Centre for Atmospheric Research, Colorado in 1994. The basic purpose of this initiative was to archive the data and analysis results of accounts which had been carried out to study the phenomena. This archive was not only well organized but some studies also had been carried out under this umbrella. The spatial distribution of smoke through out the whole period of fire on oil wells had been studied. Smoke distribution contours were generated on the basis of daily smoke monitoring data. Figure 7.1 and 7.2 are showing moderate and heavy smoke contours respectively. Numbers on contour lines are showing the number of days smoke had been covered the area. One thing is pretty clear in these figures too that the

concentration of the smoke has been towards the south of Kuwait and over the Persian Gulf instead of Iraq. The reason is wind direction.

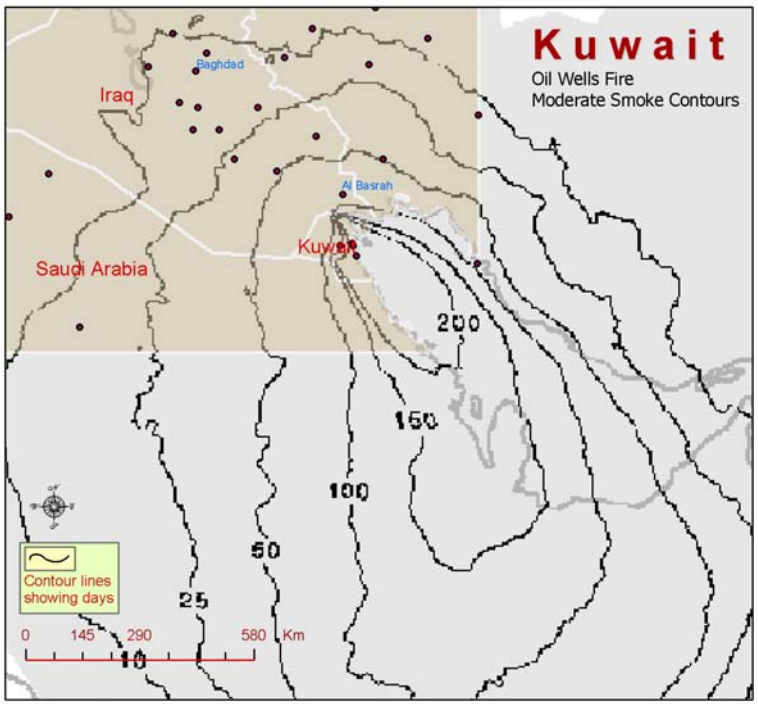

Fig. 7.1: Kuwait oil well fire, Moderate Smoke contours. Numbers on contours show the number of days. Source: Kuwait Data Archive (KuDA)

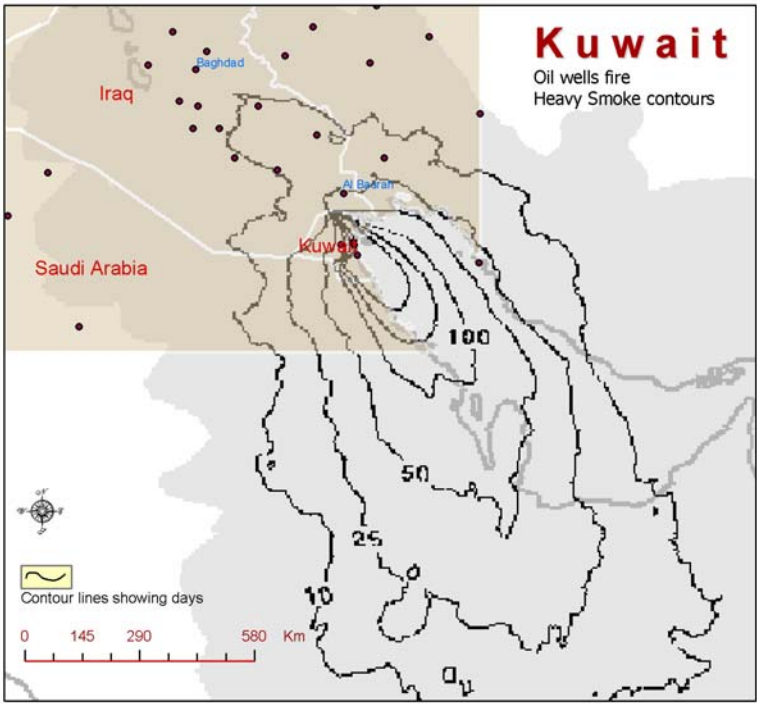

Fig. 7.2: Kuwait oil well fire, Heavy Smoke contours. Numbers on contours show the number of days. Source: Kuwait Data Archive (KuDA)

Air Research Laboratory (NOAA) has developed a model of smoke concentration areas using daily monitoring data from February 1991 to October 1991 in the Persian Gulf region. This model shows clearly the smoke concentration on Saudi Arabia, Iran, southern Kuwait, Gulf

states and on the Persian Gulf. This model doesn't show any smoke movement towards Iraq. This model also verifies the case study with satellite imageries. Figure 7.3 shows the model showing smoke coverage areas.

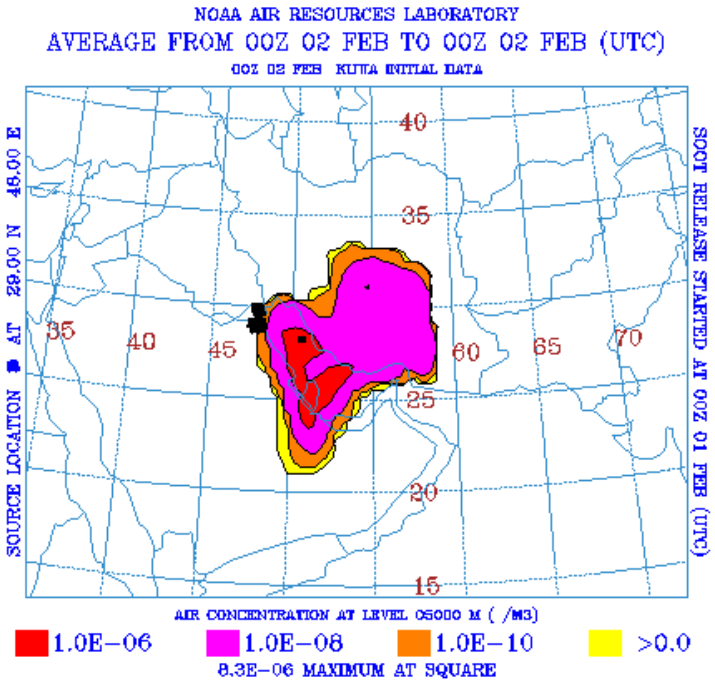

Fig. 7.3: Model showing smoke coverage areas

7.2. Temporal Study of Smoke Direction by Satellite Images:

In this research, different satellite images on different dates from different sources have been taken and analyzed. This study will verify if Kuwait oil fire smoke is one of the causes of increase in cancer incidences or not.

First three images (figure 7.4, 7.5, 7.6) have taken by NOAA-11 1Km AVHRR. These images are multi-spectral false color composites. Image one, in figure 7.4, is taken on January 15, 1991 almost one month before oil fire. It clearly shows nothing in the name of smoke and fire in it. Second image in figure 7.5 has taken on February 12, 1991. This image shows three spots in south of Kuwait and the trails of smoke traveling towards south of Kuwait and then turns towards west in the Saudi Arabia. One spot is visible along the northern border of Kuwait in the Iraq and shows one spot of fire and some is traveling towards south east of Iraq in the Persian Gulf.

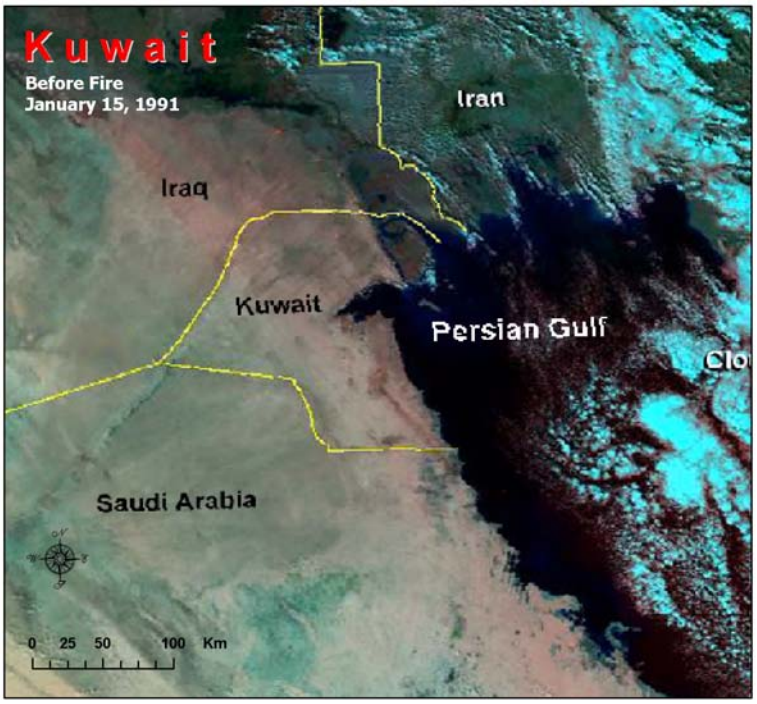

Fig. 7.4: Image taken just one day before Operation Desert Storm (NOAA-11 1Km AVHRR Multi-spectral False Color Image. January 15, 1991)

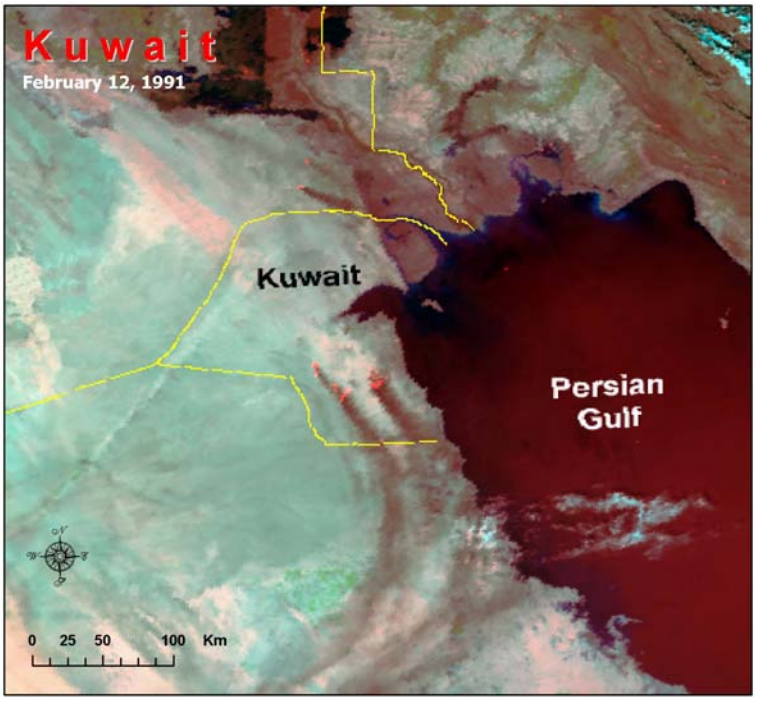

Fig. 7.5: Oil wells south of Kuwait. Smoke is visible traveling towards southeast and then southwest direction of Kuwait. (NOAA-11 1Km AVHRR Multi-spectral False Color Image. February 12, 1991)

Fig. 7.6 shows some more and aggravated activities in oil wells in the same area. Smoke plumes are thicker than previous figures and more oil wells are on fire on March 11, 1991. Another spot is visible in this image is and it's towards north of Kuwait city. The spot visible in figure 7.5 in Iraq is not visible in figure 7.6 which means that it has been caped.

In figure 7.7, we can see an image with relatively higher resolution focused on the oil well fire smoke. This inset image has taken by NASA during its mission at April 1991. One hot spot rather bigger spot is visible at the southern part of Kuwait and two spots are clearly visible at the northern side of Kuwait city in this inset image. The important thing which is visible here is again the direction of smoke. The direction of smoke is southwest. The blowup of the same image is shown in figure 7.8, which shows the situation with a closer angle.

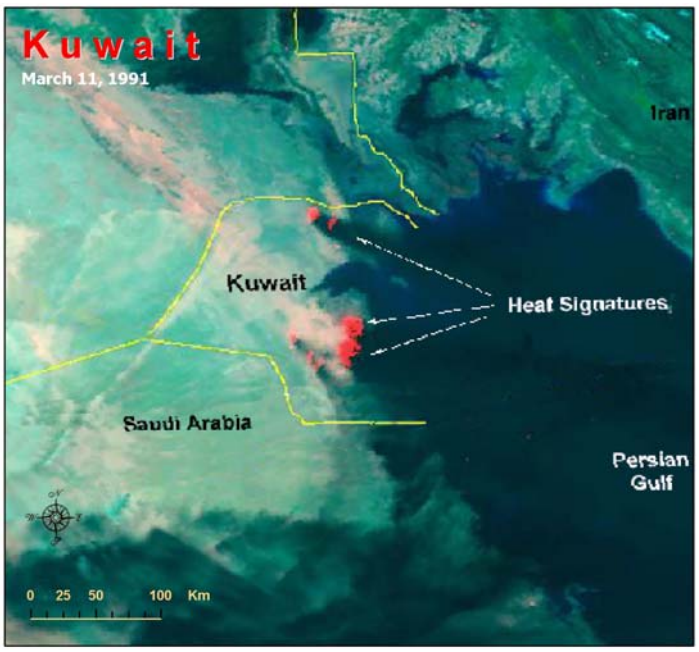

Fig. 7.6: Hundreds of oil wells continue to burn out of control. Some other oil wells are visible at north of Kuwait city in this image. Skies are filled with thick black smoke, which traveled for hundreds of miles south and east of the source. Note the accumulation of smoke in Saudi Arabia where the winds appear to be lighter and shifting more from the east. The red areas at the base of the smoke plumes indicate heat signature. (NOAA-11 1Km AVHRR Multi-spectral False Color Image. March 11, 1991)

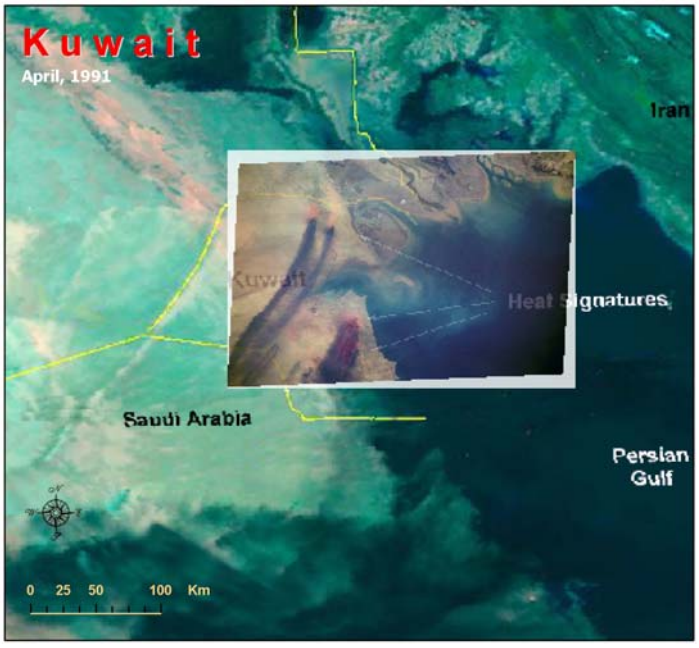

Fig. 7.7: Inset image showing clearly the heavy plumes of smoke and its direction southwest. (Mission: STS037, NASA. April, 1991)

Fig. 7.8: Blowup image of inset figure 6.8 Mission: STS037, NASA April, 1991

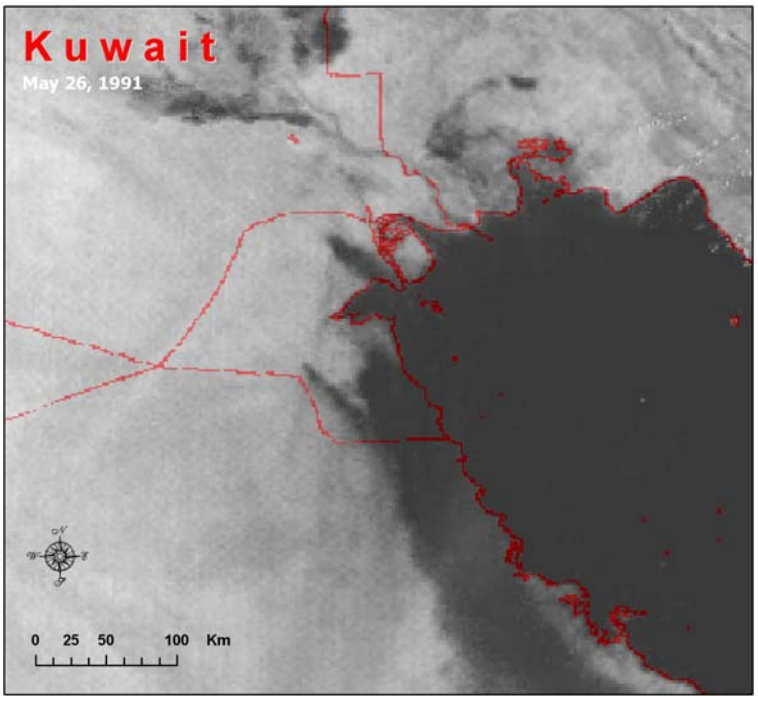

Fig. 7.9: Heavy smoke is visible. West coast of Persian Gulf is not clearly visible. (LAC visible (0.63 □m) image from the NOAA-10 AVHRR. May 26, 1991)

An image from another source has been used in figure 7.9. This figure again shows the heavy smoke from the oil wells and direction is towards southeast over the Persian Gulf on May 26, 1991.

Figure 7.10 had been taken on June 20, 1991 by DMSP-F08, DMSP-F09, DMSP-F10 and the resolution is 500m. The same situation is visible in this image too and the smoke direction is towards southwest into the Saudi Arabia.

An inset image in figure 7.11 had been taken by another mission from NASA on November 1991 after the oil wells were caped. This image shows the residuals from oil fire smoke are spread all over the ground around oil fields and the direction is again clearly visible towards south east along the Persian Gulf. The blow up of same image is shown in figure 7.12.

From all the studies on the health effects of oil fire smoke on human health and the direction of smoke, this fact can be stated safely that Kuwait oil wells fire smoke is not harm full for human health to this extent that it could cause cancer. Only some short term respiratory symptoms can be observed. The same thing can be verified from the satellite image study on different dates and its visual interpretation.

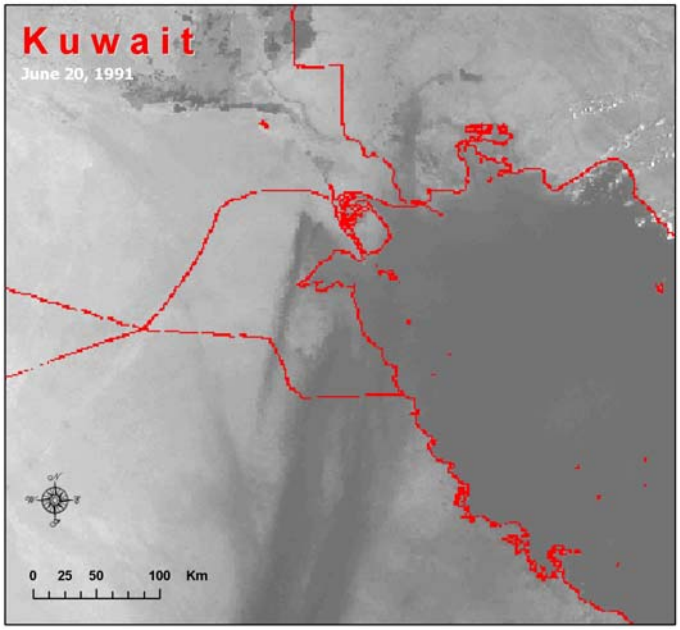

Fig. 7.10: Smoke is visible and traveling towards southward of Kuwait and spreading all over the major part of Saudi Arabia. (DMSP-F08, DMSP-F09, DMSP-F10. 500m resolution. (DMSP: Defense Meteorological Satellite Programme. June 20, 1991)

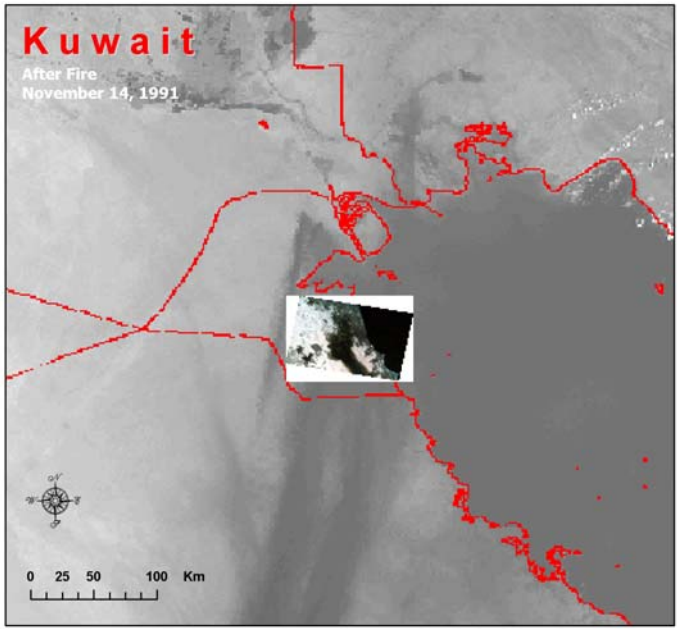

Fig. 7.11: Inset image taken after the fire. Showing the stains of oil residues in the south east direction. (Mission: STS044, NASA November, 1991)

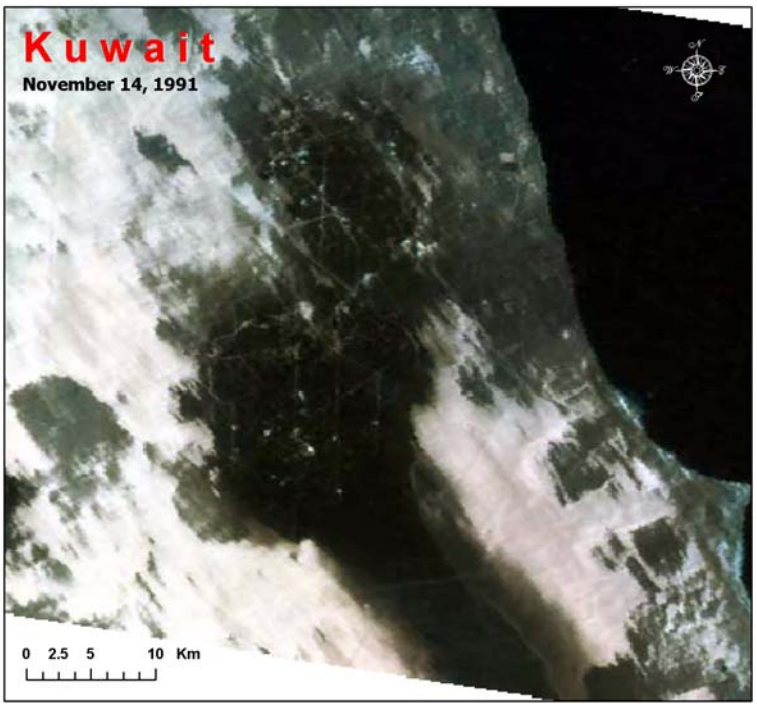

Fig. 7.12: Blowup image of inset figure 6.12. Mission STS044, NASA. November, 1991

8. Discussion and Conclusion:

After a careful review of literature on effects of Depleted Uranium on human health, couple of issues has been drawn out. One thing is common in the literature regarding DU and that is properties and uses of DU. Big gaps can be found in the literature about its long term health effects on human health. Some of the sources clearly mentioned that use of depleted uranium as weapon is not harmful enough to be a cause of cancer occurrence. Some of the researchers presented their work on the basis of assumptions. On the other hand the researchers in Iraq are trying to collect cancer incidence data and tried to prove that increase in cancer incidences is due to use of DU weapons. These Iraqi researchers not only presented their results on the basis of collected cancer incidence data but according to its morphology and its changing pattern too. The cancer types which were observed in elderly people now have been seen in children too. Secondly some of the patients have been observed having more than one cancer in the body. Third, familial cancers have been found where more than once cancer patients can be observed in one family (Al ali, 2003). These phenomena are very new in Iraq.

Dr. Doug Rokke (1999), as stated earlier, mentioned that the governments of UK and United States have enough proofs regarding negative health effects of Depleted Uranium but they don't want to open it up publicly.

The current GIS Study, to verify DU as the cause of increase in cancer incidences in Iraq, shows some results from the analysis of available data. These results show a positive increase in cancer incidences per 100,000 population in Iraq especially in south of Iraq. Basra region is the most effected region showed up in the results where percent increase in cancer incidences after Gulf War 1991 was highest. Muthana and The-Qar Governorates also show enormous increase in cancer incidences. According to the classification of data, The Governorates in southern Iraq, Muthana, The-Qar and Basrah, are gone to the maximum highest classes and the Governorates in central Iraq other than Baghdad have also entered in the next classes. Baghdad Governorate is also showing enormous increase in cancer incidences after Gulf War 1991. The Ninevah Governorate was showing the increased cancer incidences before Gulf

War 1991 and after the war it remained in the same class but increase was high in numbers though. Relative Risk of further increase in cancer cases is highest in Muthana and The-Qar Governorate. Basrah is at the second number. The overall relative risk is showing a clear picture and still the risk is higher. Percentage increase in cancer incidences is highest again in Muthana and The-Qar Governorate.

Southern Iraq is the area where increase in cancer incidences is higher than other parts of Iraq and these Governorates are at relatively high risk. The use of DU weapons can not be said the sole cause of this increase due to lack of data on this specific topic. But general trends and results doesn't present any other cause of this increase. The situation before and after Gulf War 1991 somehow shows DU the cause of increase in cancer incidences in this scenario. One thing which makes DU a stronger cause of increase in cancer cases is the analysis of soldiers who were involved in battle and exposed to the DU explosions and the soldiers who were involved in the battle but not exposed to the DU explosions. The results show the clear picture of those who were exposed to DU having much more cancer cases than those who were not exposed to DU.

The analysis of three most populated areas in Iraq, Basra, Baghdad and Mousal, tells the same story. The increase in cancer incidences is manifold in these areas after Gulf War 1991.

The confident decision cannot be taken that DU is the only cause of increase in cancer incidences due to unavailability of specifically required data.

Brick Kiln smoke study is needed to be conducted properly. There is no detailed map or location information of brick kilns available. The literature doesn't show any specific study about this issue. The fuel for these brick kilns should also be verified. If the fuel used in these kilns is the oil (fossil fuel produced in Iraq) then it's not dangerous for health according to the outcome of the studies carried out for Kuwait oil well smoke issue. According to this study the thick plumes of smoke doesn't cause any long term health problem and specifically cancer. This issue however can not be underestimated. So a proper study should be carried out in this regard with properly collected data.

Kuwait oil wells smoke study in this research clearly shows disagreement on the statement that Kuwait oil well smoke is also one of the causes of increase in cancer cases in Iraq. The direction of the smoke has been towards the south of the Kuwait. The chances of this smoke to enter into the Iraqi territory are very few. Therefore it's safe to say that Kuwait oil wells fire smoke is not a cause of increase in cancer incidences in Iraq.

The datasets are available in current situations are not quite enough to carry out a detailed GIS study. Therefore no confident results can be drawn out. The epidemiological studies with the help of GIS are acknowledged. Therefore a detailed GIS methodology has been devised which can help to verify the DU as cause for increase in cancer incidences. This model and its results are dependant on good quality data. Wind direction and speed data, DU deployed sites and cancer patients' location data is required for this analysis.

The major limitation found in this study is unavailability of enough and required data

In the light of above facts and analysis results, Depleted Uranium is the only cause left which is the most suspicious in this entire scenario. A detailed and sincere effort is required to finally figure out this issue. The only key factor which can play an important role to find out acceptable results is the data. It's not possible to get a reliable data from Iraq in current circumstances, therefore carefully collected data according to the needs of study is required before hand.

9. References:

Al Ali, Jawad. “Cancer Incidences in Basra after 1991” World Uranium Weapons Conference, Hamburg, 2003

http://www.uraniumweaponsconference.de/

Asaad A. Ameer Khalaf, “Cancer Trend in Basra after Gulf Wars” Conference of the European Network for Pease and Human Rights, European Parliament Brussels, 2005.

http://www.russfound.org/Enet/DrKhalafpap.htm

Betti Maria, “Civil use of depleted uranium” Journal of Environmental Radioactivity 64 (2003) 113-119

Bleise A., P.R. Danesi, W. Burkart, “Properties, use and health effects of depleted uranium (DU): a general overview”. Journal of Environmental Radioactivity 64 (2003) 93-112

Bordujenko A., “Military medical aspects of depleted uranium munitions” ADF Health Volume 3, 2002

Bordujenko Alex, “Risk assessment: exposure to depleted uranium” ADF Health Vol 4 (2003)

Braga M. Cesare Cislaghi, Giorgio Luppi and Carola Tasco, “A Multipurpose, Interactive Mortality Atlas of Italy” GIS and Health, Taylor & Francis Ltd. UK. 1998.

Brody Julia Green, Ann Aschengrau, Wendy McKelvey, Ruthann A. Rudel, Christopher H. Swartz, Theresa Kennedy, “Breast Cancer Risk and Historical Exposure to Pesticides from Wide-Area Applications Assessed with GIS” Environmental Health Perspectives, Volume 112, 2004

Rokke Doug, “Depleted uranium: uses and hazards” Paper presented in the British House of Commons: London, England 1999

Fetter Steve, Frank N. von Hippel, “The hazard posed by depleted uranium munitions” Science & Global Security, 1999, Volume 8:2

Gatrell Anthony C. and Markku Löytönen, “GIS and Health Research: An Introduction” GIS and Health, Taylor & Francis Ltd. UK. 1998.

Geoffrey M. Jacquez, “GIS as an Enabling Technology” GIS and Health, Taylor & Francis Ltd. UK. 1998.

Giannardi Cristina, Daniele Dominici, “Military use of depleted uranium: assessment of prolonged population exposure” Journal of Environmental Radioactivity 64 (2003) 227-236

Haag P. A. M. Uijt de., R. C. G. M. Smetsers, H. W. M. Wiltox, H. W. Krus, A. H. M. Eisenga, ”Evaluating the rist from depleted uranium after the Boeing 747-258F crash in Amsterdam, 1992”, Journal of Hazardous Materials A76 (2000) 39-58

Hjalmars U, “Epidemiological studies including new methods for cluster analysis of acute childhood leukemia and brain tumors in Sweden” Karolinska Institute, Stockholm, 1998

IAEA, International Atomic Energy Agency,

http://www.iaea.org/NewsCenter/Features/DU/faq_depleted_uranium.shtml

Lange Jeffrey L., David A. Schwartz, Bradley N. Doebbeling, Jack M. Heller, Peter S. Thorne. “Exposures to the Kuwait oil fires and their association with asthma and bronchitis among Gulf War veterans” Environmental Health Perspectives, Vol. 110, 2002.

http://www.questia.com/PM.qst?a=o&se=gglsc&d=5000664095&er=deny

Andrews John S., Congressional Testimony “Potential Adverse Health Effects of Service in the Persian Gulf War” before the Subcommittee On Hospitals and Health Care Committee on Veterans' Affairs. September 1992

http://www.atsdr.cdc.gov/testimony/testimony-1992-09-16.html

Jubury, M. A. “Environmental and Health Impacts of Aggression on Iraq” Conference on Health and Environmental Consequences of Depleted Uranium used by U.S. and British forces in the 1991 Gulf War, Baghdad. 1998.

http://www.xs4all.nl/~stgvisie/VISIE/DUREPORT/mirror_dureport.html

Haggerty Julie A., Stephan P. Carley, David B. Johnson and Amey D. Michaelis, “Development of Data Management System for the Kuwait Oil Fire Atmospheric Measurement Programme”, Kuwait Data Archive (KuDA), National Centre for Atmospheric Research, Colorado, May 1994.

http://www.atd.ucar.edu/kuwait/contour.txt.html

Kelly A. “Depleted Uranium Use in Iraq”, University of Wisconsin, USA, 2003.

http://academic.evergreen.edu/g/grossmaz/anderkel.html

Kelsall H. L., M R Sim, A B Forbes, D P McKenzie, D C Glass, J F Ikin, P Ittak and M J Abramson “Respiratory health status of Australian veterans of the 1991 Gulf War and the effects of exposure to oil fire smoke and dust storms” Thorax 2004;59:897-903

BMJ Publishing Group Ltd & British Thoracic Society, 2004

http://thorax.bmjjournals.com/cgi/content/abstract/59/10/897

Krieger Nancy, “Place, Space and Health: GIS and Epidemiology” Commentary, Epidemiology, Lippincott, Williams and Wilkins. 14(4):384-385, July 2003.

Limaye S. S, Ackerman S. A, Fry P. M, Isa M, Habib Ali, Ghulam Ali, Wright A, Rangno A, “Satellite monitoring of smoke from the Kuwait oil fires : Studies of smoke from the 1991 Kuwait oil fires” Journal of geophysical research 1992, vol. 97

http://md1.csa.com/partners/viewrecord.php?requester=gs&collection=TRD&recid=A9255465AH&q=&uid=786914074&setcookie=yes

Teppo Lyly, “Problems and Possibilities in the Use of Cancer Data by GIS – Experience in Finland” GIS and Health, Taylor & Francis Ltd. UK. 1998.

Kulldorff Martin, “Statistical Methods for Spatial Epidemiology: Tests of Randomness” GIS and Health, Taylor & Francis Ltd. UK. 1998.

Mitchel R. E. J., S. Sunder, “Depleted uranium dust from fired munitions: physical, chemical and biological properties” Health Physics Society 2004, 0017-9078/04/0

Mould R. F., “Depleted uranium and radiation-induced lung cancer and leukemia” The British Journal of Radiology, 73 (2001), 677-683

Nanja Van Den Berg, “The Development of an Epidemiological Spatial Information System in the Region of Western Pomerania, Germany” GIS and Health, Taylor & Francis Ltd. UK. 1998.

National Institute of Health (NIH) Maryland, “Geographic-Based Research in Cancer Control and Epidemiology” 2000

OTA Background Paper “The Department of Defense Kuwait Oil Health Fire Risk Assessment (The Persian Gulf Veterans’ Registry)” Health Program Office of Technology Assessment US Congress. September 1994.

http://govinfo.library.unt.edu/ota/Ota_1/DATA/1994/9438.PDF

Löfman Owe, Inger Hagström, Per Hedberg, Helle Noorlind Brage, Karin Sahlen, “Östgöten I Miljön” Utgiven av: Samhälls-Och Miljömedicinska enheten, Landstinget I Östergötland. 1996.

Pritchard Mike, “Health risks of depleted Uranium; An independent review of the scientific literature” University of Toronto 2004, (Science for peace)

Petruccelli BP, Goldenbaum M, Scott B, Lachiver R, Kanjarpane D, Elliott E, Francis M, McDiarmid MA, Deeter D. “Health effects of the 1991 Kuwait oil fires: a survey of US army troops” (1999)

http://www.ncbi.nlm.nih.gov/entrez/query.fcgi?cmd=Retrieve&db=PubMed&list_uids=10390693&dopt=Citation

Haining Robert, “Spatial Statistics and the Analysis of Health Data” GIS and Health, Taylor & Francis Ltd. UK. 1998.

Rytkönen M, “Geographical Study on Childhood Type 1 Diabetes Mellitus in Finland” Diabetologia 2001

Trinca Stefania, “GIS Applications for Environment and Health in Italy” GIS and Health, Taylor & Francis Ltd. UK. 1998.

Schærström, Anders (1996) “Pathogenic paths? A time geographical approach in medical geography” Lund University Press. 1996.

Snihs, Jan-Olof, Åkerblom, Gustav (2000) “Use of depleted uranium in military conflicts and possible impact on health and environment” Swedish radiation protection Institute, Stockholm, 2000.

Swedish Oncological Centres, “Atlas of Cancer Incidence in Sweden 1971-89” 1995

The royal society working group on the health hazards of depleted uranium munitions, “The health effects of depleted uranium munitions: a summary” Journal of Radiological Protection (2002) PII: S0952-4746(02)35527-7

Westergren A. “Eating Difficulties in Stroke Patients”, Blackwell Science Ltd, Journal of Clinical Nursing, 2001

Wilkinson Paul, Christopher Grundy, Megan Landon and Simon Stevenson, “GIS in Public Health” GIS and Health, Taylor & Francis Ltd. UK. 1998.

WHO, Department of Protection of the Human Environment “Depleted uranium: sources, exposure and health effects” World Health Organization (WHO) 2001.

DATA SOURCES:

Air Research Laboratory (ARL-NOAA)

http://www.arl.noaa.gov/ss/transport/pgulf.html

NASA, National Aeronautics and Space Administration, “Earth from Space” The NASA Space Shuttle Earth Observations Photography database of images.

http://eol.jsc.nasa.gov/sseop/EFS/

Kuwait Data Archive (KuDA), initiative taken by National Centre for Atmospheric Research, Colorado in 1994

http://www.eol.ucar.edu/kuwait/contour.txt.html

LandScan Population Data, 2003

http://www.lib.utexas.edu/maps/middle_east_and_asia/iraq_pop_2003.jpg

Results of Iraqi cancer registry 1986-88, Ministry of Health, Iraqi Cancer Board, Iraqi Cancer Registry Centre, Institute of Radiology and Nuclear Medicine, Baghdad 1996.

Results of Iraqi cancer registry 1989-91, Ministry of Health, Iraqi Cancer Board, Iraqi Cancer Registry Centre, Institute of Radiology and Nuclear Medicine, Baghdad 1993.

Results of Iraqi cancer registry 1992-94, Ministry of Health, Iraqi Cancer Board, Iraqi Cancer Registry Centre, Institute of Radiology and Nuclear Medicine, Baghdad 1996.

Results of Iraqi cancer registry 1995-97, Ministry of Health, Iraqi Cancer Board, Iraqi Cancer Registry Centre, Institute of Radiology and Nuclear Medicine, Baghdad 1999.

Results of Iraqi cancer registry 1998-2000, Ministry of Health, Iraqi Cancer Board, Iraqi Cancer Registry Centre. (This dataset has been taken personally by Dr. Iman Aloan from Iraqi Cancer Board, Iraq in year 2004 and has not been presented and published yet).

UN Cartographic section DPI, UN Habitat, HIC Iraq, “Environment in Iraq: UNEP Progress Report” October 2003.

http://www.bren.ucsb.edu/academics/courses/595E/Session%205/UNEP%20Iraq%20environment%20study%202003.pdf

WEB SOURCES:

All the web sources were valid Until August 22, 2006

Department of Health and Human Services, Centre for Disease Control and Prevention. Atlanta, USA.

http://www.cdc.gov/nceh/clusters/about_clusters.htm.

ECRR, European Committee on Radiation Risk

http://www.euradcom.org/index.html#english

National Cancer Institute. U.S. National Institute of Health.

http://www3.cancer.gov/atlasplus/

Huntington Breast Cancer Action Coalition. USA.

http://www.hbcac.org/mapping.html

Gulf Link. Office of the Special Assistant for Gulf War Illness. USA.

http://www.gulflink.osd.mil/faq_17apr.htm

World Health Organization (WHO)
http://www.who.int/mediacentre/factsheets/fs257/en/
Management Information Network. A resouece for the public, industry and the scientific community. USA.
http://web.ead.anl.gov/uranium/guide/depletedu/index.cfm.
Campaign Against Depleted Uranium (CADU), UK.
http://www.cadu.org.uk/intro.htm.
The VISIE Foundation. Netherlands.
http://www.xs4all.nl/~stgvisie/VISIE/depleted_uranium1.html.

Robust Satellite Techniques (RST) for early warnings in security applications: the case of Ceuta and Melilla

Carolina Filizzola[1*], Enrico Cadau[2], Antonio de la Cruz[3], Giovanni Laneve[2], Nicola Pergola[1,4], and Valerio Tramutoli[4,1]

1 National Research Council, Institute of Methodologies of Environmental Analysis, C. da S. Loja, 85050 Tito Scalo - Potenza (Italy)

2 Centro di Ricerca Progetto San Marco, Via Salaria 851 - 00138 Rome, Italy

3 European Satellite Centre, Torrejon, Madrid (Spain)

4 University of Basilicata, Department of Engineering and Physics of the Environment, Via dell'Ateneo Lucano 85100 Potenza (Italy)

* filizzola@imaa.cnr.it

Abstract

A Robust Satellite Technique (RST), used up to now for natural and environmental hazard monitoring, has been recently employed also in the security field. The use of the RST approach, together with geostationary satellite observations characterized by 15 minutes of repetition rate, has shown to be reliable for timely detection of different security related events.

In this paper, RST approach is applied to MSG-SEVIRI (the imager on the Meteosat Second Generation platform) data in order to monitor structures like border fences. In particular, some evidences of a danger (bonfires in immigrant camps) seem to be detectable near the Ceuta border fence few hours before its crossing due to African immigrants on 29 September 2005.

Higher spatial resolution satellite observations (ASTER and MODIS) are used in order to validate and give a better interpretation of the observed hot spots.

Introduction

Many ground surveillance systems (closed-circuit video cameras, watchtowers, infra-red rays, fibre-optic thermal sensors, etc) are usually employed for directly monitoring hot line borders. Notwithstanding the presence of these systems, when the frontier is crossed, it could be too late for guardians to successfully intervene and stop the attack. For this reason, a more effective surveillance could be performed monitoring indirect phenomena, not necessary in correspondence of the border line, which could give an early warning of a danger. Signs of instability may be represented, for example, by the appearance of temporary bonfires near the frontier, indicating the (unexpected) presence of people which cook and keep warm in precarious conditions. To his aim, satellite (rather than ground) systems could be better employed for detecting early warnings near hot border zones.

Satellite observations have shown long since to be a valid support to give information of dangerous situations along hot border lines. Anyway, up to now only Very High spatial Resolution (VHR) data have been used in the field of border monitoring. Unfortunately, due to their low time repetition rate, VHR images allow us to only monitor situations with a very low temporal dynamics (which is not the case of temporary bonfires). In this paper, geostationary

satellite records, characterized by 15 minutes of repetition rate, in spite of a very low spatial resolution (3x3 km^2), are used in the security field for monitoring border lines. Together with this kind of observations, a robust data analysis technique has to be employed in order to assure that no false alarm is detected together with (or in place of) actual dangerous events. At the same time, the technique should be also sensitive since small variations of a thermal signal (due to temporary bonfires) are required to be detected. In this context, the RST (Robust Satellite Technique) approach, already widely used in the field of natural and environmental hazard detection, mitigation and monitoring, was expected to extract reliable information from geostationary data about evidences of a danger when it may be highlighted by (even small) thermal signal variations.

The RST approach

The RST approach was initially applied to the prevision and NRT (Near Real Time) monitoring of major natural and environmental hazards: seismically active areas [Tramutoli et al., 2001; Filizzola et al., 2004; Corrado et al., 2005; Tramutoli et al., 2005; Genzano et al., 2007], volcanic activity [Bonfiglio et al., 2005; Pergola et al., 2004a; Pergola et al., 2004b; Filizzola et al., 2007], hydrological risk [Lacava et al. 2005a; Lacava et l., 2005b] as well as forest fires [Cuomo et al., 2001; Mazzeo et al., 2007] and oil spills [Casciello et al.,2007] are the main fields of RST application. In all cases, the technique demonstrated how meteorological satellites, which presently offer the highest time repetition (from few hours to few minutes), despite their low spatial resolution, can be used to detect events involving even small portions (< $100m^2$) of Earth surface. For this reason, it was expected that RST applied to meteorological satellites could be useful also in the detection of even small variations of thermal signals due, for example, to temporary bonfires.

The RST technique is based on a preliminary multi-temporal analysis performed on several years (variable in dependence of the availability of homogeneous historical data-set {T}) of satellite records, which is devoted to characterize the signal (in terms of its expected value and variation range) for each pixel of the satellite image to be processed. On this basis, anomalous signal patterns are identified by using a local change detection index, named ALICE (Absolutely Local Index of Change of Environment), [Tramutoli, 1998; Tramutoli, 2005], so defined:

$$\otimes_V (\mathbf{r},t') \equiv \frac{\lfloor V(\mathbf{r},t') - V_{ref}(\mathbf{r}) \rfloor}{\sigma_V(\mathbf{r})} \qquad (1)$$

where V(r,t) is the signal to be analysed, r≡(x,y) represents the geographic coordinates of the image pixel centre; t' is the time of acquisition of the satellite image at hand; $V_{ref}(r)$ and $\sigma_V(r)$ are, respectively, a reference field for signal V(r,t) (e.g. minimum, maximum, mean, etc.) and its standard deviation computed on the pre-selected homogeneous data-set {T} of cloud-free satellite records, collected at location r in the same time-slot (hour of the day) and period (e.g. month) of the year of the image at hand (t'∈{T}).

Depending on the specific application, a different signal is taken into account. In the case of bonfire detection, the MIR (Medium Infra Red) signal (in terms of brightness temperature, Tb) is used as variable V(r,t) in the computation of the ALICE index in order to identify anomalous thermal transients due to bonfires. Therefore, Eq. (1) becomes:

$$\otimes_{MIR} (\mathbf{r},t') \equiv \frac{\lfloor Tb_{MIR}(\mathbf{r},t') - \mu_{MIR}(\mathbf{r}) \rfloor}{\sigma_{MIR}(\mathbf{r})} \qquad (2)$$

RST for border monitoring: the case of Ceuta e Melilla fences

The use of RST for border monitoring was tested in the case of some events which involved two Spanish towns (Ceuta and Melilla) during September 2005. These cities represent fragments of Europe on North Africa's Mediterranean coast and came under Spanish control around 500 years ago. They are surrounded by Morocco, which views the Spanish presence as anachronistic and claims sovereignty.

The test was performed considering the night of 29 September 2005, when Ceuta suffered the attack of some immigrants:"...at three o'clock in the morning a group of twenty Congoleses and some Costamarfileños crossed the two fences that separates Morocco from Ceuta. With them there have been other immigrants from different origins…" (This Tuesday News, 2006). Collateral data and/or newspapers reported also that before the attack:

- the immigrants were grouped in camps in high ground with abundant vegetation;
- the immigrants set bonfires in the camps for cooking hot drink and keeping warm.

Within this framework, the use of RST was tested in the attempt of observing hot spots related to the presence of low-intensity and short-life fires (like bonfires), different from forest fires. The RST approach was applied to the data of SEVIRI (Spinning Enhanced Visible and Infrared Imager), the multispectral sensor aboard Meteosat Second Generation (MSG) platform so that changes in thermal signal could be caught at a temporal rate of 15 minutes. Following RST approach, reference fields were built slot-by-slot, on the basis of SEVIRI images acquired in September.

Fig. 1 shows, for example, the reference fields computed, for each image pixel, using two years of SEVIRI images acquired in September at 00:00 GMT: they represent the normal behaviour of the signal for that time of the day (00:00 GMT) and period of the year (September) together with its range of variability. In particular, it is possible to immediately see, over the Mean reference field, the places which are "normally" characterized by high values of brightness temperature (brighter areas).

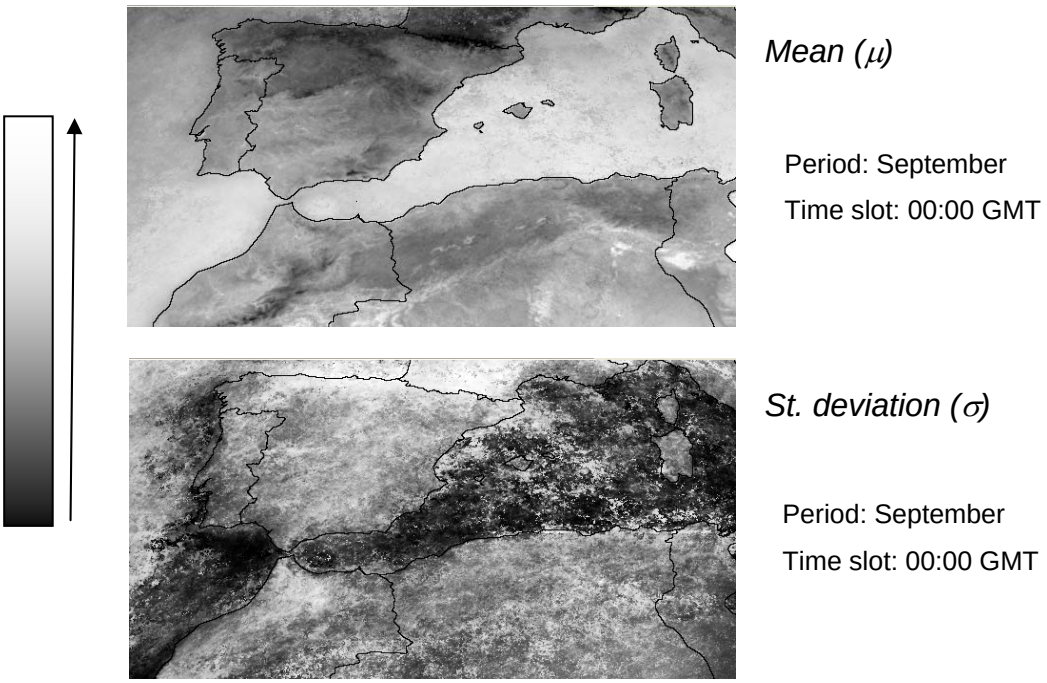

Fig. 1: Reference fields, Mean (μ) and Standard deviation (σ), computed on the basis of all SEVIRI images acquired in September at 00:00 GMT.

After building reference fields, anomalous thermal signals were identified by computing the ALICE index, which allowed us to automatically identify anomalous space-time signal transients related to actual hazardous events distinguishing them from areas which are "normally" characterized by a high temperature. Fig. 2 shows, in red colour, pixels corresponding to the ALICE values which are greater than 1.5 on the SEVIRI image of 29 September 2005, 00:00 GMT.

This result highlights that at least 3 hours before (at midnight) the crossing of the fences, the combination of RST algorithm sensitivity and the high temporal resolution of SEVIRI instrument is able to identify one hotspot very close to Ceuta.

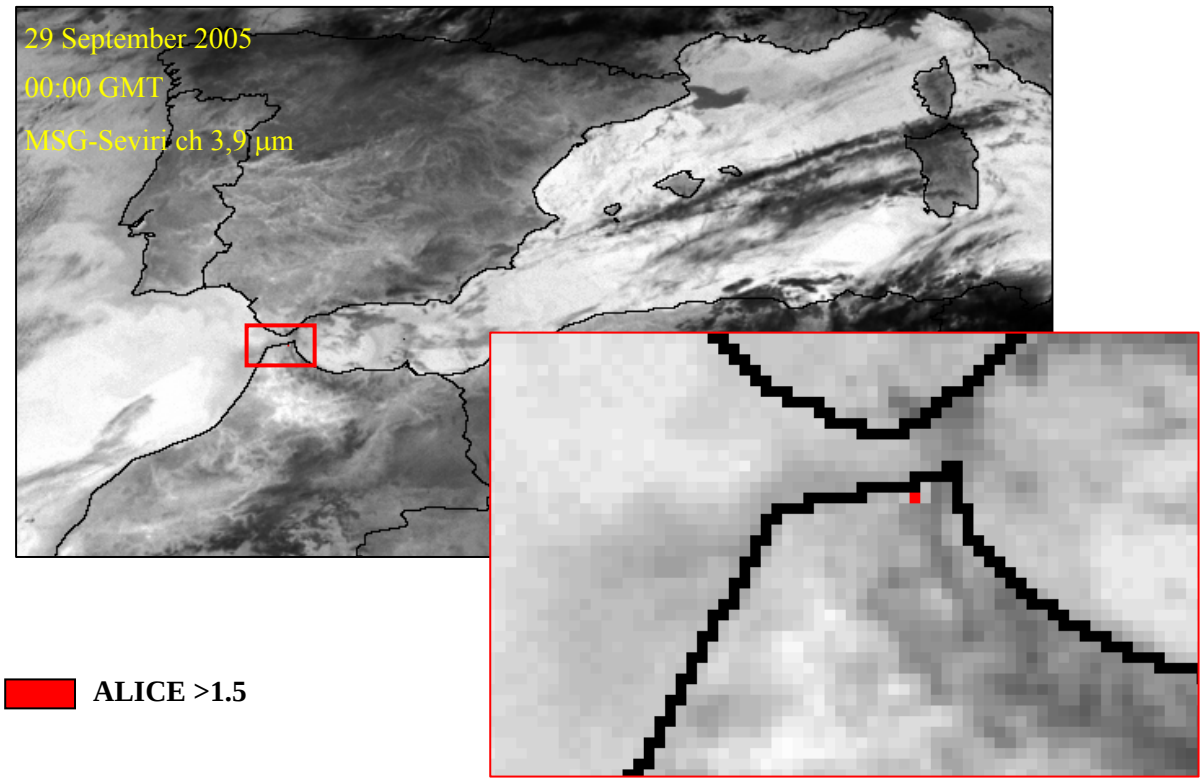

Fig. 2: SEVIRI images, analyzed by using RST technique, highlight a thermal anomaly in proximity of Ceuta, three hours before the fence crossing of the Spanish town (see text).

Discussion and Conclusions

The possibility of discriminating hot spots related to the presence of bonfires in refugee camps from the ones related to wildfires was, first of all, considered.

Using HR ASTER images covering the same area interested by the hot spot detected by RST, the presence of scar areas have been detected (see Fig. 3) testifying the occurrence of (at least) 3 wildfires between 21 September 2005 and 17 December 2005. In addition, MODIS-based products (Giglio et al., 2003) have been analysed (Fig. 4), showing that no significant (for dimension and/or duration) wildfires occurred until 30 September 2005 in the area where the RST technique detected a hot spot at 00:00 GMT on 29 September 2005. This means that such an hot spot seems not due to wildfires but, perhaps, bonfires survived on 29 September should be responsible of wildfires registered by MODIS on 30 September.

Finally, other two elements should be in favour of the hypothesis of bonfire presence rather than a wild fire:

- SEVIRI hotspot is not associated with the plumes which generally are related to forest fires;
- the hotspot coincides with the period of the border crisis and disappear thereafter.

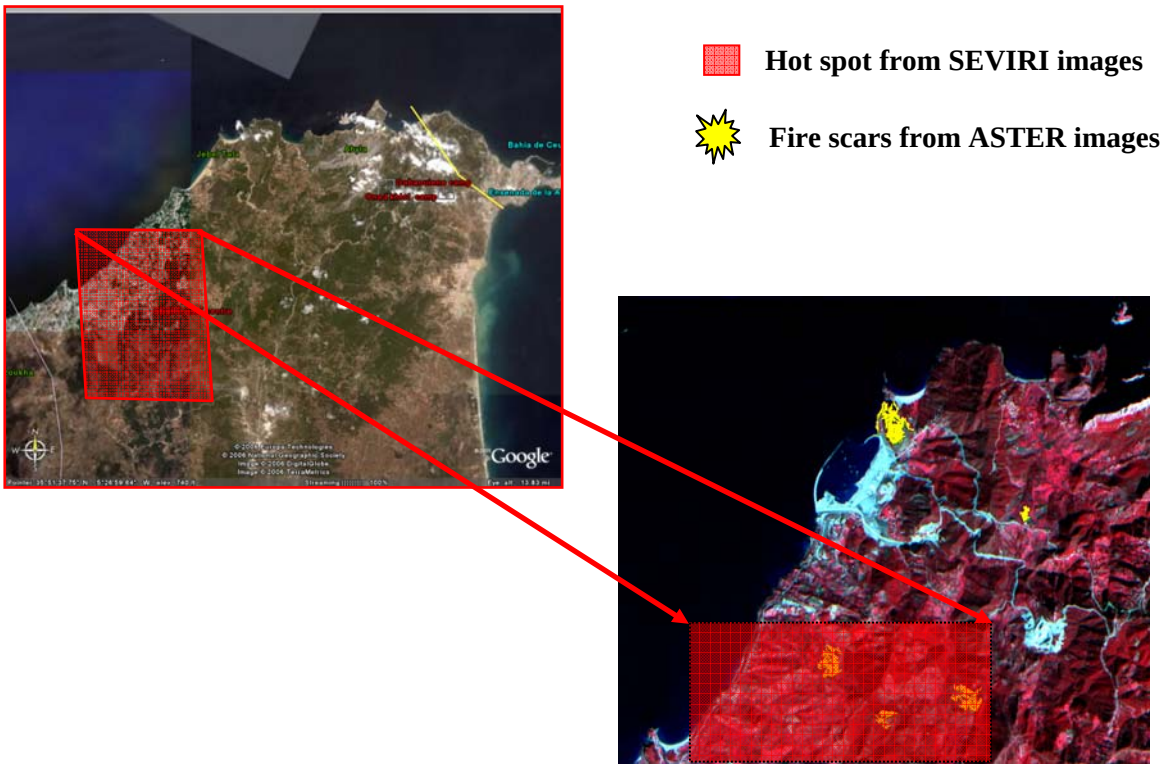

Fig. 3: Fire scars, detected by using ASTER images, are yellow coloured. They refers to possible wildfires occurred between 21 September and 17 December 2005 (see text).

After excluding the presence of a wildfire, a second step was the comparison of the position of the detected thermal anomaly with the position of known refugee camps according to collateral information (Fig. 5). The apparent lack of correspondence with known camps does not exclude a relation of the detected hot spot with the possible presence of immigrants in camps near Ceuta. In fact, the hot spot is localised at about 10 km from the town, a distance which is neither too far (it can be covered in a couple of hours) nor too close (so that the attack could be prepared without any possible control of fence guards).

In conclusion, even without ground information it is possible to suppose that the detected hot spot on SEVIRI images may be reasonably connected to the presence of immigrants who temporarily set fires for warming and cooking during the preparation of the attack in a such position that they could group in high ground with abundant vegetation far from Spanish control but not so far in order to reach quickly the frontier.

The case of Ceuta above seen certainly highlighted the capability of RST approach, used in combination with high temporal resolution satellite data (MSG-SEVIRI), to automatically detect even small and short-life thermal events. At the same time, in view of a systematic use of RST in border monitoring, the problem of automatically discriminate, among the detected hot spots, the ones actually related to the presence of immigrant bonfires from the others due to wildfires, persists.

This awareness is currently leading to develop a specific SEVIRI-based data analysis technique for the automatic distinction of anomalous thermal variations due to natural or man-made phenomena. The multi-temporal analysis of HR satellite imagery (like the one based on ASTER and MODIS images) will continue to be used on selected test cases for its validation since it showed to be useful in the case of Ceuta.

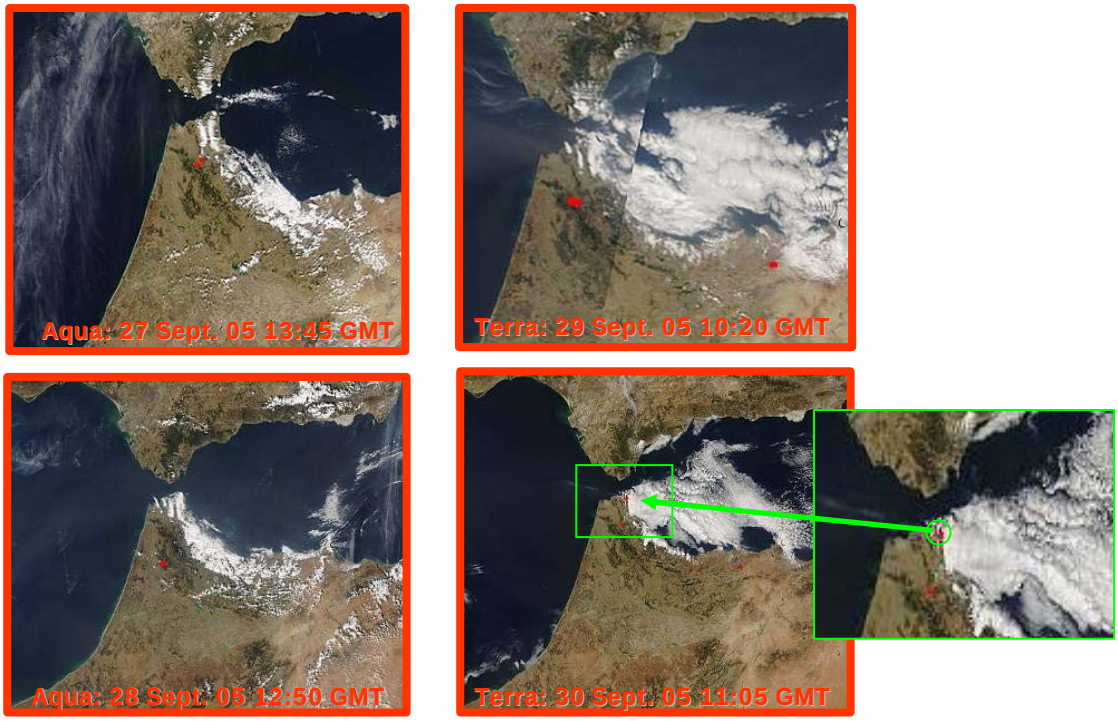

Fig. 4: Sequence of MOD14 product (based on MODIS data) for fire detection on the investigated area before and after the considered event (see text)

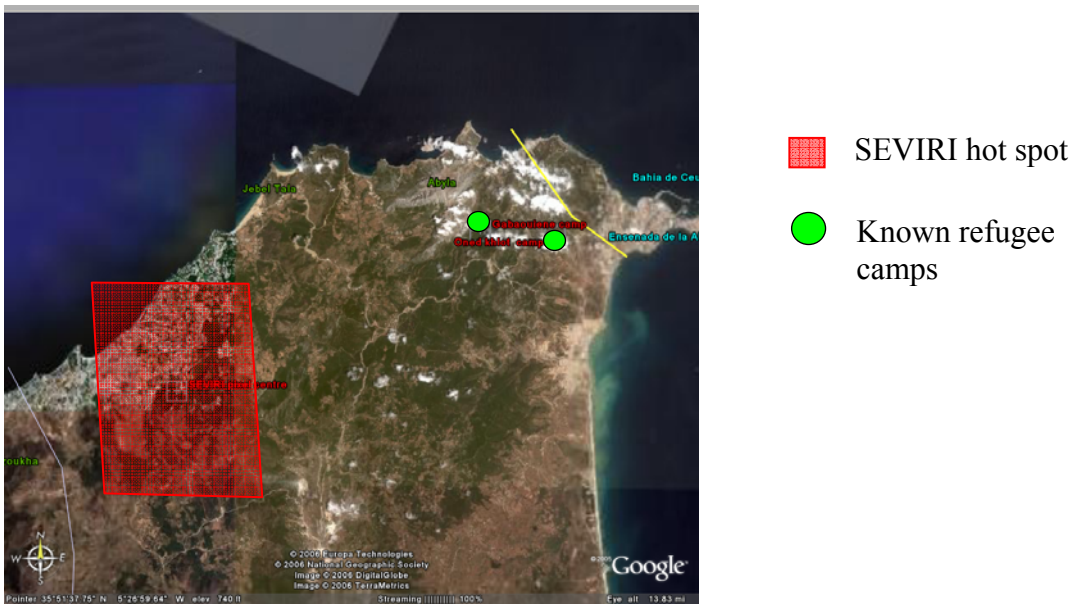

Fig. 5: Hot spot detected by applying RST to SEVIRI data and position of known refugee camps.

Acknowledgments

This work has been carried out within the framework of the GMOSS (Global MOnitoring for Security and Stability) Project, funded by the European Community (contract n° SNE3-CT-2003-503699).

References

Bonfiglio, A, M. Macchiato, N. Pergola, C. Pietrapertosa, and V. Tramutoli, "AVHRR Automated detection of volcanic clouds", *International Journal of Remote Sensing*, vol 26 (1), pp 9-27 (and reference herein), 2005.

Casciello, D., T. Lacava, N. Pergola and V. Tramutoli, "Robust Satellite Techniques (RST) for oil spill detection and monitoring" In *Proceedings Multitemp 2007*, Leuven, Belgio. Digital Object Identifier 10.1109/MULTITEMP.2007.4293040, 2007

Corrado, R., R. Caputo, C. Filizzola, N. Pergola, N. Pietrapertosa, and V. Tramutoli, "Seismically active area monitoring by robust TIR satellite techniques: a sensitivity analysis on low magnitude earthquakes in Greece and Turkey", *Natural Hazards and Earth System Sciences*, vol 5, pp 101-108, 2005.

Cuomo, V., R. Lasaponara, and V. Tramutoli, Evaluation of a new satellite-based method for forest fire detection. International Journal of Remote Sensing, vol 22, no.9, pp 1799-1826 (and reference herein), 2001.

Filizzola, C., N. Pergola, C. Pietrapertosa, and V. Tramutoli, "Robust satellite techniques for seismically active areas monitoring: a sensitivity analysis on September 7th 1999 Athens's earthquake", in *Seismo Electromagnetics and Related Phenomena*. *Physics and Chemistry of the Earth*, vol. 29, pp 517-527, 2004

Filizzola, C., T. Lacava, F. Marchese, N. Pergola, I. Scaffidi, and V. Tramutoli, "Assessing RAT (Robust AVHRR Techniques) performances for volcanic ash cloud detection and monitoring in near real-time: The 2002 eruption of Mt. Etna (Italy)", *Remote Sensing of Environment*, vol. 107, pp 440–454, 2007

Genzano, N., C. Aliano, C. Filizzola, N. Pergola, and V. Tramutoli, "A robust satellite technique for monitoring seismically active areas: The case of Bhuj–Gujarat earthquake", *Tectonophysics*, vol 431, pp.197-210, 2007, doi:10.1016/j.tecto.2006.04.024.

Giglio, L., J. Descloitres, C.O. Justice, and Y. Kaufman, "An enhanced contextual fire detection algorithm for MODIS", *Remote Sensing of Environment*, vol. 87, 273-282, 2003.

Lacava, T., M. Greco, E.V. Di Leo, G. Martino, N. Pergola, F. Romano, F. Sannazzaro, and V. Tramutoli, "Assessing the potential of SWVI (Soil Variation Index) for hydrological risk monitoring by satellite microwave observations", *Advances in Geosciences*, vol 2, pp 221-227, 2005b.

Lacava, T., V. Cuomo, E.V. Di Leo, N. Pergola, F. Romano, and V. Tramutoli, "Improving soil wetness variations monitoring from passive microwave satellite data: the case of April 2000 Hungary flood", *Remote Sensing of Environment*, vol 96 (2), pp 135-148 (and reference herein), 2005a.

Mazzeo, G., F. Marchese, C. Filizzola, N. Pergola,V. Tramutoli, "A Multi-temporal Robust Satellite Technique (RST) for forest fire detection". In *Proceedings Multitemp 2007*, Leuven, Belgio. Digital Object Identifier 10.1109/MULTITEMP.2007.4293060, 2007.

Pergola, N, V. Tramutoli, and F. Marchese, "Automated detection of thermal features of active volcanoes by means of Infrared AVHRR records", *Remote Sensing of Environment*, vol 93, pp 311-327 (and reference herein), 2004b.

Pergola, N., V. Tramutoli, I. Scaffidi, T. Lacava, and F. Marchese, "Improving volcanic ash clouds detection by a robust satellite technique", *Remote Sensing of Environment*, vol 90 (1), pp. 1-22, (and reference herein), 2004a.

This Thuesday News (2006): http://thistuesday.org

Tramutoli, V., "Robust Satellite Techniques (RST) for natural and environmental hazards monitoring and mitigation: ten years of successful applications", in: *Liang S, Liu J, Li X, Liu R, Schaepman M (eds)*, *The 9th International Symposium on Physical Measurements and Signatures in Remote Sensing*, Beijing (China), ISPRS, vol. XXXVI (7/W20), pp 792-795, ISSN 1682-1750, 2005.

Tramutoli, V., "Robust AVHRR Techniques (RAT) for Environmental Monitoring: theory and applications", in: *Cecchi G, Zilioli E (eds) Earth Surface Remote Sensing II, SPIE*, vol 3496, pp 101-1, 1998.

Tramutoli, V., G. Di Bello, N. Pergola, and S. Piscitelli, "Robust satellite techniques for remote sensing of seismically active areas", *Annals of Geophysics*, vol 44, no.2 , pp 295–312, 2001.

Tramutoli, V., V. Cuomo, C. Filizzola, N. Pergola, and C. Pietrapertosa, "Assessing the potential of thermal infrared satellite surveys for monitoring seismically active areas. The case of Kocaeli (İzmit) earthquake, August 17th, 1999", *Remote Sensing of Environment*, vol 96 (3-4), pp 409-426 (and reference herein), 2005.

Groundwater Vulnerability Mapping for Gaza Strip

Åke Sivertun* & Ramy Bader

Department of Computer and Information Science (IDA), Linköpings Universitet, S-58183 Linköping, Sweden

* akesiv@ida.liu.se

Abstract

In an already densely populated area of the Gaza Strip Palestine, there are huge problems in water quality in addition to problems of scarcity of water resources, shortage of land, climate change, etc. This article is applying vulnerability mapping in groundwater in term of hydrologic theory and use of Geographical Information System (GIS) as a tool to depict areas of high sensitivity for pollutants. Past groundwater vulnerability assessments have used overlay index methods that employ readily available data sets and weighting factors to determine vulnerability. A commonly used groundwater vulnerability assessment is the DRASTIC model. Hereby we are using a previously complied DRASTIC data set, and the ArcView GIS system to determine groundwater vulnerability for the Gaza Strip. The results of the study where we have been able to use real data from the area, have validated and modified the DRASTIC model to meet the regional range of depth to water table, the modified results shows, in a digital map, the areas in a vulnerability scale to be used for water management and physical planning.

1. Introduction

Gaza Strip is Located along the coast of the eastern Mediterranean Sea stretches over a distance of a approximately 45 km from Beit Hanoun town in the north to Rafah city in the South see (**F**ig 1) The Width is various between 7 and 12 km, and the total area is about 365 (Abu -Maylah & Aish, 1997). The total population is about 1,500,000 inhabitants, Population average annual growth is 4.8% (UNDP, 2002).

Fig.1: Gaza Strip Location

The central issue facing the Gaza Strip today is water. The availability of safe, clean water is diminishing rapidly. Demand continually outstrips renewable supply. Current water

distribution networks are sorely inadequate, and sewage collection facilities are virtually nonexistent.

A problem of growing concern is the cumulative impact of contamination of a regional aquifer from non-point sources, such as those created by intensive use of fertilizer, herbicides and pesticides. In addition, small point sources (such as numerous domestic septic tanks as semi non point sources or spills from both agriculture and industrial sources) threaten the quality of regional aquifer (NAP, 1984).

Pressure for the development of the concept of groundwater vulnerability has been generated by the worldwide concern about the problems of groundwater contamination. Groundwater quality issues are receiving widespread attention, and hydrogeologic information is essential for the effective protection and management of groundwater quality, so effective protection should be primarily aimed at the prevention of problems and requires a sound information base to determine, on a continuous basis, the groundwater quality problems that exist and those that may develop in the future.

Groundwater vulnerability maps are used as a guide for the location of future developments in an area, in order to minimize the impact the projected development will have on the surrounding water resources. (Piscopo, 2001)

Groundwater vulnerability maps are used as a guide for the location of future developments in an area, in order to minimize the impact the projected development will have on the surrounding water resources.

The fundamental concept of groundwater vulnerability is that some land areas are more vulnerable to groundwater contamination than others. The goal of the vulnerability mapping is to divide an area into several units having different potential for groundwater contamination. The results of this assessment are shown typically as polygons on a map (Yosuke, 1997).

The DRASTIC method is the most widely used method of indexing aquifer vulnerability in Canada and the US. It was developed in the US during the mid-1980s by the National Water Well Association, in conjunction with the US Environmental Protection Agency to be a standardized system for evaluating groundwater vulnerability to pollution (Aller et al, 1987.). Also DRASTIC model was successfully implemented in Israel (Melloul and Collin, 1998), which makes us confidant we can adapt the method to meet the regional factors of the study area.

The vulnerability maps could be produced by using computer mapping hardware and software geographic information system (GIS) to combine data layers such as topography, soils, and depth to water and (GIS) is widely used in hydrologic analyses and modeling, (Maidment, 1993).

Geographical Information System (GIS) allows us to deal with traditional Groundwater vulnerability mapping in a different approach; and give capability to be used for basic spatial data management tasks (data storage, manipulation, preparation, extraction, etc.), spatial data processing (overlays, buffering, etc.) and visualization of the results.

The result of DRASTIC model could be useful for the farmers because the produced map determines sensitive areas that could be contaminated by agriculture as non point sources pollution and also authorities will be interested to do some action in order to protect the sensitive areas.

2. The method

The DRASTIC method for aquifer vulnerability was developed in the late 1980s to achieve some level of consistency between individual State efforts in the United States. DRASTIC has been used for groundwater vulnerability mapping in Texas, Ohio and Nova Scotia (Agriculture Canada, 1993).

DRASTIC named for the seven factors considered in the method: ***D***epth to water, net ***R***echarge, ***A***quifer media, ***S***oil media, ***T***opography, ***I***mpact of vadose zone media, and hydraulic ***C***onductivity of the aquifer (Aller et al, 1987). The primary purpose of DRASTIC is to provide assistance in resource allocation and prioritization of many types of groundwater-related activities and to provide a practical educational tool.

DRASTIC can be used to set priorities for areas to conduct groundwater monitoring. For example, a denser monitoring system might be installed in areas where aquifer vulnerability is higher and land use suggests a potential source of pollution.

DRASTIC can also be used with other information (such as land use, potential sources of contamination, and beneficial uses of the aquifer) to identify areas where special attention or protection efforts are warranted.

The model has four assumptions:

1. The contaminant is introduced at the ground surface;
2. The contaminant is flushed into the groundwater by precipitation;
3. The contaminant has the mobility of water;
4. The area being evaluated by DRASTIC is 404690 m2 or larger.

To assess groundwater pollution potential within hydrogeologic settings, numerical ranking is used on the DRASTIC features. There are 3 significant parts, Weights, Ranges, and Ratings.

Weight

Each DRASTIC feature is assigned a weight relative to each other in order of importance from 1 to 5; the most significant is allocated five, the least significant is allocated one, see (***T***able 1).

The DRASTIC technique, by its inference, attempts to identify those features important in determining vulnerability of groundwater resources. However, each study area will need to be assessed as to the importance of each specific feature for its area. For example, topography is obviously more important in a mountainous area than in the flat plains country. Also, some features will be taken into consideration in the production of other features. For example, topography will influence the production of a depth to watertable map in a fractured rock terrain as well as represent itself in a topographic (slope) map.

Table 1. Assigned weights for DRASTIC hydrogeologic factors (Aller et al, 1987).

Hydrogeological Factor	Weight (w)
Depth to water table	5
Net Recharge	4
Aquifer media	3
Soil media	2
Topographic slope	1
Impact of the vadose zone media	5
Hydraulic Conductivity	3

As we see in the table above, the most significant factors are: Depth to water table and Impact of the vadose zone media

Ranges

For each DRASTIC feature, ranges or significant media types for the features upper and lower limits within the catchment have been devised based on its impact on pollution potential.

Ratings

The ratings for each DRASTIC feature are assigned a value between 1 and10. The rating enables the ranking of the ranges found in each DRASTIC feature map. These ratings provide a relative assessment between ranges in each feature, the typical ratings for the features ranges exist in (Aller et al, 1987).

The DRASTIC Index

The DRASTIC Index is the pollution potential (vulnerability) at any one cell or polygon on the map, is determined as:

$$DRASTIC\ Index = DrDw + RrRw + ArAw + SrSw + TrTw + IrIw + CrCw \quad \ldots(\text{Eq. 1})$$

Where:

Dr = Ratings to the depth to water table, Dw = Weights assigned to the depth to water table.

Rr = Ratings for ranges of aquifer recharge, Rw = Weights for the aquifer recharge,

Ar = Ratings assigned to aquifer media, Aw = Weights assigned to aquifer media

Sr = Ratings for the soil media, Sw = Weights for soil media

Tr = Ratings for topography (slope), Tw = Weights assigned to topography

Ir = Ratings assigned to vadose zone, Iw = Weights assigned to vadose zone

Cr = Ratings for rates of hydraulic conductivity, Cw = Weights given to hydraulic conductivity

The computed (via GIS) DRASTIC index identifies areas which are likely to be susceptible to groundwater contamination relative to one another. The higher the DRASTIC index the greater the groundwater pollution potential. It must be remembered that the DRASTIC

technique provides a relative evaluation tool and is not designed to provide absolute answers. It offers planners and developers a categorization of areas, based on the level of site investigation expectation, when considering the groundwater resources for an area.

The several DRASTIC map factors were created from the available data as follow:

1. The topography layer (***T***): the slope grid was generated from the vector topography theme, which has been digitized from contour map 1: 2500 (PWA, 2000), using intermediate elevation grid, then was reclassified as range and rating of typical DRASTIC slope ranges.
2. The soil layer (S): was generated from the vector soil theme using intermediate soil type grid, then was reclassified as range and rating of typical DRASTIC soil ranges.
3. The net recharge layer (R): because net recharge values are less precise and less easily obtained than values for other DRASTIC parameters, the ranges for net recharge are intentionally broad the estimation of net recharge, the net recharge layer was generated from equation 2, the equation is used to generate a recharge value (Piscopo, 2001). This recharge value is then grouped into a range of values that are given a rating for use in the final DRASTIC calculation.

$$Recharge\ value = Slope\ \% + Rainfall + Soil\ permeability \quad ...(\text{Eq } 2)$$

Where:

The rating of Slope, Rainfall and Soil Permeability and corresponding rating for Recharge range are given in (***T***able 2), and then by using the ArcView in Gaza strip area, we have classified the soil feature to the corresponding permeability class and the same has been done for rainfall and slope features and we added the three feature to yield the recharge values and recharge reclassified to get the final drastic rating.

Table 2: classification of of slope, rainfall and soil permeability to get the recharge values.

Slope factor		**Rainfall factor**		**Soil permeability**		**Yield reacharge values**	
Range (%)	Rating	Range(mm/y)	Rating	Range	Rating	Range	Rating
< 2	4	> 850	4	High	5	11 - 113	10
2 – 10	3	700 - 850	3	Mod-High	4	9 - 11	8
10 – 33	2	500 - 700	2	Moderate	3	7 - 9	5
> 33	1	< 500	1	Slow	2	5 - 7	3
				Very slow	1	3 - 5	1

1. The impact of vadose zone layer (I): was created according to generalized geological cross section (Melloul & Collin, 1994). it has given rating 8 as typical DRASTIC -sand and gravel- group.
2. The hydraulic conductivity layer (C): was created according to the pump test range (20 - 80 m/d), (PWA, 2000) the values of hydraulic conductivity has inversely relation with the thickness of the aquifer, thereby were distributed to the area as point theme,

the grid theme was created by Inverse Distance Weighted (IDW) interpolation, then reclassified as typical DRASTIC hydraulic conductivity range and rating.

3. The aquifer media layer (A): was digitized from a map shows characteristics materials of Gaza's aquifer (David Scarpa, 2002), a comparison was made between the map and the data to determine what the media types were rated as.
4. The other difficulty came with the depth to water factor (D). This layer was complied from the static well depths, and unconfined aquifer depths and we have used spatial analysis interpolation surface IDW to create depth to water table map, excluding some well depths that have errors. This resulted in some ranges different from the ones prescribed by the DRASTIC documentation.

The DRASTIC model was initially run using the map calculator function in the Spatial Analyst extension of ArcView. All of the factors were added to a view in an ArcView project.

It was decided the data's cell size to be 50X50 meters square. The analysis properties were set 50X50 meters square. The multiplication of the theme by the weighting factor and adding all of the themes was done in separate steps creating many intermediate themes.

Instead, the multiplication by weighting factors and the addition of the themes could have been done in one map calculation. The syntax of the expression in a map calculation is very specific and involved many sets of brackets to correctly state the expression. Although it is possible to edit the expression and re-run map calculator, often the syntax was not preserved when edited and then it was easier to recreate the entire expression.

*(([Deep to Water (D)] * 5) + ([Aquifer Recharge (R)] * 4) + ([Aquifer Media (A)] * 3) + ([Soil Media (S)] * 2) + ([Percent Slope (T)] * 1) + ([Vadose Zone (I)] * 5) + ([Hydraulic Conductivity (C)] * 3)).*

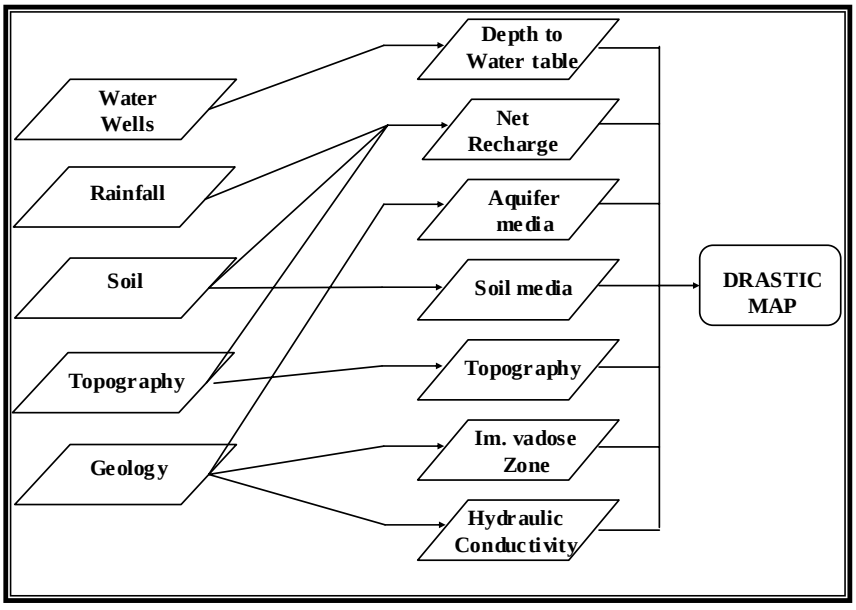

Fig 2: DRASTIC model chart and its source data

3. Results and validation

The depth of water table index map (D) shown in (Fig.3) and classified Gaza Strip area into five sub-areas, every sub-area has different color expresses the depth of water table index value (D rating x D weight) that ranges from (5 - grey) to (40 - magenta). More than 90% of

the area lies under 5-grey, that means this area lies in rating 1 and the water table depth is greater than 30m according to typical DRASTIC rating. The impact of water depth is most apparent in the middle area (Wadi Gaza). The DRASTIC vulnerability map is displayed in (**F**ig 4). Standard DRASTIC colors were used for the maps. These standard colors range from purple for the least vulnerable to yellow for the most vulnerable. The minimum possible DRASTIC index using these parameters is 23 and the maximum is 230. The DRASTIC index ranges from 93 (least vulnerable) to 176 (most vulnerable). Depth to water (D) is heavily weighted, with a weighting factor of five, and therefore has a significant influence on the index. The maximum depth considered for DRASTIC is 30 m (assigned rating 1). However, in the study area the piezometric level varies from 5.8 to 146 m, in our case 93.3% of the total area lies in the range > 30m and take rating 1, the rest 6.7% distributes to the rest rating (Fig 6), thereby the model should be validated.

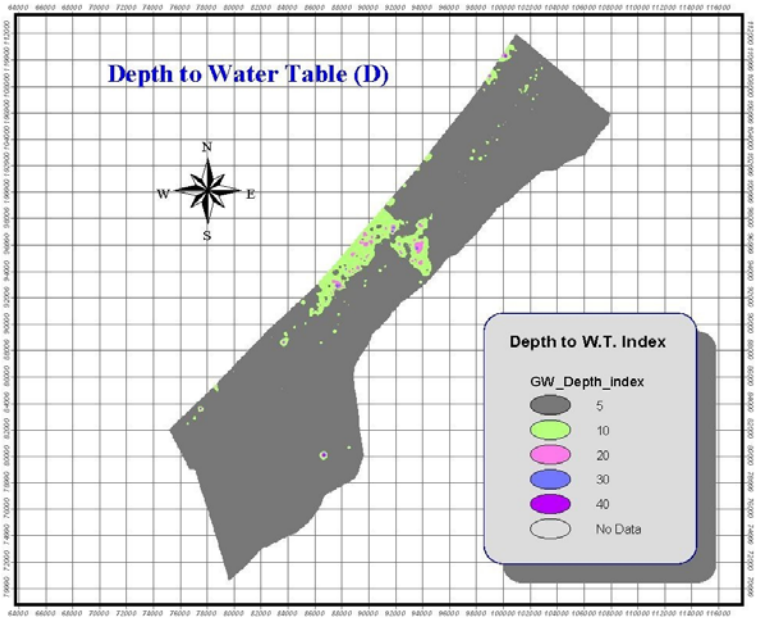

Fig 3: Index of depth to water table.

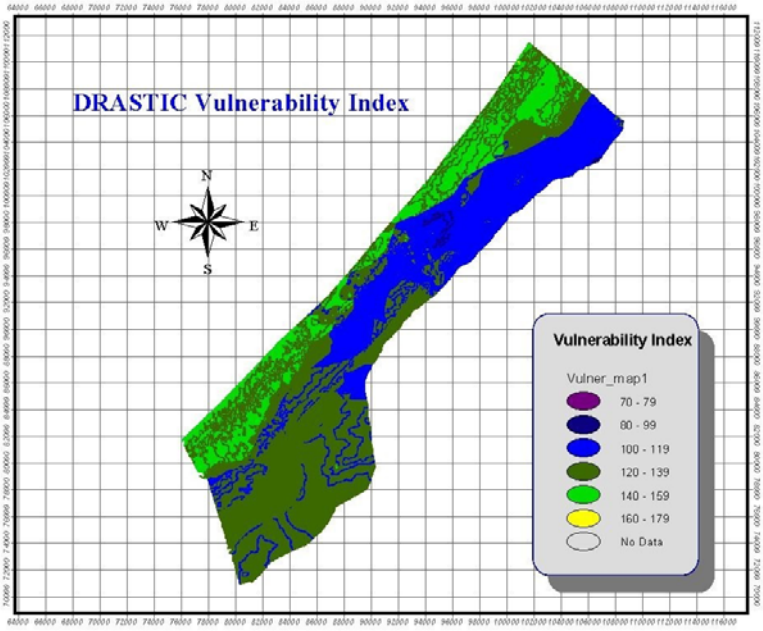

Fig 4: Drastic Vulnerability Index.

3.1 Validation

Most vulnerability maps are not validated. The use of information that is not validated can result in erroneous conclusions and subjective environmental assessments. To avoid subjectivity, parameter comparison testing and mapping validation alternatives are necessary (Ramos and Rodríguez, 2002).

If variations were detected in the selection of the rating values r for one of the factors and/or inadequate factor identification, the conceptual model was reviewed and modifications in the rating range were done.

All the seven factors contributed to yield the final DRASTIC index, the effective weight for each factor should calculate to compare it with the original weight.

The simplest expression of a weighting function could be a constant (Napolitano and Fabri, 1996; Gogu and Dassargues, 2000).

$$W_{xi} = \frac{X_{ri} X_{wi}}{V_i} \times 100 \qquad \text{.... (Eq. 3)}$$

Where;

Xri = the assigned rating for the factor X, e.g. (D, R, A, S, T, I, C)

Xwi = the assigned weight for the factor X, e.g. (D, R, A, S, T, I, C)

Vi = the vulnerability index for each point i, from Eq 3.

Each factor index (X_{ri} X_{wi}) was divided by the DRASTIC index (V_i) in order to calculate effective weight percentage for each factor by using map calculator in ArcView, the obtained results are shown in (Table 3).

Table 3: Shows the statistics of the calculated effective weights for each DRASTIC factor.

Factor	D	R	A	S	T	I	C
Min Wxi	3	3	5	4	1	22	6
Max Wxi	29	26	23	15	10	43	24
Mean Wxi	3.94	15.8	14.77	8.87	7.23	32.31	13.77
Standard Deviation	1.49	3.6	3	3.1	0.96	3.06	4.25

Then comparisons were made between the original DRASTIC weights and the mean calculated weights, the comparisons shown in (Table 4).

Table 4: Assigned and calculated effective weights for each DRASTIC factor.

Factor	D	R	A	S	T	I	C
Assigned weight,(Xwi)	5	4	3	2	1	5	3
Assigned weight, (%)	21.74	17.39	13.04	8.7	4.35	21.74	13.04
Mean calculated Weight, (Wxi) (%)	3.94	15.8	14.77	8.87	7.23	32.31	13.77
Calculated weight, (Xwi)	**0.91**	**3.63**	**3.4**	**2.04**	**1.66**	**7.43**	**3.17**

The calculated weights for each factor are close to the assigned weight except the depth of water table that asserts our primary notes about depth of ground water map. As a result of that, adjustments for the water table depth are required.

The depth to ground water is highly weighted (5), but the effective weight was calculated is 0.9, that means the effect of depth to the water table is almost negligible, in order to increase its effective weight, many processes were done by trial and error to select a new weight as follow.

- Plotting the original relation between depth and rating.
- Correlating and determining the curve equation.
- Multiplying the original depth of water table range by constant (3, 5, 7 and 9) and plotting the new curves (Fig 5).
- Determining frequencies for the original and new curves by ArcView (Fig 6).

The previous statistical operations were done considering the distribution of the water table depth overall the area. The frequency distribution is a powerful tool to look for a similar distribution of DRASTIC rating of the water table depth.

It becomes evident from the frequency distribution for each trial (Fig 6) that the histogram of depth x5 is the only one among others has a normal distribution (as Bell Shape), and the Bell Shape is the best histogram represents the real situation. We have decided to adopt the constant 5 multiplied by depth range as in (Table 5).

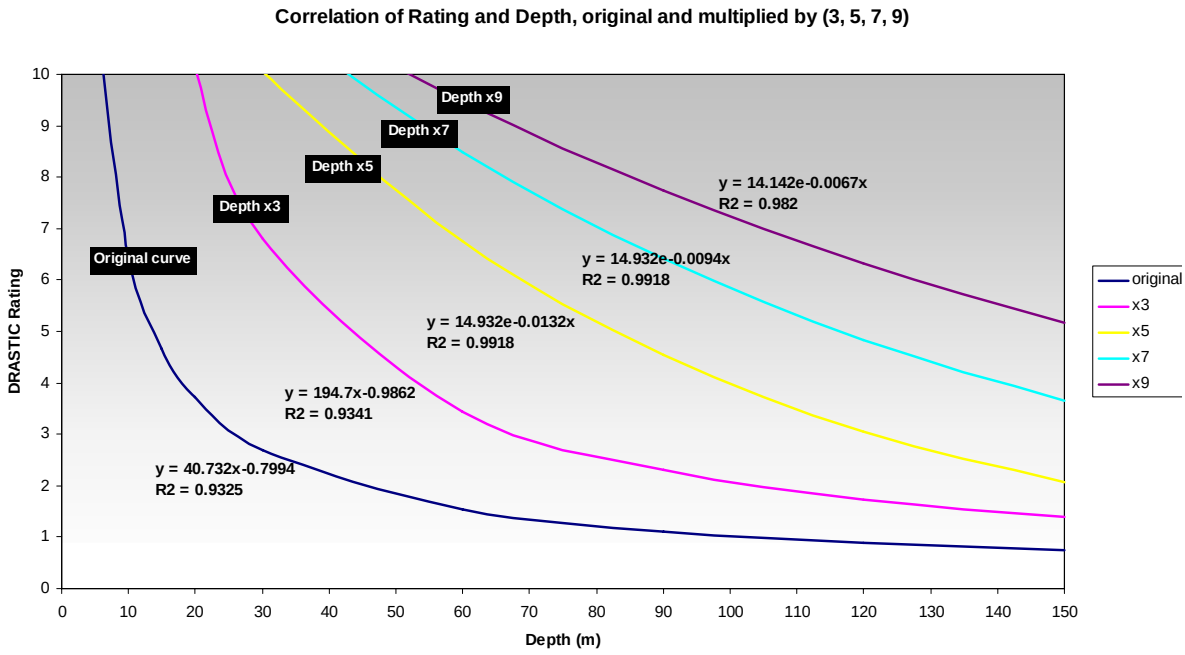

Fig 5. Correlation of curves for the original DRASTIC and depth multiplied by (3, 5, 7, 9)

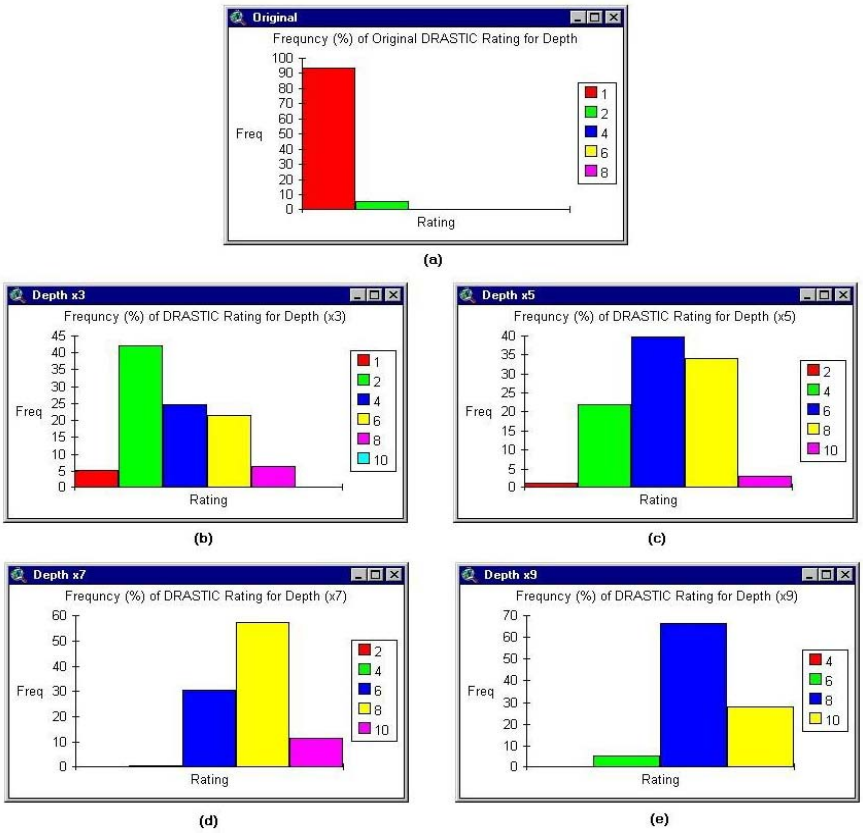

Fig 6. Rating Frequencies of the Original DRASTIC and depth of water multiplied by (3, 5, 7, 9)

3.2 Final Results

Table 5. Original and Modified Range and Rating of Depth to Water Table.

Original depth range (Aller et al, 1987.)	Depth range (Modified)	Rating
0 – 5	0 – 25	10
5 – 10	25 – 50	8
10 - 15	50 – 75	6
15 - 20	75 – 100	4
20 - 30	100 – 150	2
> 30	> 150	1

According to the modified range and rating of depth to water table shown in (Table 5), a new map was generated for depth to water table, thereby a modified DRASTIC index map was created as mentioned in the previous steps (Fig 7), and the effective weights of the seven DRASTIC factors were recalculated and tabulated in (Table 6).

Table 6. Assigned and calculated effective weights with re-rated depth to water table for each DRASTIC factor.

Factor	D	R	A	S	T	I	C
Assigned weight,(Xwi)	5	4	3	2	1	5	3
Assigned weight, (%)	21.74	17.39	13.04	8.7	4.35	21.74	13.04
Mean calculated Weight, (Wxi) (%)	20.53	13.02	11.98	7.22	5.75	26.6	11.31
Calculated weight, (Xwi)	**4.72**	**3.00**	**2.76**	**1.66**	**1.32**	**6.12**	**2.6**

If we compare Table 4 with Table 6, we notice that the calculated weights became closed to the assigned weights. As a result of rescaling the depth to water table, the effective weights of the other factors have changed and the relative error is decreased as shown in (Table 7), so it proves that all the factors have influence to each others.

Table 7. Relative Error for Original and Modified Weights

Factor	D	R	A	S	T	I	C
Assigned weight, (%)	21.74	17.39	13.04	8.7	4.35	21.74	13.04
Orig. Mean calculated weight,(Xwi) (%)	3.94	15.8	14.77	8.87	7.23	32.31	13.77
Mod Mean calculated Weight, (Wxi) (%)	20.53	13.02	11.98	7.22	5.75	26.6	11.31
Orig. Relative Error, (%)	**81.88**	**9.14**	**13.27**	**1.95**	**66.21**	**48.62**	**5.60**
Mod. Relative Error, (%)	**5.57**	**25.13**	**8.13**	**17.01**	**32.18**	**22.36**	**13.27**

The relative error in the highly weighted and most significant DRASTIC factors (D, I) were reduced as possible as shown in Table 5.5. Reducing the error in depth to water table affected to the other factors weights increasing error in some but reducing error in most of them, no modification can be done in impact of vadose zone factor because it has one category and the error has no great effect to total Index value and topography is lightly weighted, also it doesn't has big influence compared with other factors, but reflects some error to the recharge factor because the method estimates the recharge rating consider the topography, soil media and rainfall.

Accordingly this is the optimum modification we could do.

The final DRASTIC vulnerability map is presented in (Fig 7). If we compare it with the primary vulnerability map in (Fig 4), we notice the difference between them, in the first one the effect of water table depth is approximately negligible and as we mentioned before, the most significant factors are D and I, so we can say that the modification was done reflects the natural vulnerability of Gaza Strip. The standard DRASTIC colors have used to express the relative risk of areas to each other. The DRASTIC Index appears in the map within range from 95 (low vulnerable) has a magenta color to 195 (high vulnerable) has a yellow color.

The maximum possible DRASTIC Index is 230 and our maximum Index is 195, which means we have high vulnerable areas mainly, lies along the coast.

The degree of vulnerability can be determined, based on the following assessment criteria (Added and Hamza, 1999):

Low hydrogeologic vulnerability, if $V < 80$; Medium hydrogeologic vulnerability, if $80 \leq V < 120$;

High hydrogeologic vulnerability, if $120 \leq V < 160$; Very high hydrogeologic vulnerability, if $160 \leq V < 185$;

Extremely high hydrogeologic vulnerability, if $V \geq 185$

The data used in these analyses were taken from various studies and sources. The summation of mean calculated weight is less than 100% by about 4% as a result of all seven factors are not completely overlayed (the area at the Egyptian – Palestinian borders are not covered in some of the maps). Also values for some factors, such as recharge (R), were determined by different methodologies. Thus, apparent differences in vulnerability may be due to differences in methodology or interpretation. The accuracy of depth to water table is not so high, it was determined from the wells depth that is not updated in addition to use interpolation.

These maps describe the relative vulnerability of the aquifer based on available data of different levels of precision and resolution. For example the aquifer media was digitized from a low resolution image.

4. Conclusion

By using GIS, we have been able to apply the DRASTIC model to determine the vulnerability map of the Gaza Strip aquifer. DRASTIC Index provided "discrete" number which can be used to evaluate groundwater pollution potential. The DRASTIC Index of Gaza Strip is from 95 to 195. The higher the DRASTIC index means the greater the groundwater pollution potential. The index number is a relative numerical value and is of value only with respect to other numbers generated by the same DRASTIC Index.

The map reflecting the facility with which a contaminant could infiltrate the ground water shows high degrees of vulnerability in most of the study area. However, extremely high

degrees of vulnerability noted along the coast and in the northern area (Beit Lahia) where there found waste water bonds and its leaching reach the groundwater, this could incite the local community to first preserve these areas.

The reasons of high vulnerability leading to this result are:

- The soil type of the coastal and northern area is sandy, which gets higher rating (9) than the other area with clay soil (3). Pollutants transportation is easier in sandy soil than in clay and silt soils.
- The recharge rating is high in these areas because of the soil type that means more aquifer groundwater recharge of this area.
- Aquifer Media shows also higher rating at these areas.

The combination of weight of these three factors has big influence to the final results.

It is important to developed studies aiming the validation of groundwater vulnerability assessment methods, for the DRASTIC method, so that one may compare both the computed quantitative results (i.e. in terms of index values) and the qualitative values (i.e. in terms of "extremely high", "very high", "high", "medium" and /or "low") with the results of groundwater analysis. In our case DRASTIC method was not absolutely valid; e.g rescaling of depth to water table to include our range has modified the final DRASTIC index and gets more realistic results.

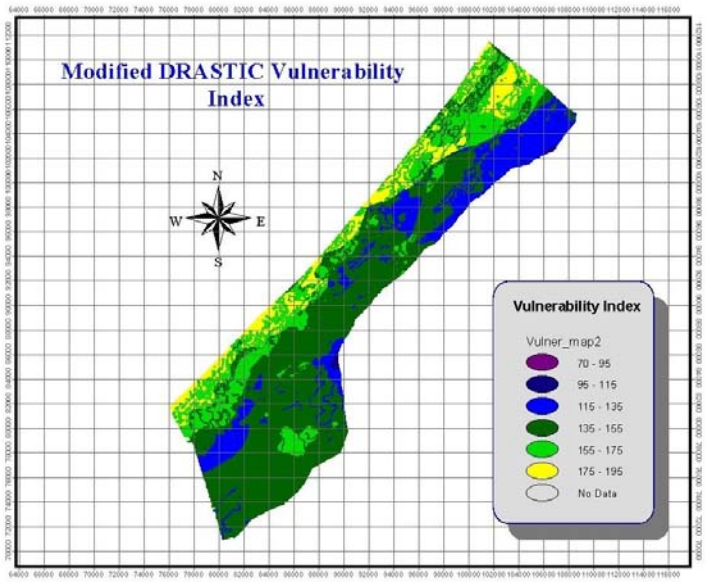

Fig 7: Modified DRASTIC Vulnerability Index (V)

Acknowledgment

To our parents that have always encouraged and supported us, without you life would not have become as good as it indeed is. To our families and friends, thank you for love, encouragement and support.
We wish to acknowledge Dr. Michel Le Duc, IDA - Linköpings Universitet, for his help, support and encouragement during preparation of this work. In addition we want to thank all those help us in IDA – Linköpings Universitet.
To the Palestinian Water Authority especially Eng. Nabil El Sharif, Eng. Sadi Ali, we would like to thank you all for your faithful efforts and cooperation to supply us by the necessary data to complete this work and for loyal and continuous support.

References

Abu –Maylah Y. and Aish A., (1997). *Water Resources Program in Gaza Strip*, Al-Azhar University - Gaza

Added A. and Hamza M.H., (1999). Evaluation of the vulnerability to pollution in Metline aquifer. (North-East of Tunisia), Université de Tunis II; Département de Géologie Faculté des Sciences de Tunis; Campus Universitaire, 1060, Tunis, Tunisie. Tel. 216-1-872600, Fax, 216-1-885408.

Agriculture Canada, (1993). Nonpoint Source Contamination of Groundwater in the Great Lakes Basin: A Review, Agriculture Canada, Research Branch.

Aller L., Bennet T., Lehr J.H., Petty R.J. and Hacket G., (1985). DRASTIC; A Standard System for Evaluation Groundwater Pollution using Hydrogeologic Setting, EPA/600/2-85/018 US EPA.

Aller L., Bennet T., Lehr J.H., Petty R.J. and Hacket G. (1987). DRASTIC: a standardized system for evaluating groundwater pollution using hydrological settings, Prepared by the National water Well Association for the US EPA Office of Research and Development, Ada, USA.

Al-Dadah J. and Yosef. Agricultural Water Management and Conservation: Methods in Gaza Governates, Palestinian Water Authority.

Al-Jamal K., and others (1996). Water Resources Management in Gaza Strip.

Al-Yaqubi and Al- Jamal, (2003). Water Resources and Management Issues, (Gaza Strip/Palestine).

Gogu R. C. and Dasargues A., (2000). Sensivitivity analysis for the EPIK method of vulnerability assessment in a small karstic aquifer, southern Belgium. Hydrogeol. J., 8, 3 337-345.

Melloul A J. & Collin M. (1994). The hydrological malaise of the Gaza Strip, Israel, Journal of Earth Sciences, 43, 105-116.

Melloul, M., and Collin, M., (1998). A proposed index for aquifer water-quality assessment: the case of Israel's Sharon region, Journal of Environmental Management, v. 54, no. 2, p. 131-142.

METAP, Mediterranean Environmental Technical Assistance Program (2003). Water Quality Management West Bank and Gaza, Room H8-133, 1818 H Street NW, Washington DC 20433, USA. Tel. (202) 473 2194, Fax (202) 477 1374/1609, E-mail: sarif@worldbank.org Website: www.metap.org

Napolitano P. and Fabbri A. G. (1996). Single parameter sensibility analysis for aquifer vulnerability assessment using DRASTIC and SINTACS in Kova K. And Nachtnebel H. P. (eds) Proc. HydrolGis Application of Geographic Information Systems in Hydrology and Water Resources Management. IAHS

Publ. 235, 559-566.

NAP, National Academy Press, (1984). Groundwater Contamination, National Research council (U.S.) Geophysics Study Committee II. Series TD223.G75 1984 628.1'68 83-27249 ISBN 0-309-03441-8.

Piscopo G. (2001). Groundwater vulnerability map explanatory notes, Centre for Natural Resources NSW Department of Land and Water Conservation

PWA, Palestinian Water Authority (1996). Integrated Water Resources Management.

PWA, Palestinian Water Authority / USAID. (2000). Coastal Aquifer Management Program (CAMP), Gaza 2000

Ramos J. A. and Rodríguez R. C. (2002). Aquifer vulnerability mapping in the Turbio river valley, Mexico: A validation study, Posgrado en Ciencias de la Tierra, UNAM, México, D.F., MEXICO. Instituto de Geofísica, UNAM, México, D.F., MEXICO

Sivertun Å, Reinelt L.E., and Castensson R. (1988). A GIS Method to Aid in Non-Point Source Critical Area Analysis, International Journal of Geographical Information Systems, 2 (4), 365-378.

Sivertun, Å, and Prange L. (2003). Non-Point Source Critical Area Analysis in the Gisselö watershed using GIS, Department of Computer and Information Science(IDA), Linköpings Universitet, Sweden, Environmental Modelling & Software 18 (2003) 877-898.

UNDP, (2002). Arab Human Development Report, Creating Opportunities for the Future Generations, UNDP.

Yosuke K. (1997). Evaluating migration potential of contaminants through unsaturated subsurface in Texas. CE 397 GIS in Water Resources, University of Texas at Austin

From change indication to fine-scale population monitoring: Disaster management, post conflict assessment and reconstruction monitoring in Harare, Zimbabwe

Stefan Lang*, Elisabeth Schöpfer, Andreas Uttenthaler, Dirk Tiede and Peter Zeil

Centre for Geoinformatics (Z_GIS), University of Salzburg, Salzburg, Austria

* stefan.lang@sbg.ac.at

Introduction

This chapter presents work carried out in the GMOSS test case Zimbabwe, demonstrating the use of remote sensing data and change analysis techniques to provide evidence for human rights violations. The study addresses different stages of damage assessment and change analysis on different scales of observation. We combine two scale-depending strategies, i.e. (1) the indication of changes in informal settlement (shanty town) areas, and (2) the counting of single houses and dwellings in order to estimate the number of people being affected by these operations. Altogether, the paper gives a concise summary on different multi-temporal remote sensing approaches as being in sub-regional and local scale in the test case Zimbabwe comprising change indication, and the mapping and monitoring of informal settlements in Harare and surrounding urban areas.

Satellite imagery has been used to gain insight and collect evidence of such operations and their impact on human rights and human security (UNOSAT, 2005; AAAS, 2006). So far, the assessment of damaged areas has been carried out by visual interpretation of corresponding before and after images. Such visual evidences – along with other change indications on regional scales, such as land use change as an implication of the fast-track land transformation process, or changes of population densities – are building blocks of a crisis-alert system for monitoring humanitarian crisis situations. Thus, in addition to mere damage assessment, remote sensing data should also be utilized to highlight ‘peaks’ in slow-onset protracted crises and/or to monitor the process of reconstruction and to evaluate the effectiveness of humanitarian support.

Operation Murambatsvina

Operation Murambatsvina, also known as Operation Restore Order, has been a country wide operation carried out by the Zimbabwean Government of forced mass evictions, the demolition of homes and informal businesses. According to figures provided by the United Nations, 700,000 people across Zimbabwe lost their homes or livelihoods or both during Murambatsvina within six weeks between May and July 2005. Harare was among the worst affected cities, but the operation was also affecting other high density urban areas in Zimbabwe including Chitungwiza, Bulawayo, Mutare, Kariba and Victoria Falls. Officials claim that this was a necessary action against illegal trading and criminality in these areas. Other sources say that it was only a clearing campaign against the Opposition, which has many voters among the urban poor. The Government of Zimbabwe has reacted to international

pressure with Operation Garikayi (Rebuilding and Reconstruction), financing the construction of houses, factory shells and market stalls (Sunday Mail, 26 June 2005), providing (plots) for those rendered homeless who build their new homes supported by loans. Evidence on the ground (UN 2005) however suggest that the operation was hastily put together, did not meet the immediate needs of the people affected, and progress of implementation was slow (Schöpfer et al., 2007). So after more than two years after the event thousands of victims are still without adequate shelter.

Study area and data sets

Harare is the largest city and the capital of Zimbabwe and is situated in the central-northern part of the country. About 1.9 million people are living in an area of less than 870 km² (UN Humanitarian Support Team, 2006). The city is characterized by different urban structures: a central business district (CBD) with high rise buildings, areas with luxurious buildings for the rich and high-density areas of the urban poor (townships).

To cover relevant sites three study areas have been chosen showing before and after situations of both operation Murambatsvina, and operation Garikayi. We obtained QuickBird imagery from 25/08/2004 for the before status of Murambatsvina sites Mbare and Glen Norah and from 22/06/2005 for the after status in Mbare and 02/08/2005 for Glen Norah, respectively. For the operation Garikayi, QuickBird data were ordered from 16/04/2005 and 17/03/2007 for the area of Hopley Farm. Additionally, IKONOS imagery has been chosen for checking additional sites of Garikayi activities[21]. The images have been orthorectified by using a SPOT-5 scene (10 metres panchromatic) and rational polynomial coefficients and a 90 m SRTM surface model. To enhance the image quality pan-sharpening was applied using a fusion model after Liu, 2000, as implemented in the software Erdas Imagine 8.7. The resulting four bands with a ground sample distance (GSD) of 0.6 m were clipped to a subset of 5 x 5 km for performing change indication and the detection of shanty towns.

For the fine-scaled change analysis of the impact of Murambatsvina two test sites were chosen (see Fig. 1). Mbare is situated south-western of the city centre and is covering an area of 12 hectares. Glen Norah, the second test site, is situated in the south-western outskirts of Harare and covers an area of 7.5 hectares.

[21] not reflected in this article

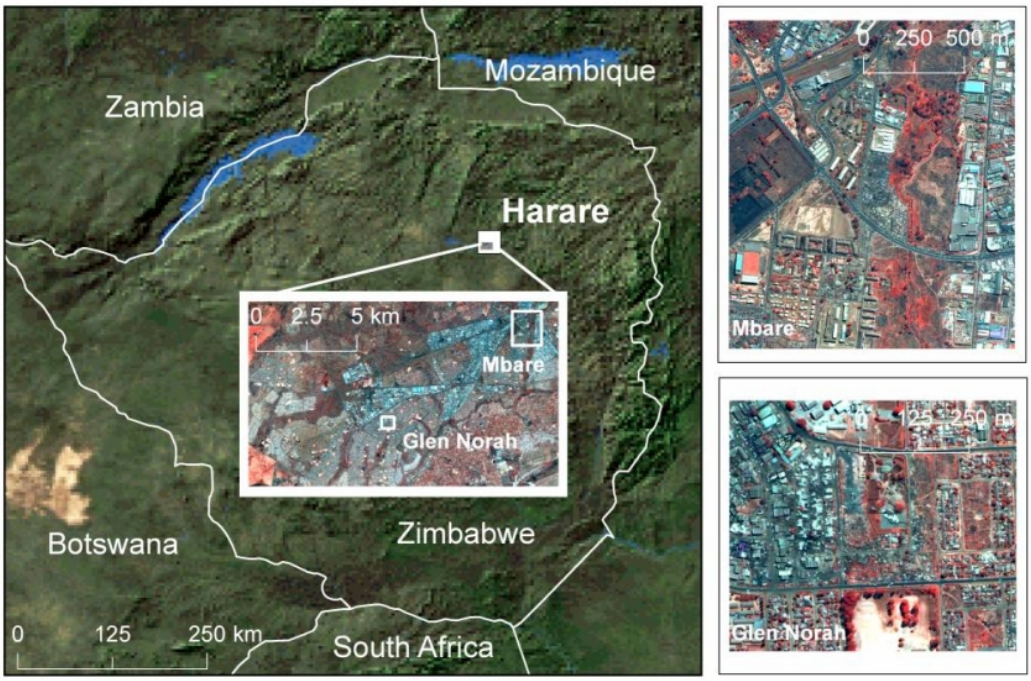

Fig. 1. Study areas affected by operation Murambatsvina in Harare/Zimbabwe

Damage assessment in informal settlements (shanty towns) using optical image data and structural hints

Informal settlements are commonly defined as urban settlement structures with mostly self–constructed buildings, built without master plan or any other governmental guidance and therefore usually considered 'illegal'. Since this definition implies legal aspects that, by remote sensing imagery, are obviously difficult to proof, we use the term 'shanty towns' to emphasize the particular structure of these settlements. Built in very high-density fashion, the buildings materials are mostly polyethylene plastics, bricks, asbestos and corrugated iron sheets. Due to the high complex structured areas with a high heterogeneity within, the delineation using conventional classification procedures is limited. The integration of spatial parameters in the process of class description elicited from expert knowledge extends the spectrum of the possibilities. Object-based class modelling enables addressing the overall structure of such settlements, by looking at the specific arrangement and the characteristics of the particular elements (buildings) such as shape, size, context and texture (Hofmann et al., 2006). In these areas tens of thousands of families used to live in the urban areas of Zimbabwe in what are known as backyard cottages or extensions – small, often brick-made structures (Amnesty International, 2006).

Detection of shanty town structures

In this first part of the research we are concentrating on cues for identifying shanty town structures in an automated, knowledge fashion and we establish a transferable and robust change analysis approach for indicating damages. The used method for damage detection combines object-based image analysis and GIS interpretation. We illustrate a workflow for information delivery by (1) transferable object-based classification on VHSR before and after images, followed by (2) spatial aggregation of results for comparative change analysis.

For detecting shanty town structures and to delineate their spatial extent, we used Definiens Cognition Network Language (CNL) for multi-scaled class modelling. For this study three segmentation levels have been created (Table 1).

Table 1: Segmentation parameters used for delineating shanty town structures

Level (scale parameter, SP)	Segmentation parameter	# of objects	¢ object size (m²)
10	Shape: 0.5 Compactness:0.9	408795	27.32
20	Shape: 0.5 Compactness:0.9	122860	90.89
100	Shape: 0.5 Compactness:0.9	5947	1877.63

In a cyclic manner, image objects are assigned to classes, based on a rule set, developed by the user or based on samples taken. On a lower level, i.e. scale parameter (SP) 10, small shacks, buildings, vegetation, small bright objects and shadows were classified. On a higher level (SP 100) the settlements, bare soil, streets, burnt areas and larger industrial buildings were identified, partly with the help of hierarchical relations to the sub-objects. Additionally, an intermediate level (SP 20) was created, that represents best the structures of larger buildings.

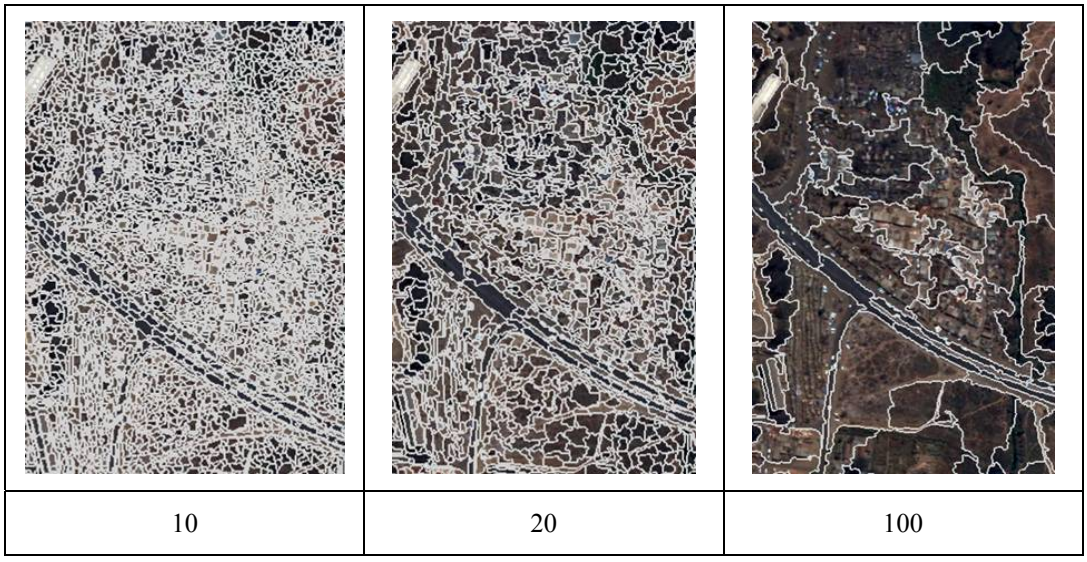

Fig. 2. Segmentation levels in the Definiens software environment

By considering the spectral attributes and information about the shape and size of buildings and shacks, mainly small quadratic structures with bright roofs could be well outlined as "informal buildings". Small shacks were classified by the rules Buildings with Shape Index <1.2 and Area of <= 25 m², whereas buildings were detected with the rule Mean Layer 1 >=240. As a next step and by the application of class-related classification rules between different segmentation levels (Relative Area of small shacks >= 0.08; Relative Area of vegetation <= 0.05) informal settlements were classified. To demarcate settlement structures a texture measure (Mean of sub-objects: stddev Layer 1 (1) >= 36) and the Relative Area of buildings >= 0.2 have been taken into account. To detect and distinguish informal settlements, the knowledge of their physiognomic structure and their spectral properties is essential. The spatial relationships between the objects (especially between super- and sub-objects) also have to be taken into consideration.

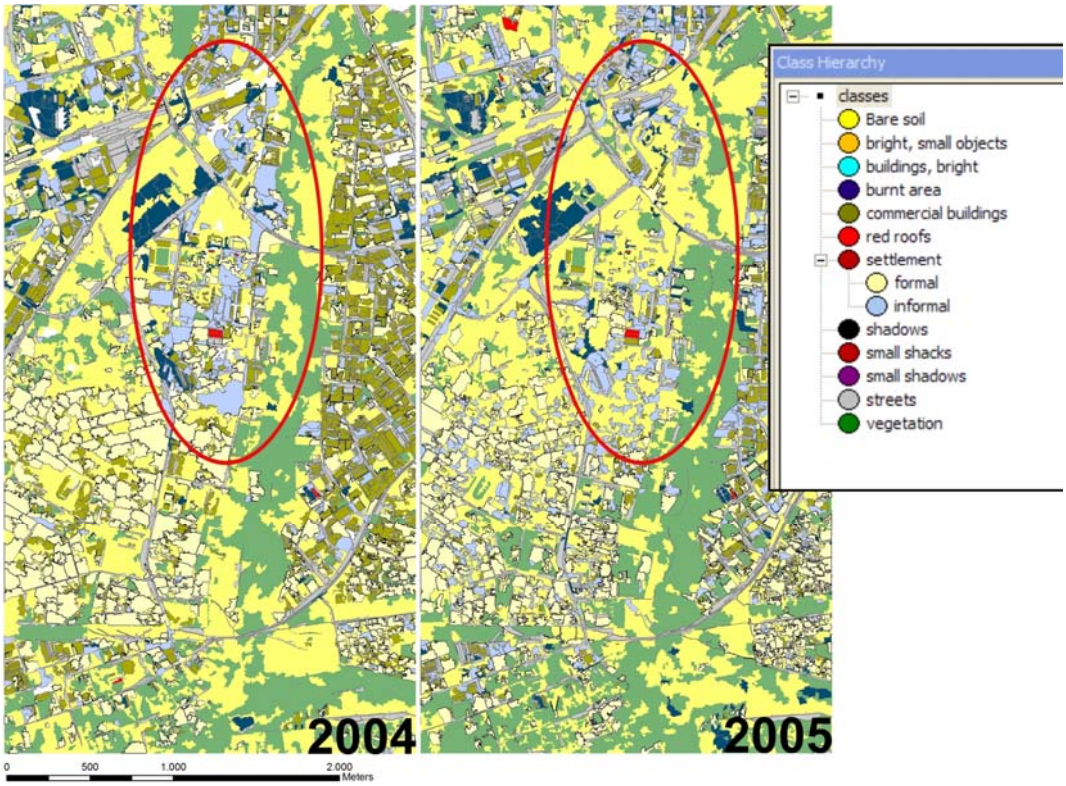

Fig. 3. Classification results for informal settlements in the Mbare area in 2004 (left) and 2005 (right)

Accuracy assessment was carried out by using sample-objects. To assess the classification result for buildings at Level 1 100 samples were taken, from which 79 were classified correctly. The overall accuracy for the detection of selected shanty town structures reached 77%.

Change indication for damage assessment

In addition to the pre-processing steps performed before, principal components (PC) were calculated to enhance spectral separability. The first three PCs were computed and PC3 (third principal component) was used for the classification.

We developed a rule set for the before image using Cognition Network Language (CNL). Steps included multi-resolution segmentation of the image and dynamic class modelling. Segmentation – as above – was performed based on a region-based, local mutual best fitting approach (Baatz and Schäpe, 2000). For the study the Normalized Difference Vegetation Index (NDVI) and the Soil Adjusted Vegetation Index (SAVI) were calculated to identify vegetated areas. In addition, an adapted feature including the blue band and PC3 was chosen to better differentiate between bare soil areas and settlements (Schöpfer et al., 2007). For the extraction of urban areas, only the most robust features were selected to maximise transferability to the 2005 scene. The developed rule set has been automatically applied to the *after* image.

The developed and applied rule set led to the results as shown in figure 4. For further analysis we overlaid the study area with 90 regular raster cells (500 * 500 m). For each cell the difference of urban area between 2004 and 2005 was determined. The standard deviation of these differences was used as a measure to remove the trend of underestimation and scatter in the after image. We could identify six cells with a standard deviation > 3 as areas with significant change (see figure 5).

Fig. 4. Extraction of urban area for the before (left) and after (right) image of the study area (from Schöpfer et al., 2007).

The identified cells serve as indicators where visual interpretation should focus to further explore destroyed townships. This automated process replaces screening large areas manually. Three out of these six cells (# 24, # 25, and # 34) were directly linked to the documentation of the township Mbare provided by UNOSAT (2005). The cell #42 also indicates changes by destruction, as being proved by the QuickBird data (see figure 5). In two other cells changes were indicated, whereas these were caused by a coal-fired power plant.

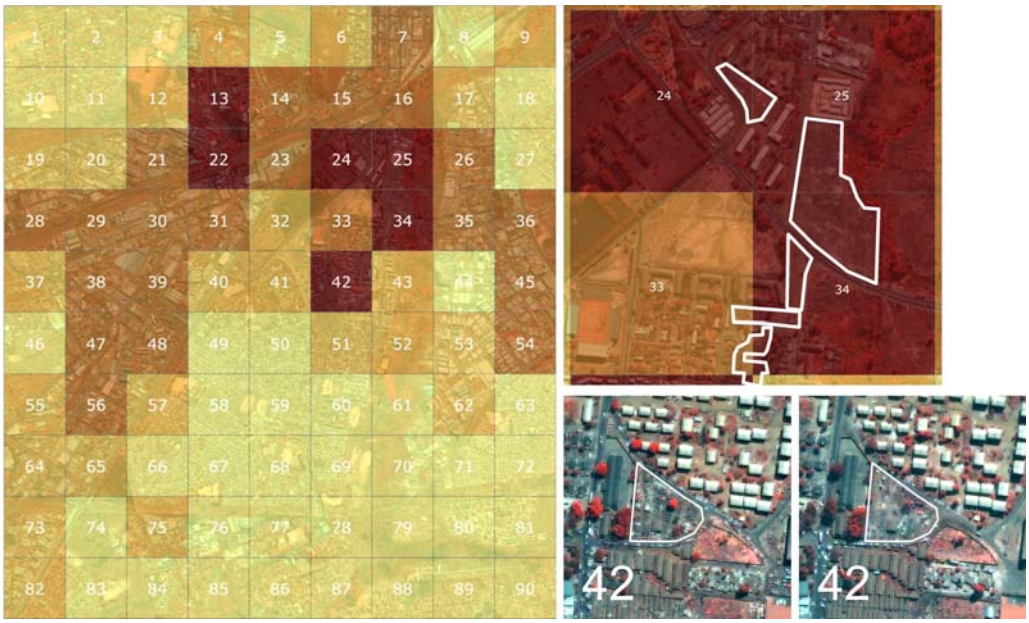

Fig. 5. Left: aggregated change of urban area between 2004 and 2005 aggregated to 90 raster cells (500 m * 500 m). Dark values indicate areas with a higher standard deviation i.e. a higher probability of change; brighter cells represent areas with minor to no change. Right above: Manual delineation of the destroyed area overlaid with the corresponding raster cells. Right below: Identified destructed area in cell # 42 in the before (left) and after (right) QuickBird images. The white outline shows the affected area. (All figures taken from Schöpfer et al., 2007)

This change indication approach may save time and – given that the algorithm applied is robust enough – users do not have to spend extra time and effort for extensive (and expensive) pre-processing and advanced classification. The user may check the images for damaged areas prior to intensive change detection analysis. Then, in a second step he or she will focus on the indicated affected areas, which are otherwise hardly detectable. Within a focused area, the number of affected houses or density of buildings can then be analyzed. The usability and reusability of rule sets enhance the efficiency of image analysis and contribute to efficient and

constant monitoring. Thus, the proposed method may help focusing response to emergencies and support rapid identification of affected areas.

Fine-scaled change analysis

Beyond the identification of changes, we also performed fine-scale mapping for detailed change analysis within the detected areas. We concentrate on two reference sites (Mbare and Glen Norah) within the city of Harare as shown in figure 1. Dwelling structures were categorized and extracted in the before and after crisis image. In addition the population was estimated to provide a rough estimate of affected people.

In a first step a visual detection of two types of building structures (i.e. small, quadratic shacks and larger, more massive buildings) was carried out in two subsets of the study areas. In the Mbare subset (before Murambatsvina) 98 shacks have been detected visually and 102 shacks have been detected automatically (see figure 6, left). In the Glen Norah subset (1) 63 shacks could be visually detected and (2) 135 were detected automatically (see figure 6, right). In this area the automatic extraction of buildings turned out to be more difficult, because of the low spectral difference within the informal settlement. Especially in the transition zones between shacks, bare soil and sandy roads confusion took place.

Fig. 6. Comparison of visual detected (dark triangles) and automatically classified (bright polygons) shacks in subsets of the study areas in Mbare (left) and Glen Norah (right). Dashed polygons are signalling erroneous classifications. Bright triangles are showing classified, but visible not detectable structures.

The differentiation between buildings/shacks and the underground was also hampered, when the roofs were dark coloured. Because of the very high density of neighbouring buildings, the delineation of single shacks was sometimes critical. In the study area of Glen Norah over-segmentation (single structures were not delineated as one object) and errors of omissions (in terms of number) can be generally assumed.

According to Brown (2001), up to twelve people live together in one shack; this number seems to be too high because of the small size of the buildings, so we limited the number to 8-10 people per shack. This would lead to a population estimation of 800-1000 people for this subset. Table 2 shows the results calculated for the whole study areas.

Table 2. Number of extracted buildings (both visual and automated) and estimated people affected according to an average occupation of 9 people (Number of people per shacks according to Brown (2001) 12 people → reduced to 9)

Test area	Visual interpretation: # of buildings (# people)	Automated delineation: # of buildings (# people)
Mbare (total area)	~ 800 (7200)	960 (8640)
Glen Norah	~ 220 (1980)	340 (3060)

Reconstruction monitoring – first experiences

Finally, reconstruction monitoring was performed to observe reconstruction efforts on the ground. In this case the rebuilding sites are investigated visually in terms of activities going on there. The construction activities of the Operation Garikayi was looked at using before and after imagery (2004/2005 and 2006/2007), in dedicated resettlement areas (Hatcliffe, Hopley Farm). As a preliminary result it turned out that while in fact reconstruction was carried out, the type and the size of the buildings as well as the space between them, did not meet basic requirements of the population settled there.

Fig. 7. Operation Garikayi: new construction sites and new densely-built dwelling structures (Hatcliffe; Left: August 2004; Middle: July, 2006; Right: magnification)

References

AAAS Science and Human Rights Program (2006): GaTHR Case study (The GaTHR Project) Zimbabwe: Community Demolitions; http://shr.aaas.org/geotech/zimbabwe.shtml

Amnesty International / Zimbabwe Lawyers for Human Rights(2006): Zimbabwe Shattered lives - the case of Porta Farm; AFR 46/004/2006, International Secretariat, London, UK.

Baatz, M., Schäpe, A., (2000): Multiresolution Segmentation: an optimization approach for high quality multi-scale image segmentation. In: STROBL, J. et al. (Hrsg.): Angewandte Geographische Informationsverarbeitung XII. Beiträge zum AGIT-Symposium Salzburg 2000, Karlsruhe, Herbert Wichmann Verlag.

Brown, A. (2001): Cities for the Urban Poor in Zimbabwe: Urban Space as a Resource for Sustainable Development, Development in Practice, Baskingstoke, Oxfam, Carfax, Taylor & Francis Limited.

Hofmann, P., J. Strobl, T. Blaschke & H. Kux (2006): Detecting informal settlements from Quickbird data in Rio de Janeiro using an object based approach. In: Lang, S. et al. (eds.): Proceedings of the 1st International Conference on Object-based Image Analysis, July 4-5, 2006.

Liu, J.G. (2000): Smoothing filter-based intensity modulation: a spectral preserve image fusion technique for improving spatial details. In: International Journal for Remote Sensing, Vol. 21, No. 18, S. 3461-3472.

Schöpfer, E., D. Tiede, S. Lang and P. Zeil (2007): Damage assessment in townships using VHSR data - The effect of Operation Murambatsvina / Restore Order in Harare, Zimbabwe. In: Urban Remote Sensing Joint Event, 11.-13. April 2007, Paris.

UN (2005): Report of the Fact-Finding Mission to Zimbabwe to assess the Scope and Impact of Operation Murambatsvina by the UN Special Envoy on Human Settlements Issues in Zimbabwe. http://www.un.org/News/dh/infocus/zimbabwe/zimbabwe_rpt.pdf

UN Humanitarian Support Team (2006): "Harare". http://www.zimrelief.info/index.php?sectid=12&articleid=389

UNOSAT (2005): Satellite image maps of Operation Murambatsvina by UNOSAT; http://unosat.web.cern.ch/unosat/asp/prod_free.asp?id=29

EO data supported population density estimation at fine resolution – test case rural Zimbabwe

Stefan Schneiderbauer[a*] & Daniele Ehrlich[b]

[a] *European Academy, Institute for Applied Remote Sensing, Viale Druso 1, 39100 Bolzano (Bz), Italy*

[b] *European Commission, Joint Research Centre, Institute for the Protection and Security of the Citizen (IPSC), Support to External Security Unit, Ispra 21027 (VA), Italy*

* stefan.schneiderbauer@eurac.edu

Abstract

The research carried out aimed at mapping Zimbabwean population density at sub-national scale. The study was conducted on a 185 x 185km area at a grid cell size of 150m. The surface modelling of population density was implemented by integrating 4 main variables: land use, settlements, road network, and slopes. During the modelling procedure, pixel weighting values were allocated according to pre-defined decision rules. In a final step the district population counts of the recent Zimbabwean census were distributed among all pixels of the relevant district according to the pixel weighting values. The results showed increased quality and spatial accuracy of population numbers compared to the latest Landscan gridded population dataset of 1 km resolution. The dataset Gridded Population of the World (GPW) available at the resolution of 2,5 km provides uniform values within the administration layers of districts, which did not match the available Zimbabwean census data

The resulting land use information and population data can be linked to vulnerability and food insecurity. The methodology developed can be extended to the whole of Zimbabwe. In order to be transferred to other countries, the modelling procedure needs to be adapted to case specific characteristics, the determination of which requires a certain level of local / expert knowledge. In addition, passive sensors might not provide sufficient cloud free satellite data for regions lying within the moist tropics.

Introduction

Population data is crucial information for disaster management, early warning systems and emergency actions. Contrary to common presumption, reliable data on population numbers and spatial distribution, as source for the exposure part of the risk equation, is rarely available for non-industrialised countries. The lack of recent population data at fine spatial resolution hampers the work in all steps of crisis management.

In developing countries population censuses have started to be conducted only in the second part of the 20th century (Vallin 1992). Censuses are typically carried out every 10 years and in less prosperous countries often supported by donor institutions. They are usually elaborated by national statistical offices and made available to the public in aggregated form as national statistical yearbooks. Aggregated statistical information at country level, often referred to as secondary data, is also available through international organisation and commercial yearbook atlases.

In developing countries population figures are also recorded within the scope of development projects and in the aftermath of disasters in order to determine dimension and type of assistance needed. The spatial extent of these surveys is usually limited due to the area selected for a project or affected by a hazardous event. They aim at generating information regarding certain aspects of population and lack the spatial and temporal continuity and coverage of traditional censuses. Due to the surveys' specific application there is no strategy to

(1) update the information or (2) make it available to wider user groups (Schneiderbauer & Ehrlich 2005).

For the integration of population datasets into spatial analysis such as agriculture, environment, disasters or communities' vulnerability/poverty estimations, the data need to match two requirements:

- Availability at finer scale units than those resulting from usual censuses.
- Storage in raster format in order to ease computation and modelling.

The research community has developed techniques to transform population vector data based on censuses into raster data, with a population number per grid cell. The raster format containing population counts is also referred to as population density representation and is increasingly used for disaster management, early warning and rapid response to crises. Current research is attempting to improve the accuracy and to increase the resolution of data on population distribution. Future work will increasingly focus on the development of attribute information determining populations' characteristics such as their vulnerability.

The work within this paper focuses on the improvement of the spatial resolution of population datasets available at district levels covering Zimbabwe. It (1) uses country specific information layers, (2) evaluates the use of medium resolution satellite imagery and map based data for a population density estimation made available at a grid size of 150 meters. The methodology developed covers a region in Zimbabwe that includes the capital Harare.

Background

Population data from censuses are commonly made available per administrative / political unit. The datum includes the spatial representation of the administrative unit as vector polygon and the associated attribute reporting the total population value. Countries are subdivided in a hierarchical system of administrative units up to 4 levels deep: country, regions / provinces, counties / districts, and municipalities / communes. Administrative borderlines are not usually drawn to represent geographical phenomena. Therefore, on vector data based choropleth population maps, the populations seem to be homogenously distributed over the area of the administrative unit, despite possibly significant variations in real population densities. The dasymetric mapping approach aims to delimit regions with similar population densities by applying ancillary data (Mennis 2003; Langford & Unwin 1994). Dasymetric mapping of populations at large and medium scale has been successfully applied in developed countries by using land use / land cover information stemming from earth observation data (Langford et al. 1991; Holloway 1999; Chen 2002; Mennis 2003; Lo 2003; Liu 2004).

A commonly used technique in population modelling is smart interpolation. Smart interpolation for population density estimation is based on two major steps:

(1) the calculation of a grid-based population potential and

(2) the allocation of population numbers, usually available at a certain administrative level, to the gridded population potential.

The population potential estimation may rely on a series of variables including the location and size of urban settlements, as well as thematic data layers such as those depicting national parks, protected areas and inaccessible areas that are supposedly not populated. A model based on these input layers and transformed into algorithm for automatic computation helps to generate population raster datasets over large areas.

The first global population density estimation in raster format was initially developed under requests from international agricultural research institutes (Deichmann 1996). Since then other raster based global population densities have been produced (Sutton et al. 2003), of which the 'Global Population of the World' (GPW) from the Center for International Earth Science Information Network (CIESIN) at the Columbia University (Balk & Yetman 2004) and Landscan (Dobson et al. 2000) have received the most attention due to their accessibility and frequent update. Landscan was developed by allocating census counts at 30" X 30" cells through a 'smart' interpolation based on the relative likelihood of population occurrence. The allocation to cell is based on weighting computed from slope categories, distance from major roads, and land cover (Mirella et al. 2005).

The global population density datasets are lacking accuracy information but they are invaluable. They are used to provide preliminary estimates of casualties in the aftermath of natural disasters such as earthquakes, tropical storms or large floods. Also, in the absence of better population figures, these datasets are used in the assessment of slow onset disasters, namely droughts or epidemics, which are typically geographically specific. However, the demand for more precise population density data at a finer scale remains unmatched.

Improvement of the smart interpolation techniques relies on the availability of country specific fine scale data and Earth Observation data. Aerial photography and satellite imagery were already tested for population density mapping in the 1980's. Remote sensing techniques have been applied in order to improve or overcome census shortcomings in developing countries' censuses (Adeniyi 1983; Olorunfemi 1984). Coarse resolution imagery has been used in improving global population density assessments (Eldvige et al. 1997), and medium resolution for zone based estimations (Lo 2003). Harvey (2002) specifically tested estimations of population numbers from satellite imagery. With the availability of very high resolution imagery, formal settlements such as cities and informal settlements such as refugee camps can be assessed for population density (Giada et al. 2003a; Giada et al. 2003b). A recent overview of techniques used for counting population in cities is provided by Mesev (2003).

This study addresses the use of medium resolution imagery for zone based estimates of population densities. It aims at further developing methodologies that allow the relatively rapid generation of information on population distribution at a fine scale that is required for improved disaster management.

The study area extends over 185 x 185 km, coinciding with the coverage Landsat TM scene path 170 and row 72 (Fig. 1). It includes the economic centre and capital Harare, and makes up part of the most productive agri-ecological zone of intensive farming in Zimbabwean's Highveld and Middleveld (Vincent & Thomas 1960). The study area covers commercial private farmland as well as government owned land, referred to as communal land22. The study is therefore representative of the land cover and land use diversity in Zimbabwe. Within the study area are three million people, accounting for 25% of the overall Zimbabwean population, living on an area of 33206 km2, which is 12% of the total land cover.

22 In southern Africa 'communal land' generally refers to an area of land owned by the State, which confers certain use rights (for cultivation, livestock grazing, timber harvesting, settlement, etc.) to rural populations that do not hold individual proprietary deeds. Many such areas in Zimbabwe are used for traditional agro-pastoral farming activities.

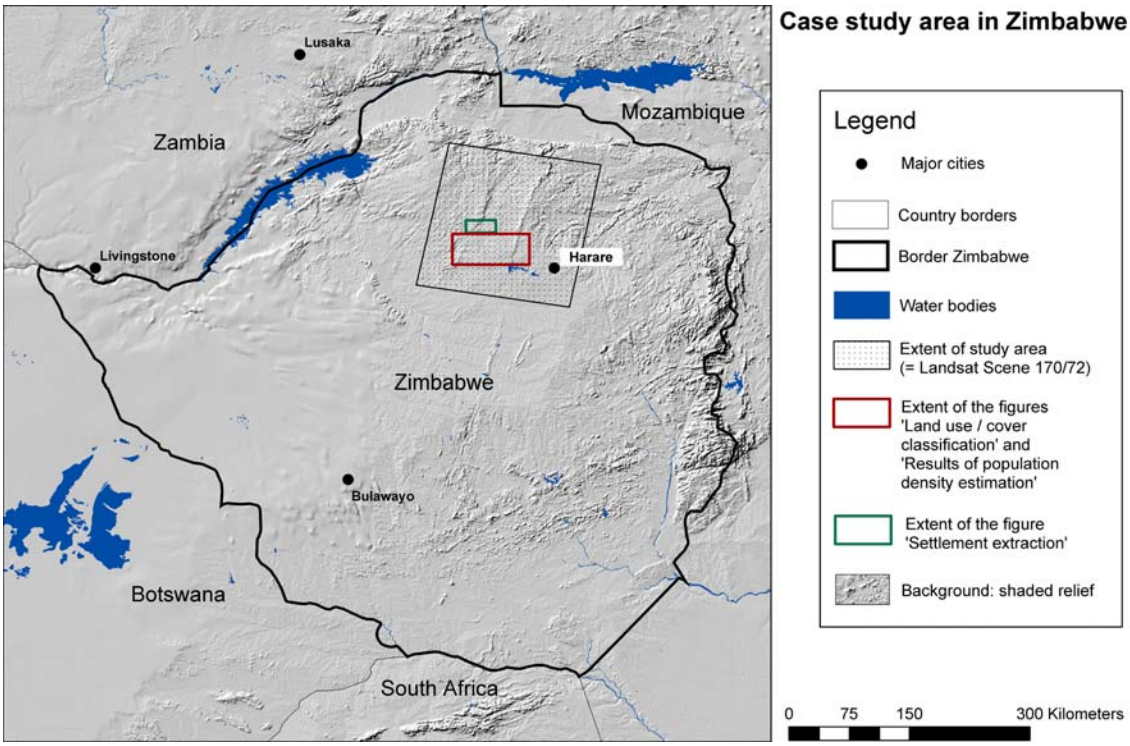

Fig. 1: Case study area in Zimbabwe including the extents of Fig. 2, "Processing stages of the extraction of human settlements from the scanned maps" (green box), Fig. 3, "Landsat imagery classification" and Fig. 5 "Results of population density model" (both red box) (source: Schneiderbauer 2007)

Methodology

The distribution of population within each district of the study area in Zimbabwe was modelled by creating a continuous surface of population density at a grid cell size of 150 m. The methodology for surface modelling of population data relies on combining information from a number of information layers listed in Table 1.

The input data were available as explicit digital information, with a spatial and attribute component, and data layers that required information extraction to provide delineation of spatial units and associated attributes. The ready-to-use information layers included the administrative borders of Zimbabwe at district level with associated population counts, protected areas, urban areas available as polygons, the road network available as lines, and towns available as point data. The raster information layers included the 1 km land cover and the digital elevation model derived from the Shuttle Radar Topography Mission (SRTM) elevation dataset. Two data sources required information extraction: Satellite imagery that needed to be classified into fine resolution land cover / land use classes and maps that were processed to extract specific features such as village location.

Table 1: Data layers used for modelling population densities within the study area (source: Schneiderbauer & Ehrlich 2005).

Dataset	Format / Resolution / Scale	Date	Coverage / Size	Theme extracted	Source
Population Census data	District level	2002	Countrywide	Population per district	Central Statistical Office Zimbabwe
Administrative subdivision of the country	Polygon	2002	60 Districts	District boundaries	Survey-General Zimbabwe

Urban areas	Polygon	NA	Areas of 8 main cities	City area boundaries	Humanitarian Information Centre
Protected areas	Polygon	NA	Countrywide	Protected area boundaries	Survey-General Zimbabwe
Road network	Line	2002	Countrywide		Humanitarian Information Centre
Settlements	Point	NA	Countrywide	Towns	DCW
Elevation	Raster / approx. 90 m (3 arc seconds)	2002	Countrywide	Slope	SRTM, United States Geological Survey
GLC 2000	Raster / 1 km	2000	Countrywide	Selected land cover classes	JRC
Landsat ETM	Raster / 15 m & 30 m	2002 / 2003	24 scenes	Land cover / Land use	LANDSAT
Topographic Maps	1:250,000	1973-1995	34 maps	Village locations	Survey-General Zimbabwe
Woody cover map	Analogue map (Printed version) 1:1 000,000	1998	Countrywide	Woodland (Photointerpreation)	Zimbabwe Forestry Commission

All data layers required pre-processing that included the standardised transformation into a common geodetic projection. A selection of significant data layers was processed in order to allow their input into the smart interpolation model.

The modelling procedure produced a weighting value for each pixel in the study area according to the relative probability of population numbers living within the pixel area. The weighting values permitted the redistribution of one population value per district to a number of grid cells within this district.

Pre-processing and information extraction

Pre-processing consisted of scanning maps, geo-coding all information layers in a common geodetic projection, and the conversion of the data into raster format. Zimbabwe is covered by two UTM zones, making standard UTM difficult to use. The national projection and the most common projection for mapping Zimbabwe as a whole country, is the Transverse Mercator projection, based on the modified Clarke 1880 spheroid (Mugnier 2003). Therefore, all the data were projected into this coordinate system. The projection of the satellite images was carried out after the classification in order to avoid information loss. After the projection, all vector layers were transferred into raster layers of 15 m pixel size, fitting with the panchromatic band of Landsat ETM. Information extraction was performed on scanned maps in order to extract the location of villages and on satellite images in order to produce a land cover map for the area.

Processing map data

The scanned topographic maps at a scale of 1:250,000 were processed in order to extract the location of small settlements. Villages and buildings such as schools and hospitals indicating the centres of settlements are represented within these maps as black dots and rectangles of slightly different size (see legend of Fig. 2). A combination of feature recognition and image processing algorithms allowed for the extraction of these objects. Figure 2 shows the working

step results for a cut-out of the study area, where mining symbols printed in the same colour as the village dots hampered the extraction procedure.

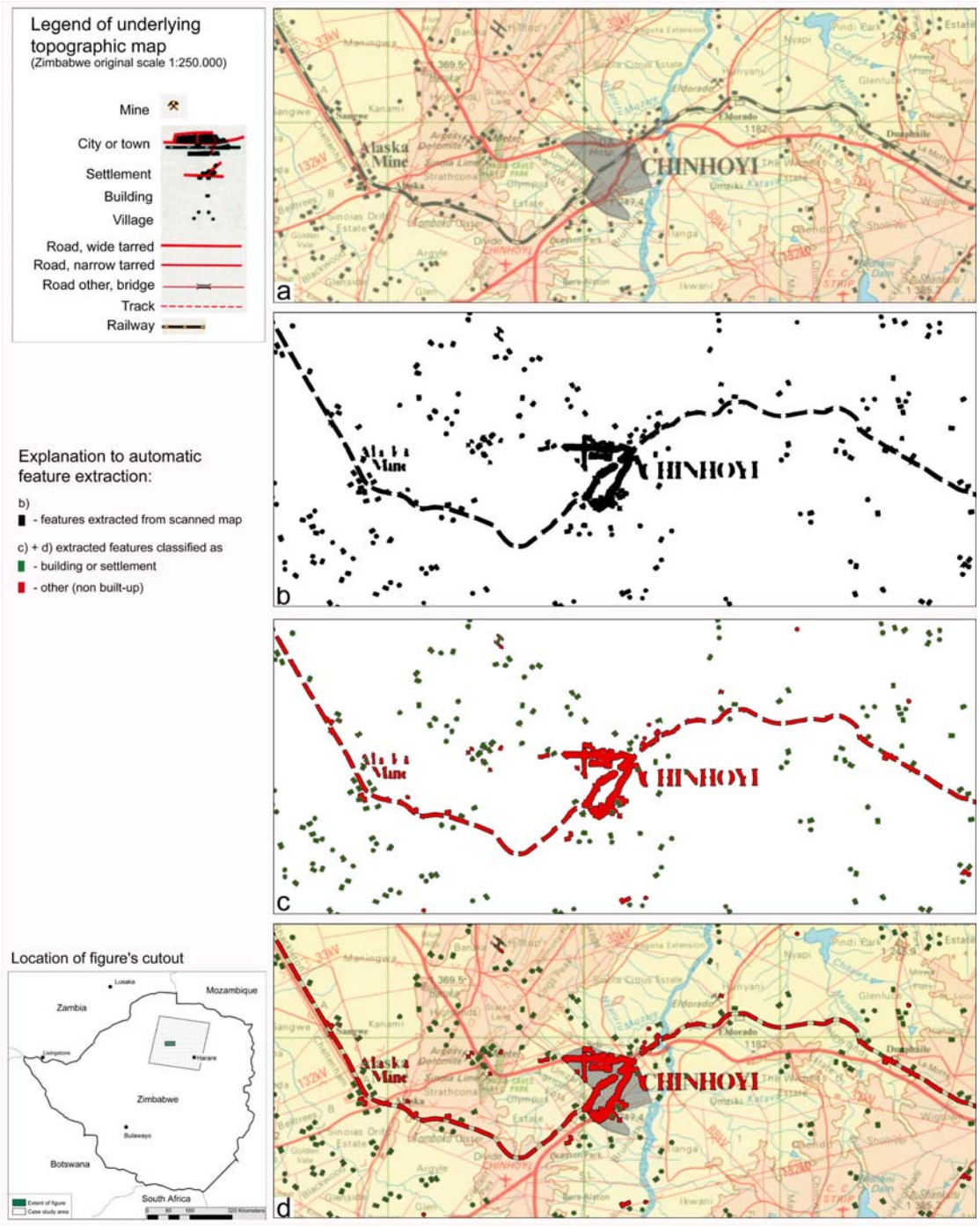

Fig. 2: Processing stages of the extraction of human settlements from scanned maps
a: Original scanned map (top),
b: Features extracted from the map (second from top)
c: Classification of extracted features (second from bottom)
d: Classified extracted features superimposed on the original map (bottom)
(source: Schneiderbauer 2007).

Figure 2 a represents the scan of the original map. In a first process step black features of a defined size were identified within the scanned maps by applying the mathematical morphological methods of erosion and dilation, resulting in the production of a binary file (Fig. 2b). Following, the erroneously selected objects, such as fragments of black labelling, were separated based on their shape and shape / size combinations (Fig 2c). Figure 2d shows

the final result superimposed on the original scanned map. This extraction process resulted in the identification of 6823 settlements within the whole study area.

Processing satellite imagery

Two Landsat ETM scenes were used in the scope of this work. The dry season image (Aug 03, 2002) was processed for the classification process, whilst the scene recorded at the end of the wet season (May 02, 2003) was selected for validation purposes. Four major land use classes were produced that included intensive small scale farming on communal land, large scale commercial farming, woodland, and land unsuitable for population. The classification process used object oriented image analysis tools available in the software package e-cognition of the company Definiens. The classification process was based on data from the Landsat ETM multi spectral band with 30m and the panchromatic band 8 at 15m resolution (Fig. 3a). The NDVI calculated from the TM band 4 and TM band 3 was used as an additional band. The image was first segmented at two different levels. The first level was used to identify relatively small objects of similar spectral characteristics such as large fields in commercial farm areas (Fig. 3b). Typical feature characteristics for object differentiation are shape, mean reflection values in a certain band or their standard deviations. The second segmentation level was used to identify larger regions with similar general land cover patterns (Fig. 3c). Each object at this level included a number of sub-objects stemming from the first segmentation level. The differentiation process at level 2 is predominantly based on the type and characteristics of the sub-objects included, combined with the sum of the area covered by sub-objects of the same class. The classification procedure required frequent verification and supervision supported by the Landsat image of the wet season and the woody classification map. 23 land cover classes based on segmentation level 1 were identified, which were converted into eight land use classes derived from segmentation level 2. For integration into the model these eight classes needed to be aggregated resulting in four final land use types (Fig. 3d).

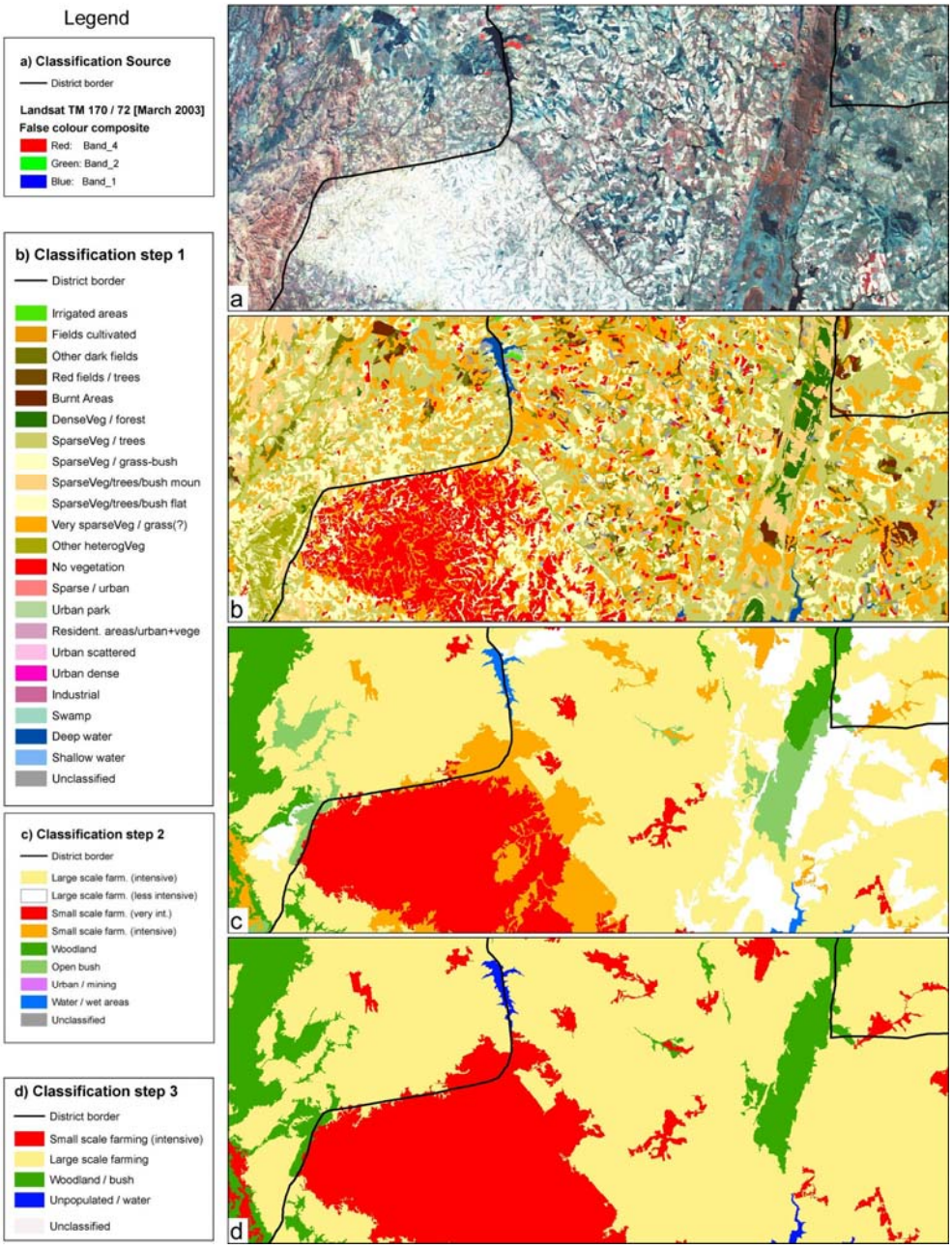

Fig. 3: Landsat imagery classification, extract of study area including commercial farms and communal land
a: Original Landsat image,
b: Level 1 segmentation resulting in 23 classes
c: Level 2 segmentation and aggregation of level 1 into eight classes
d: Aggregation of classification results into four classes for integration into the model
(source: Schneiderbauer 2007).

The results of the satellite image classification are very satisfactory. The spatial and spectral resolution of the TM Landsat scenes is sufficient for a division into main land cover classes. The quality of the analysis was significantly increased by the additional available scene and geo-datasets. The allocation of land use classes to classified groups of pixels relied on local and expert knowledge in particular regarding the main variances in population densities that exist between intensive small scale subsistence agriculture, large scale commercial farming, bush and woodland, and non-populated areas.

Geo-processing

Geo-processing consisted of geometric correction and in some cases merging the input layers into information layers to be used in the smart interpolation modelling exercise. Four final input layers were derived comprising land use, human settlements, road network, and slope classes.

Land use

The classification of different land use types is based on medium resolution satellite imagery (Landsat ETM) of the dry season in 2002, enhanced by ancillary information stemming from medium satellite imagery from the end of the wet season in 2003 (Landsat ETM), a woody cover map from 1998 and the GLC200023. The classification of the study area resulted in four main rural land use classes, each accounting for a specific average population density:

1. intensive subsistence small scale farming, which is the predominant use of communal land,
2. large scale commercial farming,
3. bush and woodland not (recently) used for agricultural purposes and
4. areas not suitable for human settlements.

Human settlements

The human settlements layer merged information from three data sources that have been allocated to four hierarchy levels:

1. A polygon vector file - that includes the eight most important Zimbabwean urban areas. This layer provided information on the urban extent of the cities Harare and Chitungwiza for the study area, classified as hierarchy level 1.
2. The settlements from the Digital Chart of the World (DCW), coded as point information and classified as level 2 when large or district capitals (only two present in the study area) and
3. coded as level 3 when towns.
4. Smaller settlements, typically villages that were not available from DCW, were derived from the 1:250,000 topographic maps and coded as level 4.

The settlements available as single pixel (level 2, 3 and 4) were buffered to produce an associated area corresponding in size to the relevant hierarchical level. Towns of level 2 were buffered with a 1500m radius, those of level 3 with 600m and the villages extracted from the map with 100m.

Road Network

Information on the road network is based on a dataset from the Humanitarian Information Centre of the UN in Zimbabwe, last updated in 2002. The roads were classified into two groups, primary and secondary roads. The class allocation was carried out by considering tarmac quality, which is included in the dataset, and level of road traffic. All roads missing

[23] Global Land Cover 2000 database. European Commission, Joint Research Centre, 2003, http://www.gvm.jrc.it/glc2000 based on SPOT VEGETATION satellite images

attribute information were classified as secondary roads. The primary and secondary roads were buffered by 300m and 150m respectively, based on the assumption that population density close to roads increases and the extension of the concerned area is correlated with road importance.

Slope

Slope information was calculated from the SRTM elevation dataset. This dataset is produced at 90 m resolution. For this study the CGIAR-CSI (Consortium for Spatial Information) SRTM data product was used on which a number of processing steps have been applied in order to represent the elevation values as continuous surfaces. The SRTM dataset served as the foundation for computing the slope, based on a 3 by 3 neighbourhood around each pixel. The results were divided into three classes of slopes with < 10 degree, 10 – 20 degree and > 20 degree. The resulting land use classification was available at 15m grid cells, corresponding to the resolution of 15m of the panchromatic band 8 of the Landsat ETM scene.

Smart interpolation

Modelling of the population density was carried out by allocating weighting factors to the pixels of each input layer by using GIS technology, according to a number of decision rules. The process of weight allocation is summarised in the decision tree diagram of figure 4. The first rule relies on the land use class input layers. The weight 0 was allocated to all pixels within the land cover class representing areas unsuitable for hosting populations. All other pixels, unless they are in the vicinity of the buffered areas of roads or human settlements, were allocated weight 1 for bush and woodland, weight 2 for large scale farming and weight 8 for small scale intensive farming (see Fig. 4).

In the second decision step, weighting values for all pixels lying within the defined vicinity of roads and human settlements were assigned. If the pixel was close to transport infrastructure, then it obtained the weight 5 or 20 respectively, according to whether the transport line crossed a wooded area or farm land. The weighting values allocated to pixels within or close to settlements depend on the hierarchy class of the settlement. Pixels associated with class 2 (small cities) and class 3 (towns) received a weighting of 60, while those related to class 1 (villages) received a weighting of 20[24]. All weights allocated to pixels concerning their vicinity to a road network and human settlements were overlaid and summed up.

The last decision rule took into account the interrelation between population density and terrain. It has been applied to all pixels lying within areas of a certain degree of slope. If the slope value is between 10 and 20 degrees the pixel weighting value was halved. If the slope was steeper than 20 degrees then it was halved again. After giving consideration to the degree of slope, each pixel received its final weighting value. For example, a pixel lying within the land use class ‘large scale farming’ in the vicinity of a road and close to a village, located on a slope of 13 degrees, would have received the value: (20 + 20) / 2 = 20.

Following this allocation procedure, the population counts at district level available from the Zimbabwean Census of 2002 were distributed according to the weighting value pw of each pixel according to Equation 1.

$$pop\ (i,j)\ [D] = a_D * pw\ (i,j) \qquad \text{(Equation 1)}$$

[24] Large cities corresponding to human settlements class 1 obtain a unique population density value that is based on the average population of the entire city. Population density estimations within cities require a different model.

In Equation 1 pop(i,j) [D] is the number of estimated people living within the area of pixel (i,j) that is lying within district D, aD is a constant, computed for district D, and pw (i,j) is the weighting factor of pixel (i,j) received from the model (**Error! Reference source not found.**). The constant aD is computed by dividing the overall population number of district D by the sum of the weighting values of all pixels within district (Equation 2).

$$a_D = \frac{pop\,[D]}{\sum \{pw(i,j)\ \forall\ (i,j) \in [D]\}} \qquad \text{(Equation 2)}$$

In Equation 2 pop [D] is the census population of district D and pw (i,j) is the weighting value of pixel (i,j). Hence, the sum of the estimated population values for all pixels within a district area is equal to the census value of the same district. For those districts of which only part of the area is overlapping with the study area the population figure considered in the model (pop [D]) was computed according to the proportion of the area lying within the study area, assuming a homogeneous population distribution.

Following the modelling process, the pixels were aggregated to a raster layer with 150m resolution. A lowpass filter was applied to smooth differences between adjacent pixel values.

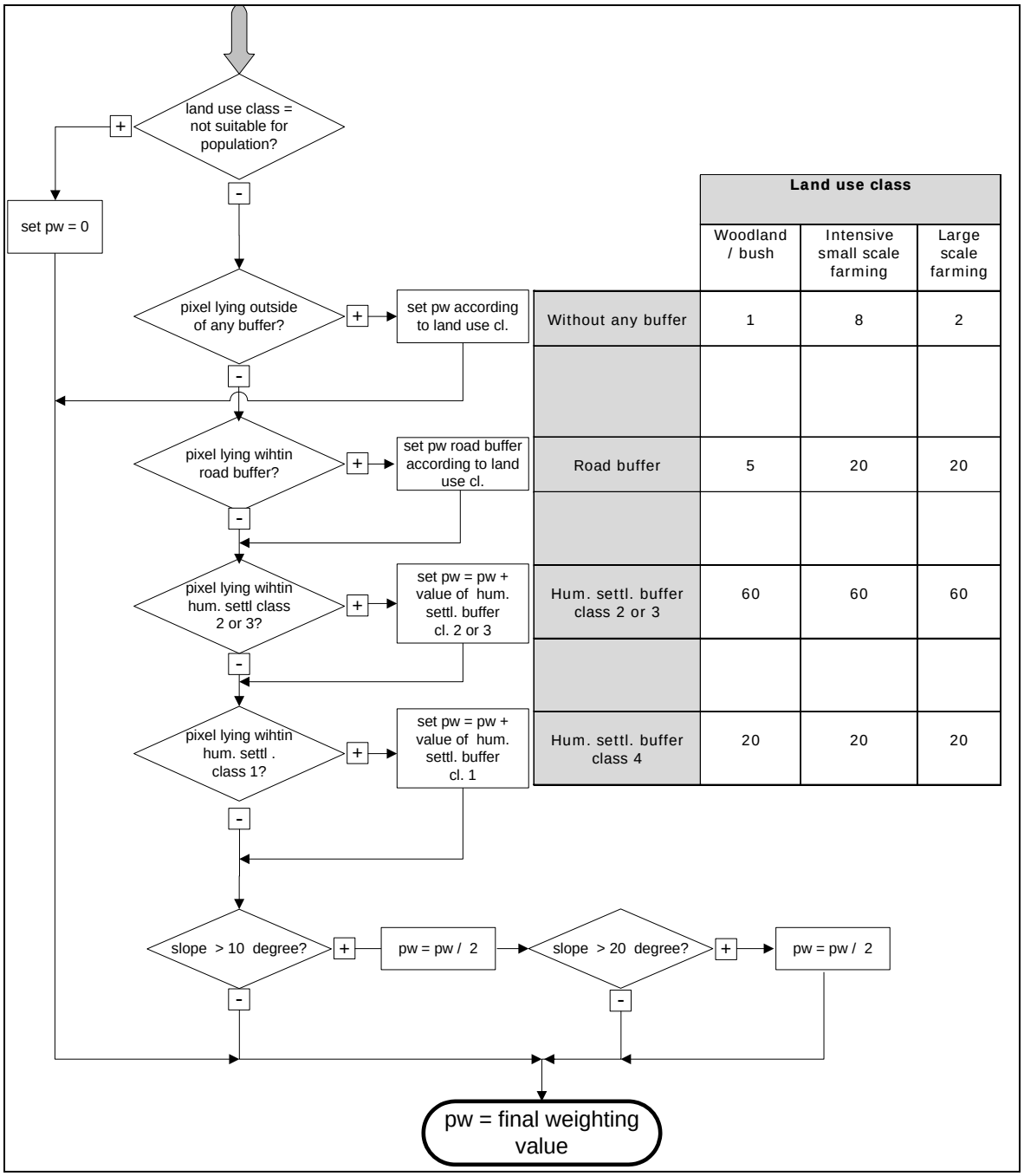

Fig: 4: Decision tree diagram used to assign weighting values to pixels (pw), (source: Schneiderbauer & Ehrlich 2005).

Results and Discussion

The resulting population density estimation for a part of the study area is shown in Figure 5 as original dataset and after lowpass filtering. The figure also shows the equivalent area as a choropleth map representing population counts at district level, and as the Landscan 2002 population dataset. Pixel in yellow represent low and red pixel represent high population densities values. The figure highlights the advantage of having population densities in grid format and at finer resolution. The choropleth map provides single counts for large areas, thus averaging areas with high and low population densities. Landscan inevitably provides coarse results. The outcome of the population modelling exercise at the fine resolution of 150 m

reflects typical population density patterns in Zimbabwe, for example communal land with high densities and commercial farm land with low population densities.

Combining different sources of input data to provide weighting for population assessment is an empirical and error prone exercise. The input datasets are of different quality and the errors accumulate when merging the dataset. Errors introduced into the model applied for this study can be linked with a number of sources. First, the location accuracy of human settlements within the DCW is probably low. The DCW are in fact derived from 1:1,000,000 maps. The quality of the topographic maps and the density of mapped villages vary with different years that they have been updated. The automatic dot detection allows for false hits and inevitably misses some villages. The location of some villages may also have changed since the production of the map.

Medium resolution Landsat imagery provides valuable information to identify land cover. The pixel size is in general sufficiently small for distinction to be made between fragmented communal land used intensively by subsistence agriculture and large scale commercial farm areas. The combination of satellite images recorded during dry and wet seasons assists in the identification of irrigation schemes and regions with little vegetation, thus accounting for areas with the likelihood of high population pressure.

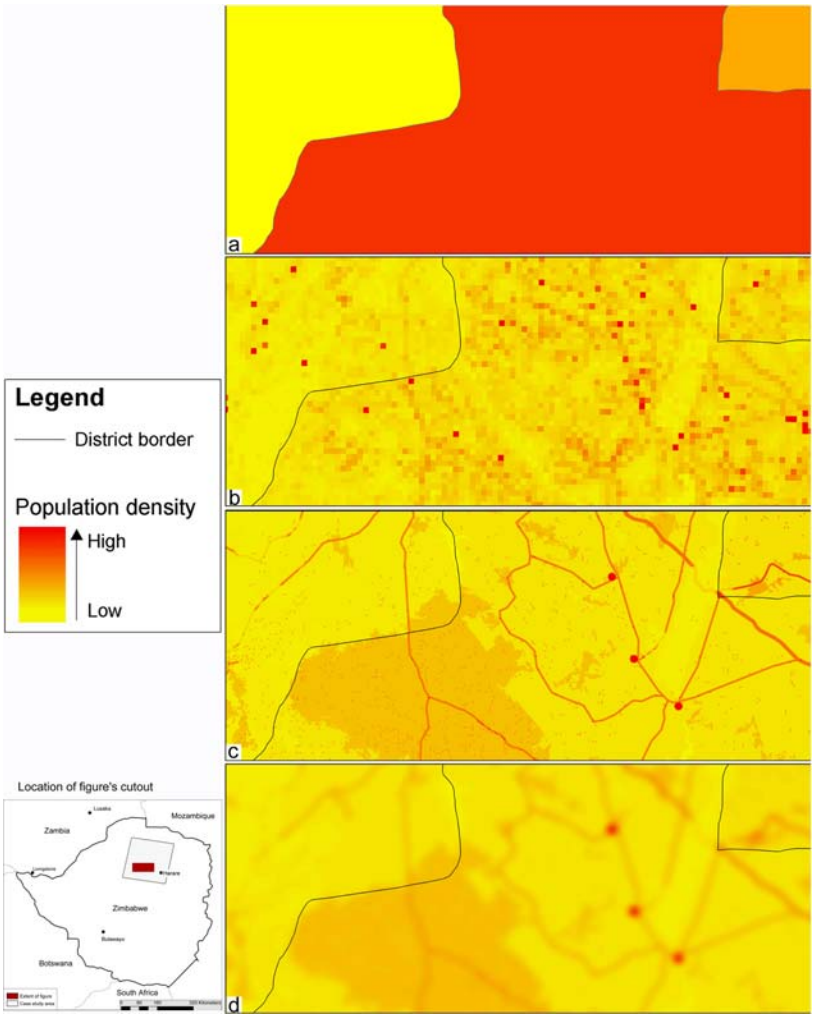

Fig. 5: Results of population density model in comparison with other population data
a: Population distribution as choropleth map (top, source: Zimbabwe census data)
b: Population density as grid with 1 km resolution (second from top, source: Landscan)
c: Modelling result of this study with 150m grid resolution (second from bottom)
d: same as c but after lowpass filtering (c and d source: Schneiderbauer & Ehrlich 2005).

The object oriented classification procedure proved effective and efficient in processing large datasets, such as a full Landsat ETM scene. The image segmentation at two different levels as a base for a land use classification of eight classes proved to be most appropriate and allowed a clear discrimination of the main Zimbabwean land use systems.

Additionally the ETM imagery with a 15m panchromatic band can be used to identify the spatial outline of larger towns. Densities within urban areas will have to be addressed with very high resolution imagery.

The global availability of the Landsat imagery makes it a unique dataset for use in population density studies in developing countries. In moist tropics however, the use of active sensors has to be considered in order to solve the problem of permanent cloud coverage.

The availability of a 90 meter resolution digital elevation model is critical for at least two reasons. It allows computation of the slope gradient, which is strongly correlated with population densities, and thus identifies areas that are not suitable for hosting any population. Also, population density may vary with the elevation. For example, in Zimbabwe, the highlands are favoured areas of settlement due to climate and geological conditions.

Finally, the selection of weighting factors allocated in the modelling process is based on subjective local and expert knowledge. The modelling result, the final population density estimation, remains very difficult to evaluate. Research findings related to the creation of continuous population surfaces in developed countries are often cross-checked with small enumeration units (Langford et al. 1991; Eicher & Brewer 2001). In Zimbabwe, population data for the smallest administrative unit, the 'ward', are available but they are often incorrect and the ward borders are continuously being changed for political reasons. An alternative method of evaluation could be to get the census' population counts before the data are aggregated into administrative units. This would require the cooperation of the relevant statistical institution and their willingness to provide the data for research purposes.

In most developing countries recent data about land use, infrastructure and population at fine scale are poor. The method applied for this study is a relatively quick way to extract information from and add value to datasets that are normally also available for developing countries. The methodology elaborated and the tools implemented are therefore of general importance for population density estimations at fine resolution in those countries. The results can feed into early warning or alert systems and support decision making in order to enhance disaster management and humanitarian aid activities. Finally, land use information and population data can also be linked to vulnerability and food insecurity. Therefore, mapping land use and population data is essential in order to come up with needs assessments in the case of drought or other disasters.

However, population distributions are determined by physical, socio-economic and historical factors that are country specific. Therefore, in order to be transferred to other countries, the modelling procedure needs to be adapted to case-specific characteristics, the determination of which requires a certain level of local / expert knowledge. In addition, passive sensors might not provide sufficient cloud free satellite data for regions lying within the moist tropics.

Comments regarding potential future activities

A centralised global data base could serve as stock for the latest available population census data at provincial or district level. The pre-requirements for this compilation is the agreement on a spatial datasets of administrative boarders of the respective administrative level to which the population data can be allocated.

Following a bottom-up approach, evolving GIS technology and new EO sensors (passive and in particular active sensors) could be exploited for the generation of worldwide population datasets. This activity requires a generic and widely accepted standard of modelling population distribution in grid layers of fine resolution.

For hot spot areas with a high potential of future critical events population distribution datasets of best possible accuracy and spatial resolution could be generated based on the here proposed methodology BEFORE an event occurs. In an evolving crisis situation these datasets could immediately be made available for decision-making of humanitarian and political relevance (for example this could have been possible and would have been very useful in the Darfur region of the Rep. of Sudan).

References

Adeniyi PO (1983) An Aerial Photographic Method for Estimating Urban Population. Photogrammetric Engineering and Remote Sensing 49: 545-560

Chen K (2002) An approach to linking remotely sensed data and areal census data. International Journal of Remote Sensing 23: 37-48

Deichmann U (1996) A review of spatial population database design and modeling. Technical Report 96-3. National Center for Geographic Information and Analysis, Santa Barbara, USA

Eicher CL, Brewer CA (2001) Dasymetric Mapping and Areal Interpolation: Implementation and Evaluation. Cartography and Geographic Information Science 28: 125-138

Elvidge CK, Baugh E, Kihn H, Kroehl ED, Davis C (1997) Relation between satellite observed visible-near infrared emissions, population, economic activity and electric power consumption. International Journal of Remote Sensing 18: 1373-1379

Giada S, De Groeve T, Ehrlich D, Soille P (2003a) Information extraction from very high resolution satellite imagery over the Lukole refugee camp, Tanzania. International Journal of Remote Sensing 24: 4251-4266

Giada S, De Groeve T, Ehrlich D, Soille P (2003b) Can satellite images provide useful information on refugee camps? International Journal of Remote Sensing 24: 4249-4250.

Harvey JT (2002) Estimating census district populations from satellite imagery: some approaches and limitations. International Journal of Remote Sensing 23: 2071-2095

Holloway SR, Schumacher J, Redmond RL (1999) People and Place: Dasymetric Mapping Using ARC/INFO. In: Morain S (ed) GIS Solutions in Natural Resource Management, Onword Press, Santa Fe, New Mexico, pp 283-291

Langford M, Maguire D, Unwin DJ (1991) The areal interpolation problem: estimating population using remote sensing in a GIS framework. In: Masser I, Blakemore M. (eds) Handling Geographical Information: Methodology and Potential Applications, Longman, New York, pp 55-77

Langford M, Unwin DJ (1994) Generating and mapping population density surfaces within a geographical information system. Cartographic Journal 31 (1) :21-6

Liu, X (2004) Dasymetric mapping with image texture. In: *Proceedings of the ASPRS 2004 Annual Conference*, Denver, USA. May 23-28.

Lo CP (2003) Zone-based estimation of population and housing units from satellite-generated land use/land cover maps. In: Mesev V (ed) Remotely Sensed Cities, Taylor & Francis, London, pp 157-180

Mennis J (2003) Generating Surface Models of Population Using Dasymetric Mapping. The Professional Geographer 55: 31-42

Mesev V (2003) Remotely Sensed Cities (ed), Taylor & Francis, London, pp 372

Mugnier C (2003): Grids and Datums, Republic of Zimbabwe. In: Photogrammetric Engineering and Remote Sensing 69, pp 1206-1207

Olorunfemi JF (1984) Land Use and Population: A Linking Model. Photogrammetric Engineering and Remote Sensing 50, pp 221-227

Schneiderbauer S (2007) Risk and Vulnerability to Natural Disasters – from Broad View to Focused Perspective. Theoretical background and applied methods for the identification of the most endangered populations in two case studies at different scales. Ph.D. dissertation, Free University Berlin, Berlin

Schneiderbauer S, Ehrlich D (2005) Population density estimations for disaster management. Case study rural Zimbabwe. In: van Oosterom P, Zlatanova S, Fendel E M (Eds.) Geo-information for Disaster Management. Proc. of the 1st International Symposium on Geo-information for Disaster Management', Delft, The Netherlands, March 21-23, 2005. Springer, 901-922.

Sutton P, Roberts D, Elvidge C, Meij H (1997) A Comparison of Nighttime Satellite Imagery and Population Density for the Continental United States. Photogrammetric Engineering and Remote Sensing 63, pp 1303-1313

Sutton P, Elvidge C, Obremski T (2003) Building and evaluating models to estimate ambient population density. Photogrammetric Engineering and Remote Sensing 69, pp 545-553

Tobler W, Deichmann U, Gottsegen J, Maloy K (1995) The global demography project, Technical Report TR-95-6, National Center for Geographic Information and Analysis, Santa Barbara

Vallin, J (1992) La population mondiale. La Decouverte, Paris

Vincent V, Thomas RG (1960) An agricultural survey of Southern Rhodesia: Part I: agro-ecological survey. Government Printer, Salisbury

Xiaohang L (2004) Dasymetric mapping with image texture. In: Proceedings of the ASP R S 2004 Annual Conference, Denver, USA, pp 23-28

Post-conflict urban reconstruction assessment using image morphological profile on 1-m-resolution satellite data in a fuzzy possibilistic approach

Application: Koidu, Sierra Leone, Africa

Elodie Pagot* & Martino Pesaresi

European Commission, Joint Research Centre, Institute for the Protection and Security of the Citizen (IPSC), Support to External Security Unit, Ispra 21027 (VA), Italy

* elodie.pagot@jrc.it

Abstract

The state of built-up features after their destruction as well as the process of their rehabilitation are assessed through the analysis of conflict and post-conflict very high spatial resolution Ikonos images. The automatic recognition procedure is based on a priori fuzzy rules formalized using two basic information derived from satellite data: structural information extracted by the derivative of the morphological profile (DMP) on the panchromatic data, and presence of vegetation derived from the multi-spectral data. The procedure is validated using a per-pixel and per-region image understanding approach.

1 Introduction

Post-war rehabilitation is one of the most important aspects for building and establishing sustainable security as well as restoring normal life in a post-conflict area. Within this context, remote sensing with earth observation satellites is of particular interest to study the anthropogenic changes engendered by a conflict. Population movements, building and infrastructure changes, environment modification can be retraced from the analysis of image time series and help in assessing the population impact and vulnerability as well as supporting the monitoring of the peace making and peace keeping operations in the area.

A variety of change detection techniques have been developed for satellite and airborne imagery including arithmetic operations, methods relying on statistical analysis as well as post-classification comparison and multitemporal classification. Nevertheless, automatic or semi-automatic classification approaches from multi-temporal satellite imagery providing accurate urban change detection remain an important challenge for the remote sensing community, especially when very high spatial resolution (VHSR) imagery is required in order to identify small scale target changes, such as those observed at the human settlement scale or beyond. Despite the advantages of the improved spatial resolution, the main difficulties arise from the different image acquisition conditions: different illumination angles and shadow formation may cause the apparition of false signal or disappearance of real changes. Moreover, the parallax displacement associated with the off-nadir angles, the lack of precise Ground Control Points (GCPs) and validated Digital Terrain Models (DTM) for an accurate orthorectification lead to unavoidable geometric distortions and the resulting misregistration of the data might be critical for change detection.

In urban areas, most of the built-up structures can be discriminated according to their shape and size. Therefore, to overcome the limitations due to radiometric changes and improve the classification results, additional information revealing the geometry of the feature and its

contrast with respect to its neighborhood should be incorporated in the study. One way to extract the structural information an image can be achieved using mathematical derived operators. Most particularly, granulometric and anti-granulometric operations (Hass and Matheron, 1967; Matheron, 1975; Serra, 1972) obtained from geodesic opening and closing filters with increasing structuring element (SE) sizes are applied to generate the multi-scale characteristics or morphological profile (Salembier and Serra, 1995; Meyer, 1997).

1.1 Derivative of the Morphological Profile in remote sensing applications

The use of advanced morphological operators in the frame of satellite remote sensing applications is described in a survey paper by Soille and Pesaresi (2002). The notion of image morphological profile (MP) extracted using gray-scale granulometries and anti-granulometries by reconstruction was introduced in remote sensing image processing for the classification of urban areas by Pesaresi and Kanellopoulos (1999). It was further developed in Pesaresi and Benediktsson (2001) with the idea to use the derivative of the morphological profile (DMP) to capture the morphological characteristics of the image, defined as the positions of the DMPs maxima, and label the regions with the same morphological characteristics in order to obtain image segmentation tasks.

In Pesaresi and Kanellopoulos, 1999, the morphologically-segmented image was classified in a neural network architecture with different input options including spectral, morphological, and shape-derived features. In this experiment, the use of morphological features as input gave better performance. Benediktsson *et al* 2003, demonstrated the interest of using directly the DMP as input of a neural network classification, without image segmentation step, for automatic recognition of urban areas in a 1-m resolution Ikonos scene. Plaza *et al*, 2004 proposed extended morphological transformations of hyper-spectral datasets to discriminate between subtle different ground covers in the classification of agricultural and urban areas, and recently, Chanussot *et al*, 2006 addressed the classification of urban areas using the fuzzy interpretation of the DMP extracted from a panchromatic Ikonos image.

1.2 Problem setting and chosen approach

This study concerns the Koidu village in the Kono district of Sierra Leone, impacted by 11-years civil war. Our approach consists of using satellite data as a source for monitoring the after-war reconstruction process four years after the events by using a bi-temporal Ikonos dataset. One scene was acquired the 23rd of April 2002 (time t_0) immediately after the conflict period, the other scene dates from the 28th of December 2005 (time t_1), during the stability phase. Each scene consists of a 1-m spatial resolution panchromatic image and four 4-m resolution multi-spectral images. The kind of destruction we are interested in is associated with built-up structures that were attacked and burnt down by hostile forces. As shown in figure 1, impacted built-up structures are those without roof and characterized by their remaining walls and debris on the ground. These built-up structures are mostly residential, low-rise buildings, hosting one of two families and having a typical size in plant of 15x15 meters. In our approach, we focused on two types of change and no change situations, with as objective the estimation of the number of built-up structures destroyed by the conflict at time t_0 and later rebuilt at time t_1 (class “Rebuilt”), and the number of built-up structures destroyed at time t_0 and remaining in the same state at time t_1 (class “Still Destroyed”).

This bi-temporal analysis was addressed in a fuzzy multi-criteria approach using structural information extracted from the image morphological profile derivative. Indeed, the detection and analysis of built-up areas can only be solved effectively by a multiple image classification approach, taking into account different image descriptors or sensors (Gamba *et al*, 2003).

Moreover, advanced grey-level morphological analysis of remotely-sensed data is an interesting technique to improve the standard earth observation image processing toolbox (Soille, 2003). Finally, a fuzzy multi-criteria approach was adopted since it demonstrated its robustness in modeling similar complex problems such as those involving VHSR satellite data and built-up damage assessment (Pesaresi *et al*, 2007).

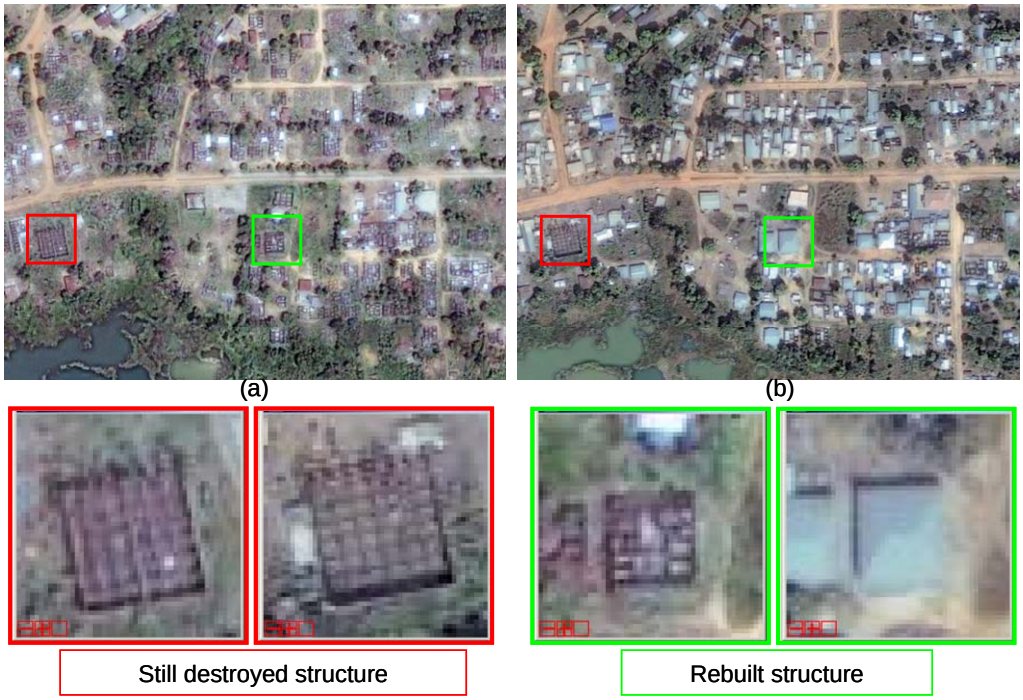

Fig. 1: Examples of the two "Still destroyed" and "Rebuilt" structures on 1-m resolution pansharpened images. The data were acquired immediately after the conflict at time t_0 (a) and four years later at time t_1 (b). The subset area represents 524×386 pixels.

In the following, we describe our methodology which has been applied on a representative study area of 3.0×3.3 km.

2 Experimental details

The procedure is based on a reduced set of fuzzy possibilistic rules derived from the formalization of a priori knowledge. The rules are established on structural information extracted from the DMP of the panchromatic (Pan) data and spectral information obtained from the multi-spectral (MS) data.

2.1 Processing flow

The processing flow follows the steps listed below:

1. Ortho-rectification of image data at time t_0 and t_1
2. Sub-pixel image co-registration of data at t_1 and t_0
3. DMP extraction from the Pan channel at t_0 and t_1
4. Processing of criteria from the DMP
5. Processing of criteria from the MS channels
6. Standardization of the criteria

7. Composition of the generic built-up criteria

In absence of precision ground control points, the first two steps ensure a sub-pixel image matching level of the two datasets at time t_0 and t_1. The data were ortho-rectified using the 90 meters resolution SRTM digital elevation model (DEM), and co-registred with the so-called moment correlation combined with the hierarchical feature vector matching techniques, implemented in the RSG software by the Institute of Digital Image Processing of the Joanneum Research. A description of the methods is available in Kropatsch and Bischof (2001) and Perko (2001). The final relative displacement error between the datasets at t_0 and t_1 corresponds to 0.6 pixels (rms).

At step 3, the DMP was derived from opening and closing by reconstruction applied to the 1-m resolution panchromatic data at t_0 and t_1. The parameters used to generate the DMP were selected in order to produce a multi-purpose morphological profile with a reasonable low number of morphological layers. In particular, a quadratic increasing size by a factor of two was chosen for the morphological structuring element (SE), with four increasing steps (scales) for opening and closing series, respectively. The DMP generated in this way forms a dataset composed of eight raster layers reporting the morphological response of the darker and brighter image structures of 1, 2, 4, and 8 pixels of half width, corresponding to SE of 3×3, 5×5, 9×9, and 17×17 pixels in the discrete grid. The larger SE of the series is considered to be able to capture the response related to the largest building of the specific area.

At step 4, basic criteria related to the size and contrast of the structures are formalized using the DMPs.

At step 5, only one criterion involving the MS data is processed and is linked to the presence of vegetation. Here, a vegetation index based on the ratio between the infra-red channel and the average of the visible (red, green, blue) bands is calculated.

At step 6, the standardization of the criteria to a unit range is performed using a simple min-max histogram stretching with 1% of saturation.

At step 7, the composition of generic built-up class membership is formalized with logical operations.

2.2 Criteria definition

The criteria definition concerns the description and formalization of *a priori* knowledge or assumptions. In this particular case we have assumed a reduced set of criteria, as follows:

- A realistic example of built-up structure ranges typically between 5x5 and 15x15 meters of size inplant. It can be indifferently brighter or darker than the surrounding background in the image;
- The vegetation is absent from the roof of built-up structures;
- The destruction or damage of built-up structures produces small structures (debris and walls remaining) with a typical width of 1 to 2 meters in-plant. In this case, bright and dark small structures are typically laid out close to each other on the ground.

The above assumptions are necessary and sufficient to describe the totality of the logic embedded in the recognition system proposed here. As consequence, any image analysis problem fitting with these above mentioned assumptions can be efficiently solved using the proposed method.

2.3 Criteria formalization

The typical phases for implementing a fuzzy multicriteria system are i) a collection of measurements from regions of interest on the image data, ii) a fuzzyfication of measurements and calculation of fuzzy memberships to specific classes, iii) a composition of elaborated classes by fuzzy logic statements and iv) an output of the decision support system including eventually a de-fuzzyfication step if crispy classes are needed (Yaochu, 2003).

The measurements collected here are : a) the responses in the DMPs from the Pan data : $DMP_{\gamma}^{t=t_0,t_1}(i)$ and $DMP_{\phi}^{t=t_0,t_1}(i)$ obtained using opening γ and closing ϕ transformations by reconstruction for different image structures of half widths $i = \{\mathbf{1,2,4,8}\}$, and b) the presence of the typical reflectance associated to the vegetation and captured by means of a NDVI index, using the MS.

2.3.1 Basic fuzzy classes

The procedure uses an ontology built on nine basic fuzzy classes. In the following formulas, the standard union, intersection and complement fuzzy logical operations are calculated as maximum, minimum, and distance to 1 of the related membership functions (Zadeh, 1965)

The membership to these classes is defined below and stands for assessing the possibility of the presence of:

Very small bright image structures:

$$\mu_{bright\_vs}^{t=t_0,t_1} = f\, DMP_{\gamma}^{t=t_0,t_1}(i=1) \tag{1}$$

Very small dark image structures:

$$\mu_{dark\_vs}^{t=t_0,t_1} = f\, DMP_{\phi}^{t=t_0,t_1}(i=1) \tag{2}$$

Small bright image structures:

$$\mu_{bright\_s}^{t=t_0,t_1} = f\, DMP_{\gamma}^{t=t_0,t_1}(i=2) \tag{3}$$

Small dark structures:

$$\mu_{dark\_s}^{t=t_0,t_1} = f\, DMP_{\phi}^{t=t_0,t_1}(i=2) \tag{4}$$

Medium bright structures:

$$\mu_{bright\_m}^{t=t_0,t_1} = f\, DMP_{\gamma}^{t=t_0,t_1}(i=3) \tag{5}$$

Medium dark structures:

$$\mu_{dark\_m}^{t=t_0,t_1} = f\, DMP_{\phi}^{t=t_0,t_1}(i=3) \tag{6}$$

Large bright structures:

$$\overset{t=t_0,t_1}{\mu}_{bright\_l} = f\,\overset{t=t_0,t_1}{DMP}_{\gamma}(i=4) \tag{7}$$

Large dark structures:

$$\overset{t=t_0,t_1}{\mu}_{dark\_l} = f\,\overset{t=t_0,t_1}{DMP}_{\phi}(i=4) \tag{8}$$

Vegetation:

$$\overset{t=t_0,t_1}{\mu}_{veg} = f\left(\frac{ir-\frac{r+g+b}{3}}{ir+\frac{r+g+b}{3}}\right)^{t=t_0,t_1} \tag{9}$$

where the function *f*, which transforms the sensor measurements into standardized fuzzy class memberships, is a simple rescaling function in the range [0...1] using a linear min-max stretching method with 1% of saturation.

2.3.2 Derived fuzzy built-up classes

The membership to the class describing generic built-up structures, i.e.: "non-vegetated small, medium or large structures, either brighter or darker than the background", can be formalized as follows:

$$\overset{t=t_0,t_1}{\mu}_{built-up} = \overset{t=t_0,t_1}{\mu}_{struct} \cap \left(1 - \overset{t=t_0,t_1}{\mu}_{veg}\right) \tag{10}$$

where

$$\overset{t=t_0,t_1}{\mu}_{struct} = \bigcup_{t=t_0,t_1} \left\{ \begin{matrix} \mu_{bright\_s}, \mu_{bright\_m}, \mu_{bright\_l}, \\ \mu_{dark\_s}, \mu_{dark\_m}, \mu_{dark\_l} \end{matrix} \right\} \tag{11}$$

Furthermore, the membership function to the class describing a generic built-up structure recognized indifferently at time t_0 or time t_1 is such that:

$$\mu_{built-up} = \overset{t=t_0}{\mu}_{built-up} \cup \overset{t=t_1}{\mu}_{built-up} \tag{12}$$

In order to formalize the notion of spatial "closeness" (co-presence of very small structures dark and bright close to each other) necessary for the description of the presence of debris on the ground in destroyed dwellings, a spatial relationship function is introduced using a Gaussian low-pass transformation Π of the membership function μ. The spatial size of the Gaussian transformation is related to the notion of "closeness" that we want to formalize. In this case a 9×9 pixels kernel was used to describe the typical situation on the field.

The membership to the destroyed built-up structure class at time t is then formalized as the intersection of the spatial low-pass Gaussian transformations of the $\overset{t=t_0,t_1}{\mu}_{bright\_vs}$ and $\overset{t=t_0,t_1}{\mu}_{dark\_vs}$ membership functions.

$$\overset{t}{\mu}_{destroyed} = \bigcap_{t=t_0,t_1} \left\{ \prod \mu^{t}_{bright\_vs}, \prod \mu^{t}_{dark\_vs} \right\} \tag{13}$$

According to (12) and (13), the membership to the class describing a generic built-up structure destroyed at t_0 and rebuilt at t_1 can be expressed as the intersection between $\overset{t=t_0}{\mu}_{destroyed}$ and the inverse of the $\overset{t=t_1}{\mu}_{destroyed}$, the result being intersected with $\mu_{built-up}$ as follows:

$$\mu_{rebuilt} = \overset{t=t_0}{\mu}_{destroyed} \bigcap \left(1 - \overset{t=t_1}{\mu}_{destroyed} \right) \bigcap \mu_{built-up} \tag{14}$$

Similarly, the membership function to the class describing the generic built-up structure being destroyed at t_0 and remaining destroyed at t_1 can be expressed as:

$$\mu_{StillDestroyed} = \overset{t=t_0}{\mu}_{destroyed} \bigcap \overset{t=t_1}{\mu}_{destroyed} \bigcap \mu_{built-up} \tag{15}$$

Equations (14) and (15) express the possibilities for an area of the image to belong to the class "Rebuilt" or "StillDestroyed", with respect to the ontology and assumptions described above. The procedure is fully automatic and does not require any training and radiometric calibration of the input data. The calibration is already included in the subsequent fuzzyfication steps.

3 Results

Figure 2 shows the outputs obtained from the computation of equations (1), (2), (3), (4), and (13) on a Pan data subset of 200×200 pixels, at time t_0.

The final outputs of the procedure deriving from equations (14) and (15) are presented in figure 3, for a different subset area. Images (3.c) and (3.d) are the fuzzy membership values to the classes "StillDestroyed" and "Rebuilt" stuctures, respectively. Naturally, they are not the results of a mutually-exclusive classification but a representation of the possibility for a pixel to belong to the "StillDestroyed" and "Rebuilt" classes.

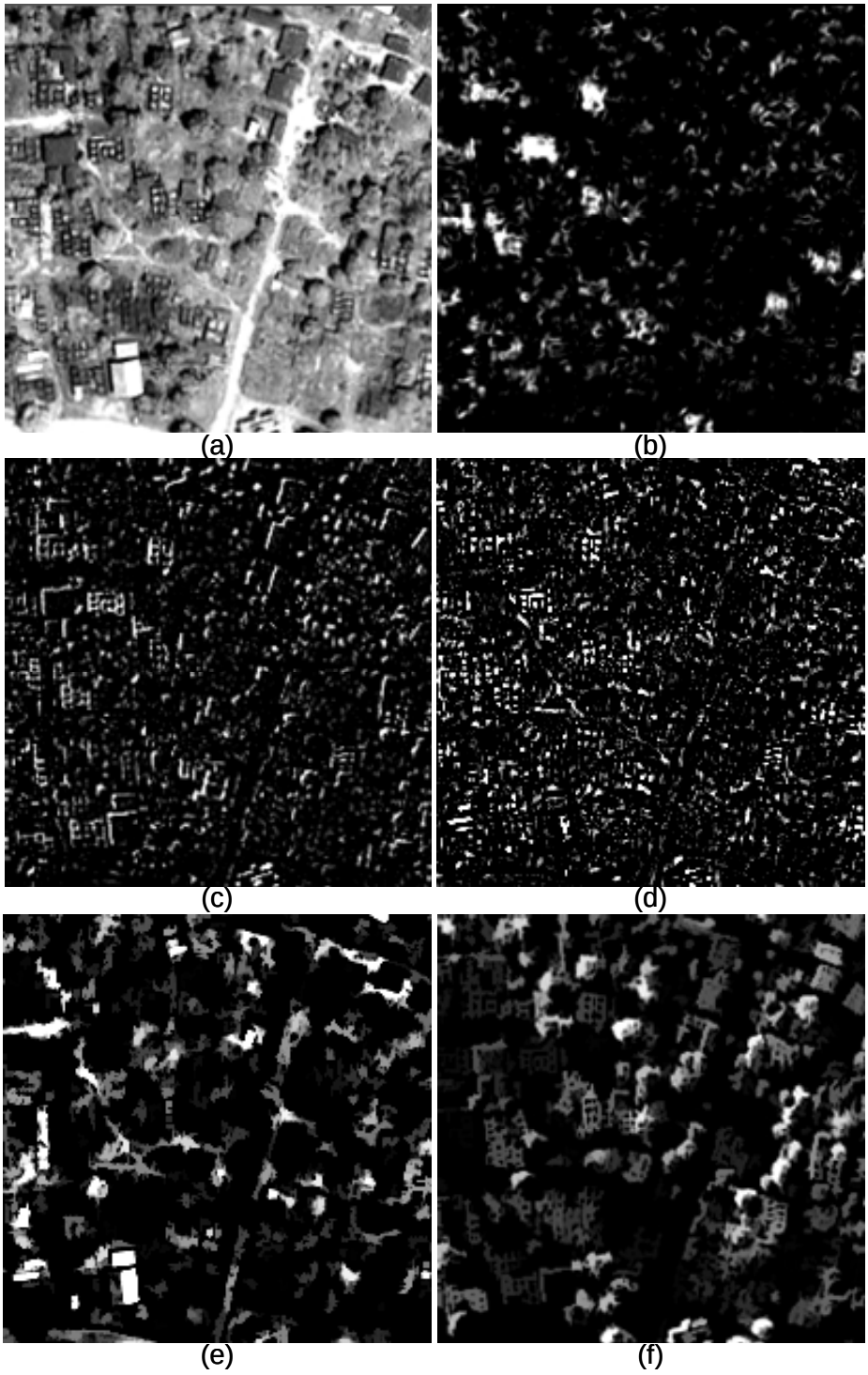

Fig. 2:. (a) Pan subset of 200x200 pixels at t_0, (b) membership to the class "destroyed" at t_0 resulting from equation (13), and memberships at t_0 linked to the presence of very small bright image structures (c), very small dark image structures (d), small bright image structures (e), small dark image structures (f) , derived from equations (1), (2), (3), and (4) respectively. The membership values are represented with a linear look-up-table from 0 (black) to 1 (white).

Consequently, the same pixel of the image belongs in a certain way to the two classes, with ideally a prevailing membership value for one class, but this is not a constraint of the procedure.

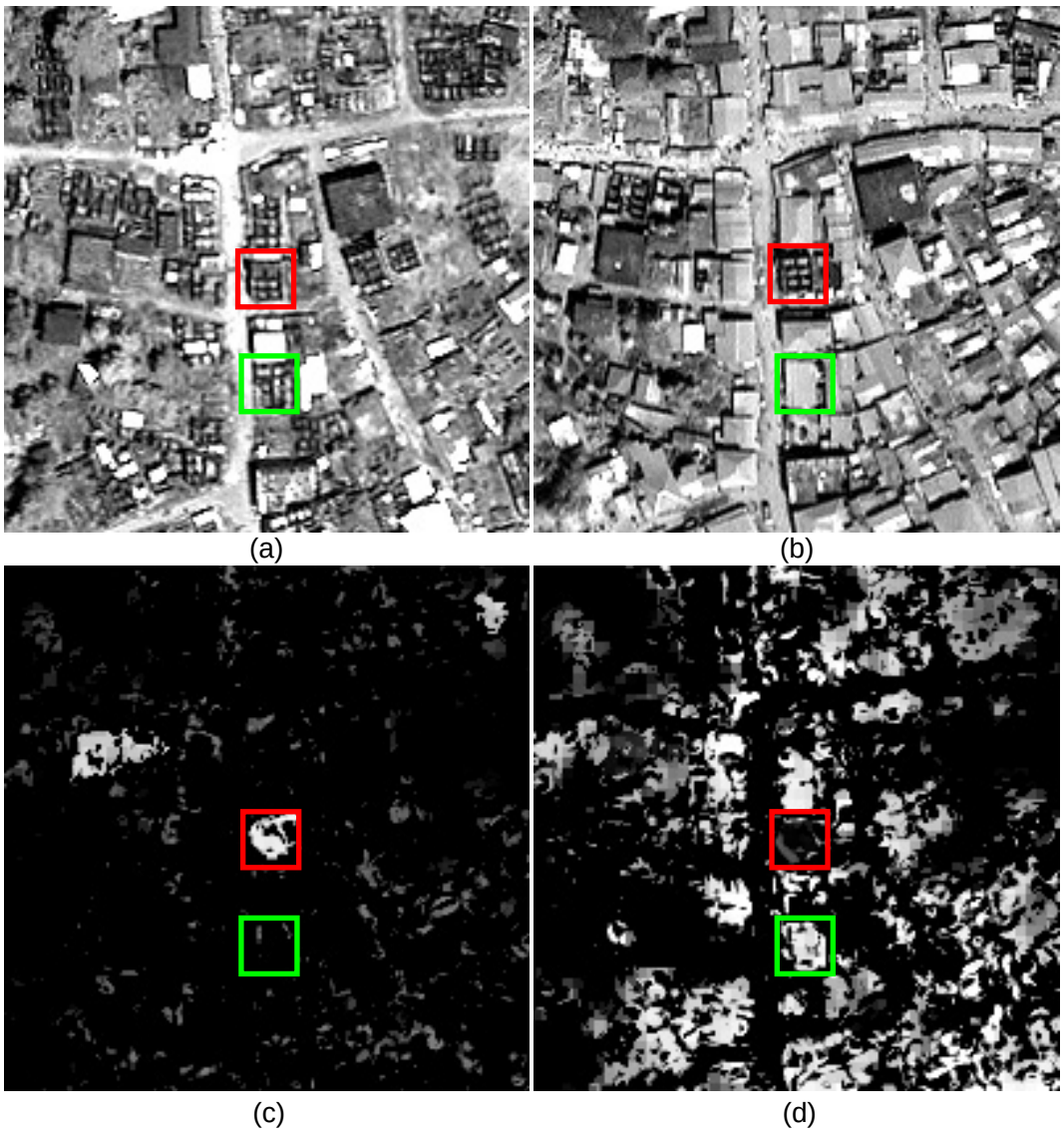

Fig. 3: Pan image subset of 200×200 pixels acquired at t_0 (a), t_1 (b) and corresponding membership values to the classes "Still Destroyed" (c) and "Rebuilt" (d). The red and green squares highlight two typical examples of the "Still Destroyed" and "Rebuilt" structures respectively. The membership values are represented with a linear look-up-table from 0 (black) to 1 (white).

The validation was realized with a total of 42 randomly-distributed region of interest (ROIs) selected in the study area. These ROIs were manually digitalized following the outline of the building plant, and classified according to human interpretation based on the available satellite imagery. They represent the built-up structure footprint of each considered class; each region contains about 200 pixels in average for a total of 7943 collected pixel samples in all the study area.

Figure 4 shows the DMP signal recorded in the 42 randomly-selected ROIs. One can a see a different behavior of the DMPs at t_0 and t_1 for the class "Rebuilt", characteristic of the *change*, whereas the DMPs behavior follows the same trend at both t_0 and t_1, emphasizing indeed *no change* for the class "StillDestroyed".

Fig. 4: DMPs signal recorded within the 42 randomly-selected ROIs labeled “Rebuilt” and “Still Destroyed” and plotted along the closing and opening series for SE of half widths 1, 2, 4 and 8 pixels respectively.

Figure 5 plots the average of the “Rebuilt” and “Still Destroyed” membership values for each ROI in the decision space defined by the two criteria (Eqs. 14 and 15). The discrimination between the two classes is here well apparent. Almost all the reference ROIs are well distant from the decision line, which discriminates between the two classes, on the basis of the prevalence of the specific membership value. Except for one ground truth, the “Rebuilt” reference ROIs are well clustered along the “Rebuilt” membership axe and far from the decision line representing equal membership values for both classes. The “Still Destroyed” reference ROIs are more scattered in the decision space: one “Still Destroyed” ROI is slightly wrongly positioned in the “Rebuilt” side of the decision space, and two others appear hazardously close to the decision line. Nevertheless, the procedure is able to discriminate with high reliability (97.5% of success rate) between “Rebuilt” and “Still Destroyed” built-up structures, with only one wrongly attributed class over 42 reference built-up structures, the assessment being done on the basis of the ROIs or connected regions of pixels belonging to the same built-up structure. In order to investigate more in-depth the quality of the procedure at the pixel level and check whether the procedure leads to contradictory outputs within the same ROI, we classified the image using a criterion of dominance, and the pixel was assigned the class with the highest membership value, with in addition the constraint of having this membership higher than a given threshold. In this case, the threshold t was set such as $t > 0$.

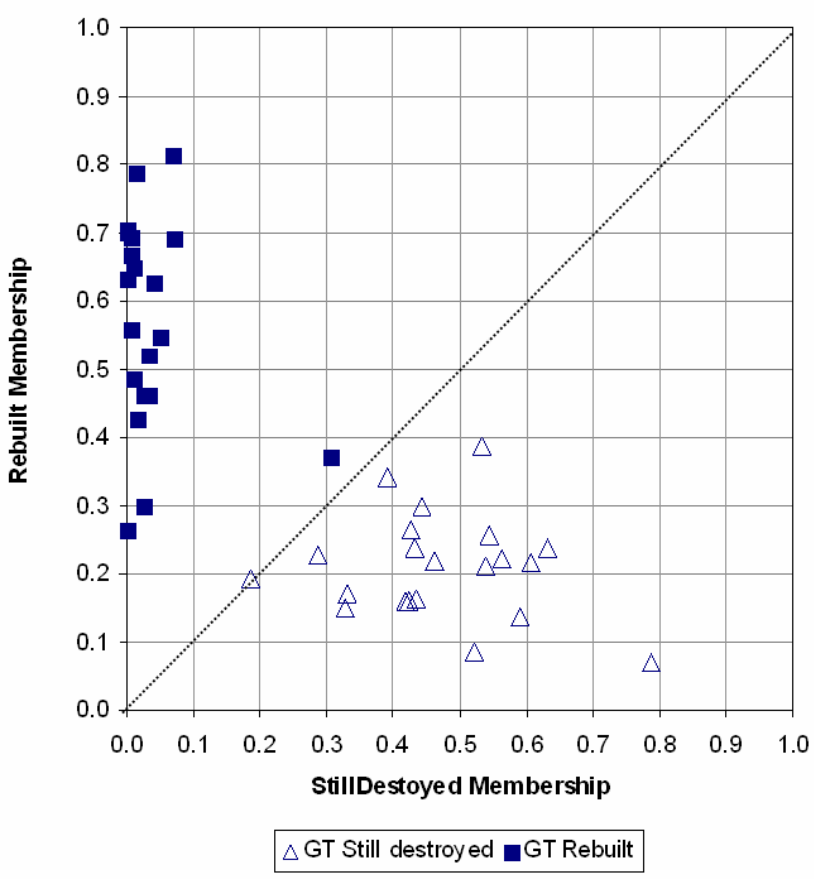

Fig. 5: Average of the membership values to the two classes "Rebuilt" and "Still Destroyed" for each of the 42 reference samples or ground truths (GT) and plotted in the decision space, defined by the two considered criteria.

The "unclassified" pixels correspond to those with both membership values equal to zero and for which the procedure gives no response. The results are shown in table 1, through a confusion matrix obtained by crossing the reference ROIs pixel-by-pixel.

The confusion matrix still shows the dominance of the correct class attribution in the reference ROIs. The producer accuracy (true / reference) is equal to 81.49% and 68.78% for the "Rebuilt" and "Still Destroyed" classes, respectively; the user accuracy (true / classified) is estimated to 85.51% and 94.56% respectively. The "Unclassified" pixels are taken into account in the producer accuracy estimation, considered as wrongly classified by the procedure. Similarly to the case of the region-based classification, the "Still Destroyed" class seems to be less well defined than the class "Rebuilt". In particular, in the pixel-based approach, 15.5% of the "Still Destroyed" reference samples have been wrongly classified as "Rebuilt" by the procedure, which is about four times more than the percentage (3.52%) of "Rebuilt" reference samples wrongly attributed the class "Still Destroyed".

Table 1: Per pixel classification confusion matrix

Classified	Reference		
	Rebuilt	***Still Destroyed***	***Total***
Unclassified	630	588	1218
Rebuilt	3424	580	4004
StillDestroyed	148	2573	2721
Total	4202	3741	7943

Moreover, it is worth mentioning that in comparison to the region-based approach, the pixel-based classification output is penalized by the indecision of the system, in presence of pixels for which both membership values to the two built-up structure classes are equal to zero. This situation does not arise in the region-based approach since the average of the membership values for all the pixels belonging to the reference region is always greater than zero.

Therefore, the region-based approach seems to be more adapted and more robust than a pixel-based classification strategy, for automatic image understanding using the proposed set of criteria.

4 Conclusion

This paper describes a procedure for automatic recognition of the state of built-up structures either rebuilt or remaining destroyed after a conflict. The procedure is based on a priori fuzzy rules formalized using two basic information derived from high spatial resolution optical satellite data: structural information extracted by the derivative of the morphological profile on the panchromatic data, and the presence of vegetation extracted from multi-spectral data. The two different kind of information are then used in a fuzzy multi-criteria approach.

This axiomatic procedure is fully automatic, it does not require any training, and the defined rules can be applied in similar problems involving the destruction/reconstruction assessment of urban areas. The procedure includes a self-calibration based on global statistics of the measurements extracted from the satellite data, and therefore does not require prior absolute radiometric calibration. Thus, it is also applicable in the case of unknown sensor model, when absolute radiometric calibration cannot be performed.

A first validation assessment shows good performance of the procedure if the criteria are used in the frame of a region-based image understanding strategy (97.5% of success rate), while a pixel-based strategy shows less overall accuracy (75.5%) due to the presence of misclassified and unclassified pixels.

The proposed procedure gives only a partial contribution to the analyses of post-conflict reconstruction dynamics on built-up areas, with the study of two specific classes. In particular, it does not assess two important classes, such as stable built-up structures that were not damaged at t_0 and remained intact at t_1, as well as new built-up structures that were not present at time t_0 and came out at time t_1. Accounting for the “Intact” class is necessary to evaluate the total destructive impact of the war on the built-up environment together with assessing the built-up stock proportion and estimate the population which might still be settled in these dwellings. The “New” class together with the “Rebuilt” class are useful to estimate the coping and reaction capacity of the local population.

The perspectives foreseen to strengthen this work are: i) the extension of the procedure for the integration of two other classes “Intact” and “New” built-up structures, ii) implementation of a

region-based image understanding approach including a specific image segmentation step, and iii) validation of the procedure on a consistent number of available satellite scenes for robustness testing.

Acknowledgement

The presented work has been supported by the institutional research activity of the Information Support for Effective and Rapid External Action (ISFEREA) of the EC Joint Research Centre, Institute for Protection of the Citizen (IPSC). We warmly thank Dr. Karlheinz Gutjahr of the Joanneum Research, Institute of Digital Image Processing, for the indispensable support in the optimization of the RSG software in the frame of knowledge shared in the Global Monitoring for Security and Stability (GMOSS) Network of Excellence.

References

Benediktsson J. A., Pesaresi M., and Arnason K., (2003) Classification and feature extraction for remote sensing images from urban areas based on morphological transformations," IEEE Trans. Geosci. Remote Sens., vol. 41, no. 9, pp. 1940–1949.

Chanussot J., Benediktsson J. A. and Fauvel M. (2006), "Classification of Remote Sensing Images From Urban Areas Using a Fuzzy Possibilistic Model", IEEE Geoscience and Remote Sensing Letters, Vol 3, No 1, pp. 40-44.

Gamba P., Benediktsson J. A., and Wilkinson G. (2003) Foreword to the special issue on urban remote sensing by satellite," IEEE Trans. Geosci.Remote Sens., vol. 41, no. 9, pp. 1903–1906.

Haas A., Matheron G., Serra J. (1967) Morphologie mathématique et granulométrie en place, Annale des Mines 11, pp. 736-753, 1967 and 12, pp. 767-782.

Kropatsch W. G., Bischof H., (2001) Digital Image Analysis. Selected Techniques and applications", Pattern recognition and image processing group, technical report, Institute of Computer Aided Automation, University of Technology, Vienna, Austria.

Matheron G. (1975), Randoms sets and integral geometry, Wiley and Sons, New York –London-Sydney.

Meyer F. (1997) Morphological connected mapping with scale space properties, Technical report, Centre Morphologie Mathématique, Fontainebleau, France.

Perko R., (2001) Correlation methods for Multi-temporal Images", Master Thesis, Institute for Computer Graphics and Vision, University of Technology, Graz (Austria).

Pesaresi M. and Kanellopoulos I. (1999) Detection of Urban Features using Morphological Based Segmentation and Very High Resolution Remotely Sensed Data, in I. Kanellopoulos, G.C. Wilkinson, T. Moons, Machine Vision and Advanced Image Processing in Remote Sensing, Berlin, pp. 271-284, Germany: Springer.

Pesaresi M., Gerhardinger A., Haag F., (2007) Rapid Damage Assessment of Built-up Structures using VHR Satellite Data in Tsunami Affected Area", International Journal of Remote Sensing, vol. 28, no 13, pp. 3013.

Plaza A., Martinez P., Perez R.M. and Plaza J. (2004) A New Approach to Mixed Pixel Classification of Hyperspectral Imagery Based on Extended Morphological Profiles, Pattern Recognition, vol. 37, no. 6, pp. 1097-1116.

Salembier P. and Serra J., (1995) Flat zones filtering, connected operators, and filters by reconstruction. IEEE Trans. Image Process. 4 (8), 1153-1160.

Serra J. (1972) Stereology and structuring elements – 3rd Int. Congress Strereology, Berne, 28-31 aug 1971, J. of Microscopy, vol 95 no.1, pp 93-103.

Soille P. (2003) Morphological Image Analysis, Principles and Applications, 2nd ed. Berlin, Germany: Springer-Verlag

Soille P. and Pesaresi M. (2002), Advances in mathematical morphology applied to geoscience and remote sensing in IEEE Transactions on Geosciences and Remote Sensing, vol. 40, pp. 2042–2055

Yaochu J. (2003), Advanced Fuzzy Systems Design and Applications, Physica-Verlag Heidelberg; 1 edition.

Zadeh L., (1965) Fuzzy sets, Inf. Control, vol. 8, pp. 338–353.

Border permeability modelling: technical specifications at global and local scale

Nathalie Stephenne* & Gunter Zeug

European Commission, Joint Research Centre, Institute for the Protection and Security of the Citizen (IPSC), Support to External Security Unit, Ispra 21027 (VA), Italy

* nathalie.stephenne@jrc.it

Abstract

Based on the concept of border permeability defined at the level of the EU25 border (Stephenne and Pesaresi 2006), this study extents the previous spatial decision support system (SDSS) framework toward a more general "accessibility" indicator that could be further used in various spatial analysis of security issues. This paper uses the permeability approach in a two scales application (continental and local): generalization and simplification of model assumption at the European level, and model focalization at fine scale using very high resolution (VHR) imagery. The technical specifications of these downscaling and upscaling applications are described.

1. Introduction

Migration is a topic of great interest to policy makers, researchers and the public. The GMOSS Border Monitoring study assessed the use of satellite imagery to monitor flows of people across national borders within the two different political and technological contexts of Europe and Africa (Stephenne et al., forthcoming). These authors introduced the use of satellite imagery in an indirect way to monitor the spatial dynamics of the population at the borders, through their integration into a conceptual model to estimate the border's geographical permeability. Due to problems regarding data quality, open source statistical databases on migration (Eurostat, OECD, UNHCR etc.) and satellite imagery, these authors concluded that existing data do not provide an appropriate tool for near-real time monitoring of land border crossings. Integration of satellite imagery products in a permeability model has then be seen by these GMOSS partners as a starting point for monitoring migratory flows in a close co-operation with border control authorities.

Based on the permeability concept extensively described by Stephenne and Pesaresi (2006), this paper extents the spatial decision support system (SDSS) framework towards a more general "accessibility" indicator that can be used in other security related spatial analysis. While the EU25 SDSS represented the geographic permeability related to a standard adult migrant having illegal behavior and deciding to cross Europe's eastern green border by foot, this application refers to the walking pattern of a standard adult without referring to a particular border.

The application of the permeability SDSS has been done at two different scales - continental and local:

- For a larger coverage, a *generalization* and simplification of model assumptions were carried out. The geographical extension for the generalized permeability model is the EU neighbouring countries. Technical settings are related to a global extent, referred in this paper as "the global approach" (Section 3.).

- For a fine scale analysis, a *focalization* using digitalized features from very high resolution (VHR) imagery (Section 4) was performed. This application refers to a section of the EU25 eastern border, the city of Uzhorod in Ukraine.

2. Background: spatial accessibility indicators

The Geographical Information Systems (GIS) provide adequate technology to integrate, combine several digital sources and perform geospatial analysis between raster and vector dataset in a common analytical system. Spatial analytical analysis are using the GIS processing in association with optimization methods of weighting different criteria in what is called a Multi-criteria decision analysis (MCE) (Geurs and vanWee, 2004). On the contrary of the simple binary techniques (good or bad), the weighted suitability models classify the layers on a relative scale and multiply each layer by its relative importance. While decision support is an important function of a GIS, only very few software provide tools especially designed for this purpose. Idrisi includes several modules that help in the construction of the multi-criteria analysis (Eastman 1993).

The potential of successful illegal border crossing can be related to the well known suitability models called accessibility indicators. GIS has been used in different disciplines(i.e. environmental researches, land use planning and transport studies) to measure the accessibility. The concept of accessibility defined as a capacity to reach/diffuse customers, services or a message, is a geographical concept that has progressively been introduced in transport planning and evaluation of projects in the 1960's and 1970's. In transport studies, the accessibility measures the situation (separation and distance) of a location in a region (Harris 2001). In the spatial analysis of population, the accessibility can be defined as the ability for interaction or contact between urban settlements throughout the neighbouring places (Deichmann, 1996), however there are a multitude of ways in which this intuitive concept has been expressed and assessed in the literature (Table 1).

Integrating criteria or spatially overlying them are two different ways to model the complexity of the reality. The integration of the geographical and spatial concept of accessibility in a decision support process deals with the complexity of representing the whole system and the difficulty to quantify the driving forces with reliable data. In the meantime, the quantitative model is a tool to simulate different scenario and alternatives proposed by decision makers.

Table 1: references of reviewed papers on accessibility measures in different disciplines

Reitsema van Eck J.R. and de Jong T.	1999	Accessibility analysis and spatial competition effects in the context of GIS-supported service location planning	Computers Environment and Urban Systems	Vol. 23 pp. 75-89
Geertman S.C.M. and Reitsema van Eck J.R.	1995	GIS and models of accessibility potential: An application in planning	International Journal of Geographical Information Systems.	9, p.67
Guagliardo M. F.	2004	Review Spatial accessibility of primary care: concepts methods and challenges	International Journal of Health Geographic	3, 1-13
Joly O.	1999	Working Group I.: Geographical Position: ''State of French art of spatial accessibility indicators''	SPESD - France	Working Paper
Lynn Mary Tischer (ed)	2001	Special Issue on Methodological Issues in Accessibility	Journal of Transportation and Statistics	Vol. 4 N°2/3

3. The global approach

A spatial decision support model is an abstraction in 2 dimensions of the reality. It allows the decision maker to study spatial alternatives representations. The reality represented in this permeability model is the suitability of walking for an average adult. The EU multi criteria model integrates earth observation and geo-spatial technologies with formal decision theory to assess the permeability, based on a presumed cost/opportunity behavioural strategy. The spatial multi-criteria analysis results depend not only on the geographical distribution of attributes, but also on the value judgments involved in the decision making process.

The multi-criteria approach is highly modular. Quite simple but also strong assumptions have been fixed at the beginning of this development process to test the permeability modeling approach. The EU25 eastern land border model calculated the permeability in cells of 1x1 kilometers size in a buffer zone of 50km on each side of the 6000 kilometers EU land border. The continental application of this EU25 model in a global context modifies the original technical settings in terms of spatial extent, resolution and projection. Not all the datasets used in the EU25 exercise are available for the global application. After selecting the input datasets, their preprocessing steps will be adapted respecting computer processing time and storage limitations. The global application has to be processed first as separated regional tiles and reassembled in a second step. Technical issues arise in terms of standardization of the extent, spatial resolution and projection.

3.1. Changes in scientific assumptions

- The spatial simulation tool is developed in order to make scenarios about the EU permeability (BP) based on the indirect use of satellite imagery in a cost function calculated on a geographical surface. The cost function is still defined by a friction surface not only along the EU land border but on the overall extent of the regional tile. The permeability is assumed to be the inverse function of the frictions.
- The first step in describing and solving any problem, such identifying the most permeable part of EU is to structure some rules that will allow a decision about which areas are most susceptible to be accessible with a definition of “easiness of walking”. The geographical permeability is not any more restricted to the illegal migrant walking across a border line but to all kind of human being in the continuous space taking decision about which areas are most suitable or not. This ease of walking has clear similarities with suitability and accessibility models.
- The green border assumption of the EU25 permeability model is released. The continental application quantifies the friction in cells of 1x1 kilometer resolution. This technical choice remains because of the availability of open-source spatial datasets and the general use of this scale to conduct analysis on global variables.
- The typology of behaviour to calculate the friction is related to a standard adult person deciding to walk on the regional space. Generally talking in the European landscape, the average walking distance to be covered by an average adult is around 6km per hour.
- Decision rules typically involve a process for the *combination of one or more criteria* (factors and constraints) into a *composite index* (Eastman et al. 1993). A criterion is some basis for a decision that can be measured and evaluated. A factor is a criterion that enhances or detracts from the suitability of a specific alternative. To be combined the different criteria must be homogenous and then pre-processed as described in the next chapter.

- GIS must have an *unambiguous and common spatial reference* of the stored information.
- GIS must have an continuous raster format.
- GIS must have an uniform range of values

- In this study, the high numbers of criteria has driven the necessary clustering of these criteria in order to increase the understanding of the model development. Three clusters has been treated separately in the EU25 permeability model, only the two first criteria (walking and hiding) have a meaning at the regional scale. The illegal and border crossing limitations are not relevant any more. Other strategies of transport are not yet developed in this version of the model. The overall friction combines these basic criteria to represent the difficulties encountered to walk throughout the region on foot. These three geographical characteristics are measured continuously from GIS layers. The overall friction is created by a multicriteria analysis.

3.2. Global extent

As a basic technical choice for the practicability of the modeling test, the permeability concept includes open-source geospatial datasets. The permeability is then measured by cells of 1x1 kilometers size because of the overwhelming use of this resolution for global grid dataset on elevation (Verdin and Greenlee, 1996), land cover (Bartholome and Belward., 2005) and population density (Tobler et al. 1995, Dobson et al. 2000). The 30-arc seconds grid cell is typical in global analysis. Based on the minimum common extension of all the input open source dataset, the extent of the global model was reduced by the pole-areas.

3.3. Projection

Due to metric distance measures modeling the behavioral patterns, a mapping projection is a necessary preprocessing step. The application cannot be conducted in a lat/long WGS 84 coordinate system. The EU tile inputs are projected with the same projection as in the EU25 eastern land border model (ETRS-LAEA).

3.4. Input datasets

The global land border model uses six datasets which are summarized in the following table. For all the vector layers the Global Discovery dataset became the only source. Finally, ERA40, Landscan 2003, Gtopo30, Glc2000 and Global Discovery were processed in the global application.

Table 2: Names of input and output files in the global application compared to the EU25 model

EU25 dataset	File names in the EU application	Global dataset
Era40	snow	Era40
Era40	tmean	Era40
Landscan2002	landscan	Landscan2003
Nightlights	night	Nightlights
Gtopo30	topo	Gtopo30
Gtopo30	topoalt	Gtopo30

GLC2000	glcwlk /glchide / glcpop/ glcwater	GLC2000
Gisco	lake	Global Discovery
GD	gdplaces	Global Discovery
GD	roads	Global Discovery
GD + Esri European map	rail	Global Discovery
gisco	river	Global Discovery
Esri European base map	tunnel	Global Discovery
GD + Esri European map	urbsprawls	Global Discovery

3.5. The processing chain for the EU tile

3.5.1. Preprocessing toward a continuous raster format (ArcGis)

The main standardization and transformation of original datasets are carried out in four general steps, respectively for the vector and the raster dataset:

- extracting the EU extent (extract by mask for the raster dataset / clip for the vector dataset) in wgs84 cartographic coordinates,
- projecting the files (project) into ETRS-1989-LAEA equal distance projection,
- defining the density (point/line/focal statistic) of objects for the vector dataset (Fig. 3) or other spatial process (i.e. slope or reclassification) for the raster ones, and
- finally transforming the files in the generic tiff-geotiff format in order to import them into Idrisi.

There are some specificities, i.e. the weather dataset provided at a monthly time period are aggregated/ averaged annually before the extraction at the EU extent. As the resolution of these dataset is 0.5 degree, the values are smoothed locally to a resolution of 1x1km. The GLC2000 dataset is reclassified in 4 different layers to be introduced in the permeability criteria.

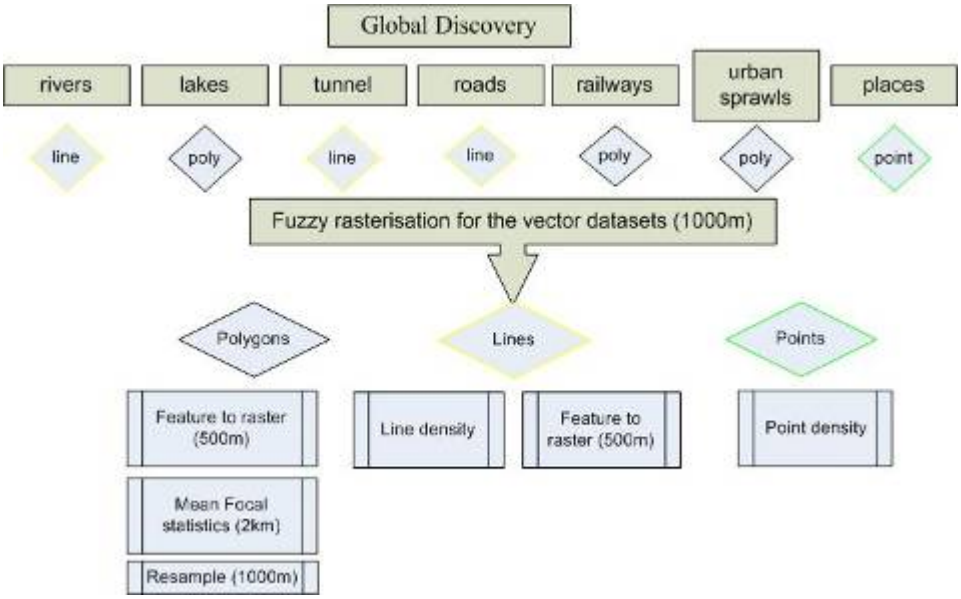

Fig. 3: Global Discovery vector files rasterisation

3.5.2. Standardization and MCE (Idrisi)

The basic criteria implemented in the current model release are built around two concepts: the rapidity of walking allowed by the terrain and the weather conditions (walk) and the possibility to hide by the physical environment (hide). The EU25 land border third criterion requiring localization of Border Control Points (BCP) cannot be included in this global application because of unavailability of a global open source dataset. In contrary the BCP used in the EU25 model have been manually digitalized based on information provided by a survey to border authorities. This time consuming work can not be carried out at the world level, even not at the level of one tile. The integration of this criterion in the global model could only be done locally, on a specific area.

The model defined in Idrisi carries out the indicator scaling and the combination of the different layers in the two criteria using respectively Boolean overlay and weighted linear combination (WLC) strategies at different stages of the modeling exercise.

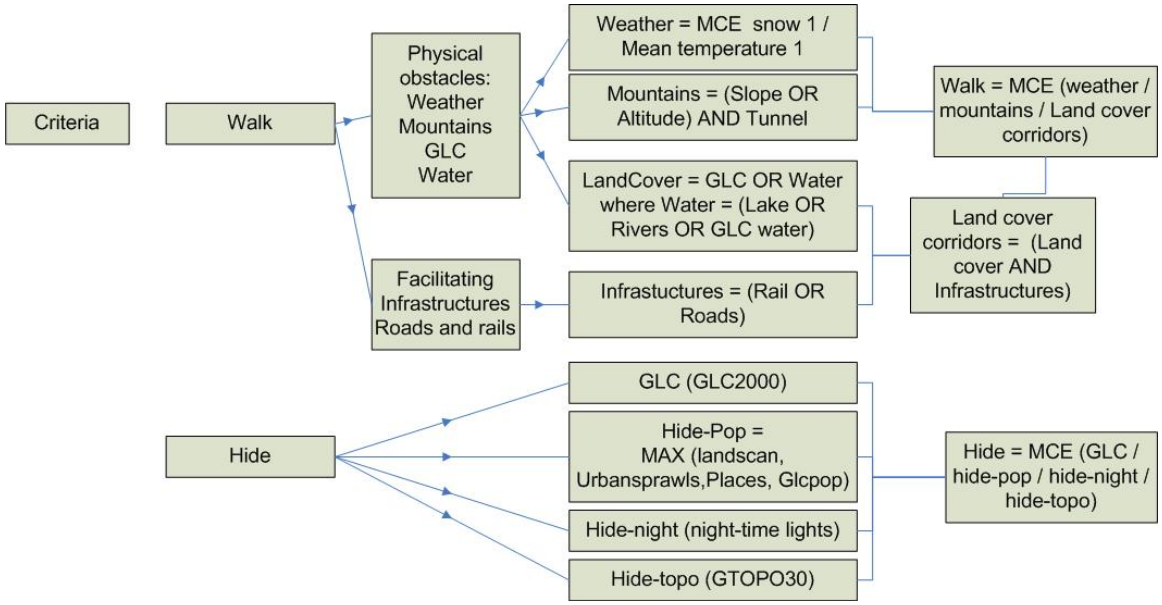

Fig. 4: Two clusters criteria in the multi-criteria evaluation (MCE) of the EU friction surface.

The model built for the EU25 eastern border has been simplified (Fig. 4). In this European tile, most of the thresholds of the fuzzy transformations have been re-used except for the weather conditions scaled with the min and max values in the study area. These have to be adapted from one tile to the other.

3.5.3. EU permeability criteria

European permeability application can be seen on the two following figures (Figure 5a and b): the walk and hide criteria. These figures illustrate the regional coverage and the spatial resolution of the model. These maps can be used to compare border segments permeability as it has been proposed in the EU25 framework. They can be respectively described as “accessibility” and “urbanized area” maps.

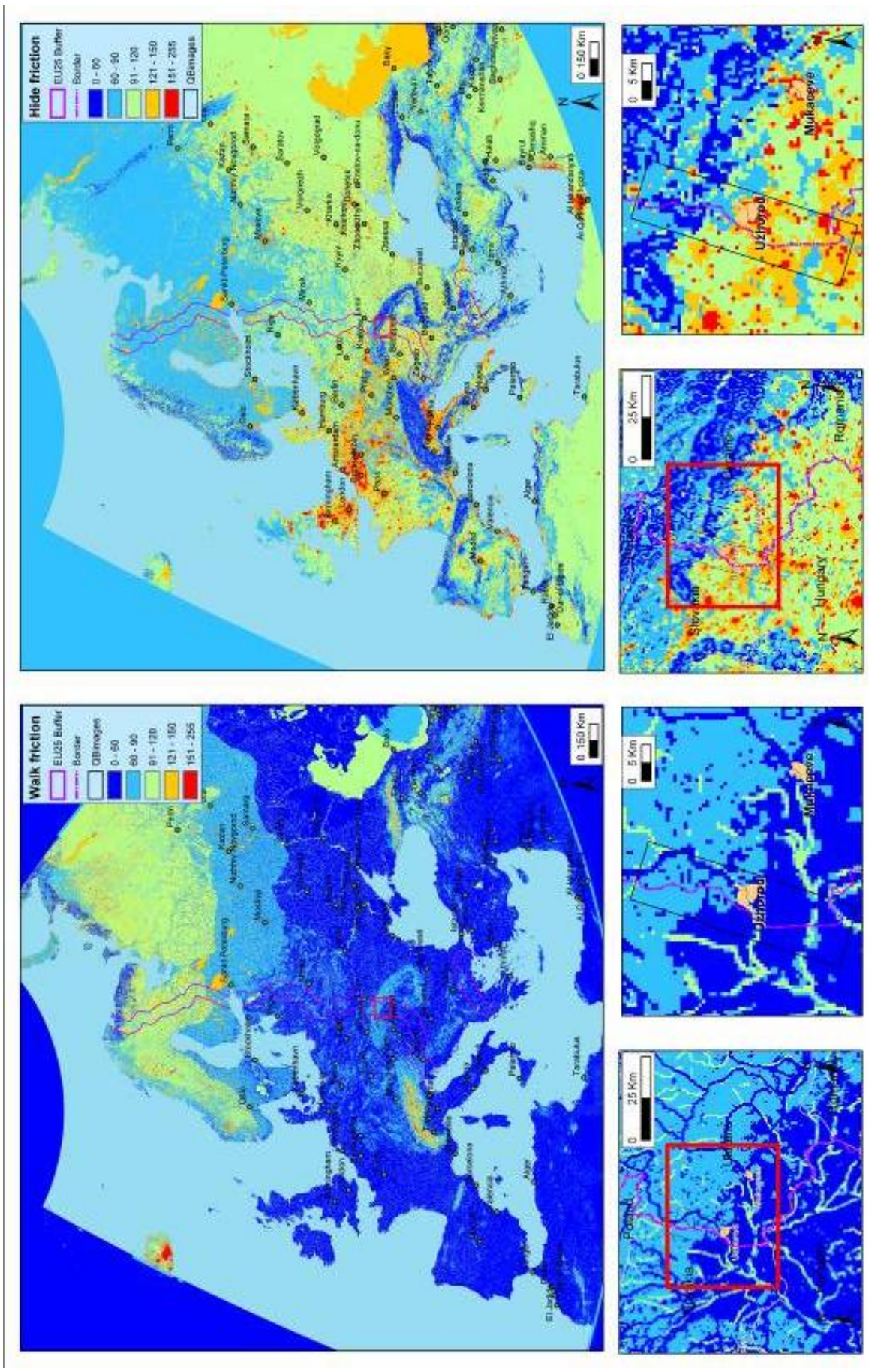

Fig. 5 a and b: walk and hide friction on the EU tile

4. The local application : Uzhorod

The local application of the permeability model is carried out on a specific border segment presenting high levels of friction in the EU25 land border permeability study (Stephenne and Pesaresi, 2006). The city of Uzhorod is located at the border section between Ukraine, Slovakia and Hungary, in Ukraine at longitude 21° 59”11’and 22° 33”51’, and latitude 48° 55”16’ and 48° 21”39’. Three Quickbird scenes have been acquired to evaluate the border permeability in this zone (Figure 4). The high political interest of this area has been highlighted by border institutions calling for strengthening co-operation between Ukraine and the EU institutions in the field of border surveillance, especially with the new EU Border Management Agency (Magoni et al., 2006). Ukraine has been referred as a corridor of entry into EU countries in the 2005 overview of illegal migration described by Europol (http://www.europol.europa.eu).

4.1. Features Digitalization on Quickbird images

Some of the geographical features defined as relevant in the permeability modeling study (annex 1) have been identified on three scenes of radiometrically corrected and pansharpened Quickbird images covering the test area. “On-the-screen photo-interpretation” of the geographical features have helped in the definition of these on the imagery itself.

- Correction/enhancing of 90m SRTM data and production of the slope feature
- Orthorectification of Quickbird (QB) multispectral imagery (MS - 2.44~2.88 meters of spatial resolution) using SRTM data (http://www.vterrain.org/Elevation/global.html) as Digital Terrain Model
- Sharpening of image at 0.8 meters of spatial resolution (image fusion with the PAN image -0.61~0.72 meters of spatial resolution-) by HSV transform technique using cubic convolution resampling method. After different tests, this method appears to comply with the objective of object digitalization, but is not interesting for the visual presentation. Spots of different colors appear throughout the image.
- Definition of complete list of features to be detected (annex 1)
- On-the-screen photo-interpretation of the fused imagery. Digitalization of features in GIS environment.

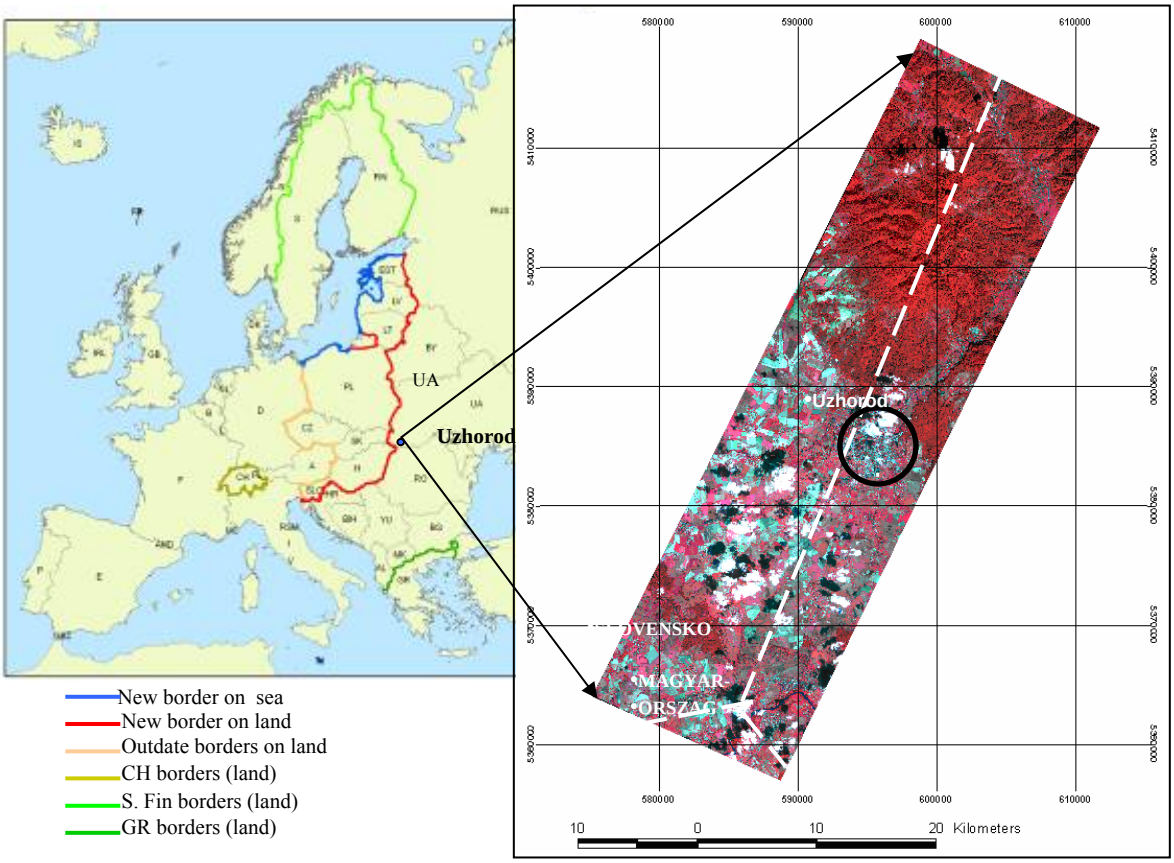

Fig. 6: Location of area under consideration and a composite mosaic of three Quick bird images covering Uzhorod and the surrounding areas

4.2. Technical issues in geographical features digitalization

The list of digitized geographical features differs from the "a priori" defined list (annex 1). Some features of the list are missing. Terrain surface characteristics and small man-made structures (point 2 and 3 in the annex) have not been identified on the image. The main reason is the high amount of time necessary to digitize these features. Priority has been given to the land cover dataset.

The border line provided by regional dataset doesn't fit with the satellite imagery and has then been digitalized based on the 100k Russian topographic map. This border has been refined manually on the QB image where the line of this administrative limit is easy to recognize. When clouds prevent the detection of this line, the former track has been kept. Based on this dataset, buffer zones can be defined.

The land cover dataset includes all the features referenced in the section 4 and 5 of the annex 1. Clouds are not distinguished from their shadows. The a priori list of land cover classes has been updated by the photo-interpreter identifying specific features (railway station, intertidal zones, young forest, …). These features represent only a small portion of the image (Table 3).

Table 3: Uzhorod land cover dataset

Land cover legend	annex1	Comments	Area in km^2	% of coverage
Forest	4.1.	extensive mass of trees	310.79	29.88%
Tree patch	4.2.	strip or patches of trees	24.40	2.35%
Grass	4.3.	natural grass	3.62	0.35%
Bare soil	4.4.	bare soil or rock	2.56	0.25%
Shrub	4.5.	shrubs or scrub	11.57	1.11%
Wetland	4.6.	wetland	0.77	0.07%
Water body	4.7.1	lakes, ponds, dams	1.33	0.13%
Wide river	4.7.2.	river greater than 10 meters wide	4.35	0.42%
Compact settlement	4.8.		15.87	1.53%
Linear settlements	4.9.	buildings along the roads	24.03	2.31%
Scattered settlements	4.10.	scattered buildings	16.35	1.57%
Industrial area	4.11.	industry, factory, processing sites	5.71	0.55%
Inhabited fields	4.12.	buildings in agricultural fields	5.81	0.56%
Uninhabited fields	4.13.	agricultural field with no buildings	494.18	47.50%
Clouds and shadow	5.00		104.04	10.00%
Railway station		railway station	5.05	0.49%
Intertidal flat		soil deposits along river banks	0.42	0.04%
Others		unclassifiable settlement	1.74	0.17%
Young forest		mass of growing trees	5.93	0.57%
Park		Open recreational areas in settled areas	0.99	0.10%
Airport		airport	0.78	0.08%
Total			1040.29	

The main issue in the digitalization of VHR images to create a land cover dataset are the clouds. Clouds and shadows related to these clouds represent one land cover category (Fig. 7). This technical choice, without any interpolation by the photo-interpreter, induces some breaks in the linear features as the roads or railways. Cloudy zones are “holes” in the land cover map as well as in the permeability map. Unfortunately, Uzhorod image contains a high proportion of these “undefined” areas (around 100 km^2 within the 843 km^2 of the overall zone).

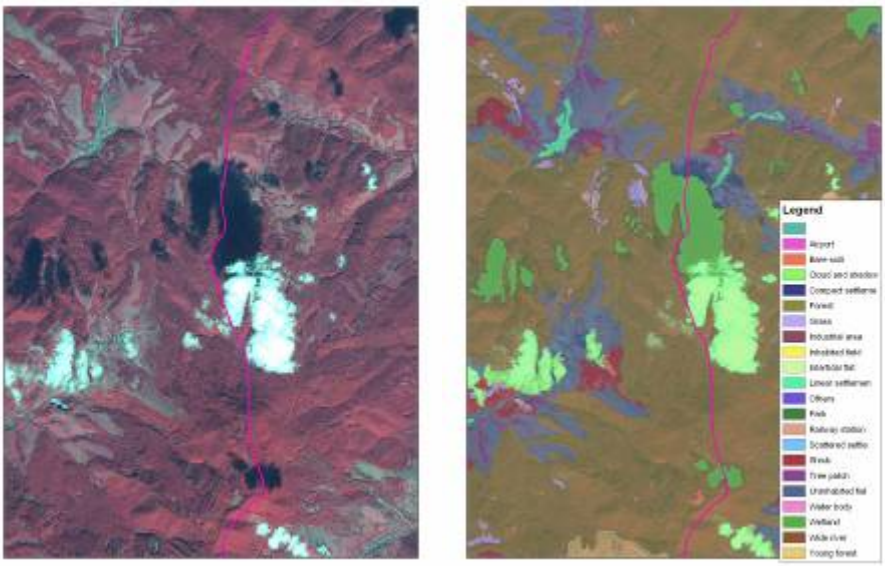

Fig. 7 : Clouds and shadows on the QB image and on the land cover digitalization

The linear vector segments have been digitilised in five different files. Four of them refer to the category called infrastructure in annex 1: bridges (bridge/ "water barrier"), roads (Highway 1.3.1./ paved roads 1.3.2./ unpaved roads1.3.3./ track 1.4.), railway line, narrow rivers and ford (6 on temporary rivers and 4 on pipes). Only one railway is crossing the entire area and in particular the town of Uzhorod (Fig. 8a). The fifth file is called "narrow river" and includes one river in the northern part of the area and one canal in the western part. This vector dataset completes the water bodies included in the land cover dataset (wide rivers and lakes/water bodies) (Fig. 8b).

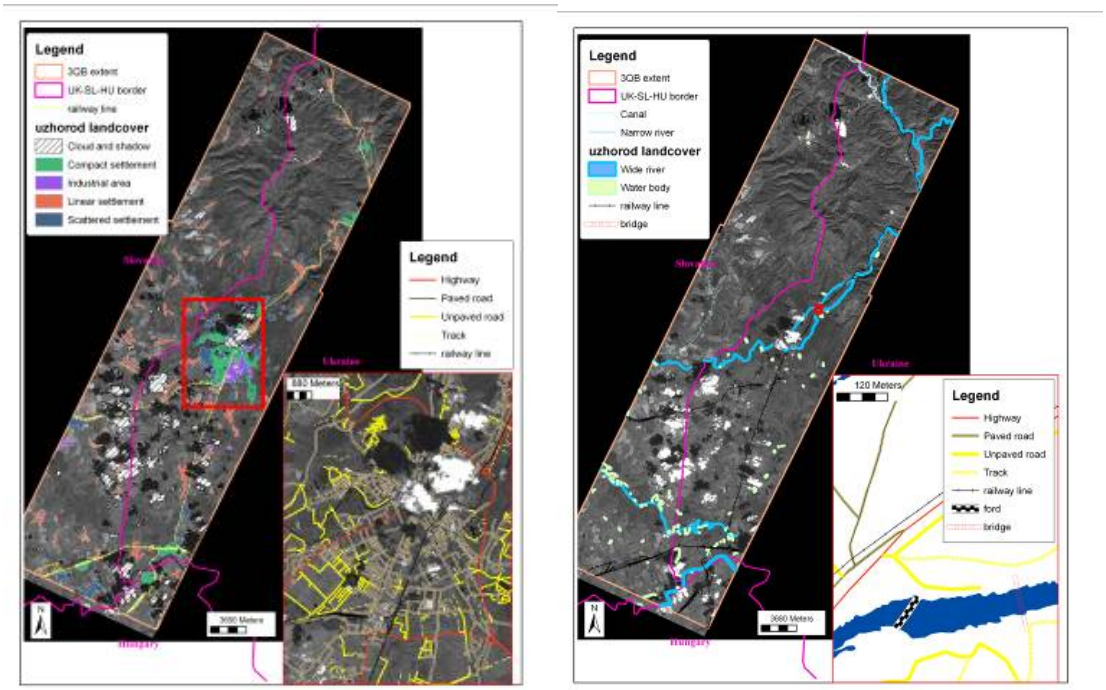

Fig. 8 : a) Rail and built-up classes in the Uzhorod landcover dataset, and clouds issue on the town and b) water bodies in the lines and polygons vector datasets and bridging structures (ford and bridge)

Bridges and fords are really specific and important features in a permeability study. They counter act the barrier effect of the river, but their identification is challenging. Annex 1 requested the identification of informal or temporary bridges (1.2) and "ford" (Fig. 9). Unfortunately, a high level of suspicion is attached to these features because of the difficulties of visual interpretation without field verification (Fig. 9). 33 bridges were identified on the wide rivers in the first digitalization process. 10 others localized on the canal and on the northern narrow river were missing. Two bridges on the wide river have been categorized as "looking as water barrier" and identified also in the "ford" dataset. In fact, as there is only one crossing path and no links with an infrastructure (roads or railway), these objects have to be deleted from the bridge dataset and kept in the ford one (Fig. 10). 10 informal river crossing points due to low level of water have been identified in the area, among them 4 pipelines, that are seen as a mean of river crossing for people, and 6 low level paths on river. The type of infrastructures and types of water bodies that is linked to each of these crossing structures have been added to the original dataset. For example on Fig. 9, the fords (number 1) are identified by the road network interrupted on each part of the river.

Fig. 9 : Difficulties in bridge identification (1) Ford and (2) informal bridge (pipeline bridge, dam)

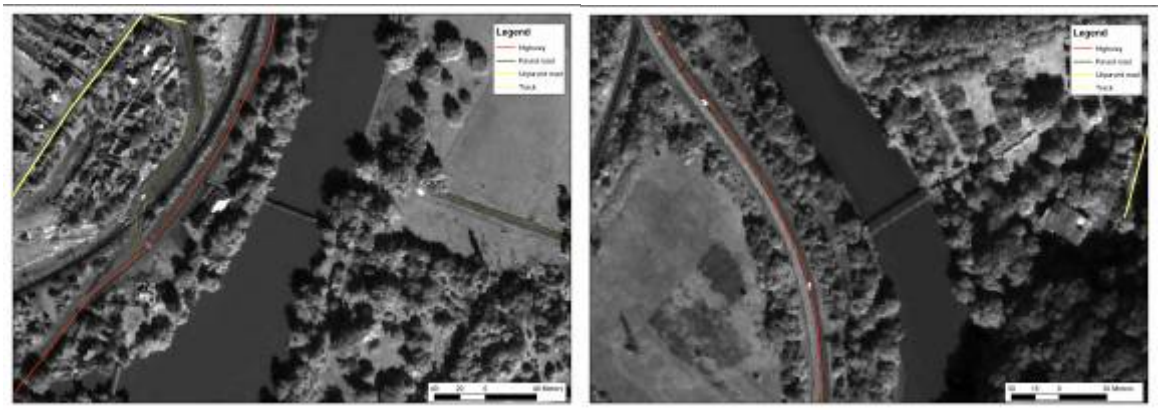

Fig. 10 a and b: Pipes, wrongly identified as bridges

Several issues in the building of this dataset have been highlighted in the first digitalization process. These specific issues have to be taken into account and further analyzed in future applications of this modeling protocol:

- The clouds and shadows coverage introducing breaks in all the features
- Necessary distinction between the road or rail infrastructure in bridge/ ford dataset.

4.3. Processing of geographical features in terms of permeability

4.3.1. Preprocessing steps (Arc Gis)

In this local application, the inputs and resolution differ from the global approach. The EU25 model processes are adapted to represent most of the part of the permeability concept (Table 4). Some inputs are released. For example, as weather and topographical conditions in their annual average values are quite homogenous in this small area, these variables are not considered in a local model. The resolution of the results is not constraint any more by the resolution of the input datasets. The vector datasets are rasterised because of the multicriteria methodology applied. The resolution of 10m keeps the accuracy of the digitalization using 1m panchromatic data and 2.5 multispectral information. The ArcGis pre-processing steps calculate the density of rivers, roads, railways, bridges or fords and reclassify the land cover datasets.

Table 4 : comparison of input files in EU25 and local models

File names in the EU25 model :	Used or not in the local application	EU25 dataset	File names in the local model	Digitalization
bcp_grid	no	JRC/GD		
border_buffer	no	JRC/Gaul		
snow	no	Era40		
tmean	no	Era40		
landscan	no	Landscan2002		
night	no	Nightlights		
topo	no	Gtopo30		
topoalt	no	Gtopo30		
tunnel	no	Esri European base map		
glc11	yes	GLC2000	lcwalk/ lchide	landcover
riverplus	yes	Gisco	narrow river	Vector narrow river
lake	yes	Gisco	lcwater	landcover
marsh	yes	Gisco	Intertidal class	landcover
gdplaces	yes	GD	lcpop	landcover
urbsprawls	yes	GD + Esri European map		
localroad	yes	GD	roads	Roads vector file
rail	yes	GD + Esri European map	railway	Rail vector file

As it has been done for the GLC2000 land cover dataset the Uzhorod landcover is reclassified in 4 categories of decreasing suitability to walk, quantifying from values of 0 to 256 in terms of friction (0/64/128/192/256) (Table 5). The same reclassification exercise is done in the context of decreasing suitability to be hidden.

Table 5: reclassification of land cover in terms of walking accessibility and hiding suitability

Land cover legend	Accessibility levels (lcwlk)	Hiding levels (lchide)
Forest	256	0
Tree patch	256	0
Grass	64	128
Bare soil	64	256
Shrub	128	64
Wetland	192	128
Water body	256	128
Wide river	256	128

Compact settlement	0	256
Linear settlements	0	192
Scattered settlements	0	192
Industrial area	0	192
Inhabited fields	0	192
Uninhabited fields	64	128
Clouds and shadow	undefined	undefined
Railway station	256	256
Intertidal flat	192	128
Others	0	192
Young forest	128	64
Park	128	64
Airport	256	256

4.3.2. SDSS model

The walk criteria integrates information about land cover, water barrier and facilitating infrastructures. The hide criteria refers to the land cover dataset. And the secure criteria uses a cost function that takes into account the six border points that are in the QB area with a friction surface corresponding to the walk criteria. As in the global applications, the threshold values in the fuzzy scaling steps have to be adapted on the frequency, minimum and maximum values of each feature.

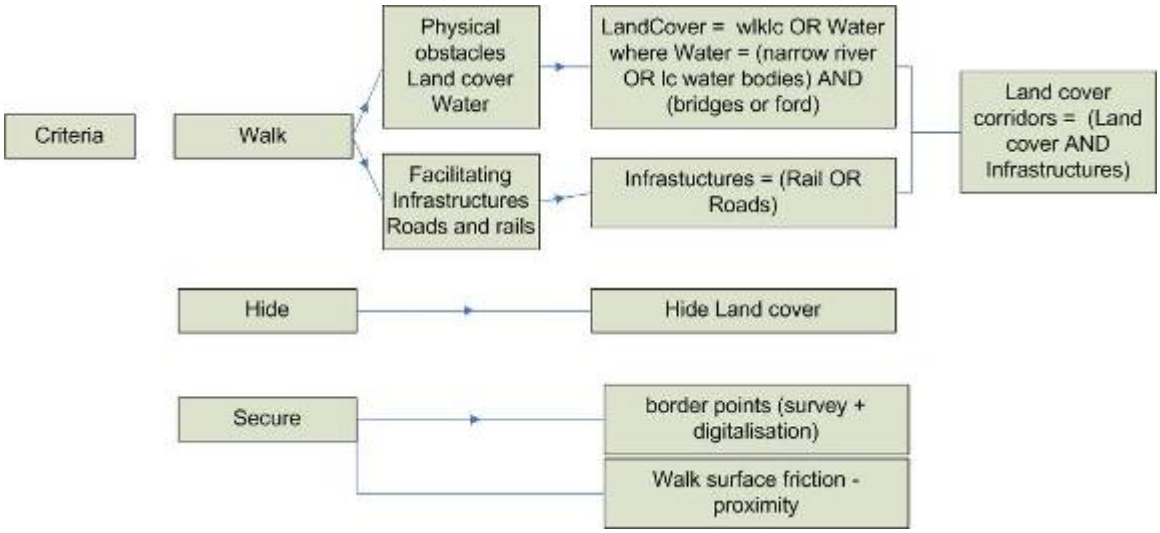

Fig. 11 : Three clusters criteria in the multi-criteria evaluation (MCE) of the Uzhorod friction surface

4. Conclusions and discussions

In order to understand the applicability of the permeability concept introduced by Stephenne and Pesaresi (2006), the modeling approach has been adapted to two different scales (continental and local). The model building processes differ while the SDSS is either generalized in a larger coverage (European tile) or applied at a finer scale (three Quickbird

scenes on the region of Uzhorod in Ukraine). The main technical differences are related to the availability of data in both applications.

Inputs of the regional model are extracted from global open source datasets. The simplification of the preprocessing and processing steps in the generalization is similar to the land border approach except for the third criteria “secure”. The unavailability of border point crossing data did not allow any kind of “border permeability” assessment. The basic assumptions of this application release the relation to a specific border. The “secure” criteria representing the cost of being captured by border guards became irrelevant.

The local dataset has been built manually through a time extensive digitalizing method. Because of the recent availability of very high resolution imagery (less than 1m of grid cell), new applications are proposed. The use of these data in the permeability of border posts could be one of these new fields of research according to the exploratory character of this application. Some basic and simple guidelines have been provided to the photo-interpreter. But either in the digitalization phase, or in the definition and description of these guidelines some issues have arisen. The discussion of these technical problems can be useful in other modeling or digitalization applications. The main problem is related to the presence of clouds in the imagery. All the vector and raster features extracted from the imagery are broken by the presence of clouds or shadows. The consecutive permeability map presents then some holes.

Besides these technical issues that can be the subject of further research. These applications prove the interest of the spatial model approach in a better understanding of regional or local characteristics. While regional permeability maps integrating BCP points can be used to compare border segments permeability as it has be proposed in the EU25 framework. They can also be respectively described as “accessibility” and “urbanized area” maps. The local application demonstrates the interest of small features as bridges and fords. In the future, some automatic procedure can be proposed by scientific research to define these structures (Cinbis and Aksoy, 2007).

Acknowledgement

We would like to thank Martino Pesaresi, Daniele Ehrlich, Raphaele Magoni and Dirk Buda for their collaboration in the definition of the permeability concept but also in previous reports redaction. The work was made possible through the support of all the staff of the Support to External Security unit at the JRC. The establishment of this particular methodology benefited also from the cooperation work carried out with Giovanni Laneve, Centro di Ricerca Progetto San Marco, Università di Roma "La Sapienza" within the Global Monitoring for Security and Stability (GMOSS) Network of Excellence.

References

Bartholomé, E., Belward, A.S. (2005), GLC2000: a new approach to global land cover mapping from Earth Observation data. International Journal of Remote Sensing 26, 9: 1959-1977.

Cinbis, R.G. Aksoy, S (2007), Relative Position-Based Spatial Relationships Using Mathematical Morphology, in IEEE International Conference on Image Processing, San Antonio, Texas, September 16-19.

Deichmann, U. (1996), A review of spatial population database design and modeling. Technical Report 96-3. National Center for Geographic Information and Analysis. Santa Barbara.

Dobson, J.E., Bright, E.A., Coleman, P.R., Durfee, R.C., Worley, B.A. (2000), LandScan: A Global Population Database for Estimating Populations at Risk. Photogrammetric Engineering & Remote Sensing 66, 7: 849-857.

Eastman, R.J. (1993), Multi-criteria evaluation and GIS, in Longley P.A., Goodchild, M.F., Maguire, D.J., Rhind, D.W. (eds.) (1999), Geographic Information Systems and Science, John Wiley & Sons, New York, US, pp. 493-502.

Geertman, S.C.M., Reitsema van Eck, J.R. (1995), GIS and models of accessibility potential: An application in planning, International Journal of Geographical Information Systems, 9, 67.

Geurs Karst T., van Wee, B. (2004), Accessibility evaluation of land-use and transport strategies: review and research directions, Journal of Transport Geography, 12, 2, pp 127-140.

Guagliardo, M.F. (2004), Review Spatial accessibility of primary care: concepts methods and challenges, International Journal of Health Geographic, 3, 1-13.

Harris, B. 2001, Accessibility : Concepts and applications, Journal of Transportation and Statistics, vol4, n° 2/3, pp. 15-30.

Joly, O. (1999), Working Group I. 1 : Geographical Position : 'State of French art of spatial accessibility indicators', SPESD - France, Working Paper.

Magoni, R., Stéphenne, N., Stančová, K., Buda, D., Pesaresi, M. (2006), Migration at the EU-25 land border: Data issues and a preliminary permeability model, EU technical report (IPSC/TN/2006017).

Reitsema van Eck, J.R., de Jong, T. (1999), Accessibility analysis and spatial competition effects in the context of GIS-supported service location planning, Computers Environment and Urban Systems, Vol. 23 pp. 75-89.

Stephenne, N.,Pesaresi, M. (2006), Spatial Permeability Model at the European Union Land Border, EUR report 22332 (Luxembourg: European Commission / DG-JRC / IPSC).

Stephenne, N., Magoni, R. (2006), Migration through the EU-25 land border: Data issues and initial results of a permeability model, presented at the second challenge training school : "security, technology, borders, EU responses to new challenges", CEPS, 6-7 October 2006, Brussels, Belgium.

Stephenne, N., Magoni, R., Laneve, G., From real time border monitoring to a permeability model, In Jasani, B. et al. Remote Sensing from Space: Supporting international peace and security, Springer Science (forthcoming).

Tischer, M.L. (ed) (2001), Special Issue on Methodological Issues in Accessibility, Journal of Transportation and Statistics, Vol. 4 N°2/3.

Tobler, W., Deichmann, U., Gottsegen, J., Maloy, K. (1995), The global demography project, Technical Report TR-95-6, National Center for Geographic Information and Analysis, Santa Barbara.

Verdin, K.L., Greenlee, S.K. (1996), Development of continental scale digital elevation models and extraction of hydrographic features. In: Proceedings, Third International Conference/Workshop on Integrating GIS and Environmental Modeling, Santa Fe, New Mexico, January 21-26, 1996. National Center for Geographic Information and Analysis, Santa Barbara, California.

Annex 1 : G (geographical) criteria/features to be detected in Quickbird imagery

1. Infrastructures
   - 1.1. Stable bridges (road or rail) {LINE}
   - 1.2. Temporary bridges or informal bridges {LINE} (2)
   - 1.3. Roads (different kind of)
     - 1.3.1. highway {LINE}
     - 1.3.2. normal paved road {LINE}
     - 1.3.3. unpaved road {LINE}
   - 1.4. Paths and other tracks {LINE} (11)
   - 1.5. Railways {LINE}
   - 1.6. Narrow Rivers, Water channels {LINE} (10)
   - 1.7. Ford {LINE} (1)
2. kind of terrain surface (physiography)
   - 2.1. not accessible (rock mountains) {POLYGON}
   - 2.2. steep slope {POLYGON}
   - 2.3. hill {POLYGON}
   - 2.4. plain {POLYGON}
3. Man-made obstacles
   - 3.1. wall {LINE}
   - 3.2. wire fences {LINE}
   - 3.3. trench {LINE}
4. land cover / landscape
   - 4.1. Forest {POLYGON}
   - 4.2. Strip or patches of trees {POLYGON} (3)
   - 4.3. Natural grassland {POLYGON}
   - 4.4. Natural bare/rock {POLYGON}
   - 4.5. Natural shrub {POLYGON}
   - 4.6. Wetland {POLYGON}
   - 4.7. Water bodies
     - 4.7.1. lakes {POLYGON}
     - 4.7.2. wide rivers {POLYGON} (12)
   - 4.8. Compact urban {POLYGON} (8)
   - 4.9. Linear settlement along roads {POLYGON} (7)
   - 4.10. Scattered residential settlement {POLYGON} (4)
   - 4.11. Industrial areas {POLYGON} (9)
   - 4.12. Inhabited agricultural areas {POLYGON} (5)
   - 4.13. Uninhabited agricultural areas {POLYGON} (6)
5. No imagery data
   - 5.1. Clouds
   - 5.2. Shadows

Cascade or Domino effects in Flood Impact Analysis in GIS

Åke Sivertun* & Vimalkumar Vaghani

GIS IDA, Linköping University, Sweden SE 58183 Linköping Sweden

* akesiv@ida.liu.se

Note: Published also in Proceedings at IASTED International Conference on Environmental Modeling and Simulation (EMS 2007) August 20 to August 22, 2007, at Honolulu, USA.

Abstract

Floods are common natural occurring disasters in most parts of the world. It results into damage of human life and environment but not seldom are the side effects of flooding causing more damages than the flood itself. To investigate such Cascade or Domino effects we have tested the possibility to merge and analyze such effects on built up areas, on land fills and polluted soils and on transports, roads and other infrastructure. The article analyze impact of flood along the demarcated risk areas of Lakes Roxen and Glan when they are flooded and how to use this information during flood emergency in GIS, thus providing spatial information for assessment of flood vulnerability. Thus to show GIS is an effective tool for developing flood emergency response as a part of disaster preparedness for decision makers and analyze the risk for Cascade or Domino effects.

1. Introduction

Natural disasters like floods, earthquakes, landslides and droughts are frequent occurring disaster. These disasters result into damage of human life, property, communication networks and infrastructures, agriculture land including crops and general environment threatening ending in crises when resources are out of range to coop with the emergency. Floods are some of the most common natural occurring disaster. Floods are of three types: flash flood, river flood and coastal flood. [34] Recent causes for frequent flooding of some areas are due to human involvement by un-planned settlement and land use as well as construction and careless operation of dams. There has been immense use of different modern technology to control flood disasters. This article tries to focus impact of flood on economic and environment damage in risk areas along the two Lakes Roxen and Glan when they are flooded.

The use of GIS and remote sensing can help decision maker with analysis, planning and providing an early warning for floods. In Sweden several areas get frequently flooded downstream of river due to high seasonal inflow of melted ice and snow and heavy rainfall. These floods are quite frequent during spring and autumn. Especially the high flow situation in 1983 and spring flood during 1995 that caused flood in most of the entire large rivers and lakes in Sweden. The recent worst rains and hurricanes winds in Northern Europe affected UK, Denmark and Sweden highly, that took three lives in Sweden and altogether 14 lives in Europe [11] Since then there has been a constant efforts by the different Swedish agencies like The Swedish Meteorological and Hydrological Institute (SMHI) that is responsible for flood forecasting and monitoring the emergency situation during flood, to provide real time information to - SRV (Räddningsverket/Swedish Rescue Agency) – to plan flood emergency response. Additionally to overcome such emergency situation the Swedish Governmental Agencies. Additionally Lantmäteriet (National Land Survey), Swedish Geological Survey

(SGU), SMHI and the National Ship Administration jointly have created the project KRIS-GIS to tackle these questions [36].

The goal with this report is - additional to earlier studies – to investigate the feasibility in identifying Cascade or Domino Effects related to at flood situations. Digitized flood risk areas were obtained from a ready flood risk map [37] data on properties and buildings, Landscape, Rivers and Roads from Lantmäteriet (National Land Survey of Sweden) and Soil maps (Swedish Geological Survey. With these data as input the ESRI software ARC Map 9 and ARC View 3.3 have been used for flood impact data preparation, integration and analysis.

2. Problem description

The floods affect human lives, destroying their homes and livelihood, moreover affecting the country business, economy and industry. As the research and development continues to overcome this vulnerability, the article tries to focus on better use of GIS i.e. asses the flood impact for rescue purpose. The goal in short;

1. To examine integrating of GIS data and flood models to determine the possibility to identify areas at risk for flood emergency prevention and response.
2. To analyze impact of flood on flood risk areas for different spatial data when the areas along the Lakes Roxen and Glan are flooded.
3. Identifying where Cascade and Domino effects can occur that is of importance for prioritization of response.

2.1 Methods

Spring floods has lead to carry out many researches and development to prepare emergency rescue plans for flood risk vulnerable regions in Sweden. In the past few years, GIS has emerged as a powerful analyze tool and being put to use to assess risk for property and life stemming from natural hazards such as floods. Internationally GIS is also used to identify vulnerable areas for Earthquakes, cyclones and other hazards and aid in the preparation and rescue work [19]. Also remotely sensed data can be used at various stages of the flood impact analysis and preparation of emergency rescue plan [5]

There are different models to calculate flood levels for emergency situations. The HBV model developed by SMHI in Sweden can forecast flood emergencies weeks before they happen. This model can be found suitable in Sweden to prepare flood hazard map using topographical data, time series of hydrological and metrological data that could be used for different purposes i.e. to assess the flood impact, flood watch, emergency situation, evacuation etc. [13][30]

Emergency response of any major disaster (flood, earthquake etc.) incident taking place where there is heavy life loss. Usually the high need of emergency operation is near the incident area but if it affects many people and environment in large areas then there is a need of different resources for rescue operation. [24] Thus a growing need of up-to-date information for various geographic features to estimate potential impact of a disaster when it occur GIS can integrate and assess all the minute details for various geographic features.

2.2 The Study area

The geographical location of Sweden is north European country covering also the Arctic Circle that makes it a more sensitive region. Lake Roxen and Glan as shown in fig. 3 is located

in the Southeast of Sweden in the Östergötlands län (county) and it shares 36 % of this surface water in Motala Ström catchments area. Lake Roxen and Glan shares its boundary with Linköping, Norrköping, and Finspång lommuner (administrative areas). It has an elevation of average 33 m from mean sea level. The main stream of Motala Ström River runs primarily from west to east passing through Lake Roxen and Glan opening into the Baltic Sea. The Lake Roxen is located on Latitude 58° 30' 0" , longitude 15° 40' 0" and Lake Glan is located on latitude 58° 38' 0", Longitude 16° 0' 0" . The surface area of Lake Roxen is approx. is 95 sq. km and lake Glan is 77 sq km.

A subset area (frame) was selected around the Lake with an area of 1258.17 sq. km and used as working area with an aim to represent the maximum extent of the lakes and surrounding environment. Also computing time is reduced to minimum in ARC Map and Arc view 3.3 and a comparative analysis could be carried out without loss of any information. There are small dams around the lake for water regulation and flood control. The Lake edges are very low - in some part of the lake just little higher than the ground surface and some reclaimed areas also below sea level protected by dams. The maximum extent of risk areas is less then 6 km from the edges of the lakes. The major urban areas of the cities Linköping, Norrköping, and Finspång are located quite far from major flood risk areas. There are small residential areas, commercial areas, infrastructure network-road, large agriculture and forested area in the surroundings of Lake Roxen and Glan which are at great flood risk if the dams are not controlled properly or there is high amount of water being pored into the lakes due to melting up of snow in upstream of Motala Ström River. The digitized flood risk areas superimposed on the topographic map is shown in Figure 1.

2.3 Flood Impact simulation

The study uses a vector based analysis approach in simulating the impact of flood using GIS software ARC Map -Arc GIS 9 and ARC view 3.3. This is one of the most basic flood modeling approaches. The article focuses on data preparation, integration and analysis to find the 1) flooding inundating areas 2) flood damage and risk. Such information can be used for flood management and planning purpose for preparing flood emergency plans and predict how much different land will be affected when the flood occurs. The most basic flood models only require the extents of flood hazards zones, without any information on movement and volume of water. In this approach, there exist calculated flood hazards zones representing flood risk areas according to calculations based on 100 years statistics of water flow (flooded area) and Risk class 1 for dam (risk areas). These flood hazard zones is obtained from the report of SRV. There are two approaches for flood management viz. structural and non structural approach, where structural approach concerns physical work like construction of dams, reservoirs, bridges, channel improvement, river diversion and other embankments to keep floods away from people and the non-structural approach is concerned with planning and analyzing the flooding situation, flood plain zoning, flood proofing for reducing the risk of flood damage and to keep people away from floods.

Results and discussions:

Flood Impact Analysis and Map products

Following is the description for types of analysis that can be performed and types of map products that can be derived in GIS for flood hazard management.

Flood hazard mapping

For town planning and floodplain management purposes, there is a need to map various hazard zones as means for setting development guidelines and establishing emergency response procedures. Mapping of flood extents have obvious uses in showing the area affected by a particular historical flood or a modeled flood of a given probability of occurrence. Once the possible flood levels have been derived, maps for each flood level can be effortlessly produced with GIS. GIS tools can readily perform different land use based overlay analysis in a planning context, and produce maps of resultant analysis. When overlaid on property or an infrastructure database, it could be analyzed what property or infrastructure is immediately at risk. Visual representation can definitely add value to the results of the numerical modeling for informed planning and hazard management.

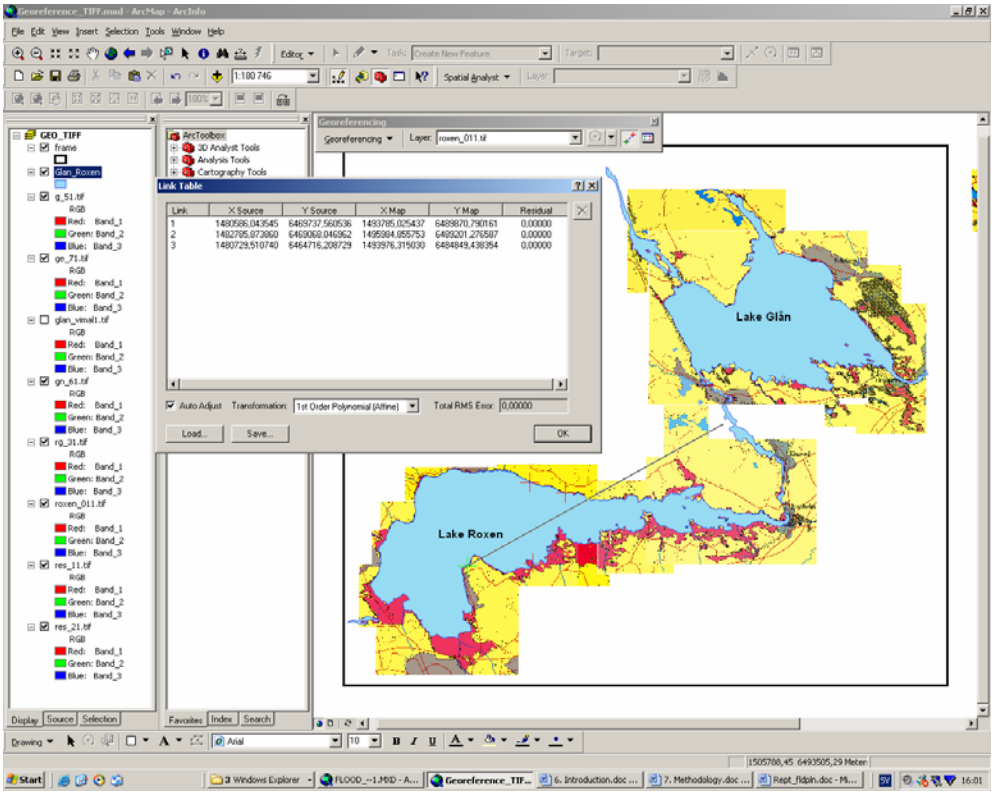

Fig. 1: A print screen window showing geo-referencing of TIFF maps with the existing Lake Shape file in ARC Map -Arc GIS 9.

Overlay analysis between land use, vegetation, road, buildings, soil type, water and extent of the flood data can be identified as vulnerable to economic damage. Figures and calculated tables below show the portion of different spatial data affected by flood data. It could very well be observed that the emergency services have been planned and located in a flood hazard proof area. These kinds of maps provide necessary inputs during land use planning exercises.

Affected Land use

Land use data shows usability of land in urban and rural areas. Specifically these data are required in GIS environment to prepare risk maps and issue early warning to urban area, thus avoiding disasters where major residential, commercial, industrial and other buildings are located at high risk, also to other rural areas where there is forest cover and agriculture vulnerable to flooding. In addition to this hospitals, schools, colleges and other building

information can be of help in identifying buildings and structure locations. These maps can be digitized to use in GIS database for future use. Fig 2 shows the various land use affected when overlaid with flood data and calculated with respect to total values affected. The total land use affected would be in risk areas - 26425909,16 sq.m and in flooded area is 32078557,20 sq.m. The agriculture land is affected the highest in risk areas 12933691, 60 sq.m and 14728364, 54 sq.m. The industrial and low rise development areas are also affected up to some extent thus arising risk for the population working & residing in it.

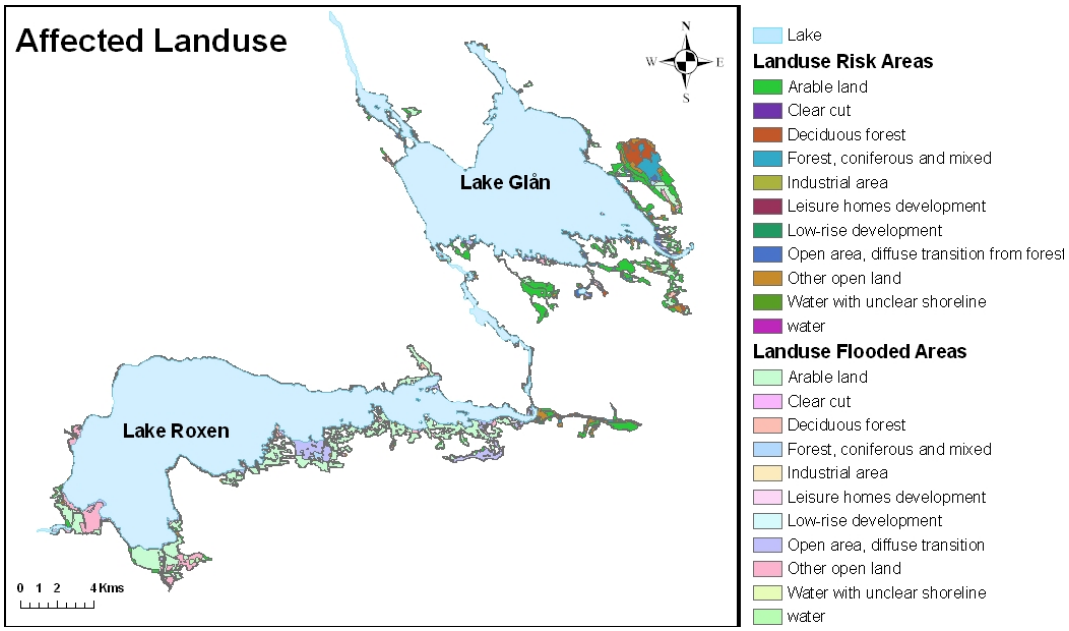

Fig. 2: A map showing affected land use types along the study area

Affected Road

Road data is the key for transportation planning in case of emergencies. With help of an "affected road map" an effective evacuation could be planned. If we have information if private, public and other roads are flooded or at risk then the population and emergency service vehicles can be guided in advance. With the help of GIS, when overlaying the affected road network data on building and population, it can be easily found out how the authorities can reach - from source (rescue centers) to their destinations (affected areas) and people could be rescued to safer location with identifying safest, shortest path calculated. Figure 3 shows the affected road network when overlaid with flood data. The total road network that would be affected in risk areas is 64389 m and in flooded area 43758 m. The private roads affected are the highest in risk areas 18355 m and in flooded area is 12303 m. The standard gauge, double track, electrified railway would be highest affected for 3720 m in risk areas and 696 in flooded areas. The public roads in risk areas 3910 m and Road > 7 m wide would be affected for 3133 m in flooded areas.

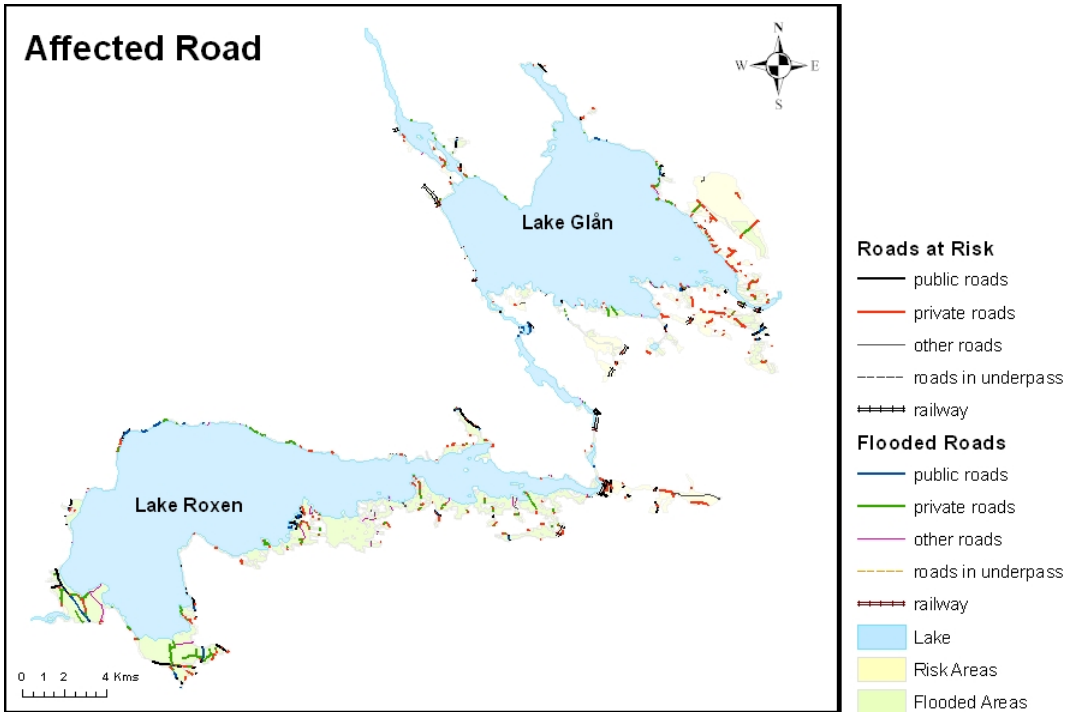

Fig. 3: A map showing affected Road network along the study area

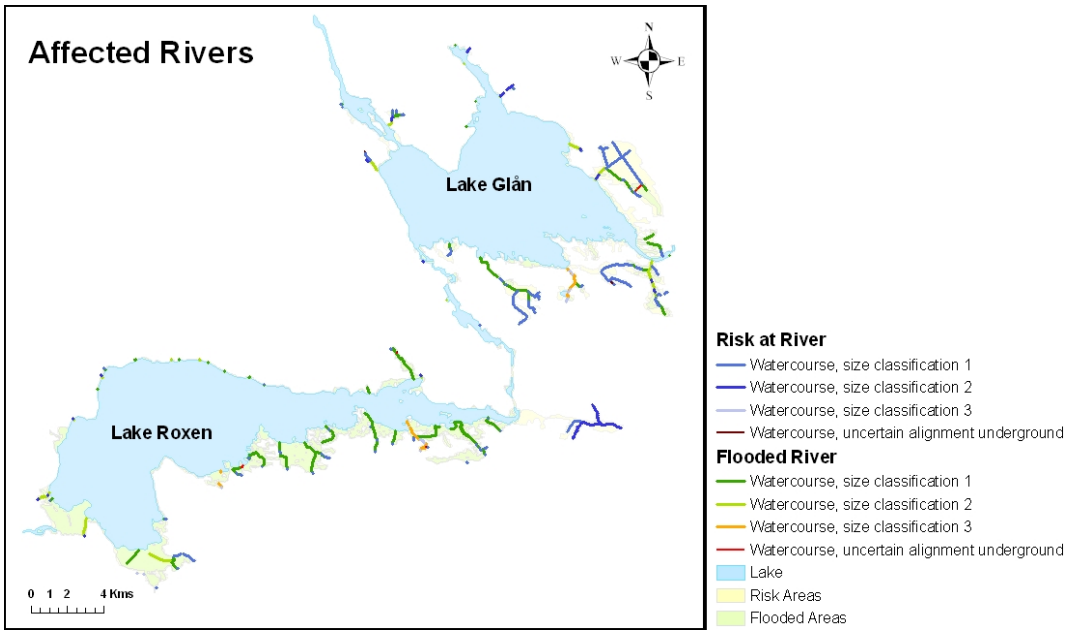

Fig. 4: A map showing affected Water network along the study area

Affected Rivers

As shown in Figure 4 different affected rivers can be flooded thus a rising state of emergency for the residential and commercial area near to it. These data can be of great use in finding what river could affect also the dams. The population and property near the rivers can be estimated for risk. It can be used in GIS environment for flood forecasting and early warning system. The total river network would be affected in risk area is 69623 m and in flooded area is 91605 m. The water course, size classification 1 would be affected for 23392 m in risk area and 35851 m in flooded area.

Affected soil type

To understand what buildings are the most likely to sustain damage, but also areas in risk for mobilizing nutrients and metals to the water due to changed hydrological conditions the rescue team need current information about affected soil type. Figue 5 shows the calculated effects.

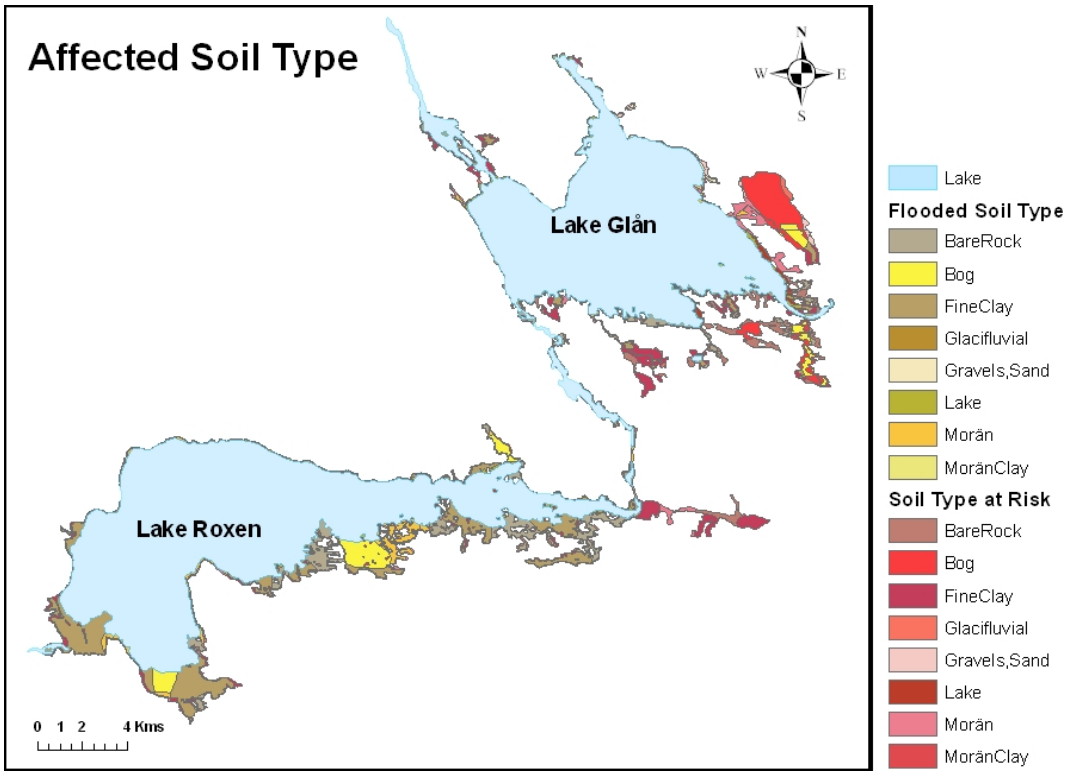

Fig. 5: A map showing affected Soil type in and around the study area

The total soil types that would be affected in risk areas are 26425909 sq m and in flooded area 32078557 sq m. The fine clay soils would be affected the most in risk areas 8693871 sq. m and in flooded areas is 14077346 sq. m.

Buildings data

Buildings and demographic data can be related together as each building depicts as some population is staying there. Further these data can be of great use in GIS environment for preparing hazard maps to identify the population that resides in the high risk area and needs to be warned and evacuated first to other places. The high density population can be at more risk during emergency as there can be loss of life in mass, therefore the need to plan high mass of people moves safely to safer place. This kind of affected data can also be useful for insurance and real estates agencies. There are total 563 parcels along the Lake Roxen and Glan and 137 commercial and residential buildings are affected in flooded areas and 164 commercial and residential buildings in risk areas. The affected area with respect to risk for flood and buildings are 563 and in flooded area 477.

3. Conclusion

By identifying the treats against important objects that should be protected and risks in a GIS it is possible to update the models for risks but also constantly plan and work for safety instead of just plan for actions in case in case of an emergency. Of course it helps to have all these data available to make wise judgments on where it can be flooded and where it is not so clever to build roads, houses or other installations as cascade and domino effects can occur. A flooded piece of land can in such case lead to a destroyed water source for a downstream community as nutrients and metals in the flooded area can be mobilised from soils or landfills into the water. A flooded road can lead to unwanted and much bigger consequences than was expected as hindering rescue work. If electric installations are affected this will lead to loss in capacity to pump away the water, loss of communications and other consequences even worse than from the flood itself. A traditional flood map analysis is in this way not sufficient if we want to create a safe community. Here we suggest a GIS based multi purpose Emergency information and management system. We must further combine flood analysis with several other layers of information to be able to judge the consequences and need for actions.

Acknowledgements

This research was made through support from the Swedish Emergency Management Agency –SEMA Swedish Rescue Services Agency RSA, Swedish National Defense College, Swedish Research Council and European Commission –GMOSS NoE. We also thank the Swedish Land Survey and the KrisGIS team for their support.

List of References:

1. Alok Gupta, Information technology and natural disaster management in India, GIS development webpage. http://www.gisdevelopment.net/aars/acrs/2000/ts8/hami0001.shtml (acc.04-10-24).

2.Andre Zerger, and David Ingle Smith, Impediments to using GIS for real-time disaster decisionsupport, Science@directwebpage,http://www.sciencedirect.com/science ?_ob=Article URL&_udi=B6V9K-468D852-&_user=650414&_coverDate=03%2F31%2F2003&_alid =218074581&_rdoc=13&_fmt=full&_orig=search&_cdi=5901&_sort=d&_st=13&_docanchor=&_acct=C000034998&_version=1&_urlVersion=0&_userid=650414&md5=add81baf3b06ab562f1f6d72e525e0f4 (acc.2004-10-11).

3. D.A. Kraijenhoff & J.R. Moll (1986), River flow modelling and forecasting. D. Reidel Publishing Company, Dordrecht, Holland

4. David Moore, GIS in Emergency Planning -A Spatial Analysis of Ambulance Services, Irish Organisation for Geographic Information web page, (2004-11-12). http://www.irlogi.ie/pdf/Emergency_Planning_IRLOGI_2003.pdf

5. Dr. Dinand Alkema, (2004); RS & GIS application in Flood forecasting, International Institute for Geo-Information Science and Earth Observation webpage, http://www.itc.nl/library/Papers_2004/n_p_conf/alkema.pdf (acc.2004-10-10).

6. Dr. Vinod K. Sharma, Use of GIS related technologies for managing disasters in India: an overview, GIS development webpage, (acc.04-09-12). http://www.gisdevelopment.net/application/natural_ hazards/overview/nho0003.htm

7. D. Z. Sui and R. C. Maggio, Integrating GIS with hydrological modeling: practices, problems, and prospects, Computers, Environment and Urban Systems, Volume 23, Issue 1, 1 January 1999, Pages 33-51.

8. Early Warning, Forecasting and Operational Flood Risk Monitoring in Asia – United Nations Environment Programme Division of Early Warning & Assessment, UNEP webpage(acc. 2004-09-21). http://www.na.unep.net/flood/FLOOD_WO.pdf

9. Er. M. Gopalakrishnan, forecasting & warning system for an effective disaster preparedness & response, Central Water Commission, UNDP webpage, (acc. 04-10-12).
www.undp.org.in/UNDMT/dpm/Day%20One/Theme/ %20I %20Presentation/GK.ppt

10. Farah Aziz, Nitin Tripathi, Mark Ole and Michiru Kusanagi Development of flood warning system, GIS development webpage, (acc. 2005-03-21).
http://www.gisdevelopment.net/application/natural_hazards/floods/nhcy0005a.htm

11. Flash Flood North-Western states, UN Developmental programme, 04 Aug 2004, Relief webpage, (acc.2004-10-12). http://www.reliefweb.int/w/rwb.nsf/unid/2a02222

12. Goodchild, M.F The state of GIS for Environmental Problem Solving, In: Goodchild, M.F., Parks, B. and Steyaert, L., Editors, 1993. Environmental modelling with GIS, Oxford University Press, New York, USA, pp. 147–167.

13. HBV-model Hydrologiska Byråns Vattenbalansavdelning, Swedish Metrological and Hydrological Institute,SMHI webpage, (acc. 04-06-21). http://www.smhi.se/foretag/m/hbv_demo/html/welcome.html

14. Jalaluddin Md. Abdul Hye, Principal Specialist, Surface Water Modelling Centre, Integration Of 3s And Mathematical Modelling In Disaster Mangement In Bangladesh (acc. 2005-04-15).
http://www.bytesforall.org/8th/DMBSeminar.PDF

15. Jiqun Zhang, Kaiqin Xu1, Masataka Watanabe, Yonghui Yang & Xiuwan Chen, Estimation of river discharge from nontrapezoidal open channel using QuickBird-2 satellite imagery, Hydrological Sciences–Journal–des Sciences Hydrologiques, 49(2) April 2004

16. John S. Gierke, Engineering Applications in the Earth Sciences: River Velocity, Michigan Technical University, 1 August 2002, Michigan Tech webpage, (acc.2004-10-15).
http://www.cee.mtu.edu/peacecorps/documents_novmeer_02/use_of_manning_equation_for_measuring_river_velocity.pdf

17. Joy Sanyal and Xi Xi Lu, Application of GIS in flood hazard mapping: A case study of Gangetic West Bengal, India, GIS development webpage,(acc.2004-10-11).
http://www.gisdevelopment.net /application/natural_hazards/floods/ma03138a.htm

18. Integrated Flood Risk Management in England and Wales Jim W. Hall1; Ian C. Meadowcroft 2; Paul B. Sayers3; and Mervyn E. Bramley4 (acc. 2005-03-06).
http://www.cen.bris.ac.uk/civil/staff/jwh/Publications/NHR4.pdf

19. Lavakare Ajay, (1997), GIS & Risk Assessment- Map India Conference, RMSI webpage, (acc.2004-04-10).
http://www.rmsi.com/PDF/gis&riskassessment.pdf

20. Lorena Montoya, Geo-data acquisition through mobile GIS and digital video: an urban disaster management perspective, Environmental Modelling & Software, Volume 18, Issue 10, December 2003, Pages 869-876,

21. Maidment, D.R., 1993. GIS and hydrological modelling. In: Goodchild, M.F., Parks, B. and Steyaert, L., Editors, 1993. Environmental modelling with GIS, Oxford University Press, New York, USA, pp. 147–167. (acc. 2005-04-05).

22. Martin Häggström, Norrköping, SMHI (1990), Application of the HBV model for flood forecasting in six Central American rivers.

23. Mr. Falak Nawaz , Mr. Mohammad Shafique, Data integration for flood risk analysis by using GIS/RS as tools, GIS development webpage, (acc.2004-10-11).
http://www.gisdevelopment.net/application/natural_hazards/floods/ma03032c.htm

24. M. Morin, J. Jenvald and M. Thorstensson, Computer-supported visualization of rescue operations, Safety Science, Volume 35, Issues 1-3, June 2000, Pages 3-27,

25 Nirupama, Role of remote sensing in disaster management, ICLR webpage, (acc. 2004-04-21).
http://www .iclr.org/pdf/Niru_report%20Simonovic.pdf

26 Ooded Areas, P. A. Brivio, R. Colombo, M. Maggi & R. Tomasoni, Integration of remote sensing data & GIS for accurate mapping of flooded area, San Francisco State University webpage, (acc. 2004-08-03).
http://bss.sfsu.edu/ehines/geog815/gis_rs%20article.pdf

27. Översiktlig översvämningskartering längs Motala ström- sträckan från Vättern till Bråviken Projekt: Översiktlig översvämningskartering Rapport 17, 2001-03-27 Räddningsverket.

28. Plate, Erich J. (2002) Flood risk and flood management, Journal of Hydrology, Volume 267, Issues 1-2, pages 2-11

29. Rego, A.J. (2001) National Disaster Management Information Systems & Networks: An Asian Overview, Asian Disaster Preparedness Centre webpage, (acc. 04-09-27). http://www.adpc.net/infores/adpc-ocuments/ paperatgdin01.pdf

30. Sanner, Håkan, Application (1994), of the HBV model to the upper Indus River for inflow forecasting to the Tarbela Dam, (SMHI hydrology, 48).

31. Shanker Kumar Sinnakaudan, Aminuddin Ab Ghani, Mohd. Sanusi S. Ahmad and Nor Azazi Zakaria, Flood risk mapping for Pari River incorporating sediment transport, Environmental Modelling & Software, Volume 18, Issue 2, March 2003, Pages 119-130.

32. Sofia Fogelberg (2003), Modelling Nitrogen Retention at the Catchment scale: Comparison between HBV-N and MONERIS.

33. Srikantha Herath: Geographical Information Systems in Disaster Reduction (acc. 2005-04-09). http://www.adrc.or.jp/publications/Venten/HP/Paper(Herath).htm

34. The Earth in Our Hands: Flooding – Geological Society of London, June 2001, (acc.2004-06-23) http://www.geolsoc.org.uk/pdfs/floods_aw.pdf

35. THOMAS J. COVA and RICHARD L. CHURCH (1997): Modelling community evacuation vulnerability using GIS (acc. 2005-03-03). http://www.geog.utah.edu/~cova/cova-church-1997.pdf

36. Yang, Xihua (2001) Predicting flood inundation and risk using geographic information system and hydrodynamic model: a technical report on the case study at Eskilstuna / Xihua Yang, Anders Grönlund and Solgerd Tanzilli, Gävle: Gävle GIS Institute, 2001 Extent: 34 s.

37. SRV,Räddningsverket (2001) Outline of areas under risk of flooding Motala Ström River basin. ”Översiktlig översvämningskartering längs Motala ström- sträckan från Vättern till Bråviken Projekt: Översiktlig översvämningskartering Rapport 17, 2001-03-27 Räddningsverket.

Pseudo-realistic and Analytical 3D Views – Conditioned Information for Security Scenarios

Dirk Tiede* & Stefan Lang

Centre for Geoinformatics (Z_GIS), University of Salzburg, Schillerstr. 30, 5020 Salzburg, Austria

* dirk.tiede@sbg.ac.at

Workflow for conditioned information

A general workflow for high standard information delivery has been outlined by Lang et al. 2006a. It foresees automatic transformation of imaged scenarios into policy-relevant information, being itself embraced (and triggered) by the decision support chain. Starting from situation analysis and needs assessment it provides targeted information, conditioned for decision support. The workflow comprises techniques of data integration, image pre-processing, feature extraction and object-based class modelling, accommodating a series of algorithms and methods exchanged in the GMOSS network and provided by different partners.

The workflow includes two further crucial elements, i.e.,

- spatial analysis of the extracted raw information (quantification, statistics and spatial dis-/aggregation etc.); and
- dissemination and communication using 3D visualization techniques (Tiede & Lang, 2007).

With respect to the latter we differentiate between two different product types, depending on the objectives or context of use: (1) Pseudo-realistic visualization aims at providing a 'true' depiction of e.g. a certain crisis area, complemented by figures, graphs and numbers describing the situation quantitatively. This may be used to directly support relief actions or other fine-scale operations (cf. Lang et al 2006a and 2006b). (2) Analytical 3D views display analytical items, and communicate scientific results, in a familiar context. We use virtual globes as tools for seamless combination of 3D enabled and geo-referenced data. Freely available virtual globes with HSR contextual data enable disseminating analytical information derived EO data to a broad audience. Analytical 3D views are information layers on different spatial aggregation levels (administrative units or regular units like grids, hexagons etc.) using extrusion as a means for displaying the crucial spatial information (Tiede & Lang, 2007).

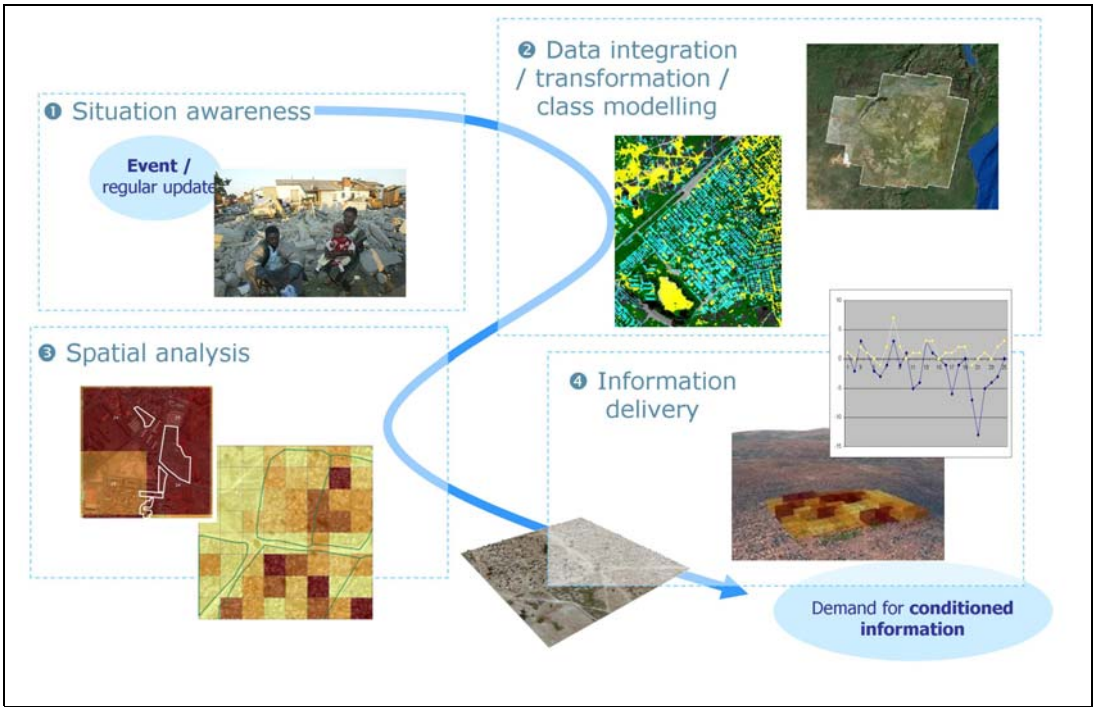

Fig. 1: Workflow for conditioned information (Lang et al., 2006a, modified)

Security scenarios

The following security scenarios were used to test, apply and validate 3D visualisations in the context of GMOSS.

- Refugee camp Goz Amer / Eastern Chad (Lang et al., 2006a), hosting people mainly originating from the Darfur/Sudan crisis (2004: about 18,000 inhabitants), prevailing dwelling structures: tents of different types and simple shelters;
- Refugee Twin-Camp Lukole A+B / Western Tanzania (Lang et al., 2006b), hosting mainly refugees from Burundi (2005: about 50,000 inhabitants), dwelling structures predominantly semi-permanent (little huts, even houses), but presently structures are bieng dismantled;
- Demolitions in Zimbawe due to government operation Murambatsvina between 2004 and 2005 (see Schöpfer et al., 2007; Lang et al, this volume; Rama et al., this volume)
- GNEX 2006, GMOSS near-real time exercise, scenario ‘population affected by contamination plume expelled by leaking nuclear power plant’
- GNEX 2007, scenario ‘damage assessment and influenza hazard in refugee camp’

Pseudo-realistic 3D representations

Pseudo-realistic 3D representations may be used to directly support relief actions or other fine-scale operations, providing a detailed overview about the situation which may be expected at place. The idea is to enrich the portfolio for security scenarios beyond ordinary 2D maps and reveal a better impression with more self explaining information, especially to people who are not experienced in reading maps (cf. Lang et al. 2006a).

In this paper we present two examples using pseudo-realistic 3D representations for both of the refugee camps mentioned above: (1) Goz Amer using QuickBird imagery from 12/2004,

pansharpened, 4 bands, 0.6 m GSD; (2) Lukole camps A & B using Ikonos imagery from 09/2000, panchromatic, 1 m GSD and multispectral, 4 bands, 4 m GSD).

The outlined workflow had to fulfil specific requirements concerning information extraction from the VHSR images, including among others: (1) Anchor points of the relevant dwelling structures had to be obtained from centroids of the extracted objects,holding attribute information about the dwelling type and main orientation (both camps exhibit semi-permanent, regular structures in terms of dwelling arrangements); and (2) land cover classification as context information (bare soil, vegetated areas, and single trees).

For a pseudo-realistic representation of dwelling structures, a 3D symbol library was created which contains different dwellings representing the dominant dwelling types in the respective camp (figure 2).

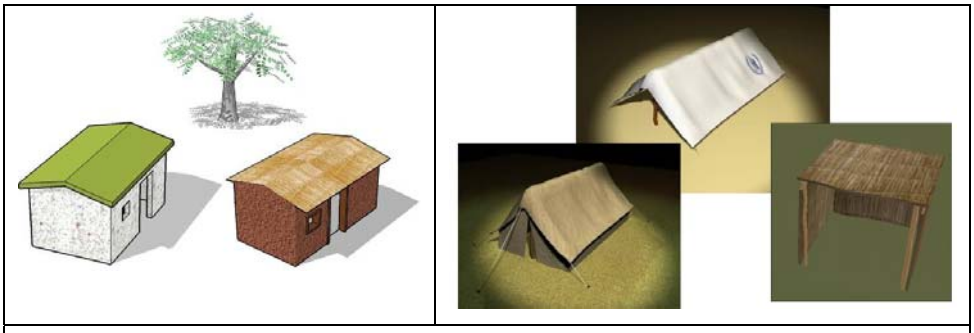

Fig. 2: 3D symbol libraries for the refugee camps Lukole (left) and Goz Amer (right), representing the dominant dwelling types (Lang et al., 2006a, 2006b)

The 3D symbols were designed and constructed in Autodesk 3D Studio Max and Google Sketchup, using photo documentation material of the camp. The limited number of dwellings types (two to three) in these examples reduces the effort for creating such a symbol library.

The 3D symbols were then linked with the extracted dwelling structures from the EO data and automatically adjusted according to the main direction of the extracted dwelling object. Auxiliary data like terrain height information from SRTM (Shuttle Radar Topography Mission) and additional satellite imagery were integrated. The resulting scene is a real-time visualisation in a 3D GIS environment (here: ArcScene, ESRI), enabling the users to change between different perspectives, navigate in the third dimension and easily create and export pre-rendered animation (Figure 3). It is a highly flexible 3D scene: data can be changed easily, the integration of new or updated information is possible and it enables the use of GIS analysis functions.

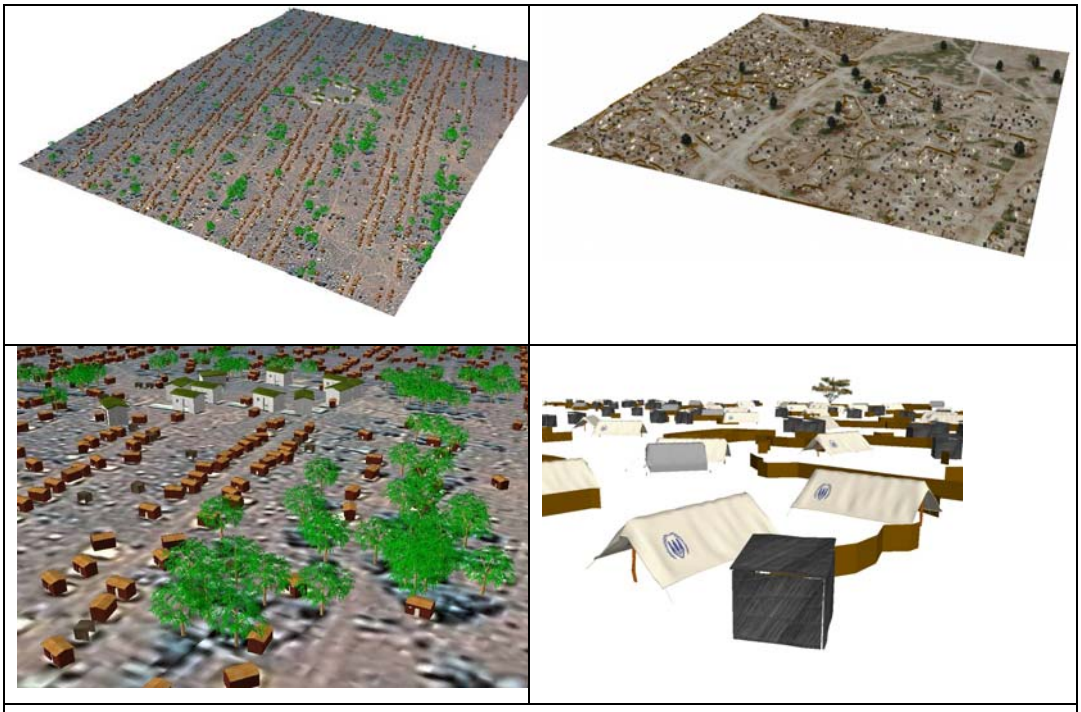

Fig. 3: Pseudo-realistic 3D representations of the refugee camps Lukole (left) and Goz Amer (right), (Lang et al., 2006a,2006b).

Pseudo-realistic 3D representations can also be integrated into different globe viewers. Figure 4 shows exemplarily the integration in ArcGlobe. But also free available virtual globe clients (like ArcGIS Explorer or ArcReader) could help to overcome problems of information dissemination due to restrictions in software licensing.

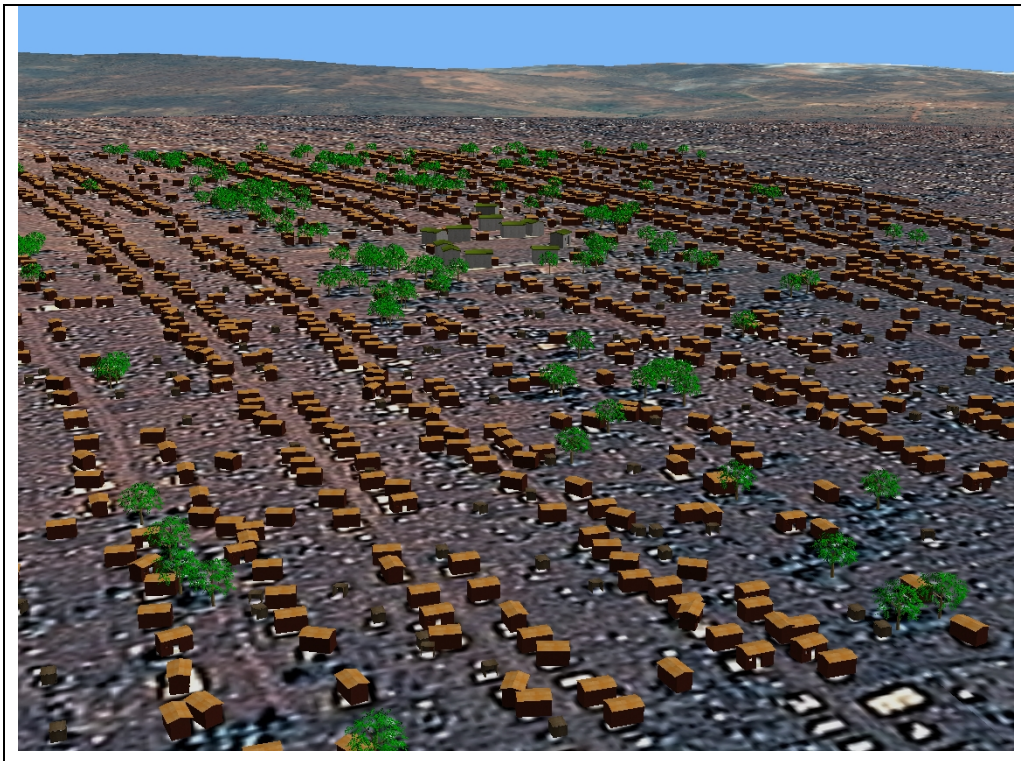

Fig. 4: Pseudo-realistic 3D representation of the refugee camp Lukole in a virtual globe environment (here: ArcGlobe with integrated Ikonos imagery)

Analytical 3D views

In contrast to the pseudo-realistic 3D representations, analytical 3D views (A3Vs) are information layers on different spatial aggregation (administrative or regular, constructed units like grids, hexagons etc.). Extrusion is used as a means for displaying the crucial spatial information through height (Tiede & Lang, 2007). A3Vs are made available in an adequate mode, depending on the envisaged virtual globe software used for publishing (data formats like *kml/kmz*, ESRI *multipatch*, extruded *shapefile* etc. can be chosen).

The extracted information from the VHSR images is post-processed using GIS analysis techniques like dasymetric mapping and the LIST extension for ArcGIS (ESRI). LIST (Landscape Interpretation Support Tool, Schöpfer and Lang 2006) provides algorithms for object quantification, object (dis-)aggregation and object-based change analysis. The third dimension of the final layers (extrusion value) is used as an additional information carrier, representing the respective aggregated variable being measured. Produced A3V layers can be used in different virtual globes (like Google Earth, NASA World Wind, ArcGIS Explorer etc.). In this case the virtual globes not only function as a visualization tool – they also provide the contextual information via the targeted virtual globe provider using a web stream. Therefore the amount of data for the delivery of conditioned information is kept very small.

In the following examples of the GMOSS test cases, as well as both GNEX exercises 2006 and 2007, regular grid cells and hexagon units are used as (dis-) aggregation basis for meaningful information delivery.

GNEX06 - Real-time exercise

In this faked crisis scenario teams across Europe were asked to reply within 33 hours to a fictitious information request by the European Commission on a nuclear leakage scenario. Satellite imagery as well as auxiliary geo-information were provided to the teams, from which up to date information on infrastructure, urban areas and land cover should be extracted and provided.

One of the goals was the estimation of affected population: By dasymetrically mapping utilizing (1) information of population figures on municipality level and (2) a land cover classification based on SPOT 5 data the population distribution in the fictitious plume of radio-active contamination could be estimated. Figure 5 shows the A3Vs in ArcGIS Explorer using a *multipatch shapefile* and in Google Earth using a *kml* file (plus a html based legend).

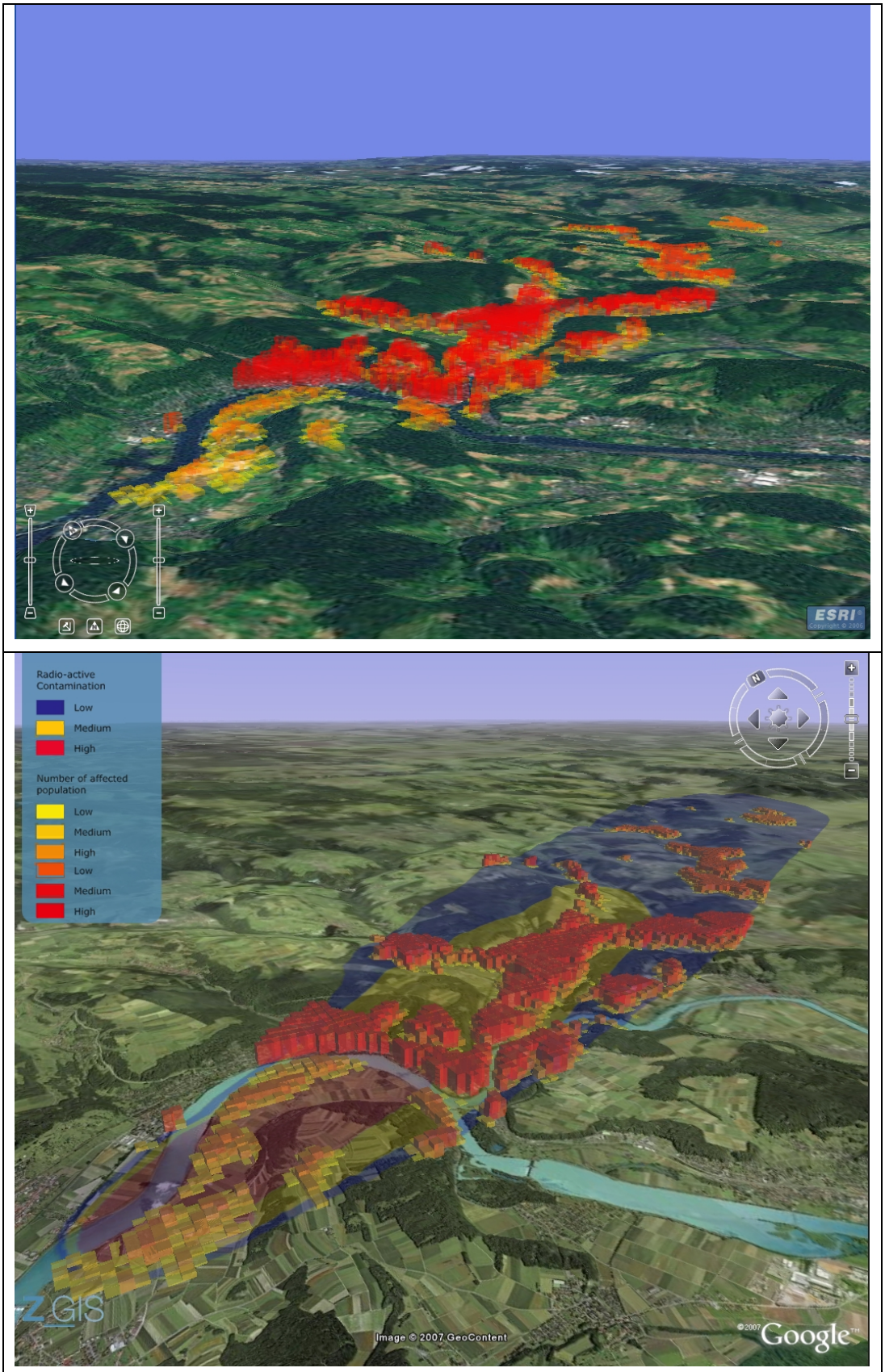

Fig. 5: Top: Dasymetrically mapped population density (multipatch shapefile) in ArcGIS Explorer. Below: The same analytical 3D view as kml file in Google Earth with underlying fictitious plume of radio-active contamination (from Tiede & Lang, 2007, modified)

GNEX07 - Real-time exercise

The GNEX07 exercise was the second near real time exercise within GMOSS. In a fictitious scenario a refugee camp in the country ‘Albenon’ has been severely damaged in the course of an armed conflict and refugees escaped to a neighbouring camp. When the refugees returned they were confronted with destroyed housing and sanitation facilities, including broken water and sewage networks. This has lead to first cases of watery diarrhoea and cholera. On top of this a severe influenza epidemic is affecting the camp and starts spreading into the country. The government of 'Albenon' has asked the European Commission for relief support and the Commission tasked the GMOSS team to provide satellite based crisis information to support the decision making (source: DLR, www.dlr.de).

Again, one of the goals was the estimation of population in the camps. The A3V in figure 6 shows the aggregation of automatically extracted houses in the refugee camp ‘Fy Ganub’ on hexagon units and visualized in Google Earth.

Fig. 6: Extracted houses in the refugee camp Fy Ganub (fictitious name, according to the specification of the real-time exercise) aggregated on hexagon units (hexagon diameter: 70 m) and visualized in Google Earth.

Zimbabwe

QuickBird data from August 25, 2004 and June 22, 2005 was used for object-based change detection in urban areas of Harare. The methodology aims for a fast change indication on a higher level, i.e. a kind of ‘pre-screening’ of the image to facilitate further change detection inspections. The results are aggregated to 500 m x 500 m raster cells and visualized according to the standard deviation of urban change per cell which reflects a higher probability of change (cf. Schöpfer et al. 2007)

Figure 7 shows the resulting analytical 3D view as *kml kmz* file in Google Earth. Darker shades indicate areas with a higher probability of destruction whereas brighter cells represent areas with minor to no change of urban area between 2004 and 2005 (see also the legend which is implemented in Google Earth via html). The idea of visualizing changes in this way is to support rapid mapping (avoiding time consuming pre-processing). The detection of likely affected areas should help to focus on these areas for further interpretation and critical review.

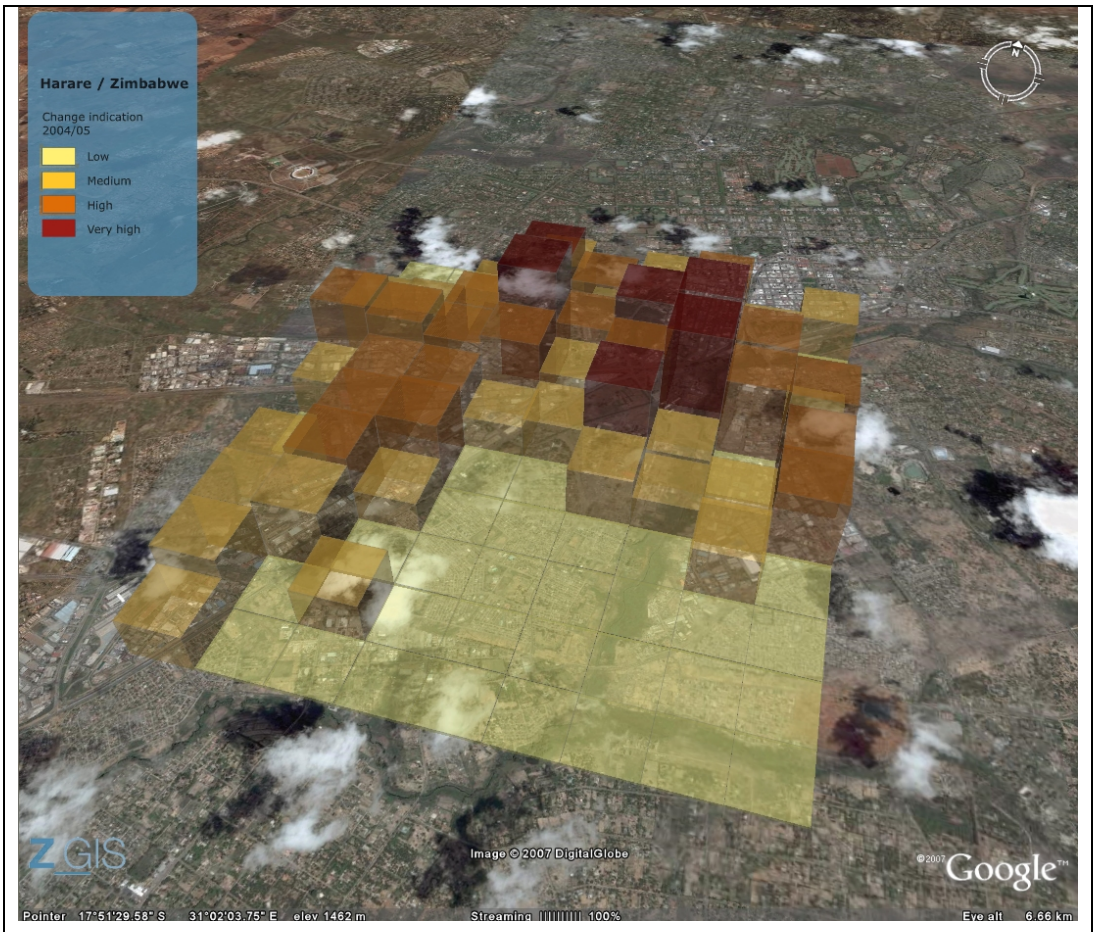

Fig. 7: Visualization of change by means of analytical 3D views in Google Earth: Ninety grid cells indicating change in Harare / Zimbabwe between 2004 and 2005 (cf. Schöpfer et al. 2007).

Lukole refugee camp, Tanzania

The analytical 3D view shows aggregated dwelling units for the whole Lukole A+B camp. The dwelling units were aggregated to 100 m x 100 m grid units. The extrusion height reflects the estimated population figure per cell. In this case data were made available in Google Earth. The contextual information which is delivered by Google (in this case by means of a QuickBird image) was captured more recently than the satellite image used for the dwelling extraction. In this case, this supports visual change detection, but at the same time it highlights the importance of metadata to be attached to the 3D layer.

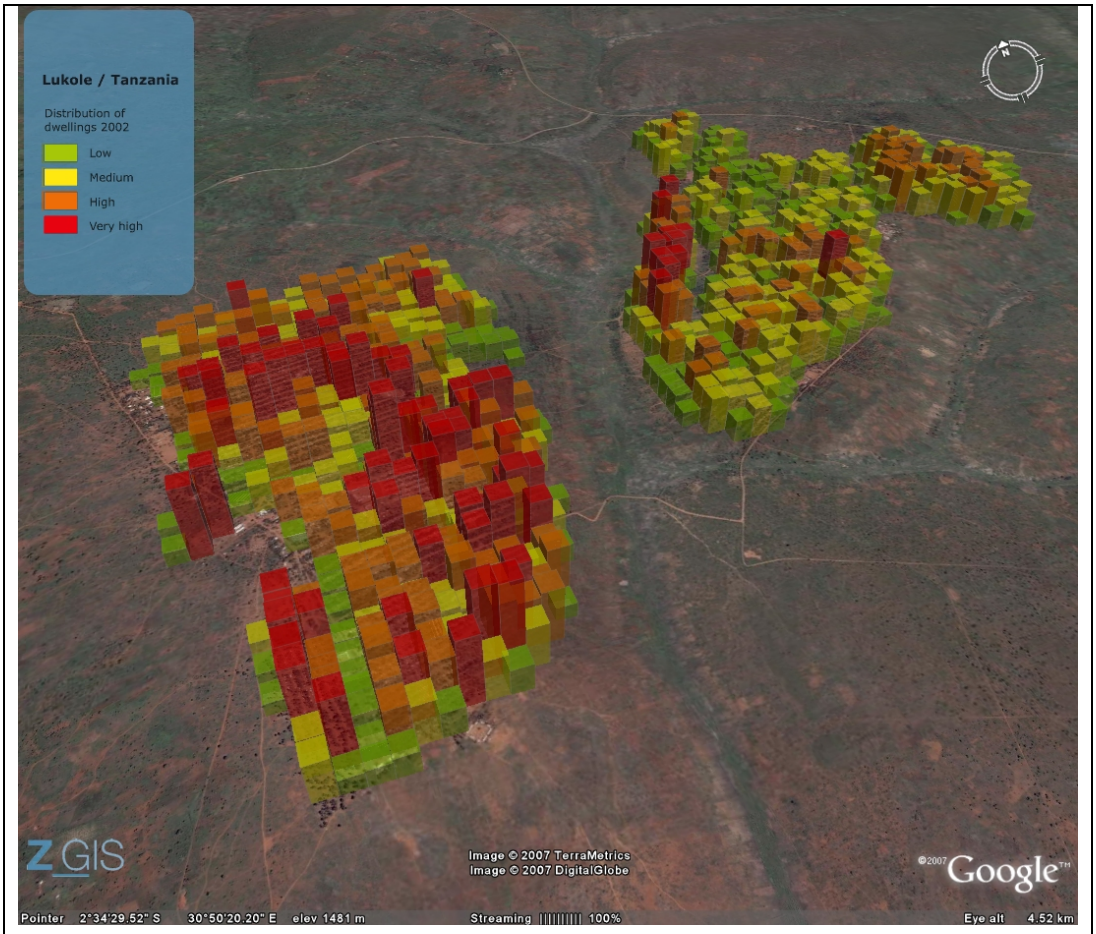

Fig. 8: Lukole refugee camp / Tanzania: Density of dwelling units (dwellings are aggregated to 100 m x 100 m grid cells), visualized in Google Earth

References

Lang, S., D. Tiede and F. Hofer(2006a): Modeling ephemeral settlements using VHSR image data and 3D visualisation – the example of Goz Amer refugee camp in Chad. In: PFG - Photogrammetrie, Fernerkundung, Geoinformatik, Special Issue: Urban Remote Sensing, 4/2006, 327-337.

Lang, S., D. Tiede and G. Santilli (2006b): Varying sensors and algorithms – an information delivery approach for population estimation in African refugee camps. In: 6th African Association of Remote Sensing of the Environment Conference (AARSE), Oct 30 - Nov 2, Cairo, Egypt.

Schöpfer E and S. Lang (2006): Object fate analysis – a virtual overlay method for the categorisation of object transition and object-based accuracy assessment. In: International Archives of Photogrammetry, Remote Sensing and Spatial Information Sciences, Vol. No. XXXVI-4/C42, Salzburg, Austria

Schöpfer, E., D. Tiede, S. Lang and P. Zeil (2007): Damage assessment in townships using VHSR data - The effect of Operation Murambatsvina / Restore Order in Harare, Zimbabwe. Urban Remote Sensing Joint Event. Paris 2007, CD-ROM

Tiede, D. and S. Lang (2007): Analytical 3D views and virtual globes – putting analytical results into spatial context. ISPRS, ICA, DGfK - Joint Workshop: Visualization and Exploration of Geospatial Data, Stuttgart

Implementation of Geographic Information and Geographic Information Systems in municipal Emergency Management

Michaël Le Duc[1]* & Åke Sivertun[2]

[1] *School of Business, Mälardalen University, Box 883, 721 23 Västerås, Sweden*

[2] *Department of Computer and Information Science, Linköpings University, 581 83 Linköping, Sweden*

* michael@leduc.se

Introduction

This paper concerns Emergency Management (EM) for local government in Sweden especially regarding support from Geographic Information (GI) and Geographic Information Systems (GIS).

The main *questions* are: (1) How can municipalities implement the use of GI and GIS for EM effectively? (2) How can risk analysis be implemented with a special focus on support from GI and GIS?

Theoretical framework

Emergency Management in local and regional government is a complex phenomenon that can be investigated with many perspectives. The implementation and use of GI and GIS in local government are nowadays also complex phenomena with many agents involved having varying background, knowledge, responsibilities and tasks. The combination of GI, GIS and EM is thus even more challenging, e.g., that the EM cycle (preparedness, response, recovery, and mitigation) works effectively and efficiently. Stallings (2002) denotes the aforementioned phases of the EM cycle as "activity clusters" or "patterns of behavior", which is fruitful to encompass their complex nature.

A theoretical framework was devised related to the diffusion and adoption of innovations as well as implementation of GIS and similar technologies in organizations. The elements on adoption of innovation stem mainly from the work of Everett M. Rogers (1995), which is supported by many scientific empirical studies, in the thousands according to Rogers (2005), during decades of research. We also have added other relevant factors from the literature and our experience, including the experience of the Swedish Land Survey.

Adoption of innovations

The part of the theoretical framework included in this section is mainly based on a conference article on Innovation Management in Computer Software and Services (Le Duc, 2000). According to Rogers (1995, p. 11) "an *innovation* is an idea, practice, or object that is perceived as new by an individual or other unit of adoption". Rogers (1995, p. 10-11) defines *innovation diffusion* as "the process by which an *innovation* is *communicated* through certain *channels* over *time* among the members of a *social system.* The four main elements are the innovation, communication channels, time, and the social system …". The diffusion process over time for a successful innovation typically forms an S-shaped curve (Foster, 1986) with

slow adoption in the beginning and faster adoption in the middle leading to saturation where the adoption level stabilizes. When an innovation is no longer useful it is typically replaced by a better alternative, however not always in a complete manner.

Adoption is a key concept in the innovation literature. Rogers (1995) also terms it the innovation-decision process, which "is the mental process through which an individual (or other decision-making unit) passes from first knowledge of an innovation to forming an attitude toward the innovation, to a decision to adopt or reject, to implementation of the new idea, and to confirmation of this decision." In other words, Rogers (1995) conceptualizes five steps in the adoption process: (1) knowledge, (2) persuasion, (3) decision, (4) implementation, and (5) confirmation.

Rogers (1995) has identified *five pivotal characteristics* that determine the adoption of an innovation. (1) *Relative advantage* is the degree to which an innovation is perceived by a potential adopter as being better than the idea it supersedes. (2) *Compatibility* "is the degree to which an innovation is perceived as consistent with the existing values, past experiences, and needs of potential adopters". (3) *Complexity* concerns the degree to which an innovation is perceived as relatively difficult to understand and use. (4) *Trialability* has to do with how much the potential adopter can experiment with the innovation. (5) *Observability* is associated with the degree to which the results of an innovation are visible or communicated to others.

The innovation adoption process in the area of software and information systems has been analyzed extensively in the research literature, e.g., Cooper and Zmud (1990), Lai and Mahapatra (1997), Wildemuth (1992), Barnett and Siegel (1988) and, Chengalur-Smith and Duchessi (1999).

Other dimensions in the software adoption process within an organization often mentioned is the role of top management support, the role of innovative champions (Beath, 1991), available slack resources, etc.

Research in GI and GIS that has used an innovation perspective for implementation in organizations includes Budic and Godshalk (1994), Cavric et al. (2004), Nedovic-Budic (1997), Nedovic-Budic (1998), Nedovic-Budic and Godschalk (1996), Chan and Williamson (1999a) and Chan and Williamson (1999b).

Further implementation principles

In the GIS area, Campbell (1992) and Obermeyr (1990) can be of further interest regarding implementation.

Therese Söderman in her bachelor's thesis at Mälardalen University (Söderman, 2000) investigated facilitating and inhibiting factors regarding implementation of GIS in municipalities. Michael Le Duc was her supervisor and provided her with literature but she also found other interesting sources. Therese Söderman created a model based on literature with the following factors.

Table 6. Success factors and obstacles for implementation of GIS in municipalities. Source: Söderman (2000)

Success factors	***Obstacles***
• Attitude of management • Availability of GIS database to the organization • Users' motivation	• Lack of appropriate knowledge among the personnel • Lack of understanding among decision makers • Cost of data

• User satisfaction • Education and training • System use • How fast implementation generates tangible benefits • Standardized systems • The existence of an IT strategy where GIS is included • Standardized data • How fast utilization is diffused in the organization • How quickly data is captured • The existence of needs and requirements analysis with user participation • The use of cost-benefit analysis before and after implementation	• Lack of coordination among the organizations • Cost of software and hardware • Software difficult to use • Lack of data • Lack of access to other organizations' data • Insufficient quality of data • Inadequacy of data

Methodology

Semi-structured telephone interviews were performed with municipalities. The aim with a qualitative method such as semi-structured telephone interviews is to generate rich information including information to add elements to and eventually revise the theoretical framework used.

Sampling of respondents, questionnaire and presentation of results

A qualitative sampling strategy was used combining different principles, including to sample by size, variation (risks for flooding, heavy sea traffic with oil tankers, proximity to nuclear plant, etc.) and opportunity, e.g., some potential respondents were difficult to reach. We performed interviews or obtained information by e-mail with two groups of respondents (1) Municipal GIS coordinators, or professionals with the equivalent function (questionnaire with 27 questions) and (2) Emergency Preparedness Officers, or professionals with the equivalent function (questionnaire with 19 questions).

We chose to present the results without the names of the municipalities and individuals so people could speak openly as well as for security reasons.

Critique of method

One weakness in the data collection procedure is that we could not obtain information from both GIS coordinators and Emergency Preparedness Coordinators in some municipalities. In addition, some professionals responded by e-mail. Furthermore, a larger sample would have yielded higher validity. We also limited the number of questions in the questionnaires to avoid putting too high demands on the respondents. A mail survey using appropriate statistical sampling would have yielded more statistically precise and valid data.

Interview results

We report some findings in this article and refer to our project report for more comprehensive data and analyses. Only the emergency management officers' responses are reported here due to space limitations.

Some respondents work in a fire and rescue services federation, thus representing several municipalities. In addition, some questions were not answered or asked. If a respondent said that he or she did not know much on the questionnaire's topic there was no point in asking all the questions.

To keep track of the specific statements and items the following table is used to link the data we use internally. Furthermore, these codes will enable the reader to see patterns more clearly in the data.

Table 7. Municipalities, Federations of Fire and Rescue Services (*) and respondent codes.

*: two persons answered.

Municipality or federation of FRS	*Number of inhabitants (approx.)*	*GIS Coordinator or similar*	*Emergency Preparedness Coordinator or similar*	*SALAR code*	*SALAR category*
Municipality A	90.000	LC_AG	LC_AS	3	Large cities
Municipality B	90.000		LC_BS¤	3	Large cities
Municipality C	>200.000	Metro_CG	Metro_CS1 Metro_CS2	1	Metropolitan municipalities
Municipality D	120.000	LC_DG	LC_DS	3	Large cities
Municipality E	70.000		LC_ES	3	Large cities
Municipality F	80.000		Sub_FS	2	Suburban municipalities
Municipality G	120.000		LC_GS1 LC_GS2	3	Large cities
Municipality H	50.000	Other25_HG		7	Other municipalities, more than 25,000 inhabitants
Municipality I	>200.000	Metro_IG		1	Metropolitan municipalities
Municipality J	80.000	LC_JG		3	Large cities
Municipality K	50.000	Other25_KG	Other25_KS	7	Other municipalities, more than 25,000 inhabitants
Municipality L	110.000	LC_LG	LC_LS	3	Large cities
Municipality M	55.000	LC_MG		3	Large cities
Municipality N	130.000	LC_NG	LC_NS	3	Large cities
Municipality O	30.000	Other25_OG		7	Other municipalities, more than 25,000

					inhabitants
FRS federation P	105.000		FFRS_PS	*	*
FRS federation Q	190.000		FFRS_QS	*	*

In the final column, the code for municipality type is noted according to the classification of The Swedish Association of Local Authorities and Regions (SALAR). The SALAR classification of municipalities, as of January 1, 2005, (Bengtsson, 2004) divides the municipalities into nine categories on the basis of structural parameters such as population, commuting patterns and economic structure. We present only the used classes' definitions. The categories of municipalities are: (1) *Metropolitan municipalities* (3 municipalities), i.e., municipalities with a population of over 200,000 inhabitants; (2) *Suburban municipalities* (38 municipalities), i.e., municipalities where more than 50 per cent of the nocturnal population commute to work in another area. The commonest commuting destination is one of the metropolitan municipalities; (3) *Large cities* (27 municipalities), i.e., municipalities with 50,000-200,000 inhabitants and more than 70 per cent of urban area; (4) *Commuter municipalities* (41 municipalities); *(5) Sparsely populated municipalities* (39 municipalities); *(6) Manufacturing municipalities* (40 municipalities); *(7) Other municipalities, more than 25,000 inhabitants* (34 municipalities), i.e., municipalities that do not belong to any of the previous categories and have a population of more than 25,000; *(8) Other municipalities, 12,500-25,000 inhabitants* (37 municipalities); *(9) Other municipalities, less than 12,500 inhabitants* (31 municipalities).

The respondent code is constructed as follows. The first part of the code indicates the type of municipality (LC = Large city; Metro = Metropolitan municipality, etc.). The last letter is used to indicate if the person is working with EM (S) or GIS (G). In the middle is the town code from A to Q in alphabetical order. FFRS represents Federation of Fire and Rescue Services.

Interviews with municipal Emergency Preparedness Officers and similar occupations

Approx. 14 government officials in EM were interviewed or responded through e-mail (six). Most had worked many years in the area (more than 10 years). In two municipalities, two persons responded.

We asked to what extent GIS is used in the municipality. See table 3 for answers and comments below the table.

Table 8. Stated extent of GIS use in general. 1= small extent, 5 = large extent

***** respondent answers for several municipalities

Possible answers	*Number of answers per alternative*	*Respondents*
1	1	FFRS_QS
2	1	FFRS_PS*
3	3	LC_AS OTHER25_KS FFRS_PS

4	9	Metro_CS2 SUB_FS LC_ES LC_DS LC_GS1 LC_GS2 FFRS_PS* FFRS_PS* LC_NS
5	3	LC_BS LC_LS Metro_CS1

Comments included that the extent of GIS use varies between different municipal departments (LC_ES). In addition, GIS is implemented in many other applications (SUB_FS). The technical departments use GIS extensively, while the "soft" departments lag behind said a person who also has worked as a GIS coordinator for three years (OTHER25_KS).

We also asked to what extent GIS is used for risk and vulnerability analysis. See table 4 for answers and comments below the table.

Table 9. Stated extent of GIS use for risk and vulnerability analysis. 1= small extent, 5 = large extent

*: respondent answers for several municipalities

Possible answers	*Number of answers per alternative*	*Answers*
1	5	OTHER25_KS LC_DS LC_GS1 FFRS_QS SUB_FS
2	5	LC_BS Metro_CS2 FFRS_PS* FFRS_PS* FFRS_PS*
3	4	LC_ES LC_LS LC_GS2 Metro_CS1
4	-	
5	1	FFRS_PS*
Don't know	1	LC_NS

One noteworthy comment was that "We do not use GIS at all. The system Geosecma is not suitable for those purposes." (OTHER25_KS) "GIS is like a heavy truck without wheels" (OTHER25_KS).

Regarding which geographic information is used in risk and vulnerability analysis we obtained diverse answers. On a general level, base maps, risks, transportation, Fire and Rescue Services, hydrology, and population were mentioned. One municipality is more advanced (Metro_CS2) using a 3D primary map with pipes and wires, property information, etc.

One reason that GI is abandoned is if the information is not updated (LC_BS). The lack of money and resources are obstacles (FFRS_PS). In one case, the system was difficult to use so the project was cancelled (LC_ES**).**

Usability problems were mentioned, including that if you seldom use the system that can create problems (LC_ES); technical skills are required to find information (LC_AS); the personnel want help continuously by GIS expertise (FFRS_PS); it is difficult to assess the quality of the information. "With GIS you can get anything" (LC_LS).

We asked to what extent geographic information and GIS are compatible with how the municipalities work with risk and vulnerability analysis. Indicators are presented in the table 5 below.

Table 10. Extent of compatibility between GI and GIS and risk and vulnerability analysis.

1= small extent, 5 = large extent

Possible answers	*Number of answers per alternative*	*Respondents*
1	-	-
2	-	-
3	1	LC_LS
4	5	LC_DS LC_GS2 Metro_CS2 LC_ES Metro_CS1
5	1	FFRS_QS
Don't know	5	SUB_FS OTHER25_KS LC_NS LC_GS1 LC_BS

We also asked if the respondents have experienced problems with the complexity of geographic information and GIS in relation to the users. Five respondents answered "yes" (LC_AS, Metro_CS2, OTHER25_KS, LC_GS2, LC_ES), six responded "no" (LC_NS, LC_LS, LC_DS, SUB_FS, FFRS_QS, Metro_CS1) while a few did not know (LC_GS1, LC_BS). Furthermore, "as I have said earlier, if you don't use GIS so often, you can experience the problems mentioned" (LC_ES).

One very clear pattern is that the professionals considered vendors to have a very limited influence on their decisions.

We further asked through which information channels the professionals learn of other's experience concerning risk and vulnerability analysis, geographic information and GIS. To reduce space requirements we skip the specific respondent information. Newspapers (2), Professional press (7), Magazines for members (-), Company information (2), Associations (3), Fairs (4), Seminars (7), Informal contacts (9), Education and training (4), Internal information (1) and Other channels (-) were selected.

We asked how adequate emergency preparedness can be assured with support of GI and GIS. Emergency Management Administration (EMA) that is well organized is needed, which means that all parties involved have *clear roles*. *Training* is also an element. In addition, you need to *plan* properly. EMA must work in day-to-day operations. In addition, you must clearly demonstrate benefits.

Discussion

Rich and complex information was obtained on the great variety of experiences and situations in the investigated municipalities and Federations of Fire and Rescue Services.

The aim of a qualitative method is to enable research to blend the unique and the general in the research area and generate new insights.

We must be careful in not generalizing the information obtained to other municipalities, other countries, other levels of EM, etc. In addition, for each municipality we have collected some opinions. More in-depth studies are required to obtain additional nuances, especially the time dimension, i.e., in case studies with multiple sources of information.

The innovation adoption perspective

GIS use varies in the different municipalities. However, the situation is decent (Table 3). On the other hand, GIS is used to a lesser extent for risk and vulnerability analysis, with ten answers below 3 (Table 4).

Education, training and exercises in the investigated area were mentioned many times as needed. In that context, incremental innovation might be the path to choose, e.g., to demonstrate simple tools and examples with GIS support.

A key dimension that can hinder adoption is if an innovation is not compatible with the potential adopters according to Rogers (1995). Table 5 contains two main groups. Seven professionals consider GI and GIS compatible with risk and vulnerability analysis, thus indicating that with time GIS adoption has the potential to increase for risk and vulnerability analysis. Five respondents do not know how compatible GI and GIS are with risk and vulnerability analysis (SUB_FS, OTHER25_KS, LC_NS, LC_GS1, LC_BS). The persons in this group have rated GIS use for risk and vulnerability analysis as low (LC_NS did not know), which is consistent with prior research. These professionals are probably early in what Rogers (2005) calls the knowledge phase of the adoption process without knowing if GIS is compatible with risk and vulnerability analysis. One interesting extreme in table 5 is the respondent from the Federation of Fire and Rescue Services Q rating compatibility of GI and GIS regarding risk analysis as high as 5. In table 4, the respondent FFRS_QS states that GIS use for risk and vulnerability analysis is very low (1). The FFRS Q is eager to get started as soon as possible. However, "the municipalities stop that initiative".

As noted by Jurison (1993) software adoption varies between users in the same organization. Different modules of a GIS can have different user groups. Tools based on Microsoft Excel and similar tools such as IBERO are used for risk and vulnerability analysis in the investigated municipalities. Simple innovations are more rapidly adopted than complex ones according to Rogers (1995). Incremental innovations are easier to adopt than radical innovations.

This analysis illustrates that a process perspective is relevant which includes a time dimension on the complex process of innovation adoption, including GI and GIS for risk and vulnerability analysis as well as other areas of emergency management.

Regarding the five pivotal characteristics that determine the adoption of an innovation by an individual or other decision-making unit, advantages and disadvantages with digital GI for risk and vulnerability analysis (*relative advantage*) are noted, with a slight dominance for negative statements. The problems include different coordinate systems used in the same organization, and quite a number of usability problems. The statements of municipality K's Emergency Preparedness Coordinator (Other25_KS) are extremely negative. They indicate clearly that there are problems of seeing the use for GI and GIS for risk and vulnerability analysis in some municipalities. *Compatibility* problems are noted. *Complexity* problems are also noted. "There is a lot to do in this area, to make systems user friendly, you have to improve that a lot" (LC_AS). *Trialability* does not seem to be significant with some exceptions like LC_ES and Metro_CS1. *Observability* is also of limited relevance, although four respondents thought that other municipalities' experience influenced their decision-making. Vendors had no influence whatsoever according to the respondents.

Implementation principles

First we discuss success factors.

Attitude of management is noted as important to succeed in implementing GI and GIS. This support varies. "It is difficult to create an understanding for GIS. You must show practical things. It is difficult to talk about GIS. However, with time the situation improves. We would need a special budget. Top management support is important." (OTHER25_OG).

Availability of GIS database to the organization is noted as paramount and problems are mentioned. For the two Federations of Fire and Rescue Services interviewed there are significant problems in this dimension. "We hope to plan an investment in a system." However, "municipalities don't give us data when we ask for them" (FFRS_PS).

Users' motivation is confirmed as a key factor. It seems that Emergency Preparedness Coordinators are less positive than GIS coordinators (data is in the full report). *User satisfaction*. In some cases, user satisfaction is low or even very low. There are however more positive statements and things are improving, e.g., with the emergence of web services. *Education, training and exercises* emerge as very important. This topic was mentioned many times by many respondents. *Standardized systems* and s*tandardized data*. Here we obtained mixed opinions. "If you mean ISO then it has not influenced us" (LC_MG). "We participate in standardization organizations" (METRO_IG). *The role of the champion/ champions* is confirmed to be important. "All is about champions. Without champions, nothing happens. It is important to find these champions". (METRO_IG).

Regarding obstacles some points are included here.

Lack of appropriate knowledge among the personnel. A majority of the GIS coordinators confirmed the problem. "Regarding crisis management and risk management there is great variation in knowledge and skills" (LC_NG). In some case, the problems are not associated with skills, rather the lack of resources (OTHER25_HG). *Cost of data*. Problems are noted

here, especially in FFRS. *Software difficult to use*. This has been extensively noted. If you seldom use the system that can create problems (LC_ES). *Lack of data* is a noted aspect.

Conclusions

The first main question of the project concerned how municipalities can implement the use of GI and GIS for EM. Collected data confirm many of the components of the theoretical framework.

The second question was similar to the first question and concerned specifically Risk and Vulnerability Analysis. GI and GIS support for Risk and Vulnerability Analysis is limited in many of the investigated municipalities. Maybe these components will diffuse in concert with other applications of GI and GIS in emergency management. For example, web services were mentioned as promising solutions to many of the existing obstacles.

The Swedish Land Survey and other central agencies for meteorology, geology, road information, etc., can play an important role in supporting municipal Emergency Management. This includes, according to the professionals' statements (GIS coordinators):

- Information, education and training material
- Education and training
- Web services
- Expertise support, e.g., for flood modeling and the analysis of landslide risks
- Products, data and maps

Project organization and acknowledgements

The project was funded by the Swedish Emergency Management Agency with management from the KRIS-GIS project at the Swedish Land Survey. Michaël Le Duc has performed the main research effort including project management, theory development, research design, main data collection, data analysis and report writing. Åke Sivertun has contributed with significant contacts and data collection as well as comments on the report.

Reference list

Barnett, G.A., and Siegel, G. "The Diffusion of Computer-Assisted Legal Research Systems," *Journal of the American Society for Information Science* (39:4) 1988, pp 224-234.

Beath, C.M. "Supporting the information technology champion," *MIS Quarterly* (15:3) 1991, pp 355-372.

Bengtsson, H. "Classification of municipalities, January 1 2005," Svenska kommunförbundet, Stockholm, 2004.

Budic, Z.D., and Godshalk, D.R. "Implementation and Management Effectiveness in Adoption of GIS Technology in Local Governments," *Comput., Environ. and Urban Systems* (18:5) 1994, pp 285-304.

Campbell, H. "The Impact of Geographic Information Systems on British Local Government," *Computers, Env. and Urban Systems* (16) 1992, pp 531-541.

Cavric, B.I., Nedovic-Budic, Z., and Ikgopoleng, H.G. "Diffusion of GIS Technology in Botswana: Process and Determinants," *International Development Planning Review* (25:2) 2003, pp 195-219.

Chan, T.O., and Williamson, I.P. "A Model of the Decision Process for GIS Adoption and Diffusion in a Government Environment," *Journal of the Urban and Regional Information Systems Association* (11:2) 1999a, pp 7-16.

Chan, T.O., and Williamson, I.P. "The different identities of GIS and GIS diffusion," *International Journal of Geographical Information Science* (13:267-281) 1999b.

Chengalur-Smith, I., and Duchessi, P. "The initiation and adoption of client-server technology in organizations," *Information & Management* (35) 1999, pp 77-88.

Cooper, R.B., and Zmud, R.W. "Information technology implementation research: A technological diffusion approach," *Management Science* (36:2) 1990, pp 123-139.

Foster, R.N. *Innovation: The Attacker's Advantage*, Summit Books, New York 1986.

Gummesson, E. *Qualitative Methods in Management Research. Revised edition.* Newbury Park: Sage Publications, 1991.

Jurison, J. "Adoption of OIS by four groups of office workers: An analysis from the perspective of innovation diffusion theory," SIGCPR '93. Proceedings of the 1993 conference on Computer personnel research, 1993, pp. 178-187.

Lai, V.S., and Mahapatra, R.K. "Exploring the research in information technology implementation," *Information & Management* (32) 1997, pp 187-201.

Le Duc, M. "Elements of Innovation Management in Computer Software and Services," Ninth International Conference on Management of Technology (IAMOT 2000), Miami, Florida, USA, 2000.

Nedovic-Budic, Z. "The Likelihood of Becoming a GIS User," *Journal of Urban and Regional Information Systems Association* (10:2) 1998.

Nedovic-Budic, Z. "GIS Technology and Organizational Context: Interaction and Adaptation," in: *Geographic Information Research: Bridging the Atlantic,* M. Craglia and H. Couclelis (eds.), Taylor & Francis, London, 1997, pp. 165-184.

Nedovic-Budic, Z., and Godschalk, D.R. "Human Factor in Adoption of Geographic Information Systems (GIS): A Local Government Case Study," *Public Administration Review* (56:6) 1996, pp 554-567.

Obermeyr, N.J. "Bureaucratic Factors in the Adoption of GIS by Public Organizations: Preliminary Evidence from Public Administrators and Planners," *Comput., Environ. and Urban Systems* (14) 1990, pp 261-271.

Patton, M.Q. *Qualitative Evaluation and Research Methods. Second edition.* Newbury Park: SAGE, 1990.

Ramamurthy, K., and Premkumar, G. "Determinants and Outcomes of Electronic Data Interchange Diffusion " *IEEE Transactions on Engineering Management* (42:4) 1995, pp 332-351.

Rogers, E.M. *Diffusion of Innovations*, (4 ed.) The Free Press, New York, 1995.

Shapiro, C., and Varian, H. *Information Rules – A Strategic Guide to the Network Economy* Harvard Business School Press, Boston, 1998.

Shapiro, C., and Varian, H.R. "The Art of Standards Wars," *California Management Review* (41:2) 1999, pp 8-32.

Stallings, R.A. "Threats to Cities: Large-Scale Disasters and September 11, 2001", *Background paper for Institute for Civic Enterprise Seminar, 4 September 2002*, School of Policy, Planning, and Development, University of Southern California, 2002.

StrateGIS-projektet "12 frågor och svar om GIS. Ett läsmaterial för chefer och beslutsfattare," 2003. http://www2.lst.se/strategis/kursmaterial/index.htm (Access May 24, 2007)

Söderman, T. "En kartläggning av hur långt kommunerna i Västmanlands län har kommit gällande införandet av GIS – identifiering av framgångsfaktorer och hinder " *Institutionen för ekonomi och informatik*, Mälardalens högskola, Eskilstuna, 2000.

Wildemuth, B.M. "An Empirically Grounded Model of the Adoption of Intellectual Technologies," *Journal of the American Society for Information Science* (43:3) 1992, pp 210-224.

Tools

Moving Targets Velocity and Direction by Using a Single Optical VHR Satellite Imagery

Martino Pesaresi[a]*, Karlheinz Gutjahr[b], and Elodie Pagot[a]

[a] *European Commission, Joint Research Centre, Institute for the Protection and Security of the Citizen (IPSC), Support to External Security Unit, Ispra 21027 (VA), Italy*

[b] *Joanneum Research ForschungsgesmbH, Institute of Digital Image Processing, Wastiangasse 6, A - 8010 Graz, Austria*

* martino.pesaresi@jrc.it

Abstract:

The present contribution demonstrates the feasibility and explores the limits of a new method for estimating the velocity and direction of moving targets using a single VHR satellite dataset. The method is based on the fact that there is a time lag between the data collection of the panchromatic (PAN) and multi-spectral (MS) sensors in the same VHR platform. Consequently, it is developed around three main steps: i) accurate image-to-image registration between MS and PAN images with a sub-pixel displacement error, ii) precise location of barycentre of targets by mathematical morphology-based image transforms, and iii) estimation of the targets ground velocity and direction using the MS-PAN spatial displacement, the known time lag, and an image-to-ground transformation taking into account the interior and exterior orientation of the sensors and a terrain height reference. An evaluation of the reliability and limits of the proposed method based on the observation of the results regarding manually-selected moving and non-moving targets is included.

1. Introduction

Most of the applications using VHR data assume that the collection of one imagery data set occurs at one point in the time line. If a multi-temporal analysis is needed, this requires a multiple collection of imagery representing the same spatial domain at different points of the time line. Then change detection techniques are usually applied in order to enhance evolving phenomena or detect moving targets. The associated intrinsic limit is to be able to observe only changes having a frequency of occurrence/change or a velocity on the ground much slower than the revisit time of the satellite platforms. These are of the order of some days in optimal conditions of cloud coverage and other tasks constraints.

The detection of moving targets with remotely-sensed data is usually done using conventional radar or imaging radar techniques, such as SAR (Meyer et al., 2006; Pettersson, 2004) and along-track SAR interferometry approaches have been proposed for traffic monitoring using SRTM/X-SAR ATI data (Suchandt et al., 2006). In alternative, optical video cameras are used for traffic monitoring (Munno et al., 1993), but they are mostly based on ground or aircraft platforms that offer technical characteristics as image spatial resolution and frequency of image collection that unfortunately are not available in the satellite platforms at the date (Toth and Grejner-Brzezinska, 2006; Reinartz et al. 2006). For security applications aircraft platforms have also limitations related to the accessibility of remote areas especially relevant in case of conflict-prone places or areas with severe security-related concerns that are not accessible by civilian missions.

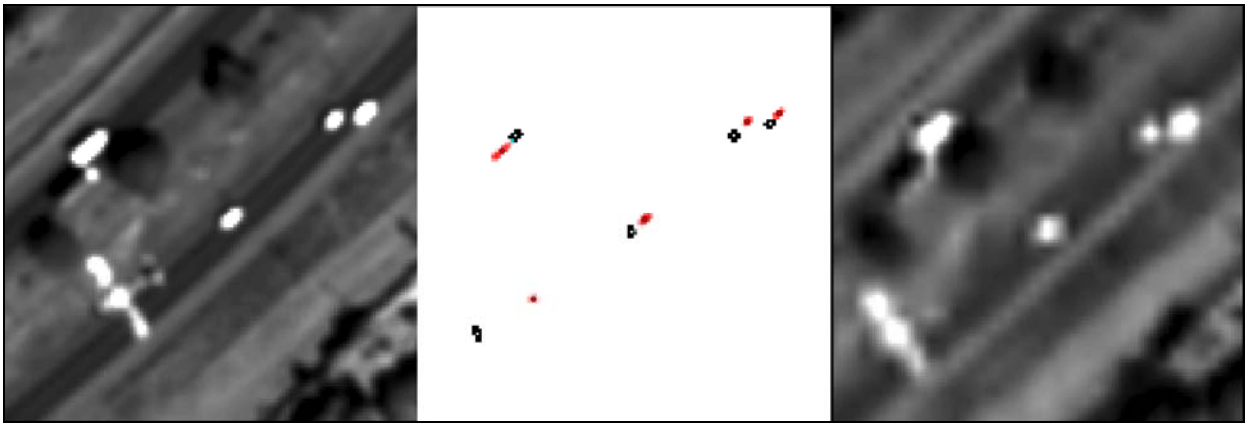

Fig. 1: sub-sample of the PAN (left) and MS (right) data used for detection of the image blobs and precise barycentres (center). In red and black the blobs coming from the PAN and MS sensors, respectively.

The proposed methodology changes radically the perspective by exploiting the fact that in reality satellite VHR optical systems have two different sensors on board, respectively multi-spectral (MS) and panchromatic (PAN), which do not capture the information instantaneously but with a given time lag between the two data collections. By knowing the exact time lag between the two data collections, it is possible to estimate the target's ground velocity with the approximation of the pixel size. The shift of fast-moving features in the PAN and MS images produced by the time lag between the two image data collections are well known characteristics of VHR data (Dial 2003), but no systematic evaluation of the reliability if this information for estimation of the target velocity is available in the literature at the date. Usually this characteristic of VHR satellite data is considered as an artefact to be fixed for improving the image-to-image matching and digital surface extraction from stereo-pairs (Baltsavias and others 2001, Jacobsen 2005).

The detection of moving targets using remotely-sensed data has a clear connection with the support to all the activities related to traffic monitoring, estimation of traffic volume, and the modelling and planning of the traffic both in the terrestrial and maritime environment. An important application field can also be related to security and defence, where it is important to know if, and possibly where, there are moving vehicles or in general targets in the scene under analysis, with the estimation of ground velocity and direction. Moving vehicles detection using remotely sensed data could be also important in case of necessity to estimate the illegal border crossing of goods and people on remote areas difficult to control with traditional approaches.

2. The Proposed Method

2.1 Processing flow

The concept presented here is tested using a part of VHR data coming from the Quick Bird® satellite of Digital Globe, having nominally 0.6 and 2.4 meter spatial resolution of the panchromatic and multi-spectral sensor, respectively. The processing flow consists on six steps as follow:

1. Fusion of the MS channels in order to simulate the spectral response of the panchromatic P
2. MS and P resolution matching

3. Image-to-image registration by correlation matching of the MS output of point (2) on the panchromatic channel using the latter as reference
4. Rough selection of potentially interesting target points (fuzzy markers)
5. Automatic refinement of the targets location
6. Estimation of the targets ground velocity

Steps 1 and 2 are functional to the preparation of the image-to-image registration, with the objective to use the multi-spectral data (MS) of the sensor for creating an MS-derived image as similar as possible to the spectral characteristics of the panchromatic (P) image. For Quickbird images the fusion is done by spectral averaging all the values of the MS sensor, simulating the frequency response of the P sensor. To ensure same gray value distributions a histogram matching is applied to the fused MS-image with the panchromatic image serving as reference. In order to reach the resolution of the P sensor, the MS-derived image was then over-sampled by a factor 4 through bi-linear resampling approach. The original P image was filtered by a 4 x 4 low-band-pass convolution filter in order to create an image with similar spatial characteristics to the MS-derived image, but without loosing the accuracy on the location of the barycentre of the targets.

Steps 3, 4, 5 are described in the following paragraph 4, and the final step 6 is detailed in paragraph 5.

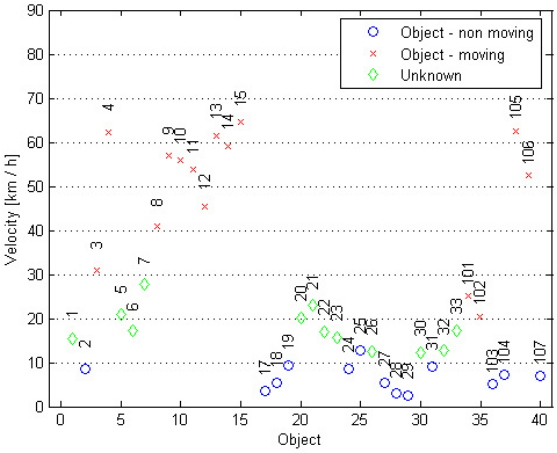

Fig. 2: estimated velocity for the selected targets (objects)

2.2 Accuracy considerations

The time lag $\Delta t_{Pan,MS}$ between the MS and P sensor acquisition is the limiting factor for the velocity determination. Obviously a coarse estimation can be found according to $v = \frac{\Delta d_{Pan,MS}}{\Delta t_{Pan,MS}}$ where $\Delta d_{Pan,MS}$ is the length of the displacement vector between the target locations in the MS and P image. In case of Quickbird, the time lag is about 0.2 sec and the nominal spatial resolution of the panchromatic and multi-spectral sensor is 0.6 and 2.4 meters, respectively. Thus a target velocity of 50 km/h corresponds to 4.7 pixels in the P image or, the other way around, a displacement of 1 pixel corresponds to about 10 km/h.

As a consequence reliable velocity results can only be achieved if sub-pixel accuracy is ensured throughout the processing flow, most particularly for the image-to-image registration and the target localization. Since the velocity can be estimated from relative displacements, the

absolute location accuracy and the quality of the reference height information are of minor importance.

3. Moving Target Detection

As the accuracy of the estimated velocity depends on the quality of the measured displacement vectors, an image-to-image registration is required. Therefore, a dense grid of points in the modified P image is identified with the fused MS image, applying image matching techniques (Paar and Pölzleitner, 1992). These points are used to calculate an affine transformation between both images. Poor identification results are filtered by the back-matching distance and additionally can be removed during the polynomial calculation by looking at the individual point residuals.

We chose a grid of 10 by 10 pixels in the area of interest (1000 by 1000 pan-pixels) yielding about 9000 tie-points (TP´s) candidates. These points where first filtered using a threshold of 0.5 pixels for the back-matching distance. When fitting an affine polynomial to the remaining 1901 points again 198 tie-points where eliminated because of their poor residual statistic. The residual statistics of the polynomial fitting is summarized in Table 1. Finally, the fused MS image is warped to the P image using the found affine transformation.

Table 1: Residual statistics of the polynomial transformation calculation

1703 TP´s	**Column [pxl]**	**Line [pxl]**	**Length [pxl]**
Std.Dev.	0.76	0.81	1.11
Mean	0.00	0.00	0.99
Minimum	-1.89	-2.02	0.04
Maximum	1.87	2.02	2.59

The rough selection of potentially interesting target points on step 4 of the processing flow has been solved by visual inspection of the images after the image-to-image automatic matching. The procedure was the following: a disk of radius r overlapping interesting targets (moving and stable objects) was manually digitised and recorded in a separate image layer. Stable targets were acquired in order to have an indirect measure of the image-to-image registration intrinsic error. The disk serves as fuzzy marker with a spatial fuzziness proportional to parameter r. In this case r=15 pixels (corresponding to a radius of 9 meters on the ground) was chosen in order to include any potential interesting target such as cars and/or trucks.

The precise location of the targets (step 5) was calculated using a procedure based on mathematical morphology and involving the detection of the image structures (blobs) related to the manually-fuzzy-selected targets together with the calculation of the precise barycentre of these image blobs.

In order to detect both targets brighter and darker than the surrounding image background, the procedure used a parallel approach based on the calculation of the residuals of morphological opening and morphological closing by reconstruction, respectively.

In particular, the image blobs of brighter targets of the image $T_{bright}(f)$ are calculated by the white top-hat by reconstruction (RWTH) morphological transform as follows:

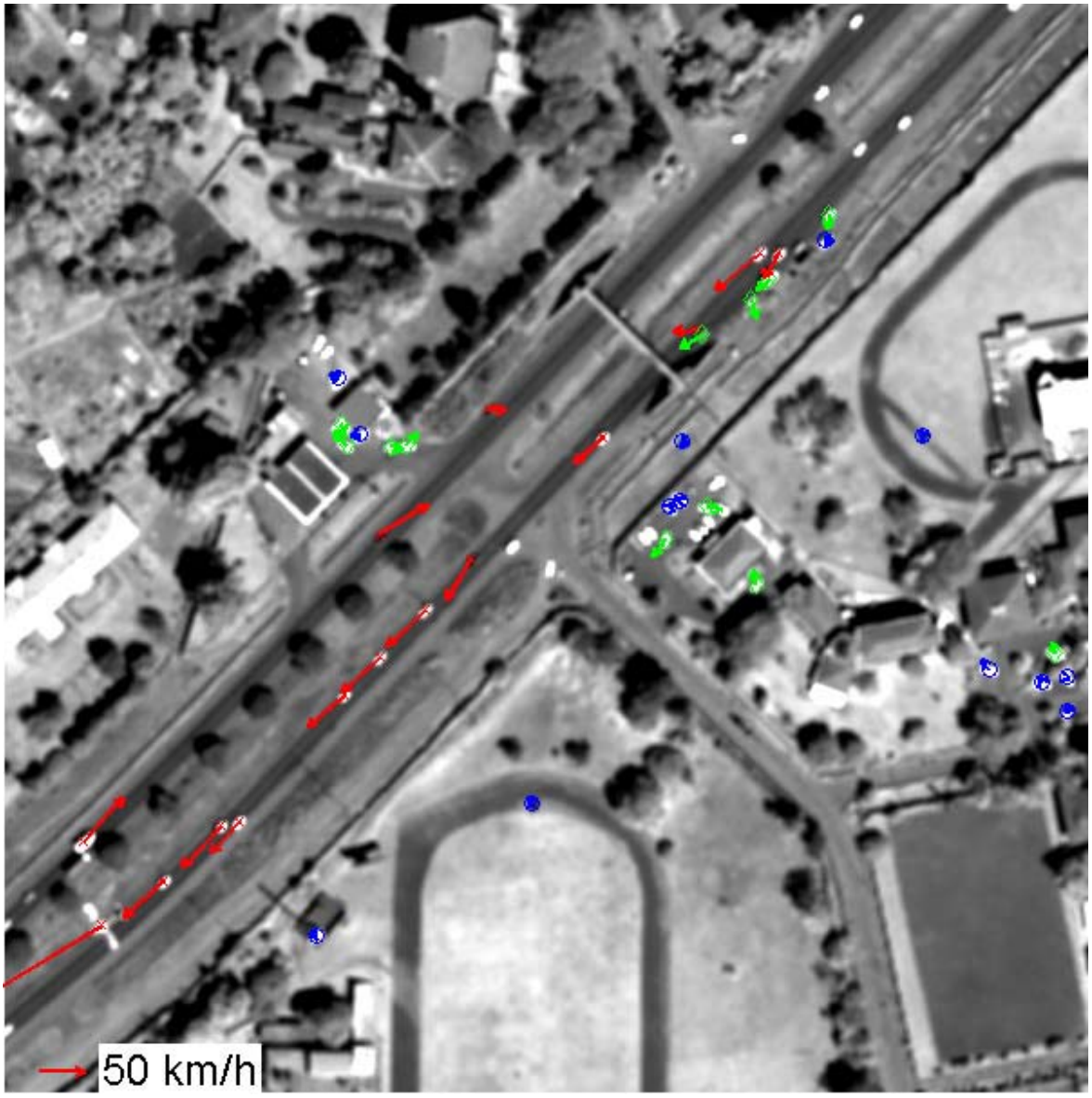

Fig. 3: estimated velocity of targets overlaid on the PAN image. Red, green and blue targets were classified as "moving", "unknown", and "non-moving", respectively, by visual inspection.

$$T_{bright}(f) = RWTH(f) > 0 \qquad f - \gamma_R^{(n)}(f) > 0 \qquad (1)$$

While the image blobs corresponding to the darker targets of the image are calculated by the black top-hat by reconstruction (RBTH) morphological transform as follows:

$$T_{dark}(f) = RBTH(f) > 0 \qquad \phi_R^{(n)}(f) - f > 0 \qquad (2)$$

Where $\gamma_R^{(n)}(f)$ and $\phi_R^{(n)}(f)$ are the opening and closing by reconstruction, respectively, with a structuring element of size *(n)* of the input image *(f)* (Soille 2003, p.212). The target blobs

were derived from the support area of the $RWTH(f)$ and $RBTH(f)$, defined as the region of pixels in the transformed image $T_{bright}(f)$ or $T_{dark}(f)$, having residuals greater than zero. The size *(n)* of the structuring element used here is of course linked to the size of the targets we want to detect as bright or dark structure in the image: in this case the minimal 3x3 box was sufficient.

The barycentre of the detected blobs is then calculated by simply averaging the x and y image coordinates of all pixels belonging to each specific blob. Other alternatives have been tested as the detection of the extrema (regional maxima and regional minima for bright and dark blobs, respectively) of the grey-level functions associated with the blobs, or the weighted average of the coordinates by the intensity of the blob contrast. However, by analysing the estimated displacement of stable targets, the results of these more complicated procedures were not reducing this displacement but increasing it by a factor of about 5 to 10 % with respect to what we obtained with the simple coordinate averaging method. Therefore, the last method was chosen in the following.

4. Estimation of the Targets' Ground Velocity

4.1 Ground-to-image and inverse transformation

To determine the velocity (step 6 of the processing flow), the barycentre pixel coordinates of the detected blobs in the pre-processed MS and PAN images had to be geo-referenced. This was based on a so-called image-to-ground transformation which requires the additional information on the interior and exterior orientation of the sensors at the acquisition time of the image and a height reference. In case of Quickbird or Ikonos sensors, the rational polynomial coefficients (RPC´s) are supplied with the image data and directly describe the ground-to-image transformation by two fractions of cubic polynomials:

$$x = \frac{f_x(X,Y,Z)}{g_x(X,Y,Z)} \text{ and } y = \frac{f_y(X,Y,Z)}{g_y(X,Y,Z)} \qquad (3)$$

The original sensor polynomials depend on geographic co-ordinates ( ) but we prefer the representation in an Earth-centred, Earth-fixed Cartesian system ( ).

4.1.1 Image-to-map transformation

Calculation of East and North ground coordinate for given height. Approximations for East and North:

$$\bar{r} = (r - r_0)/\mu_r$$
$$\bar{r} = \frac{L_{1,1} + L_{1,2}\cdot\bar{\lambda} + L_{1,3}\cdot\bar{\phi} + L_{1,4}\cdot\bar{H}}{L_{2,1} + L_{2,2}\cdot\bar{\lambda} + L_{2,3}\cdot\bar{\phi} + L_{2,4}\cdot\bar{H}} \qquad (4)$$

$$\bar{c} = (c - c_0)/\mu_c$$
$$\bar{c} = \frac{C_{1,1} + C_{1,2}\cdot\bar{\lambda} + C_{1,3}\cdot\bar{\phi} + C_{1,4}\cdot\bar{H}}{C_{2,1} + C_{2,2}\cdot\bar{\lambda} + C_{2,3}\cdot\bar{\phi} + C_{2,4}\cdot\bar{H}} \qquad (5)$$

Solve for $\overline{\phi}$ and $\overline{\lambda}$:

$$\begin{aligned}&\left(L_{1,2}-\overline{r}\cdot L_{2,2}\right)\cdot\overline{\lambda}+\left(L_{1,3}-\overline{r}\cdot L_{2,3}\right)\cdot\overline{\phi}=\\&\left(L_{2,1}+L_{2,4}\cdot\overline{H}\right)\cdot\overline{r}-\left(L_{1,1}+L_{1,4}\cdot\overline{H}\right)\end{aligned}\qquad(6)$$

$$\begin{aligned}&\left(C_{1,2}-\overline{c}\cdot C_{2,2}\right)\cdot\overline{\lambda}+\left(C_{1,3}-\overline{c}\cdot C_{2,3}\right)\cdot\overline{\phi}=\\&\left(C_{2,1}+C_{2,4}\cdot\overline{H}\right)\cdot\overline{c}-\left(C_{1,1}+C_{1,4}\cdot\overline{H}\right)\end{aligned}\qquad(7)$$

4.1.2 Inverse normalization to get ϕ and λ.

Iterate for East (X) and North (Y):

$$\begin{aligned}&r=r(\vec{X}+d\vec{X})\\&r=r(\vec{X}_0)+\frac{\partial r}{\partial\lambda}\cdot d\lambda+\frac{\partial r}{\partial\phi}\cdot d\phi+\frac{\partial r}{\partial' H}\cdot dH\end{aligned}\qquad(8)$$

$$\begin{aligned}&c=c(\vec{X}+d\vec{X})\\&c=c(\vec{X}_0)+\frac{\partial c}{\partial\lambda}\cdot d\lambda+\frac{\partial c}{\partial\phi}\cdot d\phi+\frac{\partial c}{\partial' H}\cdot dH\end{aligned}\qquad(9)$$

$$\frac{\partial r}{\partial\lambda}\cdot d\lambda+\frac{\partial r}{\partial\phi}\cdot d\phi+\frac{\partial r}{\partial H}\cdot dH=r-r(\vec{X}_0)\qquad(10)$$

$$\frac{\partial c}{\partial\lambda}\cdot d\lambda+\frac{\partial c}{\partial\phi}\cdot d\phi+\frac{\partial c}{\partial H}\cdot dH=c-c(\vec{X}_0)\qquad(11)$$

4.1.3 Calculus of the solutions

The solution of the inverse transformation can be found iteratively using Taylor series expansions. It is a well known and documented problem that the meta-information has a limited and variable absolute accuracy (Jacobsen 2005, Dial and Grodecki, 2002). Generally a sensor model optimization based on ground control points (GCP´s) is required. This is crucial for security related applications as the access to the area of interests is restricted in many cases. Anyhow, the accuracy of the image-to-ground transformation also depends on the used reference height. We used the globally available SRTM C-band DEM with a nominal resolution of about 90 m and a relative height accuracy of 10 m. Obviously this level of detail and height accuracy does not meet the requirements specified above.

In our approach we try to solve, or at least release, all these problems in the image-to-image registration step. First this registration reduces the sensor geometries to be considered and optimized to one (pan-chromatic sensor). Secondly we again have to stress that we are only interested in relative displacements. Thus the absolute pointing accuracy is of minor interest if the topography around the moving objects is changing smoothly. This is a feasible condition for vehicles as the road networks in general do not show very steep height gradients.

4.1.4 Results

Figure 2 shows the velocity estimations of 40 targets that were classified by visual inspection. Three classes were assigned: “non moving objects” such as for parked vehicles or trees, “moving objects”, and “unknown” when it was hard for the interpreter to decide whether or not the target was moving. It is evident that the “non-moving” targets are almost all clustered below the velocity line of 10km/h, which corresponds to roughly one panchromatic pixel of displacement with the given MS-PAN collection time lag (see point 3.2). This can be considered as the technological limit of the tested source given by the constraints on available resolution, MS and PAN image matching precision, and MS-PAN collection time lag. The targets with estimated velocity between 10 km/h and 30 km/h were almost “unknown” from the visual inspection, because the displacement was too small to be detected univocally by manual means, while the targets with estimated velocity greater than 30 Km/h were all labelled as “moving targets” by the visual inspection.

Moreover, if we check the direction and angle together with the velocity of the moving targets on the road, we can observe that the results are coherent with the expected opposite directions in the two road lanes (Figure 3).

5. Conclusions

The present contribution demonstrates the feasibility and explores the limits of a new method for estimating the velocity and direction of moving targets using a single VHR satellite dataset. The method is based on the fact that there is a time lag between the data collection of the PAN and MS sensor in the same VHR platform, and it is developed around three main steps: i) image-to-image registration between MS and PAN images, ii) precise location of barycentre of targets, and iii) estimation of the targets ground velocity and direction by image-to-ground transformation.

This preliminary study has shown that the theoretical limit of the estimated velocity accuracy given by the spatial resolution and MS-PAN time lag constraints can be reached using sub-pixel image-to-image warping and accurate target barycentre detection procedures. In particular, with the tested Quickbird sensor, we have estimated a limit of 10Km/h as minimal velocity of targets having the size of a car.

Further efforts will concentrate on testing the different limits associated to different VHR sensors available, and on the development of an automatic procedure able to select the potential moving targets without the manual intervention used in this methodology. The fully automatic target-selection procedure will be required in case of application of this methodology for detection of unexpected (out of road) or low-velocity moving target in the entire satellite scene, that are difficult to identify by visual inspection.

Acknowledgements

The presented work has been supported by the institutional research activity of Action ISFEREA (Information Support for Effective and Rapid External Action) of the European Commission, Joint Research Centre, Institute for Protection of the Citizen (IPSC). The research concept and his implementation have been made possible because of the effective sharing of ideas and tools inside the GMOSS (Global Monitoring for Security and Stability) Network of Excellence.

References

Baltsavias E., Pateraki M., Zhang L., 2001. Radiometric and geometric evaluation of Ikonos geo images and their use for 3D building modeling, Joint ISPRS Workshop “High Resolution Mapping from Space 2001”, Hannover, Germany, 19-21 September.

Dial G., 2003. Measuring Boat Speed, Space Imaging technical paper.

Dial G., Grodecki J., 2002. Block adjustment with rational polynomial camera models. Proceeding of ASCM-ASPRS Annual Conventions, Washington D.C., April 2002, pp.

Jacobsen K., 2005. High Resolution Satellite Imaging Systems – Overview, ISPRS Hannover Workshop 2005, High-Resolution Earth Imaging for Geospatial Information, May 17-20, 2005, Hannover, Germany.

Meyer F., Hinz S., Laika A., Weihing D., and Bamler R., 2006, Performance analysis of the TerraSAR-X Traffic monitoring concept, ISPRS Journal of Photogrammetry and Remote Sensing, 61 (3-4), pp. 225-242

Munno C.J., Turk H., Wayman J.L., Libert J.M., Tsao T.J., 1993. Automatic video image moving target detection for wide area surveillance, Security Technology Proceedings, Institute of Electrical and Electronics Engineers 1993 International Carnahan Conference on 13-15 Oct. 1993 pp. 47 – 57.

Paar G., Pölzleitner W,. 1992. Robust disparity estimation in terrain modelling for spacecraft navigation. Proc. 11th ICPR, International Association for Pattern Recognition, 1992, pp.

Reinartz P., Lachaise M., Schmeer E., Krauss T. and Runge H., 2006, Traffic monitoring with serial images from airborne cameras, ISPRS Journal of Photogrammetry and Remote Sensing, 61 (3-4), pp. 149-158.

Soille P., 2003. Morphological Image Analysis, Springer.

Suchandt S., Einedera M., Breita H., Runge H., 2006. Analysis of ground moving objects using SRTM/X-SAR data, ISPRS Journal of Photogrammetry and Remote Sensing, 61 (3-4), pp. 209-224.

Toth C.K. and Grejner-Brzezinska D., 2006, Extracting dynamic spatial data from airborne imaging sensors to support traffic flow estimation, ISPRS Journal of Photogrammetry and Remote Sensing, 61 (3-4), pp. 137-148.

Using differential SAR interferometry for the measurement of surface displacement caused by underground nuclear explosions and comparison with optical change detection results

Xiaoying Cong[1*], Jörg Schlittenhardt[1], Karlheinz Gutjahr[2], Uwe Soergel[3], Mort Canty [4], Allan Nielsen[5]

[1] *Bundesanstalt für Geowissenschaften und Rohstoffe (BGR), Stilleweg 2, 30655 Hannover, Germany*

[2] *Institute of Digital Image Processing, Joanneum Research Forschungsgeschaft mbH, Wastiangasse 6, 8010 Graz, Austria*

[3] *Institute of Photogrammetry and GeoInformation, Leibniz University Hannover, Nienburger Str. 1, 30167 Hannover, Germany*

[4] *Forschungszentrum Jülich, 52425 Jülich, Germany*

[5] *Technical University of Denmark, 2800 Lyngby, Denmark*

* Xiaoying.Cong@bgr.de

Abstract

Differential synthetic aperture radar interferometry (DInSAR) has nowadays become an important means for measuring and monitoring of surface displacements of various types. This report focuses on investigating the capability of this technique for detection and characterization of underground nuclear explosions, taking the Nevada Test Site (NTS) as an example. The analysis revealed large scale surface subsidence phenomena which were either related to the detonation itself or post-event deformation in the cm-range within the damage (spall) zone of the explosion. However, subsequent investigations of nuclear tests at other test sites also showed the limits of the DInSAR technique when mountainous topography and/or temporal and spatial baseline differences become critical factors. Although satellite data analysis is not an element of the IMS (International Monitoring System) of the UN's (United Nations) CTBTO (Comprehensive Nuclear Test-Ban Treaty Organization) currently build up in Vienna it can provide important information for the treaty verification regime, either by itself or in combination with the seismically detected explosion signal.

Introduction

Synthetic Aperture Radar (SAR) uses the microwave domain of the electromagnetic spectrum for remote sensing. Due to the active sensor principle and the long wavelength ranging from a few centimetres to metres, SAR sensors are capable of gathering mapping data independently from weather conditions or time of day. In order to achieve imagery of high spatial resolution besides the signal amplitude the phase data are also acquired. Based on the phase data interferometric processing of several images can be carried out. One standard application for such SAR Interferometry (InSAR) is to derive digital elevation models (DEM) from couples of SAR images taken from different across-track sensor positions. Recent years saw the breakthrough of an extension of InSAR: Differential SAR Interferometry technique using time series of SAR images became an important means for deformation monitoring.

This paper focuses on the application of DInSAR technique to monitor large scale surface subsidence caused by past underground nuclear explosions at Nevada Test Site, (see *Figure 1*) (Vincent et al, 2003). Five ERS SLC (Single Look Complex) images were analyzed

incorporating a given reference SRTM (Shuttle Radar Topography Mission) DEM, which was used to remove phase components induced by topography to calculate the differential interferogram. By spectral filtering non-overlapping parts of the image spectra were eliminated before the phase unwraping was calculated. After phase unwrapping the SAR line-of-sight (LOS) velocity vector fields could be derived from these phase differences according to a linear relation. Adding an additional constraint (motion is assumed to consist of vertical subsidence only without any horizontal component) and taking into account the sensor acquisition times subsidence rates can be directly calculated from the LOS vector field. The subsidence rates of coseismic and postseismic signals were finally measured from the geocoded displacement maps based on UTM coordinate system. In order to improve the accuracy of localization a GCP based geometric sensor modeling was carried out.

Based on the given SAR data mainly postseismic subsidence processes could be monitored. The deformation may cover large areas of one kilometer or more in diameter on the surface above the point of explosion. According to the local geological situation the actual point of explosion known from ground-truth may not be located in the centre of deformation area. Therefore, 3D analysis was accomplished, to extract more detailed information about the relation between the position of the test and the subsidence pattern's center of gravity. Since the observed subsidence could be composed by superposition of the effects of several individual tests nearby creating a cluster signal, this effect must be taken into account for the accurate location determination of the test position. By considering the possible variations in the geologic and hydrologic environment of the local test area and taking into account the variance of individual measurements the results for the derived decay constants and initial deformation rates did not show clear regional distinctions. Furthermore, a continuous sinking sequence was derived from the postseismic signals. A brief comparison with results from a validation of the multi-spectral change detection algorithm (Canty et al., 2005) for those underground nuclear explosions investigated also in this paper is presented.

The research of using DInSAR technique for detecting/monitoring underground nuclear explosion is of relevance for CTBT (Comprehensive Nuclear Test-Ban Treaty) verification regime (Canty & Schlittenhardt, 2001). Special emphasis will be placed on accessing whether signals detected by DInSAR could be used in the CTBT verification scenario in combination with the seismic data.

Data Processing and results

Nevada Test Site and ERS data

The Nevada Test Site is located in Nye County in southern Nevada about 105 km northwest of the City of Las Vegas, near 37°07′N, 116°03′W. In Figure 1 the site is highlighted with a black polygon. From 1962 to 1992 over 1000 underground nuclear tests were carried out there. The nuclear tests were documented in-situ with on-site-inspection or remotely by seismic and other methods. The red rectangle in *Figure 1* represents the area covered by ERS data; the green and blue rectangles depict two prominent areas called Pahute Mesa (PM) and Yucca Flat (YF).

The acquisition dates of ERS data available for the processing are shown in *Figure 2*. First ERS data were taken in 1992 when a moratorium on all U.S. nuclear tests came into effect. Last test "Divider" was conducted on 23 Sep. 1992. The other four tests that have taken place after the acquisition time of the first ERS scene are located in Yucca Flat, except for Hunters Trophy in Rainier Mesa. The 5 ERS scenes are illustrated in time diagram with the red folded line and the acquisition date, and the data were numbered consecutively with index from 1 to

5. Hence, it is possible that both of coseismic und postseismic signals as well as the long-term deformation signals could be captured.

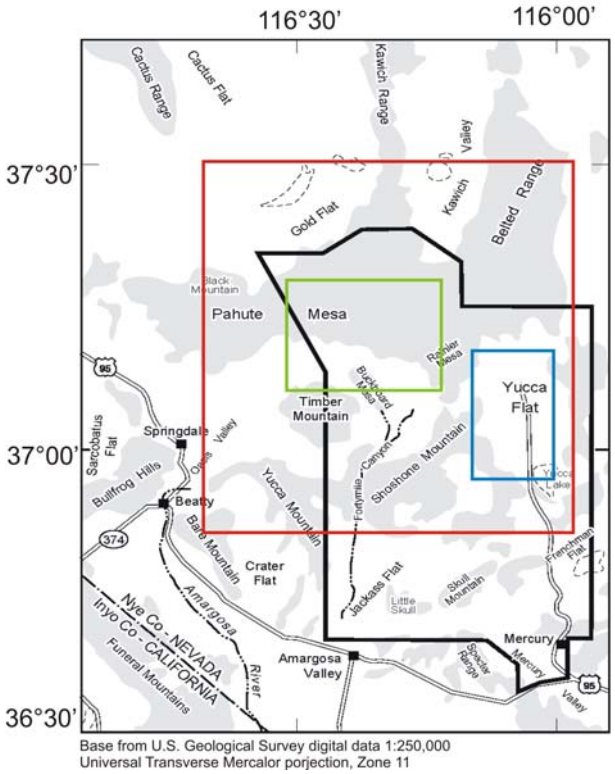

Fig. 1. Geographical overview for NTS (black polygon), ERS data (red rectangle), PM area (green), and YF (blue)

In addition to the ERS data an external DEM is essential for the processing. The SRTM X-band DEM (30 m resolution) covering the entire area was used here. Moreover, the heterogeneous seismic data were needed for the further interpretation (Springer et al., 2002).

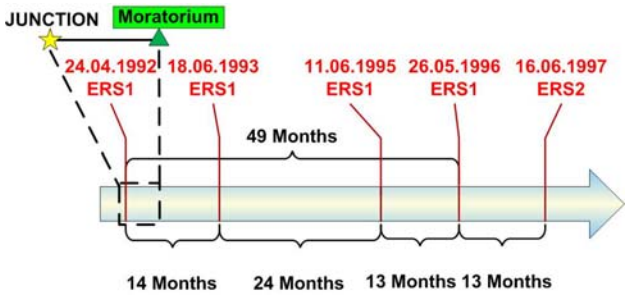

Fig. 2. Time diagram of five ERS scenes

Processing with DInSAR method

All the processing steps are carried out using the software package 'RSG' which is developed at Joanneum Research (Gutjahr, 2004). The DInSAR processing following the work flow depicted in *Figure 3* is carried out in image pairs. Two criteria have been applied for selection of the image pairs. The first was minimization of the perpendicular baseline component, and the second was to obtain orbit pairs of different time spans and epochs in order to acquire versatile deformation signals. *Table 1* lists the interferometric orbit pairs along with relevant interferometry parameters.

Table 1. InSAR orbit pairs and the relevant parameters.

Image pairs	Sensors	Epoch	Baseline	
			temporal [days]	spatial [m]
1/2	ERS 1	920424-930618	420	-41
2/3	ERS 1	930618-950611	723	-59
3/4	ERS 1	950611-960526	350	18
4/5	ERS 1 & 2	960526-970616	386	-87
3/5	ERS 1	920424-960526	386	-10
1/4	ERS 1	920424-960526	1493	-25
1/5	ERS 1 & 2	960526-970616	1879	-112

Five available ERS images were processed to seven interferograms (*Table 1*), incorporating the given reference SRTM DEM, which was used to remove phase components induced by topography via phase simulation. By spectral filtering non-overlapping parts of the image spectra were eliminated before the difference interferograms were calculated. After phase unwrapping the SAR line-of-sight (LOS) velocity vector fields can be derived from the difference of real and simulated interferometric phase. According to an additional constraint (assuming only subsidence and no horizontal movement component) and taking into account the sensor acquisition times the LOS vector field can be directly transformed into vertical subsidence rates. Then the subsidence rates of coseismic and postseismic signals were extracted from the geocoded displacement maps (*Figure 3*). The deformation signals are given in form of the depth (motion in vertical direction over the time interval of the image pair). Besides depth, the shape of the deformation crater and the location of the estimated center of gravity as auxiliary information were listed in *Table 2*. During the processing the atmospheric influence was neglected, which is assumed to be small in this arid environment.

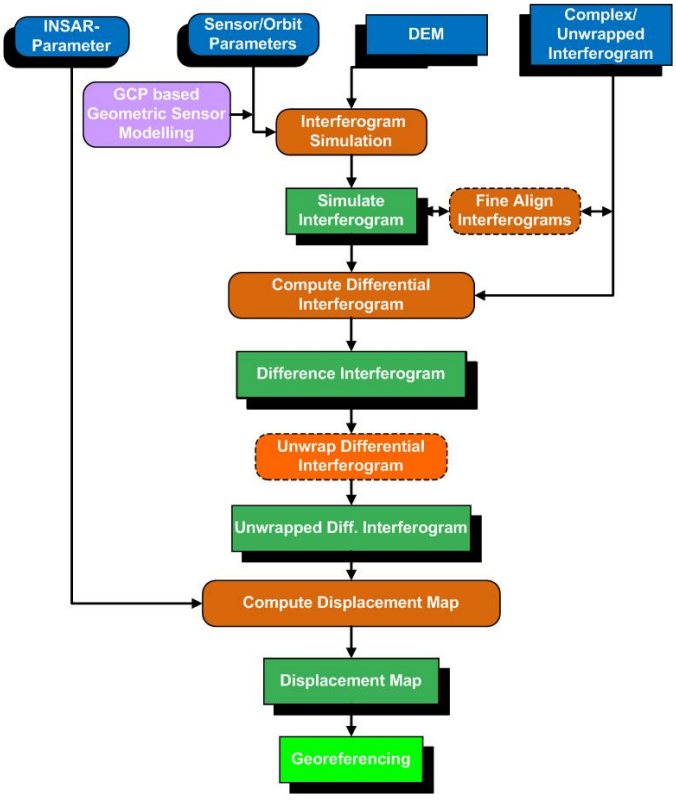

Fig. 3. Process sequence of differential SAR interferometry

Coseismic and postseismic signals

After the differential InSAR processing both coseismic and postseismic signals were derived from the image pairs. From image pair 1/2 coseismic and postseismic signals were extracted with high quality compared to ground truth (Springer et al., 2002).

Coseismic signals

Figure 4 shows two coseismic signals from the differential interferogram created using the image pair 1/2. The measured subsidence area center was located in center point of the image, (see *Table 2*). Galena (M_L = 3.9) formed an observable coseismic collapse craters measuring 134 meters in diameter and 8 meters in depth. This value exceeds by far the unambiguous measurement range in LOS of 2.83 cm of C-band (half of 5.66 cm wavelength). For this reason by using InSAR to capture coseismic signals of this size will lead to loss of information near surface ground zero. On the other hand for the detection of larger deformations (most of them occurred coseismically too) it is more suitable to apply methods which use optical EO data (Canty et al., 2005).

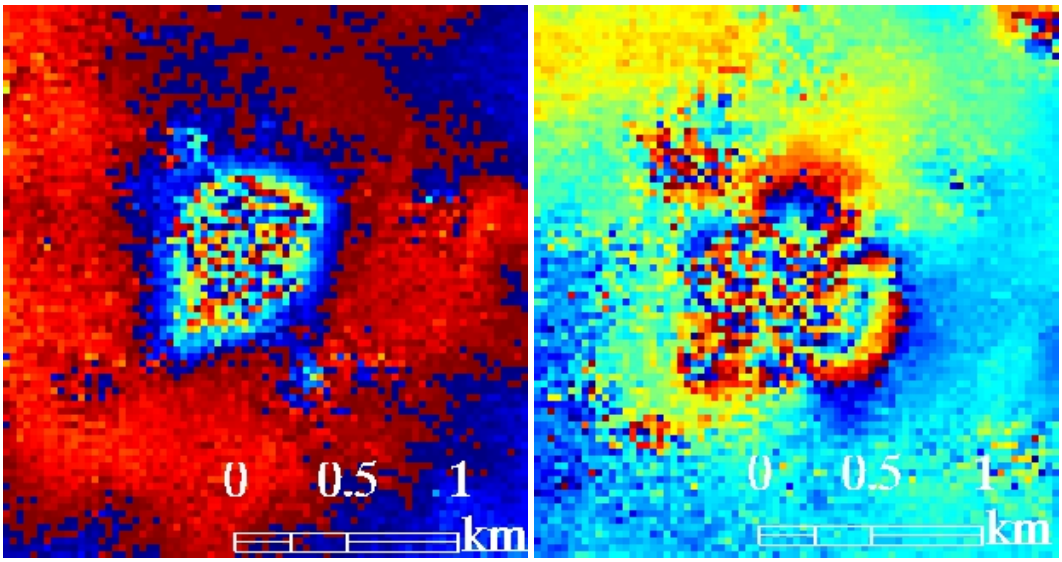

Fig. 4: Coseismic deformation signals of two of the last five underground nuclear tests conducted at NTS in 1992 captured by 14 months period InSAR pair 1/2; coseismic events Galena (left) und Divider (right), see also Table 2. Phase values are color-coded according to legend in Figure 5.

Postseismic signal

From the given data mainly postseismic subsidence signals could be obtained, e.g. all tests in PM and the most tests in YF besides Victoria, Galena and Divider occurred after the taking of the first available scene. The deformation may extend over large areas of one kilometer or more in diameter on the surface above the point of explosion (*Figure 5(1) and Figure 5(2)*). According to the local geological situation the actual point of explosion known from ground truth may not be located in the centre of deformation area. Firstly, the data in Springer et al., 2002 were given with accuracy of ca. 100 m, corresponding to a location uncertainty of three pixels. Secondly, consideration of a single exposition might not be sufficient here, because additional deformation processes caused by historical tests nearby can lead to more complex subsidence patterns. In such case the estimated center point could be biased from these superimposed contributions.

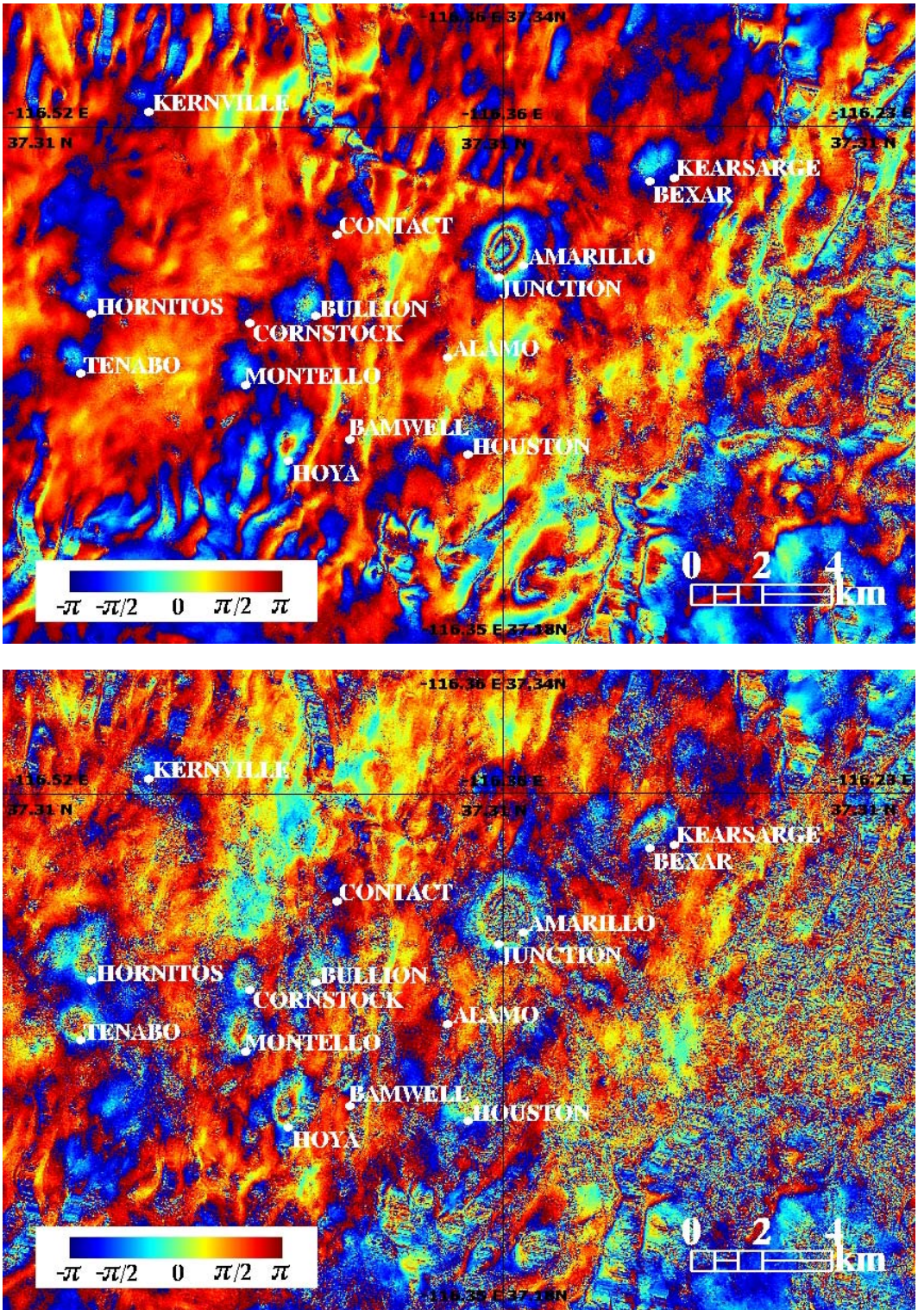

Fig. 5(1): Postseismic surface deformation signals from underground nuclear tests conducted in Pahute Mesa region of NTS (green rectangle in figure 1); the Pair 1/2 (top) spanning 14 months accumulation of deformation und 1/4 (bottom) spanning 49 months. Large white dots denote the underground tests after 1988.

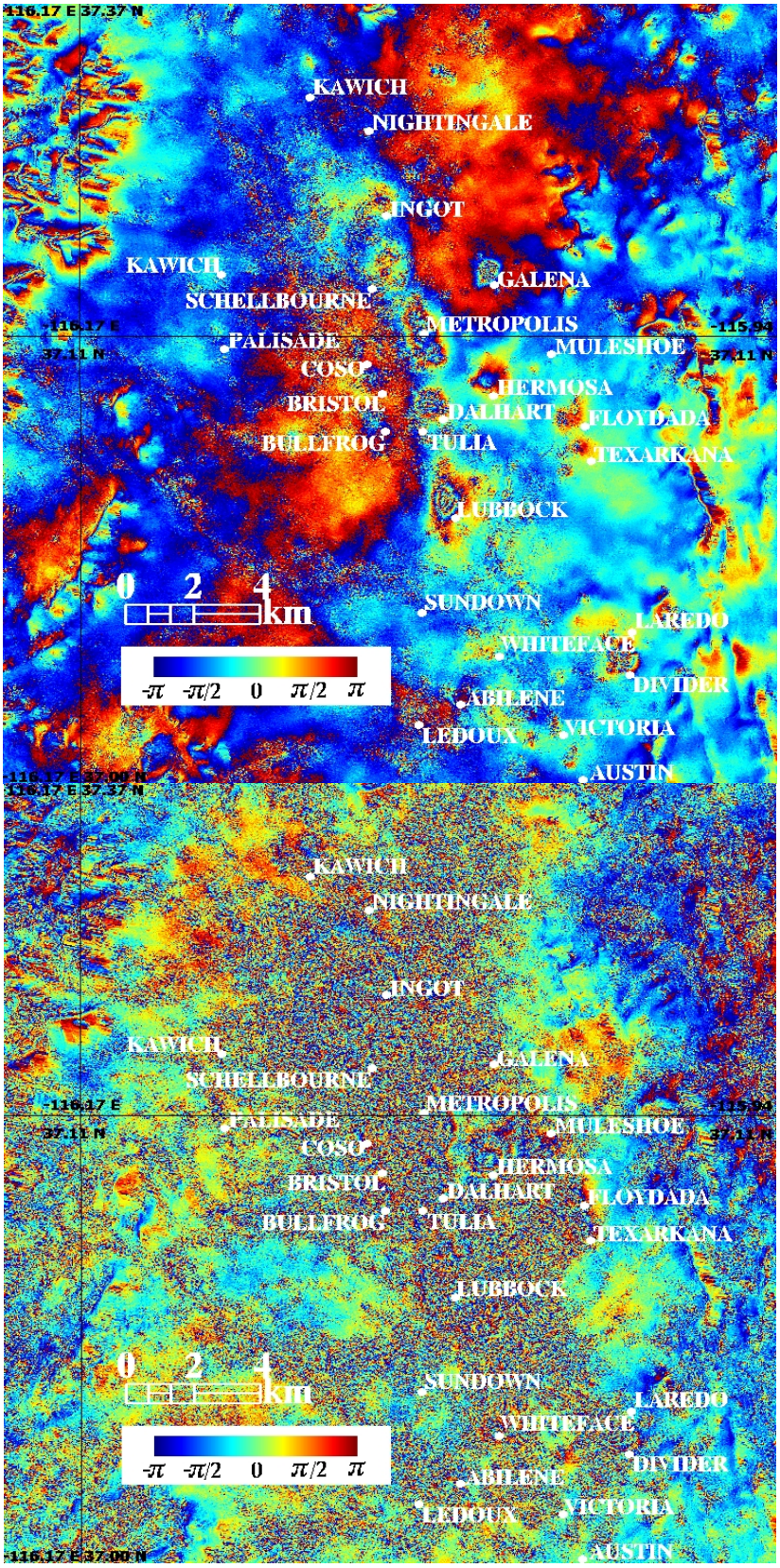

Fig. 5(2): Postseismic surface deformation signals from underground nuclear tests conducted in Yucca Flat region of NTS (blue rectangle in figure 1); the Pair 1/2 (top) spanning 14 months accumulation of deformation und 1/4 (bottom) spanning 49 months. Large white dots denote the underground tests after 1988.

Thirdly, generalization effects in the SRTM DEM lead to errors both in the phase simulation and in the geocoding step. The mentioned effects caused that in the area existed many peaks side by side. To tackle this problem, the field was analyzed in 3-D, where the deformation signals were included.

Thereby more information about the relation between the position of the test and the center of movement could be gained. The measured signals were used for the calculation of the deformation decay rate of the subsidence process with a simple exponential equation. In *Figure 5(1) and (2)* both differential interferograms present rather similar situations, actually the deformation decays quite rapidly after the period of 14 months (according to pair 1/2). However, both pairs share the same reference data of 1992. Hence, the observed subsidence signal could be composed by superposition of the effects of several tests nearby and created by a cluster signal (see *Figure 6(2)*).

Table 2: Parameters of ellipse (a and b, semi-major and semi-minor axis; φ, angle of orientation) or circle (r, radius) and of the deformation center (depth of center, location of center with latitude and longitude) of nuclear tests since 1985 derived from image pair 1/2.

Test Information				a	b	φ	Center of Ellipse/Circle			Collapes Crater Diameter [m]
Code-Name	Date	Region Code	mb	r [m]		[°]	Depth [cm]	Latitude [°]	Longtitude [°]	
Divider	23.09.1992	YF	4.4	630.0		--	-3.8	37.028	-115.992	--
Galena	23.06.1992	YF	(3.9)	570.0		--	-5.8	37.129	-116.034	134
Junction	26.03.1992	PM	5.5	1410.3	1050.4	27.1	-7.7	37.278	-116.361	--
Lubbock	18.10.1991	YF	5.2	960.0		--	-8.8	37.066	-116.050	--
Hoya	14.09.1991	PM	5.5	990.0	450.0	23.7	-3.1	37.229	-116.430	--
Floydada	15.08.1991	YF	--	600.0		--	-4.0	37.091	-116.007	--
Montello	16.04.1991	PM	5.4	750.0		--	-1.5	37.249	-116.444	--
Bexar	04.04.1991	PM	5.6	780.0		--	-2.2	37.299	-116.317	--
Houston	14.11.1990	PM	5.4	750.0		--	-1.2	37.231	-116.373	--
Tenabo	12.10.1990	PM	5.6	630.0		--	-1.9	37.251	-116.496	--
Bullion	13.06.1990	PM	5.7	750.0		--	-2.9	37.265	-116.425	--
Metropolis	10.03.1990	YF	5.0	1230.0	540.0	-31.4	-5.0	37.105	-116.052	122
Hornitos	31.10.1989	PM	5.7	750.0		--	-2.6	37.267	-116.495	164
Ingot	09.03.1989	YF	5.0	630.0		--	-3.5	37.147	-116.070	276
Texarkana	10.02.1989	YF	5.2	390.0		--	-4.4	37.075	-116.010	274
Dalhart	13.10.1988	YF	5.9	600.0		--	-5.1	37.093	-116.056	--
Cornstock	02.06.1988	PM	--	420.0		--	-0.7	37.265	-116.444	55
Kernville	15.02.1988	PM	5.3	600.0		--	-1.5	37.318	-116.475	122
Hermosa	02.04.1985	YF	--	720.0		--	-4.5	37.099	-116.037	--

Crater Modelling – Spall zone

The test JUNCTION detonated on 26th of March 1992 was the last nuclear test to be carried out underground in PM. Its seismic signal and inferred seismological epicentral parameters are shown in *Figure 6(1)*. *Figure 6(2)* shows the corresponding interferogram und displacement map from image pair 1/2. The detonation happened about a month before the first ERS image was gathered. Therefore, the captured deformation signals were purely postseismic. *Figure 6(2)* illustrates five tests (black and white dots) including JUNCTION inside of the deformation area, and one test just outside of it. The area with significant deformation could be related to many explosions inside the area (clustering signal composed by complex motion), but it is more expedient to label the area with a unique name. According to the spall zone modeling the

deformation decayed rapidly with time. Therefore, the effects of detonations before the year 1988 could be neglected compared to the later ones. Then the distance from the deformation center was taken into account. The detected subsidence area indicated an elliptical deformation pattern with semi major and semi minor axes of approximately 1.4 and 1.0 km (*Table 2)*.

Seismic Origin Time	**Seismic Magnitudes**
19920326 16:30:00.00	5.5mb 4.2MS
Lat. **Lon.**	**Geographic Region**
37.272°N 116.360° W	Southern Nevada, United States

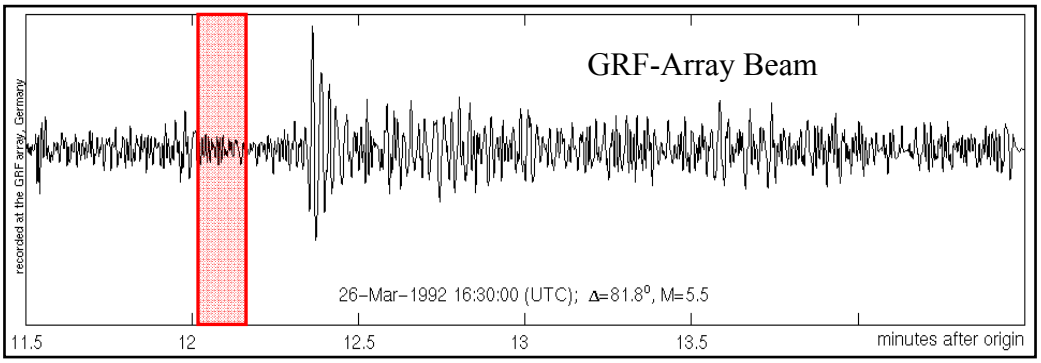

Fig. 6(1): Seismic signal of the JUNCTION underground nuclear test (red-shaded) recorded by the Graefenberg (GRF) Array in Germany (bottom) and inferred seismological epicenter data (top).

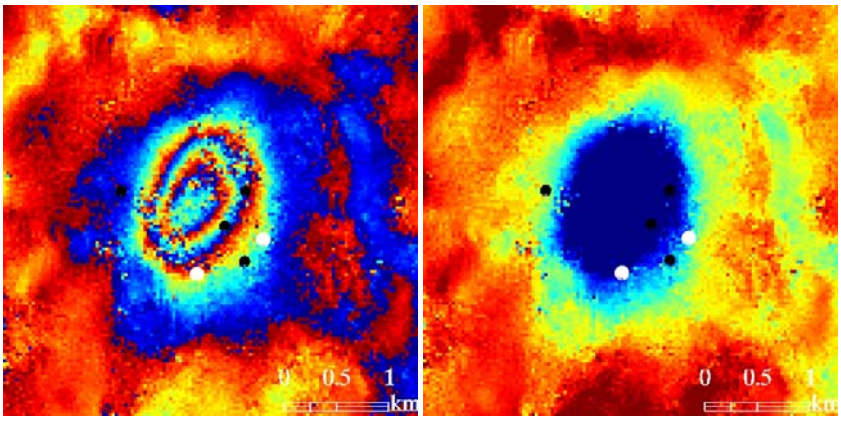

Fig. 6(2). (left): differential interferogram for search area JUNCTION; (right) displacement map for the same area. Black and white dots indicate known locations of underground tests before and after 1988, respectively;

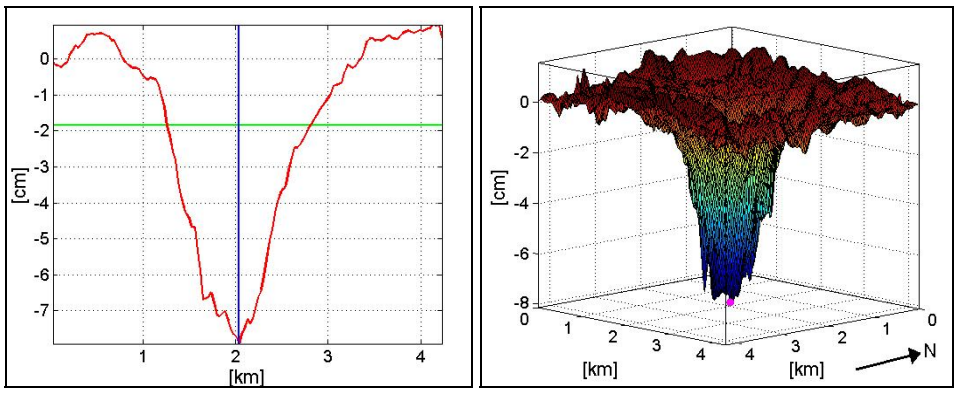

Fig. 6(3): (Left) vertical profile across the motion centre with west-east orientation; (right) 3D representation of the shape of the subsidence phenomenon.

Figure 6(3) shows the vertical profile across the deformation centre. For the determination of the depth of the subsidence, first a local reference level was estimated from the data in order to eliminate systematic effects; then the depth 'd' was measured from the deepest point along the profile to this reference surface. The measured radius exceeded the collapse crater size and agreed well with the spall zone dimension calculated using the seismic parameters from *Table 2*.

Comparison with optical multi-spectral change detection method

For a validation of the multi-spectral change detection algorithm developed within GMOSS, a case study on the detection of underground nuclear explosions using optical data was made (Canty et al., 2005). It is of interest to compare briefly the results using this method for those underground explosions that were also investigated with ERS-data in this study.

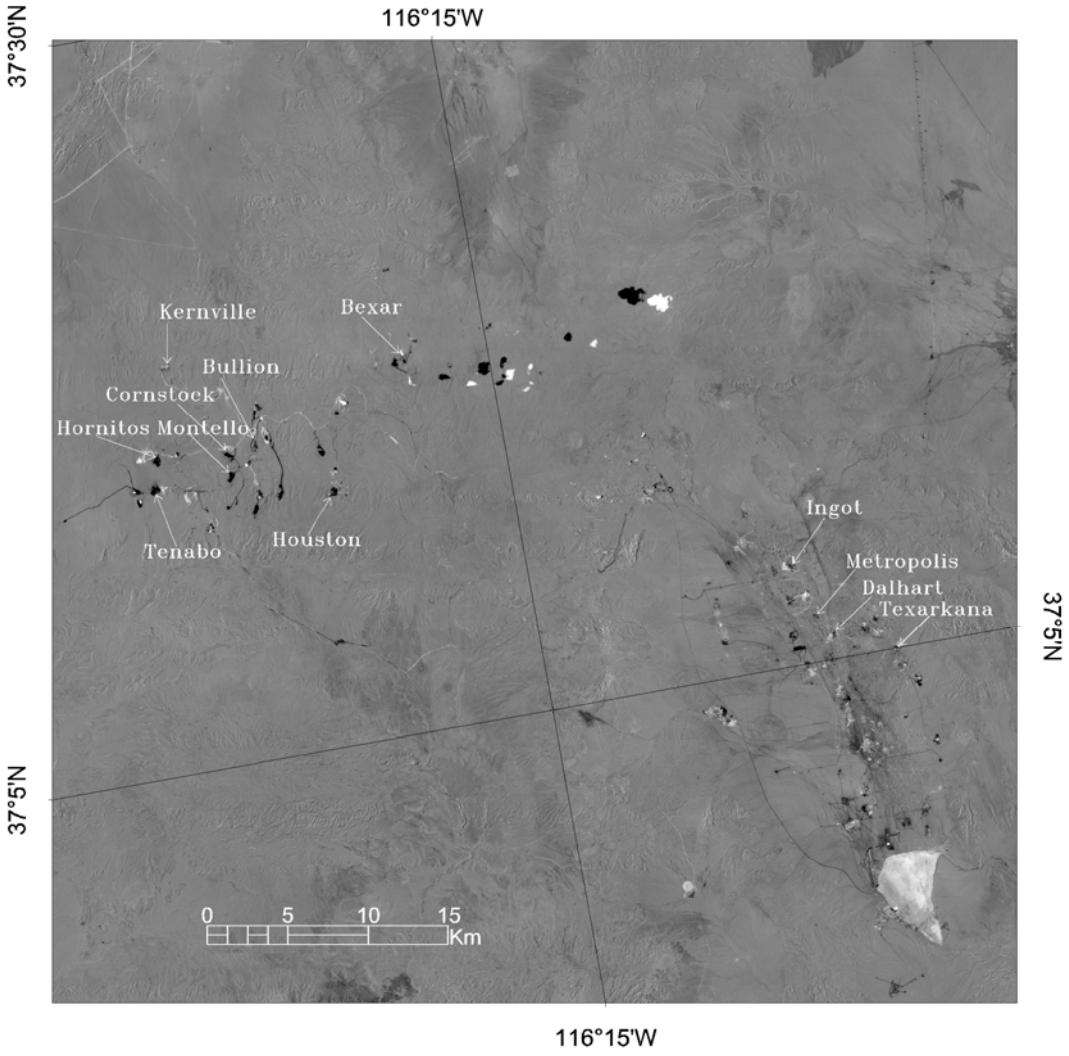

Fig. 7: Landsat TM change image of the Nevada test area between May 28, 1986 and May 26, 1991. The image shown is the first component of a MNF (Minimum Noise Fraction) transformation of the 6 iterated MAD difference images corresponding to the 6 Landsat TM VNIR/SWIR bands. The intensities are stretched to ± 8 standard deviations of the no-change pixels identified by the algorithm. Middle gray pixels indicate no change, light or dark pixels indicate changes.

Figure 7 shows a MAD (Multivariate Alteration Detection) image (Nielsen, 2007) based on two Landsat 5 TM acquisitions. It spans the time interval from May 28, 1986 to May 26, 1991 and includes the entire Nevada Test Site. Bright and dark pixels are indicative of significant changes which have occurred during the interval. Middle grey indicates no change. All of the tests in *Table 2* which occurred within this period are marked (e. g. from "Montello" to "Kernville") and can be associated with change signals in the image. The optical change detection results generally agree with the findings from the SAR data. However, due to the lack of an adequate temporal resolution of the data a one-to-one comparison of individual explosions studied with both methods is not feasible.

Discussion

In principle, the subsidence measurements could be estimated in millimeter accuracy, but this is hard to achieve in practice, owing to the influence of many errors sources, e.g. atmospheric turbulence, processing approximations, and measurement artifacts etc. In comparison to seismic methods (with about km error ellipse) the reachable accuracy by estimation of horizontal coordinates is obviously better. The selection of the absolute offsets after the phase unwrapping is 'arbitrary', since DInSAR provides relative measures only. However, this is not a critical point if large stable areas are available within the scene. Second, the geologic and hydrologic environment of the local test area is known up to a limited degree only. By lack of information the modeling of deformation is only preliminary. Nevertheless, the results for the derived decay constants (not shown) and initial deformation rates did not show many regional distinctions. If the measured signals are taken in close time intervals, a 'continuous' time series is obtained. This technology is regarded a valuable tool to supplement existing methods for monitoring compliance with the CTBT.

Conclusions

In comparison to optical EO data SAR is independent from weather conditions and time of day. The differential InSAR techniques offer the opportunity to reveal both coseismic and postseismic subsidence signals caused by underground nuclear explosions with multi-dimensional parameters. These observations open the possibility that InSAR may provide additional capabilities to supplement existing methods for monitoring compliance with the CTBT, e.g. underground nuclear explosions may not need to be captured coseismically by radar images in order to be detectable. However it should be mentioned that the data available for this study do not by far have the necessary temporal resolution needed in a CTBT verification scenario. Such data could become available in the near future since there are promising system developments under way (e.g. TerraSAR-X and RapidEye for optical and radar data, respectively) that greatly reduce the return rate for a given point on Earth with an improved spatial resolution. Clearly, such information is important for nuclear monitoring and, given the required timeliness, could be used in a CTBT verification scenario together with the seismically detected explosion signals to initiate and to guide an on-site-inspection by the CTBTO authority. This work has been carried out in part within the framework of the Global Monitoring for Security and Stability (GMOSS) Network of Excellence initiated by the European Commission.

References

Canty, M. J., Nielsen, A. A., Schlittenhardt, J., 2005, Sensitive change detection for remote monitoring of nuclear Treaties. In: *Proceedings of the 31st International Symposium on Remote Sensing of Environment, Global Monitoring for Sustainability and Security*, St. Petersburg, Russia, 20-24 June 2005

Canty, M. J., Schlittenhardt, J., 2001. Satellite data used to locate site of 1998 Indian nuclear test. *EOS Transaction American Geophysical Union*, 82(3), pp. 25-29.

Gabriel, A. K., Goldstein, R. M, Zebker. H. A., 1989, Mapping small elevation changes over large areas: differential radar Interferometry. *Journal of Geophysical research*, 94 (B7), pp. 9183-9191

Gutjahr KH., 2004. Monitoring of Alpine Glaciers via Multipass Differential SAR Interferometry. In: *Proceedings of EUSAR 2004*, pp. 75 – 78, 25-27 May 2004, Ulm

Nielsen, A. A., 2007. The Regularized Iteratively Reweighted MAD Method for Change Detection in Multi- and Hyperspectral Data. IEEE Transactions on Image Processing 16(2), 463-478.

Springer, D. L., Pawloski G.A., Ricca, J. L., Rohrer, R. F., Smith, D. K., 2002. Seismic Source Summary for All U.S. Below-Surface Nuclear Explosions. In: *Bulletin of the Seismological Society of America*, Vol. 92, No. 5, pp. 1806-1840.

Vincent, P., S. Larsen, D. Galloway, R.J. Laczniak, W.R. Walter, W. Foxall, and J. J. Zucca., 2003. New signatures of underground nuclear tests revealed by satellite radar Interferometry. *Geophys. Res Letters*, 30(22), 2141.

A Robust Satellite Techniques for oil spill detection and monitoring in the optical spectral range.

Daniele Casciello[1], Caterina S. L. Grimaldi[2] , Irina Coviello[2], Teodosio Lacava[2], Nicola Pergola[2,1] and Valerio Tramutoli[1,2]

[1] *Department of Engineering and Physics of the Environment (DIFA), University of Basilicata,85100 Potenza, Italy*

[2] *Institute for the Methodologies and the Environmental Analysis (IMAA), National Research Council,85050 Tito Scalo (PZ), Italy*

* casciello@unibas.it

Abstract

In the last years, the environmental pollution of the sea due to the oil spills out-coming from different sources (oil rigs releases, illegal discharges from vessels, tanker accidents, acts of environmental warfare, etc.) still continues to be a serious environmental problem. Satellite remote sensing could be an useful tool for the management of this kind of hazards.

Recently, a new AVHRR (Advanced Very High Resolution Radiometer) technique for near real time monitoring of the oil spilled areas, based on the general Robust Satellite Techniques (RST) approach, has been presented. In this paper, results related to several oil spills events occurred in the past are discussed. Moreover, because of the complete independence of the proposed approach on the specific satellite platform, first achievements obtained exploiting RST potentialities with MODIS (Moderate Resolution Imaging Spectroradiometer) data (which offers a better spatial resolution than AVHRR) for different test cases (also in different geographic areas) are also shown.

Introduction

In the last years, the use of satellite remote sensing for environmental monitoring has drastically increased. Sea pollution monitoring is one of the main application where satellite data have been largely used. Oil discharge, among the technological hazards, is one of the most environmentally damaging man-made marine hazards.

Up to now several satellite techniques devoted to the detection of oil spill have been developed. They are mainly based on the use of SAR (Synthetic Aperture Radar) technology. Such methods (even if not in whatever wind condition) assure good sensitivity for oil spill detection and high spatial resolution for a detailed description of the polluted area. Unfortunately, they cannot be suitable for near real-time monitoring at all latitudes because of revisiting cycles which ranges from few days up to 5 weeks moving from polar to equatorial zones respectively. Till SAR constellations (like the Italian COSMO-Skymed mission), able to increase time repetition, are not operative, the SAR technology cannot be profitably used for a near real-time monitoring of these phenomena. On the other hand, passive optical sensors, on board meteorological satellites, could be, in principle, used for oil spill monitoring, provided that suitable data analysis techniques (still lacking) are developed. In fact, thanks to a temporal resolution which is better than a few hours (up to a few minutes) and despite their lower

spatial resolution (not better than 250m in the visible spectral range) they could represent the unique possibility when a timely detection is crucial in order to mitigate the damages.

Recently (Casciello et al., 2007) a new technique for the detection and the monitoring of oil spill has been presented. It is based on the general Robust Satellite Techniques (RST, Tramutoli 1998 and 2005) approach; it exploits the multi-temporal analysis of thermal channels AVHRR (Advanced Very High Resolution Radiometer) records in order to detect, automatically and timely, the presence of the oil spill on the sea, minimizing the "false-detections" possibly caused by spurious effects.

In this paper, first we tried to verify the potential of the proposed techniques in different observational conditions. Two different test case have been chosen: i) the Seki - Baynunah events of 1994, and ii) the oil pollution due to oil extraction releases from rigs and pipelines on the Caspian Sea during May 1996.

The second aim of this work is to asses the RST intrinsic exportability on other satellite sensors. In particular, we applied RST using visible data acquired by MODIS (Moderate Resolution Imaging Spectroradiometer), the radiometer aboard the Terra and Aqua EOS (Earth Observing System) missions. MODIS visible channels have a spatial resolution of 250m, (better than AVHRR) which might improve the quality of the obtained results. The analyzed oil spill event is the Lebanon "Jiyyeh power plant", an accident occurred in July 2006.

Robust satellite techniques (RST) for oil spill detection using AVHRR data

The RST approach is an automatic change-detection scheme which has been already applied with good results in monitoring different natural and environmental risk (see for example: forest fires, Lasaponara et al., 1998, Cuomo et al, 2001; floods, Lacava et al., 2003, 2005; volcanic eruptions, Pergola et al., 2001; earthquakes, Filizzola et al., 2004).

It is based on use of historical series of satellite data for a complete signal characterization (spectral, spatial and temporal) followed by an anomaly detection step using automatic thresholds (specific for the time and the place of observation).

In the case of oil spill, the signal under investigation is the one measured in AVHRR TIR channels: this is namely due to different thermal inertia between oil polluted sea areas and sea water (Fingas & Brown, 1997a & 1997b, 2000) at these wavelengths. Due to its thermal inertia, in fact, lower than the sea water, oil polluted areas have higher brightness temperature in AVHRR TIR images collected in daytime, the opposite during the night (Casciello et al., 2007).

Starting from those considerations, two different indexes (one for the AVHRR channel 4 and another one for the channel 5) have been proposed (Casciello et al., 2007):

$$\otimes_{\Delta T_4}(\mathrm{r},t') = \frac{[\Delta T_4(\mathrm{r},t') - \mu_{\Delta T_4}(\mathrm{r})]}{\sigma_{\Delta T_4}(\mathrm{r})} \qquad (1)$$

$$\otimes_{\Delta T_5}(\mathrm{r},t') = \frac{[\Delta T_5(\mathrm{r},t') - \mu_{\Delta T_5}(\mathrm{r})]}{\sigma_{\Delta T_5}(\mathrm{r})} \qquad (2)$$

where $\Delta T_x(\boldsymbol{r},t') = T_x(\boldsymbol{r},t') - T_x(t')$ (with x being AVHRR channel 4 or 5, respectively) is the difference between the current ($t = t'$) signal value $T_x(\boldsymbol{r},t')$ at location $\boldsymbol{r}$ and the spatial average $T_x(t')$, computed in place on the image at hand considering cloud-free pixels only all belonging on the same 'sea' class in the investigated area (i.e. all the cloud-free sea pixels of the Region of Interest). $\mu_{\Delta Tx}(\boldsymbol{r})$ and $\sigma_{\Delta Tx}(\boldsymbol{r})$ are the time average and standard deviation values of $\Delta T_x(\boldsymbol{r},t')$ computed on an homogeneous data-set of cloud-free satellite records collected at location $\boldsymbol{r}$ in the same observational conditions (same month of the year, same time of acquisition) of the image under investigation.

By this way, $\otimes_{\Delta T x}(\mathrm{r},t')$ gives the excess of the current signal $\Delta T_x(\boldsymbol{r},t')$ compared with its historical mean value and weighted by its historical variability at each considered location. Remembering oil spill spectral signatures described above for both AVHRR channel 4 and 5, we expect to find, in correspondence of polluted zones, high positive values of both the indexes during the day.

AVHRR RST applications

All the RST prescriptions have been followed in order to study both the test cases: images were calibrated, geo-referenced and precisely navigated (with sub-pixel accuracy) using the SANA (Sub-pixel Automated Navigation of AVHRR) approach proposed and validated by Pergola and Tramutoli (2001, 2003). A sub scene, sized 512x512 and centred on the Region of Interest, was extracted for each pass and re-projected in the same projection in order to obtain a time sequence of co-located and superimposed images. Temporal average (i.e. $\mu_{\Delta T}(\boldsymbol{r})$) and standard deviation (i.e. $\sigma_{\Delta T}(\boldsymbol{r})$) reference fields were computed on this area using the above constructed data-sets for AVHRR thermal infrared channels 4 and 5. Finally, the two local variation indexes, defined in equation 1) and 2), have been computed.

The Seki - Baynunah event

During the night of 30th March 1994, Panamanian oil tanker "SEKI" and the oil tanker recorded to the United Arab Emirates "BAYNUNAH", had a collision near to the strait of Hormuz, 16 Km approximately from the coast of Fujairah of the UAE (United Arab Emirates) (figure 1).

One AVHRR image, taken on 31 March 1994, at 12.47 GMT (local time of 16.47 P.M.) from NOAA-11, clearly captured the initial spread of oil spill.

In Fig. 2 results obtained using the $\otimes_{\Delta T_4}$ index (Eq. 1) for this AVHRR image, the first available after the accidents, are shown. The presence of oil spill is detected with a reliability of 100% (no false alarms) over the full scene (figure 2a) by RST at very high signal-to-noise ratio (S/N) levels ($\otimes_{\Delta T_4} > 5$). Such a S/N ratio means, in the RST context, that the observed signal excess is 5 'sigmas' times higher than the historically observed expected value. In figure 2b, instead, the "adjustability" of RST technique is shown; it allows us to better investigate spatial distribution of signal anomalies of different intensity associated to oil spills of different thickness and/or at different levels of emulsion in the sea water. These results are quite important because, different detection levels may be used according to the specific application: as far as a primary and timely detection is required, higher threshold level should be used to detect the presence of the spill and then, after detecting, RST is able to better describe the extension of the polluted area using different (lower) threshold levels.

Similar results have been achieved using the $\otimes_{\Delta T_5}$ index (Eq. 2). Also in this case, higher values of the index ($\otimes_{\Delta T_5} > 5$), allow us to identify, without any false alarm, the presence of oil spill over the scene. Moreover, once again, thanks to the adjustability of RST technique was possible to reveal, and well separate, the signals due to the different oil polluted zones using lower index values (figure 2c).

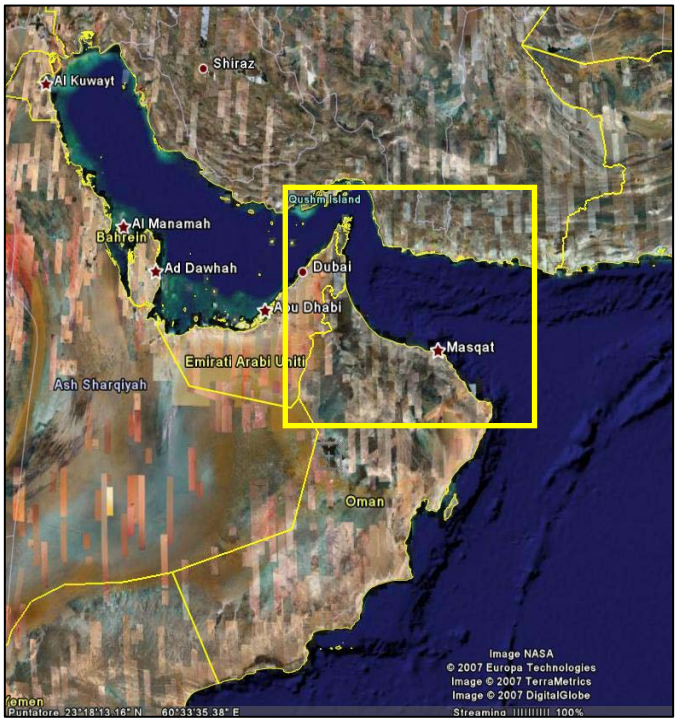

Fig. 1: Localization of the Seki - Baynunah event

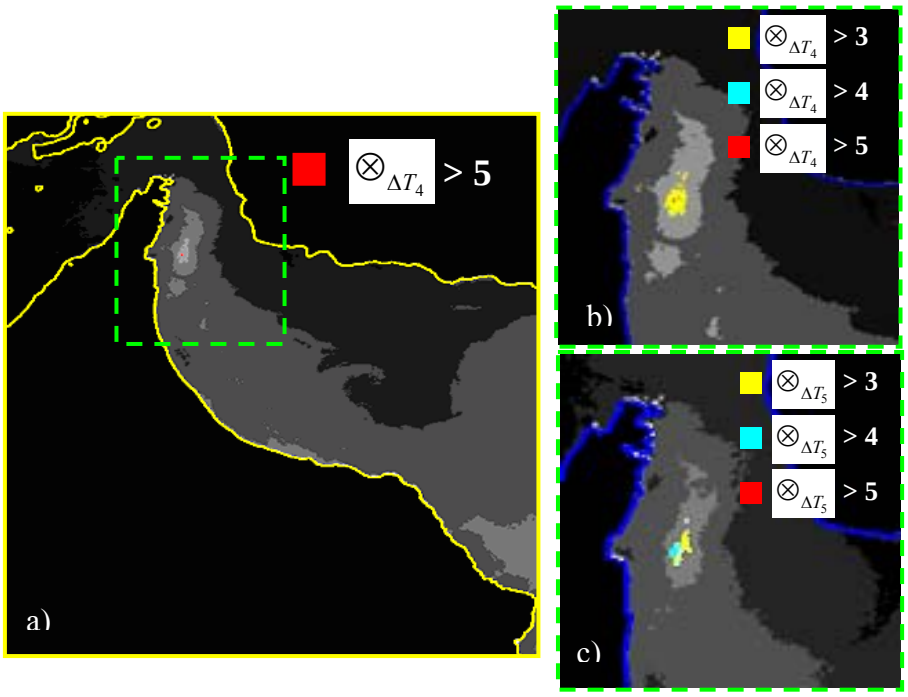

Fig. 2: Results achieved applying index $\otimes_{\Delta T_4}$ and $\otimes_{\Delta T_5}$ on the AVHRR image of 31th of March 1994. (a) Full scene, $\otimes_{\Delta T_4}$ values higher than 5 are depicted in red; (b) a zoom describing oil spilled area using different thresholds, coloured layers show the values $\otimes_{\Delta T_4} > 3, 4, 5$; (c) A zoom describing oil spilled area using different thresholds, coloured layers show the values $\otimes_{\Delta T_5} > 3, 4, 5$

Oil pollution of Caspian Sea

The above described AVHRR indexes have been also used to analyze the situation of the Caspian Sea during May 1996.

In figure 3, a map of the zone and main accumulation points (the ellipses) of oil spills due to their different sources (rigs and pipelines) (Ivanov et al., 2004) are shown.

Results achieved applying $\otimes_{\Delta T_4}$ index are shown in figure 4a for the AVHRR image of 12th of May 1996 and, as can be seen looking at this figure, using an RST threshold $\otimes_{\Delta T_4} > 5$ again it is possible to detect " for sure" the presence of oil spill on the sea (with a high level of accuracy and without any false detection). Also in this case, using different threshold levels, it is possible to map the area and the spreading of the oil spill, as is shown in figure 4b, where layers showing results achieved using $\otimes_{\Delta T_4} > 3, 4, 5$ are overlayed with different colours.

Similar results are shown in figure 4c, applying $\otimes_{\Delta T_5}$ index with the same threshold: also in this case RST was quite able to recognize and to map the extension of oil spilled areas on the sea with only slight differences.

The analysis of the above described results, obtained applying the RST AVHHR approach to both the test cases, confirms the potential of such a technique in detecting and describing oil spill, with a good accuracy and reliability and in different observational conditions.

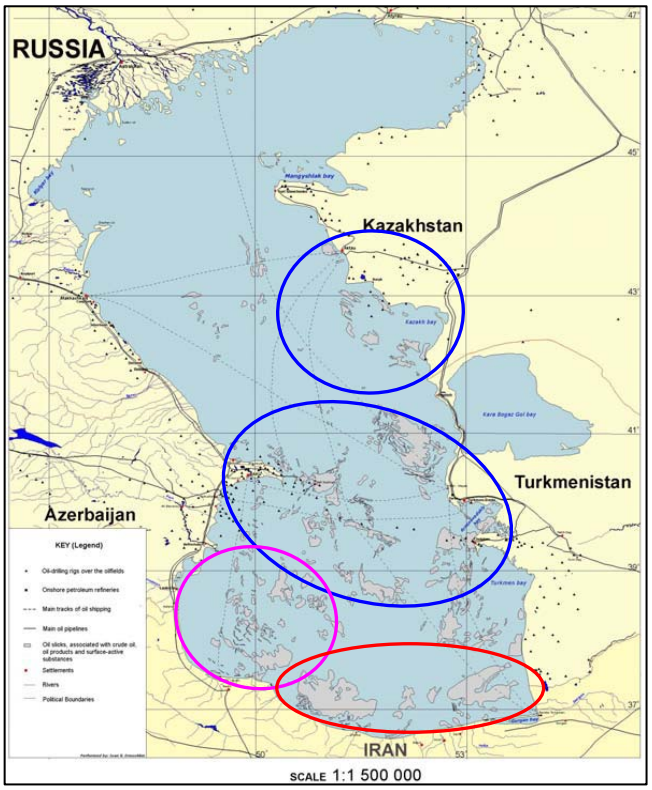

Fig. 3: Map of oil spills accumulation in the Caspian Sea areas related to crude oil, oil products and other man-made oil pollution on the surface of the Caspian Sea (May 1996). Ellipses show areas of oil slick accumulations over the oil production fields (blue), bottom seepages (violet) and river run-off (red).

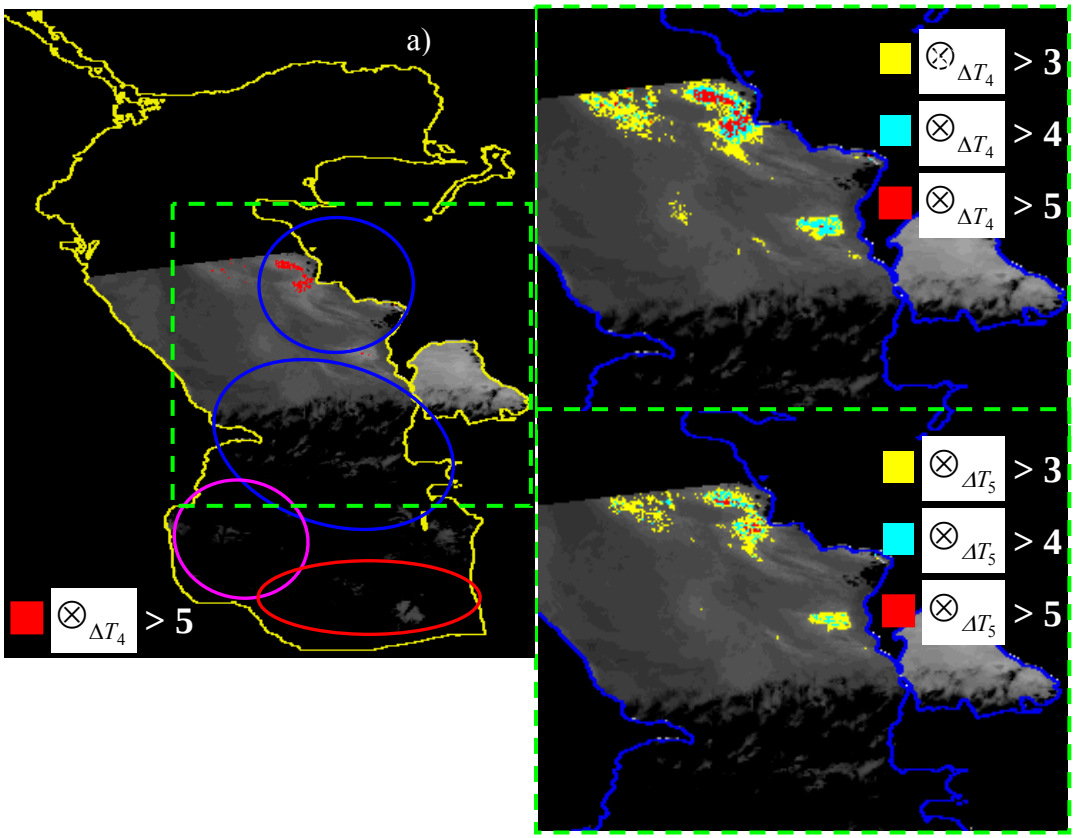

Fig. 4: As figure 2 for the AVHRR image of 12th of May 1996. (a) Full scene, $\otimes_{\Delta T_4}$ values higher than 5 are depicted in red; (b) a zoom describing oil spilled area using different thresholds, coloured layers show the values $\otimes_{\Delta T_4}$ > 3, 4 ,5; (c) A zoom describing oil spilled area using different thresholds, coloured layers show the values $\otimes_{\Delta T_5}$ > 3, 4 ,5

Oil spill detection and monitoring using MODIS visible (VIS) and near infrared (NIR) channels

One of the main advantage of the RST approach is its intrinsic exportability on different satellite sensors: what we need is just the presence of long historical data-set of satellite records. In this paper, for the first time, we tried to apply RST using MODIS data for the detection and the monitoring of oil spill. MODIS is an instrument launched by NASA in 1999 on board the Terra (EOS AM) satellite, and in 2002 on board the Aqua (EOS PM) platform. MODIS capture data in 36 spectral bands ranging in wavelength from 0.4 µm to 14.4 µm and at varying spatial resolutions (2 bands at 250m, 5 bands at 500m and 29 bands at 1000m).

Our choice felt on the two channels with the best spatial resolution, namely channel 1 (620 - 670 nm, visible) and channel 2 (841 - 876 nm, near-infrared). Oil spill reflectance, in fact, is different from that of the surrounding sea water, so that, it will be possible to detect oil spill presence.

The problem is that signal reflected by oil spill is not unique but it may change depending on several factors: solar/viewing geometry, satellite azimuth, wind speed. As a consequence, oil spill can appear, in VIS and NIR bands, less or high reflecting than the sea water (Fingas & Brown, 1997a & 1997b, 2000, Hu et al., 2003). Some automatic techniques and approaches

(e.g. Adamo et al., 2006, Hu et al., 2003; Shi et al., 2007), up to now, have been proposed but also if the efforts are appreciable, the authors reported the difficulty to detect with a good accuracy the presence of oil spill at the sea for problems mentioned before and also for other kinds of problems (e.g. algae blooms and other natural phenomena).

Starting from these considerations, two different indexes were then computed (one for each MODIS channel), that for each image-location r and acquisition time t' can be written as:

$$\otimes_{ch_x}(\mathrm{r},t') = \frac{[V_{ch_x}(\mathrm{r},t') - \mu_{ch_x}(\mathrm{r})]}{\sigma_{ch_x}(\mathrm{r})} \qquad (3)$$

being $\otimes_x(\mathrm{r},t')$ the index computed on the basis of the MODIS channel x (x = 1 and 2), Vchx the measured reflectance, $\mu_{ch_x}(\mathrm{r})$ and $\sigma_{ch_x}(\mathrm{r})$ the corresponding reference fields computed on an homogeneous data-set of cloud-free satellite records collected at location r in the same observational conditions (same month of the year, same time of acquisition) of the image under investigation.

Remembering oil spill spectral signatures described above, we should find, in correspondence of polluted zones, both high positive indexes values, where oil spill reflectance is higher than the clear sea water one (positive contrast), and negative values when oil spill reflectance is less than the clear sea water one (negative contrast).

MODIS RST application

The RST technique was implemented using MODIS channel 1 and 2 following the procedure described in previous section. In the pre-processing phase all MODIS images available were collected for the studied event. Both the month of July and August have been analyzed following RST prescription, in particular all the MODIS image acquired over the Region of Interest (ROI) in the temporal range 08:30 – 09:30 GMT have been collected. Images were calibrated, geo-referenced and precisely navigated (with sub-pixel accuracy). A sub scene centred for this event on the ROI, was extracted for each pass and re-projected in the same projection in order to obtain a time sequence of co-located and superimposed images. Temporal average (μ(r)) and standard deviation (σ(r) reference fields were computed on this area using the above constructed data-sets for MODIS VIS channels 1 and NIR channel 2 and for the two months where the event is happened. Finally the two index above described have been computed for several MODIS imagery of July and August 2006.

The Lebanon " Jiyyeh power plant " accident

The test case studied by RST MODIS approach, is the Jiyyeh power plant " accident.

On the 13th and 15th of July 2006, Israel army forces brought a serious attack to the Jiyyeh power plant in Lebanon, bombing the fuel tanks close to the coast. A huge quantity of oil, between 11 millions and 40 millions of lither, was spilled into the sea. Due to the sea surface currents, oil spill became drifting northward and extended up to 150 kilometres arriving to the neighbour coasts of Syria (figure 5).

Fig. 5: Oil spill localization (left) and extension (right) (adapted by Report UNEP, 4 August 2006 available at: http://www.indybay.org/newsitems/2006/08/05/18294908.php)

After a few days, the oil spilled became forming tar balls that subsequently sank on the sea floor. Many species were damaged by oil and also a great part of Lebanon coast was completely covered by oil. The effects were visible till the end of August 2006.

Several MODIS images were available for the Lebanon, acquired from both NASA satellites Terra and Aqua. Using automatic extraction algorithm developed by IMAA-CNR[25] laboratory, many satellites passages were extracted and collected during the months of July and August 2006 (18 Terra images and 24 Aqua Images).

Remembering oil spill spectral signatures described in previous section for both channel 1 and 2, we find, in correspondence of polluted zones, both high positive indexes values, where oil spill reflectance is higher than the clear sea water one (positive contrast), and negative values where oil spill reflectance is less than the clear sea water one (negative contrast).

In particular we chosen an image of 23th July 2006 at 08.35 GMT with an oil spill-sea positive contrast and an image of 15th August 2006 at 08.45 GMT with an oil spill-sea negative contrast.

In the case of positive contrast (figure 6), the presence of oil spill is detected by RST at very high S/N levels ($\otimes_{ch_1} > 6$, $\otimes_{ch_2} > 5$). By observing fig.6 we can see that some residual false alarms due to clouds bounds (which reflectance values are comparable with the oil spill ones) are still present. These false alarms can be however eliminated by realizing and using a more refined cloud mask technique.

[25] Institute for the Methodologies and Environmental Analysis (IMAA), National Research Council (CNR), Italy

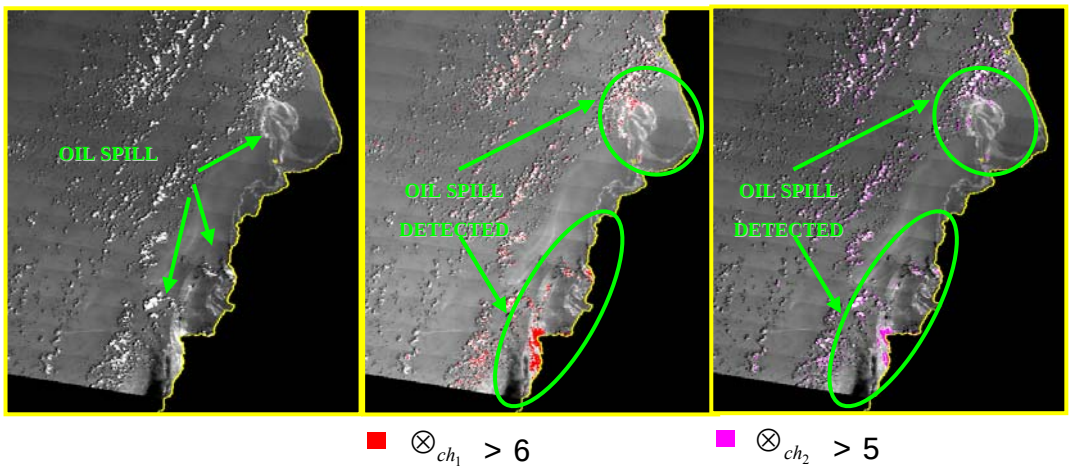

Fig. 6. Results of RST Technique. From the left to the right we have event image of 23th July 2006, the application of RST in channel 1 and in channel 2, land is masked in black.

In the case of negative contrast, where spill reflectance is lower than the clear sea water one, we have, unlike the previous case, low S/N values ($\otimes_{ch_1} <0$, $\otimes_{ch_2} <0$).

As you can see, in this case, looking for lower reflectance values, no false alarms related to clouds are present over the full scene.

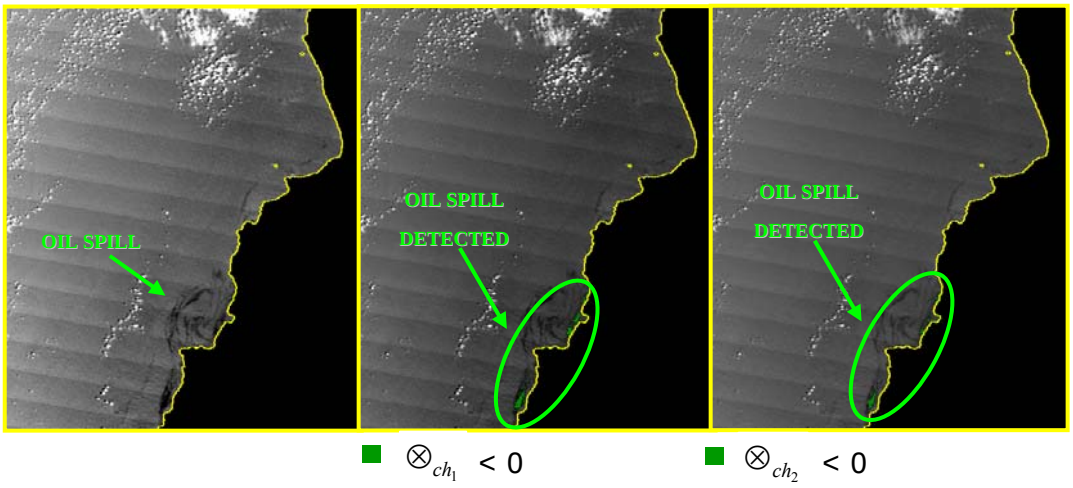

Figure 7 – Results of RST Technique. From the left to the right we have event image of 15th August 2006, the application of RST in channel 1 and in channel 2, land is masked in black.

In both cases, the results obtained for channel 1 and channel 2 are mostly comparable.

The comparison between the two different tests cases shows that the second approach needs more efforts to better understand how to improve the S/N level, for example using different reference fields or different analysis strategies, but up to now, it is scarcely applicable, since the obtained results are not far from the normal local variability.

On the other hand, results obtained in the case of positive contrast can find good application for slick description.

Conclusion

Recently a new AVHRR technique for oil spill detection and monitoring has been proposed. It is based on the RST approach, a general change-detection strategy.

Preliminary results shown in this paper confirm the potential of the proposed technique: for both the test cases analyzed, the oil spill due to different sources and in different observational conditions, has been, in fact, clearly detected with high accuracy and low rate of false alarms.

The detection was automatically performed and it was carried out using sole satellite data. The TIR anomalies identified on the images event were classified for sure as TIR anomalies due to oil spill.

Moreover, exploiting intrinsic exportability of RST approach (the complete independence of the proposed approach on the specific satellite platform) in this paper, for the first time, we applied it to MODIS data. In particular, higher spatial resolution data (250m) acquired in the first two MODIS channels have been used. Preliminary results obtained show the feasibility of such an attempt.

When positive contrast between oil spill reflectance and sea water is present, in fact, clear high anomalies have been detected on the corresponding MODIS image (with comparable results in both the channels). Some residual problems related to the clouds bounds could be corrected using a more detailed and reliable cloud mask. On the other side, deeper studies and analysis need to be carried out in the case of negative contrast to better enhance the S/N value.

The higher spatial resolution of MODIS, could help also in the detection of event whose dimension and/or intensity are not enough in order to be detected by AVHRR.

In the future, the combination/integration of both the methodologies should help the local authorities in the timely management of oil spill risk. If such positive results will be further confirmed, the AVHRR TIR approach can be used for the oil spill detection in near-real time (thanks to the higher temporal resolution), whereas, MODIS can be used for a more detailed description of the slick extension.

References

Adamo, M., De Carolis, G., De Pasquale, V., Pasquariello, G. (2006).On the combined use of sun glint Modis and Meris signatures and SAR data to detect oil slicks. *Proceedings of SPIE - The International Society for Optical Engineering*, v 6360, *Remote Sensing of the Ocean, Sea Ice, and Large Water Regions 2006*, p 63600G

Casciello, D., Lacava, T., Pergola, N., Tramutoli, V., (2007). Robust Satellite Techniques (RST) for Oil Spill Detection and Monitoring**.** *Analysis of Multi-temporal Remote Sensing Images, 2007. MultiTemp 2007. International Workshop on the. 18 – 20 July, 2007, 1-6.*

Cuomo, V., Lasaponara, R., Tramutoli, V., (2001). Evaluation of a new satellite-based method for forest fire detection. *International Journal of Remote Sensing*, 22 (9), 1799-1826.

Di Bello G., Filizzola C., Lacava T., Marchese F., Pergola N., Pietrapertosa C., Piscitelli S., Scaffidi I., Tramutoli V.**,** (2004)**.** Robust Satellite Techniques for Volcanic and Seismic Hazards Monitoring**.** *Annals of Geophysics*, 47, (1) 49-64.

Filizzola, C., Pergola, N., Pietrapertosa, C., Tramutoli, V., (2004). Robust satellite techniques for seismically active areas monitoring: a sensitivity analysis on September 7th 1999 Athens's earthquake, in *Seismo Electromagnetics and Related Phenomena*. *Physics and Chemistry of the Earth*, vol. 29 , pp 517-527.

Fingas, M., F., Brown, C., E., (1997). Review of oil spill remote sensing. *Spill Science & Technology Bulletin*, 4 (4), 199-208.

Fingas, M., F., Brown, C., E., (1997). Remote sensing of oil spills. *Sea Technology*, 38, 37-46.

Fingas, M., F., Brown, C., E., (2000). A review of the status of advanced technologies for the detection of oil in and with ice. *Spill Science & Technology Bulletin*, 6 (5), 295-302.

Hu, C., Müller-Krager, F., E., Taylor, C., J., Myhre, D., Murch, B., Odriozola, A., L., et al. (2003). MODIS detects oil spills in Lake Maracaibo, Venezuela. *EOS, Transactions, American Geophysical Union*, 84(33), 313, 319.

Ivanov, A., Yu., Fang., M., He, M., Ermoshkin, S., I., (2004). An Experience of using RADARSAT, ERS-1/2 and ENVISAT SAR images for oil spill mapping in the waters of the Caspian sea, Yellow sea and east China sea. *2004 Envisat & ERS*
Symposium. 6-10 September, Salzburg, Austria.

Lacava, T., Cuomo, V., E.V. Di Leo, Pergola, N., Romano, F., Tramutoli, V., (2005). Improving Soil Wetness Variations monitoring from passive microwave satellite data: The case of April 2000 Hungary Flood. *Remote Sensing of Environment* , vol. 96, no. 2, pp. 135-148.

Lacava, T., Di Leo, E.V., Pergola, N., Romano, F., Sannazzaro, F., Tramutoli, V., (2003). Analysis Of Multi-Temporal Satellite Records For Extreme Flooding Events Monitoring. *Proceedings of the 5rd Plinius Conference*, Ajaccio, Corsica, France.

Lasaponara, R., Cuomo, V., Tramutoli, V., (1998). Fire detection by AVHRR toward a new approach for operational monitoring. *Remote Sensing for Agriculture, Ecosystems, and Hydrology II*. Proc. SPIE, 3499.

Pergola, N., Tramutoli, V., (2000). SANA: sub-pixel automatic navigation of AVHRR imagery. *International Journal of Remote Sensing*, 21 (12), 2519-2524.

Pergola, N., Tramutoli, V., (2003). Two years of operational use of Subpixel Automatic Navigation of AVHRR scheme: accuracy assessment and validation. *Remote Sensing of Environment*, 85, 190-203.

Pergola, N., Tramutoli, V., Lacava, T., Pietrapertosa, C., (2001). Robust satellite techniques for monitoring volcanic eruptions. *Annali di Geofisica*, vol. 45, no. 2, pp. 167-177.

Shi, L.; Zhang, X., Seielstand, G., Zhao, C., He, M., (2007).Oil spill detection by MODIS images using Fuzzy Cluster and Texture Feature Extraction. *IEEE Oceans 07*, Aberdeen, UK, June 18 – 21.

Tramutoli,V., "Robust AVHRR techniques (RAT) for environmental monitoring: theory and applications". *Earth surface remote sensing II*. *Proceedings of SPIE*, vol. 3496, pp. 101-113, 1998.

Tramutoli, V., "Robust Satellites Techniques (RST) for natural and environmental hazards monitoring and mitigation: ten years and applications". *The 9th International Symposium on Physical Measurements and Signatures in Remote Sensing*, Beijing (China), ISPRS, vol. XXXVI (7/W20), pp. 792-795, ISSN 1682-1750, 2005.

From GMOSS to GMES: Robust Satellite Techniques for flood risk mitigation and monitoring.

Teodosio Lacava[1], Irina Coviello[1], Elena Vita Di Leo[1], Mariapia Faruolo[1], Nicola Pergola[1,2], Valerio Tramutoli[2,1]

[1] *Institute of Methodologies for Environmental Analyses – CNR, C.da Santa Loja, 85050 Tito Scalo (PZ), Italy*

[2] *Department of Engineering and Physics of Environment - University of Basilicata, via dell'Ateneo Lucano 10, 85100 Potenza, Italy*

Abstract

In the past, satellite remote sensing techniques have been widely used within the flood risk management cycle. Satellite data acquired in different spectral ranges, at various spatial and temporal resolutions, have been used by the decision-makers in all the phases of such a cycle. The combination of several kinds of satellite data, when they are available, could help them to have a better view of the risk scenario, taking more reliable decisions.

In this paper, a general Robust Satellite Techniques (RST) approach has been applied both using microwave data acquired by AMSU (Advanced Microwave Sounding Unit) and optical data by AVHRR (Advanced Very High Resolution Radiometer). Preliminary results related to the flooding event which hit the Carpathian Basin during April 2000 are shown. First outcomes achieved seem to demonstrate the feasibility of such a combination: passive microwave data may assure us data in whatever whether conditions with a low spatial resolution, while optical data allows us to have, in absence of clouds, more detailed information about surface situation.

1. Introduction

Remote sensing data have been widely used within the hydro-meteorological risk management cycle: two main fields of interest can be defined for the use of remote sensing data in the flood domain: (1) a detailed mapping approach, that is required for the production of hazard assessment maps and for input to various types of hydrological models. These mapping approaches are used at the regional and local scales; the user requirements are related to detailed mapping for updating (and sometimes creating) risk maps. The maps contribute to the hazard and vulnerability aspects of flooding. The other field of interest is: (2) a larger scale approach that explores the general flood situation within a river catchment or coastal belt, with the aim of identifying areas that have greatest risk and need immediate assistance; in this case, remote sensing may contribute to the initialization of numerical weather prediction models, weather forecasts and to mapping of inundated areas, mainly at the regional level (CEOS, 2001, 2003 and references herein).

Satellite optical observations of floods have been hampered by the presence of clouds that resulted in the lack of near real-time data acquisitions. Microwave sensors can achieve regular observation of the earth's surface, even in the presence of cloud cover. Therefore, the combination/integration of both of them could improve the knowledge of the territory, mainly during the crisis phase, when timely and frequently updated situation reports are particularly required by the local authorities. To this aim optical and microwave instruments aboard polar and geostationary meteorological satellites can offer, despite their low spatial resolution (from few kilometers up to few hundreds of meters), temporal resolutions (from few hours up to few tens of minutes) high enough to guarantee timely, frequent and updated situation reports.

Moreover the availability of several satellite passes per day gives more chances to achieve optical cloud-free images (Sandholt et al., 2003; Jain et al., 2006).

A Robust Satellite Techniques (RST, Tramutoli 1998 and 2005) has been already applied with good results in the framework of the hydro-meteorological risk mitigation and monitoring. In particular, two different applications have been developed: one (Lacava et al., 2005c) using data acquired by the microwave radiometer AMSU (Advanced Microwave Sounding Unit), flying aboard NOAA (National Oceanic and Atmospheric Administration) polar satellites, and another one based on the use of data collected by another sensor aboard NOAA satellite, the AVHRR (Advanced Very High Resolution Radiometer) (Lacava et al., 2004). The first is devoted to give information about soil wetness variations, while the second application concerns the mapping and monitoring of flooded areas. The current NOAA satellites constellation is able to provide at least one image every 6 hours (NOAA-OSD, 2004). This circumstance allows us to have frequent information at regional scale, making us able to give a support in the management cycle of flooding risk.

In this paper, we tried, for the first time, to combine both the applications. The flooding event whit hit the Carpathian Basin during April 2000 has been chosen as test case.

2. Methodology

The RST approach is an automatic change-detection scheme that identifies signal anomalies in the space-time domain as deviations from a normal state that has been preliminarily identified (and usually given in terms of time average and standard deviation) on the basis of satellite observations collected during several years, under similar observational conditions for each image pixel. The use of historical series of satellite records allows us a complete signal characterization (spectral, spatial and temporal) and an automatic threshold determination (specific for the time and the place of the observation) to be used for several change-detection applications.

When applied to monitoring soil wetness variations, the proposed formula is:

$$SWVI(x,y,t) = \frac{SWI(x,y,t) - \mu_{SWI}(x,y)}{\sigma_{SWI}(x,y)} \qquad (1)$$

where *SWVI(x,y,t)* is the proposed Soil Wetness Variation Index, while *SWI(x,y,t)* is a soil wetness index defined as the difference (SWI=BT89GHz–BT23GHz) between the radiance (expressed in Brightness Temperature) measured in AMSU channels 15 (at 89 GHz) and 1 (at 23 GHz), respectively (Grody, 2000). $\mu_{SWI}(x,y)$ and $\sigma_{SWI}(x,y)$ are respectively the temporal average of SWI and its standard deviation, both computed on a selected, multi-annual AMSU imagery data-set composed by records collected during the same month of the year and acquired at around the same hour of the day. The *SWI(x,y,t)* may provide useful information about surface emissivity variations, but it is unable to discriminate the amount of these variations which are actually related to different soil water contents from the ones possibly due to vegetation and/or roughness effects. On the other side the *SWVI(x,y,t)* gives, at pixel level, the actual *SWI* excess compared to its unperturbed conditions (*SWI(x,y)* - $\mu_{SWI}(x,y)$), and compares this excess with the normal variability of *SWI(x,y,t)* ($\sigma_{SWI}(x,y)$), historically observed for the same site under similar observational conditions. In order for an anomaly to be significant, its magnitude should be greater (at least) than the normal fluctuation of the signal.

The SWVI index has been already implemented and tested on several recent flooding events occurred in Europe (Lacava et al., 2005a, 2005b and 2005c), demonstrating its capabilities in following temporal dynamic of the analyzed cases, but also in indicating the presence of already wet soils (as consequences of other meteorological events, like antecedent precipitation or snow-melting) just before the occurrence of the main rain episode.

The different spectral behaviour of water and soil in the AVHRR channels 1 (0,58-0,68μ) and 2 (0,725-1μ), respectively, has been used in different combinations (difference or ratio) by several authors (Xiao and Chen, 1987; Sheng and Gong., 2001) in order to identify flooded areas. In this case, RST approach has been implemented using the following two indexes:

$$\otimes_{2-1}(x,y,t) = \frac{R_{2-1}(x,y,t) - \mu_{2-1}(x,y)}{\sigma_{2-1}(x,y)} \quad (2)$$

$$\otimes_{2/1}(x,y,t) = \frac{R_{2/1}(x,y,t) - \mu_{2/1}(x,y)}{\sigma_{2/1}(x,y)} \quad (3)$$

where, $R_{2-1}(x,y,t)=R_2(x,y,t)-R_1(x,y,t)$ is the difference, and $R_{2/1}(x,y,t)=R_2(x,y,t)/R_1(x,y,t)$ the ratio, between R_2 and R_1 AVHRR bands computed pixel-by-pixel on the AVHRR image at hand; $\mu_{2-1}(x,y)$ and $\mu_{2/1}(x,y)$ are the time averages and $\sigma_{2-1}(x,y)$ and $\sigma_{2/1}(x,y)$ the standard deviations, of $R_{2-1}(x,y,t)$ and $R_{2/1}(x,y,t)$ time series computed on a selected multi-year data set of co-located, cloud-free, AVHRR records collected around the same time of day during the same month of the year.

The index $\otimes_{2-1}(x,y,t)$ (or $\otimes_{2/1}(x,y,t)$) gives, for each location (x,y), the present $R_{2-1}(x,y,t)$ (or $R_{2/1}(x,y,t)$) deviation from its expected (in unperturbed conditions) value, $\mu_{2-1}(x,y)$ ($\mu_{2/1}(x,y)$), for the same place (x,y) and period of observation, weighted by its normal variability $\sigma_{2-1}(x,y)$ ($\sigma_{2/1}(x,y)$), as historically observed for the same place under similar observational conditions. What we expect using such indexes is, other than a general reduction of false alarms, that the lower $\otimes_{2-1}(x,y,t)$ (or $\otimes_{2/1}(x,y,t)$) index values will appear associated to flooded zones.

Also such an approach has been already applied in mapping and monitoring of several flooding events happened in the past in Europe (Lacava et al., 2004; Tramutoli, 2007).

3. Test case

The proposed approach has been applied, in order to assess its actual potential and efficiency, during the flooding event that affected the Carpathian Basin (figure 1) in April 2000. The event caused about ten victims, the evacuation of 20.000 people and a large number of damages to the infrastructures and to the farmlands (Agence France Presse, 2000). The country which was mainly affected by the flood was Hungary, and the rivers that had a key role were the Tisza and the Danube. On the 9th of April 2000 the Hungary's government declared parts of eastern Hungary as a disaster area, allowing the release of funding to combat floods. A state of emergency was declared in the region hit by the flood (Agence France Press, 2000; European Water Management News, 2000; BBC News, 2000). The event under investigation in this paper started on the morning of 5th April and ended after approximately ten days. It was caused by a rapid snowmelt due both to heavy rainfalls in northern Hungary and western Romania and to a sudden increase in temperatures (Seth, 2000; Brakenridge et al., 2003). The area hit by the flood was, in fact, affected by two different meteorological events during the beginning of April: the first one was between the afternoon of 1st April and the morning of 2nd April, and the last one, more intensive, during 5th April.

Fig. 1: The Carpathian Basin, adapted from:
http://www.panda.org/about_wwf/where_we_work/europe/what_we_do/danube_carpathian/index.cfm

4. Results

In order to implement the SWVI index to the studied test case, all the AMSU imagery acquired during the month of April since 1999 have been collected, pre-processed and co-located in the space domain. Two different data-sets have been used, one with all the NOAA morning passes, the other one with afternoon passes. Then the reference fields have been computed and finally the SWVI has been calculated for April 2000. During the generation of the reference fields, a standard test (Grody, 2000) has been used in order to discharge from the following steps all the pixels identified as rainy affected.

In figure 2 results obtained using the SWVI in order to analyze the selected test case are shown. In particular, in the figure, the temporal sequence of the SWVI maps between the 6th and the 10th of April is shown. Note as all the areas affected by the rain felt during 5th April are clearly interested by high values of SWVI, as expected. Note also as the progressive decrease of such values moving towards the last days of the sequence, indicating a slow drying phase of the soils.

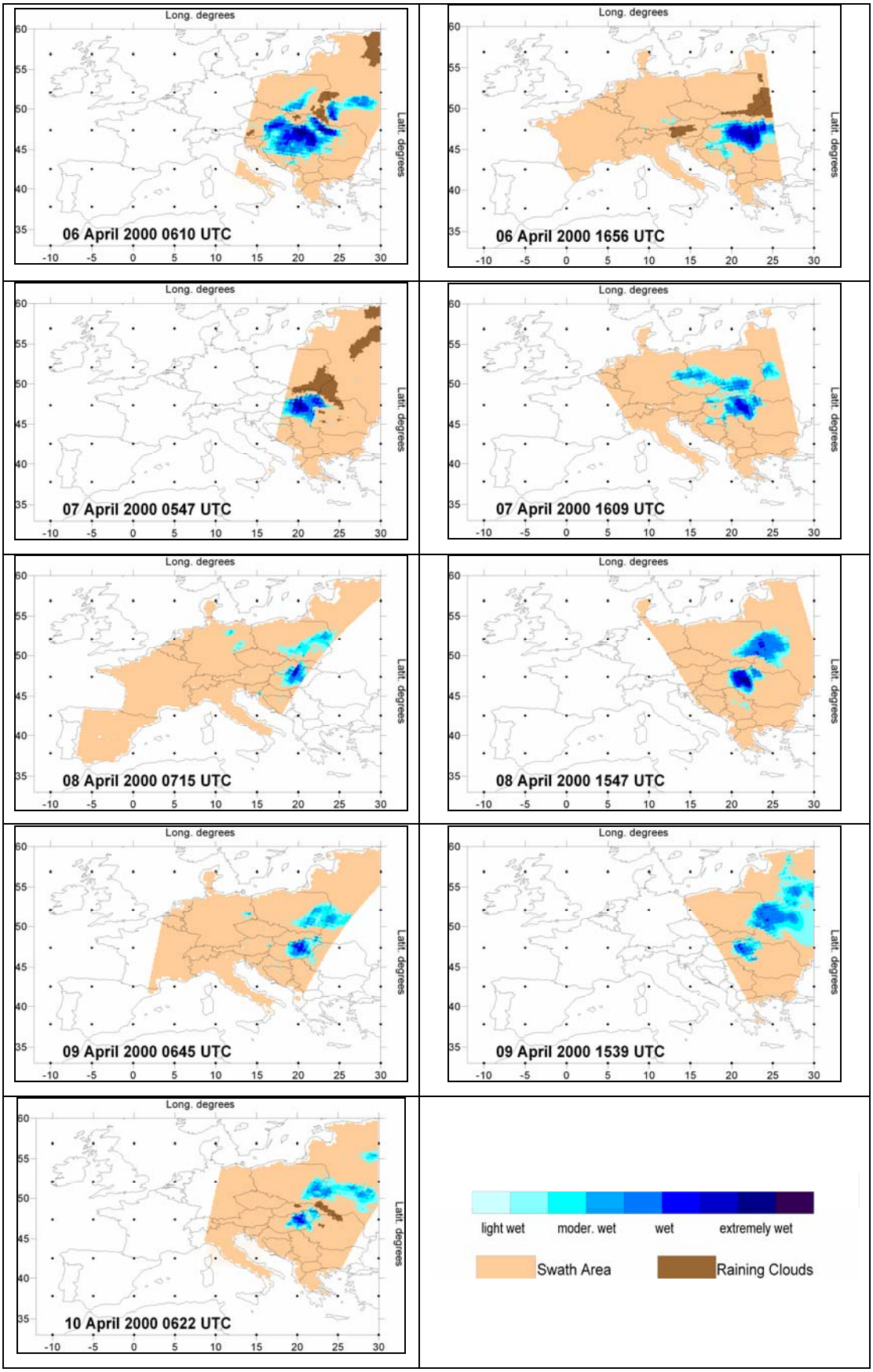

Fig. 2: Maps of *SWVI(x,y,t)* for several days of April 2000 (from the morning of 6th of April to the morning of 10th of April). Different values of SWVI have been coloured in different shades of blue (i.e. higher SWVI values are shown in darkest blue). The AMSU swath is shown in light orange. Raining clouds are depicted in brown. Colour bars show a qualitative range of fluctuation for each field.

Such results, once again, demonstrate the potential of the SWVI in following the spatial-temporal dynamics of the soil wetness variations as consequences of meteorological events.

The same approach has been used with AVHRR data, so again, all the AVHRR images acquired in the month of April since 1994 have been analyzed following again the RST prescription. Also in this case, a cloud detection test (One-channel Cloud-detection Approach - OCA, Pietrapertosa et al., 2001, Cuomo et al., 2004) has been used in order to avoid their effect on the reference fields computation.

In figure 3a the AVHRR image (channel 2) acquired on 9th April at 14.00 GMT is shown, as you can see, several clouds are still present over the region of interest, but they do not affect the SWVI map in this day (see figure 2). In particular, we analyzed the area within the yellow box where, as you can see in figure 3b, it is evident the presence of the Kiskore lake.

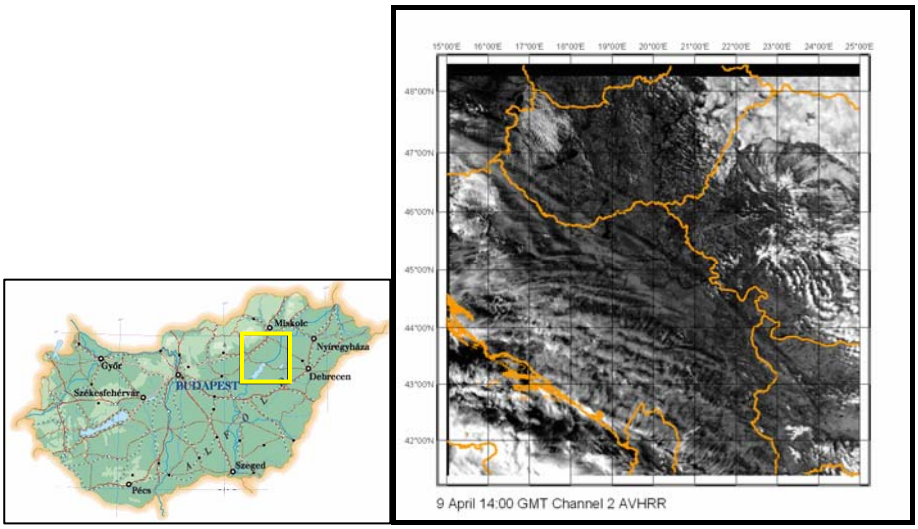

Fig. 3: a) AVHRR Channel 2 image of 9th April 2000 at 14:00 GMT. b) Localization of Kiskoere lake. The area within the yellow box has been analyzed by RST approach.

In figure 4 the results of the application of both the AVHRR indexes are shown. As you can see, they are both able to discriminate the edge of the Kiskore lake which is flooded, as well as other locations where the Tisza river overflowed.

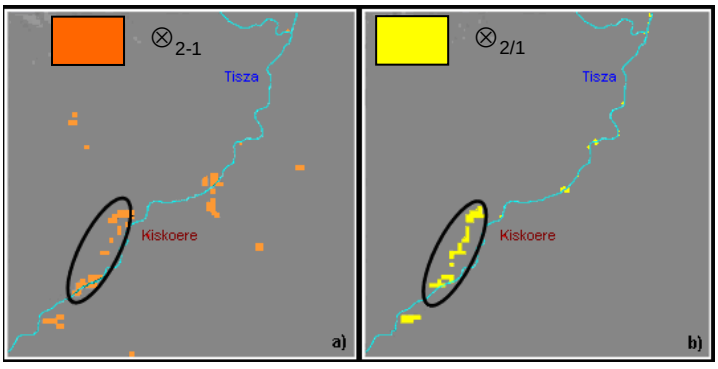

Fig. 4: Results obtained applying RST approach (pixels coloured in orange and yellow respectively) for the area within the yellow box in figure 3.

Such a result is, of course, an expected result: the intrinsic differential nature of the indexes described by expressions (2) and (3) gives us the opportunity to identify areas which are effectively flooded, discriminating them from permanent water bodies.

Unfortunately, this is the only partially cloud free AVHRR image available during the period between 6th and 10th of April 2000, so no other multi-spectral combinations are possible. However, this first result achieved, confirms the potential of such a combination: the SWVI gives us the opportunity to have a view of the soil situation at regional scale also in presence of clouds, and such an information is useful for local authorities because it frequently highlights the vulnerability of the area in terms of soil wetness variations. On the other side, both the two indexes proposed using AVHRR have been able to individuate, with a good reliability, a critical situation at local scale, that should help the decision-makers to better address their choices.

5. Conclusion

A Robust Satellite Techniques (RST) has been applied (in automatic way and by using only satellite data at hand and without any other ancillary information), in the mapping of flooded areas (using AVHRR data) as well as in the mapping of soil wetness variations (by AMSU data).

In this paper, for the first time, we tried to integrate the two different applications. As well known, in fact, microwaves assure all weather capabilities, while optical data should guarantee more detailed information, so that, a combination of both the applications could improve the quality of the obtained results. This should improve the risk scenario knowledge, helping the decision-makers to take better decisions, especially during the emergency phase.

Preliminary results showed in this paper confirm the feasibility of such an approach. The intrinsic robustness of the proposed approach allow us to identify, without false alarms, a critical situation along the Tisza River, in a contest where all the surrounded area was characterized by soil condition wetter than normal.

Such an approach is local but, for construction, globally exportable. Future works and improvements could be devoted, for AVHRR data, to the use of infrared data for a continuous monitoring during the day; in the microwaves the future developments could be devoted to better understand the space-time dynamic of such an index (especially in the phase preceding the considered event) in order to use it for prevention/prediction/mitigation purposes. Moreover, because of the complete independence from the specific satellite platform, such a technique could be easily exported to the new generation of satellite sensors with improved performances. In particular, regarding the optical application, MODIS (Moderate Resolution Imaging Spectroradiometer) aboard polar EOS mission (Earth Observing System) or SEVIRI (Spinning Enhanced Visibile and Infrared Imager) aboard geostationary MSG (Meteosat Second Generation), could be used, while the incoming MIRAS (Microwave Imaging Radiometer using Aperture Synthesis) aboard SMOS (Soil Moisture and Ocean Salinity) mission will be the future for the microwave application devoted to soil moisture measurements.

References

Agence France Presse, “Hungary: floods-Apr 2000”, available at http:www.reliefweb.int/w/rwb.nsf, 2000.

BBC news, “Flood-hit Hungary calls in army”, available at http://news.bbc.co.uk/1/hi/world/europe/707398.stm, Sunday April 9th 2000 15:22 GMT.

Brakenridge, G.R., Anderson, E., Caquard, S., “2000 Global Register of Extreme Flood Event”, Dartmouth Flood Observatory, Hanover, USA, digital media, available at http://www.dartmouth.edu/~floods/Archives/2000sum.xls, 2003.

CEOS (Committee on Earth Observation Satellites), "Disaster Management Support Project Earth Observation Satellites for Flood Management", *Flood Hazard Team Report 2001*, available at http://www.ceos.org/pages/DMSG/2001Ceos/Reports/flood.html, 2001.

CEOS (Committee on Earth Observation Satellites), "The Use of Earth Observing Satellites for Hazard Support: Assessments and Scenarios", *Final Report of the CEOS Disaster Management Support Group* (DMSG), available at http://www.ceos.org/pages/DMSG/pdf/CEOSDMSG.pdf, 2003.

European Water Management News, Wednesday April 12th 2000: "9. Hungary Declares Flood Disaster", available at http://www.riza.nl/ewa_news/news_12_april_2000.html#9, 2000.

Cuomo, V., Filizzola, C., Pergola, N., Pietrapertosa, C., and Tramutoli, V., "A self-sufficient approach for GERB cloudy radiance detection", *Atmospheric Research,* vol. 72*,* no. 1-4, pp. 39-56, 2004.

Grody, N.C., Weng, F., and Ferraro, R.R., "Application of AMSU for hydrological parameters", in: *Microwave radiomemetry and remote sensing of the earth's surface and atmosphere*, (P. Pampaloni and S. Paloscia, editors) VSP, The Netherlands, pp. 339-352, 2000.

Jain, S.K., Saraf, A.K., Goswami, A., and Ahmad, T., "Flood inundation mapping using NOAA AVHRR data", *Water Resource Manage*, vol. 20, pp. 949–959, 2006.

Lacava, T., "Sviluppo di tecniche satellitari a microonde per il monitoraggio del rischio idrometeorologico", *Ph. D. Thesis*, available at University of Basilicata, Potenza, Italy, 2004.

Lacava, T., Di Leo, E.V., Pergola, N., Romano, F., Sannazzaro, F., and Tramutoli, V., "Analysis Of Multi-Temporal Satellite Records For Extreme Flooding Events Monitoring", *Proceedings of the 5th EGS Plinius Conference* held at Ajaccio, Corsica, France, edited by J. Testud, A. Mugnai and J.F. Santucci, pp. 231-237, 2004.

Lacava, T., Greco, M., Di Leo, E.V., Martino, G., Pergola, N., Sannazzaro, F., and Tramutoli, V., "Monitoring soil wetness variations by means of satellite passive microwave observations: the HYDROPTIMET study cases", *Natural Hazards and Earth System Sciences*, vol. 5, pp. 583-592, 2005a.

Lacava, T., Greco, M., Di Leo, E.V., Martino, G., Pergola, N., Romano, F., Sannazzaro, F., and Tramutoli, V., "Assessing the potential of SWVI (Soil Variation Index) for hydrological risk monitoring by satellite microwave observations", *Advances in Geosciences*, vol. 2, pp. 221-227, 2005b.

Lacava, T., Cuomo, V., Di Leo, E.V., Pergola, N., Romano, F., and Tramutoli V., "Improving Soil Wetness Variations Monitoring From Passive Microwave Satellite Data: The Case Of April 2000 Hungary Flood", *Remote Sensing of Environment*, vol. 96*,* no. 2, pp. 135-148, 2005c.

NOAA–OSD (National Oceanic and Atmospheric Administration–Official of System Developments), available at http://www.oso.noaa.gov/poes/index.htm, 2004.

Pietrapertosa, C., Pergola, N., Lanorte, V., and Tramutoli, V., "Self Adaptive Algorithms for Change Detection: OCA (the One-channel Cloud-detection Approach) an adjustable method for cloudy and clear radiances detection", *Technical Proceedings of the Eleventh International (A)TOVS Study Conference (ITSC-XI) BUDAPEST, HUNGARY 20 - 26 SEPTEMBER 2000*, J.F. Le Marshall & J.D.Jasper eds, Bureau of Meteorology Research Centre, Melbourne, Australia, pp. 281-291, 2001.

Sandholt, I., Nyborg, L., Fog, B., Lô, M., Bocoum, O., and Rasmussen, K., "Remote Sensing Techniques for Flood Monitoring in the Senegal River Valley", *Geografisk Tidsskrift Danish Journal of Geography*, vol. 103, no. 1, pp. 71-81, 2003.

Seth, A., "April 2000", *IRI Climate Information Digest*, vol. 3(4), pp. 1-8, 2000.

Sheng, Y., and Gong, P., "Quantitative dynamic flood monitoring with NOAA AVHRR", *International Journal of Remote Sensing*, vol. 22, pp. 1709-1724, 2001.

Tramutoli, V., "Robust AVHRR Techniques (RAT) for Environmental Monitoring: theory & applications", *Earth Surface Remote Sensing II*, Giovanna Cecchi, Eugenio Zilioli Editors, SPIE, 3496, pp. 101-113, 1998.

Tramutoli, V., "Robust Satellite Techniques (RST) for natural and environmental hazards monitoring and mitigation: ten years of successful applications", *The 9th International Symposium on Physical Measurements and Signatures in Remote Sensing*, Shunlin Liang, Jiyuan Liu, Xiaowen Li, Ronggao Liu, Michael Schaepman Editors, Beijing (China), ISPRS, vol. XXXVI (7/W20), pp. 792-795, ISSN 1682-1750, 2005.

Tramutoli, V., Sannazzaro, F., Pergola, N., Lacava, T., Filizzola, C., "Improving flood monitoring by RAT (Robust AVHRR Technique) approach: the case of April 2000 Hungary flood", *Remote Sensing of Environment*, submitted 2007.

Xiao, Q., and Chen, W., "Songhua River flood monitoring with meteorological satellite imagery", *Remote Sensing Information*, pp. 37-41, 1987.

An automatic satellite system for near real time volcanic activity monitoring.

F. Marchese[1], M.. Ciampa[1], I. Coviello[2], C. Filizzola[2], N. Pergola[2,1], V. Tramutoli[1,2]*

[1] Department of Engineering and Physic of the Environment – University of Basilicata, Via dell'Ateneo Lucano 10,85100, Potenza (Italy)

[2] Institute of Methodologies for Environmental Analysis - CNR Contrada S.Loja 85050 Tito Scalo (Pz), Italy.

* fmarchese@imaa.cnr.it

Abstract

An automatic satellite system named VAMOS (Volcano AVHRR Automatic Monitoring System), based on RST (Robust Satellite Techniques) multitemporal approach, has been developed at IMAA (Institute of Methodologies for Environmental Analysis) to monitor Italian volcanoes in near real time using AVHRR data. This system is capable of generating thermal anomaly maps, Kml and text alert files reporting information on detected volcanic hotspots, a few minute after the sensing time. Some of these satellite products were occasionally provided to the Department of the Italian Civil Protection during the Etna eruptions of September 2004-February 2005, for a first experiment of a near real-time operational service. In this paper, the potential of the VAMOS monitoring system for volcanic hazard mitigation will be further assessed, analyzing some recent Mount Etna and Stromboli volcanic eruptions.

Introduction

Volcanoes represent one of the most dangerous natural hazards, causing every year damage for several billion dollar. The growing number of people populating flanks and valley of active volcanoes requires modern and efficient monitoring systems, capable of successfully supporting decision makers in case of strong eruptive events. Satellite remote sensing thanks high observational frequencies, global coverage and generally low cost of data, offers a unique opportunity to monitor volcanoes both in densely populated region and in remote areas, where ground based systems are generally difficult to use (Oppenheimer 1998).

Among the most recent satellite techniques developed to this aim an advanced multitemporal approach, named RST (Robust Satellite Technique, Tramutoli 2005), has shown a higher capability in identifying and tracking volcanic ash plumes, as well as in detecting and monitoring hot volcanic features (Di Bello et al., 2001; Filizzola et al., 2007; Marchese et al., 2006, 2007*a*, 2007*b*; Pergola et al., 2004*a*, 2004*b*, 2007). This approach considers every anomaly in the space time domain as a deviation from a "normal" state, typical of each place and time of observation, which may be derived processing satellite data following homogeneity criteria.

Recently a new satellite monitoring system, named VAMOS (Volcano AVHRR monitoring system), based on RST approach, has been developed at IMAA to monitor Italian volcanoes in near real time (Marchese et al., 2007*a,* 2007*b*). This system is capable of automatically generating thermal anomaly maps, kml and text alert files in case of hotspot detection, a few minute after the sensing time.

In this paper, the potential of this monitoring system in supporting management of eruptive crisis will be analyzed, studying recent Mount Etna and Stromboli flank eruptions.

A new satellite monitoring system for volcanic hazard mitigation

The VAMOS monitoring system implements an automatic chain of satellite data processing, based on RST approach, to identify possible hotspots over Italian volcanoes. Starting from HRPT raw data directly acquired at IMAA, and after the application of calibration (Kidwell 1991) and accurate navigation (Pergola et al., 2000; 2003) procedures, a Region of Interest (ROI), of 1024×1024 in size, is automatically extracted from the scene. A local variation index named ALICE (Absolutely Index of The Change of Environment) is then computed to provide an estimation of how much the signal deviates from the normal unperturbed condition (Tramutoli et al., 1998, 2005). This index is computed for each pixel of the ROI, comparing the image at hand with the "background reference fields" of temporal mean and standard deviation, previously derived processing long historical AVHRR MIR data sets, as:

$$\otimes_{MIR}\ (x,y,t) = \frac{\left[T_{MIR}(x,y,t) - \mu_{MIR}(x,y)\right]}{\sigma_{MIR}(x,y)} \qquad (1)$$

Where $T_{MIR}(x,y,t)$ is the thermal signal (i.e. the brightness temperature) acquired at time t for the pixel (x,y) in the AVHRR channel 3 (*MIR*) centered at around 3.5 μm, while $\mu_{MIR}(x,y)$ and $\sigma_{MIR}(x,y)$ respectively represent, the temporal mean and standard deviation obtained, for the same location (x,y), processing data following homogeneous criteria (same channel, same month, same hour of pass). An original cloud detection scheme is applied to daytime satellite data in order to mask cloud contaminated pixels (Pietrapertosa et al., 2000; Cuomo et al., 2004), while to take into account the saturation problems of the AVHRR sensor, the maximum brightness temperature measurable in the AVHRR channel 3 is associated to saturated pixels before the computation of the local variation index (Marchese et al., 2007*b*).

Lower levels of the local variation index ($\otimes_{MIR}(x,y,t) > 2$) are computed to possible identify hotspots of lower intensity, while higher values of the same index ($\otimes_{MIR}(x,y,t) > 3$) are generally used to better detect high temperature surfaces like lava flow. Hotspots detected using formula reported in (1) are reprojected on georeferenced layers of monitored volcanoes, generating thermal anomalies maps in a standard image format (i.e. JPEG). Text alert files (in ASCII format), which report geographic location (e.g. longitude and latitude of the centre-point of the hot-spot pixel) date of the observation, time of the observation (expressed in GMT or local time) and relative intensity of detected hotspots, are also automatically generated by the system together with kml files. These products, available a few minute after the sensing time, are attached to the alert email which are automatically sent by the system in presence of significant thermal volcanic activity.

In the following section, results provided by the VAMOS-RST monitoring system during recent Mount Etna and Stromboli eruptions will be shown and discussed.

Results Mount Etna eruption of 6-15 December 2006

Since 13 October 2006 and until 15 December 2006 a significant effusive activity occurred at Mount Etna with a lava flow emitted from a fissure opened at base of the SE crater, and from a vent located at 2800 m elevation on the W headwall of the Valle del Bove. On 6 December a strombolian activity occurred at SEC with lava and ash emission. On the morning of 8 December any significant thermal activity was visible at different eruptive vents, and the following days only a low level of activity was recorded. On 11 December, around 03:30 LT,

new Strombolian explosions occurred at SEC, while a new lava body, emitted from the 2800 m vent, formed a flow that slowly descended toward Valle del Bove (INGV 2006).

In figure 1 a daily sequence of thermal anomaly maps (one per day), automatically generated by the VAMOS monitoring system over Mount Etna between 6 and 15 December 2006, is reported. Hotspots having different local variation index values were depicted in different colors on the maps. As can be seen from the figure detected hotspots, generally characterized by high values of the local variation index ($\otimes_{MIR}(x,y,t) > 3$), showed significant variations in number in the analyzed time series. Many thermal anomalies were flagged on 6 December, in accordance with a new eruptive event occurred at SEC, a general reduction of the same features was observed between 9-10 December, and finally, after an new increase in hotspot number observed between 12 and 13 December, a significant reduction of these features was once again correctly flagged.

These results confirm the reliability of the VAMOS-RST system in correctly monitoring thermal volcanic activity, as already tested in previous studies (Marchese et al., 2007*a*, 2007*b*). Geographic location of detected hotspots, their intensity and variation in number, observed during time period analyzed, well fitted in fact with the space-time evolution of the actual lava flows emitted by the Etna volcano.

As previously described, the VAMOS monitoring system has been developed to provide, together with thermal anomaly maps, also kml and ASCII files, in case of hotspot detection. Kml files report information about latitude and longitude (centre of the flagged anomalous pixel), date and hour of observation, relative intensity of the detected hotspots, etc., for a quick visualization on Google Earth. Text Alert files report similar information in ASCII format to be easily ingested in every GIS environment.

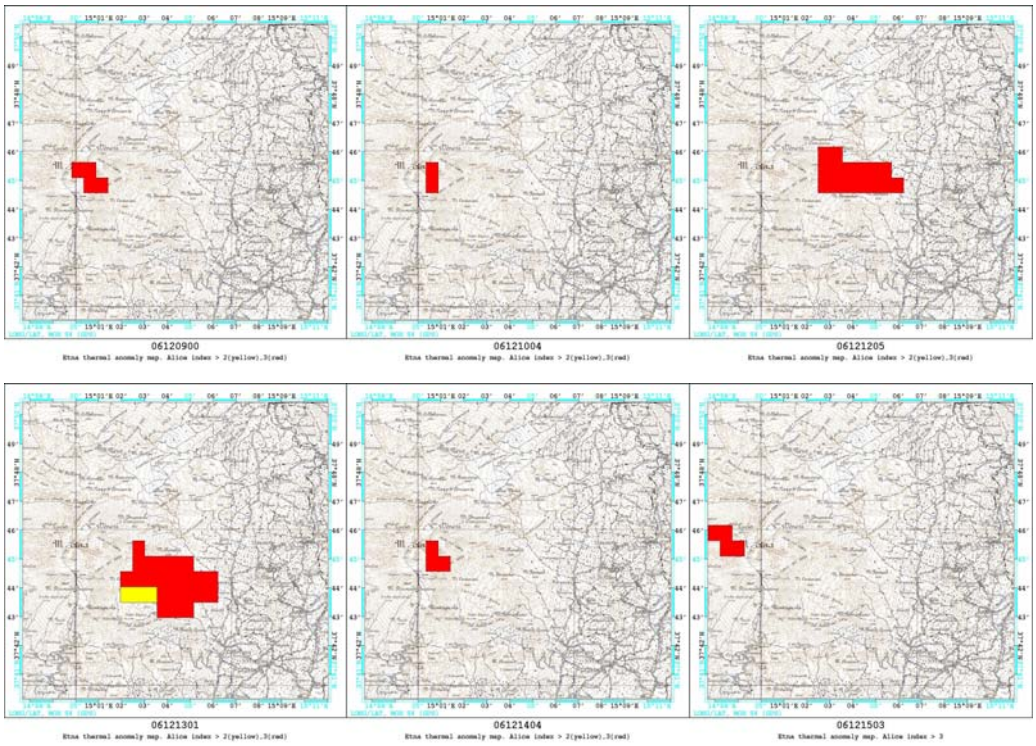

Fig.1: Thermal anomalies maps (with data format YYMMDDHH) automatically generated by the VAMOS monitoring system during Mount Etna eruption of December 2007. Different colors on the maps indicate hotspots having different values of the local variation index.

In figure 2 an example of kml product, automatically generated by the VAMOS monitoring system during Stromboli eruption of 27 February 2007, is reported. As can be seen from the figure, two hotspots were flagged over Stromboli in accordance with a lava flow emitted by a new eruptive vent opened below NE crater (Smithsonian 2007). For each detected thermal anomaly basic information, already described above, were available on Google Earth.

Results shown in this paper highlight the capability of the VAMOS satellite system in successfully detecting and monitoring volcanic hotspots. Both the recent Mount Etna and Stromboli eruptions analyzed were, in fact, correctly recognized by this satellite system, which provided reliable information about location and intensity of the hot volcanic features related to strombolian activity and lava flow. These result show that RST approach if implemented in automatic way may provide suitable information to contribute to volcanic hazard mitigation.

Fig.2: Kml file automatically generated by the VAMOS monitoring system during the Stromboli eruption of 27 February 2007 around 00GMT (01 Local Time).

Conclusions

Results shown in this paper confirm the VAMOS-RST capability in successfully monitoring thermal volcanic activity. The recent eruptive events of Mount Etna and Stromboli were well monitored by a fully-automated system, based on the use of AVHRR data, which is capable of providing up to four thermal anomaly maps per day of monitored volcanoes.

These products, generated by the system together with ASCII and kml files, are immediately attached to the email alert to promptly identify geographic location and relative intensity of detected hotspots. RST products were already occasionally provided to the Department of the Italian Civil Protection during the Mount Etna eruptions of September 2004-February 2005, showing that a near real-time operational service may be successfully carried.

Further improvements of the VAMOS monitoring system, like the integration of RST prescriptions for ash cloud detection and tracking, will allow us to better monitor volcanoes,

providing reliable satellite products suitable to support decision makers in management of strong eruptive crisis.

Reference

Cuomo, V., Filizzola, C., Pergola, N., Pietrapertosa, C., Tramutoli, V. (2004). A self sufficent approach for Gerb cloudy radiance detection. *Atmospheric Research*, vol.72, 39-56.

Di Bello, G., Filizzola, C., Lacava, T., Marchese, F., Pergola, N., Pietrapertosa, C., Piscitelli, S., Scaffidi, I., Tramutoli, V. (2004). Robust Satellite Techniques for Volcanic and Seismic Hazards Monitoring, *Annals of Geophysics*, 47 (1).

Filizzola, C., Lacava, T., Marchese, F., Pergola, N., Scaffidi, I., Tramutoli, V. (2007). Assessing RAT (Robust AVHRR Technique) performances for volcanic ash cloud detection and monitoring in near real-time: The 2002 eruption of Mt. Etna (Italy). *Remote sensing of the environment*, 107, 440-454.

INGV (2006) Reports on volcanic activity-U.F. Vulcanologia e Geochimica. Available at web site *http://www.ct.ingv.it/Report/Etna%2022Nov-12Dec%202006.pdf*

Kidwell, K. (1991). NOAA Polar Orbiter Data User's Guide. NCDC/SDSD. National Climatic Data Center, Washington, DC.

Marchese, F., Telesca, L., Pergola, N. (2006). Investigating the temporal fluctuations in satellite advanced very high resolution radiometer thermal signals measured in the volcanic area of Etna (Italy). *Fluctuations and Noise Letters*, 6, no.3, 305-316.

Marchese, G. Malvasi, M. Ciampa, C. Filizzola, N. Pergola, V. Tramutoli (2007*a*). A robust multitemporal satellite technique for volcanic activity monitoring: possible impacts on volcanic hazard mitigation. *In Proceedings Multitemp 2007*, Leuven, Belgio, doi: 10.1109/MULTITEMP.2007.4293056

Marchese, F., D'Angelo, G., Ciampa, M., Filizzola, C., Pergola, N., Tramutoli V. (2007*b*). Assessing the potential of a robust satellite technique for volcanic activity monitoring: possible impacts on volcanic hazard mitigation. *Journal Volcanology and Geothermal Research* (under review).

Oppenheimer, C. (1998). Volcanological applications of meteorological satellites. *International Journal of Remote sensing*, vol.19, no.15, 2829-2864.

Pergola, N., and Tramutoli, V. (2000). SANA: Sub-pixel Automatic Navigation of AVHRR imagery. *International Journal of Remote Sensing*, vol.21, no.12, 2519-2524.

Pergola, N., Tramutoli, V. (2003). Two years of operational use of SANA (Sub-pixel Automatic Navigation of AVHRR) scheme: accuracy assessment and validation. *Remote Sensing of Environment*, vol. 82, no.2, 190-203.

Pergola, N., Tramutoli, V., Scaffidi, I., Lacava, T., Marchese, F. (2004*b*). Improving volcanic ash clouds detection by a robust satellite technique. *Remote sensing of environment*, vol.90, no.1, 1-22.

Pergola, N., Marchese, F., Tramutoli, V. (2004*a*). Automated detection of thermal features of active volcanoes by means of Infrared AVHRR records. *Remote Sensing of Environment*, Vol. 93, no.3, 311-327.

Pergola, N., Marchese, F, Tramutoli, V., Filizzola, C., Ciampa, M. (2007). Advanced Satellite Technique for the Monitoring and the Early Warning of volcanic activity. *Annals of Geophysics* (in press).

Pietrapertosa, C., N. Pergola, V. Lanorte, V. Tramutoli (2000): Self-adaptive algorithms for change detection: OCA (the One-channel Cloud-detection Approach) – an adjustable method for cloudy and clear radiances detection. *XI TOVS Study Conference*, Budapest, 281-291.

Smithsonian (2007). Global Volcanism Program, Smithsonian Institution. Available at web site *http://www.volcano.si.edu*

Tramutoli, V. (1998). Robust AVHRR Techniques (RAT) for Environmental Monitoring theory and applications. In Earth Surface Remote Sensing II, Giovanna Cecchi, Eugenio Zilioli; Editors, *SPIE* 3496, 101-113.

Tramutoli, V. (2005). Robust Satellite Techniques (RST) for natural and environmental hazards monitoring and mitigation: ten years of successful applications. *In The 9th International Symposium on Physical Measurements and Signatures in Remote Sensing*, Shunlin Liang, Jiyuan Liu, Xiaowen Li, Ronggao Liu, Michael Schaepman Editors, Beijing (China), ISPRS, Vol. XXXVI (7/W20), pp.792-795, 2005. ISSN 1682-1750.

From GMOSS to GMES: Robust TIR Satellite Techniques for Earthquake active regions monitoring

Carolina Aliano[1], Rosita Corrado[1], Carolina Filizzola[2], N. Genzano[1], Nicola Pergola[1,2],Valerio Tramutoli[1,2]

[1] *University of Basilicata, Department of Engineering and Physics of the Environment, Via dell'Ateneo Lucano 85100 Potenza (Italy).*

[2] *National Research Council, Institute of Methodologies of Environmental Analysis, C. da S. Loja, 85050 Tito Scalo - Potenza (Italy)*

Abstract

Since 1980 some authors have suggested space-time enhancements of Thermal Infra Red (TIR), observed by satellite during a time (from months to weeks) before the occurrence of earthquakes, as pre-seismic anomalies.

Several physical models have been proposed as possible causes of the short-lived TIR signal variations in some connection with seismic activity. A certain agreement exists about the possible occurrence of thermal anomalies prior to earthquakes, even if, despite of the growing number of such studies in last decades and some claimed success in earthquake prediction, some skepticism of the scientific community appears justified about the used methods of analysis and interpretation of satellite TIR images. In fact, the main problems regard the lack of a rigorous definition of anomalous TIR signal fluctuations, the absence of a convincing validation/confutation test and the scarce attention paid to the possibility that other causes (e.g. meteorological) than seismic activity could be responsible for the observed TIR variations.

In this context, a robust data analysis technique (RST) was developed which permits a statistically based definition of a signal "anomaly", even in the presence of a noisy contributions from atmospheric (e.g. transmittance), surface (e.g. emissivity and morphology) and observational (time/season, but also solar and satellite zenithal angles) conditions. It was already tested in the case of tens of earthquakes occurred in Europe, Africa, Asia and America, by using a suitable validation/confutation approach, devoted to verify the presence/absence of anomalous space-time TIR transients in the presence/absence of seismic activity.

In this paper the main results achieved on several earthquakes happened in different geo-tectonic contexts by using diverse satellite sensors will be compared emphasizing the RST intrinsic exportability on different geographic areas and/or satellite sensors.

1. Introduction

Since 1980 several authors have suggested space-time Thermal Infra Red (TIR)[26] anomalies, observed by satellite from months to weeks before the occurrence of earthquakes, as precursors.

Several natural processes have been considered as possible causes (which do not exclude one another) of the short-lived (i.e. unstable) thermal anomalies.

According to this model the fluid filtrates upwards from the higher depth to the Earth's surface to provide a temperature enhancement of the ground in the vicinity of fault system.

[26] Earth's thermally emitted radiation measured from satellite in the Thermal Infrared (8-14μm) spectral range is usually referred to as TIR signal and given in units of Brightness Temperature (*BT*) measured in Kelvin degrees.

Therefore, a certain agreement exists about the possible occurrence of thermal anomalies prior to earthquakes, even if, and in spite of the results presented in last decades, some skepticism appears justified about the used methods of analysis and interpretation of satellite TIR images. In fact, the main problems in the above-mentioned studies were the lack of a rigorous definition of anomalous TIR signal fluctuations, the absence of a convincing testing step based on a validation/confutation approach and the scarce attention paid to the possibility that other causes (e.g. meteorological) than seismic activity could be responsible for the observed TIR variations.

Within this context, a different approach has been proposed which, unlike preceding methods, permits a statistically based definition of TIR anomaly even in the presence of highly variable contributions from atmospheric (e.g. transmittance), surface (e.g. emissivity and morphology) and observational (time/season, but also solar and satellite zenithal angles) conditions. It was initially proposed for AVHRR-NOAA[27] data, therefore was named RAT (Robust AVHRR Technique, Tramutoli, 1998), but its full exportability on different satellite systems suggested then the more generic name RST (Robust Satellite Technique, Tramutoli 2005)

RST possible application to satellite TIR surveys in seismically active regions has already been tested (in the case of tens of earthquakes occurred in Europe, Africa, Asia and America, see a selection in Table 1) by using a validation/confutation approach, devoted to verify the presence/absence of anomalous space-time TIR transients in the presence/absence of seismic activity.

This article compares the main results achieved on several earthquakes happened in different geo-tectonic areas by using different satellite sensors, emphasizing the RST intrinsic exportability.

2. A robust satellite-based TIR index

As mentioned earlier, the RST approach was firstly applied to the AVHRR sensor and named for this reason RAT (Tramutoli, 1998). Its implementation on different satellite sensors to monitor seismic areas can be found in successive papers (Tramutoli et al., 2001a; Di Bello et al., 2004; Filizzola et al., 2004; Corrado et al., 2005; Tramutoli et al., 2005; Genzano et al., 2007). In some cases a specific index, RETIRA (Robust Estimator of TIR Anomalies), was used which belongs to the more general class of ALICE (Absolutely Llocal Index of Change of the Environment) indexes (see Tramutoli, 1998 for all details), which give a statistically based definition of *llocal*[28] signal anomalies.

In a quite general formula, ALICE indexes are computed on the image at hand as:

$$\otimes_V (\mathbf{r},t) = \frac{V(\mathbf{r},t) - \mu_V(\mathbf{r})}{\sigma_V(\mathbf{r})} \quad (1)$$

where:

$\mathbf{r}\equiv(x,y)$ represents location coordinates on a satellite image;

[27] Advanced Very High Resolution Radiometer onboard NOAA (National Oceanographic and Atmospheric Administration) platforms.

[28] According to Tramutoli (1998) the double *l* will will be hereafter used to highlights a reference not only to a specific place ***r'*** but also to a specific time *t'*

t is the time of image acquisition with $t \in \tau$, where τ defines the homogeneous domain of satellite imagery collected during the years in the same time-slot of the day and period of the year;

$V(\mathbf{r},t)$ is the value of a variable V at the location $\mathbf{r}\equiv(x,y)$ and at the acquisition time t

$\mu_V(\mathbf{r})$ is the time average value of $V(\mathbf{r},t)$ at the location $\mathbf{r}\equiv(x,y)$ computed on cloud free records belonging the selected data set ($t \in \tau$)

$\sigma_V(\mathbf{r})$ is the standard deviation of $V(\mathbf{r},t)$ at the location $\mathbf{r}\equiv(x,y)$ computed on cloud free records belonging the selected data set ($t \in \tau$)

The choice of the variable $V(\mathbf{r},t)$ depends on the specific application and on particular effects that we want to take into account. For its application to the seismic area monitoring different indexes were used:

(2) $$\otimes_T(\mathbf{r},t) = \frac{T(\mathbf{r},t) - \mu_T(\mathbf{r})}{\sigma_T(\mathbf{r})}$$

where $V(\mathbf{r},t) \equiv T(\mathbf{r},t)$ and $T(\mathbf{r},t)$ is simply the TIR radiance at the sensor;

(3) $$\otimes_{\Delta T}(\mathbf{r},t) = \frac{\Delta T(\mathbf{r},t) - \mu_{\Delta T}(\mathbf{r})}{\sigma_{\Delta T}(\mathbf{r})}$$

where $V(\mathbf{r},t) \equiv \Delta T(\mathbf{r},t) \equiv T(\mathbf{r},t) - T(t)$; and $T(t)$ is a spatial average of $T(\mathbf{r},t)$ computed on the same satellite image. The $\otimes_{\Delta T}(\mathbf{r},t)$, index is also named RETIRA index.

(4) $$\otimes_{\Delta LST}(\mathbf{r},t) = \frac{\Delta LST(\mathbf{r},t) - \mu_{\Delta LST}(\mathbf{r})}{\sigma_{\Delta LST}(\mathbf{r})}$$

where $V(\mathbf{r},t) \equiv \Delta LST(\mathbf{r},t) \equiv LST(\mathbf{r},t) - LST(t)$; and and $LST(t)$ is a spatial average of $LST(\mathbf{r},t)$[29] computed on the same image.

Spatial averages $T(t)$ and $LST(t)$ are computed *in place* on the image at hand considering cloud-free pixels only, separately for land and sea: only sea pixels are used in (3) and (4) to compute $\Delta T(\mathbf{r},t)$ and $\Delta LST(\mathbf{r},t)$ if $\mathbf{r}$ is located on the sea; only land pixels are used instead if $\mathbf{r}$ is located on the land. The use of the excess $\Delta T(\mathbf{r}, t)$ and $\Delta LST(\mathbf{r},t)$, instead of the simple $T(\mathbf{r}, t)$ and $LST(\mathbf{r},t)$, is expected to reduce the possible contributions (e.g. occasional warming) to the signal due to the year-to-year climatic changes and/or season time-drifts which usually affect near-surface temperature at a regional scale.

By construction, the ALICE indexes turn out to be a useful tool for a robust identification of TIR anomalies and allows us to estimate them in terms of the Signal-to-Noise (S/N) ratio. In

[29] LST (Land Surface Temperature) is a product of satellite data analysis, which is expected to give an estimate of Earth's Surface Temperature corrected for the effects of (variable) atmospheric water vapour content (see Di Bello et al. 2004)

fact, the local excess $V(\boldsymbol{r},t) - \mu_V(\boldsymbol{r})$, which represents the Signal (S) to be investigated for its possible relation with seismic activity, is evaluated by comparison with the corresponding observational/natural Noise (N) represented by $\sigma_V(\boldsymbol{r})$. It is important to note that $\sigma_V(\boldsymbol{r})$ includes all (natural and observational, known and unknown) sources of the overall (llocal) variability of S as historically observed at the same site in similar observational conditions (same platform, time of day, month, etc). This way, the relative importance of the measured TIR signal (or the intensity of anomalous TIR transients) can naturally be evaluated in terms of S/N ratio by the ALICE indexes.

As a result, the ALICE index is intrinsically resistant to false alarms and, in addition, may assure a complete exportability to different geographical areas and a free choice of sensors to be used.

As a matter of fact, the robustness and potentials of RST approach were widely assessed (see Table 1) in monitoring of areas with a very different extension (from rather limited regions like Italian peninsula to very wide areas like Indian Subcontinent), with highly variable morphology and very different geo-tectonic settings (compressive, transcurrent and distensive fault zones), considering different kinds of earthquakes for localization (both boundary plate and intra-plate events) and magnitude (from 4.0 to 7.9). Furthermore, RST intrinsic exportability on different satellite instrumental packages was evaluated on the basis of several years of NOAA/AVHRR, Meteosat and GOES[30] observations and allowed us to verify, for example, the improvement of S/N achievable by RST moving from polar to geo-stationary satellites.

3. RST exportability on different geographic areas and/or satellite sensors

The first application of RST approach to seismically active areas was performed using polar satellite data (NOAA-AVHRR) and RETIRA index (3) on the Irpinia-Basilicata (23 November 1980, Ms=6.9) earthquake (Tramutoli et al., 2001a). In that case the monthly average of $\otimes_{\Delta T}(\boldsymbol{r},t)$ index was considered in order to compare the mean signal behaviour during the month (November 1980) of the earthquake with the signal observed during the same month in different years. These preliminary results (see, for example, figure 1) showed how RST approach is able to strongly reduce site effects (e.g. related to orography, land cover, etc). In addition, during the year of the event (validation), anomalous pixels ($\otimes_{\Delta T}(\boldsymbol{r},t)$ index greater than 0.6) were found more numerous than in "unperturbed" years (confutation) and in a better correlation with spatial distribution of seismogenic areas.

The index (2) reduces the noisy contribution of variable atmospheric conditions (Di Bello et al., 2004). In fact, the use of a Land Surface Temperature, LST ($\boldsymbol{r},t$), AVHRR based product, instead of the simple AVHRR TIR signal collected around 11 μm, gives an estimate of the land surface temperature corrected by the effects of atmospheric water vapour content. As a result, the use of $\otimes_{\Delta LST}(\boldsymbol{r},t)$ index, instead of $\otimes_{\Delta T}(\boldsymbol{r},t)$, reduces the local noise $\sigma_{\Delta LST}(\boldsymbol{r},t)$ (compared to $\sigma_{\Delta T}(\boldsymbol{r},t)$) permitting to halve residual signal variability.

Moreover, as before, the use of a differential variable (ΔLST), computed *in place* as a difference between the punctual value LST(r,t) and its spatial average LST*(t)*, allows us to reduce year-to-year and seasonal drift effects.

The above-mentioned improvement can be clearly shown by a visual comparison between figure 3 (where $V(\boldsymbol{r},t) = \Delta T(\boldsymbol{r},t)$, i.e. the brightness temperature difference without correction

[30] Geostationary Operational Environment Satellites operated by NOAA.

for atmospheric water vapour) and figure 2 (where $V(\boldsymbol{r},t) = \Delta LST$): for November 1980 (validation) the spatial distribution of anomalous pixels is rather similar to the case in figure 1, but for unperturbed years (confutation) anomalous pixels almost disappear. The comparison turns out to be useful also in confirming the possible extension of anomalous space-time transients far away (up to several hundred kilometres) from the epicentral zone, reinforcing the idea that spatial resolution is not the main constraint for satellite packages devoted to such studies.

It should be noted that also in this second case, the $\otimes_{\Delta LST}(\boldsymbol{r},t)$ index was averaged on a monthly basis.

Successive studies on AVHRR data showed significant increase of the achievable S/N ratio moving from monthly average of $<\otimes_{\Delta LST}(\boldsymbol{r},t)>$ to daily $\otimes_{\Delta LST}(\boldsymbol{r},t)$ products (see fig. 2 and 3). This is the case of the daily analysis (Filizzola et al., 2004) of $\otimes_{\Delta LST}(\boldsymbol{r},t)$ index which was performed for Athens's earthquake (Ms=5.9), occurred on 7 September 1999 (fig. 3). In this case, the $\otimes_{\Delta LST}(\boldsymbol{r},t)$ appears to be greater 1.5 and the sequence of its daily values allowed us also to identify the temporal dynamics of TIR anomalies which affected the epicentral area some days before (with a maximum four days before) the seismic event. It should be emphasized that daily analysis (rather than the monthly one) demonstrated to be useful not only to describe the space-time evolution of TIR anomalies but also in identifying their temporal and spatial persistence as useful indicator for discriminating meaningful anomalous transients from signal outliers with similarly high S/N values (see, for example, Tramutoli et al., 2005; Genzano et al., 2007). In fact, as demonstrated in Tramutoli et al. (2005), other effects could be responsible for TIR anomalies with comparable intensity, but such anomalies have to be isolated in the space and in time in order to escape from the selection processes subtended by the application of the RST approach.

For the same seismic event (7 September 1999 Athens's earthquake), a comparison is presented in Filizzola et al. (2004) between the results achieved on AVHRR polar data (accounting for atmospheric water vapour by using $V(\boldsymbol{r},t)=\Delta LST(\boldsymbol{r},t)$) and the ones achieved on Meteosat geostationary observations (by using simply $V(\boldsymbol{r},t)=\Delta T(\boldsymbol{r},t)$).

The same good performances on geostationary data (Meteosat-7, in this case) are recorded also in the case of medium-low magnitude events like the series of Greek-Turkish earthquakes. For some of them, TIR anomalies appear more clearly in correspondence of known tectonic lineaments as shown in figure 5 where results of the validation step are presented in the case of a series of three seismic events which started on 28 May (Patras) and carried on with the earthquakes on 29 May (Cyprian region) and 3 June (Crete) 1995 (see Corrado et al., 2005, for details).

Anyway, within the series of seismic events we studied, the most spectacular case is probably represented by Gujarat's earthquake (26 January 2001, Ms=7.9), where the boundary plate seems to be drawn by the TIR anomalies obtained by computing $\otimes_{\Delta T}(\boldsymbol{r},t)$ index on Meteosat-5 images as illustrated in figure 5 (see Genzano et al., 2007, for details). The indication for possible large scale effects also in this case suggests that high spatial resolution is not a requirement for this kind of studies.

The spatial correlation between TIR anomalies and tectonic structures was highlighted, however, even by using $\otimes_{T}(\boldsymbol{r},t)$ the most simple of the ALICE indexes (where $V(\boldsymbol{r},t)$ is the simple TIR radiance at the sensor), instead of the more robust $\otimes_{\Delta T}(\boldsymbol{r},t)$ RETIRA index as demonstrated in the test case of Izmit's earthquake (17 August 1999, Ms=7.8), studied using both indexes on the same Meteosat-7 geostationary data (figure 6). Notwithstanding the presence of same spurious effects introduced by a seasonal warming over the region (reduced mainly by using instead $\otimes_{\Delta T}(\boldsymbol{r},t)$ index in Tramutoli et al., 2005), some thermal anomalies

with an intensity of $\otimes_T$ $(\boldsymbol{r},t)$ index greater than 2 clearly show a trend which seems to gather along the North Anatolian Fault some days before the occurrence of the earthquake.

It should be highlighted that, in comparison with polar data, the application of RST approach to geostationary images leads to a significant increase of the S/N ratio even in the case of using the simple TIR signal, confirming the improved performance assured by the stability of observational conditions associated to the geostationary attitude. On the other hand, the comparison with results achieved by using the more robust index $\otimes_{\Delta T}(\boldsymbol{r},t)$ shown in figure 7 (see Tramutoli et al. 2005, for details), straddling the day of Izmit's earthquake, clearly shows the effectiveness of RETIRA index in reducing spurious effects related to occasional (at the regional scale) warming due to meteorological or even climatological changes and/or season time/drifts.

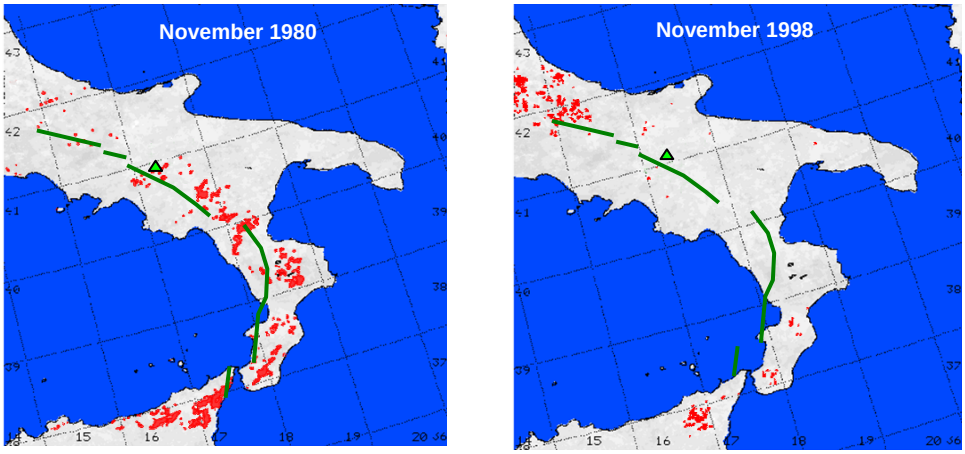

Fig. 1: RST approach applied to polar satellite data (NOAA-AVHRR). Results of the analysis on monthly average $<\otimes_{\Delta T}(r)>$ of the $\otimes_{\Delta T}(r,\ t)$ index computed for (top) November 1980 (year of Irpinia's earthquake) and (bottom) November 1998, one of seismically unperturbed (i.e. no earthquakes with M >4 in the study area) years. Unperturbed signal behaviour, in terms of $\mu_{\Delta T}(r,t)$ and $\sigma_{\Delta T}(r,t)$, was determined on the basis of five years of NOAA-AVHRR records collected in similar observational conditions (see tab. 1). Thermal anomalies with $<\otimes_{\Delta T}(r)>$ > 0.6 are depicted in red. Green triangle locates the epicentral area; green lines draw main seismogenic faults of the area (adapted from Tramutoli et al., 2001a).

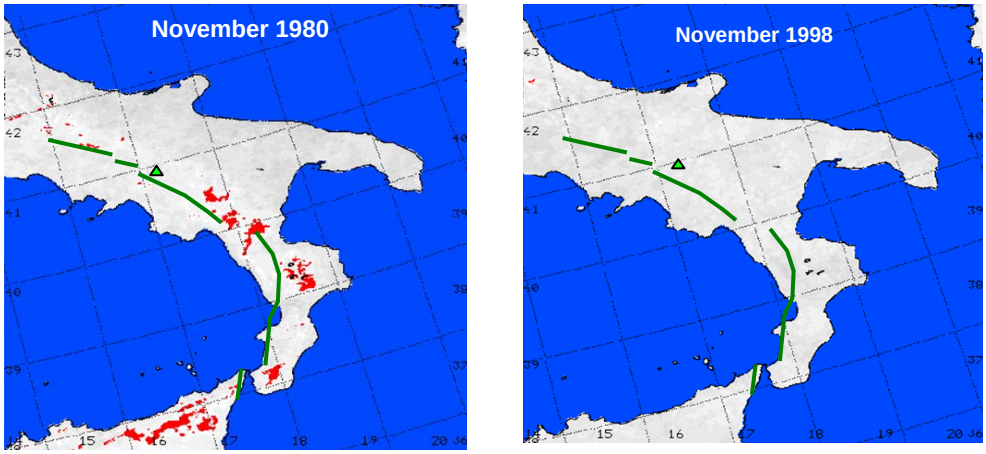

Fig. 2: – RST approach applied to polar satellite data (NOAA-AVHRR). Results of the analysis on monthly average $<\otimes_{\Delta LST}(r,\ t)>$ of $\otimes_{\Delta LST}(r,\ t)$ index computed for (top) November 1980 (year of Irpinia's earthquake) and (bottom) November 1998 (unperturbed) years. Unperturbed signal behaviour, in terms of $\mu_{\Delta LST}(r,t)$ and $\sigma_{\Delta LST}(r,t)$, was determined on the basis of five years of NOAA-AVHRR records collected in similar observational conditions (see tab. 1). Thermal anomalies with $<\otimes\Delta LST\ (r,\ t) > > 1$ are depicted in red. Green triangle locates the epicentral area; green lines draw main seismogenic faults (as in Valensise et al., 1993) of the area (adapted from Di Bello et al., 2004).

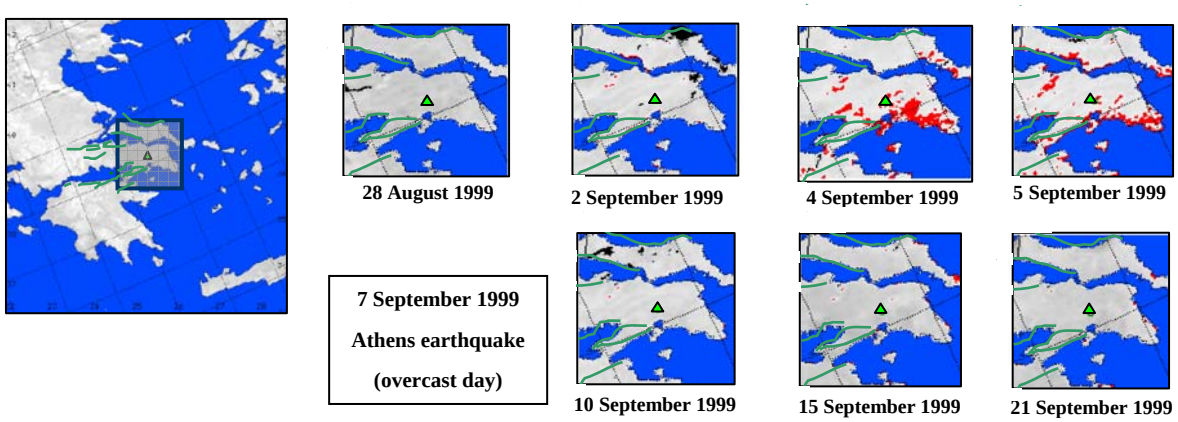

Fig. 3 - RST approach applied to polar satellite data (NOAA-AVHRR). Results of the analysis of daily $\otimes_{\Delta LST}(r, t)$ index computation on the epicentral area before and after the 7 September 1999 Athens's earthquake. Mostly overcast days have been excluded by the sequence. Thermal anomalies with $\otimes_{\Delta LST}(r, t) > 1.5$ are depicted in red. Unperturbed signal behaviour, in terms of $\mu_{\Delta LST}(r)$ and $\sigma_{\Delta LST}(r)$ was determined on the basis of four years of satellite records collected in similar observational conditions (see tab. 1) during August and September (which were considered as a "unique month", in order to increase the number of satellite records to build of the reference fields). Green triangle indicates the epicentre; green lines are the main tectonic lineaments (COMET, 2006); black areas are cloudy pixels (adapted from Filizzola et al., 2004)

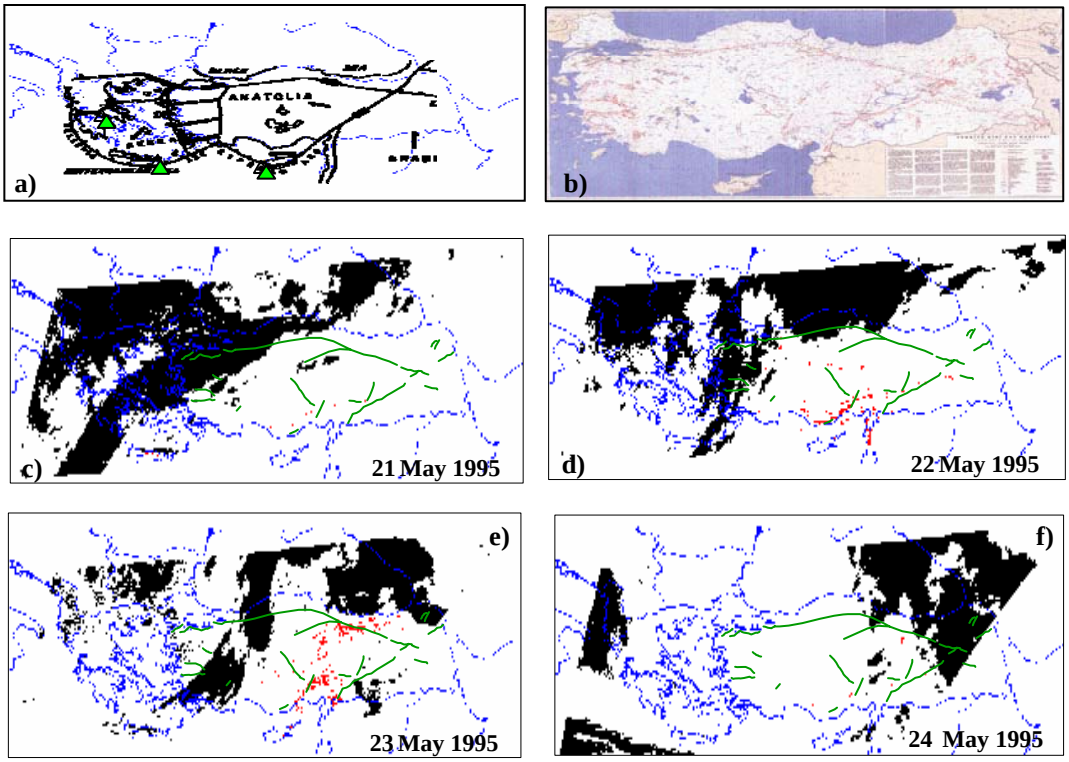

Fig. 4 a) Schematic map of the principal tectonic structures of the Eastern Mediterranean Sea (adapted from Rodstein and Kafka, 1982); b) Active fault map of Turkey (produced by Geological Research Department MTA - MADEN TETKIK ARAMA - Ankara); c-f) Thermal anomalies with $\otimes_{\Delta T}(r, t) > 3$ are depicted in red. Unperturbed signal behaviour, in terms of $\mu_{\Delta T}(r)$ and $\sigma_{\Delta T}(r)$, was determined on the basis of eight years of Meteosat TIR records collected in similar observational conditions (see tab. 1). TIR anomalies overlapped the main active faults: the spatial distribution of TIR anomalies seems to follow the tectonic structures of the region. Green triangles indicate epicentres (adapted from Corrado et al., 2005).

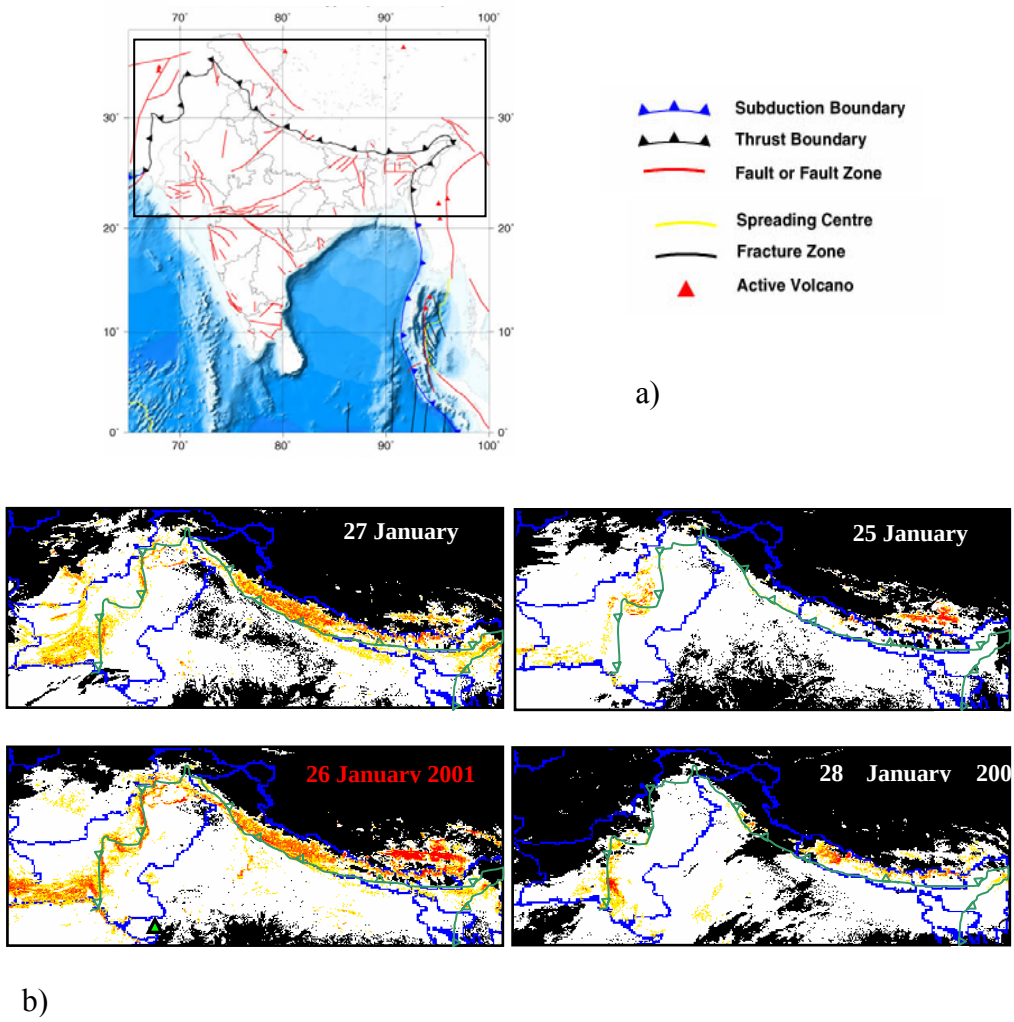

Fig. 5 a) Tectonic map (faults active since the Quaternary period) of the Indian subcontinent (adapted from ASC, 2004); b) RST approach applied to geostationary satellite data (Meteosat). Results of the analysis of daily $\otimes_{\Delta T}(r, t)$ index computation on the epicentral area of the Gujarat' earthquake. TIR anomalies with $\otimes_{\Delta T}(r, t) \geq 3$ are depicted in red, while the lower values (≥ 2.5 and ≥ 2) of the index are in orange and yellow. Unperturbed signal behaviour, in terms of $\mu_{\Delta T}(r)$ and $\sigma_{\Delta T}(r)$, was determined on the basis of six years of satellite records collected in similar observational conditions (see tab. 1). Lower intensity TIR anomalies straddling the day of Gujarat earthquake seem to follow in great detail the trend of the tectonic boundary. Green solid triangle indicates the epicentre of the seismic event, while the green line outlines the trend of Himalayan plate boundary. Cloudy pixels are black coloured (adapted from Genzano et al., 2007).

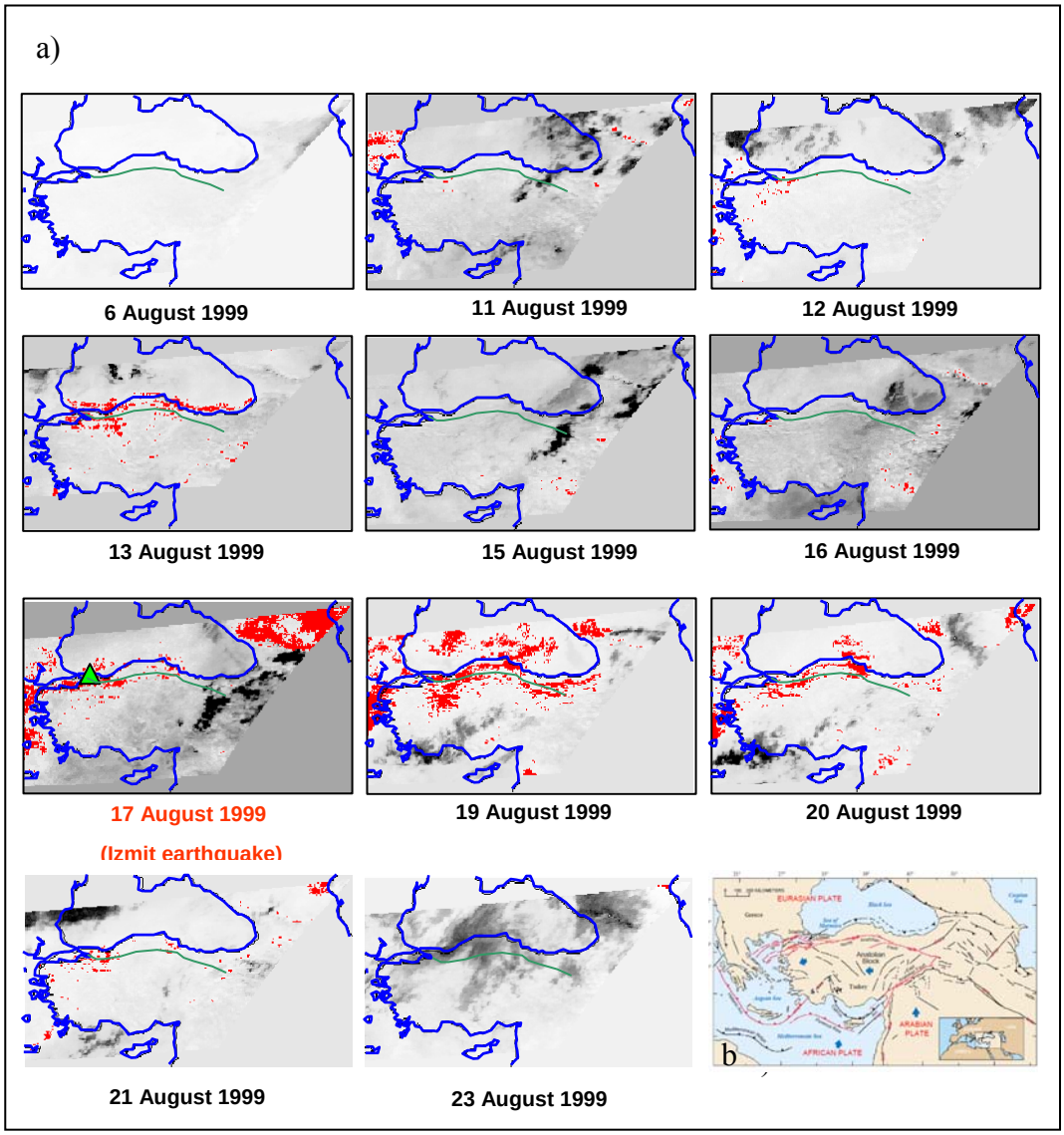

Fig. 6: a) RST approach applied to geostationary satellite data (Meteosat). Results of the analysis of daily $\otimes_{TIR}$ (r, t) index computation on the epicentral area before and after the 17 August 1999 Izmit's earthquake. TIR anomalies with $\otimes_T (r, t) > 2$ are depicted in red. Unperturbed signal behaviour, in terms of $\mu_T(r)$ and $\sigma_T(r)$, was determined on the basis of six years of satellite records collected in similar observational conditions (see tab. 1). Green triangle indicates the epicentre; green line draws North Anatolian Fault; b) tectonic map of the region including the North Anatolian Fault (Credits: U. S. Geological Survey, in USGS, 2000, modified from Barka, 1992).

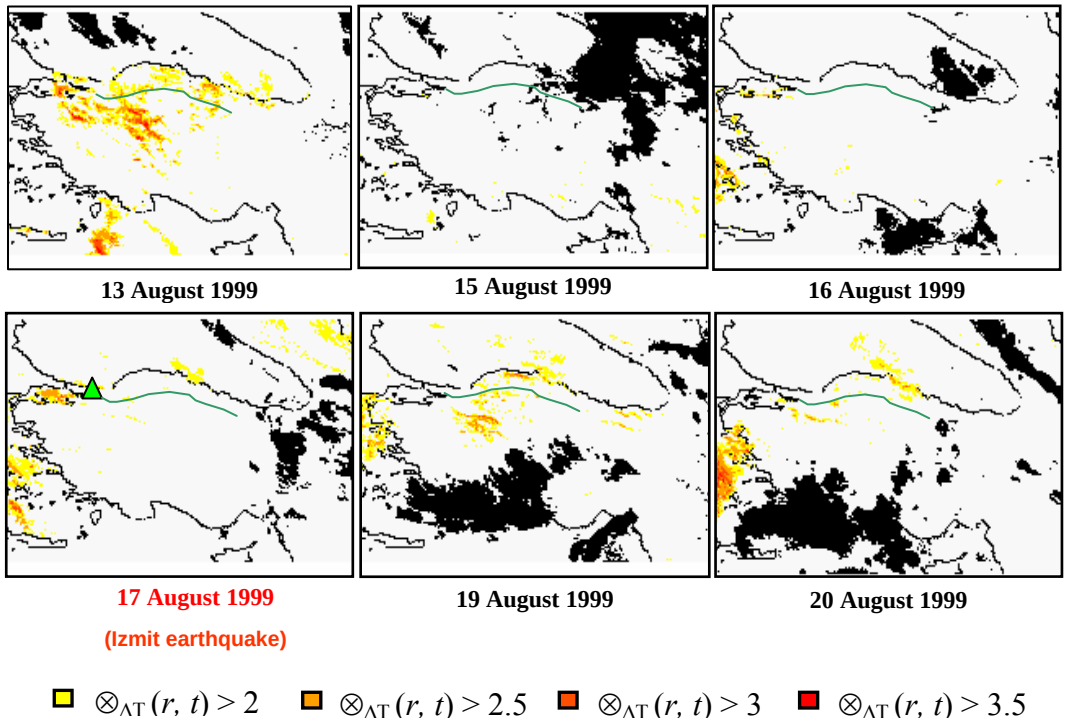

Fig. 7: RST approach applied to geostationary satellite data (Meteosat). Results of the analysis of daily $\otimes_{\Delta T}$ (r, t) index computation on the epicentral area of the day of Izmit's earthquake. TIR anomalies with $\otimes_{\Delta T}(r, t) > 3$ are depicted in red, while the low-level signal anomalies ($3.5 < \otimes_{\Delta T}(r, t) > 2$) of the index are depicted in different colours. Unperturbed signal behaviour, in terms of $\mu_{\Delta T}(r)$ and $\sigma_{\Delta T}(r)$, was determined on the basis of eight years of satellite records collected in similar observational conditions (see tab. 1). Green triangle indicates the epicentre; green line draws the North Anatolian Fault (adapted from Tramutoli et al., 2005).

5. Conclusions

This paper compared the main results achieved in the last ten years testing RST approach in the framework of the application of satellite TIR observation to seismically active areas monitoring.

The use of RST approach, as we have seen, permits to strongly reduce all the environmental factors (independent from seismic activity) which could affect the Earth's emitted thermal signal (possible earthquake precursor?), overcoming one of the most important obstacles in this kind of Earth observing satellite applications. A long experience in the image analysis let us understand the role that TIR anomaly shape and the space-time persistence plays in order to decide if or not it can be related to seismic activity. At the same time, this persistence analysis allowed us to suppose a relation with seismicity even when TIR transients are found in a spatial (up to several hundred kilometres from epicentral area) and temporal (days to weeks from the time of earthquake occurrence) correspondence. Sometimes a surprising connection between TIR anomalies and tectonic lineaments was also observed.

Up to now RST approach has been applied for such studies using both polar (like NOAA-AVHRR) and geostationary (like Meteosat-5 /7) satellites, obtaining always encouraging results.

Anyway, RST on geostationary images showed the best performances, in terms of Signal-to-Noise ratio, clearly pointing out the advantages offered by the use of this kind of data.

Acknowledgments

This work was supported by the Italian Space Agency (Contract No. I/R/173) within the framework of "SeisMASS" (Seismic area Monitoring by Advanced Satellite System) Project and by EC and ESA through the Network of Excellence "GMOSS" (Contract No. SNE3-CT-2003-503699) in the framework of GMES Program.

References

ASC (Amateur Seismic Centre) (2004), available at the WEB site http://www.asc-india.orgBONFIGLIO, A., M. MACCHIATO, N. PERGOLA., C. PIETRAPERTOSA, V. TRAMUTOLI (2005): AVHRR automated detection of volcanic clouds, in *International Journal of Remote Sensing*, **26** (1), 9–27.

COMET (Centre for the Observation and Modelling of Earthquakes and Tectonics, 2006), available at the WEB site http://comet.nerc.ac.uk

CORRADO, R., R. CAPUTO, C. FILIZZOLA, N. PERGOLA, C. PIETRAPERTOSA, V. TRAMUTOLI (2005): Seismically active areas monitoring by robust TIR satellite techniques: a sensitivity analysis on low magnitude earthquakes occurred in Greece and Turkey since 1995, in *Natural Hazards and Earth System Sciences*, **5**, 101-108.

DI BELLO, G., C. FILIZZOLA, T. LACAVA, F. MARCHESE, N. PERGOLA, C. PIETRAPERTOSA, S. PISCITELLI, I. SCAFFIDI, V. TRAMUTOLI, (2004): Robust Satellite Techniques for Volcanic and Seismic Hazards Monitoring, in *Annals of Geophysics*, **47** (1), 49-64.

FILIZZOLA, C., N. PERGOLA, C. PIETRAPERTOSA, V. TRAMUTOLI (2004): Robust satellite techniques for seismically active areas monitoring: a sensitivity analysis on September 7th 1999 Athens's earthquake, in *Physics and Chemistry of the Earth*, **29**, 517-527.

GENZANO, N., C. ALIANO, C. FILIZZOLA, N. PERGOLA, V. TRAMUTOLI (2007): A robust satellite technique for monitoring seismically active areas: The case of Bhuj–Gujarat earthquake, in *Tectonophysics* **431**, 197-210.

TRAMUTOLI, V., (1998): Robust AVHRR Techniques (RAT) for Environmental Monitoring: theory and applications, in *Earth Surface Remote Sensing II*, Giovanna Cecchi, Eugenio Zilioli, Editors, SPIE, 3496, pp. 101-113.

TRAMUTOLI, V, G. DI BELLO, N. PERGOLA, S. PISCITELLI, (2001a): Robust Satellite Techniques for Remote Sensing of Seismically Active Areas, in *Annali di Geofisica*, **44** (2), 295-312.

TRAMUTOLI, V., N. PERGOLA, C. PIETRAPERTOSA (2001b): Training on NOAAAVHRR of robust satellite techniques for next generation of weather satellites: an application to the study of space–time evolution of Pinatubo's stratospheric volcanic cloud over Europe, in *Smith, W.L., Timofeyev, Yu.M. (Eds.), IRS 2000: Current Problems in Atmospheric Radiation. VA' Deepak Publishing, Hampton*, 36–39.

TRAMUTOLI, V., (2005): Robust Satellite Techniques (RST) for natural and environmental hazards monitoring and mitigation: ten years of successful applications, in *ISP MSRS 2005 Conference Proceedings, Beijing, China.*

TRAMUTOLI, V., V. CUOMO, C. FILIZZOLA, N. PERGOLA, C. PIETRAPERTOSA (2005): Assessing the potential of thermal infrared satellite surveys for monitoring seismically active areas: the case of Kocaeli (Izmit) earthquake, August 17, 1999, in *Remote Sensing of Environment* **96**, 409-426.

Texture Analysis on Time Series of Satellite Images with Variable Illumination Conditions and Spatial Resolution

Giovanni Laneve*, Enrico G. Cadau, Giancarlo Santilli

CRPSM – University of Rome "La Sapienza", Via Salaria, 851, 00138 – Roma, Italy

* laneve@psm.uniroma1.it

Abstract

Very recently satellite systems for remote sensing are required to provide images with a spatial and temporal resolution suitable to be applied for disaster management. High resolution (HR) satellite imagery can provide a good insight into the magnitude of a disaster and a detailed assessment of the damage. To meet these objectives, HR imagery has to be collected immediately after the disaster and precisely in the areas that have been damaged by the event. Presently, space based remote sensing systems result unsuitable to provide useful information when disastrous events require simultaneously high temporal and spatial resolutions. Furthermore, due to the technological limits of the transmission systems, a very high resolution is usually coupled with a reduced sensor swath. This means that the observation can be carried out when the area to be imaged is known. Low-resolution satellites (e.g. geostationary satellite) could also provide, in principle, some information with the required promptness in presence of event characterized by sudden temperature increases (fires, explosions, volcanic eruption, etc).

The University of Rome (Centro di Ricerca Progetto San Marco, CRPSM) is studying the suitability of a satellite based system able to monitor national borders and/or given regions of the Earth in a quasi-continuous way with an adequate spatial resolution. To meet this requirement, the so-called Multi-Stationary (MS) orbits have been introduced. A constellation of few (4) satellites located on this kind of orbits allows a quasi-continuous monitoring of a selected region of the Earth. The images acquired quasi-continuously from a satellite located on such an orbit, are characterized by a continuously changing spatial resolution and illumination conditions.

This paper aims to present firstly the results of the analysis of the impact of the images spatial resolution and illumination conditions variability on change detection methods based on a time-series of these and secondly the application of the texture analysis on these time-series images in order to detect small changes in the scene.

Introduction

Remote sensing systems on board of satellites represent the best way to observe the earth without any constraint on the location of the region of interest. As a consequence of this possibility to access practically any place of the Earth satellites can be used to gather information everywhere without any restriction related to geographical and/or political reasons.

When the observation requirements are not involving temporal constraint, spatial images at the required spatial resolution (down to 0.6 m) can be easily acquired. In the recent years the interest in applying information provided by satellite systems for remote sensing in disaster management issues has been constantly increasing. In general, these applications are characterized by the fact that they need a high spatial and temporal resolution. High resolution (HR) satellite imagery can provide a good insight into the magnitude of a disaster and a detailed assessment of the damage, but this information could be of invaluable importance in the aftermath of a disaster if there are provided few hours after the event.

Presently, space based remote sensing systems result unsuitable to provide useful information when high temporal and spatial resolutions are simultaneously required. Mainly this is due to the fact that, even if many high resolution satellites are available they are not organized in a constellation and the image acquisitions, for observational reasons, are concentrated around convenient local time. Further, due to the technological limits of the transmission systems a very high resolution is usually coupled with a reduced sensor swath (typically 10 km x10 km). This means that the observation can be carried out when the area to be imaged is known.

On the other side low-resolution satellite could provide, in principle, some information with the required promptness in presence of event characterized by sudden temperature increases (fires, explosions, volcanic eruption, etc.). In fact, in this case the poor spatial resolution is compensated by the high sensitivity of the short wave infrared channels (SWIR) to high temperatures.

In the framework of the activities of the Network of Excellence (NoE) GMOSS (Global Monitoring for Stability and Security) aiming to explore the possibility of using satellite images for security related applications, the University of Rome (Centro di Ricerca Progetto San Marco, CRPSM) is studying the suitability of a satellite based system able to monitor national borders and/or given regions of the Earth in a quasi-continuous way with an adequate spatial resolution. To meet this requirement, the so-called Multi-Stationary (MS) orbits have been introduced. As for the Molnya orbit case the MS orbits are characterized by having an orbital inclination equal to the critical inclination (63.43°). However, apart from the different orbital period (8 h instead of 12 h) for the design of the orbit a constraint on the satellite-Earth relative velocity is introduced in order to optimize the observation conditions. A constellation of few (4) satellites located on this kind of orbits allows a quasi-continuous monitoring of a selected region of the Earth.

The images, acquired quasi-continuously from a satellite located on such an orbit, are characterized by a continuously changing spatial resolution and illumination conditions. When the information required need a change detection analysis of the acquired images the variation associated with the observation condition must be considered. This paper aims at presenting the results of the analysis of the impact of the images spatial resolution and illumination conditions variability on change detection methods based on a time-series of these. Different techniques to automatically geo-referencing the images have been introduced and a texture analysis of the images time-series has been exploited in order to detect small changes in the scene.

2. Data and Method

2.1 Orbit Design

A constellation of few satellites located on a MS orbit (Laneve at al. 2000, 2004) allows a quasi-continuous monitoring (Fig. 1) of a selected region of the Earth. With respect to the well known Molnya orbits a constraint on the satellite-Earth relative velocity is introduced in order to optimize the observation conditions.

A preliminary analysis of the spatial resolution obtainable by using an optical sensor on board of a satellite located on this kind of orbit, taking into account the satellite altitude and the sensor-surface relative velocity has been carried out.

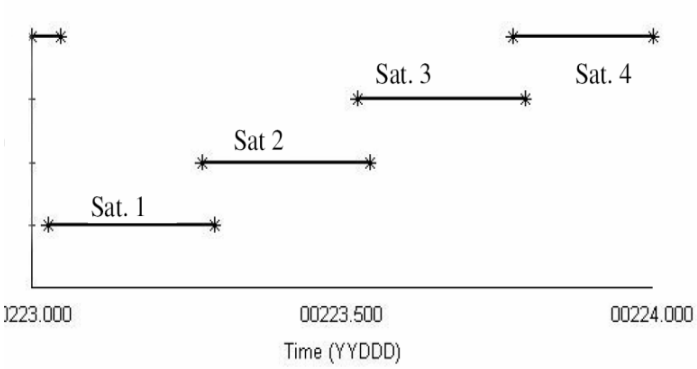

Fig. 1: MS constellation daily coverage of the area of interest with elevation higher than 45°

A spatial resolution better than 100 m could be easily obtained with the present technology but, due to the variation of the observation conditions (altitude and view angle) during the acquisition time, the resolution can change as shown in Fig. 2.

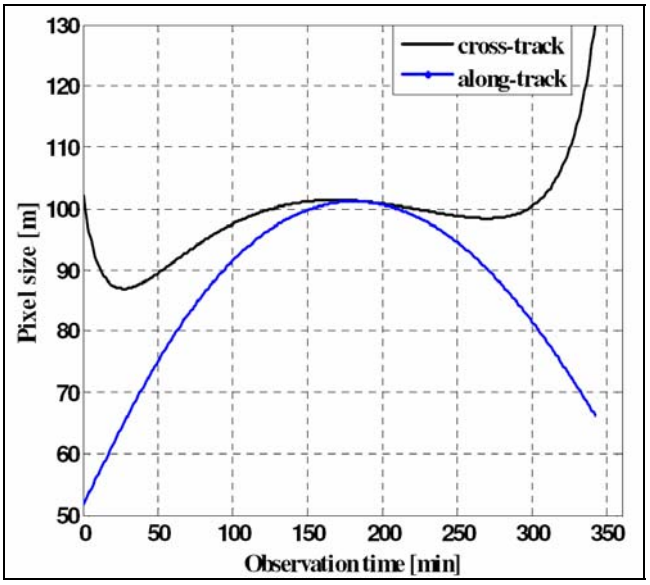

Fig. 2: Variation of the pixel sizes (along and cross-track) during the observation time

The selection of the orbit has been made considering the following requirements:

- Quasi-synchronous condition when the satellite over-flies the zone of interest.
- Perigee altitude high enough to avoid the atmospheric drag.
- Orbital inclination equal to critical inclination to minimize apsidal drift and eccentricity variation.An orbital period sub-multiple of the Earth's nodal period.

In this example the orbit is characterized by the following parameters:

Semi-mayor axis:	20261.75 Km
Eccentricity:	0.5939
Inclination:	63.43 deg
Perigee argument:	312.817 deg
RAAN:	260.275 deg
Mean anomaly:	0 deg

With this choice, an orbital period of about 8 hours results. The time interval during which the area of interest can be observed in quasi-stationary conditions is about 6 hours long. A continuous coverage can be obtained locating 4 satellites on 4 orbital planes in according with the Right Ascensions (RAAN) and mean anomalies given in Table 1:

Table 1. Right ascensions and mean anomalies of the four satellite of the constellation

Parameter	**Sat 1**	**Sat 2**	**Sat 3**	**Sat 4**
RAAN (deg)	80.275	170.275	260.275	350.275
Mean Anomaly (deg)	180.0	270.0	0	90

2.1 Image Processing

The problem of processing a time series of images taken from a MS satellite, and in general from highly eccentric orbit satellites by applying change detection techniques, in the knowledge of the authors, has never been addressed. The problems to deal with synthetically require the development of:

- an automatic technique for the co-registration of the images acquired with high temporal frequency,
- a procedure to detect changes in the scenario imaged by the sensor able to take into account the apparent changes due to the variation of the spatial resolution of the consecutive images.

A series of images have been simulated with GCI-Toolkit, reproducing the ground scenario related to the sensor view on board of a hypothetic satellite flying on a MS orbit. Further, simulations of the orbital motion, carried out using the STK software, allow knowing the orbital parameters of the MS orbit, in particular the altitude of the satellite above the Earth's surface. The creation of the scenario is obtained through several steps: a satellite image of the desired area is used as input of a classification process that produces a map in which a suitable mixture of materials, with known thermo-optical characteristics, is associated to each pixel; the sensor characteristics are chosen, in particular the IFOV is set; from STK simulations the attitude of the satellite (the focal plane angle and the focal plane stare point) and the sensor position are computed. We have chosen an area centered on the Italian peninsula. Starting from all these inputs, the GCI software produces a radiance map at sensor, with a user-defined spatial and spectral resolution and in accordance with a given atmospheric model. Several Image Processing techniques have been investigated for the automatic, real-time registration of the images of the series, for change detection purposes.

We suppose that the area of interest is imaged every 10 minutes. Based on orbital and attitude data a preliminary coarse registration is performed by geo-referencing the images. For the moment we neglect projective image deformation, considered the relatively small inter-frame motion, and address the problem of finding the translation, rotation and scale parameters that bring the coordinate system attached to the image to be registered to the coordinate system attached to the base image:

$$\begin{bmatrix} x_1 \\ y_1 \end{bmatrix} = \begin{bmatrix} x_0 \\ y_0 \end{bmatrix} + sR(\theta) \begin{bmatrix} x_2 \\ y_2 \end{bmatrix}$$

being s the scale, $R(q)$ the rotation matrix associated to the rotation θ around the image centre and:

$$\begin{bmatrix} x_0 & y_0 \end{bmatrix}^T$$

the displacement of the image centre. The changes in the pixels scale of two consecutive images, due to altitude and view angle changes, can be precisely estimated when the satellite orbit and is attitude are accurately known. Fig. 3 shows the variation of the pixel size between two consecutive images (acquired at 10 min time interval) during the single satellite acquisition time of about 6 hours.

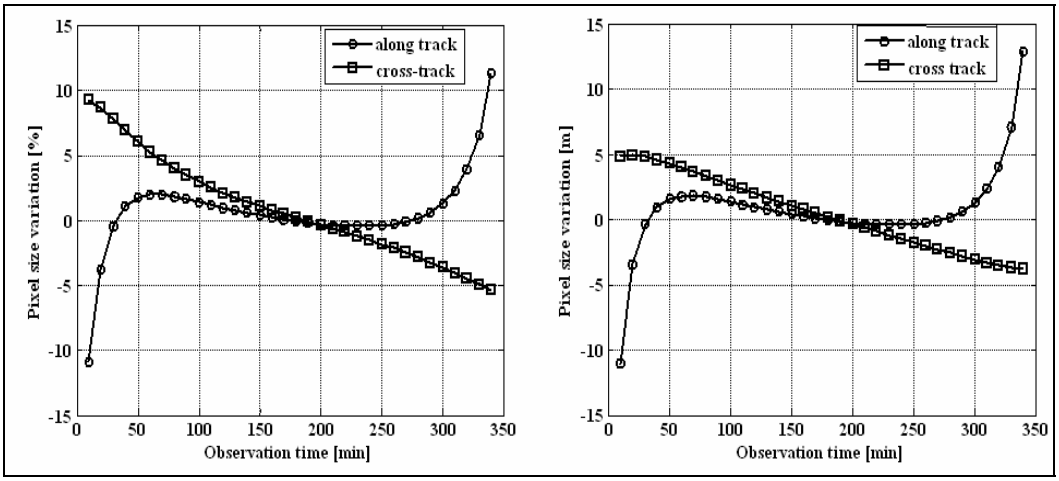

Fig. 3: Behaviour of the pixel sizes variation between two consecutive images (acquired 10 min. apart each other) during the acquisition time of about 6 hours: absolute variation (right) [m], percentage variation (left).

As it can be observed most of the time the pixel size variation is of the order of few percent (lower than 5%); of course its impact on the change detection based analysis depends on the amount of the searched/expected changes.

2.2 Feature detection (Harris) and tracking (cross-correlation)

Feature points detection and tracking can be used to select automatically Ground Control Points on the image and keep track of them through the series. Selection at step k is based on a modified Harris detector (Harris et al. 1988), whilst tracking of points, detected at previous k-1 step, is based on the correlation between: the region of image at step k corresponding to the selected points (the template) whole image k or region of image k corresponding to the location of points detected at step k-1 or region of image k corresponding to the expected location of points tracked at step k (based on orbit and attitude data).

2.3 Mutual Information

Images can be registered also by using the Mutual Information (MI) technique. The image to be registered (I_2) is scaled, rotated and translated and the MI with respect to the base image (I_1) is evaluated as:

$$MI(I_1; I_2) = H(I_1) + H(I_2) - H(I_1, I_2)$$

where $H(I_1)$ and $H(I_2)$ are the marginal entropies, evaluated as:

$$H(I) = \sum_i p_i \log_2 p_i$$

being p_i the marginal probability distribution function, and $H(I_1,I_2)$ is the joint entropy of the two images, evaluated as:

$$H(I_1, I_2) = \sum_{i,j} p_{ij} \log_2 p_{ij}$$

being p_{ij} the joint probability function, which is evaluated as the joint histogram of the two images, where the co-occurrences of image levels are binned. The process is iterated for the opportune range of the translation-rotation-scale space and maxima are searched in a MI accumulator (Fig. 4).

The process is very slow if the registration parameter space is large, although MI is very accurate.

2.4 Mutual Information with Image Pyramid

The novel approach (Chen et al. 2003) consists in applying the MI to image pyramids. An image pyramid is obtained by using the base image and the image to be registered. Than the rotation and translation parameters are estimated using a coarse-to-fine approach: as the image pyramid is descended, the parameter space is narrowed and its discretization is thickened. This allows increasing the result accuracy, while decreasing the global processing time.

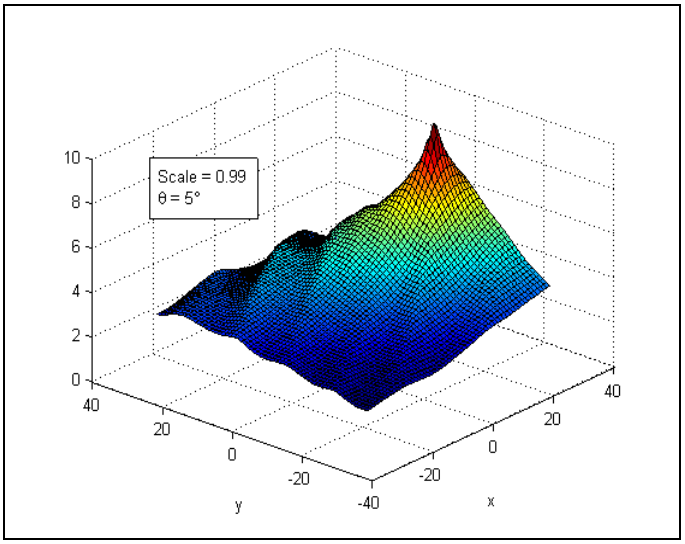

Fig. 4: Visualization of the Mutual Information

2.5 Texture Analysis

Although no formal definition of texture exists, commonly this descriptor describes measures of properties like smoothness, coarseness, and regularity of an image. Image texture, defined as a function of the spatial variation in pixel intensities (gray values), is useful in a variety of applications and has been a subject of intense study by many researchers. One immediate application of image texture is the recognition of image regions using texture properties. Three are the principal approaches used in image processing to describe the texture of a region, statistical, structural and spectral. In this work we will use the first technique based on the research of the statistical moments of the gray-level histogram of an image.

In particular the moment adopted is an *average entropy* defined as:

$$e = -\sum_{i=0}^{L-1} p(z_i) \log_2 p(z_i)$$

where z_i is a random variable indicating intensity, p(z) is the histogram of the intensity levels in a region and L is the number of bins of the histogram. Entropy is, in other words, a measure of variability and it is 0 for a constant image (Gonzales et al. 2002, Tuceryan et al. 1998).

3. Results and Discussion

Fig. 5 (a) and (b) show an example of the images simulated with GCI-Toolkit for a sensor on-bard of a satellite located on a MS orbit, with nadir pointing. Images are taken around the orbit apogee, with a 10-minute interval. As it can be seen, the main variation in the image is the rotation, whereas translation, scale and illumination change slightly. At the centre of the image we simulated a **toxic cloud**, which we aim to detect. The processing is initialised by using orbital parameters and attitude data. Fig. 5 (c) shows the absolute difference between the base image and the registered image. Registration errors are visible as red/yellow pixels, especially along the coasts. Such errors are mainly due to: image sampling (when resizing and rotation of the images is performed); changes in light conditions between images; inaccuracy in the image scale model, which does not take into account the Earth sphericity (leading to a registration error of about 3 pixels at image borders in this case).

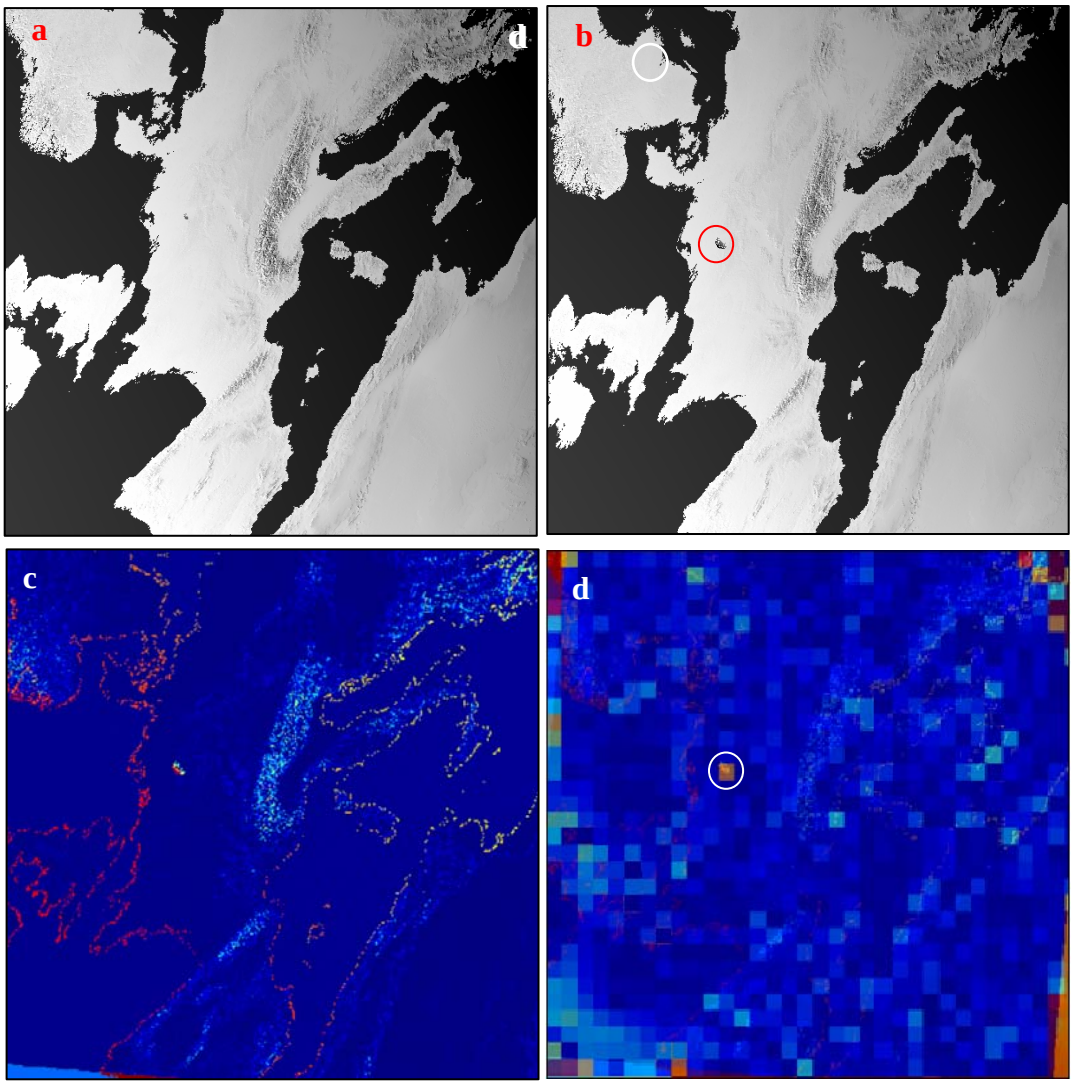

Fig. 5: Pair of images acquired 10-minute apart (simulated) to be registered (a) and (b), difference between base image and registered image (c), a texture analysis imaged with detected change (d).

Figure 5d shows the application of the entropy moment of the textural analysis with an 18x18 pixel-floating window on the co-registered images; the results are superimposed on the original image. As it can be observed, the simulated toxic cloud can be easily detected in the scene. The high values of the entropy moment, in fact, denote the occurrence of high changes. Actually, over the borders of the image high values are also visible but these are due to the different crop of the Total Field of View of the sensor.

A second example (Fig. 6a) shows the textural analysis applied on two simulated SPOT-5 images (Band-1), where a hypothetic **polluted spill** (10 meters radius) on the river (Fig. 6c) has been added. The two simulated images are characterized by different illumination conditions and spatial resolution. As the two images have been acquired with a 10-minutes interval from a different position along the orbit. Major differences are due to the different solar illumination conditions. In this case the texture analysis is applied with a 15x15 pixel window after the co-registration process between the two-series images. Figure 6d represents the differences between the two textural images. It is clear how, even in this case, the texture analysis can reveals small changes in the scene, the white spot indicates in fact the polluted anomaly detected effectively over the water.

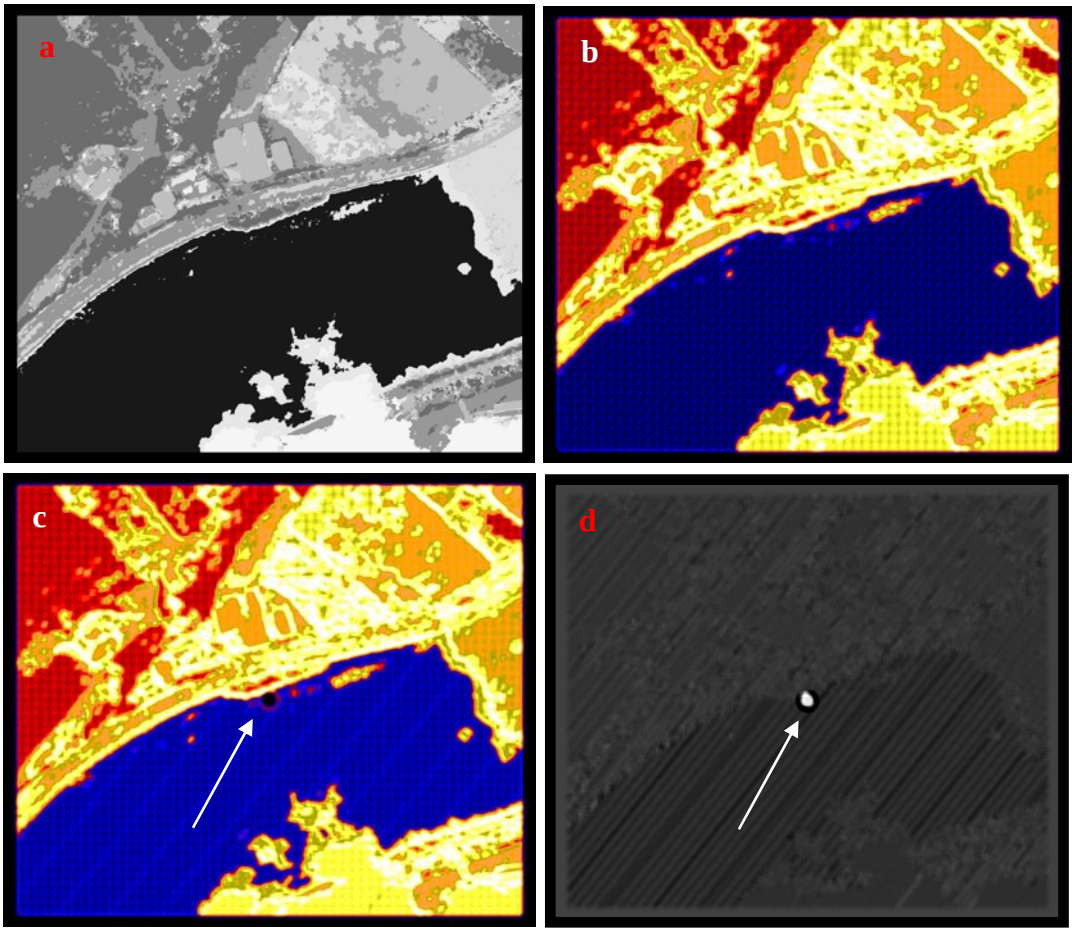

Fig. 6: Simulated SPOT-5 images (a), entropy moment applied two a pair of simulated images (b) and (c), difference of the texture analysis with detected changes (d).

Further studies aim at improving the co-registration process taking into account the effect of the earth shape.

4 References

G. Laneve and M.M. Castronuovo (2000), A Satellite Constellation for Early Fire Detection, 51st IAF Congress, Brazil.

G. Laneve, M. M. Castronuovo and L. Naticchioni (2004), Flower Constellations for a Continuous Regional Observation, 55th IAF Congress, Vancouver, Canada.

C. G. Harris and M. A. Stephens (1988), Combined Corner and Edge Detector, Proceedings of the 4th Alvey Vision Conference, 147-151

J. P. Lewis, Fast Normalized Cross-Correlation, Industrial Light & Magic

H.M. Chen, P.K. Varshney (2003), A pyramid approach for multimodality image registration based on mutual information, in Proceedings of the Third International Conference, Info. Fusion 1, 3-9.

R.C. Gonzales, R.E. Woods (2002), Digital Image Processing, International Edition.

M. Tuceryan, A.K. Jain, Texture Analysis (1998), The Handbook of Pattern Recognition and Computer Vision (2nd Edition) pp. 207-248, World Scientific Publishing Co.

Versatility of the Mathematical Morphology to Detect any Kind of Target on High and Medium Resolution Images

Giovanni Laneve*, Giancarlo Santilli, Enrico Cadau

CRPSM – University of Rome "La Sapienza", Via Salaria, 851, 00138 – Roma, Italy

* laneve@psm.uniroma1.it

Abstract

In the framework of the European project GMOSS (Global Monitoring for Security and Stability) the CRPSM (Centro di Ricerca Progetto San Marco) has successfully developed automatic techniques devoted to detect different types of targets (civilian, military, etc.) available on high and medium spatial resolution satellite images (Quickbird, Ikonos, Spot 5, ASTER, aerial).

The paper aims at describing the results obtained by applying new techniques based on Mathematical Morphology (MM), in order to shown the versatility of this theory in the detection of objects, belonging to very different contexts, like dwelling units in refugee camps, roads of complex shapes and different background, main structures in nuclear plants, etc.

The purpose described above is obtained by using a series of algorithms based on the Mathematical Morphology (MM) theory. These algorithms have been developed exploiting the functions available in the Matlab Image Processing Toolbox. In particular, some techniques able to automatically extract potential made-man structures, which could be present in complex images, have been developed. These techniques have been applied to a "mosaic of images" (about 4 GB, in the considered cases, corresponding to 40 ASTER images) covering the Kashmir region. MM has been used to develop automatic procedures for detecting and counting dwelling units in several refugee camps located in Africa (Goz Amer, Mille, Lukole, etc) using very high spatial resolution (VHSR) images (Ikonos and Quickbird), to build automatic procedures for detecting roads of complex shape in the Kashmir region using SPOT 5 images and finally, to developed techniques able to extract the main structures inside to nuclear plants using VHSR images (Quickbird).

1. Introduction

Remote sensing systems on board of satellites represent the best way to observe the earth without any constraint on the location of the region of interest. As a consequence of this possibility to access practically any place of the Earth satellites can be used to gather information everywhere without any restriction related to geographical and/or political reasons.

In the framework of the activities of the Network of Excellence (NoE) GMOSS (Global Monitoring for Stability and Security) aiming to explore the possibility of using satellite images for security related applications, the CRPSM (Centro di Ricerca Progetto San Marco – Sapienza Università di Roma) has developed a set of algorithms, based on the *Mathematical Morphology Theory,* able to detect and extract in an automatic way, on high and medium spatial resolution satellite images (Quickbird, Ikonos, Spot5, ASTER, etc.), any kind of target.

The above-mentioned objectives are dictated from the requirements we met in the latest three years of the GMOSS activity. These requirements regard:

- The detection and automatic counting of dwelling units in refugee camps located in several African countries (Chad, Sudan, Kenya) in order to estimate in an independent way the population present,

- The automatic research and extraction of the roads having complex shape in order to create an updated database of them (often needed for many African regions), or simply to make a quick monitoring of those hit from a disastrous event in order to verify their state,
- The automatic detection of complex made-man structures like airports, nuclear plants, etc to monitoring national boundaries and verify the observance of the international treaties, etc.

2. Data and Method

The methods proposed by CRPSM rely on an object-oriented approach that is based on a theory for the analysis of spatial structures called *Mathematical Morphology* (Gonzales et al., 2002, Soille et al., 2002, Dougherty et al., 2003, Gonzales et al., 2004). It is called morphology because it aims at analysing objects shape and form. It is mathematical in the sense that the analysis is based on the set theory, integral geometry, and lattice algebra.

Mathematical Morphology has proven to be a powerful image analysis technique. In Mathematical Morphology, two-dimensional grey tone images are seen as three-dimensional sets by associating each image pixel with an elevation proportional to its intensity level. An object of known shape and size, called the structuring element, is then used to investigate the morphology of the input set.

This is achieved by positioning the origin of the structuring element to every possible position of the space and testing, for each position, whether the structuring element either is included or has a non-empty intersection with the studied set. The shape and size of the structuring element must be selected according to the morphology of the sought structures in the image.

2.1 Refugee Camps.

Besides the method used by JRC (Giada et al., 2002), CRPSM has explored a spectrum of different morphological approaches to solve, using Ikonos and Quickbird VHSR images, the tents counting problem for Goz Amer and Mille refugee camps located in western Chad, and Lukole camp in Tanzania.

The first method developed by CRPSM is based on the observation that each considered area, at least within the Goz Amer camp, has a "good behaviour", in the sense that it shows all the characteristics (shapes, dimensions and neat contrast with respect to the background) necessary to obtain good results by means of MM. In fact, in this camp, tents appear as objects with a well-defined geometry and dimensions, namely squares of about 4 by 4 pixels and rectangles of about 10 by 5 pixels, and a very high digital number (around 255), quite different from the image background. Once the tents are recognised, the counting is performed using suitable Matlab toolbox functions (Gonzales et al, 2004, Matlab, 2003).

The basic idea of the second new approach is to define a family (base) of structuring elements (Soille et al. 2002) selected according to the shape and dimensions of the tents. The process consists in extracting the features matching with each structuring element of the base and in subtracting them from the image (Fig.1). The process is repeated for each element of the base until all tents in the image have been masked. A third method is based on the Template Matching (or cross-correlation) technique. This technique, initially applied to the Mille refugee camp, allows a sufficiently accurate detection of the tents for about ¾ of the camp, where suitable contrast, shape and size characteristics are met.

It is worthwhile to recall that the morphological techniques are applicable on grey-tones images for which the spectral information, associated with high-resolution multi-spectral detectors, results not exploited. This limit can be overcome using a Principal Component Analysis (PCA) (Laneve et al., 2006) able to synthesize mostly of the spectral information in a couple of uncorrelated new spectral bands. The application to the Mille camp of the template matching technique, after a pre-processing phase aiming at extracting the PC bands, allows counting the tents with a good approximation everywhere in the camp (Fig.2, portion of Quickbird panchromatic image of the 12 June 2004). Thus, in an automatic way, an estimate of the number of tents, even in the parts of the camp less favourable from the point of view of the object/background separability, has been obtained (Lang et al., 2006).

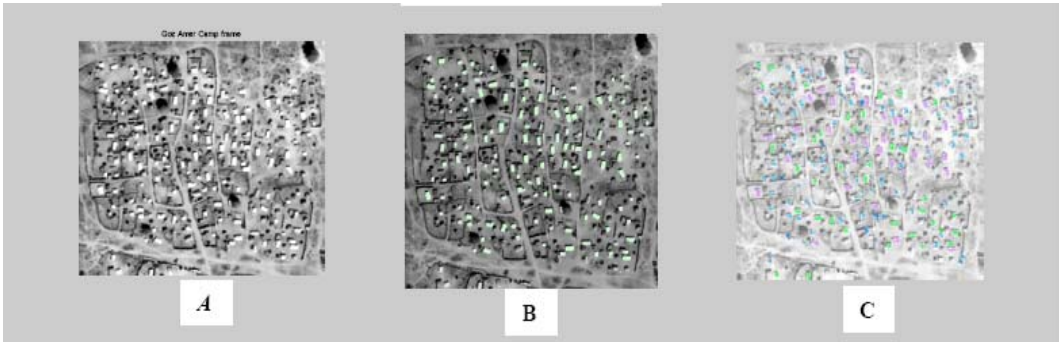

Fig. 1: Original and processed image of the Goz Amer camp obtained using the second one of the methods developed at CRPSM and the eCognition s/w. Coloured objects of image B represent tents correctly detected using the automatic procedure. Coloured objects of image C represent tents correctly detected using eCognition (User Guide, 2004) s/w package.

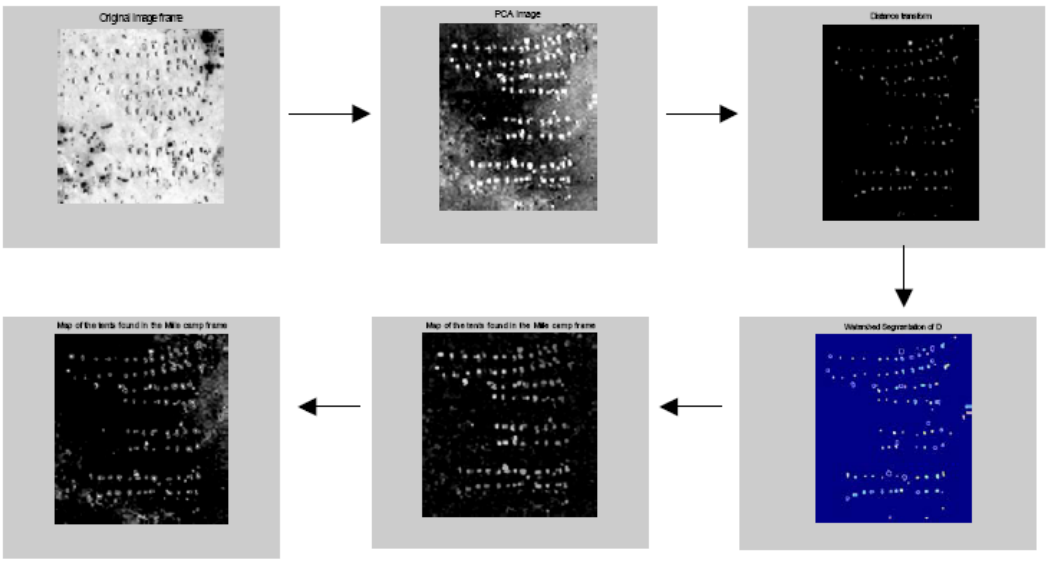

Fig. 2: Tents detection using Template Matching technique (third CRPSM method): summary of the methodology on an image sample of the Mille camp.

2.2 Automatic Extraction of Man-Made Structures from Mosaics.

CRPSM has also developed some techniques able to automatically extract potential made-man structures, which could be present in a complex image, that's in a "mosaic of images". In particular, the considered satellite images mosaic has very big sizes (about 4 GB, in the considered cases, corresponding to 40 ASTER images) and the main goal of this research is to develop a technique that allows the automatic detection of given objects of interest.

In particular, we are interested in detected man made structures like, roads, airports, etc. then only the first 3 VIS/NIR channels of this sensor, having a spatial resolution of 15 m are used. The images have been downloaded by a NASA website. Two big mosaics of ASTER images have been considered, one is covering the Libya/Chad border and the other one refers to the Pakistan/India (Kashmir region) border. Figure 3 shows the extent of the area of interest in Africa. The red square shows the part of mosaic reported in Fig. 4. To cover the whole border about 40 ASTER images are needed.

Fig. 5 shows a part of the mosaic covering the Kashmir area around the Pakistan/India border. The difference in the landscape characteristics, with respect to the previous case, can be clearly observed.

The basic idea of this study is to extract, in automatic way, information from big size images (like mosaics) exploiting not only the spectral characteristics, but also the morphological characteristics in order to simplify the images analysis by the users.

Fig. 3. Libya/Chad border considered as an example in this paper. The superimposed ground tracks pattern corresponds to that of SPOT 4 and 5.

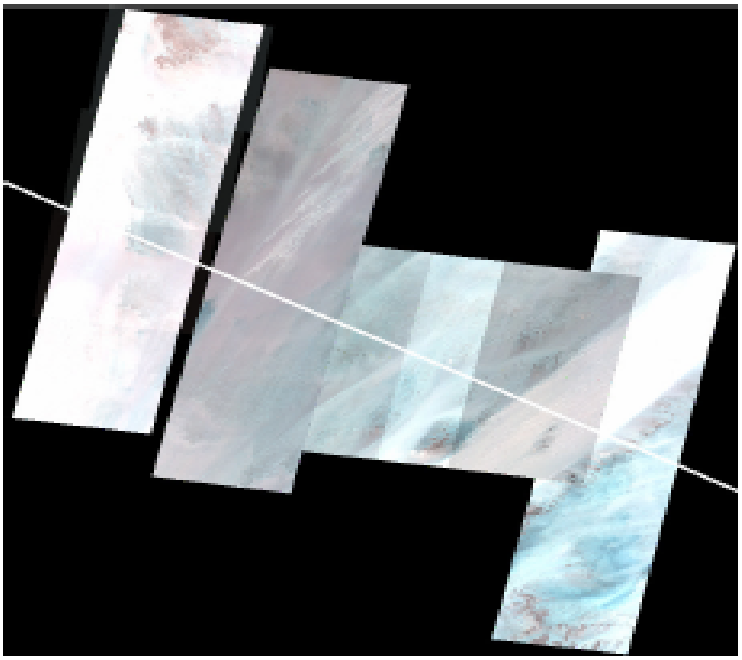

Fig. 4: One of the ASTER images mosaics, covering the Libya/Chad border, on which the analysis has been carried out. It is made of 20 images.

The mosaic is automatically subdivided in smaller frame in order to increase the efficiency of the processing chain, then, using suitable structuring elements, any object of a given shape, size and orientation can be detected. At the end of the process the frames with the detected object are recombined in a mosaic. The removal of not interesting objects can be carried out exploiting the geometric characteristics of them (area, length, width, solidity, centre of gravity, etc), since these information are gathered during the object detection process. The purpose described above is obtained by using an algorithm comprised of the following steps (see Fig. 6):

- The RGB image is converted to a grey image since, as we know MM (on which our algorithm is based) is only applied to grey tone or binary images. The grey tone image can be obtained by selecting the more suitable band, or applying a transformation technique like PCA or a dedicated function like the one available in Matlab Image toolbox called *rgb2gray*. This function converts a RGB image to grey-scale image by eliminating the hue and saturation information while retaining the luminance. The result of this function is shown in Fig. 7. That image represents a mosaic of 10 ASTER images (covering part of the Libya-Chad border), it is 242 MB in size.
- The grey-tone image is pre-processed in order to highlight the required objects (for example, tracks) with respect to the background. This can be obtained by using a top-hat transformation, with a suitable structuring element. The original grey-scale image is divided in several parts (sector) of suitable size, than we proceed to the automatic detection of the objects that can potentially be man-made structures.
- The automatic analysis of each part of the mosaic is made by using tools provided by the MM theory since we can easily choose suitable structuring elements, which allow us to find objects of any given shape, size and orientation. This technique, tested within GMOSS objectives (Laneve et al. 2006, GMOSS rep., 2006), allows to search exactly for the objects of interest. In the case that the target is an airport or similar objects, using a suitable structuring elements, a precise angular scansion of the image can be

performed. The scene can be analysed by using a probe image (structuring element) having the expected characteristics (length, width, inclination) of the "human-structure" that we are seeking. The original shape and size of the interesting objects can be re-obtained by means of the morphological reconstruction process. This allows the reconstruction of these objects using the marker image (represented by the processed frame) on the mask image, which is obtained by a binarization process of the marker. The most important think we have to emphasize is that these thresholds are computed in an entirely automatic way, by using image depending characteristics, eliminating the need of a human-operator.

- The previous process is repeated for every sector. Finally, all the processed sectors are reorganized in a single image equal, in size, to the original one.
- Generally, the processed image presents several objects: our objects of interest plus some unwanted objects. These latter can be removed by using a morphological filtering, which, exploiting the characteristics of "sought objects", allows to meet the final purpose.

The efficiency and robustness of the method is demonstrated by reporting the results obtained by applying the method to the Libya/Chad (Fig. 8) and Pakistan/India (Kashmir region) borders (Fig. 9) mosaics.

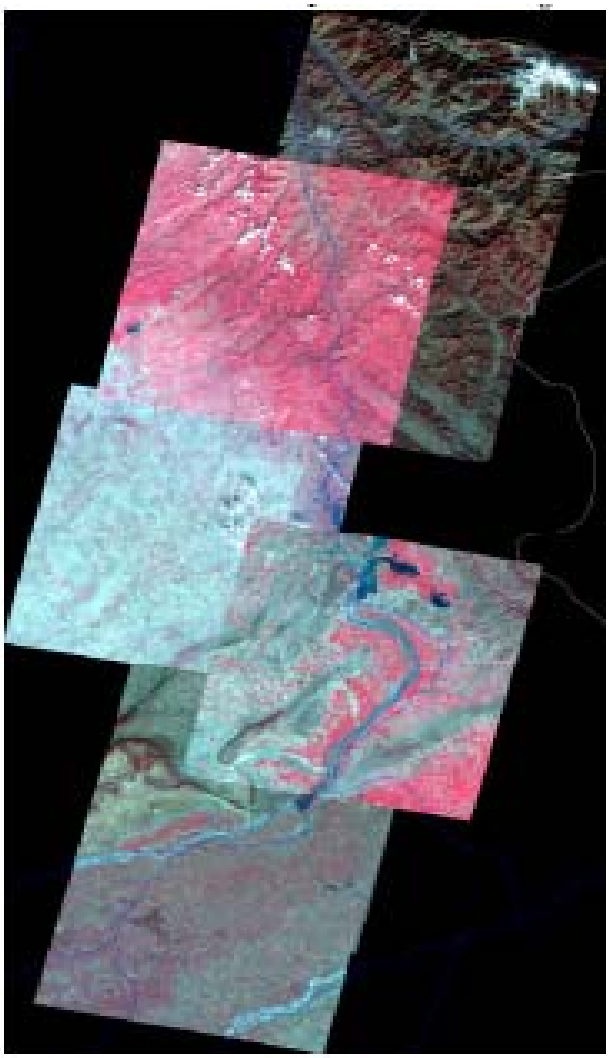

Fig. 5: Part of ASTER images mosaic of the Pakistan/India border (Kashmir region) on which the analysis has been carried out.

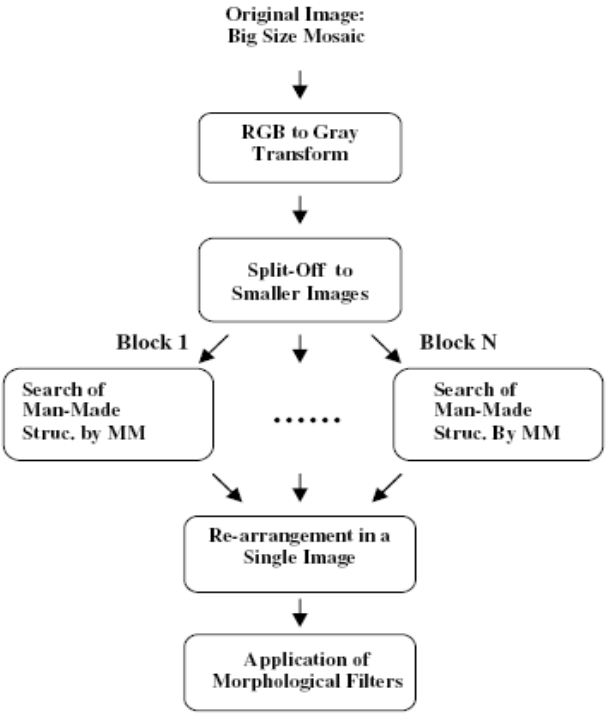

Fig. 6: Schematic diagram of the steps involved in the man-made structures detection procedure.

Fig. 7: ASTER mosaic: grey image obtained as described in the test. The red square indicates the airport position.

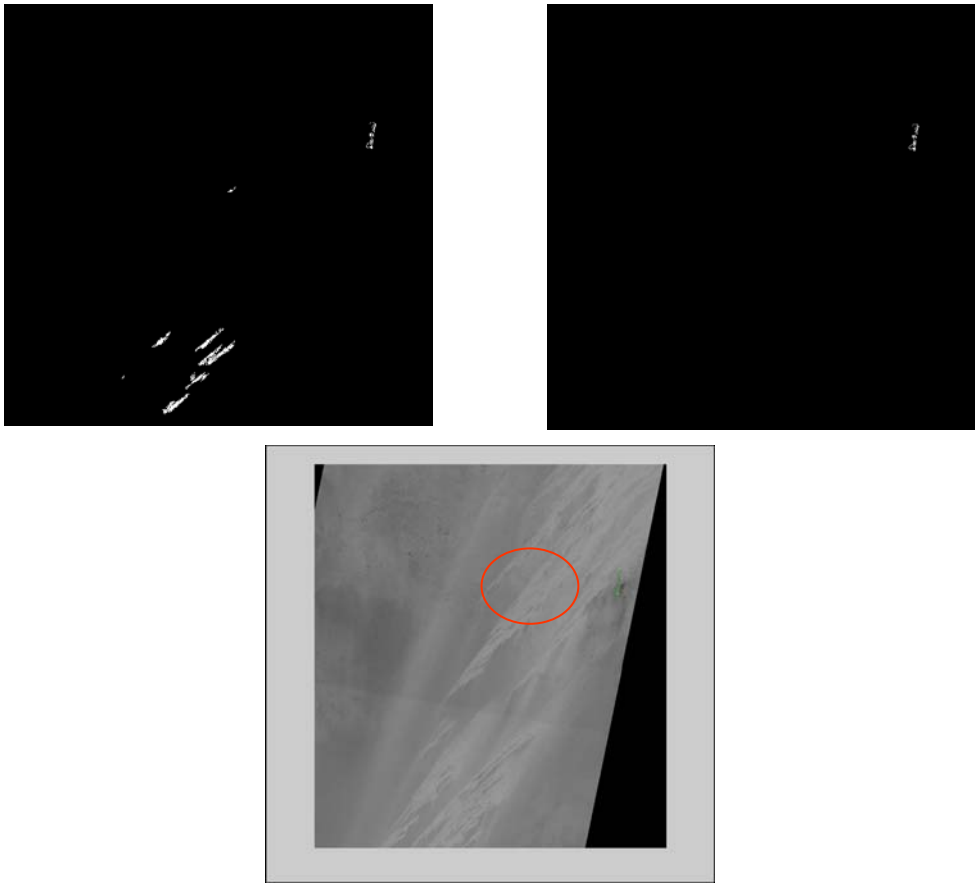

Fig. 8: Several objects found after processing (left), Remaining objects after filtering (right) and final image with superimposed the found objects (bottom).

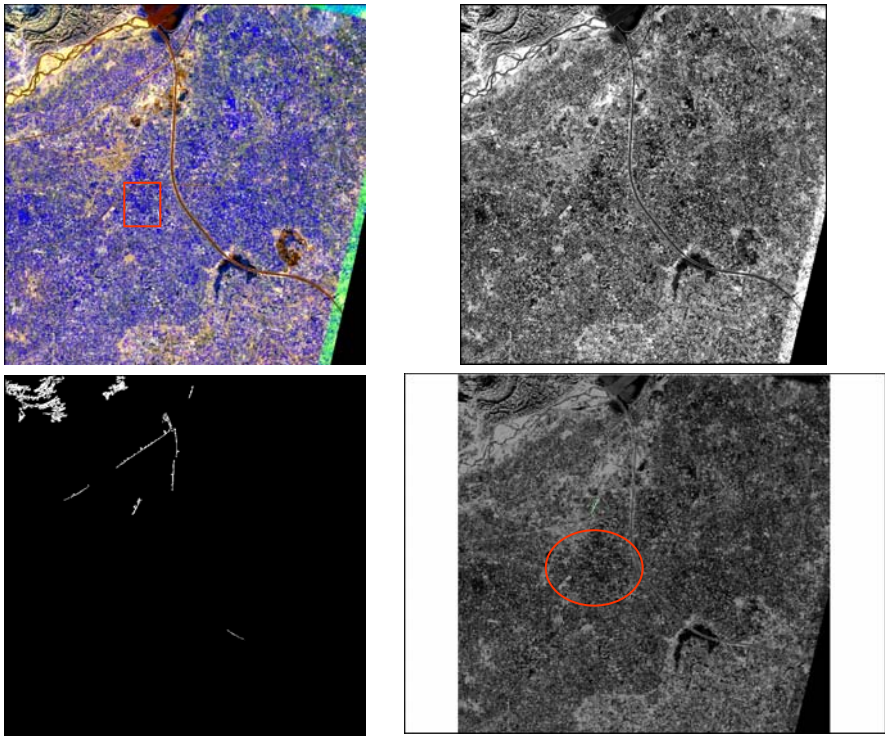

Fig. 9: (top-left) Image in false colour. (top-right) corresponding grey tone image, (bottom-left) object detected after application of MM, (bottom-right) result after morphological filtering application the detected structure (in green has been super-imposed to the original image). Mandi Bahauddin airport.

2.3 Automatic Roads Detection

The same principles has been applied to the problem of automatically detecting structures like roads (Laneve et al. 2006) having any complex shape to create an updated database of them, often needed for many African regions or simply to make a quick monitoring of the those hit from a disastrous events to verify the their state, as we did on the Kashmir region, which was struck from an Earthquake in October 2005.

The basic idea is again the exploitation of the Mathematical Morphology characteristics using suited structuring elements (like appropriate lines) to individuate and to extract any kind of roads. Further this approach was used to create a tool able to extract, in the Kashmir region, the roads having a complex shape. In this way it was possible to monitoring the their state after the Earthquake, occurred in this region on October 8, 2005. Figure 10 shows a Spot 5 frame covering the studied region before (10/06/2005) and after (10/21/2005) the event. The figure on the right shows an intermediate step of the whole morphological processing chain before suited shape filters will be applied. Figure 11 shows the extracted road (before and after) in above-mentioned region superimposed on the original frames. The red circle on the second image allows highlighting that the earthquake has made the road unusable.

Fig. 10: Spot 5 Images on Kashmir Region Before (10/06/2005, left) and After (10/21/2005, center) the Earthquake. Results after Morphological Processing (right)

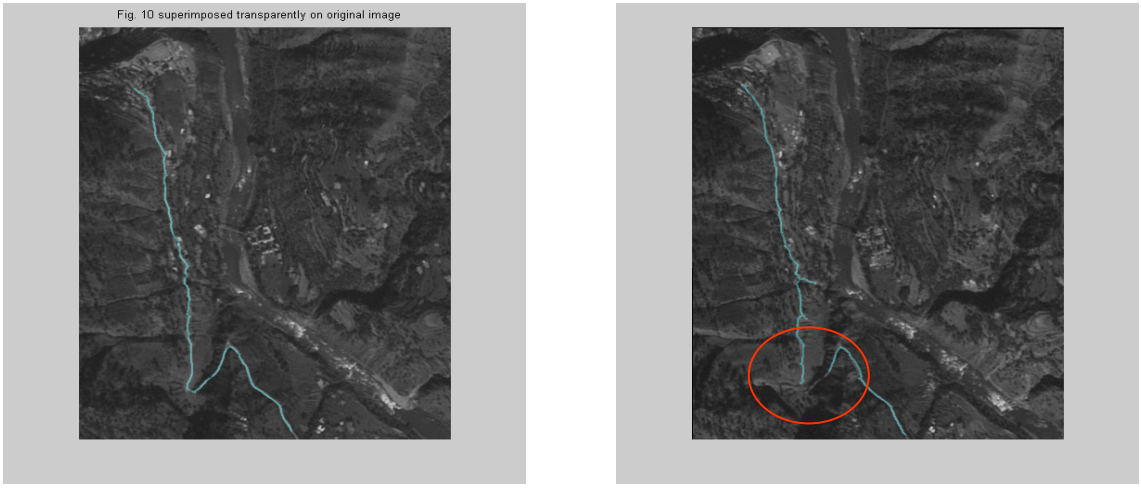

Fig. 11: The change in the detected roads allows highlighting the earthquake has made the road unusable.

3. Results and Discussion

This paper aims at presenting the interesting results reached in the latest three years of GMOSS activity, thank to the ***versatility*** and ***robustness*** of the Mathematical Morphology theory.

This theory is very versatile and robust, allowing the detection of any kind of target on the base of the following observations:

- Defining "probe images" (the structuring elements) having any shape and dimension, gives us the possibility to search the objects of interest with more suited elements.
- Set of operations very powerful (Set Theory applied to the images) which act like not-linear space filters, and that if applied in sequence allow us to get the desired result.

To use the elementary morphological operators is very important since starting from not much basic concepts that define them, is possible create a important variety of operators useful in the more heterogeneous application fields. This fact allows exploiting the knowledge and the experiences gained in many fields to develop heuristic solutions to problems connected with the extraction of objects from an image. In particular, it is possible to obtain versatile and fast algorithms useful for a first approach to the image analysis, which can be extended to problems growing in complexity. The versatility of the morphological algorithms allow also to describe a wide range of problems from a point of view of the complexity of the topological description.

The velocity of the algorithms is due to the use of the Boolean algebra (in the binary case) or to the calculation of maximum and minimum (in the N grey levels) in the pixels that are examined and also to various expedients, which we can implement in a simple and effective way.

The thing emerged clearly from the previous examples is the existence of a narrow dependence between the usable strategies and the objective of interest. Such dependence brings to develop basic instruments able to cooperate to provide a solution to the problems of extracting all objects/structures/features we can meet.

References

R. Gonzalez and R. Woods (2002), Digital Image Processing, 2nd ed., Prentice Hall, Upper Saddle River, NJ.

P. Soille and M. Pesaresi (2002), Advances in mathematical morphology applied to geoscience and remote sensing, IEEE Transactions on Geosciences and Remote Sensing, vol. 40, pp. 2042-2055.

E. R. Dougherty and L. A. Lotufo (2003), Hands-on Morphological Image Processing, SPIE - International Society for Optical Engin.

R. Gonzalez, R. Woods, and S. Eddins (2004), Digital Image Processing using Matlab, Pearson-Prentice Hall, Upper Saddle River, NJ.

S. Giada, T. De Groeve, D. Ehrlich, and P. Soille (2002)**,** Information extraction from very high resolution satellite imagery over Lukole refugee camp, Tanzania, Int. J. Remote Sensing, vol. 24, N° 22, pp. 4251-4266.

G. Laneve, G. Santilli, I. Lingelfelder (2006), Development of Automatic Techniques for Refugee Camps Monitoring using Very High Spatial Resolution (VHSR), IGARSS 2006, Denver - U.S.A.

S. Lang, D. Tiede, G. Santilli (2006), Beyond Sensors and Algorithms: An Information Delivery Approach for Population Estimation in African Refugee Camps, 6th AARSE Conference, Cairo – Egypt.

eCognition User Guide (2004), Definiens Imaging.

G. Laneve, G. Santilli (2006), Automatic Detection of Man-Made Structures in Big Size Mosaics of Spaceborne Images, Image information Mining for Security and Intelligence ESA-EUSC Conference, Madrid - Spain.

GMOSS WP20600 24-30 months report, 2006, http://gmoss.jrc.it/index.asp.

Modeling of Buildings in Urban Areas from high resolution stereo Satellite Images for Population Estimation and Change Detection

Thomas Krauß*, Manfred Lehner and Peter Reinartz

German Aerospace Center (DLR), Remote Sensing Technology Institute PO Box 1116, 82230 Weßling, Germany

* thomas.krauss@dlr.de

Abstract:

Models of urban areas are an important input for many applications in the field of urban monitoring. Besides the creation and updating of maps from sprawling urban settlements the models are also used for simulation and planning in case of catastrophic events like flooding, tsunamis or earth quakes. With the availability of very high resolution (VHR) satellite data investigations of large urban areas regarding their three dimensional shape can be performed fast and relatively cheap in comparison to aerial photography especially for cities in developing countries. Most of the actual methods used for the generation of city models depend on a large amount of interactive work. A method for automatic derivation of - in a first step - coarse models of urban structure is therefore of great use. In this paper the methods used for such an automatic modeling is presented. The methods are based on stereo images from VHR satellite stereo imagery provided by satellite sensors like IKONOS or QuickBird. In a first step a digital surface model (DSM) is derived from the stereo data. Subsequently a digital terrain model (DTM) is generated from the DSM. Orthoimages are created in parallel using the derived DSM. Based on the local height differences between DSM and DTM and the normalized difference vegetation index (NDVI) a coarse classification of the orthoimages is performed. The classification divides the images in four classes: low level and no vegetation, low level with vegetation, higher level and no vegetation and higher level with vegetation. Based upon this classification object models are selected and object parameters are adapted to create an object-based representation of the satellite image scene - especially of man made buildings. The used processing steps are evaluated and the results for IKONOS stereo pairs of the cities of Athens and Munich are presented and discussed.

Introduction

Urban areas all around the world – especially in developing countries – grow rapidly. So more and more 3D models of large city areas are needed for planning and monitoring purposes. For the usage in developing countries such models should be relatively cheap and can be relatively simple. This can be achieved by a fully automatically generation from very high resolution (VHR) satellite image stereo pairs from satellites like Ikonos, QuickBird or the upcoming WorldView series [DigitalGlobe, 2007].

Starting with a stereo scene – a very high resolution satellite image pair – it is possible to generate in a first step a high resolution digital surface model (DSM) by suitable stereo evaluation of the image pair ([Lehner and Gill, 1992], [Krauß et al., 2005], [Hirschmüller, 2005]). Since the ground resolution of the satellites is in the range of one meter the resolution of the surface model is rather coarse in comparison to surface models from airborne camera or lidar data.

Furthermore there exists no additional data in rapidly growing cities. So the proposed automatic process is often limited to only one single stereo image pair. From this only source of information all needed parameters for the generation of a – in a first step coarse – city model have to be extracted.

After the generation of the DSM a digital terrain model (DTM) can be derived from the surface model giving the ground plane (without buildings/trees etc.). Using the high resolution DSM and the satellite images also a true orthophoto can be calculated. Since the satellite data contain four channels (blue, green, red, near infrared) a simple classification based on the orthophoto can be accomplished. This classification uses only a mask of high objects derived from the DSM and DTM and a vegetation mask calculated from the NDVI of the orthophoto [Krauß et al., 2007].

From this classification all high, non-vegetation objects can be extracted and modeled as described in this paper.

Currently already many approaches exist for city modeling. But these methods are mostly based on cadastral data, aerial images, aerial and terrestrial laser scanner data, terrestrial photographs and more information since the aim of these methods are near photorealistic city models in industrial countries. These models integrate data from several of these sources in often intense manual work for the urban models [CyberCity, 2007, 3D Geo, 2007].

In this paper one part of this processing chain – the automatic extraction of buildings – is described. Many approaches exist which use high resolution airborne lidar data or digital image data. A method often used is the calculation of tensors of inertia and their eigenvectors as main axes of a building. This and a search for maximum diameters of objects and rectangular deviations for describing building outlines as described in [Müller, Zaum, 2005] work only well for convex buildings. A better top-down approach is the recursive rectangle approximation as shown by [Gross, U. et al., 2005]. But in this paper a bottom-up approach for the building outline extraction will be described.

In the approach described here rather simple urban 3D models are generated only from one stereo satellite image pair. Such images are provided at the moment, e.g., by Space Imaging (Ikonos, [SpaceImaging/GeoEye, 2007]) with a ground resolution of about 1 meter panchromatic and 4 m multispectral or in the near future, e.g. by WorldView I (2007) and II (2008), offering half-meter panchromatic and 1.4 to 1.8 m multispectral resolution ([DigitalGlobe, 2007]).

Data

The fully automatic processing chain relies on stereo image pairs which are best acquired in the same orbit with the same illumination conditions, two distinct viewing angles and known internal and external orientation of the satellite (e.g. orbital positions and look angles or RPCs). The processing chain and the building extraction are demonstrated for one Ikonos stereo image pair of the city of Munich.

The scene was acquired on 2005-07-15 at 10:28 GMT with a ground resolution of 83 cm. The viewing angles of the forward and backward image were +9.25° and –4.45°. The images were available only as level 1A product, which are only corrected for sensor orientation and radiometry (0) but contain no further geometric changes.

Fig. 1: Section 600 m × 400 m from the Munich scene (area of Technical University), left and right stereo image

Processing Chain

The proposed fully automatic processing chain consists of the following steps which are explained shortly in the next sections:

1 Preprocessing of the raw imagery

2 Creating the digital surface model (DSM)

3 Extracting the digital terrain model (DTM)

4 Creating true orthophotos

5 Classification

6 Object extraction

7 Object modeling

8 Representing the object models through geometric primitives and exporting in suitable 3D format

The part "modeling building objects" of "object modeling" is explained in detail in chapter 0.

Preprocessing of the raw imagery

In the preprocessing the images are imported and the metadata and the rational polynomial coefficients (RPCs) delivered with the VHR imagery is interpreted. These coefficients are mandatory since they are used to transform the geographical coordinates longitude X, latitude Y and ellipsoid height Z to image coordinates (x,y) by division of two polynoms with 20 coefficients each [Jacobsen et al., 2005, Grodecki et al., 2004]. These geometric calculations are used throughout the generation of the DSM and further for absolute georeferencing and orthophoto generation.

In a further preprocessing step the multispectral channels with much coarser resolution (one pixel multispectral correspondents to four by four pixel in the pan image) than the panchromatic channel are pansharpened.

Creating the digital surface model (DSM)

In the first processing step a digital surface model is created from the image stereo pair. For implementation of this step in the processing chain some DSM generation methods where evaluated. A classical area based matching approach as described in [Lehner and Gill, 1992] depends on images with few occlusions which means in the case of urban scenes a very narrow viewing angle and so also larger height errors.

More useful for urban scenes seem to be dense stereo algorithms used in computer vision. Such methods depend however on strict epipolar geometry. A good overview of a selection of such algorithms is given on the Stereo Vision Research Page of the Middlebury College maintained by Daniel Scharstein and Richard Szeliski [Scharstein and Szeliski, 2007].

Beside these also two more algorithms based on dynamic programming described in [Krauß et al., 2005, "dynamic line warping"] and [Hirschmüller, 2005, "semi-global matching"] where found applicable for inclusion in the processing chain.

All following investigations were done with results of modified versions of these two dynamic programming algorithms, which becomes necessary due to the non-epipolar geometry of the image pairs. This is due to the fact that the satellite image pair doesn't allow the creation of a true epipolar image – only so called quasi-epipolar images are possible since the viewing angles of the two satellite images are not parallel.

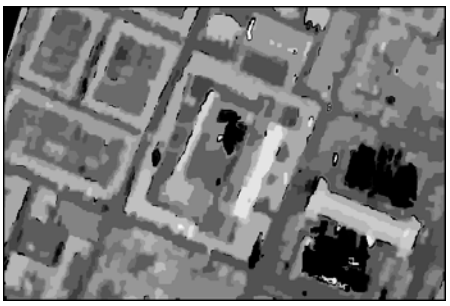

Fig. 2: Digital surface model calculated for a section of 600 m × 400 m from the Munich scene using the "dynamic line warping" approach

Extracting the digital terrain model (DTM)

Using this calculated DSM the digital terrain model describing the ground can be derived. This is accomplished by calculating a morphological erosion with a filter size of the maximum of the smallest diameter of all buildings. This results in a height image with every pixel representing the minimum height in this area around the pixel. For calculating the DTM in contrast to [Weidner and Förster, 1995] in reality a median filter returning a rather low order value will be applied instead of the morphological erosion to avoid the domination of the generated DTM by single outliers from the calculated DSM. After filtering an averaging using the same filter size is applied to obtain a smoother DTM. In the Munich example parts above the DTM are reduced to a flat plane on street level

Creating true orthophotos

Thanks to the rather dense DSM, the RPCs from the original imagery and the pansharpened multi-spectral stereo images it is possible to derive true orthophotos.

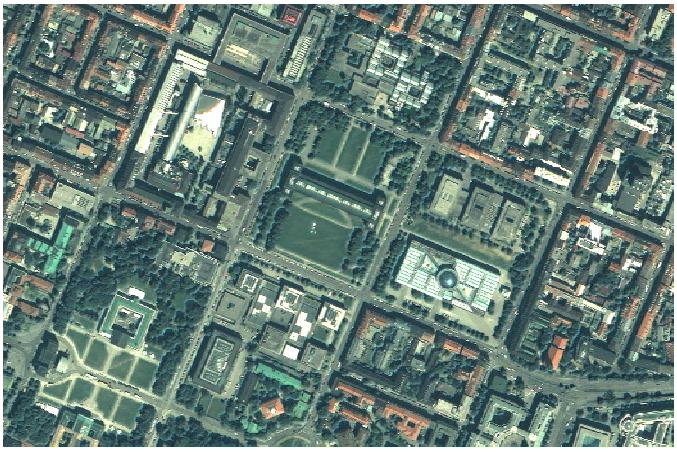

Fig. 3: Pan sharpened orthophoto based on the left stereo image and the DSM from the Munich scene

Classification

Calculating the difference image between DSM and DTM and applying a threshold of "high" (about 4 m) gives the so called "high objects mask" as shown in 0.

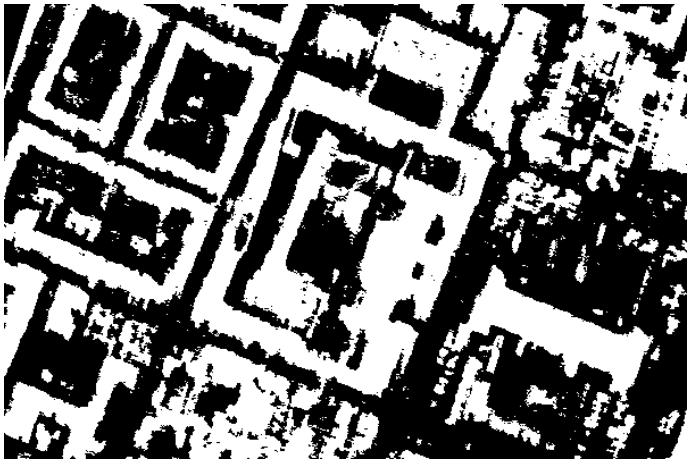

Fig. 4: High objects mask calculated from the DSM and the derived DTM applying a height threshold of 4 m (section 600 m × 400 m)

The "vegetation mask" is derived from the normalized difference vegetation index (NDVI) which is calculated from the red and near infrared channels of the pansharpened multispectral true orthophoto by applying a suitable vegetation-threshold (0).

$$NDVI = (NIR - Red) / (NIR + Red)$$

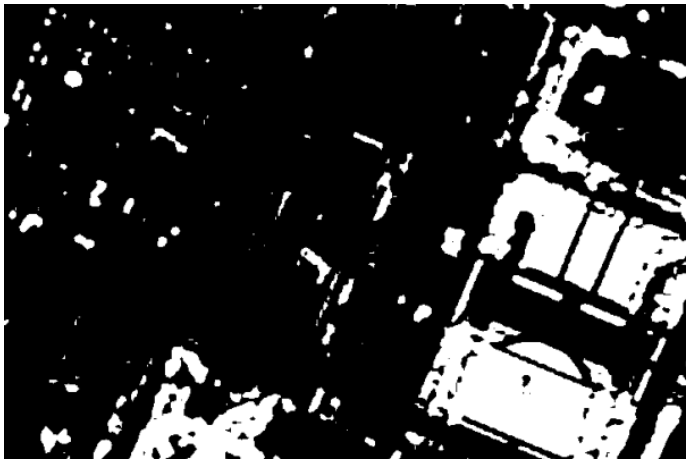

Fig. 5: Vegetation mask based on the thresholded NDVI calculated from the orthophoto (600 m × 400 m)

Combining these two binary masks leads to four classes:

- low and no vegetation: streets, plain soil, . . .
- high and no vegetation: buildings, . . .
- low and vegetation: meadows, grass, . . .
- high and vegetation: trees, bushes, . . .

Fig. 6. shows these classifications for the used section from the Munich scene:

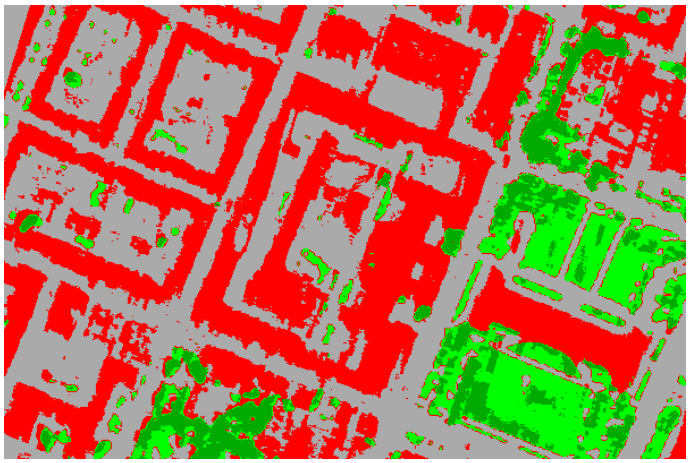

Fig.6: Classification of the Munich scene using a height mask derived from DSM and DTM and a vegetation mask based on the NDVI from the pan-sharpened orthophotos

Object extraction

For extracting objects the DSM and the orthophoto will be masked with one or more of the derived classes. Extracting the “high vegetation” class yields trees and bushes. The “high non vegetation” class will result mostly in man made buildings. Extracting all “low” objects will result in a ground plane.

Object modeling

For the simple modeling of the extracted objects following base models are used:

Model “ground” (class “low”, any type of vegetation)

Model “tree” (class “high” and “vegetation”)

Model “building” (class “high” and “no vegetation”)

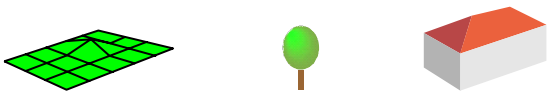

Fig.7: Simple models used

The “ground” is inserted as a height field extracted from the DTM with an optional texture directly from the true orthophoto.

“Trees” are described by a crown diameter and a treetop height extracted from the classification and the DSM respectively.

“Buildings” are represented as prismatic models restricted to rectangular edges as shown in the next section. In the future the prismatic models will be split to cuboids with optionally parametric roofs.

Representing the object models through geometric primitives and exporting in suitable 3D format

The coarse models will be represented through geometric primitives. A height field derived from the DTM for “ground” (one for full scene if textured from the true orthophoto), an ellipsoid supported by a cylinder for trees and rectangular vertical walls following the extracted circumference and a horizontal polygonal roof in the first version. A texture may be extracted from the original images by projecting the resulting polygons backward using the RPCs. The optionally textured geometric primitives have to be exported into a suitable 3D vector format. 0 shows the area around the technical university from the Munich scene as shown by a VRML viewer.

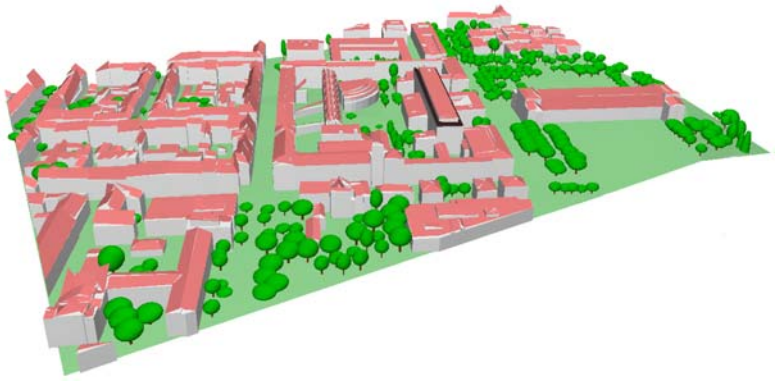

Fig.8: Simple 3D view generated from the Munich scene, size 640 m × 400 m, center: Technical University of Munich, right Old Pinacotheca

Building extraction

For the extraction of buildings the DSM will be masked with one of the objects of type “high, non-vegetation” extracted from the classification. So only one object – the mask enlarged slightly by a morphological dilation – remains in the DSM image.

This (masked) DSM is classified to “height classes” by means of height and optional also by gradients of a small surrounding area of every point. This classification process calculates a height-parameter for each pixel and joins subsequently pixels with height differences below a given threshold together.

Due to this process only clearly by height separable objects remain as classes characterized by the average height of all contributing DSM elements. For example gabled roof will join to one class of half the roof height if the height-join threshold parameter is large enough to join adjacent pixels on the slanted roof together (height-join parameter of about 1 m, larger as a GSD-step on a roof and smaller than the height of a floor).

In the next step for each of these extracted height classes of the masked object the object outline is extracted. These are shown in green for four selected objects in a section from the Munich test scene in 0.

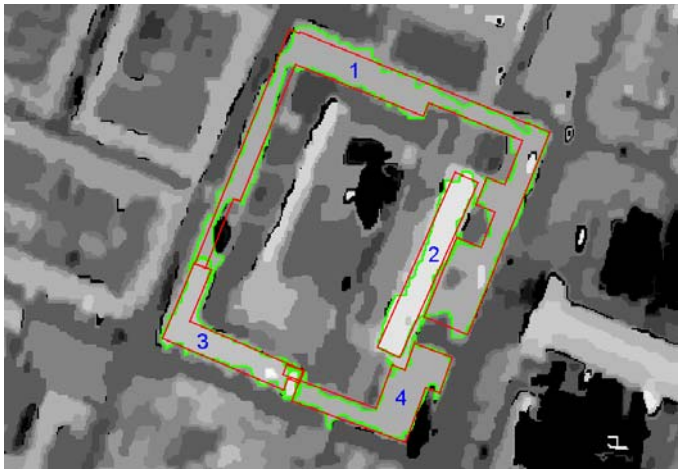

Fig. 9: Four selected outlines for building extraction in the Munich scene (full classified DSM of the examined area, not only the one extracted object – image size: 600 m × 400 m)

Based on these outlines of the height class objects a rectangular outline will be calculated. The outline is first parameterized to a vector containing for every pixel the position and an averaged direction between four preceding and four successive points. The angles are combined to full degrees and statistics, showing how many points of the outline possess which direction, is calculated as shown in 0.

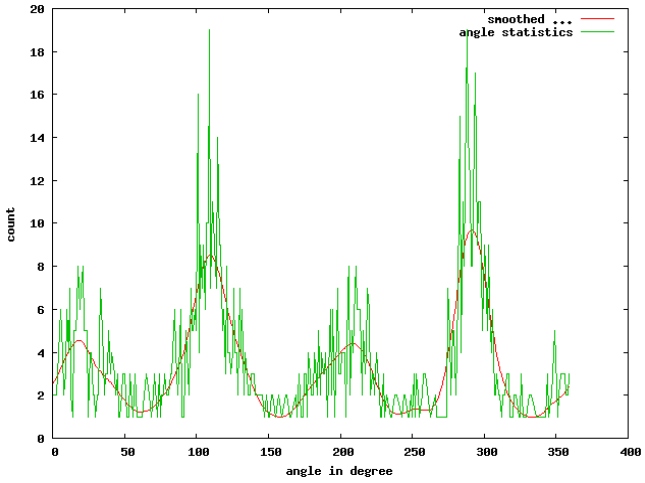

Fig. 10: Statistics of measured angles for outline “1” (green outline in 0, right: angle in degree, up: count)

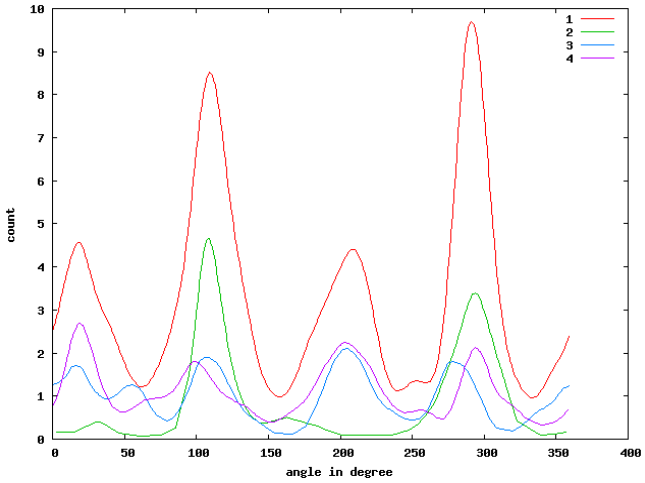

Fig. 11: Smoothed distribution for all 4 borders

Smoothing this angular distribution yields Figure 11 and allows the extraction of maxima. These found maxima will be used as the main directions of the outline. For polygon 1 the maxima can be located at 22°, 112°, 202° and 292°.

After filtering and grouping angles together to these found main directions (0) in a last step consecutive line segments (0) are intersected and the closed red polygons shown in 0 above are generated.

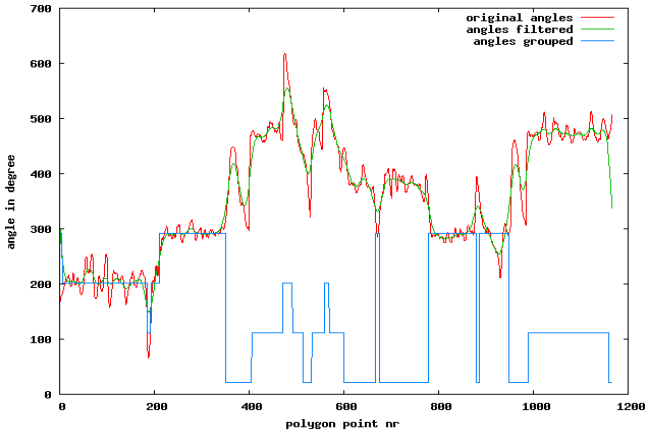

Fig. 12: Grouping angles of border elements together to found main directions

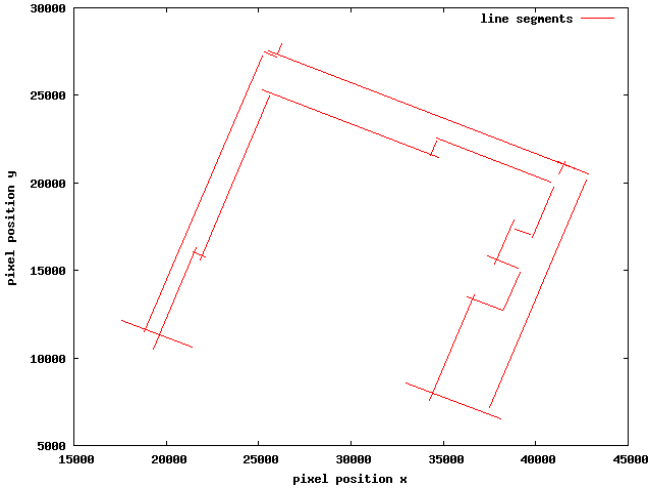

Fig. 13: Derived line segments of polygon 1 after grouping of angles

In a first version the coarse modeling is done by simply generating prismatic models with these perpendicular polygons as footprints and flat tops with an average height extracted from the DSM.

Since the accuracy and resolution of the derived DSM is in most cases not sufficient a detailed modeling of the roof shape is difficult. In future versions the polygonal circumference will be divided into rectangles. Using these rectangles an averaged section along and across these rectangles may give a hint if it is a gabled or a flat roof and lead to the selection of a more detailed bottom-up model. In the following example this is evaluated for outline “2” from 0:

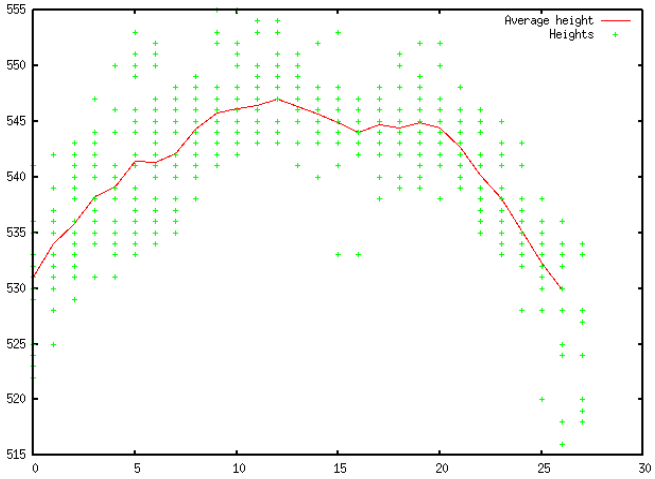

Fig. 14: Statistics of DSM heights from object 2 across roof direction (green dots: DSM values all along the roof, red line: averaged profile)

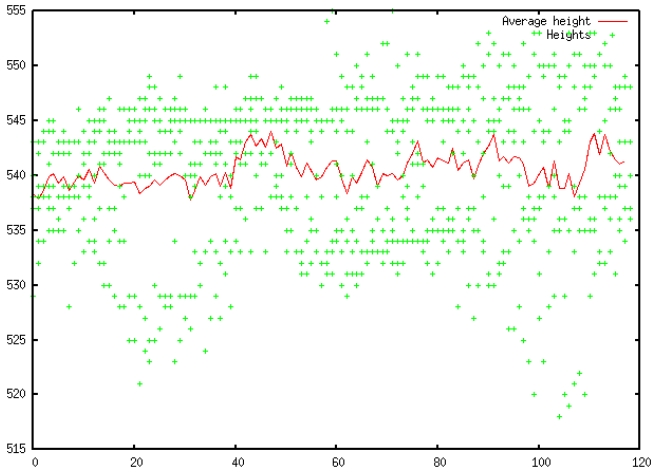

Fig. 15: Statistics of DSM-heights from object 2 along roof direction (green dots: DSM values all across the roof, red line: averaged profile)

Since the digital surface model generated from the satellite stereo image pair is in all used generation methods very coarse and noisy, a statistical approach is the only possibility for further estimation of model parameters like the roof type. Also the extraction of smaller roof features like dormers or chimneys are not possible based on the given data.

Since this approach depends on the classification based on height and vegetation it will fail in case of steep rocks not covered by vegetation or buildings covered with roof top gardens or greened roofs.

Summary and Outlook

In this paper a rather simple method for a coarse building extraction and modeling is shown. Also a quick overview of a processing chain for the automatic extraction of three-dimensional city models directly from high-resolution stereo satellite images is given. The processing chain is still in development. So the DSMs generated are not satisfying up to now. Also the automatic extraction of objects from the classified images exist only in a first evaluation version. The texturing is still missing up to now. But the results gained from each step are encouraging enough to follow the path and refine every step of the chain to receive a new fully automatic system for generating coarse three-dimensional urban models from stereo satellite imagery in a short time.

References

3D Geo: http://www.landxplorer.net/ (accessed 07/2007).

Birchfield, S. and Tomasi, C., 1998: Depth discontinuities by pixel-to-pixel stereo. Proceedings of the 1998 IEEE International Conference on Computer Vision, Bombay, India, pp. 1073–1080.

CyberCity: http://www.cybercity.tv/. (accessed 07/2007).

DigitalGlobe: http://www.digitalglobe.com/about/imaging.shtml. (accessed 07/2007).

Förstner, W. and Gülch, E., 1987: A fast operator for detection and precise location of distinct points, corners and centres of circular features. In: ISPRS Intercommission Workshop, Interlaken.

Grodecki, J., Dial, G. and Lutes, J., 2004: Mathematical model for 3D feature extraction from multiple satellite images described by RPCs. In: ASPRS Annual Conference Proceedings, Denver, Colorado.

Gross H., U. Thoennessen U., v. Hansen W., 2005: 3D-Modeling of Urban Structures. Proceedings of the ISPRS Workshop CMRT 2005, Vienna.

Hirschmüller, H., 2005: Accurate and efficient stereo processing by semi-global matching and mutual information. In: IEEE Conference on Computer Vision and Pattern Recognition (CVPR).

Jacobsen, K., Büyüksalih, G. and Topan, H., 2005: Geometric models for the orientation of high resolution optical satellite sensors. In: International Archives of the Photogrammetry, Remote Sensing and Spatial Information Sciences, Vol. 36 (1/W3). ISPRS Workshop, Hannover.

Krauß, T., Reinartz, P., Lehner, M., Schroeder, M. and Stilla, U., 2005: DEM generation from very high resolution stereo satellite data in urban areas using dynamic programming. In: International Archives of the Photogrammetry, Remote Sensing and Spatial Information Sciences, Vol. 36 (1/W3). ISPRS Workshop, Hannover.

Krauß, T., Reinartz, P. Lehner, M., 2007: Modeling of urban areas from high resolution stereo satellite images. In: Proceedings of ISPRS Workshop "High-Resolution Earth Imaging for Geospatial Information", Mai 29 – Juni 1, 2007, Hannover.

Lehner, M. and Gill, R., 1992: Semi-automatic derivation of digital elevation models from stereoscopic 3-line scanner data. ISPRS, 29 (B4), pp. 68–75.

Müller S., Zaum D., 2005: Robust Building Detection in Aerial Images. Proceedings of the ISPRS Workshop CMRT 2005, Vienna.

Otto, G. and Chau, T., 1989: Region growing algorithm for matching of terrain images. Image and vision computing (7) 2, pp. 83–94.

Scharstein, D. and Szeliski, R. Middlebury stereo vision page: http://cat.middlebury.edu/stereo. (accessed 07/2007).

Weidner, U., Förstner, W., 1995: Towards automatic building extraction from high resolution digital elevation medels. ISPRS J. 50 (4), 38–49.

SpaceImaging/GeoEye: http://www.geoeye.com/ (accessed 07/2007).

Industrial area detection during GNEX06

Charles Beumier*

Signal and Image Centre, Royal Military Academy, Brussels Belgium

* Charles.Beumier@elec.rma.ac.be

Abstract

Since the availability of Very High Resolution satellites like Ikonos and Quickbird, the resolution and multi-spectral nature of the related images enable the detection of medium or large size buildings. In the current paper, we present the localization of industrial areas in the context of risk assessment as industrial plants are potential targets in crisis situation. The approach, rapidly designed and developed during the real-time exercise GNEX06 of the European Network of Excellence GMOSS, is based on the detection of long linear segments on an image whose intensity is related to the vegetation index. Automatic detection of candidate industrial areas was qualitatively assessed by human observation relatively to the map of industrial zones provided in the context of the exercise.

1 Introduction

Very High Resolution images from satellites like Quickbird and Ikonos are available for more than five years. The automatism of the acquisition process, delivering regularly images with small revisit time, large area covers and precise geographical localization has opened the era of discrete and remote earth observation with high reso-lution. Typical applications are risk or change assessment where the presence or absence of key features allows for the establishment of conditions regarding pre or post crisis management.

In the context of risk assessment, the localization of industrial areas is of particular importance as industrial plants typically contain high level technology or dangerous products. These sites represent potential targets in cri-sis situations and may constitute a real danger for the neighboring population in case of hazard conditions even in normal situations.

An increasing number of works are published in the field of man-made structure detection thanks to VHR sat-ellite images like Ikonos or Quickbird. For instance, the ORFEO initiative (http://smsc.cnes.fr/PLEIADES/ and [1]) headed by CNES contains a research program to study the potentials of the new satellite constellation con-sisting of visible (Pleiades, France) and SAR (Cosmo-Skymed, Italy) sensors with VHR (metric) resolution.

Classical man-made structures of interest are the road network and the buildings. Consult for instance the re-view by Mena about the state of the art on automatic road extraction for GIS update [2]. One year and a half after the launch of Ikonos satellite, Fraser et al [3] published a work about the geometric potential and suitability for 3D building reconstruction. An example of building extraction in urban areas using structural, contextual and spectral information is given in Jin et Al. [4].

In the current work, the difficulty of man-made structure detection has been relaxed in the sense that only me-dium or large structures are of interest (minimum 25 m). We intend to filter out small buildings and highlight ar-eas corresponding to industrial plants. Results are presented in the form of a digital map overlapped with high-lighted segments to draw the operator's attention. The operator typically confirms the automatically highlighted areas after observation of the underlying original image data.

The next section details the methodology for the detection of large and linear image segments on a vegetation index image. Section 3 presents the results and section 4 concludes the paper.

2 Methodology

Industrial plants are usually made of buildings of large extent with linear outlines. They are often distinguished from their neighborhood thanks to the difference in vegetation content. Contiguous parking lots are additional visible cues easily revealed by their multi-spectral characteristics (grey color and little vegetation).

We propose to detect industrial areas in VHR satellite images thanks to the presence of large straight segments with high contrast in the NDVI image.

Contrary to urban areas where many small straight segments are typically encountered, industrial buildings present in top view images large straight segments corresponding to building limits or man-made roads and park-ing lots.

Built-up areas are made of a material contrasting with vegetation. The vegetation index (NDVI) obtained from the combination of near infrared and red channel of the multi-spectral images is a valuable cue to separate vegeta-tion and non-vegetation areas.

The dark areas corresponding to the shadow casts so characteristic of elevated buildings give an additional support to the built up area presence and are detected thanks to the magnitude of the edge gradient.

2.1 Vegetation index

We followed the definition of the Normalized Difference Vegetation Index:

$$NDVI = (NIR - RED) / (NIR + RED)$$

with NIR and RED the respective intensities of the infrared and red spectral channels. As the live green plants appear rather dark in the RED channel (energy absorption for photosynthesis) and bright in the near infrared NIR channel (little absorption that would turn into heating, bad for plant life expectancy), values for NDVI are posi-tive (max +1) for vegetation and negative (min -1) for non vegetation areas. This formula is applied to all the pix-els of the image independently.

2.2 Segment detection

The NDVI image obtained in the previous section is first applied a low-pass filter to reduce noise. We limited the filter to a 3x3 uniform average corresponding to 3.6 m as each pixel is 1.2 m large. This reduces significantly the noise without blurring the image at the scale of large buildings (at least 25 m).

A classical edge detector was performed on the low-pass filtered image. The mask (-1_0_1) was applied hori-zontally and vertically to derive the directional gradient values from which to compute the gradient magnitude and orientation.

An edge follower helped grouping edge pixels with sufficient gradient into contiguous segments based on the gradient magnitude and orientation. For each pixel with sufficient gradient and not yet assigned to a segment, the three neighbors in the direction consistent with the gradient orientation are compared. The pixel with maximal gradient magnitude and consistent gradient orientation is added to the segment.

2.3 Segment filtering

Detected segments are filtered based on geometrical constraints. Segments shorter than 25 m are rejected to keep large buildings and those longer than 200m are not considered as they are likely to correspond to roads. The standard deviation of the segment points relative to the minimal inertia axis has been used to constrain the straightness of the candidate segments. This straightness measure, detailed in [5], possesses an intuitive interpre-tation of the threshold (standard deviation, expressed in pixels) and allows for an incremental straightness meas-ure, computationally efficient.

3 Results

The localization of industrial areas has been one of the contributions of the Signal & Image Centre (Royal Mili-tary Academy of Belgium) to the real-time exercise GNEX'06 organized by the European Network of Excellence GMOSS.

A few partners of the team designed a fictitious crisis scenario (http://www.zki.dlr.de/events/2006/gnex06/5_en.html) based on real data in the region of the nuclear power plant of Leibstadt, Switzerland. On the specified day, we were informed of the scenario and organized how to answer specific questions raised by the virtual crisis centre.

One of our contribution consisted in the localization of industrial plants as they represent a possible target or a possible danger for the population. We retrieved by ftp the image data of the area provided by the GNEX06's or-ganizers.

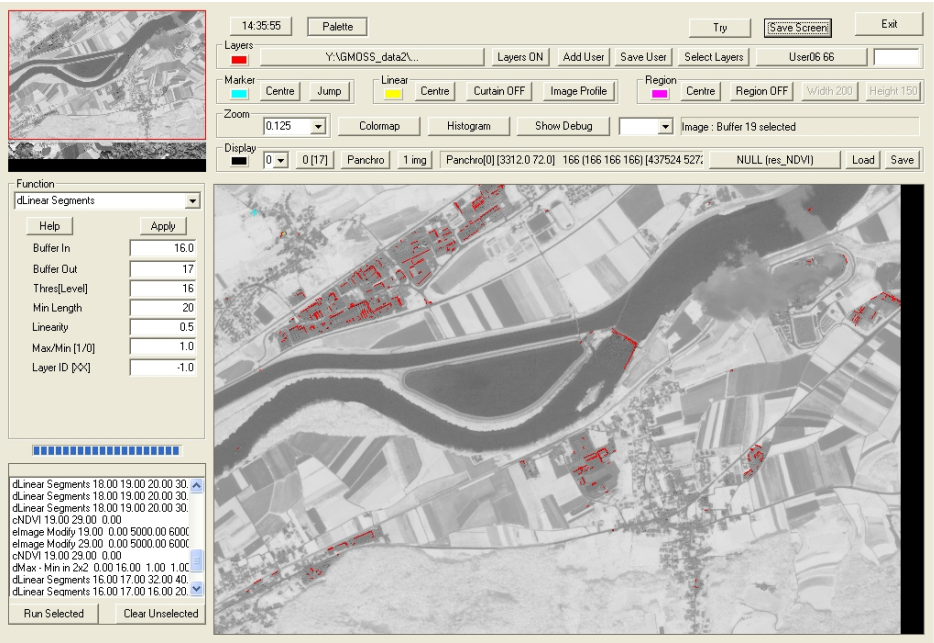

Fig. 1: NDVI image and superimposed detected segments in red.

We applied the algorithm described in the previous section to the red and near infrared band of a Quickbird image over the region of Leibstadt, Switzerland. We derived the NDVI image (see Fig. 1) and the long and straight segments with high contrast. Observe the darker area corresponding to the plume in the top right quadrant above the nuclear plant, close to the river.

A ground truth image was created from the map available during the GMOSS GNEX06 exercise. The map was converted into a grey image, converting pixels assigned to industrial areas to a specific value represented in red in the results. Detected straight segments were superimposed in green on that ground truth image (see Fig. 2).

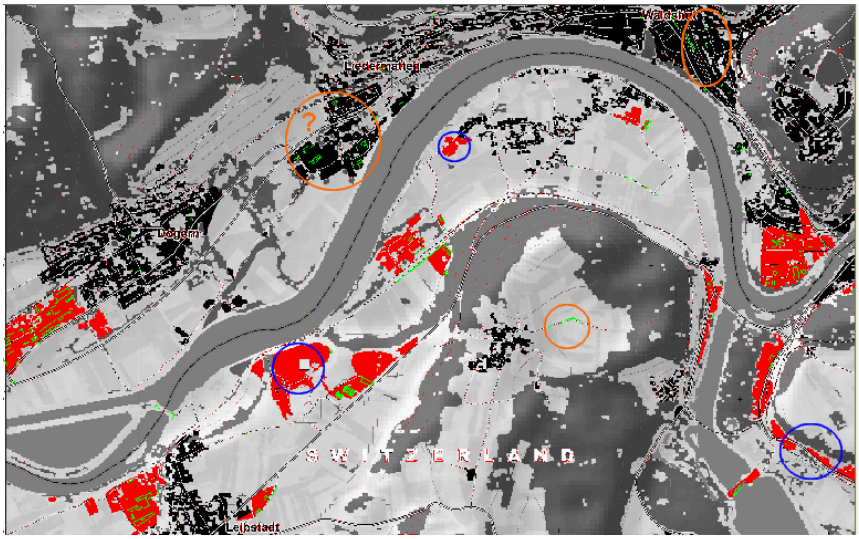

Fig. 2: Vectors of automatically detected industrial plants (in green) superimposed on the ground truth map with industrial areas drawn in red.

We observe that most detected segments (in green) overlap industrial (red) areas. False detection is marked by an orange circle while missed industrial areas are marked with a blue circle. The orange circle with a question mark seems to be a ground truth error.

4. Conclusions

This paper presents automatic industrial area detection based on the localization of long and straight linear seg-ments detected in the NDVI image. The methodology has been applied in the context of the GNEX06 real-time exercise. Although not perfect, the automatically highlighted segments represent valuable information to guide a human observer when searching for industrial areas.

A possible improvement to the approach consists in the explicit use of elevation so characteristic of built-up areas, and possibly gathered by stereoscopy or shadow extraction.

Acknowledgments

This work has been undertaken in the context of the GMOSS Network of Excellence thanks to which satellite data has been gracefully obtained.

References

[1] A. Baudoin, "Beyond SPOT 5: Pleiades, Part of French-Italian Program ORFEO" Proceedings of ISPRS 2004, Istanbul, Turkey, July 12-23, 2004.

[2] J.B. Mena, “State of the art on automatic road extraction for GIS update: a novel classification”, In Pattern Recognition Letters 24 (2003), pp 3037-3058.

[3] Fraser, C.S., Baltsavias, E. & Gruen, A., “3D building reconstruction from high-resolution IKONOS stereo images”. Proc. of 3rd int. Symposium on Automatic Extraction of Man-made Objects from Aerial and Space Images, Ascona, Switzerland, 10-15 June 2001: 331-344.

[4] X. Jin, C. Davis, "Automated Building Extraction from High-Resolution Satellite Imagery in Urban Areas Using Structural, Con-textual, and Spectral Information", In EURASIP Journal on Applied Signal Processing, 2005:14, 2196-2206.

[5] C. Beumier, “Straight-line Detection Using Moment of Inertia”, IEEE International Conference on Industrial Technology 2006 (ICIT 2006), Mumbai, India, Dec 15-17, 2006.

Advances in Statistical Change Detection Methods within the GMOSS Network of Excellence

Morton J. Canty[1*] & Allan A. Nielsen[2]

[1] *Institute for Chemistry and Dynamics of the Geosphere, Jülich Research Center, D-52425 Jülich, Germany*

[2] *Danish National Space Center, Technical University of Denmark, DK-2800 Kgs. Lyngby, Denmark*

* m.canty@fz-juelich.de

1 Introduction

Over the period of GMOSS funding, beginning 2004 until the present, an intensive collaboration has been taking place within the Treaty Monitoring WP 20400 on the further development and application of the Multivariate Alteration Detection (MAD) algorithm originally proposed by Nielsen et al. (1998). The research complements that carried out with other change detection techniques in WP 20300. Methodological extensions and improvements of MAD resulting from the work have been recently published in peer-reviewed journals and conference proceedings, applications to Treaty Monitoring have been reported at several conferences and symposia devoted to security applications and, last but not least, Matlab and IDL software implementing the methodology has been made freely available to researchers within the network. In this paper, the progress within GMOSS in the field of change detection is summarized and some of the main achievements highlighted. These include the introduction of an iterative re-weighting scheme into the MAD algorithm, the use of regularization to avoid numerical instabilities with high-dimensional data, the application of MAD to automatic radiometric normalization of image time series and the unsupervised clustering of changes in the MAD feature space. Reference is made to published work for those interested in technical details.

2 The MAD transformation

Consider two N-band multispectral images of the same scene acquired at different times, between which ground reflectance changes have occurred at some locations, but not everywhere. Assume without loss of generality both images to have pixel intensities with zero mean. Representing observations (pixel intensities) in the first multispectral image by a random vector $\boldsymbol{F} = (F_1 \ldots F_N)^\top$, we can make a linear combination of the intensities for all spectral bands, creating a scalar image characterized by the random variable $U = \boldsymbol{a}^\top \boldsymbol{F}$. The vector of coefficients $\boldsymbol{a}$ is as yet unspecified. We do the same for the second image, represented by $\boldsymbol{G}$, forming the linear combination $V = \boldsymbol{b}^\top \boldsymbol{G}$, and then look at the scalar difference image $U - V$. This combines all of the change information into a single image, but one has of course still to choose the coefficients $\boldsymbol{a}$ and $\boldsymbol{b}$ in some suitable way. In Nielsen et al. (1998) it is suggested that they be determined by applying standard Canonical Correlation Analysis (CCA) (Hotelling, 1936) to maximize the correlation between images $\boldsymbol{F}$ and $\boldsymbol{G}$. This leads to coupled generalized eigenvalue problems which can be solved for the projection directions

$\boldsymbol{a}$ and $\boldsymbol{b}$. Solution of the eigenvalue problems generates new multispectral images $\boldsymbol{U} = (U_1 \ldots U_N)^\top$ and $\boldsymbol{V} = (V_1 \ldots V_N)^\top$, the components of which are called the *canonical variates* (CVs). The CVs are ordered by similarity (correlation) rather than, as in the original images, by wavelength. The canonical correlations $\rho_i = \mathrm{corr}(U_i, V_i)$, $i = 1 \ldots N$, are the square roots of the eigenvalues of the coupled eigenvalue problem and $\boldsymbol{a}_i$ and $\boldsymbol{b}_i$, $i = 1 \ldots N$, which determine $\boldsymbol{U}$ and $\boldsymbol{V}$ from $\boldsymbol{F}$ and $\boldsymbol{G}$, are the eigenvectors. The pair (U_1, V_1) is maximally correlated, the pair (U_2, V_2) is maximally correlated subject to being orthogonal to (uncorrelated with) both U_1 and V_1, and so on. Performing paired differences (in reverse order) then generates a sequence of transformed difference images

$$M_i = U_{N-i+1} - V_{N-i+1}, i = 1 \ldots N, \qquad (1)$$

which are referred to as the *MAD variates*.

The first MAD variate has maximum variance in its pixel intensities. The second MAD variate has maximum variance subject to the condition that its pixel intensities are statistically uncorrelated with those in the first variate, the third has maximum variance subject to being uncorrelated with the first two, and so on. Depending on the type of change present, any of the components may exhibit significant change information. Interesting small-scale anthropogenic changes, for instance, will generally be unrelated to dominating seasonal vegetation changes or stochastic image noise, so it is quite common that such changes will be concentrated in higher order MAD variates. This is illustrated in Figure 1, which shows an application of change detection for monitoring the Comprehensive Nuclear Test Ban Treaty. In fact one of the nicest aspects of the method is that it sorts different categories of change into different, uncorrelated image components.

3 Iteratively re-weighted MAD (IR-MAD)

Next consider two images of a scene, acquired at different times under similar illumination conditions, but for which no ground reflectance changes have occurred whatsoever. Then the only differences between them will be due to random effects like instrument noise and atmospheric fluctuation. In such a case we would expect that the histogram of any difference component that we generate would be very nearly Gaussian. In particular, the MAD variates of Equation (1), being uncorrelated, should follow a multivariate normal distribution with diagonal covariance matrix.

The MAD variates associated with change observations will deviate more or less strongly from such a multivariate normal distribution. Therefore, in the presence of genuine change, we expect an improvement of the sensitivity of the MAD transformation if we place emphasis on establishing an increasingly better background of no change against which to detect change. This can be done in an iteration scheme in which observations are weighted by the probability of no change, as determined on the preceding iteration, when estimating the sample means and covariance matrices which determine the MAD variates for the next iteration (Nielsen, 2007).

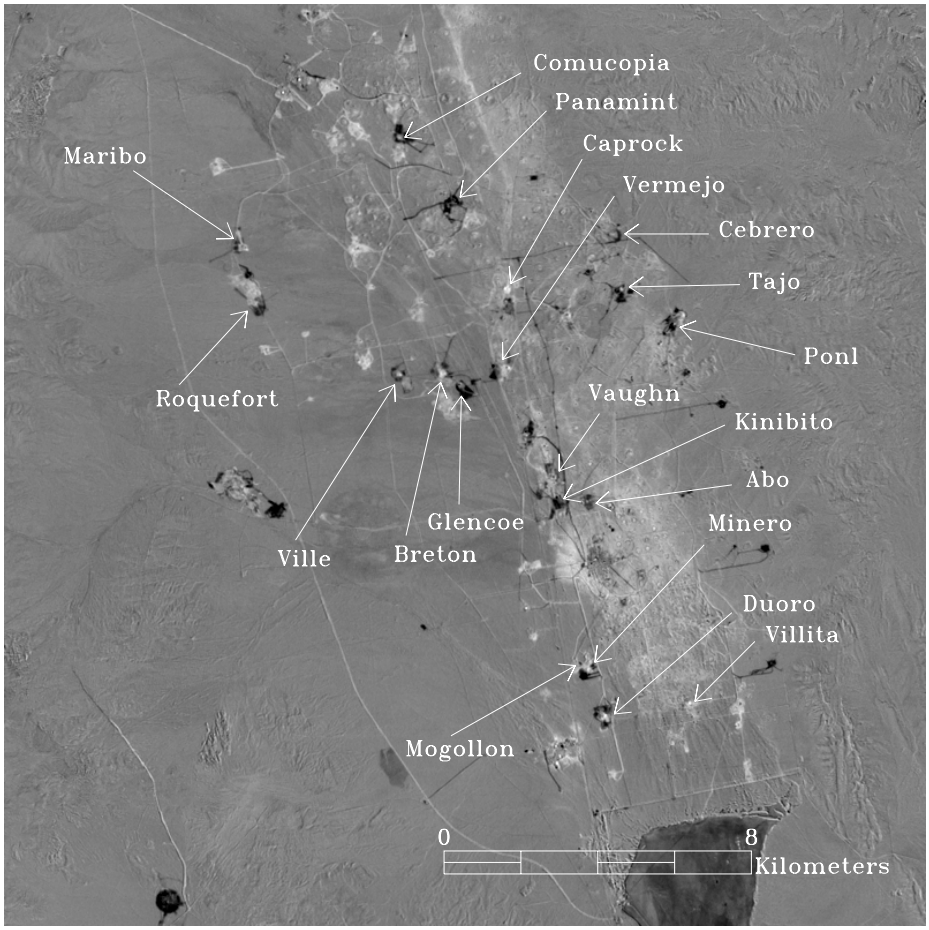

Fig. 1: Landsat TM change image over the Nevada Test Site betweenMay 6, 1984 and May 28, 1986. The 6th MAD variate is shown, stretched +-8 standard deviations. Middle gray pixels indicate no change, light or dark pixels indicate changes. Many significant changes can be associated with preparation activities for underground nuclear tests that took place during this time interval (indicated by their code names).

The probability weights may be obtained by examining the MAD variates directly. Let the random variable Z represent the sum of the squares of the standardized MAD variates

$$Z = \sum_{i=1}^{N} \left(\frac{M_i}{\sigma_{M_i}} \right)^2, \tag{2}$$

where σ_{M_i} is the standard deviation of no-change part of MAD variate M_i. Then, since the no-change observations are normally distributed and uncorrelated, their realizations should be chi-square distributed with N degrees of freedom (distribution function $P_{\chi^2;N}(z)$). For each iteration, the observations z (realizations of the random variable Z) can then be given weights determined by the chi-square distribution, namely

$$\Pr(\text{no change}) = 1 - P_{\chi^2;N}(z). \tag{3}$$

Pr(no change) is the probability that a sample z drawn from the chi-square distribution could be that large or larger. A small z implies a large probability of no change. Other weighting schemes are possible, for instance using unsupervised classification of change/no-change

observations, see below. The improvement that can be obtained using iteration is illustrated in Figure 2.

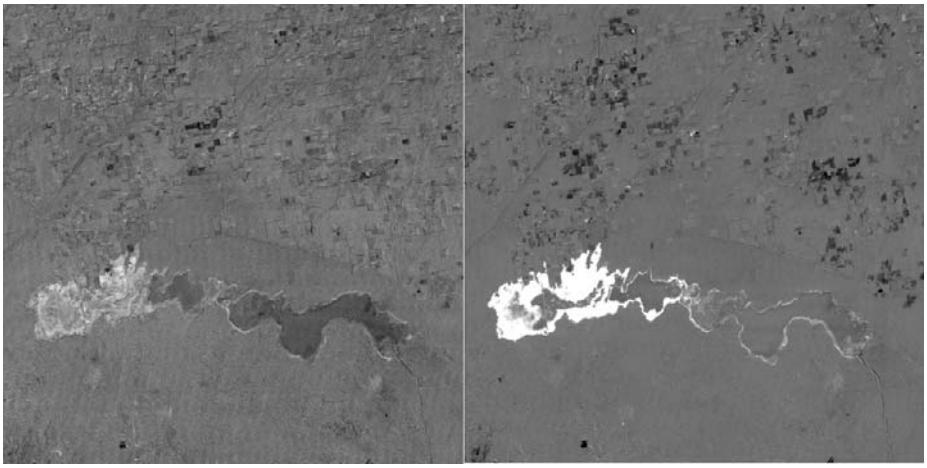

Fig. 2: Left: The sixth MAD variate for a bitemporal Landsat TM image over a reservoir in Hindustan, India, without iteration of the MAD transformation, shown in an unsaturated linear histogram stretch. Right: The sixth IR-MAD variate after iteration to convergence, shown on the same intensity scale. Bright and dark pixels indicate change.

4 Regularization

Nielsen (2007) describes the iterative extension sketched above as well as several regularization schemes to the MAD method. When we work with hyperspectral data we have many (correlated) variables and the solutions to the CCA generalized eigenvalue problem may become unstable. This is due to (near) singular variance-covariance matrices that enter into the CCA eigenproblem, causing small changes in the data to lead to dramatically different solutions for the eigenvectors $\boldsymbol{a}$ and $\boldsymbol{b}$ A possible solution to such (near) singularity problems in hyperspectral data change detection may be regularization (also known as penalization) where, inspired by ridge regression, we add a small, positive scalar times a unit or other matrix to the variance-covariance matrices. Using a second order derivative-type matrix rather than the unit matrix we may choose to penalize curvature of the elements in $\boldsymbol{a}$ and $\boldsymbol{b}$ considered as functions of wavelength. Using the unit matrix penalizes the lengths of $\boldsymbol{a}$ and $\boldsymbol{b}$.

Alternatively, the invariance of the MAD variates to linear (affine) transformations of the original variables can be exploited. Possible (near) singularities may also be remedied by means of principal component analysis (PCA), maximum autocorrelation factor (MAF), projection pursuit (PP) analysis or other dimensionality reducing projections applied to the variables at the two points in time separately before doing canonical correlation and MAD analysis.

If regularization is needed or desired, one may use either the former, the latter or a combined scheme. The ordering of the projection variates in the dimensionality reducing regularization scheme is by some projection index (such as variance, autocorrelation, deviation from normality or other) rather than by wavelength. This ordering makes penalizing for example curvature un-natural. So the two regularization schemes do not readily combine.

To work around this problem we may apply the dimensionality or feature reduction scheme above to adjacent, non-overlapping groups of spectral bands. For example, we may replace bands 1, 2, and 3 with one projection, 4, 5 and 6 with another etc. In this way we reduce the dimensionality of the data (in the example by a factor of three) while retaining the main spectral features of the original data and their order. This preservation of order facilitates the

application of further regularization by penalizing for example curvature as described in the former regularization scheme above.

If we use this combined regularization scheme, the general MAD transformation invariance may be lost depending on the choice of dimensionality reduction scheme. If we choose the MAF transformation, we retain the invariance to any transformations that are linear (or affine) in the individual original variables.

5 Radiometric normalization

Ground reflectance determination from satellite imagery requires, among other things, an atmospheric correction algorithm and the associated atmospheric properties at the time of image acquisition. For most historical satellite scenes such data are not available and even for planned acquisitions they may be difficult to obtain. A relative normalization using the radiometric information intrinsic to the images themselves is an alternative whenever absolute surface reflectances are not required.

In performing relative radiometric normalization, one usually makes the assumption that the relationship between the at-sensor radiances recorded at two different times from regions of constant reflectance can be approximated by linear functions. The critical aspect is the determination of suitable time-invariant features upon which to base the normalization.

In Canty et al. (2004) we suggested a fully automatic procedure for determining time-invariant observations which takes advantage of the invariance properties of the MAD transformation. The method was validated with unbiased statistical tests for equal means and variances of the normalized image bands and compared favorably to much more time-consuming manual selection of pseudo invariant features for normalization.

The IR-MAD procedure described in Section 3 is superior to the ordinary MAD transformation in identifying significant change, particularly for data sets in which the fraction of invariant pixels is relatively small, e.g., scenes which undergo large seasonal changes in vegetation or land use. It therefore also performs better in isolating the no-change pixels suitable for use in relative radiometric normalization. In our investigations (Canty and Nielsen, 2007) this has been confirmed by comparing radiometric normalizations obtained with the original and with the iterated versions of the MAD transformation. Figures 3 and 4 illustrate the use of radiometric normalization with iteratively re-weighted MAD for image mosaicking. The success of the normalization is particularly evident on the left hand edge of Figure 4, where a coherent arid area with no vegetation change can be followed from top to bottom of the mosaic with no discernible transitions, although very significant and real changes occur elsewhere in the scene. Note that the substantial cloud cover in the April 9, 2001 image has no effect on the quality of its normalization as all cloud and cloud shadow pixels are correctly identified as change.

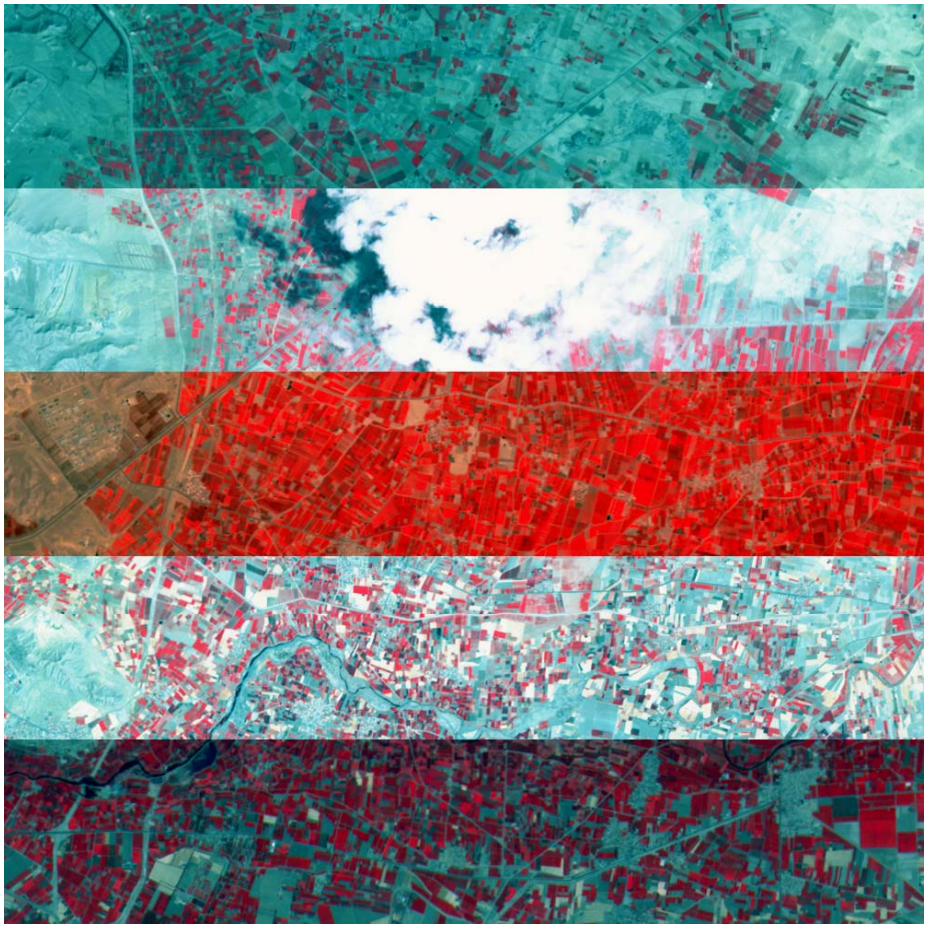

Fig. 3: Mosaic of 5 ASTER images over Iran prior to radiometric normalization, RGB color composite equalization stretch: band 1 (blue), band 2 (green), band 3N (red). The acquisition dates are, from top to bottom: March 11 2002, April 9 2001, May 22 2005, July 30, 2001 and September 11 2005.

6 Unsupervised clustering

In Canty and Nielsen (2006) we investigated the unsupervised classification (clustering) of change and no-change pixels using a multivariate Gaussian mixture model fitted with the EM algorithm. The method allows for hyper-ellipsoidal clusters and clusters of differing sizes, and includes a criterion for choosing the best number of classes. Advantage is also taken of the probabilistic interpretation of class memberships determined by the algorithm to apply post classification processing to improve the spatial coherence of the change classes obtained. Unsupervised classification facilitates the *a posteriori* interpretation of the MAD variates and permits quantification of surface areas that have undergone significant changes of different kinds, see Figure 5.

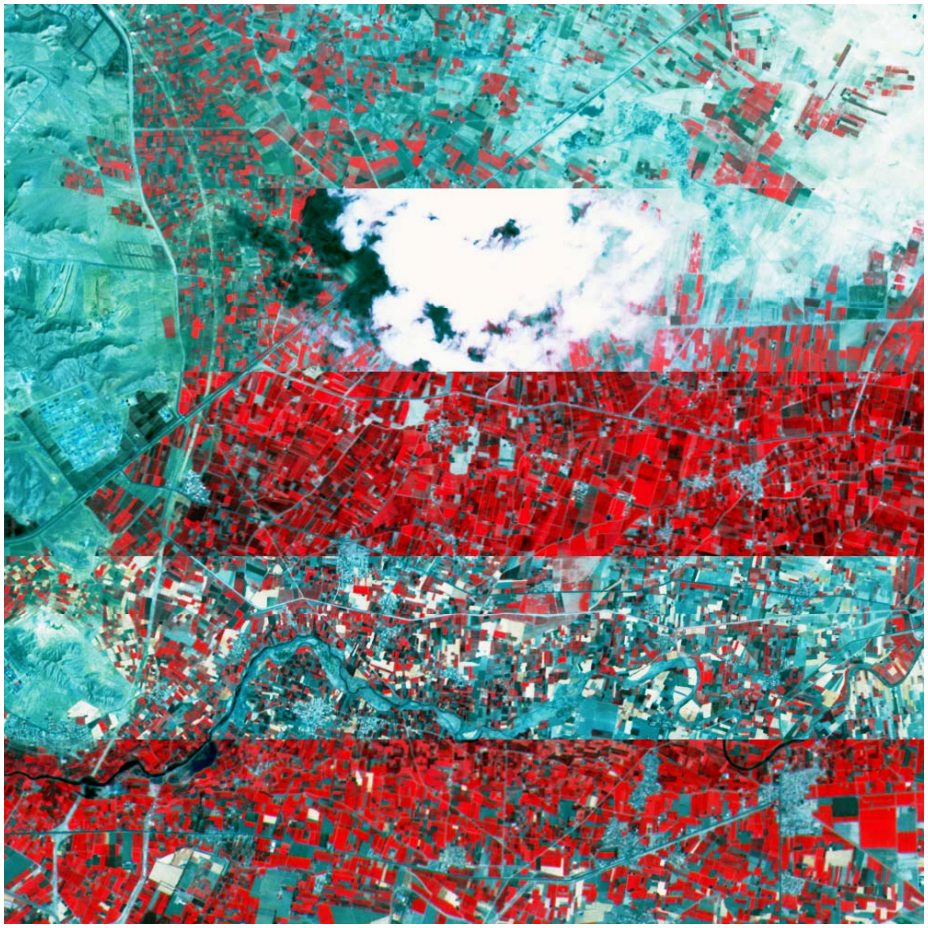

Fig. 4: As Figure 3 after IR-MAD radiometric normalization.

7 Conclusions

In conclusion, the IR-MAD procedure provides the image analyst with change information as well as no-change information. The former is interesting in its own right and the latter can be used as a basis for completely automatic, orthogonal regression analysis-based, radiometric normalization of multi-temporal imagery. Also, the method provides a wide range of ways to interpret multi-temporal imagery: direct inspection of the MAD variates for change signals, analysis of chi-square images and the change probabilities derived from them, examination of unsupervised classification thematic maps, interpretation of correlations between original and transformed data and of eigenvector weights, etc.

For future research, many extensions and modifications of IR-MAD can be envisaged, such as the use of mutual information (rather than correlation) as a similarity measure or the application of nonlinear transformations with kernelized CCA, artificial neural networks or the alternating conditional expectation (ACE) algorithm.

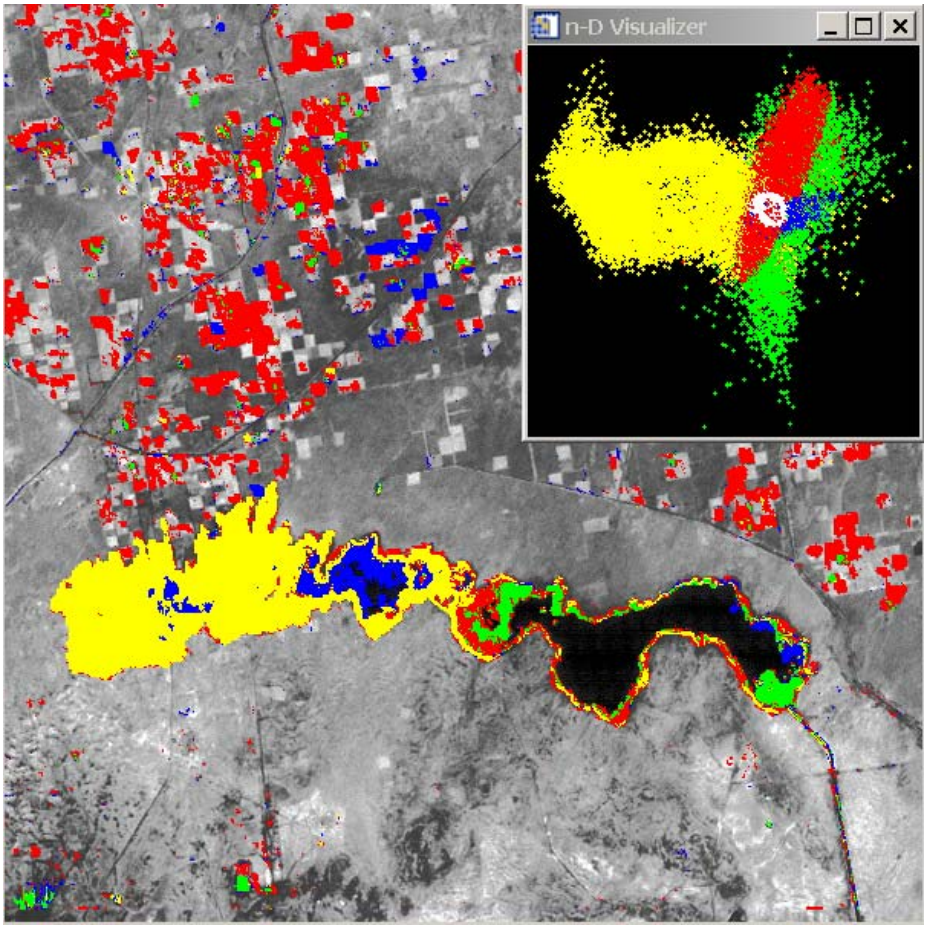

Fig. 5: Unsupervised classification of the MAD variates for the reservoir scenes of Figure 2. Five clusters were used, including no change. The four change clusters are shown superimposed onto spectral band 5 of the first image. The insert displays the clusters in feature space. The partially obscured white cluster near the center is no-change.

Available software

Software for all of the image processing algorithms discussed here has been made available during the lifetime of the GMOSS Network of Excellence, both in IDL and in Matlab, the former as easy-to-use extensions to the ENVI remote sensing image analysis environment (ITT Visual Information Solutions), see Canty (2007) and http://www.imm.dtu.dk/∼aa.

References

Canty, M. J. (2007). Image Analysis, Classification, and Change Detection in Remote Sensing, With Algorithms for ENVI/IDL. Taylor and Francis.

Canty, M. J. and Nielsen, A. A. (2006). Visualization and unsupervised classification of changes in multispectral satellite imagery. International Journal of Remote Sensing, **27**(18), 3961–3975. Internet http://www.imm.dtu.dk/pubdb/p.php?3389.

Canty, M. J. and Nielsen, A. A. (2007). Automatic radiometric normalization of multitemporal satellite imagery with the iteratively re-weighted MAD transformation. Accepted for Remote Sensing of Environment Internet http://www.imm.dtu.dk/pubdb/p.php?5362.

Canty, M. J., Nielsen, A. A., and Schmidt, M. (2004). Automatic radiometric normalization of multitemporal satellite imagery. Remote Sensing of Environment, **91**(3-4), 441–451. Internet http://www.imm.dtu.dk/pubdb/p.php?2815.

Hotelling, H. (1936). Relations between two sets of variates. Biometrika, **28**, 321–377.

Nielsen, A. A. (2007). The regularized iteratively reweighted MAD method for change detection in multi- and hyperspectral data. IEEE Transactions on Image Processing, **16**(2), 463–478. Internet http://www.imm.dtu.dk/pubdb/p.php?4695.

Nielsen, A. A., Conradsen, K., and Simpson, J. J. (1998). Multivariate alteration detection (MAD) and MAF post-processing in multispectral, bitemporal image data: New approaches to change detection studies. Remote Sensing of Environment, **64**, 1–19. Internet http://www.imm.dtu.dk/pubdb/p.php?1220.

Achievements & Challenges

The Way Forward

Peter Zeil*

with contributions by Vinciane Lacroix, Nathalie Stephenne, Hans-Joachim Lotz-Iwen, Stefan Schneiderbauer, Gunter Zeug, Ola Dahlman, and Klaus Granica.

Centre for Geoinformatics (Z_GIS), University of Salzburg, Salzburg, Austria

* peter.zeil@sbg.ac.at

At the onset of GMOSS, there were wide-spread uncertainties about what the instrument 'Network-of-Excellence' should achieve. The concept of NoEs had been newly established by the Commission for the 6th Framework Programme, and a common understanding still had to be developed between the scientific officer and the consortium about the key criteria to be used for the evaluation of progress.

A work programme should be performed 'aimed at tackling fragmentation of existing research capacities....to assemble the critical mass of resources, activities, and expertise needed to ensure that they reach their ambitious objective, e.g. the durable integration of the participants' capacities in the area considered'. The activities to be carried out towards these results were supposed to be threefold: integrating activities, implementing a joint research programme, and spreading of excellence. In order to highlight this, the EC-contribution was labeled 'grant for integration' , and based on the number of researchers involved from the participating institutions.

For the consortium, which actually had planned for an integrated project, the framework of a NoE posed quite a challenge. With perceptions still firmly embedded in 'workpackages' and 'product deliverables', partners from research organizations - civil and military -, companies and consultancies, felt pushed into integration by first of all having to understand each others language (e.g. security, threat, COP), then to effectively communicate (across sectoral boundaries between 'military' and 'civilian' domains), before being able to explore the benefits of efficient collaboration.

As a matter of fact, integration did not just happen by itself. The initial attempt to use gaming (understood as a near-real time exercise under a given scenario) as a mean to develop a common understanding of problems at an early stage of GMOSS faced criticism and reluctance. In order to establish a 'culture for integration' the consortium had to follow subsequent steps to facilitate the exchange at specific levels:

- inter-working groups (integration meetings, information markets, test-cases)
- inter-institutions (staff exchange, training seminars)
- inter-sectoral (summer schools, GNEX – near-real time exercises)
- science-policy (user meetings, panel discussions, summer schools, seminars, GNEX, test-cases)
- inside-outside of GMOSS (meeting with other GMES project consortia, summer schools, test-cases)
- EU-global (summer schools, test-cases)

The result of this process is not only a network of institutions and organizations, but a community of researchers exploring synergies evolving from corresponding skills, knowledge and infrastructure. Participants experienced to act within a Network, and to perform strategic planning based on consensus, effective network management and the efficient implementation of a joint research program. An essential component of the 'culture of integration' is the capacity to provide feedback to each others work. Even though working in a highly competitive environment, the GMOSS community was able to build the confidence and mutual trust required to evaluate individual and/or joint achievements (algorithms, tools, workflows) by establishing procedures for validation and benchmarking (test cases, GNEX).

The interdependency which is inherent to an NoE helps to remove stumbling blocks common to competitive, and even more to industry-driven research and development projects. Well managed and wisely using the flexibility of the instrument, a NoE is perfectly suited to explore new R&D-fields of interdisciplinary and intersectoral nature, and to facilitate the development of research strategies.

Achievements

GMOSS, in the first place, is a network of people. Inspiring personal contacts were established through meetings, joint research and integrating activities such as working on test cases, collaboration during summer schools and near-real time exercises. Partners are now well aware of each others institutional capacity, activities and expertise. This is the fundament of effective communication and an important pre-requisite for integration. Collaboration, partnership (some even formalized through Memoranda of Understanding, MoUs), friendship, are all synonyms for the new dimension, which GMOSS as a process was able to create during the four years of implementation.

A true network of researchers emerged over time, capable to develop a concept for integration. The components of this culture -as mentioned above- maintain communication and flow of expertise between pure and applied natural sciences and socio-political analysis. Bridging the communities of social and political scientists with engineers and remote sensing experts offered great opportunities for insights and advances in security related research. GMOSS lived up to its objective of providing an integrating platform for monitoring security and stability.

The wealth of expertise contributed by partners and the advances made during the implementation of the joint research program enabled GMOSS to establish application-oriented workflows, starting with the analysis of issues and priorities of European security policy towards the identification and ranking of major threats to security and stability, and the definition of scenarios to be assessed by GMOSS researchers. The results are used for the identification of early warning indicators and 'keys' (fingerprints), which can be monitored and evaluated. They guide the selection of available and relevant information sources (RS, intelligence, public) for respective scenarios. For selected test cases (Iran, Iraq, Kashmir and Zimbabwe) a wide spectrum of methodologies and tools was applied in order to evaluate optimized procedures for information extraction. Efficiency and effectiveness of the information extraction procedures were assessed, (i.e. for geo-referencing and feature-extraction) following a benchmarking and validation protocol. At user meetings, summer schools and the GNEX exercises – the relevance of these products for security-related interventions was evaluated by EU representatives and end users.

Moving from gender reporting (as an obligation) to gender action, GMOSS began to consider the gender dimensions related to security issues. A GMOSS Gender and Security Workshop organised with the Women and Science Unit, DG Research and the Equal Opportunities Unit,

DG Administration, convened GMOSS scientists with researchers and experts in the analysis of gender issues in the domain of Security. The workshop focused on the perspective of women in conflict, post conflict reconstruction and peace building. One of the recommendations from this exchange, was that the gender dimension has to be incorporated in concepts for a future network of excellence on security research. For this purpose, connections with other NoEs were established to explore and evaluate potential gender action concepts.

GMOSS put in a variety of efforts to reach out to other GMES projects, experts outside of the European research area and end users. GMOSS considers other GMES projects in implementation as scientific end users, which need to be exposed to the results and concepts developed by the network. The network intends to engage partners of respective consortia in training measures as a way to stimulate the exchange of expertise. Users from the communities-of-practice are involved in training events (such as GNEX, summer schools and seminars) to increase the awareness about the benefits of using spatial information for decision making in security situations. The activities of the training program cater not only for outreach, but also strongly facilitate the integration within the partnership. The year 2007 may serve as an example: following the presentation of the test cases in an integrated analysis framework during the Review Meeting in The Hague (April), the third Summer School on 'Early Warning and Monitoring of Agreements' in Madrid (September), and a Seminar on 'Environment and Conflict' in Bonn (October) provided platforms for exchange between different communities. It is by these 'interfaces' that the network attracted a substantial number of institutions from sectors such as policy analysis, science and technology and service providers to apply for associated partnership. The implementation of near-real time exercises (GNEX'06, '07) is a clear indicator for the progressing integration within GMOSS.

So, in the end, the concept of gaming under realistic scenarios as a tool for problem analysis and validation was broadly accepted by the participants, from GMOSS and outside.

Challenges

Where do we go from here? Based on the described outcome, the impact of the activities on GMES projects and the conviction of the consortium that new territories in research and collaboration have been ventured, concepts and ideas towards future network(s) of excellence have been discussed in several brainstorming sessions. The issues raised so far address challenges in thematic priority areas, integration and network organization.

The topic of the recent seminar on 'Environment and Conflict' responded to a growing recognition that the stability of livelihoods is in many ways influenced by environmental factors as well as governance. Safeguarding human security then certainly requires to extend existing scenarios by incorporating the global and climate change dimension. This should also include investigations into the linkage of security & health and security & migration as demonstrated for epidemics or even pandemics during the GNEX'07. A future research corridor to be explored and structured by a NoE may be associated with 'Environment and Security', in which the concept of human security applies.

However, we, as a monitoring and verification community, can only effectively contribute meaningful information if the characteristics of the relevant processes are identified. The analysis of scenarios – and the evaluation of information products afterwards – show that EO expertise alone is not sufficient. Therefore, the integration of the socio-political domain has to be continued and deepened by incorporating social sciences as 'full' partners. The dialogue between the interdisciplinary communities is fundamental to a future network, as the issues concerned are not resolved by one science at a time but by many simultaneously. In the ideal

case, such an endeavor is closely accompanied by interested users, who feel the strong urge for support, define test cases on their own, and validate the relevance of the information provided.

As a deliberate counterbalance to the operational GMES services, a NoE faces specific organizational challenges. A strong leading team needs to guide the integration of work-package teams, ascertaining consensus-based management. The experience from GMOSS shows that effective communication and the movement of staff across participating institutions are key elements of a 'networking-culture'. By using the flexibility of the NoE wisely, GMOSS has paced towards a 'European Think Tank for the development and benchmarking of new tools and methodologies for the application of EO technology in the security domain'.. The challenge for a future network is to flower out by acting as an advisory group for decision makers in security applications and to further develop the benchmarking concept as support for the operational GMES Core Services.

GMOSS produced evidence that a NoE is a perfect platform for medium-career staff to present the results of their research to a European auditorium. The wealth of new ideas – pre-operational as well as service-improving in nature – can be tapped better by the facilitation the network provides. In this respect, the training concept developed by GMOSS (e.g. summer schools and near-real time exercises) can and should be extended as an integrated component of all GMES services and development projects,

During a brainstorming session a month ago attended by GMOSS and associated partners the participants reached consensus on a working title for a future GMES-NoE: Integrating political, social and remote sensing based monitoring for security. The corridor is wide open for addressing the challenges.

Contributors

Anthony John Cragg
Bhavini Rama

King's College London (KCL)

Department of War Studies, King's College London, Strand, London WC2R 2LS, UK
http://www.kcl.ac.uk/schools/sspp/ws

Dirk Buda
Clementine Burnley
Daniele Ehrlich
Francois Kayitakire
Elodie Pagot
Martino Pesaresi
Christof Roos
Nathalie Stephenne
Gunter Zeug

European Commission - Joint Research Centre (JRC)

Via E. Fermi 2749, I-21027 Ispra (VA), Italy

http://ipsc.jrc.ec.europa.eu/

http://ses.jrc.it/

Albert Nieuwenhuijs
Bert van den Broek

Netherlands Organisation for Applied Scientific Research (TNO)

NL-2597 AK The Hague, Netherlands

http://www.tno.nl

Richard Göbel

Hochschule Hof – University of Applied Sciences

Fachhochschule Hof
Alfons-Goppel-Platz 1
D-95028 Hof, Germany

http://www.fh-hof.de

Daniele Cerra
Antonio de la Cruz
Gracia Joyanes
Marcin Mielewczyk

European Union Satellite Centre (EUSC)

Torrejon de Ardoz, Madrid, Spain E-28850

http://www.eusc.europa.eu

Charles Beumier
Vinciane Lacroix

Royal Military Academy - Signal and Image Centre (SIC-RMA)

Ecole Royale Militaire, Chaire d'électricité, BE-1000 Bruxelles, Belgium

http://www.sic.rma.ac.be/

Stefan Lang
Elisabeth Schöpfer
Dirk Tiede
Andreas Uttenthaler
Peter Zeil

Centre for GeoInformatics - Salzburg University (Z_GIS)

Zentrum für Geoinformatik, Universität Salzburg, A-5020 Salzburg, Austria

http://www.zgis.at

Klaus Granica
Karlheinz Gutjahr

Joanneum Research (JR)

Institut für Digitale Bildverarbeitung, DIB, A-8010 Graz, Austria

http://www.joanneum.at/fb3/dib.html

Irmgard Niemeyer

Technische Universität Bergakademie Freiberg (TUBAF)

Institut für Markscheidewesen und Geodäsie, D-09599 Freiberg, Germany

http://www.geomonitoring.tu-freiberg.de/

Stefan Schneiderbauer

EURAC research

Institute for Applied Remote Sensing
Drususallee/Viale Druso, 1
39100 Bozen/Bolzano

http://www.eurac.edu

Mort Canty

Forschungszentrum Jülich GmbH (FZJ)

D-52425 Jülich, Germany

http://www.fz-juelich.de

Ramy Bader
Michaël Le Duc
Hassan Muammad
Åke Sivertun
Vimalkumar Vaghani

Linköpings Universitet (IDA/LiU)

Institutionen för datavetenskap, Linköpings universitet
SE-581 83 Linköping, Sweden

http://www.ida.liu.se/index.en.shtml

Iman Aloan
Linköping Hospital, Sweden

Thomas Krauß
Manfred Lehner
Peter Reinartz
Deutsches Zentrum für Luft- und Raumfahrt (DLR)
DLR Oberpfaffenhofen, D-82230 Wessling, Germany
http://www.dlr.de/

Xiaoying Cong
Jörg Schlittenhardt
Bundesanstalt für Geowissenschaften und Rohstoffe (BGR)
Seismic Data Analysis Center
D-30655 Hannover, Germany
http://www.seismologie.bgr.de

Uwe Soergel
Universität Hannover -Institut für Photogrammetrie und GeoInformation
Nienburger Straße 1
D-30167 Hannover
http://www.ipi.uni-hannover.de/

Enrico Cadau
Giovanni Laneve
Giancarlo Santilli
Centro di Ricerca Progetto San Marco – Università di Roma "La Sapienza" (CRPSM)
Via Salaria, 851, I-00138 – Rome, Italy
http://www.psm.uniroma1.it/

Allan A. Nielsen
Technical University of Denmark
IMM, Building 321
DK-2800 Lyngby, Denmark

Carolina Aliano
Daniele Casciello
M. Ciampa
Rosita Corrado
N. Genzano
Francesco Marchese
Nicola Pergola
Valerio Tramutoli
Dipartimento di Ingegneria e Fisica dell'Ambiente – Università della Basilicata (UNIBAS)
I-85100 Potenza – Italy
http://www.difa.unibas.it

Irina Coviello
Mariapia Faruolo
Carolina Filizzola
Caterina Grimaldi
Teodosio Lacava
Elena Vita Di Leo

Instituto di metodologie per l'Analisis Amientale (IMAA)
I-85050 Tito Scalo (PZ), Italy
http://www.imaa.cnr.it/

Ana Silva
Einar Bjorgo

UNOSAT – UNITAR
Palais des Nations
CH - 1211 Geneva 10
Switzerland

European Commission

EUR 23033 EN – Joint Research Centre – Institute for the Protection and Security of the Citizen

Title: Global Monitoring for Security and Stability (GMOSS) – Integrated Scientific and Technological Research Supporting Security Aspects of the European Union

Editors: Gunter Zeug & Martino Pesaresi

Luxembourg: Office for Official Publications of the European Communities

2007 – 396 pp. – 21 x 29.7 cm

EUR – Scientific and Technical Research series – ISSN 1018-5593

ISBN 978-92-79-07584-1

Abstract

This report is a collection of scientific activities and achievements of members of the GMOSS Network of Excellence during the period March 2004 to November 2007. Exceeding the horizon of classical remote-sensing-focused projects, GMOSS is characterized by the integration of political and social aspects of security with the assessment of remote sensing capabilities and end-users support opportunities. The report layout reflects the work breakdown structure of GMOSS and is divided into four parts.

Part I *Concepts and Integration* addresses the political background of European Security Policy and possibilities for Earth Observation technologies for a contribution. Besides it illustrates integration activities just as the GMOSS Gender Action Plan or a description of the GMOSS testcases.

Part II of this book presents various *Application* activities conducted by the network partners. The contributions vary from pipeline sabotage analysis in Iraq to GIS studies about groundwater vulnerability in Gaza Strip, from Population Monitoring in Zimbabwe to Post-Conflict Urban Reconstruction Assessments and many more.

Part III focuses on the research and development of image processing methods and *Tools*. The themes range from SAR interferometry for the measurement of Surface Displacement to Robust Satellite Techniques for monitoring natural hazards like volcanoes and earthquakes. Further subjects are the 3D detection of buildings in VHR imagery or texture analysis techniques on time series of satellite images with variable illumination and many other more.

The report closes with Part IV. In the chapter ‘The Way Forward’ a review on four years of integrated work is done. *Challenges and achievements* during this period are depicted. It ends with an outlook about a possible way forward for integrated European security research.

The mission of the JRC is to provide customer-driven scientific and technical support for the conception, development, implementation and monitoring of EU policies. As a service of the European Commission, the JRC functions as a reference centre of science and technology for the Union. Close to the policy-making process, it serves the common interest of the Member States, while being independent of special interests, whether private or national.

LB-NA-23033-EN-C

ISBN 978-92-79-07584-1